

# **BIOLOGICAL REMOVAL OF ZINC FROM INDUSTRIAL EFFLUENT**

## **A THESIS**

*Submitted in partial fulfilment of the requirements for the award of the degree*

*of*

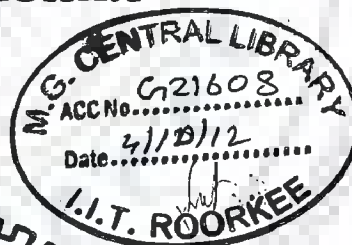
**DOCTOR OF PHILOSOPHY**

*in*

**CHEMICAL ENGINEERING**

*by*

**VISHAL MISHRA**

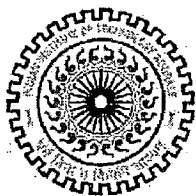


**DEPARTMENT OF CHEMICAL ENGINEERING  
INDIAN INSTITUTE OF TECHNOLOGY ROORKEE  
ROORKEE-247 667 (INDIA)**

**MARCH, 2012**



**©INDIAN INSTITUTE OF TECHNOLOGY ROORKEE, ROORKEE- 2012  
ALL RIGHTS RESERVED**

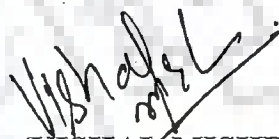


# INDIAN INSTITUTE OF TECHNOLOGY ROORKEE ROORKEE

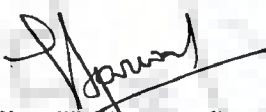
## CANDIDATES DECLARATION

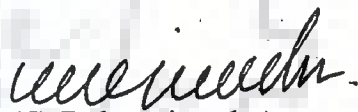
I hereby certify that the work which is being presented in the thesis entitled **BIOLOGICAL REMOVAL OF ZINC FROM INDUSTRIAL EFFLUENT** in partial fulfillment of the requirements for the award of the degree of doctor of philosophy and submitted in the Department of Chemical Engineering, Indian Institute of Technology Roorkee, Roorkee is an authentic record of my own work carried out during the period from August 2008 to February 2012 under the supervision of Dr. C. Balomajumder, Associate professor and Dr. Vijay K. Agarwal, Professor, Department of Chemical Engineering, Indian Institute of Technology Roorkee, Roorkee.

The matter embodied in this thesis has not been submitted by me for the award of any other degree at this or any other institute.

  
(VISHAL MISHRA)

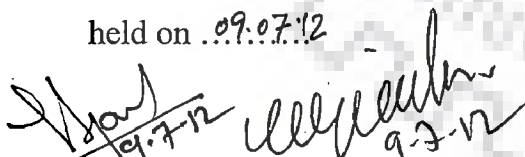
This is to certify that above statement made by the candidate is correct to the best of our knowledge.

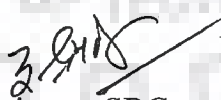
  
(Vijay K. Agarwal)  
Supervisor

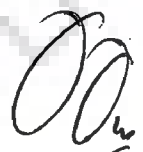
  
(C. Balomajumder)  
Supervisor

Date: 5.3.12

The Ph.D. Viva – Voce examination of **Mr. Vishal Mishra**, Research Scholar, has been held on 09.07.12

  
Signature of Supervisors  
Examiner

  
Chairman SRC

  
Signature of External

  
Head of Department/ Chairman ODC

## ABSTRACT

---

With the development of civilization and industrialization during last few decades, the level of heavy metal ions in natural water resource has increased substantially. Zinc is one such type of heavy metals, presenting in the list of hazardous chemicals, produces various ranges of zinc toxicity to the environment when it is discharged from various industrial effluents with higher concentration. In the present work, the heavy metal zinc in its divalent form along with copper and iron has been considered since these are usually found associated with zinc in various types of industrial effluents. The limit of zinc in wastewater laid down by various environment protection agencies such as USEPA (United States Environment Protection Agency), World Health Organization (WHO) and Central Pollution Control Board (CPCB) is  $5 \text{ mg l}^{-1}$ . Various conventional metal ion remediation technologies have been extensively practised in past. Most of these technologies are not cost effective, eco friendly, has technical shortcomings and also produces secondary pollutants. According to the literature review, bioremediation can be a viable possibility for the zinc removal, since it is not only cost effective, also does not produce any secondary pollutants. Hence, the present investigation aimed at the bioremoval of zinc along with copper and iron from synthetic simulated wastewater and real industrial wastewater. In the present work, both the batch and continuous column studies have been performed. The bioremoval of Zn (II), Cu (II) and total Fe (II, III) was performed by biosorption on the surface of various biomasses and on isolated dead cells of *Zinc sequestering bacterium VMSDCM* accession no. HQ108109. Four types of metal ion combinations namely pure zinc, Zn (II)- Cu (II), Zn (II)- total Fe (II, III) and Zn (II)- Cu (II) – total Fe (II, III) have been studied in the present work. Nine different bioadsorbents namely *Cedrus deodara* sawdust, Eucalyptus leaf powder, Eucalyptus bark sawdust, Pine apple peel powder, Mango bark sawdust, Jack fruit peel powder, Egg shell with egg shell membrane, Orange peel and dead cells of *Zinc sequestering bacterium VMSDCM* accession no. HQ108109 have been used in the present work. The physico-chemical characterization of adsorbents revealed the fact that these bio-adsorbents have high content of carbon. The surface characterization of adsorbents, performed by Scanning electron microscopy (SEM) and Fourier transformation infrared analysis (FTIR), revealed the fact that the surfaces of adsorbents are quite heterogeneous, non-crystalline, rough and highly enriched with

negatively charged functional groups such as amine, amide, carboxyl, carbonyl and hydroxyl stretching. The sorption of Zn (II), Cu (II) and total Fe (II, III) ion was performed on all the adsorbents. The adsorption of these metal ions was performed in various combinations. The individual metal ion system was studied and subsequently various physical process parameters such as pH, temperature, initial concentration of Zn (II), Cu (II) and total Fe (II, III), agitation rate, particle size, and contact time were optimized. Through the physical parameter optimization, two out of nine adsorbents namely *Cedrus deodara* sawdust and dead cells of *Zinc sequestering bacterium VMSDCM* accession no. HQ108109 were found highly efficient to remove Zn (II), Cu (II) and total Fe (II, III) in various combinations in liquid phase. The maximum removal of zinc obtained in pure zinc, Zn (II) - Cu (II), Zn (II)- total Fe (II, III) and Zn (II)- Cu (II)- total Fe (II, III) were 89.19%, 69.12%, 74.31% and 69.11%, respectively in case of *Cedrus deodara* sawdust. The removals of total Fe (II, III) and Cu (II) ion obtained in Zn (II) - total Fe (II, III), Zn (II) - Cu (II) and Zn (II)- Cu (II)- total Fe (II, III) in metal ion systems were 37.19%, 71.11%, 32.14% and 65.5%, respectively. In case of dead cells of *Zinc sequestering bacterium VMSDCM* accession no. HQ108109, the maximum removals of Zn (II) ion obtained in pure zinc, Zn (II) - Cu (II), Zn (II)- total Fe (II, III) and Zn (II)- Cu (II)- total Fe (II, III) was 100%, 86.66%, 88.19% and 74.61%, respectively. The removal of total Fe (II, III) and Cu (II) ion in case of dead cells of *Zinc sequestering bacterium VMSDCM* accession no HQ108109 was 81.1%, 88.19%, 73.34% and 81.23% respectively. The initial concentrations of metal ions were taken as 150 mg l<sup>-1</sup>. Various isotherm models, kinetic, mechanistic and thermodynamic modeling have been performed on both the biomasses. Results showed that the Freundlich, Temkin, pseudo second order and Bangham models were found suitable to interpret the sorption of Zn (II) ion on the surface of *Cedrus deodara* sawdust. Additionally, the sorption of Zn (II) ion on the surface of *Cedrus deodara* sawdust seemed to be endothermic and spontaneous in nature. However, in case of sorption of Zn (II) ion on dead cells of *Zinc sequestering bacterium VMSDCM* accession no. HQ108109, a modified isotherm model has been proposed. The model constant was calculated through code written in C++ language. The modified and proposed isotherm model was validated between 298 K to 308 K. Kinetic, mechanistic and thermodynamic modeling of sorption of Zn (II) ion indicated that the binding of Zn (II) ion on surface of dead cells of *Zinc sequestering bacterium VMSDCM* accession no. HQ108109 followed pseudo

second order and intra particle model. Thermodynamic analysis proved that the biosorption of Zn (II) ion on dead cells of *Zinc sequestering bacterium VMSDCM* accession no. HQ108109 was spontaneous and endothermic in nature. *Cedrus deodara* sawdust and dead cells of *Zinc sequestering bacterium VMSDCM* accession no. HQ108109 were used to treat synthetic simulated wastewater and real industrial wastewater. The industries considered in present work for the purpose of treatment of synthetic simulated waste and real wastewater were copper smelting plant, zinc-plating industry and zinc-producing unit situated SIDCUL, HARDWAR, UTTRAKHAND. The order of removal of metal ions in liquid phase was Cu (II) > Zn (II) > total Fe (II, III). The present work also embodies surface, biochemical and phylogenetic characterization of *Zinc sequestering bacterium VMSDCM* accession no. HQ108109. The 16s rRNA sequencing of *Zinc sequestering bacterium VMSDCM* accession no. HQ108109 was performed and the sequences were submitted to National Center Biotechnology Information (NCBI, US) under the accession no. HQ108109. The phylogenetic and biochemical characterization of *Zinc sequestering bacterium VMSDCM* accession no. HQ108109 revealed the fact that the bacterium seemed to cluster up with arsenite oxidizing bacteria when plotted in a maximum likelihood tree. The isolated microbial strain was grown in various environments of zinc, copper and iron. The growth curve of the bacterium was made in absence of metal ions (standard curve) and in presence of metal ions in various combinations. The growth curve of the bacterium in ternary metal ion system revealed the fact that 167.52 g l<sup>-1</sup> of total iron and 190.62 g l<sup>-1</sup> of copper with 457.66 g l<sup>-1</sup> of Zn (II) ion was found as optimum concentration for growth of *Zinc sequestering bacterium VMSDCM* accession no. HQ108109. The microbial strain of cell was immobilized on the bed of *Cedrus deodara* sawdust. The immobilization of microbial cell was carried out in column reactor and simultaneous biosorption and bioaccumulation of metal ion was performed. The real wastewater, treated in lab scale column reactor was pumped into the column at various flow rates ranging between 109 ml h<sup>-1</sup> to 318 ml h<sup>-1</sup>. The break through curve of metal ions was obtained at various flow rates and time interval. The flow rate of 109 ml/h offered the maximum removal of metal ions from industrial effluent. Present investigation reveals that the treatment, i.e., simultaneous biosorption and bioaccumulation (SBB) gives the best result for the removal of Zn (II), Cu (II), Fe (II, III) from industrial wastewater. We believe that this can be applied in practice for the successful removal of ternary metal ion complex.

## ACKNOWLEDGEMENTS

---

The author takes the opportunity to express his deepest gratitude to all those, who have made it possible for him to submit this work in the hands of learned elite.

The author expresses his deep sense of gratitude and indebtedness to his revered guides Dr. C. Balomajumder, Associate professor, Department of Chemical Engineering and Dr. V. K. Agarwal, Professor, Department of Chemical Engineering, Indian Institute of Technology Roorkee, who provided wholehearted co-operation, never ending inspiration and guidance, throughout the duration of this work.

Author is very thank full to Student Research Committee (SRC) members, Dr. Sri Chand, Dr. B. Choudhary and Dean's representative for their time and invaluable input to the present research.

Author takes this opportunity to put on record his respect to Dr. Vijay K. Agarwal, Head of Department for providing various facilities during the course of present investigation.

The author also likes to extend his thanks to Mr. Akhiesh Sharma, Mr. Manga Ram, technical staff of the department and Institutes Instrumentation Center (IIC) for extending their technical support.

The author likes to deeply acknowledge the ministry of human research development (MHRD) – New Delhi, Government of India for providing funds for this research.

Finally, author would like to thanks and want to express his gratitude to his esteemed father Dr. Shiv Narain Mishra and Mrs. Sangeeta Mishra for their endless support and motivation.

Author also want to thanks his wife Divya, sister and brother in law, friends and colleagues who always supported him when he was dealing with the research problem.

  
(Vishal Mishra)

## LIST OF CONTENTS

		Page no.
	ABSTRACT	i-iii
	ACKNOWLEDGEMENT	iv
	LIST OF CONTENTS	v-xi
	LIST OF TABLES	xii- xxiv
	LIST OF FIGURES AND PHOTOGRAPHS	xv-xxix
	NOMENCLATURE	xxx-xxxii
CHAPTER 1	INTRODUCTION	1-4
CHAPTER 2	LITERATURE REVIEW	5-38
2.0	Introduction	5
2.1	Sources, effect and toxicity of zinc	5 - 11
2.1.1	Sources of zinc pollution	5 - 6
2.1.2	Effect of zinc pollution	7
2.1.3	Limit of zinc discharge	7 - 8
2.1.4	Characterization of various industrial wastewaters containing zinc	8 - 11
2.2	Available technologies for the removal of zinc from wastewater and their limitations	11-22
2.2.1	Physical adsorption	12-13
2.2.2	Chemical adsorption	13
2.2.3	Biosorption and bioaccumulation	13 -14
2.2.4	Biological removal of zinc by microorganism	14-17
2.2.5	Biological removal of zinc by algae and fungi	17 - 21
2.2.6	Biological removal of zinc by various agricultural waste, resins, clay and industrial byproduct	21 - 22
2.2.7	Biosorption isotherms, kinetics and mechanisms	22 - 27
2.2.7.1	Langmuir model	22-23
2.2.7.2	Freundlich model	23-24



2.2.7.3	Temkin model	24
2.2.7.4	Dubinin- Radushkevich (D-R) model	24
2.2.8	Kinetic and mechanistic modeling	25 - 27
2.2.8.1	Pseudo first order model	25-26
2.2.8.2	Pseudo second order model	26
2.2.8.3	Mechanistic modeling	27
2.2.8.4	Intra particle model	27
2.2.8.5	Bangham's model	27
2.3	Review literature	27 - 39
2.4	Concluding remarks	39
CHAPTER 3	EXPERIMENTATION	
3.0	MOTIVATION	40
3.1	PREPARATION OF BIOSORBENT SAMPLE	40
3.2	CHARACTERIZATION OF BIOSORBENT	41-43
3.2.1	Surface area of the biosorbent	41
3.2.2	Presence of various functional groups on biosorbent surface	41-42
3.2.3	Roughness of the surface of biosorbent	42
3.2.4	Carbon, hydrogen, nitrogen and sulphur content	42
3.2.5	pH of the biosorbent surface	43
3.2.6	Physico-chemical characterization of biosorbents	43
3.3	Growth and harvesting of living microorganism	43-44
3.3.1	Preparation of biomass bed	44
3.3.2	Immobilization of microbial cells	44
3.4	SORPTION EXPERIMENTS OF Zn (II) ION	44 - 45
3.4.1	Effect of other co-ions	45
3.5	TYPES OF WASTEWATER TREATED	47
3.6	PHYSICAL PARAMETERS STUDIED IN BATCH BIOSORPTION STUDY	47- 55
3.6.1	Continuous column study	55

3.7	COMPLETE SEQUENCE OF EXPERIMENTS	56 - 57
3.8	CALIBRATION OF MEASURING INSTRUMENTS	57-
3.8.1	Calibration of pH meter	57
3.8.2	Calibration of D. O meter	57
3.8.3	Calibration of O. R. P meter	58
3.8.4	Calibration of Atomic absorption spectrophotometer	58
3.8.5	Element analyzer	58
3.8.6	Electronic weighing balance	58
3.8.7	Calibration of batch experiments and continuous column reactor	58
3.9	EXPERIMENTAL PROCEDURE	58 - 62
3.9.1	Biosorption of zinc in batch and continuous column studies	59
3.9.2	Studies on biosorption of zinc on the surface of various biosorbents in batch reactor	59
3.9.3	Studies on biosorption of Zn (II) at various biosorbent dose	60
3.9.4	Studies on biosorption of Zn (II) at various contact time	60
3.9.5	Studies on biosorption of Zn (II) at various initial concentration	60
3.9.6	Studies on biosorption of Zn (II) at various range of pH	61
3.9.7	Studies on biosorption of Zn (II) at various range of temperature	61
3.9.8	Studies on biosorption of Zn (II) at various range of agitation rate	61
3.9.9	Studies on biosorption of Zn (II) at various range of particle sizes	61-62
3.9.10	Studies on biosorption of total Fe (II, III) and Cu (II) in the presence of zinc	62
3.10	BIOSORPTION AND BIOACCUMULATION OF Zn	62

(II), TOTAL Fe (II, III) AND Cu (II) ION BY  
 IMMOBILIZED ZINC SEQUESTERING BACTERIUM  
 VMSDCM ACCESSION NO. HQ108109

3.11	CONTINUOUS COLUMN STUDY	63-64
	Concluding remark on the section 3.2	64
CHAPTER 4		
4.0	Motivation	65
4.1	DESIGN CONSIDERATION	65
4.1.1	Batch study	65-66
4.1.2	Continuous column study	68
4.1.3	Up –flow column reactor instrumentation	73
4.1.4	Double walled isotherm chamber	76
4.2	AUXILIARY AND ANALYTICAL INSTRUMENT USED IN THE PRESENT WORK	78
	Concluding remark of the section 4.2	85
CHAPTER 5		
	RESULTS AND DISCUSSION	86-
5.0	INTRODUCTION	86
5.1	Characterization of biosorbents	87 - 118
5.1.1	Physico-chemical analysis	87-88
	Concluding remarks of the section 5.1.1	118
5.2	BIOSORPTION OF Zn (II) ION and ALSO IN PRESENCE OF TOTAL Fe (II, III), Cu (II) IN BATCH STUDIES	119
5.2.1	Optimization of pH	114- 148
	Concluding remarks of the section 5.2.1	147-148
5.2.2	Optimization of temperature	148- 171
	Concluding remark of the section 5.2.1	171
5.2.3	Optimization of adsorbent dose	172 - 190
	Concluding remarks of the section 5.3.3	189 - 190

5.2.4	Optimization of initial concentration of Zn (II) ion	190-
	Concluding remarks of the 5.2.4	208-209
5.2.5	Optimization of initial concentration of total Fe (II, III) and Cu (II)	213-224
	Concluding remarks on the section 5.2.5	223 - 224
5.2.6	Optimization of particle size	224-239
	Concluding remarks of the section 5.2.6	239
5.2.7	Optimization of contact time	239-257
	Concluding remark of the section 5.2.7	257 - 258
5.2.8	Optimization of agitation rate	258-277
	Concluding remark of the section 5.2.8	277
	Conclusion of the section 5.2	277
5.2.9	Modeling Using Selected Adsorbents	278- 315
5.2.9.1	Isotherm, Kinetic, Mechanistic and Thermodynamic Modeling of Sorption of Zn (II) Ion in Liquid Phase on the Surface of <i>Cedrus deodara</i> Sawdust	278 - 294
5.2.9.1.1	Isotherm modeling of sorption of Zn (II) ion on <i>Cedrus deodara</i> sawdust	278-282
	Concluding remark of the section 5.2.9.1.1	283
5.2.9.1.2	Kinetic modeling	283-287
5.2.9.1.3	Mechanistic and thermodynamic modeling	288-293
	Concluding remarks of the section 5.2.9.1.3	293-294
5.2.9.2	Isotherm, Kinetic, Mechanistic and Thermodynamic Modeling on the Surface of Dead Cells of <i>Zinc sequestering bacterium VMSDCM</i> accession No. HQ108109	294- 315
5.2.9.2.1	Isotherm modeling	295 - 299
5.2.9.2.2	Isotherm model development	299 - 307
	Concluding remarks on the section 5.2.9.2.2	307
5.2.9.2.3	Kinetic modeling on dead cells of <i>Zinc sequestering</i>	307 - 311

	<i>bacterium VMSDCM</i> accession no. HQ108109	
5.2.9.2.4	Intra particle diffusion, Bangham's film diffusion model and thermodynamic modeling	311 - 315
	Concluding remarks of the section 5.2.9.2.4	315
5.3	BIOSORPTION OF Zn (II), Fe (II, III) AND Cu (II) IN SYNTHETIC SIMULATED WASTEWATER AND REAL WASTEWATER	315-320
5.3.1	Studies on Synthetic Simulated Wastewater	315 - 318
5.3.2	Studies on biosorption using real wastewater	318- 320
	Concluding remark of the section 5.3	320
5.4	Isolation, Purification and Characterization of Zinc Resistant Microbial Strain	320 -
5.4.1	Isolation of microbial strains and purification	320
5.4.2	Genomic DNA isolation	322
5.4.3	Polymerase Chain Reaction (PCR)	322
5.4.4	Submission of sequence	322 - 323
5.4.5	Phylogenetic, biochemical and Scanning Electron microscopic characterization of Zinc Resistant Microbial Strain	323-329
5.4.5.2	Biochemical characterization of <i>Zinc sequestering bacterium VMSDCM</i> accession no. HQ108109	325-329
	Concluding remarks of the section 5.4.5	331
5.5	SIMULTANEOUS BIOSORPTION AND BIOACCUMULATION (SBB) OF ZN (II) ION IN LIQUID PHASE IN BATCH STUDY	331 - 339
5.5.1	Batch study	331
5.5.1.1	Standard growth curve of bacterium	331 - 332
5.5.2	Growth curve of bacterium in Pure zinc, Zn (II)- total	332 - 338

	Fe(II, III), Zn (II) – Cu (II) and Zn (II)- total Fe(II, III)- Cu (II) environment	
5.5.2.1	Growth of <i>Zinc sequestering bacterium VMSDCM</i> accession no. HQ108109 in pure zinc environment	332 - 334
5.5.2.2	Growth of <i>Zinc sequestering bacterium VMSDCM</i> accession no. HQ108109 in presence of copper and zinc	334 - 335
5.5.2.3	Growth of <i>Zinc sequestering bacterium VMSDCM</i> accession no. HQ108109 in presence of iron and zinc	335 – 336
5.5.2.4	Growth of <i>Zinc sequestering bacterium VMSDCM</i> accession no. HQ108109 in presence of iron, zinc and copper	337-338
	Concluding remark of the section 5.5.2	338-339
5.5.3	Biosorption of Zn (II), Cu (II) and total Fe (II, III) by Immobilized <i>Zinc sequestering bacterium VMSDCM</i> accession no. HQ108109	339-340
5.6	CONTINUOUS COLUMN STUDY USING REAL WASTEWATER	341-350
5.6.1	Studies on variation of height of the column and its correlation with mass transfer zone	343-350
	Concluding remarks of the section 5.6.1	350
CHAPTER 6	CONCLUSIONS AND SCOPE FOR FUTURE WORK	351-355
	LIST OF PUBLICATIONS	356 - 357
	REFERENCE	358-374
	ANNEXURE (A-1to A-3)	375 – 417
	APPENDIX (A-1)	418 - 420

## LIST OF TABLES

	Page no.
Table 1: Guidelines frame work delineated by various government agencies	8
Table 2: Various metallurgical units releasing zinc	9 - 10
Table 3: Limitations of various conventional metal ion remediation methodologies	11-12
Table 3.3 (a): Composition of minimal agar media	43
Table 3.3 (b): Composition of Luria Bertani media	43
Table 3.5 (a): Composition of synthetic simulated wastewater	47
Table 3.5 (b): Composition of real wastewater	47
Table 3.6 (a): Experimental work for the removal of zinc ion from pure zinc solution, from binary system of Cu – Zn, from binary system of Fe – Zn and from ternary metal ion system Cu-Fe-Zn in batch studies	48-54
Table 3.6.1 (a): Various studies conducted in the present work for the removal of zinc ion from ternary metal ion system Cu-Fe-Zn in continuous column reactor	55
Table 4.2 (a): Specification of auxiliary and analytical instruments used in the present work.	84
Table 5.1 Physico chemical properties of various biomasses	87-88
Table 5.1 (i): Detailed study of CDS sawdust before adsorption	98
Table 5.1 (j): Detailed study of orange waste before adsorption	99-100
Table 5.1 (k): Detailed study of pineapple fruit peel powder before adsorption	102
Table 5.1 (l): Detailed study of eucalyptus leaf powder before adsorption	103 - 104
Table 5.1 (m): Detailed study of mango bark powder	106
Table 5.1.1 (n): Detailed study of eggshell powder before adsorption	108
Table 5.1.1 (o): Detailed study of Eucalyptus bark sawdust before adsorption	110
Table 5.1 (p): Detailed study of Jackfruit peel powder before adsorption	112

Table 5.2.1: Uptake capacities of zinc by various living and non-living microorganism	144 – 147
Table 5.2.2: Uptake capacities of Zn (II) by various algae	167 – 168
Table 5.2.3: Uptake capacities of Zn (II) ion by various fungal biomasses in terms of their Zn (II) ion uptake capacities	169 – 170
Table 5.2.4: Uptake capacities of Zn (II) ion by agricultural biosorbents	209 – 212
Table 5.2.9.1 (a): Detailed analysis of isotherms and their regression coefficient	281 - 282
Table 5.2.9.1.2 (a): Study of pseudo first and pseudo second order model	286- 287
Table 5.2.9.1.3 (a): Study of intra particle and Bangham's model	290
Table 5.2.9.1.3 (b): Study of Gibb's free energy at three different temperatures	293
Table 5.2.9.2.1 (a): Study of various isotherm model between 298 to 308 K	298-299
Table 5.2.9.2.2 (a): Study of proposed model at 308 K	301
Table 5.2.9.2.2 (b): Study of various isotherm models at 308 K for the boundary conditions $t'$ to $t''$ towards the attainment of equilibrium	302
Table 5.2.9.2.2 (c): Results of equation [5.9] and [5.10] at boundary conditions	304
Table 5.2.9.2.2 (d): Results of equation [5.11] at various temperature and concentration ranges between 298 to 308 K, respectively	306
Table 5.2.9.2.2 (e): Value of model constants between 298 to 308 K	306
Table 5.2.9.2.3 (a): Tabulation of kinetic model equations	310
Table 5.2.9.2.3 (b): Tabulation of kinetic model equations constants	310-311
Table 5.2.9.2.4 (a): Tabulation of mechanistic model equations	313
Table 5.2.9.2.4 (a): Tabulation of mechanistic model equations constants	313-314
Table 5.2.9.2.4 (c): Study of Gibbs free energy and distribution coefficient at various temperature ranges	315



Table 5.3.1 (a): Results of biosorption of Zn (II) and total Fe (II, III) ions in synthetic simulated wastewater (Zinc plating industry, wastewater containing Zn (II) and total Fe (II,III))	316
Table 5.3.1 (b): Results of biosorption of Zn (II),total Fe (II, III) and Cu (II) ions in synthetic simulated wastewater (Copper smelting plant, wastewater containing Zn (II), Cu (II) and total Fe (II,III))	317-318
Table 5.3.2 (a): Results of biosorption of Zn (II), Cu (II) and total Fe (II, III) ions in real industrial wastewater (Zinc manufacturing industry, wastewater containing Zn (II), Cu (II) and total Fe (II,III))	319
Table 5.6.1 (a): Effect of the height of column and flow rate on the Mass Transfer Zone (cm)	343-344
Table 5.6.1.(b): Influence of height of column and flow rate on mass transfer zone and uptake capacities in continuous system	348-349
Table 5.6.1 (c): Results of biosorption of Zn (II),total Fe (II, III) and Cu (II) ions in SBB reactor for real industrial wastewater (real wastewater contains zinc, iron and copper)	350

## LIST OF FIGURES

	Page no.
Figure 3.4.1 (a): Schematic diagram batch sorption studies	46
Figure 3.7 (a): Schematic representation of sorption of Zn (II) ion in batch studies	56
Figure 3.7.(b): Schematic representation of sorption of Zn (II) ion in continuous column studies	57
Figure 4.1.1 (a): Photograph of batch reactor in incubating cum shaking process	67
Figure 4.1.2 (a): Schematic diagram of column reactor used in present work	69
Figure 4.1.2 (b): Front view of column reactor	70
Figure 4.1.2 (c): Front view of feed mixing tank	71
Figure 4.1.3 (a): Photograph of column reactor and mixing tank	73
Figure 4.1.3 (b): Photograph of feeding tank	74
Figure 4.1.3 (c): Photograph of steam generator in continuous column reactor	75
Figure 4.1.4 (a): Details of double walled isotherm chamber (not to scale)	77
Figure 4.2(a): Laminar airflow unit, Research Equipment	79
Figure 4. 2(b): Muffle furnace, Wishwani scientific, India	79
Figure 4.2 (c): Phase contrast microscope, Nikon ECILIPSE Ti	80
Figure 4.2 (d): Mill Q water unit	80
Figure 4.2 (e): FTIR, Thermo model AVATAR 370	81
Figure 4.2 (e): Hot air oven, Thermotech TiC 4000	81
Figure 4.2 (f): SEM, FEI Quanta 200 F	82
Figure 4.2 (g): Surface area analyzer, Micrometrics, model ASAP 2010	82
Figure 4.2(i): AAS unit, GBC, Avanta	83
Figure 4.2(j): Autoclave, Rivotek	83

Figure 5.1 (a): SEM photograph of <i>Cedrus deodara</i> sawdust (CDS) before adsorption	90
Figure 5.1 (b): SEM photograph of Orange waste biomass before adsorption	90
Figure 5.1 (c): SEM photograph of Pine apple peel waste biomass before adsorption	92
Figure 5.1 (d): SEM photograph of Eucalyptus bark sawdust before adsorption	92
Figure 5.1(e): SEM photograph of Eucalyptus leaf powder before adsorption	94
Figure 5.1 (f): SEM photograph of Mango bark powder before adsorption	94
Figure 5.1 (g): SEM photograph of Eggshell waste before adsorption	96
Figure 5.1 (h): SEM photograph of Jackfruit peel before adsorption	96
Figure 5.1 (i): FTIR spectrum of CDS sawdust before adsorption	98
Figure 5.1 (j): FTIR spectrum of orange waste before adsorption	101
Figure 5.1(k): FTIR spectrum of pineapple fruit peel powder before adsorption	104
Figure 5.1 (l): FTIR spectrum of eucalyptus leaf powder before adsorption	106
Figure 5.1 (m): FTIR spectrum of mango bark powder before adsorption	108
Figure 5.1 (n): FTIR spectrum eggshell powder before adsorption	110
Figure 5.1(o): FTIR spectrum of Eucalyptus bark sawdust before adsorption	113
Figure 5.1(p): FTIR spectrum of Jackfruit peel powder before adsorption	116
Figure 5.2.1 (a): Effect of pH on biosorption of Zn on the surface of Mango bark sawdust	120
Figure 5.2.1 (b): Effect of pH on biosorption of Cu and Fe in presence of Zn on the surface of Mango bark sawdust	122
Figure 5.2.1 (c): Effect of pH on biosorption of Zn on orange peel	123

Figure 5.2.1 (d): Effect of pH on biosorption of Cu and Fe in presence of Zn on orange peel	125
Figure 5.2.1 (e): Effect of pH on biosorption of Zn on Pineapple powder	126
Figure 5.2.1 (f): Effect of pH on biosorption of Cu and Fe ions in presence of Zn on Pineapple peel powder	127
Figure 5.2.1 (g): Effect of pH on biosorption of Zn on Jackfruit peel powder	128
Figure 5.2.1 (h): Effect of pH on biosorption of Cu and Fe in presence of Zn on the surface of Jackfruit peel powder	130
Figure 5.2.1 (i): Effect of pH on biosorption of Zn on <i>Cedrus deodara</i> sawdust	131
Figure 5.2.1 (j): Effect of pH on biosorption of Cu and Fe in presence of Zn on <i>Cedrus deodara</i> sawdust	132
Figure 5.2.1 (k): Effect of pH on biosorption of Zn on Eucalyptus bark sawdust	134
Figure 5.2.1 (l): Effect of pH on biosorption of Cu and Fe on Eucalyptus bark sawdust in presence of Zn	135
Figure 5.2.1 (m): Effect of pH on biosorption of Zn on Eucalyptus leaf powder	136
Figure 5.2.1 (n): Effect of pH on biosorption of Cu and Fe in presence of Zn (II) on Eucalyptus leaf powder	138
Figure 5.2.1 (o): Effect of pH on biosorption of Zn (II) on Eggshell and membrane powder	139
Figure 5.2.1 (p): Effect of pH on biosorption of Cu and Fe in presence of Zn on Eggshell and membrane powder	140
Figure 5.2.1 (q): Effect of pH on biosorption of Zn on dead cells of <i>Zinc sequestering bacterium VMSDCM</i> accession no. HQ108109 (dead cells)	142
Figure 5.2.1 (r): Effect of pH on biosorption of Cu and Fe in presence of Zn on dead cells of <i>Zinc sequestering bacterium VMSDCM</i> accession no. HQ108109	143

Figure 5.2.2 (a): Effect of temperature on biosorption of Zn on Mango bark sawdust	149
Figure 5.2.2 (b): Effect of temperature on biosorption of Cu and Fe in presence of Zn on Mango bark sawdust	150
Figure 5.2.2 (c): Effect of temperature on biosorption of Zn ions on orange peel.	151
Figure 5.2.2 (d): Effect of temperature biosorption of Cu and Fe in presence of Zn on orange peel	152
Figure 5.2.2 (e): Effect of temperature on biosorption of Zn on Pineapple peel.	153
Figure 5.2.2 (f): Effect of temperature on biosorption of Cu and Fe in presence of Zn on Pineapple peel	154
Figure 5.2.2 (g): Effect of temperature on biosorption of Zn on Jackfruit peel powder	155
Figure 5.2.2 (h): Effect of temperature on biosorption of Cu and Fe in presence of Zn on Jackfruit peel powder	156
Figure 5.2.2 (i): Effect of temperature on biosorption of Zn on <i>Cedrus deodara</i> sawdust	157
Figure 5.2.2 (j): Effect of temperature on biosorption of Cu and Fe in presence of Zn on <i>Cedrus deodara</i> sawdust	158
Figure 5.2.2 (k): Effect of temperature on biosorption of Zn on Eucalyptus bark sawdust	159
Figure 5.2.2 (l): Effect of temperature on biosorption of Cu and Fe in presence of Zn on Eucalyptus bark sawdust	160
Figure 5.2.2 (m): Effect of temperature on biosorption of Zn Eucalyptus leaf powder	161
Figure 5.2.2 (n): Effect of temperature on biosorption of Cu and Fe in presence of Zn on Eucalyptus leaf powder	162
Figure 5.2.2 (o): Effect of temperature on biosorption of Zn on Eggshell and membrane	163

Figure 5.2.2 (p): Effect of temperature on biosorption of Cu and Fe in presence of Zn on Eggshell and membrane	164
Figure 5.2.2 (q): Effect of temperature on biosorption of Zn on dead cells of <i>Zinc sequestering bacterium VMSDCM</i> accession no. HQ108109	165
Figure 5.2.2 (r): Effect of temperature on biosorption of Cu and Fe in presence of Zn on dead cells of <i>Zinc sequestering bacterium VMSDCM</i> accession no. HQ108109	167
Figure 5.2.3 (a): Effect of adsorbent dose on biosorption of Zn on mango bark sawdust	172
Figure 5.2.3 (b): Effect of adsorbent dose on biosorption of Cu and Fe ions in presence of Zn on mango bark sawdust	173
Figure 5.2.3 (c): Effect of adsorbent dose on biosorption of Zn on orange peel	174
Figure 5.2.3 (d): Effect of adsorbent dose on biosorption of Cu and Fe in presence of Zn on orange peel	175
Figure 5.2.3 (e): Effect of adsorbent dose on biosorption of Zn on Pineapple peel	176
Figure 5.2.3 (f): Effect of adsorbent dose on biosorption of Cu and Fe in presence of Zn on Pineapple peel	177
Figure 5.2.3 (g): Effect of adsorbent dose on biosorption of Zn on Jackfruit peel	178
Figure 5.2.3 (h): Effect of biosorbent dose on biosorption of Fe and Cu in presence of Zn on Jackfruit peel	179
Figure 5.2.3 (i): Effect of adsorbent dose on biosorption of Zn on <i>Cedrus deodara</i> sawdust	180
Figure 5.2.3 (j): Effect of adsorbent dose on biosorption of Fe (II, III) and Cu (II) ions in presence of Zn (II) ion on <i>Cedrus deodara</i> sawdust	181
Figure 5.2.3 (k): Effect of adsorbent dose on biosorption of Zn on Eucalyptus bark sawdust	182

Figure 5.2.3 (l): Effect of adsorbent dose on biosorption of Cu and Fe in presence of Zn on Eucalyptus bark sawdust	183
Figure 5.2.3 (m): Effect of adsorbent dose on biosorption of Zn on Eucalyptus leaf powder	184
Figure 5.2.3 (n): Effect of adsorbent dose on biosorption of Cu and Fe in presence of Zn on Eucalyptus leaf powder	185
Figure 5.2.3 (o): Effect of adsorbent dose on biosorption of Zn on Eggshell and membrane	186
Figure 5.2.3 (p): Effect of adsorbent dose on biosorption of Fe and Cu ions in presence of Zn on Eggshell and membrane	187
Figure 5.2.3 (q): Effect of adsorbent dose on biosorption of Zn on dead cells of <i>Zinc sequestering bacterium VMSDCM</i> accession no. HQ108109	188
Figure 5.2.3 (r): Effect of adsorbent dose on biosorption of Cu and Fe ions in presence of Zn on dead cells of <i>Zinc sequestering bacterium VMSDCM</i> accession no HQ108109	189
Figure 5.2.4 (a): Effect of initial concentration of Zn on biosorption of Zn on Mango bark sawdust	191
Figure 5.2.4(b): Effect of initial concentration of Zn on biosorption of Cu and Fe on Mango bark sawdust	192
Figure 5.2.4 (c): Effect of initial concentration of Zn on biosorption of Zn on Orange peel	193
Figure 5.2.4 (d): Effect of initial concentration of Zn on biosorption of Cu and Fe on Orange peel	194
Figure 5.2.4 (e): Effect of initial concentration of Zn on biosorption of Zn on Pineapple peel	195
Figure 5.2.4 (f): Effect of initial concentration of Zn on biosorption of Cu and Fe on Pineapple peel	196
Figure 5.2.4 (g): Effect of initial concentration of Zn on biosorption of Zn on Jackfruit peel powder	197

Figure 5.2.4 (h): Effect of initial concentration of Zn on biosorption of Cu and Fe on Jackfruit peel powder	198
Figure 5.2.4 (i): Effect of initial concentration of Zn ion on biosorption of Zn on <i>Cedrus deodara</i> sawdust	199
Figure 5.2.4 (j): Effect of initial concentration of Zn on biosorption of Cu and Fe on <i>Cedrus deodara</i> sawdust	200
Figure 5.2.4 (k): Effect of initial concentration of Zn on biosorption of Zn on Eucalyptus bark sawdust	201
Figure 5.2.4 (l): Effect of initial concentration of Zn on biosorption of Cu and Fe on Eucalyptus bark sawdust	202
Figure 5.2.4 (m): Effect of initial concentration of Zn on biosorption of Zn on Eucalyptus leaf powder	203
Figure 5.2.4 (n): Effect of initial concentration of Zn on biosorption of Cu and Fe on Eucalyptus leaf powder	204
Figure 5.2.4 (o): Effect of initial concentration of Zn ion on biosorption of Zn in presence of Cu and Fe on Eggshell and membrane	205
Figure 5.2.4 (p): Effect of initial concentration of Zn on biosorption of Cu and Fe on Eggshell and membrane	206
Figure 5.2.4 (q): Effect of initial concentration of Zn on biosorption of Zn on dead cells of <i>Zinc sequestering bacterium VMSDCM</i> accession no. HQ108109	207
Figure 5.2.4 (r): Effect of initial concentration of Zn on biosorption of Cu and Fe on dead cells of <i>Zinc sequestering bacterium VMSDCM</i> accession no. HQ108109	208
Figure 5.2.5 (a): Effect of initial concentration of Cu and Fe on biosorption of Cu and Fe in presence of Zn on Mango bark sawdust	214
Figure 5.2.5 (b): Effect of initial concentration of Cu and Fe on biosorption of Cu and Fe in presence of Zn on Orange peel	215
Figure 5.2.5 (c): Effect of initial concentration of Cu and Fe on biosorption of Cu and Fe in presence of Zn on Pineapple peel	216



Figure 5.2.5 (d): Effect of initial concentration of Cu and Fe on biosorption of Cu and Fe in presence of Zn on Jackfruit peel	217
Figure 5.2.5 (e): Effect of initial concentration of Cu and Fe on biosorption of Cu and Fe in presence of Zn on <i>Cedrus deodara</i> sawdust	218
Figure 5.2.5 (f): Effect of initial concentration of Cu and Fe on biosorption of Cu and Fe in presence of Zn on Eucalyptus bark sawdust	219
Figure 5.2.5 (g): Effect of initial concentration of Cu and Fe on biosorption of Cu and Fe in presence of Zn on Eucalyptus Eucalyptus leaf powder	220
Figure 5.2.5 (h): Effect of initial concentration of Cu and Fe on biosorption of Cu and Fe in presence of Zn on Eggshell and membrane	221
Figure 5.2.5 (i): Effect of initial concentration of Cu and Fe on biosorption of Cu and Fe in presence of Zn on dead cells of <i>Zinc sequestering bacterium</i> VMSDCM accession no. HQ108109	223
Figure 5.2.6 (a): Effect of particle size on biosorption of Zn on Mango bark sawdust	224
Figure 5.2.6 (b): Effect of particle size on biosorption of Cu and Fe in presence of Zn on Mango bark sawdust	225
Figure 5.2.6 (c): Effect of particle size on biosorption of Zn on Orange peel	226
Figure 5.2.6 (d): Effect of particle size on biosorption of Cu and Fe in presence of Zn on Orange peel	227
Figure 5.2.6 (e): Effect of particle size on biosorption of Zn on Pineapple peel	228
Figure 5.2.6 (f): Effect of particle size on biosorption of Cu and Fe in	229

presence of Zn on Pineapple peel	
Figure 5.2.6 (g): Effect of particle size on biosorption of Zn on Jackfruit peel powder	230
Figure 5.2.6 (h): Effect of particle size on biosorption of Cu and Fe in presence of Zn on Jackfruit peel powder	231
Figure 5.2.6 (i): Effect of particle size on biosorption of Zn on <i>Cedrus deodara</i> sawdust	232
Figure 5.2.6 (j): Effect of particle size on biosorption of Cu and Fe on in presence of Zn <i>Cedrus deodara</i> sawdust	233
Figure 5.2.6 (k): Effect of particle size on biosorption of Zn on Eucalyptus bark sawdust	234
Figure 5.2.6 (l): Effect of particle size on biosorption of Cu and Fe in presence of Zn on Eucalyptus bark sawdust	235
Figure 5.2.6 (m): Effect of particle size on biosorption of Zn on Eucalyptus Leaf powder	236
Figure 5.2.6 (n): Effect of particle size on biosorption of Cu and Fe in presence of Zn on Eucalyptus Leaf powder	237
Figure 5.2.6 (o): Effect of particle size on biosorption of Zn on Eggshell and membrane	238
Figure 5.2.6 (p): Effect of particle size on biosorption of Cu and Fe in presence of Zn on Eggshell and membrane	239
Figure 5.2.7 (a): Effect of contact time on biosorption of Zn on Mango bark sawdust	240
Figure 5.2.7 (b): Effect of contact time on biosorption of Cu and Fe in	241

presence of Zn on Mango bark sawdust

Figure 5.2.7 (c): Effect of contact time on biosorption of Zn on Orange peel. 242

Figure 5.2.7 (d): Effect of contact time on biosorption of Cu and Fe in presence of Zn on Orange peel 243

Figure 5.2.7 (e): Effect of contact time on biosorption of Zn on Pineapple peel 244

Figure 5.2.7 (f): Effect of contact time on biosorption of Cu and Fe in presence of Zn on Pineapple peel 245

Figure 5.2.7 (g): Effect of contact time on biosorption of Zn on Jackfruit peel 246

Figure 5.2.7 (h): Effect of contact time on biosorption of Cu and Fe in presence of Zn on Jackfruit peel 247

Figure 5.2.7 (i): Effect of contact time on biosorption of Zn on *Cedrus deodara* sawdust 248

Figure 5.2.7 (j): Effect of contact time on biosorption of Cu and Fe in presence of Zn on *Cedrus deodara* sawdust 249

Figure 5.2.7 (k): Effect of contact time on biosorption of Zn on Eucalyptus bark sawdust 250

Figure 5.2.7 (l): Effect of contact time on biosorption of Cu and Fe in presence of Zn on Eucalyptus bark sawdust 251

Figure 5.2.7 (m): Effect of contact time on biosorption of Zn on Eucalyptus leaf powder 252

Figure 5.2.7 (n): Effect of contact time on biosorption of Cu and Fe in 253

presence of Zn on Eucalyptus leaf powder	
Figure 5.2.7 (o): Effect of contact time on biosorption of Zn on Eggshell and membrane	254
Figure 5.2.7 (p): Effect of contact time on biosorption of Cu and Fe in presence of Zn on Eggshell and membrane	255
Figure 5.2.7 (q): Effect of contact time on biosorption of Zn on dead cells of <i>Zinc sequestering bacterium VMSDCM</i> accession no. HQ108109	256
Figure 5.2.7 (r): Effect of contact time on biosorption of Cu and Fe in presence of Zn on dead cells of <i>Zinc sequestering bacterium VMSDCM</i> accession no. HQ108109	257
Figure 5.2.8 (a): Effect of agitation rate on biosorption of Zn on Mango bark sawdust	258
Figure 5.2.8 (b): Effect of agitation rate on biosorption of Cu and Fe in presence of Zn on Mango bark sawdust	259
Figure 5.2.8 (c): Effect of agitation rate on biosorption of Zn on Orange peel	260
Figure 5.2.8 (d): Effect of agitation rate on biosorption of Cu and Fe in presence of Zn on Orange peel	261
Figure 5.2.8 (e): Effect of agitation rate on biosorption of Zn on Pineapple peel	262
Figure 5.2.8 (f): Effect of agitation rate on biosorption of Cu and Fe in presence of Zn on Pineapple peel	263
Figure 5.2.8 (g): Effect of agitation rate on biosorption of Zn on	265

Jackfruit peel

Figure 5.2.8 (h): Effect of agitation rate on biosorption of Cu and Fe in presence of Zn on Jackfruit peel 266

Figure 5.2.8 (i): Effect of agitation rate on biosorption of Zn on *Cedrus deodara* sawdust 267

Figure 5.2.8 (j): Effect of agitation rate on biosorption of Cu and Fe in presence of Zn on *Cedrus deodara* sawdust 268

Figure 5.2.8 (k): Effect of agitation rate on biosorption of Zn on Eucalyptus bark sawdust 269

Figure 5.2.8 (l): Effect of agitation rate on biosorption of Cu and Fe in presence of Zn on Eucalyptus bark sawdust 270

Figure 5.2.8 (m): Effect of agitation rate on biosorption of Zn on Eucalyptus leaf powder 271

Figure 5.2.8 (n): Effect of agitation rate on biosorption of Cu and Fe in presence of Zn on Eucalyptus leaf powder 272

Figure 5.2.8 (o): Effect of agitation rate on biosorption of Zn on Eggshell and membrane 273

Figure 5.2.8 (p): Effect of agitation rate on biosorption of Cu and Fe in presence of Zn on Eggshell and membrane 274

Figure 5.2.8 (q): Effect of agitation rate on biosorption of Zn on dead cells of *Zinc sequestering bacterium VMSDCM* accession no HQ108109 275

Figure 5.2.8 (r): Effect of agitation rate on biosorption of Cu and Fe in presence of Zn on dead cells of *Zinc sequestering bacterium VMSDCM* accession no. HQ108109 276

Figure 5.2.9.1(a): Langmuir isotherm for the biosorption of Zn (II) ion on the surface of <i>Cedrus deodara</i> sawdust	279
Figure 5.2.9.1 (b): Study of Freundlich model for the biosorption of Zn (II) ion on the surface of <i>Cedrus deodara</i> sawdust	280
Figure 5.2.9.1 (c): Study of Temkin model for the biosorption of Zn (II) ion on the surface of <i>Cedrus deodara</i> sawdust	280
Figure 5.2.9.1.2 (a): Study of pseudo first order reaction model	283
Figure 5.2.9.1.2 (b): Study of pseudo second order reaction model	284
Figure 5.2.9.1.3 (a): Study of intra particle model	288
Figure 5.2.9.1.3 (b): Study of Bangham's model	289
Figure 5.2.9.1.3 (c): Plot of $\ln K_c$ versus $1/T$	292
Figure 5.2.9.2.1 (a) : Study of langmuir isotherm model between 298 K to 308 K	295
Figure 5.2.9.2.1 (b): Study of Freundlich isotherm model between 298 K to 308 K	296
Figure 5.2.9.2.1 (c): Study of Temkin model between 298 K to 308 K	297
Figure 5.2.9.2.1 (c): Study of D-R model between 298 K to 308 K	298
Figure 5.2.9.2.2 (a): Study of the proposed isotherm at 308 K	300
Figure 5.2.9.2.2 (b): Study of proposed model between 298 K– 308 K	307
Figure 5.2.9.2.3 (a): Pseudo first order model study of Zn (II) ion biosorption on surface of <i>zinc sequestering bacterium VMSDCM</i> accession no. HQ108109	308
Figure 5.2.9.2.3 (b): Pseudo second order model study of Zn (II) ion	309

biosorption on surface of *zinc sequestering bacterium VMSDCM*  
accession no. HQ108109.

Figure 5.2.9.2.4 (a): Study of Intra particle diffusion model at various  
temperature ranges 311

Figure 5.2.9.2.4 (b): Study of Bangham's film diffusion model at various  
temperature ranges 312

Figure 5.4.1 (a): Petri plates showing the growth of *Zinc sequestering*  
*bacterium VMSDCM* accession no. 108109 321

Figure 5.4.5 (a): Phylogenetic tree of 16S rRNA amplified products for  
*Zinc sequestering bacteria*. The percentage of replicate trees in which  
the associated taxa cluster together in the boot strap test (1000  
replicates) are shown next to the branches 324

Figure 5.4.5.1 (a): Gram stained photograph of bacterium *Zinc*  
*sequestering bacterium VMSDCM* accession no. HQ108109 326

Figure 5.4.5.1 (b): Gram stained of *Zinc sequestering bacterium*  
*VMSDCM* accession no. HQ108109 327

Figure 5.4.5.1 (c): SEM photograph of *Zinc sequestering bacterium*  
*VMSDCM* accession no. HQ108109 328

Figure 5.4.5.1 (d): SEM photograph of *Zinc sequestering bacterium*  
*VMSDCM* accession no. HQ108109 (after adsorption) 330

Figure 5.5.1.1 (a): Standard growth curve of *Zinc sequestering*  
*bacterium VMSDCM* accession no. HQ108109 332

Figure 5.5.2.1(a): Growth curve of *Zinc sequestering bacterium*  
*VMSDCM* accession no. HQ108109 333

Figure 5.5.2.2 (a): Growth curve of the bacterium in the environment of  
zinc ( $457.66 \text{ g l}^{-1}$ ) and copper 334

Figure 5.5.2.3 (a): Growth curve of the bacterium in the environment of zinc (457.66 g l <sup>-1</sup> ) and iron	336
Figure 5.5.2.4 (a): Growth curve of the bacterium in the environment of zinc (457.66 g l <sup>-1</sup> ), iron and copper	337
Figure 5.5.3 (a): Effect of initial concentration of Zn on biosorption of Zn by immobilized <i>Zinc sequestering bacterium VMSDCM</i> accession no. HQ108109	340
Figure 5.6 (a): SEM Photograph of <i>zinc sequestering bacterium VMSDCM</i> accession no. HQ108109 immobilized on surface of sawdust	342
Figure 5.6.1 (a): Effect of flow rate on concentration of zinc (break through curve).	345
Figure 5.6.1 (b): Effect of flow rate on concentration of copper (break through curve).	346
Figure 5.6.1 (c) Effect of flow rate on concentration of total Fe (II, III) (break through curve).	347



## Nomenclature

C		Carbon
$C_{bm}$		Adsorbate species concentration in liquid phase ( $\text{mmolel}^{-1}$ )
H		Hydrogen
O		oxygen
A		Ash
S		Sulphur
N		Nitrogen
NCBI		National Center of Biotechnology Information
$C_0$	$\text{mg l}^{-1}$	Initial concentration of metal ion
$C_{bm}$		Adsorbate species concentration in liquid phase ( $\text{mmolel}^{-1}$ )
$C_e$	$\text{mg l}^{-1}$	Final concentration of metal ion
$D_f$	$\text{cm}^2 \text{s}^{-1}$	Film Diffusion coefficient
$D_p$	$\text{cm}^2 \text{s}^{-1}$	Pore Diffusion coefficient
$D_{vM}$		modified model constant
$\Delta G$	$\text{kJ mol}^{-1}$	Gibbs free energy
h	$\text{mg}^{-1} \text{g}^{-1} \text{min}^{-1}$	Initial sorption rate
$\Delta H$	$\text{kJ}^{-1} \text{mol}^{-1}$	Enthalpy
I		Value of intercept
$K_c$		Dimensionless, Equilibrium constant
$K_{id}$	$\text{mgg}^{-1} \text{min}^{-0.5}$	Intra particle diffusion model constant
$K_L$		Langmuir model constant
$K_f$		Freundlich model constant ( $\text{mmol g}^{-1}$ )
$K_0$		Bangham's model constant
$K_1$	$\text{min}^{-1}$	First order reaction constant
$K_2$	$\text{mg g}^{-1} \text{min}^{-1}$	Second order reaction constant
m/M	g	Mass of biosorbent in grams
$q_e$	$\text{mgg}^{-1}$	Uptake capacity
$q_e \text{ (exp)}$	$\text{mgg}^{-1}$	Experimental uptake capacity
$q_{\max}$	$\text{mgg}^{-1}$	Maximum uptake capacity

$q_e$ (Th)	$\text{mgg}^{-1}$	Theoretical uptake capacity
$q_t/q$	$\text{mgg}^{-1}$	Uptake capacity in time t
R	$\text{J mol}^{-1}\text{K}^{-1}$	Universal gas constant
$R_p$		Radius of the adsorbate particle
SSE		Sum of square errors
$\Delta S$	$\text{kJmol}^{-1}\text{K}^{-1}$	Entropy
t		Time
$t^{0.5}$		Square root of time
$t^{1/2}$		Half of the time required for total biosorption
T	K	Absolute temperature
$v/V$	l	Volume of Solution
$\chi$		Chi
$\alpha$		Bangham's model constant
$\varepsilon$	cm	Thickness of the film
$B_t$		Temkin model constant
$K_t$		Temkin model constant
$\beta$		Dubinin- Radushkevich model constant
$\varepsilon$		Polayni potential
USEPA		United States Environmental Protection Agency
$V_m$		Constant of point function in proposed model
WHO		World Health organization

# INTRODUCTION



INTRODUCTION

---

Modernization of society and industrialization during last few decades has made an increase in the heavy metal pollution in natural water bodies. The series of heavy metals consists of many elements some of which are chromium, cadmium, zinc, iron, lead, copper etc. Among heavy metals, zinc is one of the elements, which is used in many mechanical and chemical unit operations. Zinc stands at 74<sup>th</sup> rank in the list of toxic metals. The United States Environmental Protection Agency (USEPA) and World Health Organization (WHO) have demarcated the permissible limit of zinc in waste and potable water as 5 and 3 mg l<sup>-1</sup> respectively. The contamination of zinc on water surface mainly occurs through the effluent coming out from acid mine drainage, spent pickling acid from metallurgical industries and copper smelting plant effluent. The range of discharge of zinc from various industries lies between 0.142 g/l to 81986.52 g/l. The effluent released from these plants consists of many other metals such as iron, cadmium, lead etc. The zinc in its divalent state is quite toxic. Earlier, it was found that zinc is involved in reversible allergic reactions and gastrointestinal disorder. Nevertheless, the latest research indicates that excessive intake of zinc leads to nephrological, neurological and circulatory disorders. Not only the human beings are affected by the toxicity of zinc but also the toxicity of zinc substantially affects the natural fauna. In plants, very small concentration of zinc is sufficient to cause the micronucleus induction. The defined concentration of zinc induces apoptosis or programmed cell death (PCD) in human cells. Zinc in combination with chromium (hexavalent) has a tendency to cause chromosomal instability and DNA double strand breaks in human lung cells. Nano particles of zinc present as particulate matter in air severely effects lungs and induces inflammatory responses. The inhalation of zinc as zinc chloride and pure zinc in particulate form generates edema and increases the probability of asthma. The compounds of zinc used in endodontic medication have potential capacity to induce clastogenic changes. The toxicity of zinc is significantly increased in presence of other metal ions. The Maximum Concentration Limit (MCL) range of iron and copper in water bodies is 3.0 mg/l as per demarcations of WHO and Indian standards. There is huge difference in limit of discharge of zinc from various mechanical

operations and the permissible limit of discharge in various water bodies. Therefore, with the above-mentioned reasons the present investigation has been taken up for the removal of zinc from industrial effluent. The industry selected, for the present study was metallurgical cum zinc production unit, Hindustan Zinc Limited, Vedanta Industries, situated at SIDCUL, Hardwar, India. The most pronounced form of the zinc in the effluent is its divalent state, i.e., zinc (II) as chloride or any other derivative. Many remediation technologies meant for metal ion removal have been practised in the past. These are adsorption, electro coagulation and flocculation, osmosis, reverse osmosis, liquid - liquid extraction, hydroxide, sulphide precipitation etc. All these technologies are quite expensive at mass scale as well as they are not effective in removing the metal ions from liquid phase below a minimum threshold concentration. Furthermore, the conventional metal removal technologies require the usage of additional chemicals resulting in generation of secondary chemical sludge, which makes the disposal of sludge questionable. Contrary to this, the biosorption of metal ion across liquid phase onto surface of various sorts of biomass has gained the significant importance in last few years. A number of biomasses have been used to remove zinc from liquid phase such as plant biomass, agricultural by products, activated carbon, algae, fungi, bacteria etc. Most of the studies have focused on the removal of metal ion across liquid mediated by biosorption onto the surface of either living or nonliving biomass.

The main considering parameters, which significantly influence the removal of zinc (II) are pH, temperature, agitation rate, contact and equilibrium time, initial concentration of zinc (II) ion, mass of the biomass used, particle size of the biomass and volume of the solution. The other factors relevant to biomass like bulk density, surface area, types of functional groups on the biomass surface, surface texture/ morphology of biomass surface, porosity, surface pH of the biomass and  $pH_{zpc}$  also influences the sorption of zinc (II) ion up to an extent. Another factor that considerably affects the biosorption of Zn (II) ion is the interference of other metal ions present in the effluent discharge of various industries. The composition of these effluents also varies significantly. Some of the agricultural by products, bacterial strains, fungus, and algae used as biosorbents for removal of heavy metals are baggase, almond shell, birch wood, hazel nut, *Pseudomonas syringae*, *Streptomyces nouresi*, *Penicillium digitatum*, *Penicillium chrysogenum* and *Sargassum natans*. An another significant improvement in case of removal of zinc (II) ion was phytoremediation. However, the living microbial cell mediated sorption

of heavy metal ions has gained significant interest due to (i) high capability of withdrawing heavy metals from wastewater (ii) huge quantity of small size cell development in controlled conditions (iii) flexibility towards the changing environmental conditions (iv) diverse genetic constitution coupled with feasibility of genetic engineering methodology, metabolic pathways, presence of mechanisms such as bioleaching, metal ion sequestering property, oxidoreduction, detoxification, presence of metalloenzymes, metalloproteins, bioaccumulation (active transport), biosorption (passive transport) and negatively charged functional groups such as hydroxyl, phosphate, amino, sulphate and carboxylate group on the surface of microbial cell surface. The main mechanism that operates in case of microbial cells is either biosorption or bioaccumulation or a combination of both. The primary one is the passive adsorption of metal ions on to the surface of cells. The sorption of metal ion in biosorption is mediated by the functional groups present on the cell surface. However, in bioaccumulation the metal ion accumulates inside the microbial cell by various mechanisms such as methylation and intracellular precipitation.

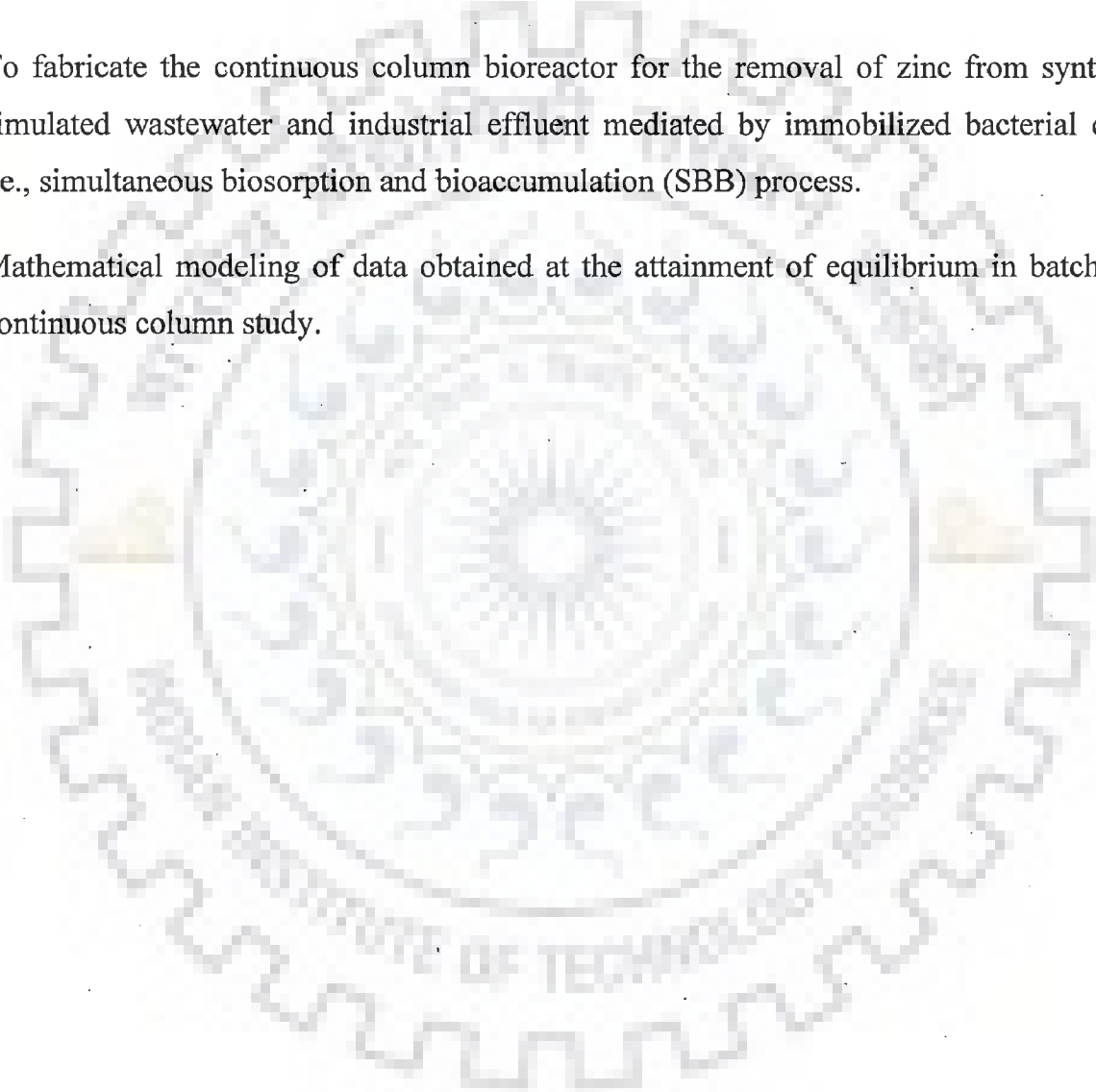
Use of free and immobilized bacterial cells systems for the removal of zinc from liquid have been reported in literature. The microorganisms used in various investigations were well known and undoubtedly have contributed significantly in this contemporary field. Furthermore, various investigations have also adopted the dead biomass of the microbial cells obtained after pretreatment. However, relatively less information is available on microbial cell and use of immobilized microbial cell in continuous column bioreactor.

The above mentioned facts motivated the present investigation meant to remove heavy metals from industrial effluent, utilizing the biosorption (passive adsorption) and bioaccumulation (active adsorption) mediated by nonliving and living biomass individually and a combination of both sorts of biomasses in batch and in continuous mode studies.

The major objectives of the present investigations have been given below.

- (i) To determine the optimum process parameters for maximum removal of zinc (II) ion from liquid phase in presence and in absence of various other heavy metal ions mediated by biosorption onto surface of various sorts of natural non living biomass and microbial cell in batch studies.

- (ii) To identify and to screen out the most zinc (II) resistant bacterium isolated from industrial pollution site, to evaluate the biosorption potential of the isolated bacterium in terms of removal of zinc from liquid phase in batch study and to investigate the capability of the identified efficient microbial cells in immobilized phase to remove zinc from synthetic simulated wastewater and industrial wastewater in batch studies.
- (iii) To perform the genomic and biochemical characterization of the isolated resistant strain of bacterium and to find out the phylogenetic relationship of the bacterium.
- (iv) To fabricate the continuous column bioreactor for the removal of zinc from synthetic simulated wastewater and industrial effluent mediated by immobilized bacterial cells, i.e., simultaneous biosorption and bioaccumulation (SBB) process.
- (v) Mathematical modeling of data obtained at the attainment of equilibrium in batch and continuous column study.



LITERATURE REVIEW

---

**2.0 Introduction**

The rapid industrialization has made a significant impact on the ground water, surface water and on natural water reservoirs due to enormous discharges of heavy metals and other chemicals. One of the significant elements that contribute significantly to the water pollution is zinc. Zinc is one of the essential elements of enzymes such as superoxide dismutase (Mukhopadhyay et al., 1998). The Comprehensive environment response, Compensation and Liability act - 2007 (CERCLA) has ranked zinc at 74<sup>th</sup> position with respect to water pollution with total score of 932.89 points (Mishra et al., 2010). The European Union Dangerous Substance Directive (76/464/EEC) has categorized zinc as list 2 element (Arshad et al., 2008). Very often, the zinc in the effluent discharged from various industrial units is accompanied by iron and zinc. The most prominent form of zinc available in industrial effluent is zinc (II) ions (Mishra and Patel, 2009). According to the list of organic and inorganic pollutants prepared by United States Environmental Protection Agency (USEPA), the zinc has been kept in the list of toxic metals with other 13 metals (Kumar et al., 2006, Ceur and Balkaya, 2007).

**2.1 Sources, effect and toxicity of zinc****2.1.1 Sources of zinc pollution**

Pollution due to various heavy metals is a matter of serious concern in the present scenario. The usage and importance of a particular metal gives a clear indication of pollution caused due to the particular metal. Zinc is essentially important element for many economic growth-supporting sectors of the world such as metallurgical operation units, electroplating industry, mining industry and mine drainage operations. Some specific sources of zinc pollution in natural water and reservoirs include effluents discharged from galvanization industry, wood preservative industry, rubber vulcanization plant, zinc and brass metal alloy industry, ceramics, textiles, brass plating, fertilizers, paint and pigments, automobile emission and batteries industries (Arshad et al., 2008, Baig et al., 2009, Lee et al., 2004, Gokhale and Khare, 2007, Mukherjee, 2007). Some more pronounced sites of zinc pollution include electroplating



units and acid mine drainages site. Recently, over  $620 \text{ mg l}^{-1}$  of zinc has been reported in the effluent releasing out from the abandoned copper mines in Monsanto, United States (Volsky 2003). The extensive mining activities in Nent Valley (UK) over two centuries for lead and zinc have left the river water and land tremendously polluted. Usually in mine drainage, zinc is present in liquid phase as zinc (II) ions. However, the mine drainage from Nent Valley has very high alkalinity, therefore, zinc persists in liquid phase as carbonate complex ( $\text{ZnCO}_3$ ). The level of zinc that comes in Nent valley mine drainage ranges between  $3 - 8 \text{ mg l}^{-1}$  (Nuttal and Younger 2000). The sample obtained from mines in Oruro, Bolivia indicated the presence of  $8709.2 \text{ mg}$  of zinc (equivalent to  $1.34 \text{ mM}$ ) /  $500 \text{ ml}$  (working volume is considered) (Alvarez et al., 2007).

However, the occurrence of zinc or any other heavy metal also depends on the specific site. Concentration of heavy metals in storm water runoff concentrations of various heavy metals were zinc  $0.008 - 0.720 \text{ mg l}^{-1}$ , copper  $0.001 - 0.079 \text{ mg l}^{-1}$ , manganese  $0.001 - 0.516 \text{ mg l}^{-1}$  and lead  $0.003 - 0.010 \text{ mg l}^{-1}$  respectively (Vijayaraghavan et al., 2008, Asaf et al., 2004). Walker et al., 1999) characterized the urban runoff, the range of heavy metals observed in urban runoff water included zinc ( $0.0007 - 22.0 \text{ mg l}^{-1}$ ), copper ( $0.00006 - 1.41 \text{ mg l}^{-1}$ ) and lead ( $0.00057 - 26.0 \text{ mg l}^{-1}$ ).

Zinc contamination in natural environment has been found in 985 sites out of 1662 national priority risk sites identified by USEPA (Agency for Toxic Substances and Disease Registry, 2005). Wastes containing zinc have been categorized as hazardous waste under the Basal convention and European Union (Agarwal et al., 2004).

The secondary waste generated during the metallurgical operations, i.e., zinc ash, zinc dross, flux, flue dust from electric arc furnace, automobile junks and sludge contains very high amount of zinc in the form of some sort of compound or derivative. Frequently, the zinc in secondary waste is accompanied by various other toxic heavy metals. The rising requirement of alkaline zinc manganese batteries and their disposal have posed a more potent source of zinc pollution in the environment (Ostroski et al., 2009). Since the zinc is involved in almost all-metal polishing and metallurgical works, hence zinc (II) ions are most habitually encountered in wastewater treatment (Pejic et al., 2008).

### 2.1.2 Effect of zinc pollution

Though zinc is an essential element required for the growth of plants, animals and humans (Sengil et al., 2009). However, excessive intake of zinc can be fatal. Metal zinc is non-biodegradable and it accumulates in the body of the organism through food chain (Ucun et al., 2009). Toxicity of zinc has several reversible and irreversible effects on natural flora and fauna. For example, very low exposure of zinc is responsible for gastrointestinal disturbance, i.e., irritability, nausea, loss of appetite, metal fume fever and muscular stiffness (Ruiz et al., 2007, Lesmana et al., 2009, Bhattacharya et al., 2006, Vilar et al., 2007, Marin et al., 2009).

The level of zinc beyond a threshold concentration in soil affects the fertility of soil very adversely (Agorboude and Navia, 2009, Das 2003). The exposure of zinc also leads to lethargy, hyperamylasemia, pancreatitis, cholestatic jaundice, anemia, thrombocytopenia, pulmonary edema, renal failure, circulation and neurological disturbances (Marin et al., 2009, Klein 2000). 120- $\mu$ M concentration of zinc leads to the micronucleus induction in plant *Vicia faba* (Mishra et al., 2010). In case of aquatics, the ionic form of zinc is lethal to invertebrates and vertebrate fish (Shek et al., 2009).

Small amount of free zinc ions can cause heavy damage to ambient environment, kill some microorganism and excessive intake of zinc can also cause the deficiency of other dietary minerals (Shek. et al., 2009). The inhalation of zinc as particulate matter at work place and in ambient environment leads to zinc intoxication resulting in pale mucous membrane, jaundice, numerous heinz bodies, anemia and pediatric asthma (Cooper 2008, Hirshon et al., 2008). The concentration of zinc determines its role as apoptosis blocker or apoptosis inducer. There are several examples where zinc has behaved as apoptosis or programmed cell death inducer (Formigari et al., 2007, Wilson et al., 2007). The genotoxic character of zinc has been demonstrated in microorganisms, i.e., *Salmonella typhimurium* and *Escherichia coli* (Codina et al.2000). The pulmonary exposure to particulate sized zinc particle and sub chronic inhalation of zinc sulphate could be responsible for cardiotoxicity (Wallenborn et al., 2009, Wallenborn et al., 2008).

### 2.1.3 Limit of discharge of zinc pollution

The guidelines for discharge of zinc in ground water, fresh water and estuaries mentioned by government agencies of various countries have been shown in table 1.

Table 1: Guidelines frame work delineated by various government agencies

Name of agency	Type of water	Limit of discharge	Reference
World Health Organization (WHO)	Drinking water	5 mg l <sup>-1</sup>	Kumar et al., 2006, Mishra and Patel (2009), Mohan and Singh, 2002
Minimum National Standards (MINAS), Ministry of Environment and Forest, Government of India	Surface water	5 mg l <sup>-1</sup>	Srivastava et al., 2007
Minimum National Standards (MINAS), Ministry of Environment and Forest, Government of India	Potable water	3 mg l <sup>-1</sup>	Srivastava et al., 2006
Central Pollution Control Board, India	Wastewater	5 mg l <sup>-1</sup>	Naiya et al., 2008
United States Environment Protection Agency	Drinking water	5 mg l <sup>-1</sup>	Naiya et al., 2008

### 2.1.4 Characterization of various industrial wastewaters containing zinc

Various industrial sectors and anthropogenic sources contribute to the pollution of zinc in environment. In India, some of the industries that cause zinc pollution are Binani Zinc in Kerla (Thomas, 1998), Hindustan Zinc Limited in Rajasthan (Mackenzie and Smith, 1981, Sharma, 1989, 1998), Debari Smelter Plant Rajasthan (Bhatnagar and Jancy, 1998, Basu and Swarnkar, 1990, Jaju, 1998, Sharma, 1989, Solanki and Singh, 1981), Zinc Lead smelter plant (Sharma, 1998, Solanki and Singh, 1981, Thomas, 1998), Sun rise zinc Goa (Bhatnagar and Jancy, 1998) and Bharat zinc. Most of these industries either dump their effluents in landfill sites or store in industrial premises in pond like structures. Except Zinc Lead smelter plant,

none of the industries is involved in recycling of zinc, and undoubtedly, their effluents and leach residue contain huge amount of zinc ranging between 1.26 % - 60% of the total waste generated. Table 2 represents the concentrations of zinc and other heavy metals present in wastewater discharging from various industrial sources.

Table 2: Various metallurgical units releasing zinc in the effluent

Name of plant	Location	Effluent	Constituents	Concentration	Reference
Belos hot dip galvanization plant	Bielsko-Baila, Poland	Spent pickling acid	Zn (II)	80000 mg l <sup>-1</sup>	Grzeszczyk and Rosocka 2007
N.D.	Minas Gerais state, Brazil	Spent pickling acid	Fe (II) HCl Cl <sup>-</sup> Zinc (II)	30000 mg l <sup>-1</sup> 2.5 M 6 M 70200 mg l <sup>-1</sup>	Mansur et al., 2008
N. D	N. D	Spent pickling acid	Zinc (II) Fe (II) Fe (III) Cr Acidity	33900 mg l <sup>-1</sup> 9000 mg l <sup>-1</sup> 2200 mg l <sup>-1</sup> 40 mg l <sup>-1</sup> 0.25 M	
N. D	N. D	Spent pickling acid	Fe	2.0 M 137500 mg l <sup>-1</sup>	Csicsovszki et al., 2005
N. D	N.D	Copper industry industrial effluent	Zn Pb Ni Cu Al HCl Zn	26120 mg l <sup>-1</sup> 91 mg l <sup>-1</sup> 83 mg l <sup>-1</sup> 27 mg l <sup>-1</sup> 87 mg l <sup>-1</sup> 17890 mg l <sup>-1</sup> 142 mg l <sup>-1</sup>	Basha et al., 2008
			Fe Pb Cu Ni Antimony Cr Co	188 mg l <sup>-1</sup> 4.6 mg l <sup>-1</sup> 93 mg l <sup>-1</sup> 12 mg l <sup>-1</sup> 1.5 mg l <sup>-1</sup> 2.3 mg l <sup>-1</sup> 0.04 mg l <sup>-1</sup>	

			Cd	24 mg l <sup>-1</sup>	
			Bi	85 mg l <sup>-1</sup>	
			As	1628 mg l <sup>-1</sup>	
N.D	N.D	Acid mine drainage	pH	0.6	Valiente et al., 1991
			Fe (III)	3600 mg l <sup>-1</sup>	
			Fe (III)	1300 mg l <sup>-1</sup>	
			Fe (II)	4700 mg l <sup>-1</sup>	
			Fe (II)	1800 mg l <sup>-1</sup>	
			Cu	250 mg l <sup>-1</sup>	
			Cu	140 mg l <sup>-1</sup>	
			Zn	1800 mg l <sup>-1</sup>	
			Zn	520 mg l <sup>-1</sup>	
			Al	620 mg l <sup>-1</sup>	
			Al	700 mg l <sup>-1</sup>	
			Mn	90 mg l <sup>-1</sup>	
			Mn	60 mg l <sup>-1</sup>	
			P	10 mg l <sup>-1</sup>	
		P	10 mg l <sup>-1</sup>		
		As	25 mg l <sup>-1</sup>	Carrera et al., 2008	
		As	20 mg l <sup>-1</sup>		
		Zn	81986520 mg l <sup>-1</sup>		
		Fe	95941710 mg l <sup>-1</sup>		
		Mn	173604.08 mg l <sup>-1</sup>		
		Al	38043.21 mg l <sup>-1</sup>		
		Pb	103600 mg l <sup>-1</sup>		
		Cr	18.718 mg l <sup>-1</sup>		
		Ni	18781.76 mg l <sup>-1</sup>		
		Cd	26978.64 mg l <sup>-1</sup>		
		Spent pickling acid			

N. D: Not defined

In United Kingdom (U. K), the average rate of acid waste production is about 32000 tones per year from 87 sites. Acid waste of the pickling acid made at galvanization plants in U. K. contains 193000 mg l<sup>-1</sup> of iron and 192000 mg l<sup>-1</sup> of zinc. The acid waste is moved to special

treatment facility, where all the valuable metals are being lost (Stocks et al., 2005). The technologies used to recycle effluent require huge cost.

## 2.2 Available technologies for the removal of zinc from wastewater and their limitations

There is a long series of technologies (Reddy et al., 2011) involved in the removal of zinc or any other heavy metal from various types of industrial wastewater and mine drainage. These include chemical precipitation, solvent extraction, sulphide precipitation, membrane filtration, ion exchange, reverse osmosis, electro dialysis, oxidation - reduction, ultrafiltration, evaporation, chemical coagulation/ flotation and flocculation, cementation, sorption, biosorption, phyto separation/remediation, activated sludge process, anaerobic-anoxic-oxic (A2O), heavy metal removal from biosurfactants, immobilized microorganisms in rotating biological contractor, solid-liquid- solid extraction, active filtration, adsorption and high gradient magnetic separation (Gavrilesco 2004, Tofan et al., 2008, Janson et al., 1982, Grosse et al., 1982, Grezesczky et al., 2007, Baig et al., 2009, Ucum et al., 2009, Tuppirainen et al., 2002, Mulligan et al., 2001, Wu et al., 2007, Hammami et al., 2003, Chang, et al., 2006, Berg et al., 2005, Costely and Wallis 2001, Sprynskyy 2009, Anand et al., 1985, Jain et al., 2009). The conventional heavy metal ion remedial technologies have some major technical shortcomings. (Eccles 1999, Miretzky et al., 2006). Some of the shortcomings of the conventional metal ion remediation methodologies have been represented in table 3.

Table 3: Limitations of various conventional metal ion remediation methodologies

Methodology	Shortcomings	Reference
Ion exchange	Input cost is very high and maintenance cost is very high	Aderhold et al., 1996
Adsorption	Efficiency of the process depends on type of adsorbent and chemical pretreatments are required to improve performance of adsorbent	Crini 2005
Chemical Precipitation	Input of chemicals is required, problem of secondary sludge generation, disposal of secondary	O'Connell et al., 2008, Aderhold et al., 1996

chemical sludge

Membrane separation and ultrafiltration	Input cost is very high, maintenance is very costly, fouling of membrane, operation cost is very high, limitation of flow rates and removal of other metal decrease in presence of other metals	Farooq et al., 2010, Madaeni and Mansourpanah 2003, Qin et al., 2002
Electrochemical treatments	Input cost is very high, filtration is required for removal of flocs, initial pH and current density of the solution is required to be adjusted	Farooq et al., 2010, Kongsricharoen and Polprasert 1995, Kongsricharoen and Polprasert 1996
Floataation	Input cost, maintenance cost and operation cost are very high	Rubio et al., 2002
Chemical Coagulation and flocculation	Input cost is very high, involves huge amount of chemicals and generation of secondary chemical sludge	Aderhold et al., 1996, Farooq et al., 2010, O'Connell et al., 2008

---

Against the conventional methodologies, the biosorption of heavy metals is a very cheap, eco friendly and efficient methodology. Bioremediation processes include the use of biomass or microorganisms. These are not only cheap, also does not produce any secondary chemical sludge. The biosorbents are readily available and they are quite efficient to remediate heavy metals below a threshold concentration of  $100 \text{ mg l}^{-1}$ . The nature of bonding between the adsorbate and the surface of the adsorbent distinguishes between the types of adsorption. Based on nature of bond or sharing of electrons, the biosorption of the metal ions on the surface of adsorbent is categorized as physical adsorption and chemical adsorption.

### 2.2.1 Physical adsorption

In physical adsorption or physiosorption the particles of the adsorbent bind to the surface of the adsorbate via weak interaction due to Vander walls force (Crowell, 1966) and there is no

rearrangement or sharing of electrons between adsorbate and adsorbent surface. The physisorption energy lies between 2 – 10 kcal mole<sup>-1</sup>. Additionally, Kuyucak and Volesky, (1988) reported the biosorption of various heavy metals (Uranium, Cadmium, Zinc, Copper and Cobalt) on dead mass of algae, fungi and yeast, mediated by electrostatic interaction between ions and cell wall moieties of dead biomass.

### 2.2.2 Chemical adsorption

In chemical adsorption the particles of the adsorbate bind to the adsorbent with strong bonds (covalent bond, ionic bond, etc.). The adsorbate particle perturbs its electronic configuration upon adsorption (Masel , 1951) lies typical chemisorption energy between 15 – 100 kcal mole<sup>-1</sup>. The chemisorption or chemical adsorption was mediated by various mechanisms such as ion exchange between cell wall moieties and adsorbate species, complexation of adsorbate particles with cell wall functional entities, precipitation, chelation etc. Precipitation can work in dual mode, i.e., metabolism dependent or metabolism independent. The biosorption of copper on the surface of fungi (*Ganoderma lucidum* and *Aspergillus niger*) (Muraledharan and Venkobachar, (1990), Venkobachar, 1990) was mediated by ion exchange process.

### 2.2.3 Biosorption and bioaccumulation

The removal of heavy metal ions such as Cd<sup>2+</sup>, Cu<sup>2+</sup>, Zn<sup>2+</sup>, Pb<sup>2+</sup>, Cr<sup>2+</sup>, Hg<sup>2+</sup>, Co<sup>2+</sup>, Ni<sup>+</sup>, etc. passively by dead biomass is called biosorption (Davis et al., 2003, Volesky and Holan, 1995). This mechanism is mediated by interaction of the cell wall functional groups and metal ions. The cell walls of microbial cells are made up of polysaccharides, lipids and proteins. These constituents play a diverse role in metal ion binding, i.e., these components create the sites for binding of metal ion. Biosorption process of metal ions is quite fast and independent of cell metabolism. (Kadukova and Vircikova , 2005, Veglio and Belochini 1997). This process is also called as passive biosorption.

Intracellular accumulation of metal ions is called bioaccumulation. Bioaccumulation is usually mediated by binding of metal ions by intracellular compounds, methylation, intracellular precipitation and other mechanisms. Since bioaccumulation belongs to active biosorption, hence the bioaccumulation may get influenced by metabolic inhibitors, change of



temperature and lack of energy. According to the classification of the processes, i.e., biosorption and bioaccumulation, the energy of activation also differs. Biosorption involves  $\sim 21 \text{ kJ mol}^{-1}$  activation energy whereas bioaccumulation mechanism needs activation energy  $\sim 63 \text{ kJ mol}^{-1}$ . (Kadukova and Vircikova, 2005).

#### **2.2.4 Biological removal of zinc by microorganism**

Various research workers (Cabral, 1992, Mattuschka and Straube, 1993, Mameri et al., 1999, Salehizadeh and Shojaosadait, 2003, Chen et al., 2005) have demonstrated biological removal of zinc and other toxic chemicals (Srivastava and Srivastava, 2007) mediated by microorganism. Both living and dead microorganism have been used in past to remove metal from liquid phase (Malik, 2004, Wang and Chen, 2009, Liu et al. 2004, Velasquez and Dussan, 2009). The bacterial biomass has gained substantial and significant interest in remediation of heavy metals in the series of various biomasses relatively. The rationale behind the supremacy of bacterial cell usage are (i) bacteria are biomass that contribute to the tremendously large fraction of biomass present on earth  $\sim 10^8 \text{ g}$  (Mann, 1990), they are smaller in size, (ii) they have capability to grow in controlled conditions, and (iii) they are flexible towards the changing environmental conditions (Urrutia, 1997). Usually, dead microorganism binds with the heavy metal ion through physiochemical mechanism. The biosorption can occur with one type of mechanisms or a combination of more than one or more mechanism. Some of the physicochemical mechanisms are physical adsorption, surface complexation, surface micro precipitation, ion exchange etc (Chojnacka, 2009, Veglio and Belochini, 1997). Cell wall of the microorganism contains polysaccharide, proteins and lipids (Chojnacka, 2009). These cellular entities provide negatively charged functional groups like carboxylate, hydroxyl, sulphate, phosphate and amino groups on the surface of dead microorganism. The negatively charged functional groups on the surface of bacterial cell surface renders living bacterial cells with tremendously higher removal capacity of metal ion from liquid phase (Wang and Chen, 2009, Liu et al., 2004, Kazy et al., 2000, Wakatsuki, 1995, Chaterjee et al., 2010). The bioaccumulation of heavy metal ions in living microorganisms is a multistage process. Usually, the multistage of bioaccumulation consists of biosorption followed by intra or extracellular accumulation of metal ions. Various

researches have proved that teichoic and teichuronic acid have significant role in metal ion binding (Moat et al., 2002, Prescott et al., 2002, Remacle, 1990, Utrrutia, 1997). Comparatively, the cell wall gram-negative bacterium is quite complex. The cell wall of the gram negative bacterium contains lipopolysacchrides (LPS), proteins and phospholipids. The presence of LPS on the cell wall of gram-negative bacterium renders the net negative charge on bacterium outer surface. The phosphate and carboxyl groups present in LPS and phospholipids are primary sites of metal ion binding (Moat et al., 2002, Prescott et al., 2002, Remacle, 1990, Utrrutia, 1997). Other sorts of microorganism repertoire secrete outside their cell wall an acidic slime or capsule. The array of these capsules is an interesting site for metal ion binding (Madigan et al., 2000, Urrutia, 1997). Yee and Fein (2001) suggested that the structures giving rise to metal and proton adsorption on the bacterial cell walls are common in almost all the bacterial species involved in metal adsorption. Ozdemir et al., 2009 performed study on the removal of cadmium, copper nickel, manganese and zinc by dead cells of *Goebacillus toebii sub sp. decanicus* and *Goebacillus thermoleovorans sub sp. stromboliensis* in batch stirred system. The authors reported that the stretching of O-H and N-H mediated the metal ion binding on microbial cell surface. The Fourier Transformation Infra Red Spectrum (FTIR) peaks were obtained at 3315  $\text{cm}^{-1}$ , 1661  $\text{cm}^{-1}$ , 1545  $\text{cm}^{-1}$ , 1403  $\text{cm}^{-1}$ , 2930  $\text{cm}^{-1}$  and 2990  $\text{cm}^{-1}$ . These peaks indicated the involvement of O-H, N-H,  $\text{-C=O}$ ,  $\text{-C=C}$ , C-H bending in aromatic ring and aliphatic stretching. These groups indicated the involvement of amine, carboxyl and aromatic groups. Silva et al., 2009 reported the biosorption of chromium, copper and zinc by *Pseudomonas auriginosa* AT18. The authors reported the preferential mechanism of biosorption as metal ion precipitation. Velasquez and Dussan 2009 reported the biosorption of As, Hg, Co and Fe was mediated by S layer proteins of the microbial cell. However, the authors have mentioned that the living cells have tendency to actively efflux the metal ion after accumulation. The dead cells go through cell microaeration process that can break the cell wall making more sites for binding of metal ion. Vullo et al., 2008 used the free and immobilized cells of *Pseudomonas veronii* 2E to remediate the zinc, cadmium and copper from liquid waste. The authors observed the changes in the negative charge on the cell surface and obtained 50% removal of zinc in ternary metal ion system. The authors also reported that increase in initial concentration of metal ion led to the decrease in density of negative

charges. Esposito et al., 2001 investigated the characterization of biomass (*Sphaerotilus natans*). The authors hypothesized that the two main functional groups namely carboxylic and phosphate group have tremendous potential to bind with metal ion in liquid phase. Choudhury and Srivastava, 2001 studied the detailed mechanism of zinc resistance in bacterium. The study revealed that the zinc resistant bacterium have series of mechanisms such as metal ion sequestration, active efflux of metal ions, bioprecipitation and changes in the cell wall of the bacterium cell to resist the toxicity of zinc. Either the single mechanism or a combination of these well regulatory mechanisms helps the bacterial cell to retain essential quantity of zinc and to avoid the toxic concentration of zinc to build up inside the cell. Lodi et al., 1998 reproduced the results of biosorption of cadmium, chromium, zinc, copper and silver metal from liquid phase. The authors reported that under the theory of mass transfer, metal ion biosorption on microbial cell surface was mediated by simple biosorption as well as by the movement of metallic ions in well inside the cells. Various researches indicate that the uptake of metal ion is a biphasic process. The first step of the process consists of rapid biosorption followed by slower uptake of metal ions inside the cell (bioaccumulation) (Malik, A., 2000). The metal ions diffuse inside bacterial cell, associate with intracellular proteins or metal chelators before being captured in vacuoles during the detoxification process of metal ions. Frequently, this process is irreversible and there is less chance of release of metal ions back into the environment (Gekeler et al., 1998). Apart from adsorption on the cell wall, metal resistance has been reported in a wide range of gram negative as well as gram-positive bacteria. Many of which have been reported to have a resistance against several different toxic heavy metals. This kind of resistance also comes from genes located within the bacterial genome or plasmids such as pMOL 28 or pMOL 30 (Mergay et al., 2003, Siddiqui et al., 1989, Lieseig et al., 1993). The zinc resistance is harbored by the *czc* operon, which apart from zinc, also imparts resistance to  $\text{Cd}^{2+}$  and  $\text{Co}^{2+}$ . Table 5.2.1 enlists the biosorption capacities of various living and non-living microorganisms with respect to zinc ions.

As mentioned earlier, the uptake of heavy metals by non-living bacterial biomass is accomplished by physico chemical interactions. Contrary to this, uptake of heavy metal by living biomass (bioaccumulation) is the result of bacterial cell resistance towards the heavy metal ions. Three independent mechanisms operate in case of bioaccumulation. They are as

follows (i) efflux of metal ion by permeability and active transport (ii) intra cellular physical and extracellular sequestration (by metallothionein protein) and (iii) detoxification and detoxification (mediated by redox reactions).

### **2.2.5 Biological removal of zinc by algae and fungi**

Like other microorganism, algae and fungi has the capability of removing heavy metal ions from liquid phase (Lesmana et al., 2009), Davis et al., 2003, Romera et al., 2007, Klimmek et al., 2001). Recent studies in the field of biosorption of heavy metals have focused on brown, green and red algae (Holan et al., 1993, Matheickal and Yu, 1999, Davis et al., 2003, Holan and Volesky, 1994).

The biosorption of metal ion on the surface of algae depends upon the chemistry of cell wall. Various types of mechanisms such as electrostatic attraction, ion exchange, complexation etc. get involved in metal ion binding.

Majority of the algal species contain embedded amorphous, non crystalline polysaccharides matrix. According to the classification of species, the algae contains xylan, mannan, alginate with fucoidan polysaccharide and sulphated galactans. These groups have tremendous capacity of metal ion binding on the surface of the algal cell wall. The carboxyl, hydroxyl, sulphate, sulphonic acid, amino acid in the polysaccharide matrix of the algal cell wall provide the key predominant sites for the biosorption of heavy metal ions. Areco et al., (2010) worked on biosorption of copper, zinc, cadmium and lead ions on the surface of *Gymnogongrus torulosus*. *Gymnogongrus torulosus* (Rhodophyta) is in high demand in Argentina as this seaweed has high content of carrageen, a polysaccharide, frequently used in hydrocolloid industry. Usually seaweeds contain high quantity of carboxyl, hydroxyl, phosphate and amine. These groups significantly improve the efficiency biosorption of seaweeds. The authors studied various isotherms, kinetic and mechanistic models for the data obtained at the attainment of equilibrium. Among the various isotherms, kinetic and mechanistic models, Langmuir, pseudo second order and intra particle model were found more suitable to interpret the biosorption of ions on *Gymnogongrus torulosus* surface. The authors concluded that the biosorption of zinc and copper is highly dependent on pH and the maximum removal of zinc and copper was obtained above pH 7. However, the biosorption of

lead has shown a little dependency on pH variation. Biosorption of Cu (II) and Zn (II) ion on the surface of macro alga *Chaetomorpha linum* was performed by Ajjabi and Chouba, 2009. The maximum adsorption of both the heavy metal ions was reported at pH 5. There was a sharp decline in biosorption of Zn (II) and Cu (II) ion in liquid phase above pH 5. The decrease in biosorption of Zn (II) and Cu (II) ion with the increase in pH from 5 to 7 was due to the formation of anionic hydroxide complexes and their competition with active sites. However, at lower pH values, the concentration of hydrogen ions was significantly higher which poses extreme competition between hydrogen ions and heavy metals for active binding sites resulting in lowering of biosorption of heavy metal ions. The surface characterization of *Chaetomorpha linum* with the help of FTIR spectrum showed the presence of O-H, C-O, N-H, N-H, C-N, N-H, S=O and P-O stretching. The shift in the FTIR vibration showed that the binding of metal ion on the surface of *Chaetomorpha linum* was mediated by these negatively charged functional groups. Sari and Tuzen, 2008 studied the effect of process parameters such as pH, temperature, contact time and biomass dosage on biosorption of total chromium on the surface of *Ceramium virgatum*. The authors optimized these process parameters and the the data obtained at equilibrium was used for isotherm, kinetic and thermodynamic modeling. The results of the investigation showed that Langmuir and pseudo second order model has better suitability in explaining the biosorption of total chromium on *Ceramium virgatum*. Results of thermodynamic study indicated that the biosorption of total chromium on *Ceramium virgatum* as exothermic in nature. The surface characterization of *Ceramium virgatu* before the binding of metal ions (metal unloaded biomass) revealed the fact that surface of *Ceramium virgatum* has carboxyl, hydroxyl and amine group. These groups participate in metal ion sequestration in liquid phase depending on the values pH. Biosorption of Cadmium, Nickel and Zinc on the surface of six different types of algae (*Codium vermilaria*, *Spirogyra insignis*, *Asparagopsis armata*, *Chondrus crispus*, *Fucus spiralis* and *Ascophyllum nodosum*) was performed by Romera et al., 2007. The authors reported that the maximum sorption of various heavy metals was at pH 5 and pH 6. The biosorption of zinc, nickel and copper were almost same. The most preferential adsorption among all the heavy metals considered was of lead followed by copper and cadmium. All the species of algae used by authors have shown similar trend of affinity for the metal ions. However, the behavior of

lead on the surface of algae was somewhat different from normal trend. The different behavior of lead metal ions during biosorption over algal surface was due to variation in mechanism of metal ion binding on algal surface. The reported trend of biosorption of metal ions was  $Pb > Cd > Cu > Ni > Zn$ . The authors also concluded that efficiency of six various strains of algae in terms of bioremoval of heavy metal ions was more effective compared to bacteria and fungi. Chromophyta, potential biosorbent contains very significant quantity of alginate and fucoidan in their cell wall. Cellular structures, storage polysaccharides, intracellular and extracellular polysaccharide together with alginate and fucoidan provide tremendous opportunities for the binding of heavy metal ion from liquid phase. On the other hand, *Rhodophyta* and *Chlorophyta* contain *cellulose*, sulphated polysaccharides, agar, carragenates, glycoprotein etc. These entities provide negatively charged functional groups (as mentioned above) for the biosorption of heavy metal ions (Romera et al., 2007, Davis et al., 2003, Lesmana et al., 2009). Table 5.2.2 represents the comparative analysis of various algae in terms of their Zn (II) ion uptake capacities.

Various fungus used like are *Sterptomyces*, *Rhizopus*, *Aspergillus*, *Penicillin*, *Saccharomyces*, *Mucor* also have capacity of removing Zn (II) ion from liquid phase (Mameri et al., 1999, Kapoor and Viraraghavan, 1995). Yang et al., 2009 reported the biosorption of Aluminium, iron, lead and zinc from liquid waste on the surface of *Aspergillus niger*. Yang et al., 2009 concluded that there was an increase in biosorption efficiency of *Aspergillus niger* with the increase of pH from 3 to 6.5. The modeling of the data obtained at equilibrium of sorption of metal ion showed that pseudo kinetic first order model and Langmuir isotherm model were found suitable to interpret the kinetics and mechanism of biosorption of metal ion on *Aspergillus niger* surface. Zafar et al., 2007 performed the biosorption of Cadmium, Nickel, Copper, Cobalt and Nickel on filamentous fungi isolated from metal ion contaminated soil. Isolated fungal species derived from soil contaminated with metal ion sample were *Aspergillus*, *Penicillium*, *Alternaria*, *Geotrichum*, *Fusarium*, *Rhizopus*, *Monilia* and *Tricoderma*. The treatment of cell wall material with alkali at higher temperature was found more promising for the sorption of metal ions. The research also indicated that there is hardly any correlation between metal tolerance and biosorption of metal ions on isolated fungi. Bayramoglu et al., 2003 attempted the biosorption of copper, lead and zinc ions on the surface

*Trametes versicolor* immobilized on CMC beads. The biosorption of Cu (II), Pb (II) and Zn (II) on immobilized *Trametes versicolor* was found to be maximum between pH 4.0 to 6.0. The maximum uptake capacity reported for immobilized living fungal cell was 1.51, 0.85 and 1.11 mmol/ g of biomass for Cu (II), Pb (II) and Zn (II) ions respectively. Mameri et al., 1999 used the non-living *Streptomyces rimosus* biomass derived from antibiotic fermentation industry for the biosorption of Zn (II) ion in liquid phase. Furthermore, the pretreatment of biomass was performed by NaOH (1 mol/L). Usage of pretreated biomass in biosorption of Zn (II) ion in liquid phase showed an enhanced efficiency of biosorption. The two types of the biomasses differed in their surface functional groups. The crude biomass showed the FTIR peaks for carboxyl and amine stretching whereas in the pretreated biomass these two bands were absent. Authors also reported the variation in pH in case of crude biomass. There was no change in pH during biosorption of Zn (II) ion in case of pretreated biomass. These results indicated that preferential mode of biosorption was ion exchange. Zn<sup>2+</sup> biomass exchanged with the H<sup>+</sup> ion in case of crude biomass and in pretreated biomass the ion exchange occurred between Zn<sup>2+</sup> ion and Na<sup>+</sup> ion. The biosorption of Ni (II) ions by white rot fungus *Polyporous Versicolor* was carried out by Dilek et al., 2002. The authors reported the effect of pH, time, temperature, initial concentration of metal ion and mixing density. The research showed that with the increase in temperature and initial concentration of Ni, the adsorptive capacity of *Polyporous Versicolor* increased. Both Langmuir and Freundlich models were found consistent with the biosorption of Ni ions on the surface of *Polyporous Versicolor*. The cell wall of the fungus consists of polysaccharides, lipids, protein, phosphates and inorganic matter. Polysaccharide fraction of fungal cell wall is significantly higher, about 80 – 90%. Chitin, nitrogen containing N-acetylglucosamine flexible polysaccharide makes two layers of cell wall. Inner thick layer of chitin are present in parallel fashion. The cell membrane of fungi is made up of phospholipids and cholesterol, i.e., sterol. Usual type of widely accepted structure of cell membrane is fluid mosaic model with outward and inward projection of polar heads and non polar heads with several embedded globular proteins. The cell wall of the fungi contains the negative charged groups such as carboxyl, hydroxyl, amine, sulfhydryl and phosphate. These negatively charged functional groups involve themselves in biosorption of metal ions. The biosorption of metal ions primarily on fungal cell wall is mediated by ion

exchange and complexation. The intracellular uptake and detoxification of metal ions by fungi is due to the presence of metallothioneins, metal excess pool, internal storage and metal sequestration by heat stable proteins. Table 5.2.3 represents the uptake capacities of various fungal biomasses in terms of Zn (II) ion uptake.

### **2.2.6 Biological removal of zinc by various agricultural waste, resins, clay and industrial byproduct**

The agricultural wastes are also used for the removal of heavy metal ions. The biosorption efficiency or uptake capacity of biomasses depends upon many factors like particle size, surface morphology, functional groups present on the surface of the biomass, porosity, surface area, pH, temperature, initial concentration of metal ions etc (Rocha et al., 2008, Agouborde and Navia, 2009, Sheha 2007, Arshad et al., 2008). The industrial byproducts and clays are also readily available (Vengris et al., 2001, Srivastava et al., 2007), to be used as biosorbent for metal ion removal from liquid phase. Resins, certainly ion exchange resins, are quite expensive; hence, their usage is not a cost effective option for biosorption of heavy metal ion.

Tofan et al., 2008 used the thermal power plant ash for the biosorption of Cu (II) and Zn (II) ion in liquid phase. Authors obtained thermal fly ash as by product of thermal power plant. Langmuir isotherm model was studied to evaluate the data obtained at the attainment of equilibrium. The monolayer sorption capacities obtained through Langmuir model were 5.75 mg g<sup>-1</sup> and 4.71 mg g<sup>-1</sup> for zinc and copper respectively. Dynamic modeling of the data showed that the Lagergren pseudo first order model seemed to be more suitable to interpret the sorption of Zn (II) and Cu (II) ions on the ash of thermal power plant in liquid phase.

Naiya et al., 2008 performed the biosorption of Zn (II) and Cd (II) ions by sawdust and neem bark in liquid solution. The optimum pH for the biosorption of Zn (II) and Cu (II) ion was 5 and 6 respectively. Dynamic modeling of the data represented the pseudo second order model to interpret the kinetics of sorption of Zn (II) and Cd (II) ions. The isotherm modelling of data showed equal inclination towards both Langmuir and Freundlich isotherms. The research also evidenced the presence of various negatively charged functional groups such as carboxylic



acid, amino, amine, amide and sulphonated groups on the surface of sawdust and neem bark before the adsorption of metal ions.

Cesur and Balkaya, 2007 performed the biosorption of zinc (II) ion using and industrial by product phosphogypsum. Freundlich isotherm was found suitable to interpret the sorption of Zn (II) ion on phosphogypsum. The maximum adsorption of zinc was obtained between pH 9 and 10. The uptake capacity of  $2.57 \text{ mg g}^{-1}$  of biomass was reported. The adsorption equilibrium was reached in 40 minutes. Biosorption of Cu (II), Zn (II), Cd (II) and Hg (II) by rice straw was attempted by Rocha et al., 2008. The authors reported that the biosorption of metal ions was exothermic in nature. The maximum adsorption of metal ion was obtained at pH 5 and at  $25 \pm 1^\circ\text{C}$ . The characterization of the rice straw showed the presence of O-H stretching, C-H stretching, C=C stretching, Si-O stretching and Si-O bending on the surface of rice straw. The Freundlich isotherm parameter analysis showed the preferential trend of sorption of metal ions as  $\text{Cd (II)} > \text{Cu (II)} > \text{Zn (II)} > \text{Hg (II)}$ . The equilibrium was obtained in 1.5 hour. Table 5.2.4 represents the comprehensive view of uptake capacities of various biosorbents in terms of zinc ion uptake.

### **2.2.7 Biosorption isotherms, kinetics and mechanisms**

Isotherm modeling of the data obtained at the attainment of the equilibrium in batch or continuous biosorption studies is a very imperative concept to elucidate the partition of metal ions in between solid and liquid phase. Various isotherm models have been used in literature.

#### **2.2.7.1 Langmuir model**

This is widely used model in the study of adsorption of metal ion on the surface of adsorbent. However, Sengil and Ozacar, 2009 reported the lower goodness of fit for Langmuir isotherm in terms of biosorption of Zn (II) on valonia tannin resin against Freundlich isotherm. However, Langmuir isotherm was found superior to Temkin and Dubinin - radushkevich isotherms.

Demirbas et al., 2005 performed the sorption of Cu (II), Zn (II), Ni (II), Pb (II) and Cd (II) in liquid phase on the surface of Amberlite IR-120. The work evidenced that the goodness of fit of the isotherm for Langmuir model for Zn (II) ion was quite less compared to

Freundlich model. The model assumes that the sorption of metal ions occurs in monolayer coverage of biosorbent surface, all active sites are same and symmetrical (homogeneous surface), adsorbate binding is independent of adjacent site occupancy, single site is occupied by single adsorbate particle and rate of adsorption is equal rate of desorption (dynamic isotherm). The linear model of Langmuir isotherm has been shown in Appendix (Appendix A-1, equation no. A-1). The other linear forms of the Langmuir equation has been shown in Appendix (Appendix A-1, equation no. A-2 to equation no. A-5).

### 2.2.7.2 Freundlich model

Yang et al., 2009 evaluated Freundlich and Langmuir isotherm to study the biosorption of zinc ions on the surface of *Aspergillus niger*. The study was conducted in the presence of aluminum, iron and lead. The findings of the investigation showed that the Langmuir model with high  $R^2$  was found more suitable to interpret the biosorption of Zn (II) ion on the surface of *Aspergillus niger*. Biosorption of zinc ions in liquid phase on the surface of phosphogypsum was performed by Cesur and Balkaya, 2007. The authors presented both the linear and non-linear Langmuir and Freundlich isotherm and used both isotherm models to fit the data obtained at the attainment of equilibrium. Freundlich model was found superior to interpret the sorption of zinc ions in liquid phase between both the models. Demirbas et al., 2005 used Freundlich isotherm to effectively interpret the sorption of  $\text{Cu}^{2+}$ ,  $\text{Zn}^{2+}$ ,  $\text{Ni}^{2+}$  and  $\text{Cd}^{2+}$  on the surface of Amberlite IR-120. Farooq et al., 2010 showed in their literature review about the applicability of Freundlich isotherm in biosorption Cr (III) ions on wheat based biosorbent. Biosorption of Hg (II) removal from aqueous solutions by *Bacillus subtilis* biomass was attempted by Wang et al., 2010. The curve fitting of data obtained at equilibrium showed that none of the Langmuir and Freundlich isotherm has effective explanation of sorption of Hg (II) ions on *Bacillus subtilis* biomass. The authors finally found the suitability of Sips isotherm (a combination of Langmuir and Freundlich isotherm) to explain the sorption of Hg (II) ions on *Bacillus subtilis* biomass. Nonlinear exponential and linear form of Freundlich equation has been shown in Appendix (A-1, equation no. (A-6) and equation no. (A-7)). Freundlich isotherm is unable to predict metal ion sorption equilibrium condition at extreme conditions in other words the Freundlich model works from very low range of

concentration gradient of adsorbate ion to intermediate concentration (Febrianto et al., 2009, Liu and Liu, 2008).

### 2.2.7.3 Temkin model

Very scarce research has been made on the applicability of Temkin model in biosorption of heavy metals from liquid phase. However, Liu and Liu (2008) reported that this model is not sufficient to interpret the  $\text{Ni}^{2+}$  biosorption on the surface of *Saragassum wightii*. The Temkin isotherm relation has been shown in Appendix (Appendix A- 1), equation no. (A -8)).

### 2.2.7.4 Dubinin- Radushkevich (D-R) model

Naiya, et al., 2008 applied Dubinin- Radushkevich isotherm for the curve fitting of the data obtained at the attainment of equilibrium. The authors reported very high value of correlation coefficient ( $r^2$ ). The value of correlation coefficient indicated the suitability of Dubinin-Radushkevich isotherm to explain the biosorption of Zn (II) ion in liquid phase on the surface of sawdust and neem bark. The authors also used the model parameters to evaluate the mean biosorption energy and it was found that biosorption of Zn (II) on the surface of sawdust, and neem bark was mediated by physical adsorption. However, in the same investigation, the authors also mentioned that the biosorption of Cd (II) on the surface of sawdust and neem bark was mediated by chemisorptions mechanism. Sari and Tuzen, 2008 used this isotherm to evaluate the biosorption of total chromium on the surface of red algae *Ceramium viratum*. The investigation concluded the fact that Dubinin- Radushkevich model was suitable to explain the biosorption of total chromium in liquid waste on the surface of *Ceramium viratum*. With the help of Dubinin- Radushkevich the mean biosorption energy was calculated and it was found that the mean biosorption energy was 9.7 kJ/mol. The value of mean biosorption energy calculated through Dubinin- Radushkevich isotherm indicated that chemisorptions was the main mechanism of metal ion sorption on the surface of *Ceramium viratum*. The model equation has been shown in Appendix (Appendix A-1, equation no. (A - 9)) (Sari and Tuzen, 2009). The model assumes the sorption of metal ions on energetically non-uniform surface, the model provides the significant explanation of equilibrium data (Igwe and Abia, 2007, Cabuk et al., 2007).

## 2.2.8 Kinetic and mechanistic modeling

Kinetic studies are required to find out the rate and mechanism of reaction coupled with determination of rate controlling step (Metacaf 2001, Sheri fetal., 1992). The rate model study also helps in the design of continuous adsorption columns (Basha et al., 2009). In the present work pseudo first order, pseudo second order, intra particle model and Bangham's model and diffusion coefficients have been studied to chalk out the rate limiting step of Zn (II) ion biosorption on the surface of various biomasses.

### 2.2.8.1 Pseudo first order model

Areco et al., 2010 studied the pseudo first order model to elucidate the mechanism of sorption of lead (II), cadmium (II), zinc (II) and copper (II) on the surface of *Gymnogongrus torulosus*. The authors reported very small values of correlation coefficient coupled with the large difference between the theoretical  $q_e$  and experimental  $q_e$ . The investigation finally concluded with the fact that the pseudo first order model was not suitable to explain the sorption of metal ion on the surface of *Gymnogongrus torulosus*.

Chegrouche et al., 2009 extensively studied the sorption of strontium in liquid phase on the surface of activated carbon. The authors analyzed the data obtained at the equilibrium through the pseudo first order model. The modeling of the data fitted well with pseudo first order model having significantly higher values of  $R^2$  ranging between 0.98 – 0.99 at various values of pH, initial concentration of metal ion, temperature and particle sizes.

Pseudo first order model was also used by Fan et al., 2008 to elucidate the mechanism of biosorption of cadmium (II), zinc (II) and lead (II) on the surface of *Penicillium simplicissimum*. The authors represented both non-linear and linear model of pseudo first order model. The constant of the model was obtained as the slope of the linear model. The investigation evidenced that pseudo second order model with higher correlation coefficient was far more better to explain the sorption of metal ions on the surface of *Penicillium simplicissimum* against pseudo first order model between 20-40 °C. The investigation also concluded that the value of Pseudo first order model constant ( $K_1$ ) did not vary significantly with the rise in temperature.

This model assumes the presence of physical forces of attraction between adsorbate and adsorbent particles. The binding of adsorbate with adsorbent is reversible and non-dissociative. The model also considers that the rate of binding of adsorbate species with adsorbent particle is directly proportional to the number of vacant active sites present on the surface of adsorbent. The non-linear form of pseudo first order reaction model has been shown in Appendix (Appendix A-1, equation (A -10 and A - 11)) (Sari and Tuzen, 2009). Pseudo first order reaction model works on the principle of linear driving force (Liu and Liu, 2009). Tremendous number of researches on heavy metal bioremediation has focused on the successful application of pseudo first order model (Hanif et al., 2007, Preetha et al., 2007, Pamukoglu and Kargi, 2007).

#### **2.2.8.2 Pseudo second order model**

Ozdemir et al., 2009 performed the study on the biosorption of cadmium, copper, nickel and zinc. The authors used the linear form of pseudo first and pseudo second order model to explain the biosorption of heavy metal ions in liquid phase on the surface of *Geobacillus toebii* and *Gebacillus thermoleovorans*. Results of the investigation evidenced that pseudo second order model has better suitability to explain the sorption of heavy metal ions on the surface of *Geobacillus toebii* and *Gebacillus thermoleovorans*. The correlation coefficient values for the pseudo second order model was quite higher compared to pseudo first order model. The research also concluded that the difference between theoretical uptake capacity and experimental uptake capacity in case of pseudo second order model was quite small where as the difference in the theoretical uptake capacity and experimental uptake capacity in case of pseudo first order model was quite higher. Biosorption of hexavalent chromium on the surface of dead fungal biomass of marine *Aspergillus niger* was studied by Khambhaty et al., 2009. The authors reported that pseudo second order model was the suitable model to interpret the sorption of hexavalent chromium on the surface of *Aspergillus niger*. The non-linear and linear form of pseudo second order has been shown in Appendix (Appendix A – 1, equation no. (A -12) and (A-13)) (Abdelwaha, 2007, Mohanty et al., 2005).

### **2.2.8.3 Mechanistic modeling**

Convective mass transfer of metal ions in cylindrical coordinates of liquid phase together with mesoporous openings present on biomass is a three phase mediated process consisting of (i) transport of metal ions from bulk liquid phase including boundary layer to the surface of biomass known as film diffusion (ii) binding of metal ions onto surface of biomass, this step is quite rapid and (iii) transport of metal ions inside the pores of biomass across liquid filled inside pores or by solid phase diffusion from one binding active site to another.

### **2.2.8.4 Intra particle model**

Intra particle model is well documented in various literatures. Literature shows that alone intra particle model itself was not capable of explaining the biosorption of Zn (II) ion in liquid phase at various stages of adsorption process.

Areco et al., 2010 studied the intra particle model for the biosorption of copper, zinc, cadmium and lead. The investigation evidenced that the the curve of intra particle diffusion did not pass through the origin. The authors also reported very small values of goodness of fit of the intra particle model. These evidences led to the conclusion that intra particle diffusion is not only rate determining step in step in biosorption of heavy metals. Intra particle model has been shown in Appendix (Appendix A-1, Equation no. (A-14)).

### **2.2.8.5 Bangham's model**

Very scarce study has been made on the study of Bangham's model. Literature shows that this can be the better suitability to interpret the sorption of Zn (II) ion in liquid phase on the surface of *Cedrus deodara* sawdust against intra particle model. Bangham's model has been shown in Appendix (Appendix A-1, Equation no. (A-15)). If the data suits well into equation (A – 15), then it can be concluded that the film diffusion was the rate-controlling step.

## **2.3 Review of Literature**

### **2.3.1 Ajjabi and Chouba 2009**

#### **2.3.1.1 Objective**

The investigation focused on the biosorption of zinc (II) and copper (II) from liquid phase on the surface of *Chaetomorpha linum*.

#### **2.3.1.2 Materials and methods**

The seaweed *Chaetomorpha linum* was collected from south side of Lake of Tunis. The seaweed was washed with the Milli Q water and dried in an oven until the attainment of constant weight. The dried biomass was crushed in homogenizer in various particle sizes ranging between 100  $\mu\text{m}$  to 800  $\mu\text{m}$ . The powdered biomass was mixed with metal ion solution of desired concentration. After the attainment of equilibrium, the biomass was separated through filtration and the samples were analyzed through atomic absorption spectrophotometer (AAS). Langmuir isotherm model was used to find out the mechanism of biosorption of metal ions on the surface of *Chaetomorpha linum*. The study of surface of *Chaetomorpha linum* was studied through FTIR.

#### **2.3.1.3 Results and discussion**

The biosorption of zinc (II) and copper (II) was quite low at low pH range ( $\text{pH} < 2$ ). The increase in pH value from 2 to 5 led to the increase in biosorption of zinc (II) and copper (II) in the liquid phase on the surface of *Chaetomorpha linum*. The increase in removal of zinc and copper with the increase in pH was due to the reduction in competition between hydrogen ions and metal ions for the same active sites present on the surface of *Chaetomorpha linum*. The maximum removal of zinc (II) and copper (II) was obtained at pH 5. Above pH 5, the sorption of zinc (II) and copper (II) ion decreased substantially due to the formation of anionic hydroxide complex and their competition with active sites.

The surface characterization of the *Chaetomorpha linum* performed through FTIR indicated the presence various negatively charged functional groups on the surface of biomass. The groups found on the surface of *Chaetomorpha linum* were carboxyl group, hydroxyl stretching, amine, amide, sulphonyl and phosphate vibrations. These groups tremendously

attracted the metal ions on the surface of *Chaetomorpha linum*. The biosorption experiments conducted at various particle sizes ranging between whole thallus to 100  $\mu\text{m}$  indicated that the sorption of metal ion and uptake capacity was maximum at lowest particle size. The increase in metal ion concentration and contact time increased the removal and uptake capacity of metal ions and *Chaetomorpha linum* respectively. Initially, the biosorption of metal ions was quite fast and almost 80% of the metal ion sorption occurred in first two hours. Afterwards, the sorption of metal ions reached equilibrium. Langmuir isotherm model was applied on the biosorption equilibrium data and the isotherm parameters were solved with the help of non-linear regression analysis.

#### **2.3.1.4 Conclusion**

The physical process parameters like pH, particle size and initial concentration of metal ions significantly influenced the removal of metal ions from liquid phase. The maximum biosorption capacities of dried biomass for copper (II) and zinc (II) were 1.56 mmol/ g and 1.97 mmol/g respectively. The sorption of copper (II) and zinc (II) was very rapid initially up to first two hours of biosorption. The investigation also concluded that biosorption of copper (II) and Zn (II) was quite higher compared to biosorption efficiency of various green algae.

#### **2.3.2 Silva et al., 2009**

##### **2.3.2.1 Objective**

The aim of authors was to study the biosorption of Zn, Cr, Cu and Mn by *Pseudomonas aeruginosa* AT 18 in single and multi ion system at various pH values ranging between 3 to 7.72.

##### **2.3.2.2 Materials and Methods**

The microbial strain was isolated from soil obtained from petroleum refinery plant situated at Cuba. The strain was maintained in nutrient agar slant and grown in nutrient broth at  $28 \pm 3^{\circ}\text{C}$ . The biomass grown was isolated through centrifugation at 10509 g for 15 minutes. The stock solution of metal ion was prepared up to the desired strength using Chromium ( $\text{Cr}_2\text{O}_3$ ),



Copper ( $\text{CuNO}_3$ ), Manganese ( $\text{MnSO}_4$ ) and Zinc ( $\text{ZnSO}_4$ ). The pH of the stock solution was maintained by 0.1 M sodium hydroxide and 0.1 M nitric acid.

Batch study was conducted by adding cell suspension to the 100 ml of metal ion solution in conical flask of 250 ml capacity for 72 hours. At the completion of 72 hours the biomass was separated through centrifugation at 10000 rpm and the supernatant was analyzed by ICPMS.

### **2.3.2.3 Results and discussion**

The maximum growth rate of the bacterium was obtained in presence of pure zinc followed by copper, chromium and manganese. Freundlich isotherm model was found suitable to predict the sorption of zinc ion. The maximum removal of zinc ions was obtained at pH 7. The removal of zinc ions in pure zinc phase was higher than the removal of zinc ions in presence of chromium, copper and manganese.

### **2.3.2.4 Conclusion**

87.72 mg  $\text{Zn}^{2+}$ / g of biomass were obtained in pure zinc phase. However, 74.5 mg  $\text{Zn}^{2+}$ / g of biomass were obtained in presence of other metal ions. The study revealed that the removal of metal ions in liquid phase was significantly affected by precipitation process, pH and presence of competitive metal ions. The metal ion removal in liquid phase above pH 5.8 is due to the other mechanism other than biosorption. Solution pH and ionic strength of liquid phase are very crucial factors for the biosorption of heavy metal ions in liquid phase.

## **2.3.3 Ozdemir et al., 2009**

### **2.3.3.1 Objective**

The study aimed at characterization of biosorption of various metal ions like  $\text{Cd}^{2+}$ ,  $\text{Cu}^{2+}$ ,  $\text{Mn}^{2+}$ ,  $\text{Ni}^{2+}$ , and  $\text{Zn}^{2+}$  on the surface of *Geobacilli toebii* sub. sp. *decanicus* (G1) and *Geobacilli thermoleovorans* sub. sp. *stromboliensis* (G2). The study also aimed at optimization of various physical parameters such as pH, temperature, initial concentration of metal ions, contact time and amount of biomass.

### 2.3.3.2 Materials and Methods

The bacterial cells obtained from Istituto di Chimica Biomolecolare, CNR, Italy were grown nutrient medium containing 0.4% yeast extract, 0.8% peptone and 0.2% NaCl at pH 7.0 in 250 ml of Erlenmeyer flask placed on a shaker at 70<sup>0</sup> C for 24 hours. The cells after growth were centrifuged at 10000 rpm for 10 minutes. The cell pellet obtained after centrifugation was washed twice with 0.9% NaCl. The cell pellet was dried in an oven at 80<sup>0</sup> C for 24 hours. The powdered biomass of bacterial cells was obtained by crushing the cells in porcelain mortar.

### 2.3.3.3 Results and discussion

The results indicated that the maximum removal of Zn (II) ion by G1 and G2 was obtained at pH 5 and pH 4 respectively. Furthermore, the results indicated that the sorption of Zn (II) ion on the surface of biomass was independent of temperature. However, the sorption of Cu (II) and Ni (II) shown variation with variation of temperature from 30 – 80 <sup>0</sup>C. The maximum removal of Zn (II) ion was obtained at 80 <sup>0</sup>C in case of G1. The maximum removal of Cu (II) was obtained at 60 <sup>0</sup>C in case of G1. The maximum removal was obtained Cu (II) in case of G2 was obtained at 60 <sup>0</sup>C. The maximum removal of Zn (II), Ni (II), Cd (II) and Mn (II) was obtained at 70 <sup>0</sup>C in case of G2. The study evidenced that increase in concentration of metal ions and biomass dose the removal of metal ions increased significantly. However, the uptake capacities (mg/ g) of the biomass decreased very significantly with the increase of biomass dose. This was due to the interference between the active sites at higher biomass dose. The binding of Cu (II) ion on the surface of G1 and G2 occurred between very rapidly between 5 to 15 minutes. The rapid sorption of metal ions on the surface of G1 and G2 was due to the advective flow and mixing. Among the various isotherms models namely Langmuir, Freundlich and D-R, the most suitable adsorption isotherm was Langmuir isotherm with highest non-linear regression coefficient ( $r^2$ ) ranging between 0.89 to 0.99. The mean biosorption energy of the sorption of metal ions was found less than 8 KJ/ mol, which indicated that binding of ions on the surface of G1 and G2 was mediated by physical adsorption. The kinetic and thermodynamic modeling of data indicated that the pseudo second

order model with spontaneous binding of metal ions on the surface of G1 and G2 were quite feasible describe the metal ion sorption.

#### **2.3.3.4 Conclusion**

The biomass surface characterization revealed that surface of G1 and G2 was quite enriched with functional groups like hydroxyl, amine, ketonic, methyl group stretching. Langmuir isotherm model together with pseudo second order model was found proficient to elucidate the biosorption of metal ions on the surface of G1 and G2. The binding of metal ions on the surface of G1 and G2 was physical and spontaneous in nature. The positive value of entropy indicated the increase in randomness at the solid liquid interface during sorption of metal ions.

#### **2.3.4 Sengil and Ozacar 2009**

##### **2.3.4.1 Objective**

The major objective of the investigation was to study the biosorption efficiency of pretreated valonia tannin resin for Pb (II), Cu (II) and Zn (II) ion. The study also aimed at evaluation of physical parameters like pH and particle size in batch biosorption studies.

##### **2.3.4.2 Materials and Methods**

Valonia tannin resin was added to the 50 ml of  $\text{NH}_3$  solution at room temperature with 65 ml of formaldehyde. The mixture was agitated for 5 minutes. The beads of valonia tannin resin were obtained after filtration were crushed in lab scale ball mill and sieved in various sieve sizes ranging between -100  $\mu\text{m}$  to + 250  $\mu\text{m}$ . The crushed beads of valonia tannin resin were added to the metal ion solution in 250 ml conical flask. The mixture was agitated constantly for 180 minutes at 150 rpm. The pH of the experimental solutions was maintained by adding HCl and NaOH.

##### **2.3.4.3 Results and discussion**

The investigation evidenced that the decrease in particle size yielded the higher internal surface area. Hence, the maximum removal of metal ions in liquid phase was obtained at -100

$\mu\text{m}$ . The rise in pH from 3 increased the removal of metal ions from liquid phase. The maximum removal of metal ions was obtained at pH 5. 28%, 8% and 12% removal of Pb (II), Cu (II) and Zn (II) was obtained at pH 2. However, with the increase of pH from 3 to 5 increased the percentage removal of Pb (II), Cu (II) and Zn (II) ion up to 98.2%, 44% and 37.5 % respectively. This was due the acidic dissociation phenolic hydroxyl groups of tannins, which in turn led to the strong metal ion binding capacity of valonia tannin resin. However, the pH 5 resulted in precipitation of metal ions. Among the various isotherms namely Langmuir, Freundlich, Temkin and D- R isotherm, the Langmuir isotherm was found more suitable with higher non-linear regression coefficient ( $r^2$ ). The values mean free energy indicated that physical forces of attraction mediated the sorption of heavy metal ions. The kinetic modeling of the data indicated that sorption of metal ions was quite lucratively described by pseudo second order model coupled with very higher values of non-linear regression coefficient compared to pseudo first order, elovich and intra particle models.

#### **2.3.4.4 Conclusion**

Lowest particle size offered the maximum removal of metal ions from liquid phase.

Langmuir and pseudo second order model were found superior to other isotherm and kinetic models. Physical adsorptive forces mediated the sorption of heavy metal ion. The preferential order of adsorption of metal ions was  $\text{Pb}^{2+} > \text{Cu}^{2+} > \text{Zn}^{2+}$ .

#### **2.3.5 Shek et al., 2009**

##### **2.3.5.1 Objective**

The study aimed at the removal of zinc ions from liquid phase mediated by sodium immidodiacetate ion exchange resin, the uptake capacity of resin was compared with the uptake capacities of two other synthetic resins.

##### **2.3.5.2 Materials and Methods**

The stock solution of zinc was prepared by dissolving desired amount of zinc chloride in de ionized water. The chelating resin was soaked in two successive stages in HCl (4% w/w) and NaOH (8% w/w) for more than 45 minutes. The resin was finally washed with de ionized

water, dried at 100<sup>o</sup> C- 110<sup>o</sup> C for three days and crushed in particle sizes ranging between 450 µm – 600 µm, 600 – 710 µm and 710 – 1000 µm. The mixture of resin and metal ion solution was agitated together in polypropylene bottles at 200 rpm and at 25 ±2<sup>o</sup> C. The samples were withdrawn at predetermined time intervals and the samples were further analyzed by ICP-AES. A 2 L plastic vessel of 0.13 m diameter, to retain 1.70 L metal ion solution, fitted with flat plastic impeller of 0.065 m diameter with a blade height of 0.013m was used as a batch reactor.

### **2.3.5.3 Results and discussion**

The authors studied various isotherms and kinetic models such as Langmuir, Freundlich, Redlich Peterson, pseudo first order and pseudo second order. The results indicated that the sorption of zinc ions on the surface of sodium immidodiacetate ion exchange resin was more profoundly explained by Redlich –Peterson isotherm compared to other isotherms. The Redlich Peterson isotherm showed very insignificant value of sum of square errors (SSE) compared to other isotherms. Through batch kinetic studies, it became evident that the lowest values of sum of square errors (SSE) were obtained from elovich model against the pseudo first and pseudo second order model.

### **2.3.5.4 Conclusion**

Among all the selected models of isotherm and kinetics, Redlich -Peterson and elovich model produced the lowest value of sum of square errors (SSE). The most probable mechanism of metal ions sorption was chemisorptions ion exchange mechanism process.

### **2.3.6 Naiya et al., 2009**

#### **2.3.6.1 Objective**

The main objective of the investigation was to assess the biosorption efficiency of sawdust and neem bark in terms of Zn (II) and Cd (II) from liquid phase. Various process parameters like pH, temperature, initial concentration of metal ions were also optimized, isotherm and kinetic modeling modeling was performed to understand the mechanism of metal ion sorption.

### **2.3.6.2 Materials and methods**

Sawdust and neem bark was collected from local campus premises. The sawdust and neem bark was washed thoroughly with distilled water. Both the samples were soaked in 0.1 N NaOH to remove lignin and colored material. After chemical pretreatment of the neem bark and sawdust, the samples were washed again with distilled water followed by drying in an oven at  $105 \pm 1$  °C. the drying of the adsorbents were performed till the samples attained the constant weights. The stock solution of the metal ions was prepared by dissolving 1000 mg/l of zinc and cadmium in the form of zinc sulphate and cadmium nitrate (AR grade). Bulk density, FTIR and BET surface area were determined to perform surface characterization of the adsorbent.

### **2.3.6.3 Results and discussion**

The surface characterization of the sawdust and neem bark indicated that the surface of the adsorbents was porous, irregular and enriched with various negatively charged functional groups like carboxylic acid, amine, amino, amide and sulphonate. The optimum values of pH for both the adsorbents were 5 and 6 for the maximum biosorption of Zn (II) and Cd (II) ions, respectively. The maximum sorption of Zn (II) and Cd (II) ion at optimized pH in case of sawdust was 85.8% and 94.25%, respectively. The maximum sorption of Zn (II) and Cd (II) ion at optimized pH in case of neem bark was 82.2% and 84.5%, respectively. The authors concluded that at lower pH, sorption of Zn (II) ion was less, which was due to the excessive repulsion between hydrogen ion and metal ion present in the liquid phase. However, with the increase of pH, the repulsion decreased resulting in increase in sorption of Zn (II) ion on sawdust and neem bark. However, in case of cadmium, the sorption of metal ion was dependent upon the ion exchange mechanism. The increased sorption of Cd (II) with the rise in pH was due to condensation reaction between hydrolyzed cadmium ions and sites carrying hydroxyl group on the surface of the adsorbents. Increase in concentration of metal ions from 3 to 100 mg l<sup>-1</sup> resulted in the decrease of sorption of Zn (II) and Cd (II) ion on the surface of adsorbents. The reason behind the lowering in the removal of metal ions from liquid phase was the saturation of high-energy active sites, which led to the sorption of metal ions at lower energy active sites. The increase in dose of the adsorbents from from 2.5 g l<sup>-1</sup> to

10 g l<sup>-1</sup> increased the sorption of Zn (II) and Cd (II) ions. At 10 g l<sup>-1</sup> of sawdust and neem bark the maximum removal of Zn (II) ion was 85.76% and 81.6%, respectively. However, at 10 g l<sup>-1</sup> of sawdust and neem bark the maximum removal of Cd (II) was 94.5% and 84.5%, respectively. The increase in adsorbent dose resulted increase surface area, which lead to the increase in percentage removal of metal ions. The study on contact time (0- 5 hours) led to the conclusion that during the first 2 hours, the sorption of metal ions was quite rapid followed by slow attainment of equilibrium of metal ion sorption at the end of 5 hours. The authors used three models of reaction kinetics namely pseudo first order, pseudo second order and intra particle diffusion model. The applicability of the kinetic models yielded significantly higher values of correlations coefficient ( $r^2$ ) for pseudo second order model against pseudo first order model and intra particle model. Various isotherm models used by authors were Langmuir, Freundlich and D-R model. Between Langmuir and Freundlich model, Langmuir model yielded significantly higher values of correlation coefficient and lower values of statistical error function ( $\chi^2$ ) compared to Freundlich model. The values of mean sorption energy derived from D-R model were in range of 1 kJ mol<sup>-1</sup> – 8 kJ mol<sup>-1</sup> in case of Zn (II) ion sorption on sawdust and neem bark. However, in case of Cd (II) sorption on the surface of sawdust and neem bark, the sorption energy was in range of 8 kJ mol<sup>-1</sup> – 16 kJ mol<sup>-1</sup>.

#### **2.3.6.4 Conclusion**

The authors concluded that the sorption of Zn (II) and Cd (II) ion on the surface of sawdust and neem bark was highly pH dependent. Initial concentration of metal ions and adsorbent dose significantly affects the sorption of heavy metal ions significantly. Among various isotherm models, Langmuir model was found satisfactory to elucidate the sorption of Zn (II) and Cd (II) ions on sawdust and neem bark. The values mean sorption energy indicated that sorption of Zn (II) was physical adsorption. However, in case of Cd (II) ion sorption on sawdust and neem bark, the values of sorption energy indicate that the chemisorptive forces mediated the sorption of Cd (II) ion. Thermodynamic feasibility study indicated that the sorption of Zn (II) and Cd (II) was spontaneous in nature. Surface characterization of the adsorbents indicated that the sorption of Zn (II) and Zn (II) was mediated by function groups present on the surface adsorbents such as C-O, C=O and C- N etc.

### **2.3.7 Chaterjee et al., 2010**

#### **2.3.7.1 Objective**

The main objective of the authors was to establish the biosorption efficiency of *Geobacillus thermodentrificans* in terms of removal of iron, chromium, nickel, cobalt, chromium, zinc, silver and iron from liquid phase.

#### **2.3.7.2 Materials and methods**

Samples of Damodar River were taken from Kalajharia site situated at West Bengal, India. Samples of river water were sown in nutrient broth to grow the bacterial colonies at 65 °C for 48 hours. The pH for the growth of the bacterium was kept at 6.5. Pure culture of the bacterium was obtained by isolation of bacterium in nutrient agar plates (Hi Media, Mumbai, India). Total 30 colonies were isolated and were investigated for morphological characteristics. The colonies were stored at 4 °C in slants. The cells of *Geobacillus thermodentrificans* were grown in Luria Broth at 65 °C and the growth of the bacterium cells were analyzed through measurement of absorbance by spectrophotometer at 600 nm.

The dead mass of bacterium cell was prepared by harvesting the mid log phase cells of bacterium by centrifugation at 9000 rpm for 30 minutes at 4 °C. The pellet was washed three times with distill water and dried at 80 °C. Langmiur and Freundlich isotherm were modeled with optimization of various parameters like pH and initial concentration of metal ions.

#### **2.3.7.3 Results and discussions**

Thirty different types of microbial isolates were obtained. Out of 30 isolates only one isolate BAC -2 (*Geobacillus thermodentrificans*) was found tolerant to higher concentration of heavy metals. *Geobacillus thermodentrificans* was characterized as gram positive, anaerobic, rod shaped, motile and endospore forming. The bacterial cell colonies were having rhizoidal border and were off white in colour. The experimental results of parameter optimization revealed the fact that the dead cells of *Geobacillus thermodentrificans* were very sensitive to pH. The optimum pH for the removal of iron, chromium, cobalt, copper, zinc, cadmium, silver and lead was 6.5, 7.0, 4.5, 7.5, 5, 6, 7.5 and 4.5 respectively. The difference in the



values of optimum pH for various types of ions was due the difference in chemical interactions between metal ions and biomass. The increase in metal ion concentrations led to increase in metal ion uptake efficiency of dead *Geobacillus thermodentrificans* cells of from 25 mg/l to 175 mg/l. Between Langmuir and Freundlich isotherm model the Langmuir model was found more suitable with the higher values of linear regression coefficient ( $R^2$ ).

#### **2.3.7.4 Conclusion**

The investigation concluded that the dead cells *Geobacillus thermodentrificans* can be potential biosorbent for the removal of heavy metal ions from liquid phase or industrial effluent. The results also indicated that the biosorption efficiency of dead cells of *Geobacillus thermodentrificans* was significantly affected by pH and initial metal ion concentration. Langmuir isotherm model was found satisfactory to interpret sorption of metal ions on the surface of dead cells of *Geobacillus thermodentrificans*.

#### **2.3.8 Areoc and Afonso 2010**

##### **2.3.8.1 Objective**

The study focused on the removal of copper, zinc, cadmium and lead from liquid phase mediated by *Gymnogongrus torulus*. The study also aimed at isotherm, kinetic and thermodynamic modeling of the data obtained during the sorption of metal ions.

##### **2.3.8.2 Materials and methods**

The sea weed was collected from Cabo Corrientes at Mar del Plata City, Argentina. The seaweed was thoroughly washed with water, dried at 60 °C, desiccated in desiccators and finally crushed in homogenizer in various particle sizes ranging between 0.5 mm to 2 mm. The stock solution of metal ions was prepared by dissolving suitable amount of zinc sulphate, copper sulphate and lead nitrate in de ionized water. The concentrations of metal ions were determined with atomic absorption spectrophotometer and by colorimetric method.

##### **2.3.8.3 Results and discussion**

Pseudo first order, pseudo second order, ligand binding model and intra particle model was used to perform kinetic modeling of the batch biosorption data. Among all the kinetic models, the best suitable model was pseudo second order kinetic model to describe the

sorption of metal ions on the surface of *Gymnmogongrus torulus* with significantly higher values of linear regression coefficient ( $R^2$ ). The increase in temperature from 7 – 25 °C led to the increase in pseudo second order rate constant increased 2, to 10.5 times. With further increase in temperature from 25 to 55 °C lead to the decrease in sorption rate constant for lead, copper and cadmium. However, the sorption constant increased 1.1 times for zinc. Various isotherm models like Freundlich, Langmuir, Temkin and D-R isotherms were used by the authors. Among all the isotherms, Langmuir isotherm was found most suitable to predict the sorption of metal ions on the surface of *Gymnmogongrus torulus* with significantly higher value of linear regression coefficient ( $R^2$ ) against the other ISOTHERMS models. The thermodynamic feasibility study revealed the fact that the sorption of metal ions was exothermic and spontaneous in nature. However, the value of  $\Delta G$  decreased with the elevation of temperature. The behavior of  $\Delta G$  with the increase in temperature indicated the inverse relationship of spontaneity with temperature.

#### **2.3.8.4 Conclusion**

The results of the investigation indicated that the dried mass of *Gymnmogongrus torulus* has tremendous potential to biosorb the metal ions on its surface indeed. Metals ions considered in the work shown difference in their biosorption behavior at different ranges. The sorption of metal ions on the surface of the dried mass of *Gymnmogongrus torulus* was found exothermic and spontaneous in nature.

#### **2.4 Concluding remarks**

In view of the literature a track on the increasing repertoire of publication in biosorption field, it is concluded that the biosorption of heavy metals have been extensively studied on various sorts of biomasses. Extensive research has also been made on the data modeling with the help of isotherm, kinetic and mechanistic models. However, there is tremendous growth in the field of biosorption, yet very scarce research has been done on the usage of immobilized microbial strain and continuous column study. Moreover, the research in the field of biosorption have many more fruitful possibilities are to be endeavored. Perhaps, the research in the field of bacterium cell immobilization on the surface of biomass is to remove heavy metal quite scarce.



# EXPERIMENTATION

**EXPERIMENTATION**

---

**3.0 Motivation:**

For every research work, planning and detailed experimental programme is the key for successful carry out of the aimed work to get goal. In this chapter, a detailed programme of work done has been given along with all methodology, used in the various section of the work. The aim of the present work was the biological removal of zinc from industrial wastewater. The main objective of the present work motivated the investigation to evaluate the biosorption efficiency of various biosorbents and isolated microbial cell for the removal of zinc from liquid phase or industrial effluent. The primary aim of the investigation also provided the motivation to utilize the capacity of microbial cell immobilized on biosorbent leading to the simultaneous biosorption and bioaccumulation of Zn (II) ion and other associated metal ions in liquid phase.

In the present investigation, biosorption of Zn (II) ion was performed by various biosorbents selected for this study. Microbial removal of zinc has also been carried out. Simultaneous removal using both adsorbent and microbes was done batch wise and continuously in the column reactor. The preparation and characterization of biosorbents, isolation of microorganism, characterization and identification of microorganism, microbial cell immobilization, types of wastewater treated, composition of wastewaters, experimental program and detailed experimental procedures have been given in this chapter.

**3.1 PREPARATION OF BIOSORBENT SAMPLE**

The selected samples were washed three times with distilled water, dried in oven at 60 °C for overnight. The dried biosorbent samples were crushed in ball mill resulting in powdered form of various particle sizes (0.05 mm- 4 mm). The biosorbents were kept in polyethylene bags and stored in cool and dry condition at room temperature (30±1 °C).

## 3.2 CHARACTERIZATION OF BIOSORBENT

Following characterization of the biosorbent that usually affect the biosorption capacities, have been performed.

- (i) Surface area of the biosorbent,
- (ii) Presence of functional groups on biosorbent surface,
- (iii) Roughness of the surface,
- (iv) Carbon, hydrogen, nitrogen and sulphur content,
- (v) pH of the biosorbent surface and
- (vi) Physico-chemical characterization of biosorbents

### 3.2.1 Surface area of the biosorbent

The surface area of the biosorbent significantly affects the biosorption of heavy metal ion on its surface. Greater the surface area of the biosorbent, the more is the opportunity for metal ions to bind. For the estimation of surface area, all the powdered biosorbent samples were dried at 373 K for 24 hours to ensure the complete removal of moisture. Before and after the removal of moisture, the weight of the samples were measured by Electronic balance, model AW220, Shimadzu Corporation Japan. In the present work, the surface area of the biosorbents was measured by Micrometrics limited model ASAP 200 doped with the software ChemiSoft TPx V1.02. The desorption was carried out with the help of liquid nitrogen. The flow rate of the gas was kept at  $10 \text{ ml min}^{-1}$  at standard temperature and pressure (STP).

### 3.2.2 Presence of various functional groups on biosorbent surface

The functional group on the surface of biosorbent helps in the binding of metal ion with its surface. Most of the heavy metals are positively charged in their ionic state, hence negatively charged functional groups on the surface of biosorbent are preferred. In the present work, the surface groups of the biosorbent were analyzed by Fourier Transformation Infrared Spectroscopy (FTIR) in Thermo FTIR, model AVATAR 370 Csl coupled with EZOMNIC software (version 6.2). The wave number of the equipment for all the samples was kept in the range  $400 - 4000 \text{ cm}^{-1}$ . The samples were dried at room temperature followed by formation

of 1% pellet of potassium bromide (KBr, spectroscopic). The liquid samples were directly coated on glass plates and were subjected to infrared radiation. The spectrum was recorded in 34 cumulative scans.

### **3.2.3 Roughness of the surface of biosorbent**

The roughness of the biosorbent surface signifies the external surface area, internal surface area and pores. The more heterogeneous is the biosorbent surface, better is the probability of higher surface area. In the present work, all the adsorbent samples were analyzed by Scanning Electron Microscopy (SEM). The samples were degassed until the complete generation of vacuum occurred. After the vacuum generation, the samples were subjected to gold coating by means of sputtering. In case of living microbial cells, the culture, grown in LB broth, was centrifuged at 8000 xg for 10 minutes. The supernatant was discarded and the pellet was washed 2 times with phosphate buffer solution. The washed pellet was resuspended in glutaraldehyde (4% v/v) for 30 minutes. The resuspended pellet was spinned at 8000 xg for 10 minutes. The supernatant was discarded and the pellet was treated with serial dilution of ethanol. The serial dilutions ranged from 60% to 100%. Every dilution of ethanol was applied on pellet for 10 minutes individually. The pellet was left to stand under atmospheric conditions to allow evaporation of ethanol. The pellet was subjected to gold sputtering under vacuum followed by degassing. The equipment used to observe the surface texture of the samples was FEI Quanta 200F, Germany make. The voltage of the machine was shifted from 15 kV to 20 kV depending upon the type of the biosorbent.

### **3.2.4 Carbon, hydrogen, nitrogen and sulphur content**

The carbon, hydrogen, nitrogen and sulphur content of the biosorbent samples were analyzed by ultimate, proximate and CHNS analysis performed in bomb calorimeter (Toshniwal electronics limited – Ajmer, India make), Muffle furnace (Wishwani Scientific traders and Instruments) and CHNS analyzer (CE- 440 Elemental Analyzer, Eai Exter Analytical, Inc), respectively. These analyses decipher out the chemical composition of biosorbents.

### 3.2.5 pH of the biosorbent surface

The pH of the biosorbent surface was measured by adding suitable amount of biosorbent in distilled water. The mixture was allowed to agitate overnight (100 rpm), the sample was withdrawn and the final pH was measured by digital pH meter (Toshniwal make – Ajmer, India).

### 3.2.6 Physico-chemical characterization of biosorbents

The value of high heating value (HHV,  $\text{kJg}^{-1}$ ) has been calculated by equation [3.1].

$$HHV(\text{kJg}^{-1}) = 0.3491C + 1.1783H - 0.1034O - 0.0211A + 0.1005S - 0.10151N \quad [3.1]$$

### 3.3 Growth and harvesting of living microorganism

Living biomass was grown in pre sterilized flasks of 500 ml capacity in minimal agar media and Luria Bertaini media. The growth curve of the bacterium was plotted at predetermined time interval. The minimal growth medium also contained predetermined amount of zinc (1 to 7 moles  $\text{l}^{-1}$ ). The composition of minimal media and Luria Bertani has been shown in table 3.3 (a) and table 3.3 (b).

Table 3.3 (a): Composition of minimal agar media

Component	Amount ( $\text{gl}^{-1}$ )
$\text{NH}_4\text{Cl}$	0.1
$\text{K}_2\text{HPO}_4$	0.1
$\text{KH}_2\text{PO}_4$	0.05
$\text{MgSO}_4 \cdot 7 \text{H}_2\text{O}$	0.1
$\text{FeSO}_4$	0.001
KCl	0.01
$\text{CaCl}_2$	0.001
Yeast extract	0.08

Table 3.3 (b): Composition of Luria Bertani media

Component	Amount (%)
Tryptone	1
Yeast extract	0.5
Sodium Chloride	1
pH	7

The microbial cells in the growth medium were harvested in sterilized, dried and pre weighed centrifuge tubes by centrifuging at 8000 xg for 10 minutes at 298 K (Remi Instruments Ltd., Mumbai, India). The final and initial dry weights of the tubes were observed in electronic balance, model AW220, SHIMAZDU Corporation Japan.

### **3.3.1 Preparation of biomass bed**

Biosorbent particles of various sizes ranging from 0.5 mm to 2 mm were sieved and the particles were soaked in hot water at 333 K for 1 hour. Soaked particles were then dried at 353 K. Finally, the dried sawdust particles were steam sterilized at 394 K for 15 minutes at 15 psi.

### **3.3.2 Immobilization of microbial cells**

Immobilization of bacterial cell was done by dispensing weighed amount of pre-sterilized sawdust (2000 mg) on 48-hour-old culture of *zinc sequestering bacteria VMSDCM* Accession no. HQ108109 growing in 50 ml LB medium contained in 500 ml round bottom flasks. The flasks were incubated at 308 K for another 48 hours. Microbial cell immobilization was confirmed by observing a small amount of microbial treated sawdust through scanning electron microscope.

## **3.4 SORPTION EXPERIMENTS OF Zn (II) ION**

The predetermined concentration of zinc was added to the 500 ml flask at predefined pH, temperature, adsorbent dose and at fixed agitation rate. The range of various parameters used in various sorption experiments were pH (1-8), temperature (298 to 318 K), initial concentration of Zn (II) ion (1 – 150 mg l<sup>-1</sup>), biomass dose (0.1 – 5 g l<sup>-1</sup>), agitation (25 – 1000 revolution per minute, RPM) and particle size (0.05 – 4 mm). The samples were withdrawn at regular time of interval, centrifuged and the supernatant was analyzed by atomic absorption spectrophotometer (AAS) at 213.9 nm wavelength.



### 3.4.1 Effect of other co-ions

The other co-ions studied in present investigation were Copper (II) and total Fe (II, III). The concentration range tried for them in batch sorption experiments ranged between (1 to 150 mg l<sup>-1</sup>). The concentration of Cu (II) and total Fe (II, III) was determined by AAS measured at 324.5 and 248.3 nm wavelength, respectively. The calibration curves have been given in Annexure A-1. The schematic diagram of sorption studies given in figure 3.4.1 (a).



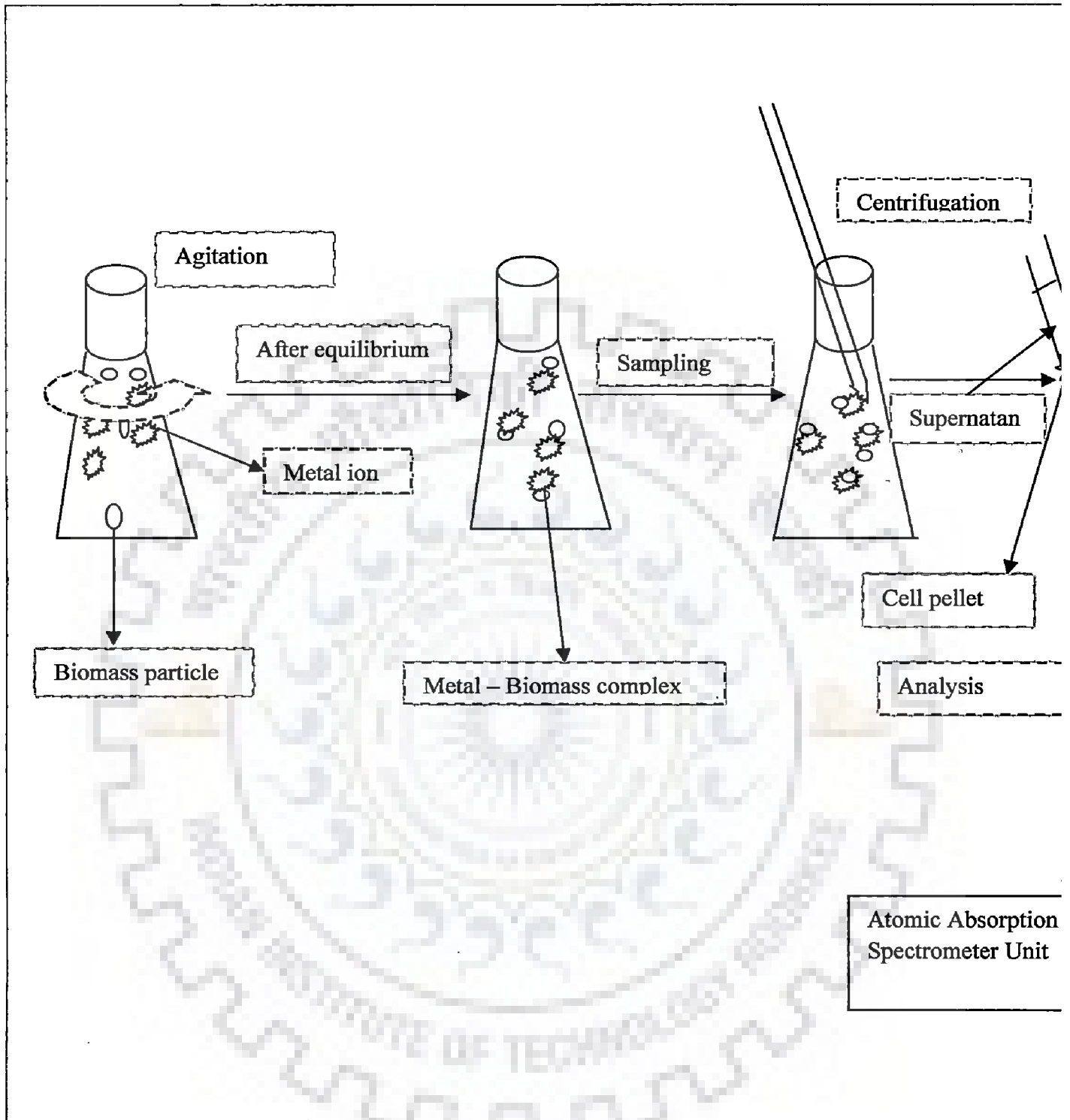


Figure 3.4.1 (a): Schematic diagram batch sorption studies

### 3.5 TYPES OF WASTEWATER TREATED

In the present work, the effluent discharging from zinc plating industry, copper smelting plant and zinc production plant were considered. The effluent from zinc production unit, SIDCUL, Hardwar, India was used as real wastewater and treated to remove Zn (II), total Fe (II, III) and Cu (II) ions from liquid phase. Composition of synthetic simulated wastewater and real wastewater has been given in table 3.5 (a) and table 3.5 (b), respectively.

Table 3.5 (a): Composition of synthetic simulated wastewater

Name of industry	Zn (II) (mg l <sup>-1</sup> )	Cu(II) (mg l <sup>-1</sup> )	Fe (II) (mg l <sup>-1</sup> )	Fe(III) (mg l <sup>-1</sup> )	Total Fe (mg l <sup>-1</sup> )	pH
Zinc plating industry	70200 - 33900	N.D	222400 - 90000	8510 - 2200	203910 - 92200	2.5
Copper smelting plant	142	93	N. D	N. D	188	0.6

Table 3.5 (b): Composition of real wastewater

Name of industry	Zn (II) (mg l <sup>-1</sup> )	Cu(II) (mg l <sup>-1</sup> )	Total Fe (mg l <sup>-1</sup> )	pH
Zinc producing industry, Hindustan Zinc Limited	4000	123	2389	5.28

The major metals considered in the present work were Zn (II), total Fe (II, III) and Cu (II). The upper limits of the Zn (II), total Fe (II, III) and Cu (II) in mg l<sup>-1</sup> were considered.

### 3.6 PHYSICAL PARAMETERS STUDIED IN BATCH BIOSORPTION STUDY

In the present work, physical parameters involved in biosorption of Zn (II) were studied in detail. The parameters selected for present work were pH, temperature, particle size, contact time, biosorbent concentration (g l<sup>-1</sup>), initial concentration of Zn (II) ion (mg l<sup>-1</sup>) and agitation rate. Furthermore, the complete microbial characterization, study of growth curve of isolated microbial strain in presence of Zn (II) ion and other associated metals, immobilization of microbial cells, its characterization and simultaneous biosorption and bioaccumulation were

also studied in the present work. The experiments were performed with the motivation to optimize various physical parameters to obtain maximum removal of zinc from liquid phase. The details of all these experiments have been shown in table 3.6 (a).

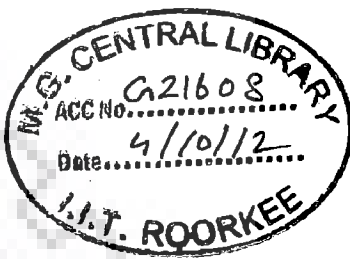
Table 3.6 (a): Experimental work for the removal of zinc ion from pure zinc solution, from binary system of Cu – Zn, from binary system of Fe – Zn and from ternary metal ion system Cu-Fe-Zn in batch studies

Name of the experiments	Materials used (Adsorbents/ Bacteria)	Parameter optimized/ physical property studied	Characterization parameters	Metal ion
Characterization of biosorbent	<i>Cedrus deodara</i> sawdust, Eucalyptus leaf powder, Eucalyptus bark sawdust, Pine apple peel powder, Mango bark sawdust, Jack fruit peel powder, Egg shell with egg shell membrane and Orange peel	-	FTIR, SEM, EDAX, pH of the surface and ultimate and proximate analysis, CHNS analysis	Zn (II)
Parameter optimization	<i>Cedrus deodara</i> sawdust, Eucalyptus leaf powder, Eucalyptus bark sawdust, Pine apple peel powder, Mango bark sawdust, Jack fruit peel powder, Egg shell with egg shell membrane and Orange peel	pH and Temperature	-	Zn (II)

Parameter optimization	<i>Cedrus deodara</i> sawdust, Eucalyptus leaf powder, Eucalyptus bark sawdust, Pine apple peel powder, Mango bark sawdust, Jack fruit peel powder, Egg shell with egg shell membrane and Orange peel	Particle size and contact time	-	Zn (II)
Parameter optimization	<i>Cedrus deodara</i> sawdust, Eucalyptus leaf powder, Eucalyptus bark sawdust, Pine apple peel powder, Mango bark sawdust, Jack fruit peel powder, Egg shell with egg shell membrane and Orange peel	Adsorbate concentration, biosorbent dose and agitation rate	-	Zn (II)
Parameter optimization	<i>Cedrus deodara</i> sawdust, Eucalyptus leaf powder, Eucalyptus bark sawdust, Pine apple peel powder, Mango bark sawdust, Jack fruit peel powder, Egg shell with egg shell membrane and Orange peel	pH and Temperature	-	Zn – Cu

Parameter optimization	<i>Cedrus deodara</i> sawdust, Eucalyptus leaf powder, Eucalyptus bark sawdust, Pine apple peel powder, Mango bark sawdust, Jack fruit peel powder, Egg shell with egg shell membrane and Orange peel	Particle size and contact time	-	Zn – Cu
Parameter optimization	<i>Cedrus deodara</i> sawdust, Eucalyptus leaf powder, Eucalyptus bark sawdust, Pine apple peel powder, Mango bark sawdust, Jack fruit peel powder, Egg shell with egg shell membrane and Orange peel	Adsorbate concentration, biosorbent dose and agitation rate	-	Zn – Cu
Parameter optimization	<i>Cedrus deodara</i> sawdust, Eucalyptus leaf powder, Eucalyptus bark sawdust, Pine apple peel powder, Mango bark sawdust, Jack fruit peel powder, Egg shell with egg shell membrane and Orange peel powder	pH and Temperature	-	Zn (II)– total Fe (II, III)

Parameter optimization	<i>Cedrus deodara</i> sawdust, Eucalyptus leaf powder, Eucalyptus bark sawdust, Pine apple peel powder, Mango bark sawdust, Jack fruit peel powder, Egg shell with egg shell membrane and Orange peel powder	Particle size and contact time	Zn – total Fe (II, III)
------------------------	--	--------------------------------	-------------------------



Parameter optimization	<i>Cedrus deodara</i> sawdust, Eucalyptus leaf powder, Eucalyptus bark sawdust, Pine apple peel powder, Mango bark sawdust, Jack fruit peel powder, Egg shell with egg shell membrane and Orange peel powder	Adsorbate concentration, biosorbent dose and agitation rate	Zn – total Fe (II, III)
------------------------	--	---	-------------------------

Parameter optimization	<i>Cedrus deodara</i> sawdust, Eucalyptus leaf powder, Eucalyptus bark sawdust, Pine apple peel powder, Mango bark sawdust, Jack fruit peel powder, Egg shell with egg	pH and Temperature	Zn – total Fe (II, III)-Cu(II)
------------------------	--	--------------------	--------------------------------

	shell membrane and Orange peel powder			
Parameter optimization	<i>Cedrus deodara</i> sawdust, Eucalyptus leaf powder, Eucalyptus bark sawdust, Pine apple peel powder, Mango bark sawdust, Jack fruit peel powder, Egg shell with egg shell membrane and Orange peel powder	Particle size and contact time	-	Zn – total Fe (II, III)-Cu(II)
Parameter optimization	<i>Cedrus deodara</i> sawdust, Eucalyptus leaf powder, Eucalyptus bark sawdust, Pine apple peel powder, Mango bark sawdust, Jack fruit peel powder, Egg shell with egg shell membrane and Orange peel powder	Adsorbate concentration, biosorbent dose and agitation rate	-	Zn – total Fe (II, III)-Cu(II)
Isolation of bacterium	<i>Zinc sequestering bacterium VMSDCM</i> Accession no “HQ108109”	Cell wall of the bacterium studied by gram staining. Phylogenetic analysis of the bacterium was studied by PHYLIP	-	Biochemical and phylogenetic characterization



			software using neighbor joining method and Jukes cantor method	
Bacterial cell shape	<i>Zinc sequestering bacterium</i> VMSDCM Accession no "HQ108109"	-	Cell shape	By phase contrast microscopy
Growth curve of bacterium	<i>Zinc sequestering bacterium</i> VMSDCM Accession no "HQ108109"	-		By optical density measurement Zn (II)
Growth curve of bacterium	<i>Zinc sequestering bacterium</i> VMSDCM Accession no "HQ108109"	-		By optical density measurement Zn (II) – total Fe (II, III)
Growth curve of bacterium	<i>Zinc sequestering bacterium</i> VMSDCM Accession no "HQ108109"	-		By optical density measurement Zn (II) – total Fe(II, III), Cu(II)
Dead biomass of bacterium	<i>Zinc sequestering bacterium</i> VMSDCM Accession no "HQ108109"	-		FTIR, SEM, EDAX, pH of the surface and ultimate and proximate analysis, CHNS analysis
Immobilization of bacterial cells	<i>Zinc sequestering bacterium</i> VMSDCM Accession no "HQ108109"	-		-
Immobilized bacterial cells	<i>Zinc sequestering bacterium</i>	-		FTIR, SEM, EDAX, pH of the surface and

	<i>VMSDCM</i> Accession no "HQ108109"			ultimate and proximate analysis, CHNS analysis
Biosorption	<i>Zinc</i> <i>sequestering</i> <i>bacterium</i> <i>VMSDCM</i> Accession no "HQ108109" (dead mass)	-	-	Zn (II)
Biosorption	<i>Zinc</i> <i>sequestering</i> <i>bacterium</i> <i>VMSDCM</i> Accession no "HQ108109" (dead mass)	-	-	Zn (II)-total Fe(II, III)
Biosorption	<i>Zinc</i> <i>sequestering</i> <i>bacterium</i> <i>VMSDCM</i> Accession no "HQ108109" (dead mass)	-	-	Zn (II)-Cu(II)
Biosorption	<i>Zinc</i> <i>sequestering</i> <i>bacterium</i> <i>VMSDCM</i> Accession no "HQ108109" (dead mass)	-	-	Zn (II)-total Fe(II, III)- Cu(II)
Simultaneous biosorption and bioaccumulation	Immobilized <i>Zinc</i> <i>sequestering</i> <i>bacterium</i> <i>VMSDCM</i> Accession no "HQ108109"	-	-	Real wastewater

### 3.6.1 Continuous column study

In the present investigation, the simultaneous biosorption and biaccumulation of Zn (II) in liquid phase was also studied in continuous column reactor. The column study was performed at various flow rates, length and column diameter. The details of the flow rates have been given in section 3.5. The experiments carried out in continuous column reactor for optimization of physical process parameters have been shown in table 3.6 (b).

Table 3.6.1 (a): Various studies conducted in the present work for the removal of zinc ion from ternary metal ion system Zn (II) – Cu (II)-Fe (II, III) in continuous column reactor

Name of the experiments	Materials used (Biosorbent/ Bacteria)	Parameter optimized	Metal ion(s)
Real Industrial Waste water	Immobilized <i>Zinc sequestering bacterium</i> VMSDCM Accession no "HQ108109" on <i>Cedrus deodara</i> sawdust	Flow rate	Zn(II) - Cu(II) - total Fe(II, III)
Real Industrial Waste water	Immobilized <i>Zinc sequestering bacterium</i> VMSDCM Accession no "HQ108109" on <i>Cedrus deodara</i> sawdust	Height of the column	Zn(II)- Cu(II) - total Fe(II, III)

All the experiments were carried out in triplicate and their average values were used in the results. The errors in experiments were calculated using equation [3.2] and equation [3.3].

$$\text{Sum of square errors (SSE)} = [q_{e(\text{th})} - q_{e(\text{exp})}]^2 \quad [3.2]$$

$$\chi^2 = [q_{e(\text{th})} - q_{e(\text{exp})}]^2 / q_{e(\text{th})} \quad [3.3]$$

### 3.7 COMPLETE SEQUENCE OF EXPERIMENTS

In the present work, the complete sets of experiments were divided into batch and continuous studies on biosorption of Zn (II) in liquid phase. The complete sets of experiment were also classified according to metal ion system used in the study. Figures 3.7 (a) and 3.7 (b) delineate the complete sequence of the experiments followed in the present investigation during batch and continuous column study.

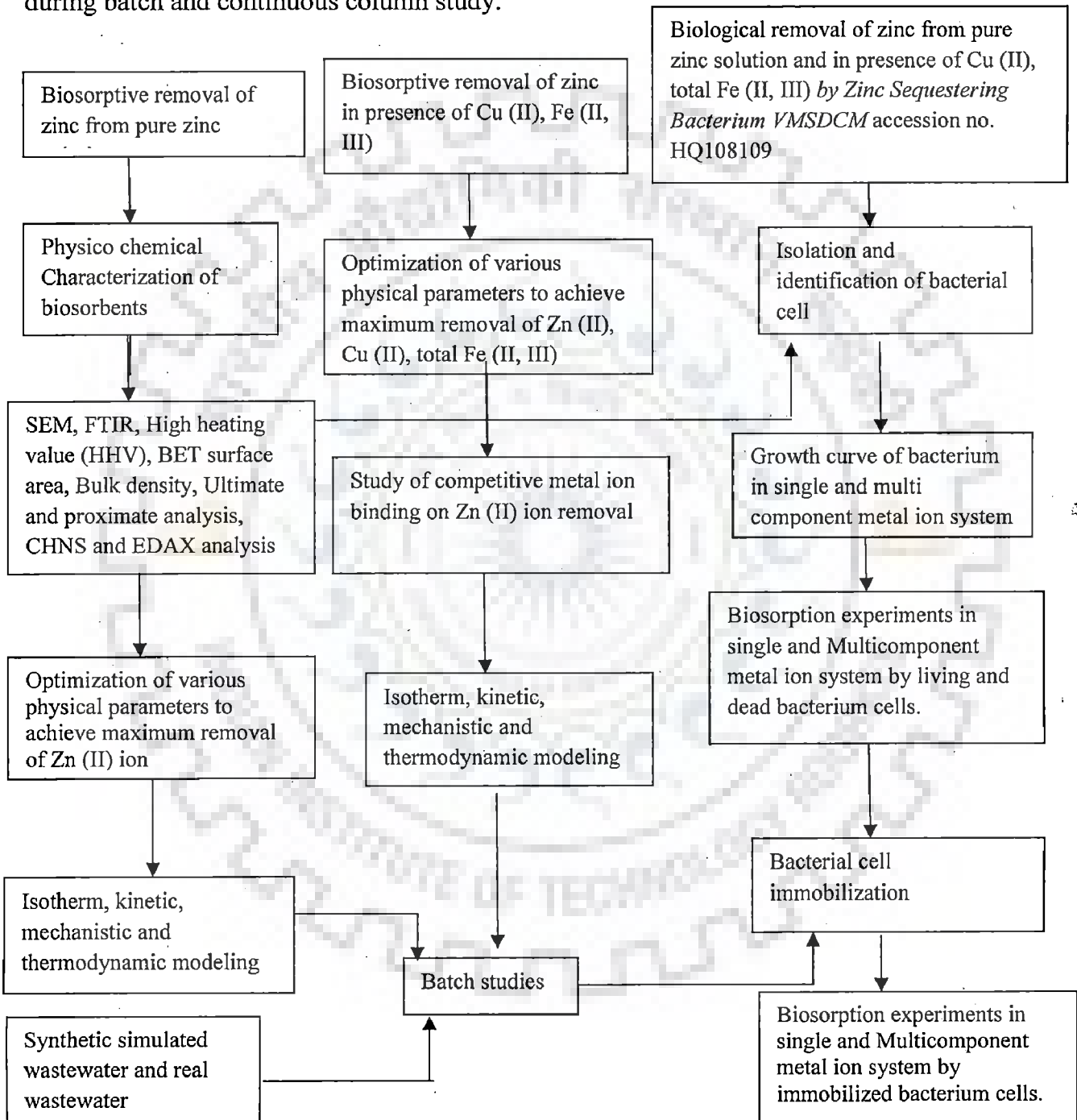


Figure 3.7 (a): Schematic representation of sorption of Zn (II) ion in batch studies

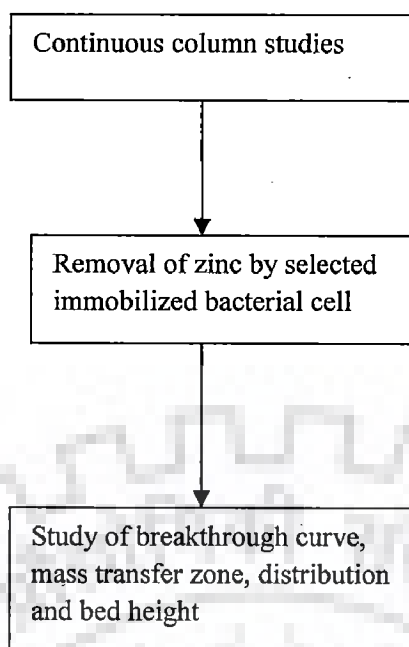


Figure 3.7 (b): Schematic representation of sorption of Zn (II) ion in continuous column studies

### **3.8 CALIBRATION OF MEASURING INSTRUMENTS**

The measuring instrument used in the present work were pH meter, D. O. meter, O. R. P. meter and Atomic absorption spectrophotometer, Element analyzer, UV – visible spectrophotometer and Electronic weighing balance. The reliability of experiments can only be assured by the proper calibration of measuring instruments. The calibration of pH meter, D. O. meter, O. R. P. meter, Atomic absorption spectrophotometer, Element analyzer, UV – visible spectrophotometer and Electronic weighing balance are mentioned below.

#### **3.8.1 Calibration of pH meter**

Calibration of pH meter was done according to instruction manual provided by manufacturer.

#### **3.8.2 Calibration of D. O meter**

D. O meter was calibrated by sodium thiosulphate solution as described in the instruction manual provided by the manufacturer.

### **3.8.3 Calibration of O. R. P meter**

O. R. P meter was calibrated according to the instruction manual provided by the manufacturer.

### **3.8.4 Calibration of atomic absorption spectrophotometer**

Atomic absorption spectrophotometer (AAS) was calibrated as per the instruction manual provided by the manufacturer using standard solution of respective metal salts. The calibration curve has been shown in Annexure A-1.

### **3.8.5 Element analyzer**

Element analyzer was calibrated according to the instruction manual provided by the manufacturer.

### **3.8.6 Electronic weighing balance**

Electronic weighing balance was calibrated according to the instruction manual provided by the manufacturer.

### **3.8.7 Calibration of batch experiments and continuous column reactor**

The batch experiments were carried out in incubator cum shaker. These incubators were calibrated with the help of thermometers. For continuous column study, peristaltic pump with variable flow rates were calibrated by using the instruction manual provided by the Miclins India Limited. Rotameters with pre-calibration certificate were purchased and calibration was done using primary standard flow meter.

## **3.9 EXPERIMENTAL PROCEDURE**

The experiments were conducted according to the scheme represented in figure 3.7.1 and 3.7.2. Each experiment was replicated in triplicate and the average reading was recorded. Detailed procedure of all the experiments has been shown below.

### **3.9.1 Biosorption of zinc in batch and continuous column**

The biosorption of zinc was studied in pure zinc solution in presence of total Fe (II, III) and Cu (II) ions in batch studies. Experiments related to synthetic simulated wastewater and real wastewater obtained from zinc producing unit were also performed in batch studies. However, the experiments with synthetic simulated wastewater and real wastewater were mainly conducted in continuous column reactor. The pH of the sample was measured after every two hours interval. After the completion of experiments, the sample was withdrawn, centrifuged and the supernatant was analyzed by AAS. All the experiments were repeated in triplicate and the average values were used for data modeling.

### **3.9.2 Studies on biosorption of zinc on the surface of various biosorbents in batch reactor**

Batch experiments of biosorption of Zn (II) ion was studied with other associated metals to obtain and to fit the data obtained at the attainment of equilibrium through various kinetic, mechanistic, thermodynamic and isotherm models. Effect of various physical parameters like pH, temperature, biosorbent to adsorbate dose ratio, agitation rate and particle size on the removal of zinc from liquid phase was studied. The effect of initial concentration of Zn (II) ion on the removal of total Fe (II, III) and Cu (II) was also studied. Simultaneously, the effect of initial concentration of total Fe (II, III) and Cu (II) ion on removal of Zn (II) from liquid phase was studied. The removal of total Fe (II, III) and Cu (II) ions from liquid phase was studied as a function of maximum removal of Zn (II) ion at optimum pH, temperature, biosorbent to adsorbate dose ratio, agitation rate, contact time and particle size. The microbial cells, immobilized microbial cells and dead cells of *Zinc sequestering bacterium VMSDCM* Accession no. "HQ108109", were also used in the present work to remove zinc from liquid phase in the absence and presence of other associated metals. The immobilization of living bacterium cell was performed on the surface of various non-living biosorbents.

### **3.9.3 Studies on biosorption of Zn (II) at various biosorbent dose**

The biosorbent dose ranging between 0.5 to 20 g l<sup>-1</sup> was distributed in doses of 0.5, 1, 2, 3, 5, 8, 12, 16, and 20 g l<sup>-1</sup>. These experiments were performed in two steps. In the first step, predetermined amount of biosorbent was added to the 150 mg l<sup>-1</sup> of Zn (II). In the another set of experiment, the predetermined amount of biosorbent was added in liquid solution containing 150 mg l<sup>-1</sup> of Zn (II) ion, 150 mg l<sup>-1</sup> of total Fe (II, III) and 150 mg l<sup>-1</sup> of Cu (II). The combination of metal ions with predetermined amount of biosorbent was agitated together in round bottom flask of 500 ml capacity at room temperature (308 ±0.5 K) and pH 7±0.5 for 40 hours. (Annexure A- 2).

### **3.9.4 Studies on biosorption of Zn (II) at various contact time**

The optimization of contact time for all biosorbents was performed in two sets of experiments. Initially Zn (II) ion was agitated with the fixed and predetermined amount of biosorbent for a time period ranging between 0.5 to 40 hours at pH 7±0.1 and temperature 303±0.5 K in a round bottom flask of 500 ml capacity. The sampling of reaction mixture was performed at predetermined time interval, i.e., 0.5, 1, 2, 4, 6, 10, 14, 18, 22, 26, 32, 36, and 40 hours. Similarly, the other set of experiment was performed in the presence of other associated metal ions (150 mg l<sup>-1</sup> of total Fe (II, III) and 150 mg l<sup>-1</sup> of Cu (II)). (Annexure A- 2)

### **3.9.5 Studies on biosorption of Zn (II) at various initial concentration**

Various initial concentrations of Zn (II) ion ranging between 1 to 150 mg l<sup>-1</sup> were used in the present work. Multiple concentrations of zinc used were 1 mg l<sup>-1</sup>, 5 mg l<sup>-1</sup>, 10 mg l<sup>-1</sup>, 20 mg l<sup>-1</sup>, 40 mg l<sup>-1</sup>, 80 mg l<sup>-1</sup>, 100 mg l<sup>-1</sup>, 120 mg l<sup>-1</sup> and 150 mg l<sup>-1</sup>. The fixed and predetermined amount of biosorbent was added to the various concentrations of Zn (II) ion, agitated at pH 7±0.1 and temperature 303±0.5 K in a round bottom flask of 500 ml capacity for 40 hours. Like other experiments, the another set of experiment was conducted in the presence of various concentration of total Fe (II, III) and Cu (II) ions (150 mg l<sup>-1</sup> of total Fe (II, III) and 150 mg l<sup>-1</sup> of Cu (II)). (Annexure A- 2)



### **3.9.6 Studies on biosorption of Zn (II) at various range of pH**

In the present work, studies on effect of pH on biosorption of Zn (II) ion were performed in the range of 1- 8. Fixed and predetermined amount of biosorbent and adsorbate were added to the round bottom flask of 500 ml capacity and agitated at  $308 \pm 0.5$  K for 40 hours and at various pH, i.e., 1, 2, 3, 4, 5, 6, 7 and 8. In the other set of experiment, the pH test was performed in the presence of other associated heavy metals  $150 \text{ mg l}^{-1}$  of total Fe (II, III) and  $150 \text{ mg l}^{-1}$  of Cu (II)). (Annexure A- 2)

### **3.9.7 Studies on biosorption of Zn (II) at various range of temperature**

The influence of temperature on biosorption of Zn (II) ion was investigated in range 298 – 313 K. The fixed amount of biosorbent with Zn (II) was agitated at pH  $7 \pm 0.1$  in round bottom flask of 500 ml capacity for 40 hours. An another set of experiment was conducted in the presence various concentration of of total Fe (II, III) and Cu (II) ions ( $150 \text{ mg l}^{-1}$  of total Fe (II, III) and  $150 \text{ mg l}^{-1}$  of Cu (II)). The temperature range was divided as 298 K, 303 K, 308 K and 313 K. (Annexure A- 2)

### **3.9.8 Studies on biosorption of Zn (II) at various range of agitation rate**

Influence of agitation rate on biosorption of Zn (II) was studied in range of 25 – 1000 rpm. The fixed amount of biosorbent and Zn (II) ions were added to the round bottom flask of 500 ml at pH  $7 \pm 0.1$  and temperature  $308 \pm 0.5$  K and agitated at various agitation rates, i.e., 25, 50, 75, 100, 200, 300, 400, 500, 600, 700, and 800 for 40 hours. An another set of experiments were conducted in the presence of various concentration of total Fe (II, III) and Cu (II) ions ( $150 \text{ mg l}^{-1}$  of of total Fe (II, III) and  $150 \text{ mg l}^{-1}$  of Cu (II)). pH of the reaction mixture was measured after every two hours. (Annexure A- 2)

### **3.9.9 Studies on biosorption of Zn (II) at various range of particle sizes**

The various particle sizes used in the present investigation ranged between 0.05 – 4 mm. The biomass of various particle sizes, i.e., 0.05 mm, 1 mm, 2 mm, 3 mm and 4 mm were added in fixed amount to fixed concentration of Zn (II) ion, agitated in the round bottom flask of 500

ml at pH  $7\pm 0.1$  and temperature  $308\pm 0.5$  K for 40 hours. An another set of experiments were conducted in the presence of various concentration of total Fe (II, III) and Cu (II) ions ( $150 \text{ mg l}^{-1}$  of Fe (II), Fe (III) and  $150 \text{ mg l}^{-1}$  of Cu (II)) (Annexure A- 2).

### **3.9.10 Studies on biosorption of total Fe (II, III) and Cu (II) in the presence of zinc.**

Influence of Zn (II) ion concentration on the removal of total Fe (II, III) and Cu (II) ions has been studied in the present investigation. The concentration of total Fe (II, III) and Cu (II) ion ranged between 1 to  $150 \text{ mg l}^{-1}$ . The concentration of Zn (II) ion was kept constant ( $150 \text{ mg l}^{-1}$ ). A fixed concentration of total Fe (II, III) and Cu (II)-ion 1, 5, 25, 50, 75, 100, 125 and  $150 \text{ mg l}^{-1}$  was added to the round bottom flask containing  $150 \text{ mg l}^{-1}$  of zinc and fixed amount of biosorbent. The flask was agitated at pH  $7\pm 0.1$  and temperature  $308\pm 0.5$  K for 40 hours. (Annexure A- 2).

### **3.10 BIOSORPTION AND BIOACCUMULATION of Zn (II), TOTAL Fe (II, III) AND Cu (II) ION BY IMMOBILIZED ZINC SEQUESTERING BACTERIUM VMSDCM ACCESSION NO. HQ108109**

The isolated and selected microbial strain was grown in LB medium and minimal nutrient medium. The compositions of mediums have been shown table 3.1 and table 3.2. The concentration of total Fe (II, III) and Cu (II) ranged between 1 to  $7 \text{ moles l}^{-1}$ . The concentration of Zn (II) ions in both the mediums ranged between 1 to  $7 \text{ moles l}^{-1}$ . The experiments were conducted in conical flask of 1 liter capacity. The bacterium culture was inoculated in broth containing various amounts of Zn (II), total Fe (II, III) and Cu (II), i.e.,  $1 \text{ mole l}^{-1}$ ,  $2 \text{ moles l}^{-1}$ ,  $3 \text{ moles l}^{-1}$ ,  $4 \text{ moles l}^{-1}$ ,  $5 \text{ moles l}^{-1}$ ,  $6 \text{ moles l}^{-1}$  and  $7 \text{ moles l}^{-1}$ . The growth of the growing bacterium cell was measured at 600 nm wavelength at the time interval of 1 to 24 hours. The combination of metals used were either single metal ion system, pure Zn (II)  $65.38$  to  $523.04 \text{ g l}^{-1}$ . The other combinations of metal ion systems used were Zn (II) – total Fe (II, III), Zn (II) – Cu (II), Zn (II) – total Fe (II, III) – Cu (II). The growth of the bacterium was performed at 308 K. The pH of the medium was fixed at 6.8.

### 3.11 CONTINUOUS COLUMN STUDY

The synthetic simulated wastewater (~ 2 l) containing 2 g/l of LB in mixing tank, was taken into the feed tank, and pumped using the peristaltic pump into the column. The feed rate was kept at 1.88 ml /min. To condition the biomass bed, the solution was kept inside the column for 4 days. At the completion of 4<sup>th</sup> day, the column was drained off and the solution containing the inoculum of screened *Zinc sequestering bacterium VMSDCM* Accession no. HQ108109 and 2 g/l of LB medium was pumped into the column at a feed flow rate of 1.88 ml/min. Under this situation, the column was kept for 4 days to precondition the screened bacterium. After the completion of four days, the solution was drained off. The preconditioning of the bacterium was performed on every 7<sup>th</sup>, 10<sup>th</sup> and 14<sup>th</sup> day. The next phase of the experiment extended for 11 days for every test run. The synthetic simulated wastewater and real wastewater were pumped into the the reactor in two different experimental sets. The flow rates of the wastewaters were 109 ml/ h, 160 ml/h, 296 ml/h and 318 ml/h. The O. R. P, D. O, and pH of inlet and outlet (ports P1 to P5) were constantly measured for a period of 11 days and compared. All the experiments were repeated twice and the average values were used for data modeling. The values obtained in continuous column study were used in calculating mass transfer zone bed capacity  $T_v$  at break point  $T_{bp}$  and total capacity of bed  $T_c$ . Equation [3.4] and equation [3.5] represent the break point obtained at equilibrium.

$$T_v = \int_0^{t_{bp}} \left(1 - \frac{C}{C_0}\right) dt \quad [3.4]$$

$$T_c = \int_0^{\infty} \left(1 - \frac{C}{C_0}\right) dt \quad [3.5]$$

where  $C$ ,  $C_0$  and  $dt$  were concentration of zinc ions at differential time ( $dt$ ) and initial concentration of zinc ions. To estimate the mass transfer, the mass transfer zone (MTZ) was calculated using equation [3.6]

$$\left(1 - \frac{T_v}{T_c}\right)h \quad [3.6]$$

The capacity of bed (mg/ g) at break point and at saturation (mg/ g) is given by equation [3.7] and

[3.8], respectively.

$$q_{tb} = \left( \frac{C_0 FT_v}{M} \right) \quad [3.7]$$

$$q_s = \left( \frac{C_0 FT_c}{M} \right) \quad [3.8]$$

where  $C_0$ ,  $F$  and  $M$  were initial concentration of zinc ion (mg/ l), flow rate (ml/h) and mass of bed (g) respectively.

### **Concluding remarks on the section 3.2**

The present chapter has dealt with the development of complete experimental programme for the removal of Zn (II) ion and other associated metal ions Cu (II) and total Fe (II, III) from synthetic metal ion solution, synthetic simulated wastewater and real industrial wastewater. Batch studies mediated by physical adsorption, microbial removal of metal ions, simultaneous biosorption and bioaccumulation in batch and continuous column reactor study were performed successfully in various experimental sets.

Various combinations of metal ions in various concentrations were used in the present work. These studies led to the optimization of physical parameters and data obtained from parameter optimization were used in data modeling. The complete experimental programme delineated the detail methodology of experiments performed in the present work and met efficiently with with the aims and scope of the present work.



# EXPERIMENTAL SETUP

**EXPERIMENTAL SETUP**

---

**4.0 Motivation:**

Present investigation aimed at removal of Zn (II) ion from industrial effluent. The main objective was fulfilled by carrying out the reaction in the batch (figure 4.1.1 (a)) and continuous column study (figure 4.1.2 (a)). Various auxiliary equipments were used for characterization of biosorbent and microbial cell, sterilization of the glass wares, double walled isotherm room, and other instruments used in the present investigation has been shown in figure 4.1.4 (a), 4.2 (a) to figure 4.2 (j).

In the present investigation, the biological removal of zinc from liquid phase has been studied from pure zinc solution, simulated and real wastewater with the objectives detailed in chapter 1. In this chapter, the design consideration in batch and column studies, details of set ups, specification of various auxiliary instruments, and analytical instruments have been given.

**4.1 DESIGN CONSIDERATION**

Designing of batch and column study needs the accurate data at the attainment of equilibrium, for the removal of Zn (II) ion from pure zinc solution, simulated and real industry wastewater.

**4.1.1 Batch study**

Batch studies were performed to obtain the optimized process parameters, rate constants, mechanistic modeling constants and isotherm constants. The batch studies were further aimed at the evaluation of biosorption capacity of various biosorbents considered in the present investigation. In batch study, 200 ml of sample volume was used throughout the study. The samples underwent biosorption in round bottom flask of 500 ml capacity. The 500 ml capacity flasks were used to ensure the proper mixing of biosorbent with adsorbate ions. The mouth of the flask was sealed with sterilized cotton to avoid any type of contamination in the

sample. At one time maximum of 20 samples can be agitated in incubator cum shaker unit. The growth of the bacterium was done in conical flask of 1 l capacity. Figure 4.1.1 (a) shows the experimental set up for batch studies.



Temperature and  
agitation regulation unit



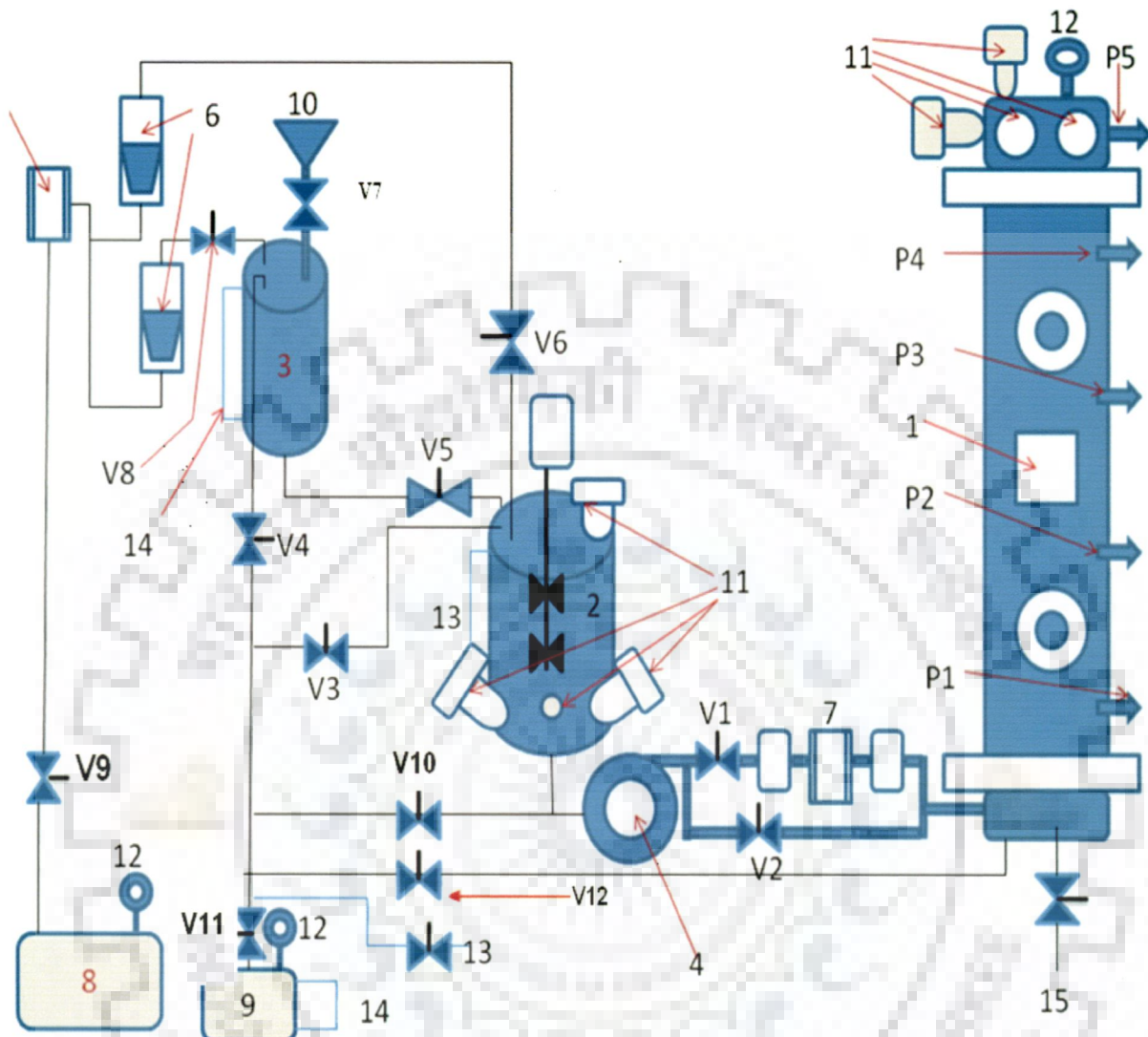
Batch reactor in incubator cum shaker

Figure 4.1.1 (a): Photograph of batch reactor in incubating cum shaking process



#### 4.1.2 Continuous column study

Biological removal of heavy metals is relatively a slow process. Therefore, in the present investigation, an up flow column reactor was preferred. The continuous experiments were performed in the column reactor (figure 4.1.2 (a)). The column of up flow reactor, feed tank, mixing vessel and connecting pipelines were made up of stainless steel (SS). Total empty volume of the column was  $4.94 \pm 0.0024$  l. The sample ports were provided at equal distance of 15.25 cm. The column was fastened over two flange joints, fitted with mesh (mesh no. 16 BSS, width aperture 0.3 mm). The upward flow of the liquid with defined flow rate from the bottom of the column was maintained by peristaltic pump. The bed of adsorbent particles was packed in the column up to 100 cm and the microbial culture (grown in LB broth) was immobilized on the bed of adsorbent. The complete experimental set up (figure 4.1.2 (a)) was kept in an isothermal chamber made up of wood and stuffed with glass wool. The chamber was set at temperature 303 K. The detailed front view of mixing and feed tank with respective dimensions has been shown in figure 4.1.2 (b) and figure 4.1.2 (c).



1. Bio Column Reactor 2. Mixing Tank with Stirrer 3. Effluent Feed Tank 4. Peristaltic Pump 5. Air Filter Units 6. Rotameters 7. Water Filter Notice 8. Compressor 9. Steam Generator 10. Feed Port in Mixing Tank 11. Electronic Probe Ports for Temperature, pH, O. R. P (Oxidation Reduction Potential) and Dissolved Oxygen (D. O) Measurements 12. Pressure Gauge 13. Drainage Line 14. Level Indicator 15. Back Washing Line, P1 – P5 Sampling Ports and V1 – V12. Flow Valves.

Figure 4.1.2(a): Schematic diagram of column reactor used in present work

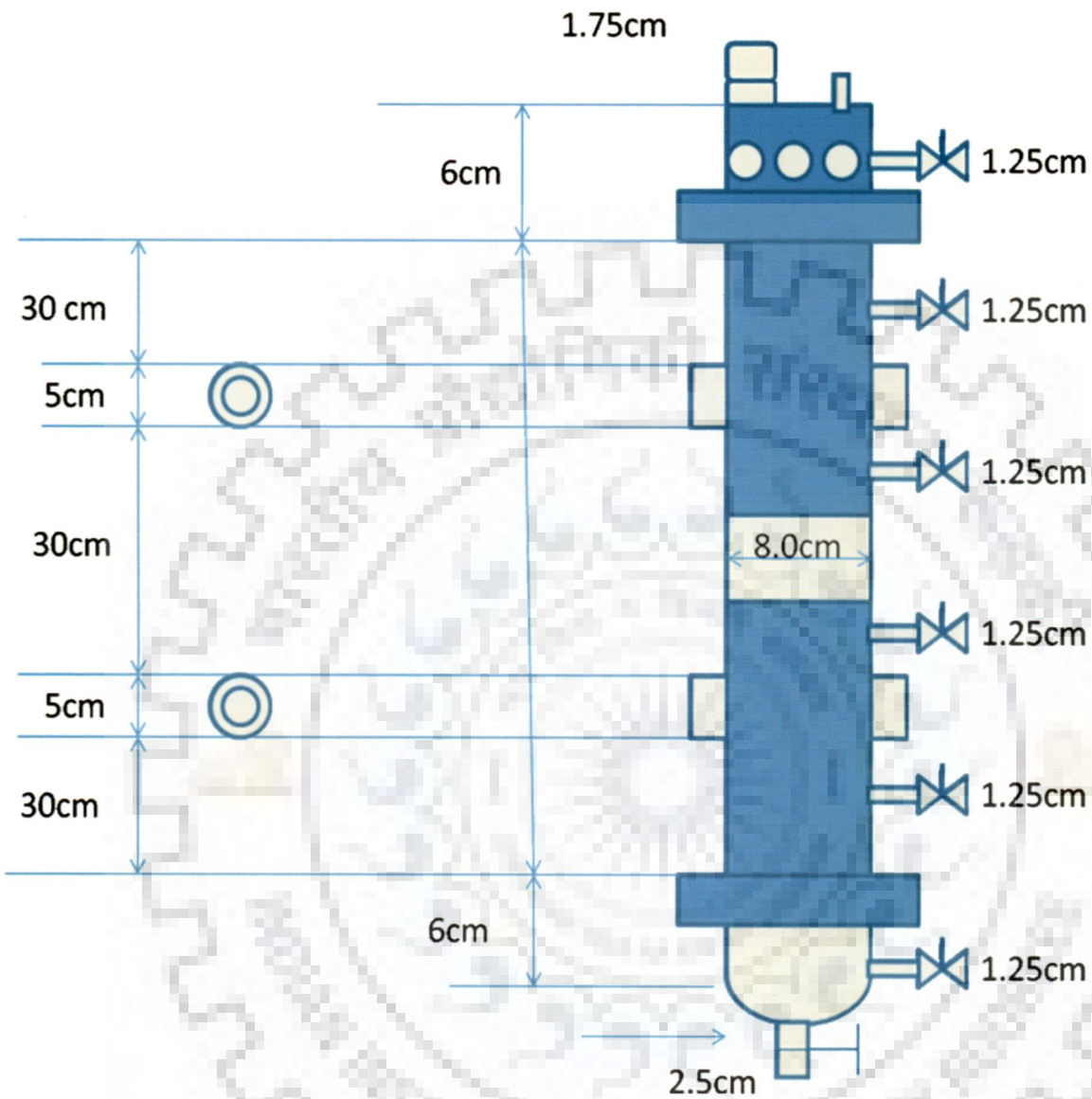


Figure 4.1.2 (b): Front view of column reactor

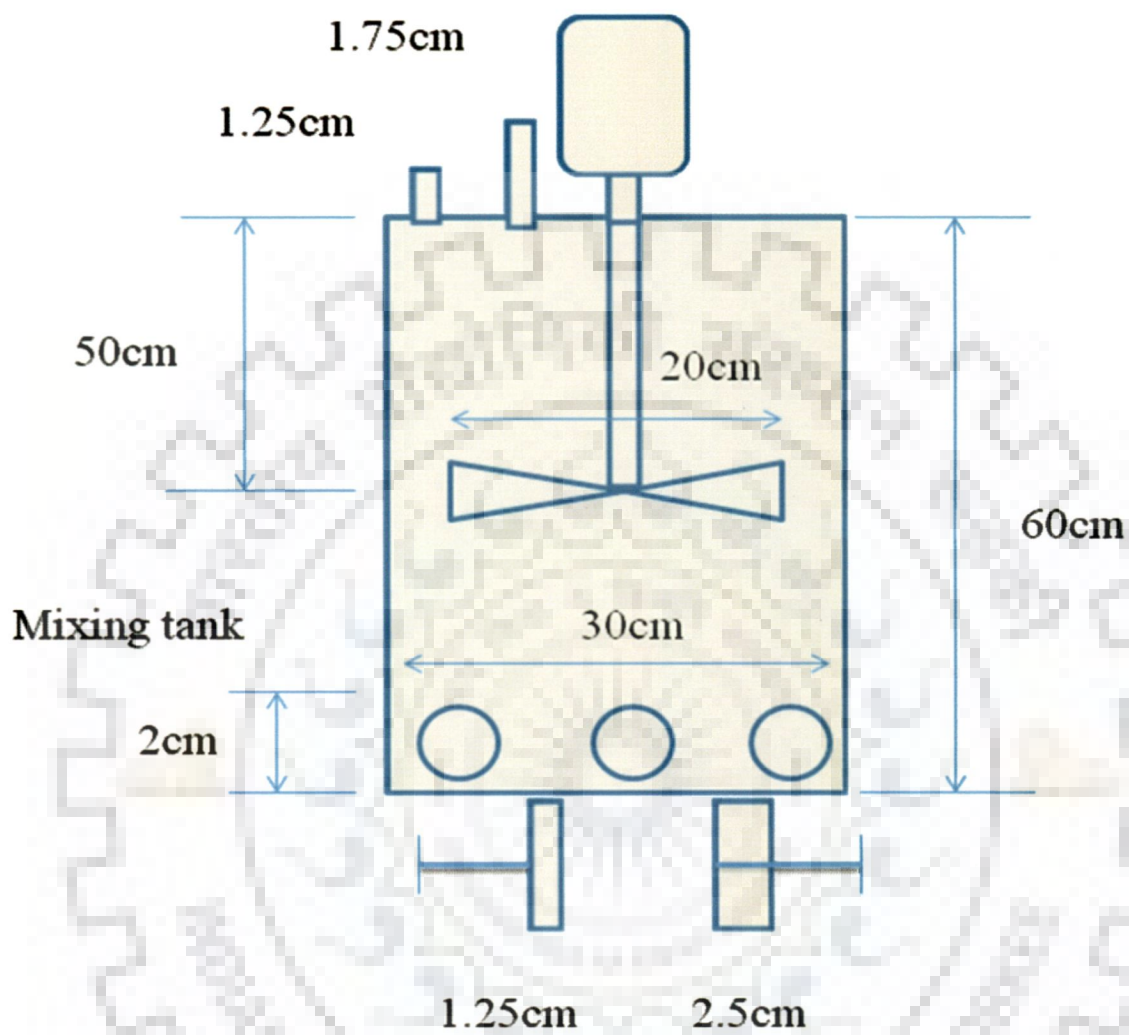


Figure 4.1.2 (c): Front view of feed mixing tank

### 4.1.3 Up –flow column reactor instrumentation

The flow rate of the feed was controlled by calibrated peristaltic pump (model-PP-20) manufactured by Miclins India, Chennai, India. The calibrated rotameters was used to measure airflow rate. Pressure of the steam was measured by pressure gauge and pressure was controlled by pressure control unit associated with steam generator. Digital Oxidation-reduction potential (O. R. P) meter, pH and dissolved oxygen probe were installed to measure conductivity, pH and D. O online. Figure 4.1.3 (a) represents the photograph of column reactor (mixing tank and reactor section). Figures 4.1.3 (b) and 4. 1. 3 (c) represent the outer section of the reactor with feeding tank, electrical fittings and steam generator for sterilization of the reactor. Steam pressure was measured by pressure gauge installed in the steam generator.



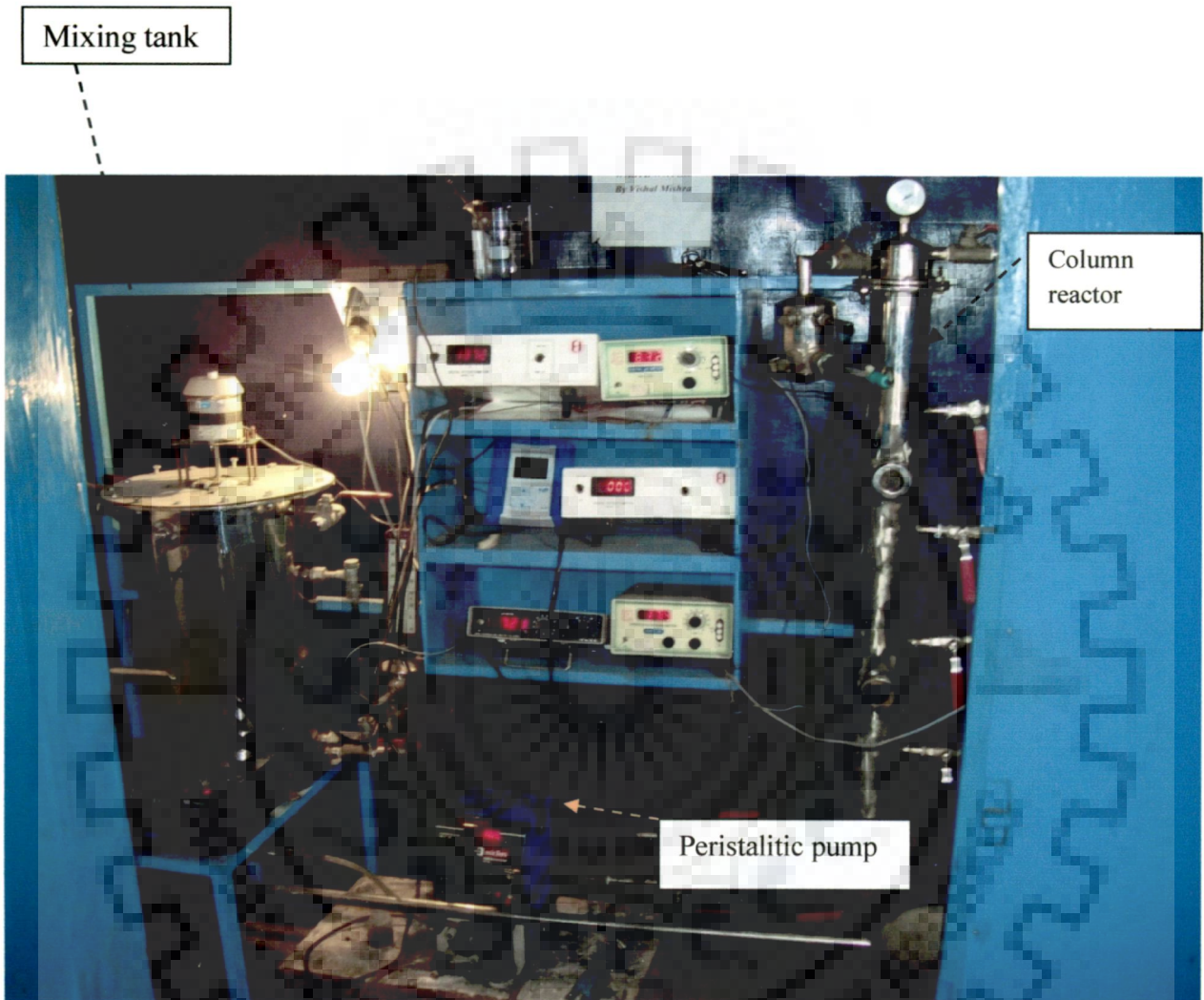


Figure 4.1.3 (a) Photograph of column reactor and mixing tank

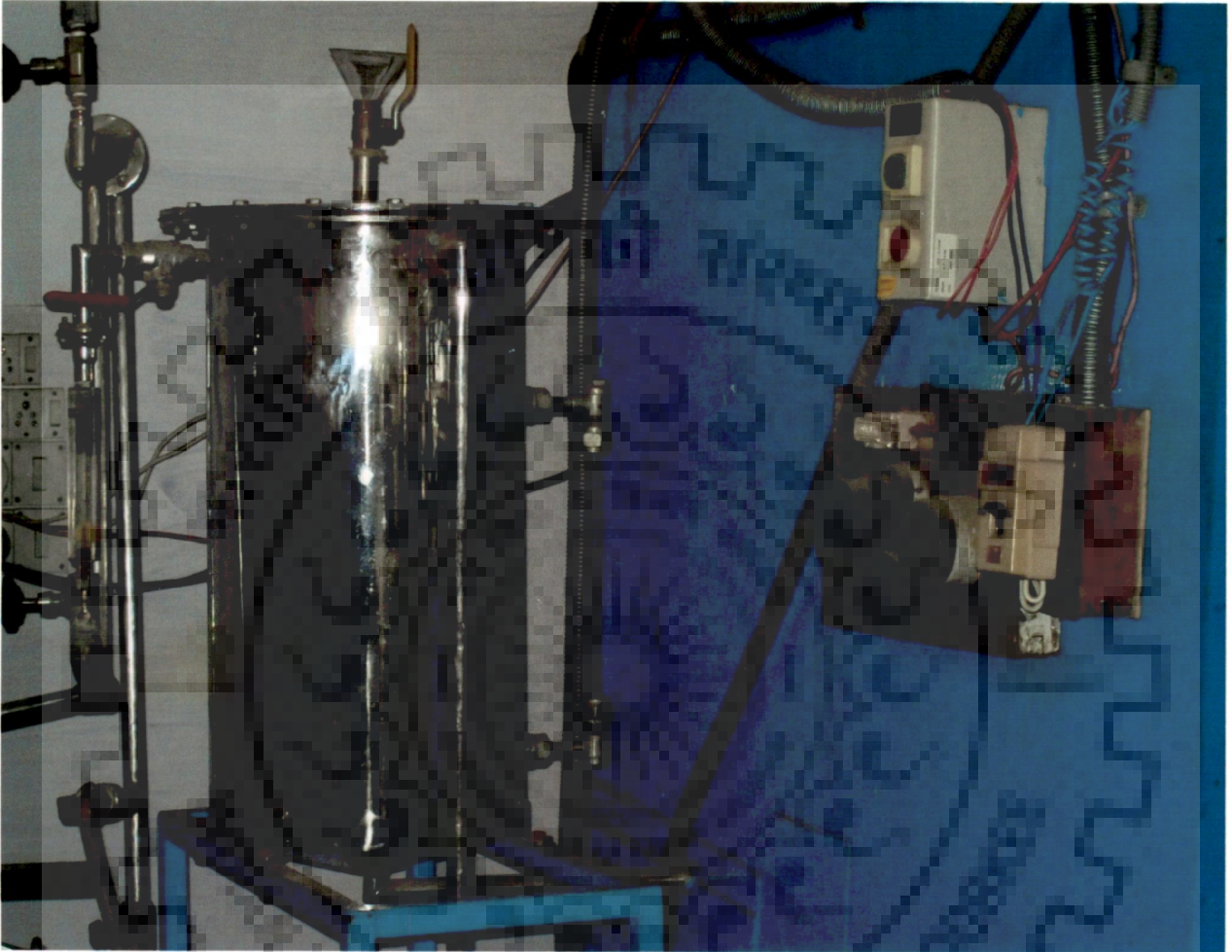


Figure 4.1.3 (b): Photograph of feeding tank

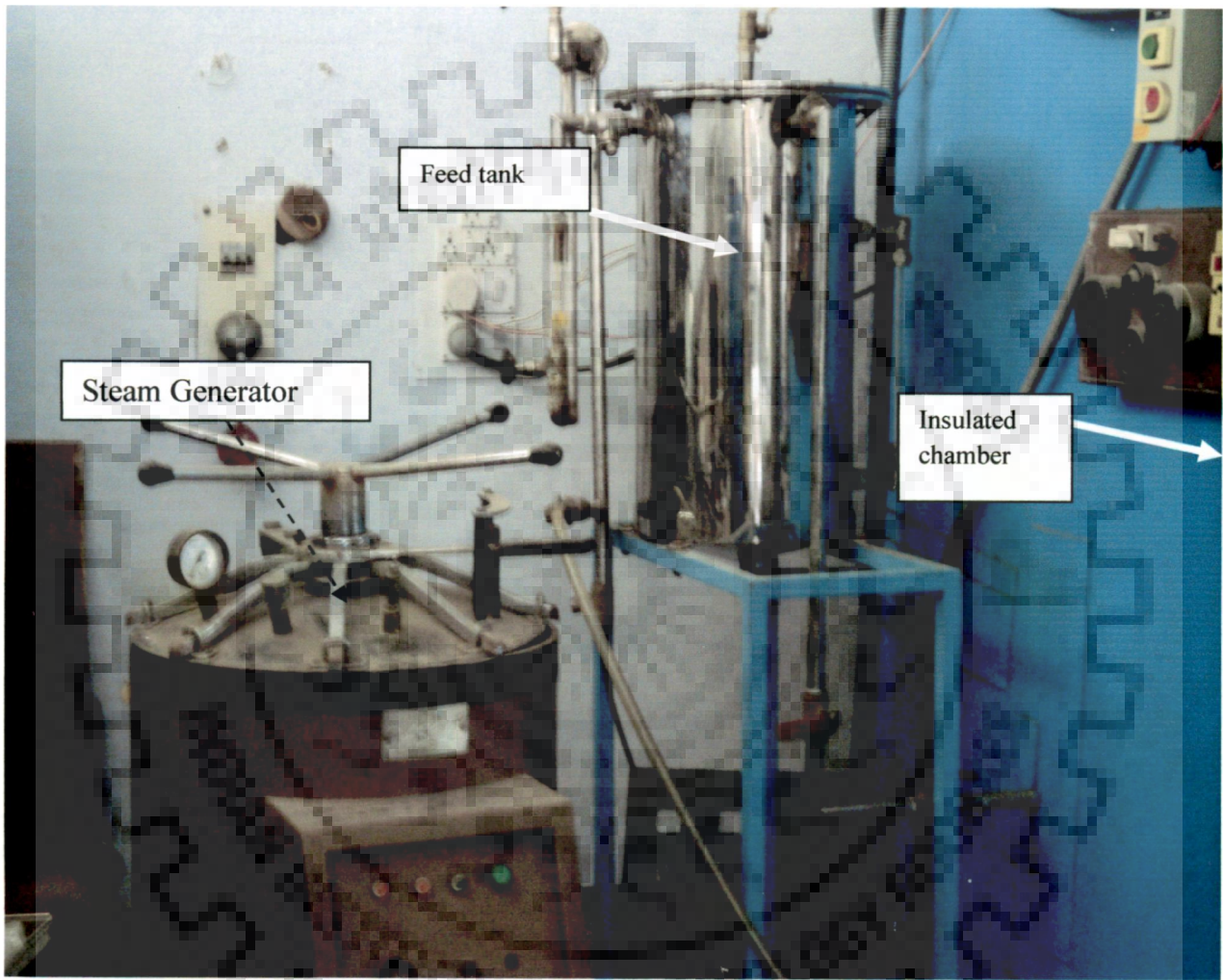


Figure 4.1.3 (c): Photograph of steam generator in continuous column reactor



### 4.1.3 Double walled isotherm chamber

The whole setup of the column bioreactor was kept inside the isothermal chamber to maintain the constant temperature throughout all experimental runs. All the experiments were performed at  $303 \pm 0.5$  K. The chamber was made up of 6 mm thick plywood. The dimensions of the double walled chamber were 1.2 m x 1.2 m x 2.2 height. Glass wool was filled in between the walls of the reactor to insulate the chamber. Temperature controller cum thermostatic heating device (ESCORT, Japsin Pvt. Ltd, New Delhi, India) along with digital display was fitted into the chamber. The thermostat used can work up to 343 K with a accuracy of  $\pm 0.2$  K. Figure 4.1.4 (a) represents the double walled isotherm chamber.



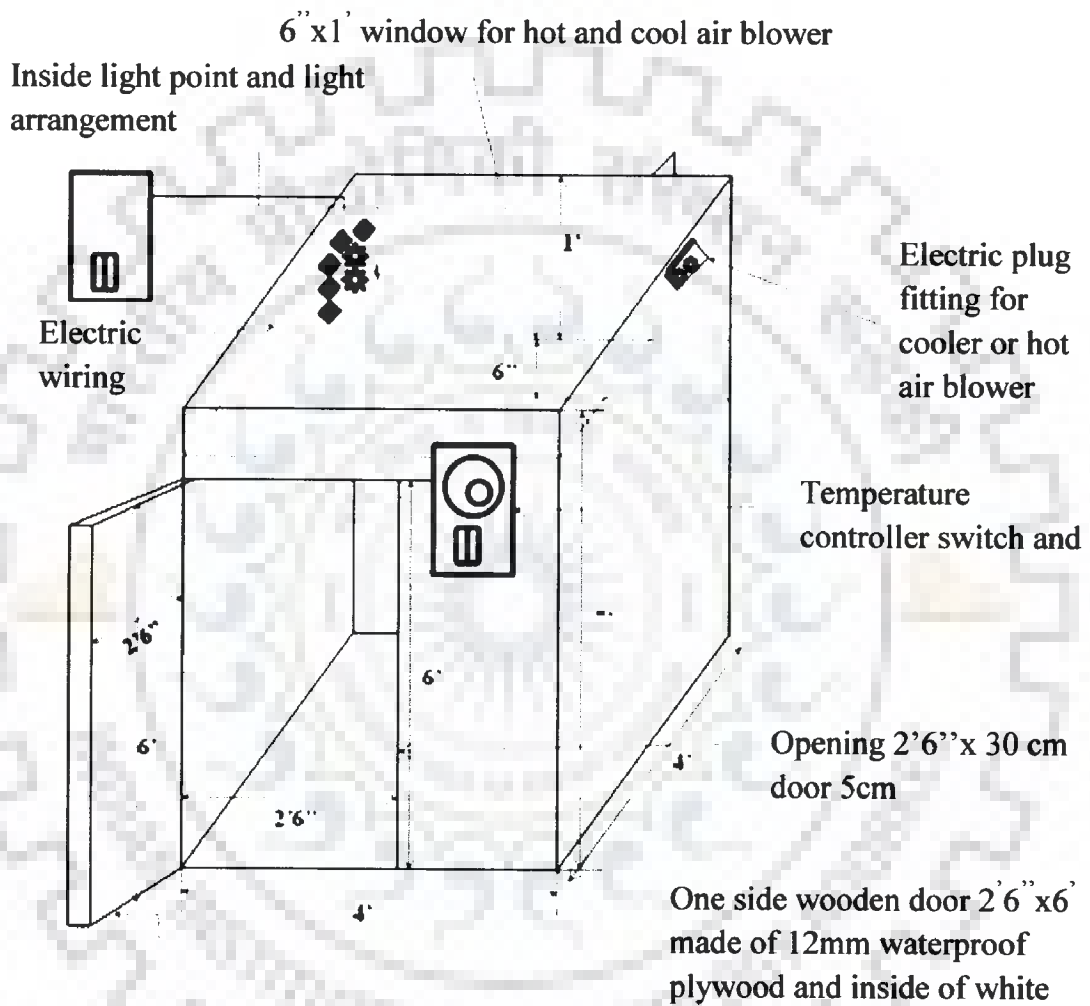
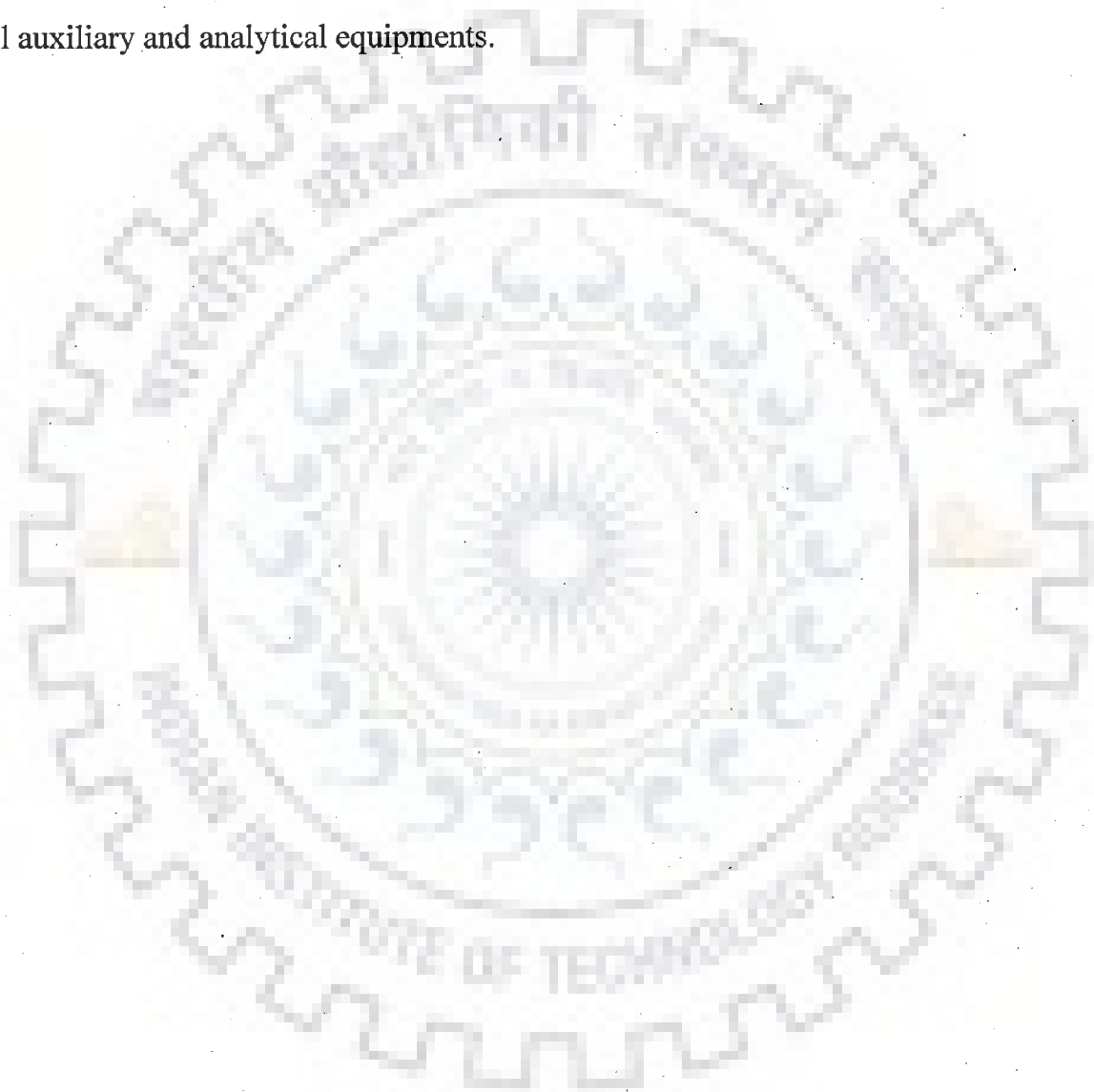


Figure 4.1.4 (a): Details of double walled isotherm chamberc (not to scale)

#### **4.1 AUXILIARY AND ANALYTICAL INSTRUMENTS USED IN THE PRESENT WORK**

The auxiliary and analytical equipment used in the present investigation were laminar chamber, centrifuge, muffle furnace, phase contrast microscope, autoclave, Milli Q water unit, electronic weighing balance, Fourier transformation infra red microscopy, Elemental analyser, Atomic Absorption Spectrophotometer, Scanning Electron Microscopy (SEM), Hot air oven and BET surface area analyzer etc. Table 4.2 (a) provides the details of specifications of all auxiliary and analytical equipments.



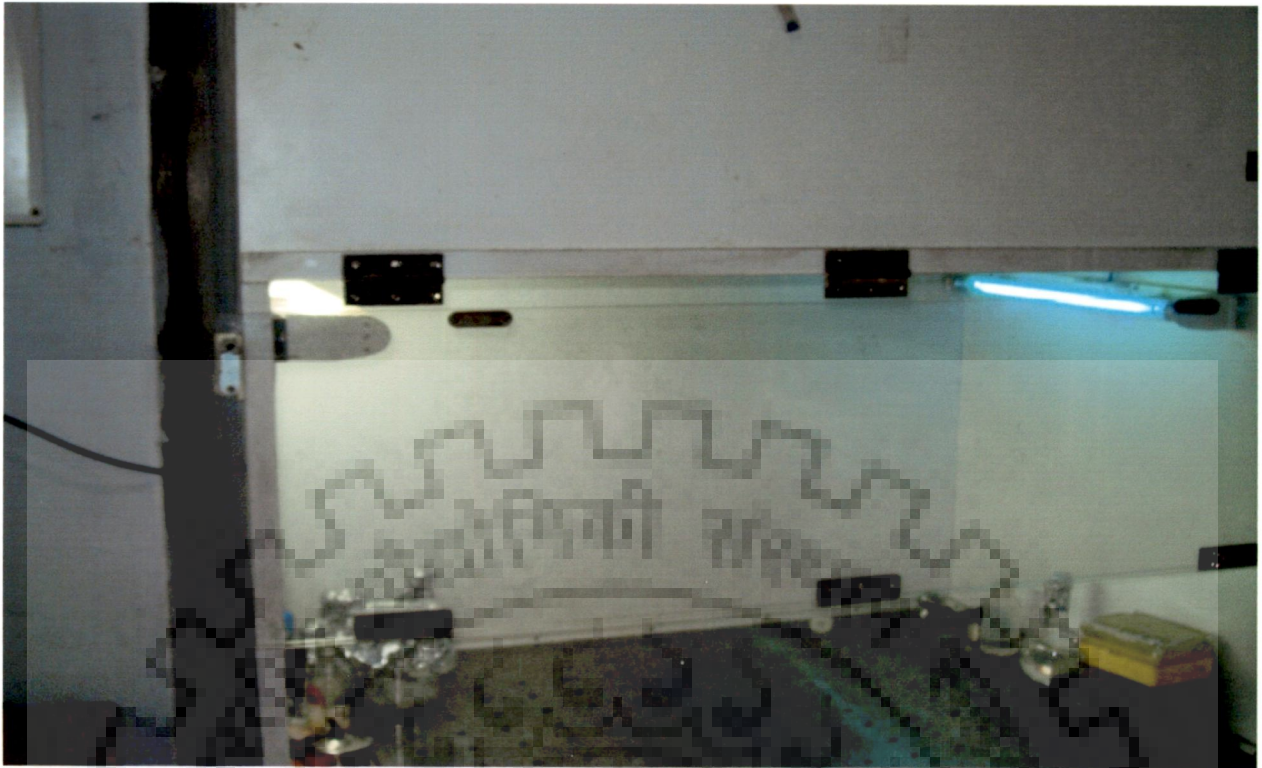


Figure 4.2 (a): Laminar airflow unit, Research Equipment



Figure 4.2 (b): Muffle furnace, Wishwani scientific, India

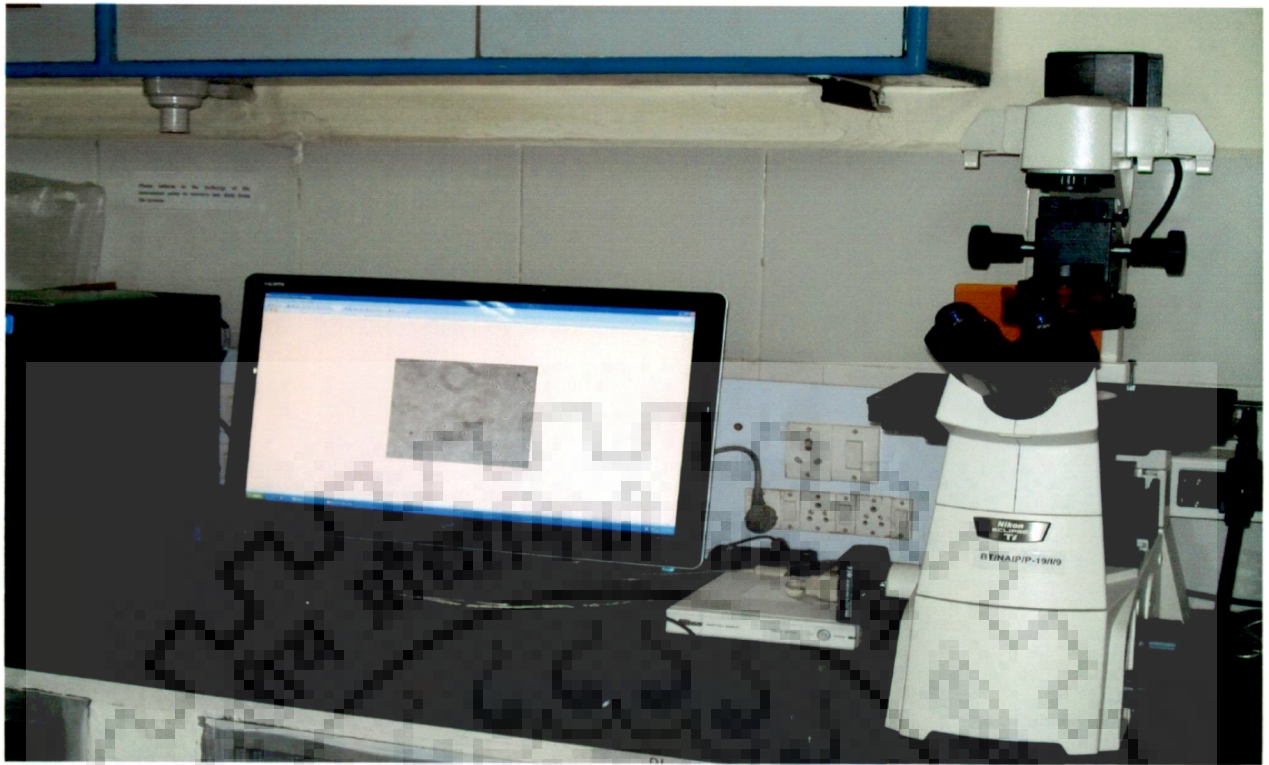


Figure 4.2 (c): Phase contrast microscope, Nikon ECILIPSE Ti



Figure 4.2 (d): Milli-Q water unit



Figure 4.2 (e): FTIR, Thermo model AVATAR 370



Figure 4.2 (f): Hot air oven, Thermotech TiC 4000

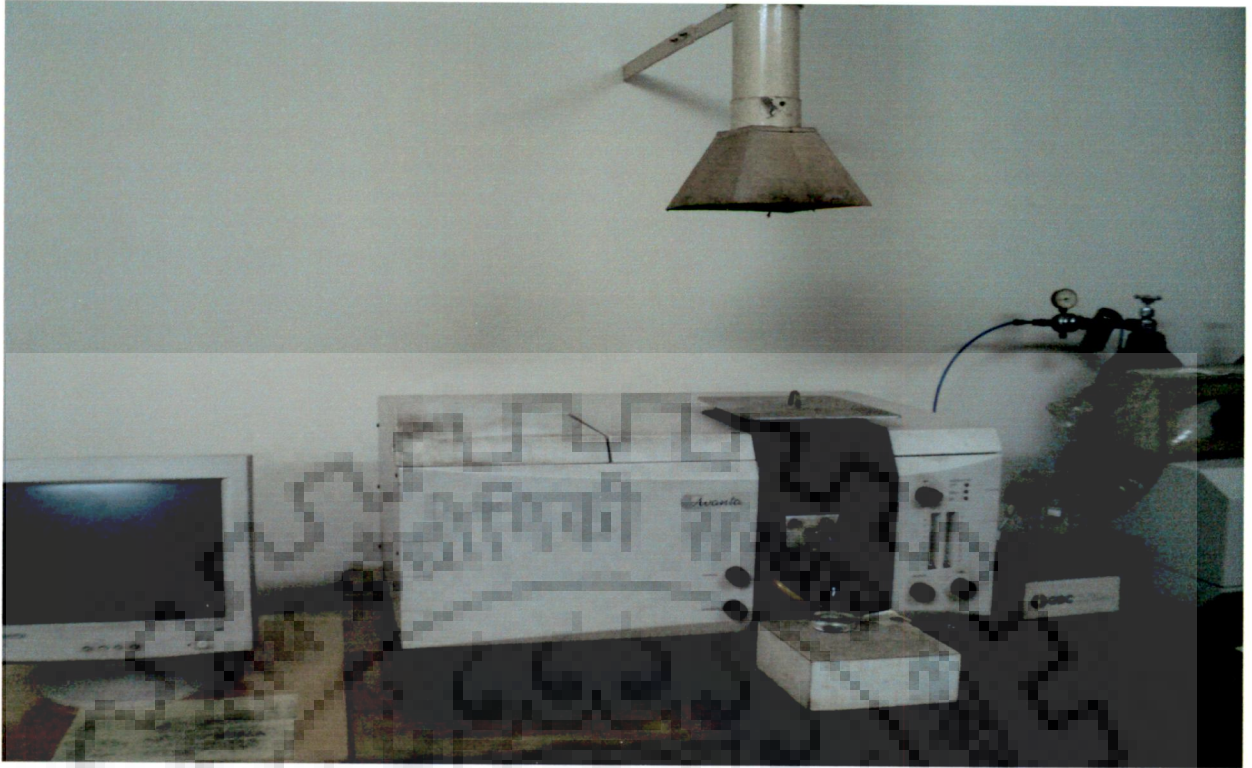


Figure 4.2 (i): AAS unit, GBC, Avanta



Figure 4.2 (j): Autoclave, Rivotek

Table 4.2 (a): Specification of auxiliary and analytical instruments used in the present work

<b>Name of equipment and its use</b>	<b>Model and make</b>	<b>Operating conditions</b>	<b>Remarks</b>
AAS (Detection of total Fe, Cu and Zn)	GBC, avanta, Australia	Air acetylene flame	Detection limit: Fe 0.05 mg/ l, Cu 0.025 mg/ l, Zn 0.008 mg/l
Elemental analyzer (Measurement of C, H, N and S content of biosorbent)	CE- 440 Elemental Analyzer, Eai Exter Analytical, Inc.	High temperature decomposition up to 1200 °C (1800 °C during decomposition) for analytical accuracy	Required sample volume <1 mg to 1 g depending on sample composition
FTIR spectra (Spectra of various biosorbent)	Themo FTIR model AVATAR 370 CSI coupled with EZOMNIC software (version 6.2)	KBR plate method, 10 mg of dried sample was dispersed in 100 mg of spectroscopic grade	-
Scanning electron microscope (SEM)	Quanta, FEI 200 F	Voltage requirement: maximum 30 kV, Resolution 6 nm wavelength and 4 nm wavelength in HV and VP	Magnification range: 10 X to 500000 X
Surface area analyzer (analyses surface area and porosity)	Micrometrics, model ASAP 2010	Liquid nitrogen is used as cold bath at ~77 K	Brunauer – Emmette- Teller (BET) method



### **Concluding remark of the section 4.2**

Present investigation was successfully accomplished by utilizing various electrical and analytical equipment. It is believed that the equipment used in the present work provided the best and accurate results in all batch and continuous studies.





# **RESULTS AND DISCUSSION**

**RESULTS AND DISCUSSION**

---

**5.0. INTRODUCTION**

This chapter covers the interpretation and discussion of results of present investigation. Studies incorporated in this chapter have been divided into five sections namely 5.1, 5.2, 5.3, 5.4, 5.5 and 5.6.

Section 5.1: Characterization of biosorbents

Section 5.2: Biosorption of Zn (II) ion from pure zinc solution and in presence of copper and iron in batch studies. This section also includes optimization of various physical process parameters.

Section 5.3 Biosorption of Zn (II), total Fe (II, III) and Cu (II) in synthetic simulated wastewater and real wastewater in batch studies.

Section 5.4: Isolation, purification and growth studies of zinc resistant microbial strain.

Section 5.5: Simultaneous biosorption and bioaccumulation (SBB) of Zn (II) ion in liquid phase in batch reactor

Section 5.6 Continuous column study using real industrial wastewater

The calibration curve and data have been shown in annexure A-1, A-2 and in A-3, respectively. The experimental setup and detail program of experimentation have been provided in chapter 3 and chapter 4, respectively. Biosorption of Zn (II) ion alone and also in presence of other associated metal ions in liquid phase in batch studies have been studied on selected biosorbents, living microbial cells and on immobilized microbial cells using synthetic simulated wastewater and real wastewater. The continuous column studies were also performed to study biosorption and bioaccumulation of zinc alone and also in presence of other associated metal ions like total Fe (II, III) and Cu (II) on surfaces of biosorbents and on immobilized microbial cells from synthetic simulated wastewater and real wastewater. The compositions of synthetic simulated wastewater and real wastewater have been given in table 3.5 (a) and table 3.5 (b), respectively. Calibration curves have been provided in annexure A – 1.

## 5.1 Characterization of biosorbents

In the present work, following adsorbent have been selected based on literature review (table 5.2.1, table 5.2.2, table 5.2.3 and table 5.2.4): *Cedrus deodara* sawdust (CDS), orange fruit waste, pine apple peel powder, jack fruit peel powder, eucalyptus bark sawdust, eucalyptus leaf powder, mango bark sawdust, egg shell and membrane, and *Zinc sequestering bacterium* VMSCM accession no. HQ108109 (dead cells).

### 5.1.1 Physico-chemical analysis

Physico-chemical analysis of selected biosorbents was performed to elucidate the elemental composition, surface texture, surface chemistry and High Heating Value (HHV). Table 5.1, figures 5.1 (a) to 5.1 (h) and figures 5.1 (i) to 5.2 (p) represent the physico chemical properties, surface texture and surface chemistry of selected biosorbents, respectively.

Table 5.1 Physico-chemical properties of various biomasses

Biosorbent	Elemental analysis (%)	Proximate analysis (%)	BET surface area (m <sup>2</sup> /g)	Pore volume (m <sup>3</sup> /g)	Bulk density	High heating value (kJg <sup>-1</sup> )
<i>Cedrus deodara</i> sawdust	C: 48.84 H: 5.56 N: 0.00 S: 00 Others 45.60	Moisture: 44.00 Ash: 23.70 Volatile compounds: 4.30 Others: 28.00	24.55	0.0124	139.2	18.43
Orange fruit waste	C: 41.48 H: 12.19 N: 21.63 S: 0 Others: 24.70	Moisture: 3.40 Ash: 24.90 Volatile compounds: 59.90 Others: 11.80	12.835	0.0115	98.21	26.17
Pine apple fruit peel powder	C: 38.92 H: 5.5 N: 0.9 S: 0 Others: 54.68	Moisture: 4.60 Ash: 13.60 Volatile compounds: 69.60 Others: 12.20	15.90	0.008f0	103.61	19.87

Jack fruit peel powder	C: 40.21 H: 3.26 N: 1.11 S: 0 Others: 55.42	Moisture: 4.30 Ash: 9.90 Volatile compounds: 69.80 Others: 16.00	11.014	0.0055	54.61	16.29
Eucalyptus bark sawdust	C: 41.52 H: 3.50 N: 0.02 S: 0 Others: 54.96	Moisture: 4.60 Ash: 21.30 Volatile compounds: 35.00 Others: 39.10	28.37	0.0143	113.61	28.24
Eucalyptus leaf powder	C: 38.92 H: 5.92 N: 0.96 S: 0 Others: 54.2	Moisture: 4.40 Ash: 4.10 Volatile compounds: 67.84 Others: 23.66	16.39	0.0083	108.91	20.4
Egg shell powder	C: 20.83 H: 1.6 N: 2.33 S: 0 Others: 75.24	Moisture: 7.78 Ash: 4.79 Volatile compounds: 81.40 Others: 6.03	8.8	0.0044	22.12	13.61
Mango bark powder	C: 48.2 H: 4.99 N: 16.3 S: 0 Others: 30.51	Moisture: 7.88 Ash: 47.37 Volatile compounds: 21.7 Others: 23.05	5.65	0.0028	113.21	16.22
Zinc sequestering bacterium VMSDCM Accession no. HQ108019	C: 13.21 H: 16.88 N: 44.61 S: 21.55 Others: 3.75	Moisture: 26.11 Ash: 13.21 Volatile compounds: 29.11 Others: 31.57	16.32	11.18	96.32	28.28

Figure 5.1 (a) represents the scanning electron micrograph of *Cedrus deodara* sawdust. It became apparent from figure 5.1 (a) that the surface texture or topology of CDS that the biosorbent surface is highly mesoporous, rough and heterogeneous in nature consisting of protrusions. The protrusions seemed to be elongated deeply inside surface of biosorbent with

deep void space, which in turn lead to heterogeneous and rough surface texture. The roughness of surface indicates the high surface area meant for metal ion adherence (Mishra et al. 2011). The SEM micrograph was analyzed at 15.0 KV at 1000 times magnification.

Before SEM analysis, the samples were coated with gold followed by degassing of the sample. After degassing, the samples were placed inside the voltage chamber followed by the generation of vacuum inside the chamber. Six samples at a time were placed inside the chamber and for every sample analysis, the sample heads were rotated at 60<sup>0</sup> angle.

Figure 5.1 (b) represents the scanning electron micrograph of orange peel sawdust. It became evident from figure 5.1 (b) that the surface of biosorbents was quite porous and heterogeneous. Additionally, several protrusions seemed to elongate inside the matrix of biomass (Ahmad et al. 2009). The SEM micrograph was analyzed at 1000 times magnification. Before SEM analysis, the samples were coated with gold followed by degassing of the sample. After degassing, the samples were placed inside the voltage chamber followed by the generation of vacuum inside the chamber. Six samples at a time were placed inside the chamber and for every sample analysis, the sample heads were rotated at 60<sup>0</sup> angle.

Figure 5.1 (c) represents the scanning electron micrograph of pine apple peel powder. It became evident from figure 5.1 (c) that surface of pineapple peel waste biomass was quite rough, heterogeneous and porous in nature. The rough and heterogeneous surface of the Pineapple peel waste biomass indicated the presence of tremendous surface area meant for the biosorption of metal ion in liquid phase.

The SEM micrograph was analyzed 1000 times magnification. Before SEM analysis, the samples were coated with gold followed by degassing of the sample. After degassing, the samples were placed inside the voltage chamber followed by the generation of vacuum inside the chamber. Six samples at a time were placed inside the chamber and for every sample analysis, the sample heads were rotated at 60<sup>0</sup> angle.

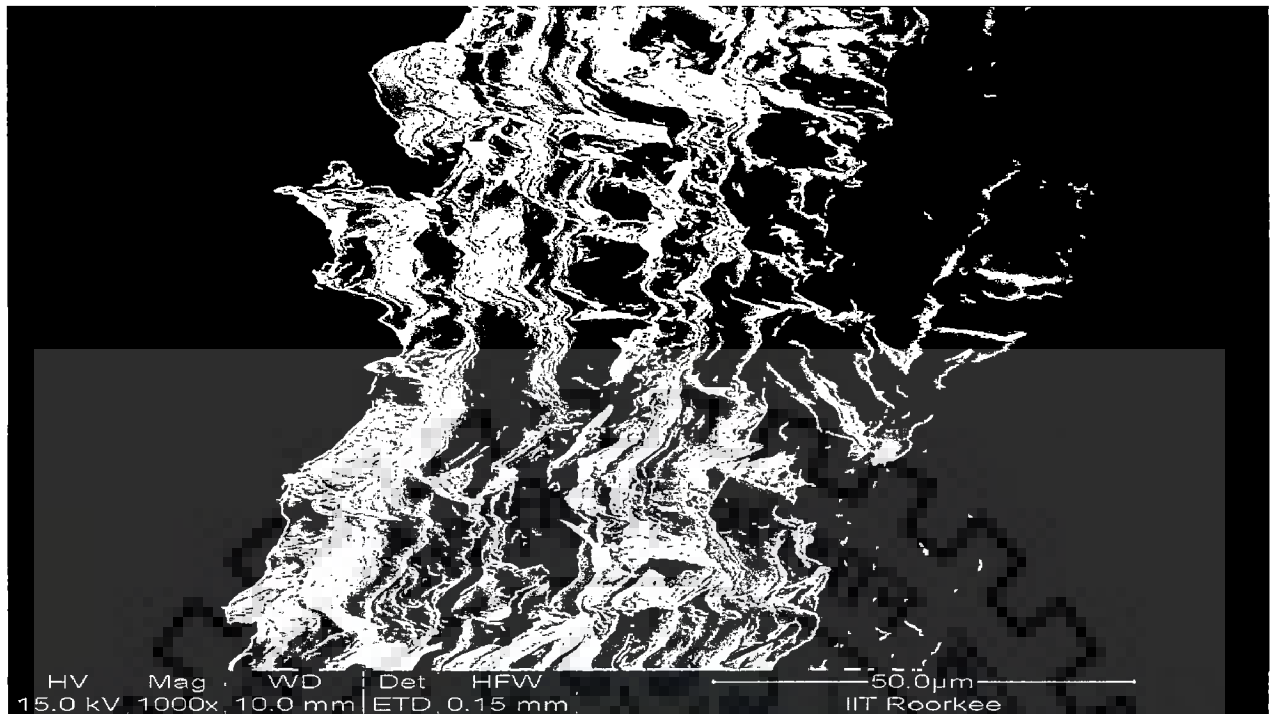


Figure 5.1 (a): SEM photograph of *Cedrus deodara* sawdust (CDS) before adsorption

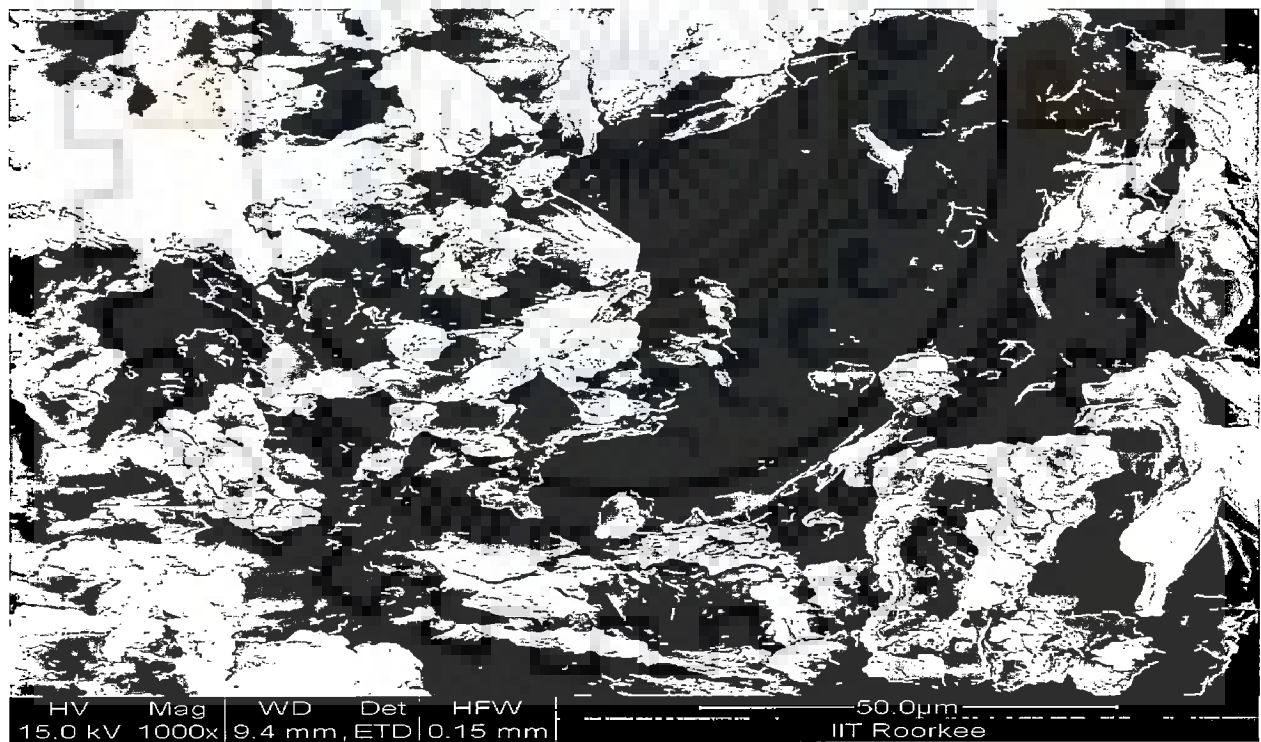


Figure 5.1 (b): SEM photograph of Orange waste biomass before adsorption

Figure 5.1 (d) represents the scanning electron micrograph of eucalyptus bark sawdust. It became obvious from figure 5.1 (d) that the surface of eucalyptus bark sawdust was quite porous, rough and heterogeneous with tremendous number of protrusions.

These protrusions elongate inside the matrix of the biomass. The SEM micrograph was analyzed at 1000 times magnification. Before SEM analysis, the samples were coated with gold followed by degassing of the sample. After degassing, the samples were placed inside the voltage chamber followed by the generation of vacuum inside the chamber.

Six samples at a time were placed inside the chamber and for every sample analysis, the sample heads were rotated at  $60^{\circ}$  angle. Figure 5.1 (e) represents the scanning electron micrograph of eucalyptus leaf powder (ELP). It became obvious from figure 5.1 (e) that the surface of eucalyptus leaf powder was quite porous, rough and heterogeneous with tremendous number of protrusions. These protrusions elongate inside the matrix of the biomass.

It can be easily pointed out that surface of ELP was highly porous (mesoporous) and heterogeneous. High porosity of ELP provided immense rise in biosorption of Zn (II) ion on to biosorbent surface. The SEM micrograph was analyzed at 1000 times magnification.

Before SEM analysis, the samples were coated with gold followed by degassing of the sample. After degassing, the samples were placed inside the voltage chamber followed by the generation of vacuum inside the chamber. Six samples at a time were placed inside the chamber and for every sample analysis, the sample heads were rotated at  $60^{\circ}$  angle.



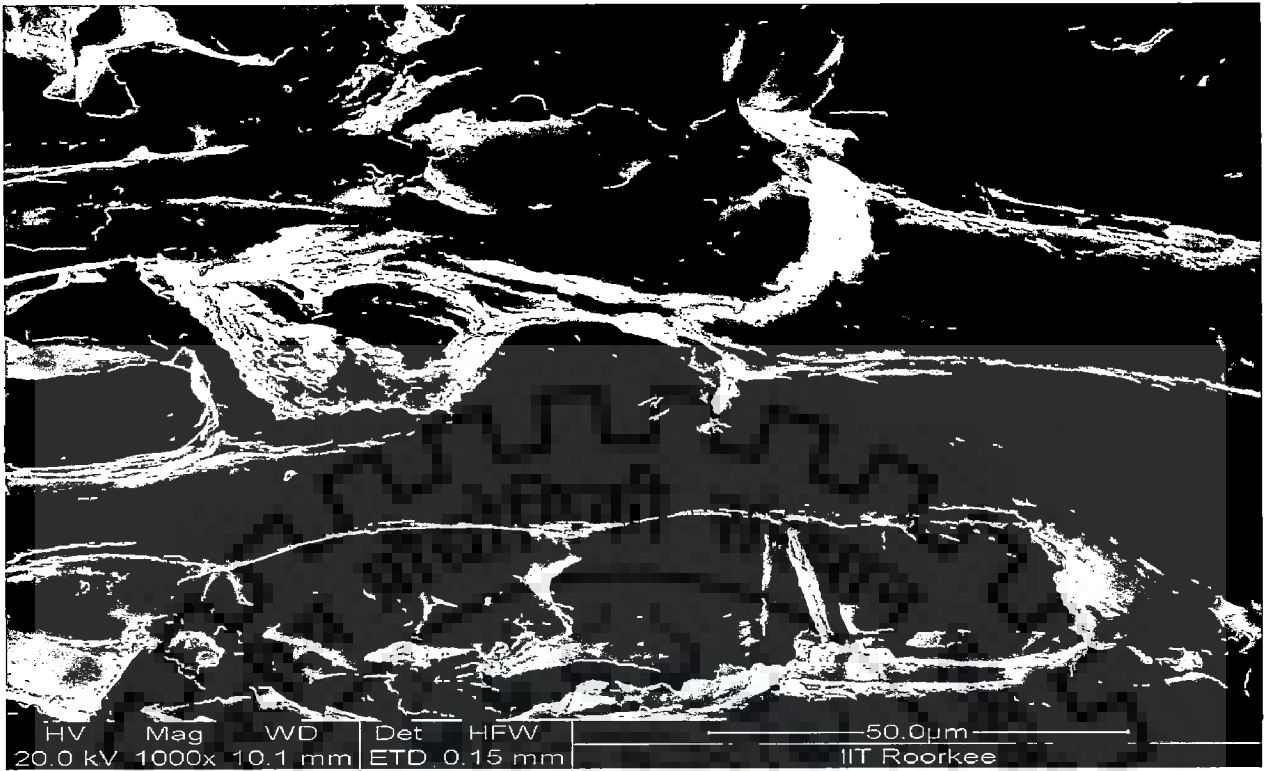


Figure 5.1 (c): SEM photograph of Pineapple peel waste biomass before adsorption

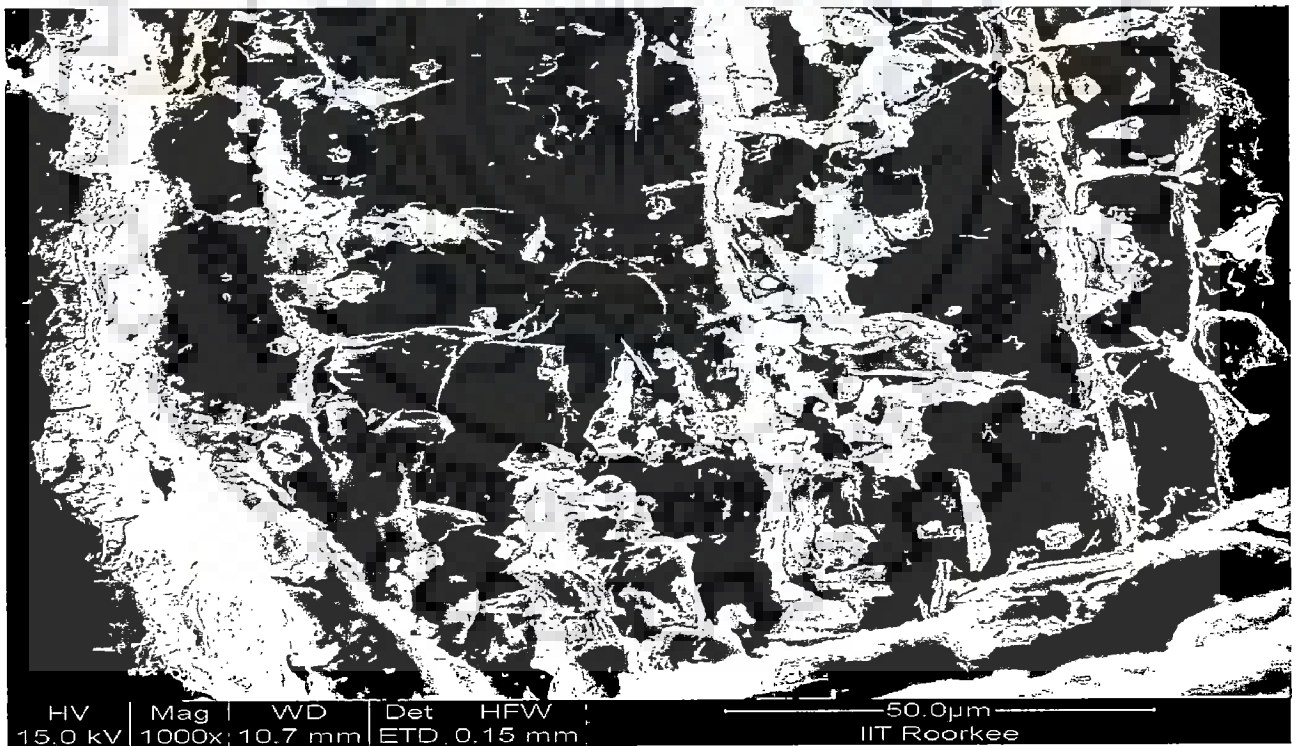


Figure 5.1 (d): SEM photograph of Eucalyptus bark sawdust before adsorption

Figure 5.1 (f) represents the scanning electron micrograph of mango bark powder. It became obvious from figure 5.1 (f) that the surface of mango bark powder was quite porous, rough and heterogeneous with tremendous number of protrusions. These protrusions elongate inside the matrix of the biomass. The SEM micrograph was analyzed at 1000 times magnification.

Before SEM analysis, the samples were coated with gold followed by degassing of the sample. After degassing, the samples were placed inside the voltage chamber followed by the generation of vacuum inside the chamber. Six samples at a time were placed inside the chamber and for every sample analysis, the sample heads were rotated at  $60^{\circ}$  angle.

Figure 5.1 (g) represents the scanning electron micrograph of eggshell waste. It became obvious from figure 5.1 (g) that the surface of eggshell waste was quite non-porous, crystalline and homogenous in nature.

These features of eggshell waste surface indicated towards less surface area meant for the biosorption of metal ions. The SEM micrograph was analyzed at 1000 times magnification.

Before SEM analysis, the samples were coated with gold followed by degassing of the sample. After degassing, the samples were placed inside the voltage chamber followed by the generation of vacuum inside the chamber. Six samples at a time were placed inside the chamber and for every sample analysis, the sample heads were rotated at  $60^{\circ}$  angle.

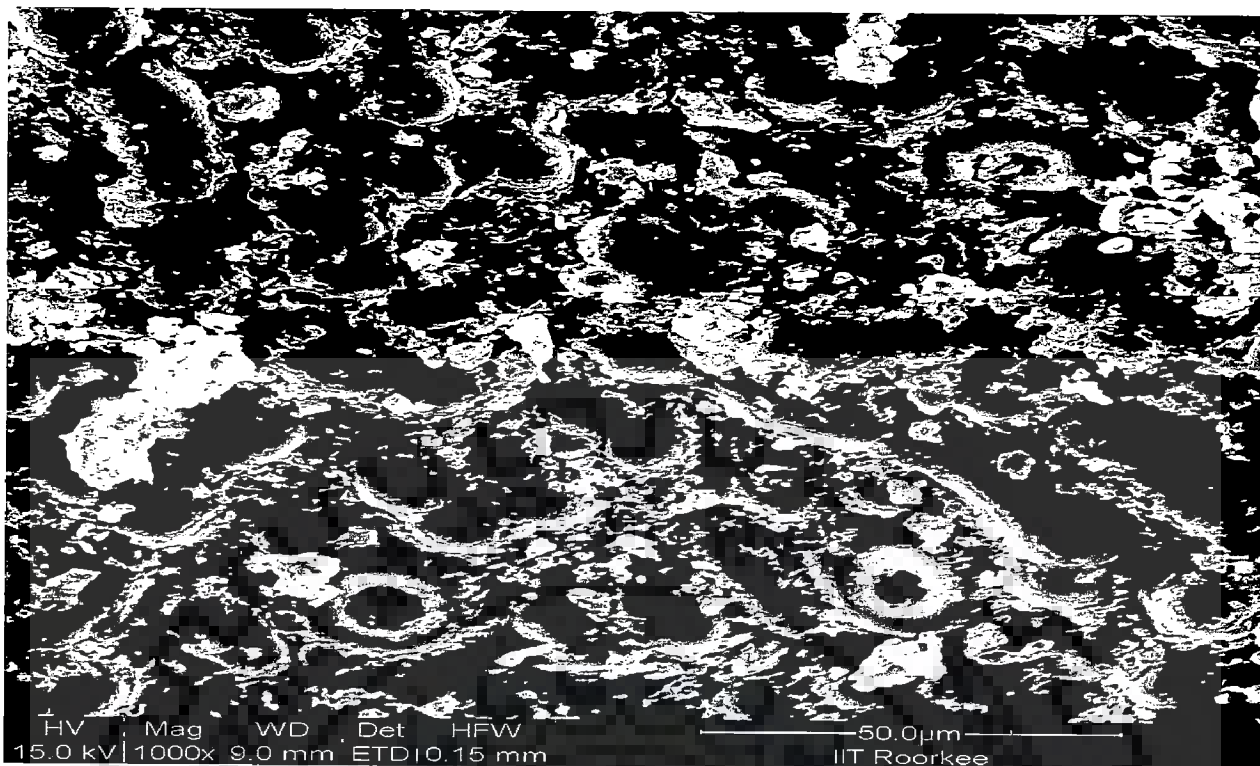


Figure 5.1(e): SEM photograph of Eucalyptus leaf powder before adsorption

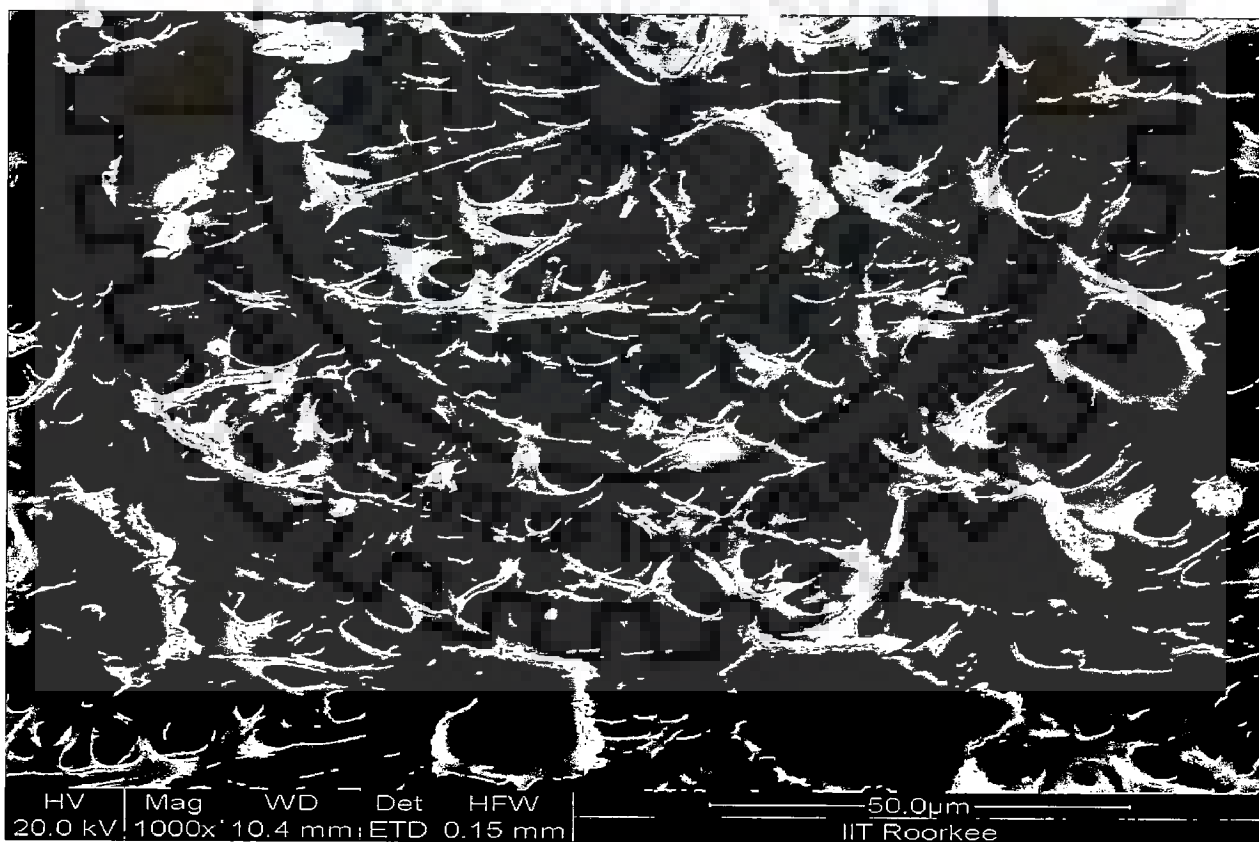


Figure 5.1 (f): SEM photograph of Mango bark powder before adsorption

Figure 5.1 (h) represents the scanning electron micrograph of Jackfruit peel. It became obvious from figure 5.1 (h) that the surface of Jackfruit peel was quite porous, rough and heterogeneous with tremendous number of protrusions. These protrusions elongate inside the matrix of the biomass.

The SEM micrograph was analyzed at 1000 times magnification. Before SEM analysis, the samples were coated with gold followed by degassing of the sample. After degassing, the samples were placed inside the voltage chamber followed by the generation of vacuum inside the chamber. Six samples at a time were placed inside the chamber and for every sample analysis, the sample heads were rotated at  $60^{\circ}$  angle.



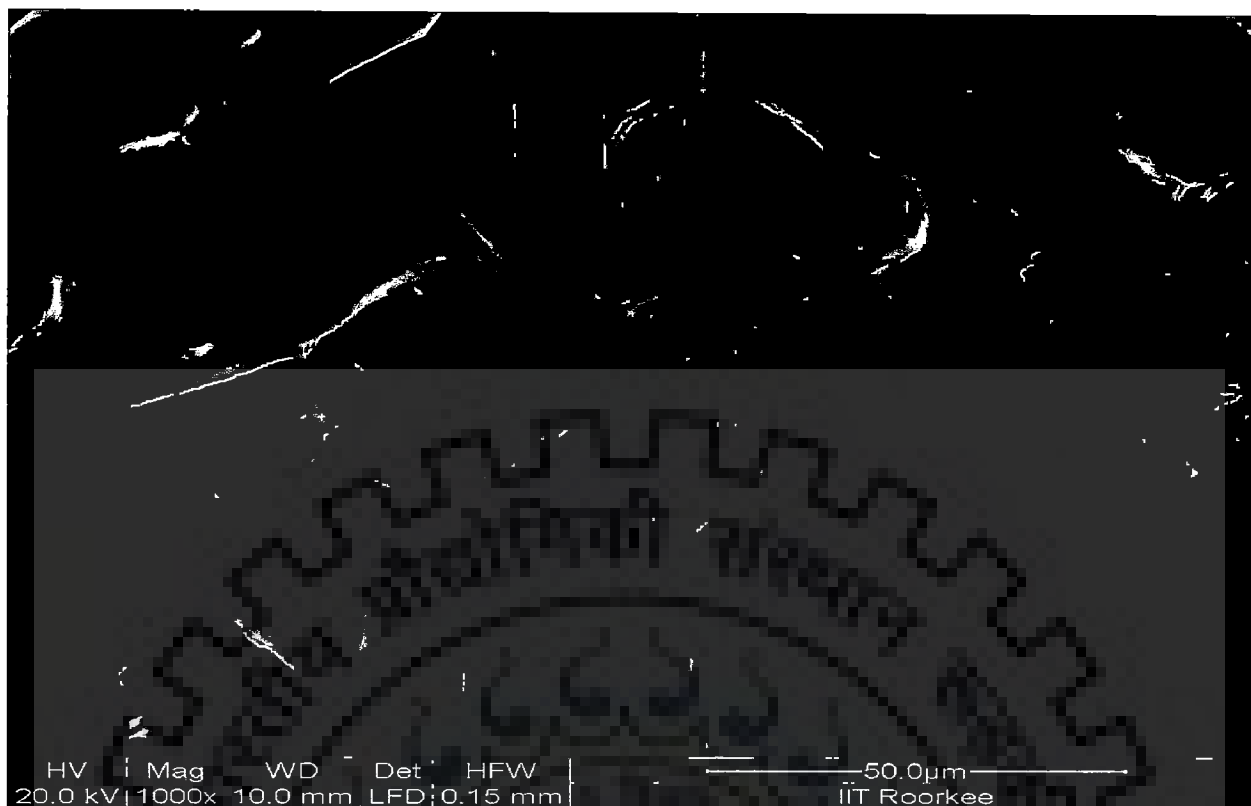


Figure 5.1 (g): SEM photograph of Eggshell waste before adsorption

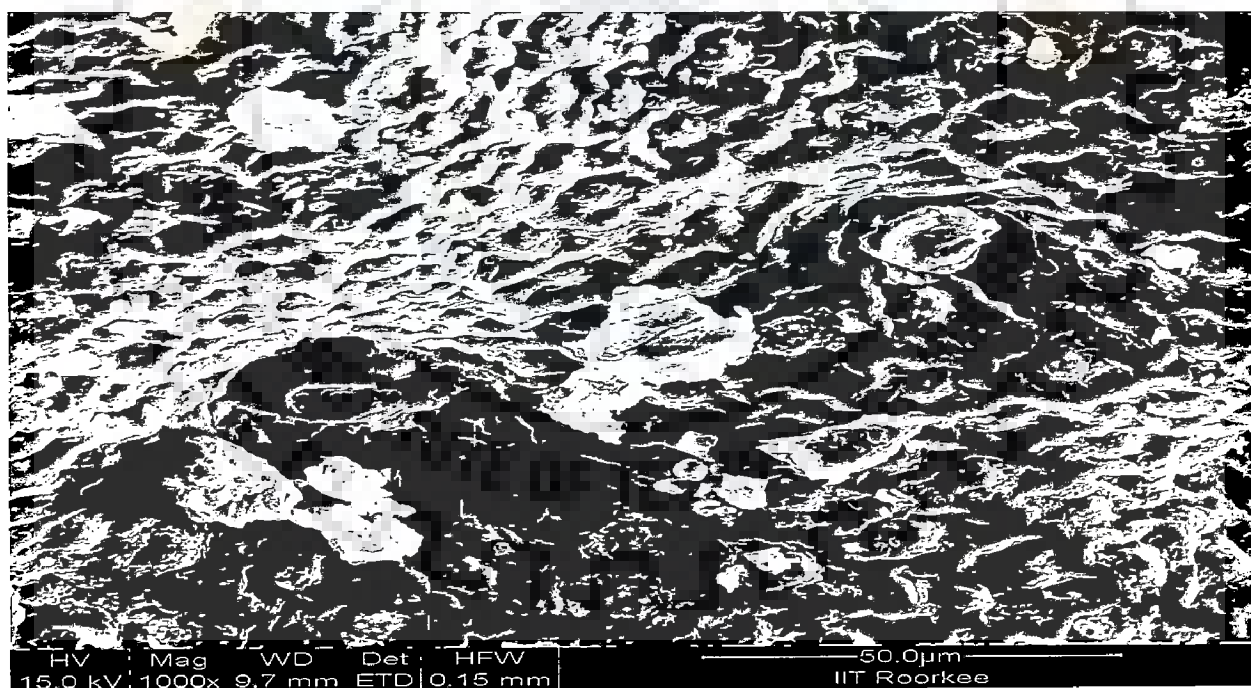


Figure 5.1 (h): SEM photograph of Jackfruit peel before adsorption

Figure 5.1 (i) to 5.1 (p) represent the FTIR spectrum of various metal unloaded biomasses.

Figure 5.1 (i) and table 5.1 (i) represents detailed analysis CD sawdust (CDS) before the sorption of metal ion. The samples for FTIR analysis of CDS was prepared by making 1% pellet of sample with photometric grade potassium bromide (KBR). The pellet was placed in the path of infrared ray for a total cumulative 32 scans. Before placing the pellet in the path of infrared ray, the background was collected for continuously for every 32 cumulative scans. The collected background was used as reference for sample FTIR analysis. The range of wave number was kept between  $4000\text{ cm}^{-1}$  –  $400\text{ cm}^{-1}$ . The spectrum was extrapolated between wave number and % transmittance.

It became evident from figure 5.1 (i) that the surface of metal unloaded CDS was quite enriched in peaks obtained between  $4000\text{ cm}^{-1}$  –  $400\text{ cm}^{-1}$ . The spectrum did not indicate any vibration for moisture in the sample, since the curve was smooth and the peaks obtained were sharp. The detailed analysis of CDS has been shown in table 5.1(i).

Table 5.1 (i): Detailed study of CDS sawdust before adsorption

Metal unloaded biomass (Wave numbers $\text{cm}^{-1}$ )	Functional group	Reference
3500 – 3000	Hydroxyl and amide groups	Mishra et al., 2011
2925.22	Methyl group asymmetric stretching	Mishra et al., 2011
1728.04 – 1450.17	C= C aromatic ring and C= H stretching	Mishra et al., 2011
1428.48 – 1061.97	C= C aromatic ring and C-O stretching	Mishra et al., 2011
878.38 – 476.06	C- H stretch with outward deformation and miscellaneous oxides and symmetrical vibrations of S-O group	Mishra et al., 2011

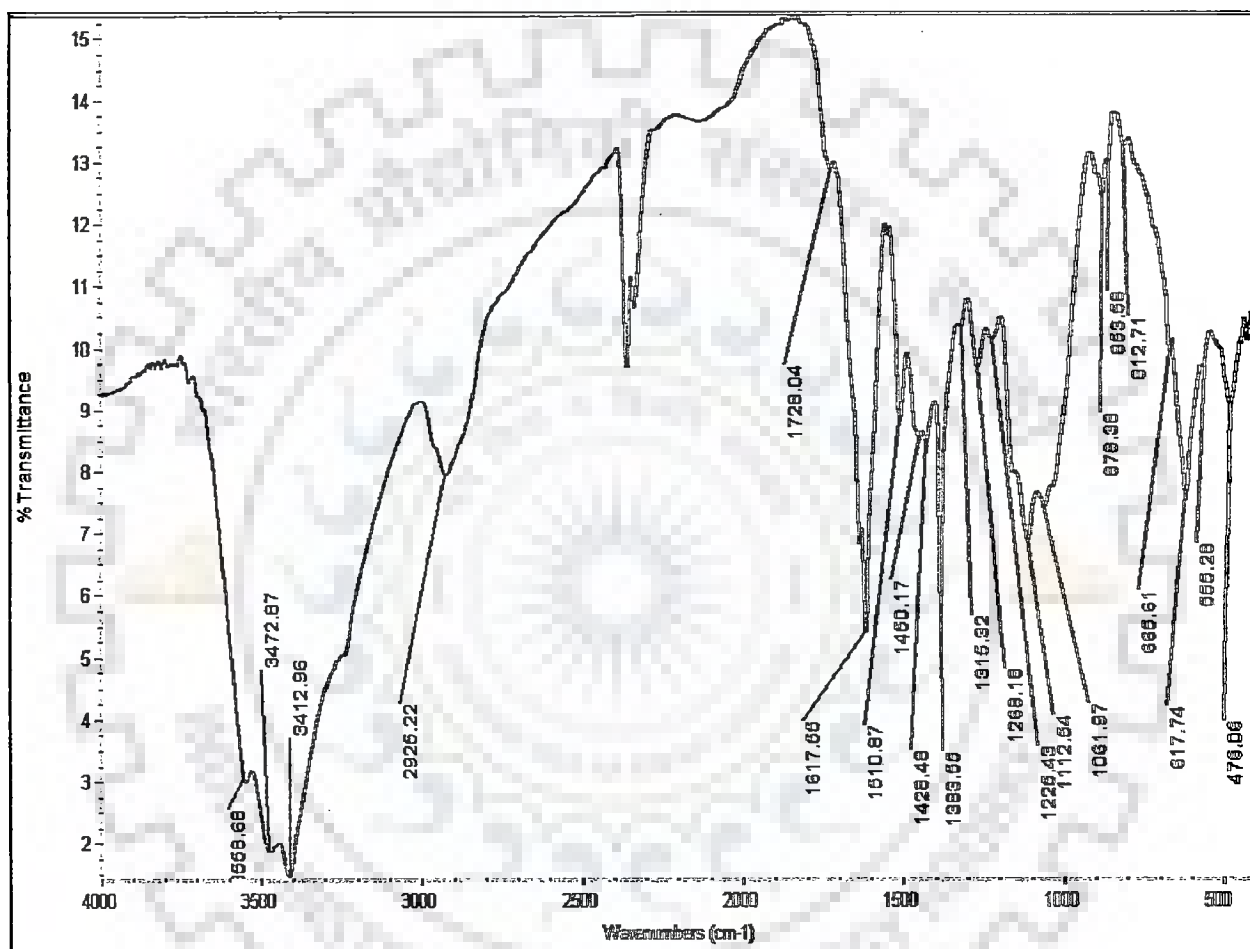


Figure 5.1 (i): FTIR spectrum of CDS sawdust before adsorption

It became evident from figure 5.1 (i) and table 5.1 (i) that the functional groups, which contribute significantly to metal ion binding on biomass surface like carboxyl, methyl, hydroxyl, carbonyl and methyl were present in sufficient amount on metal unloaded CDS sawdust surface. In the extrapolation of the curve, no smoothing factor was used. The lines of spectrum were drawn at regular interval of  $500\text{ cm}^{-1}$  wave number. The lines of the spectrum were interpreted as the function of their respective wave numbers.

Figure 5.1(j) and table 5.1 (j) represent the detailed study of orange waste. The samples for FTIR analysis of orange waste was prepared by making 1% pellet of sample with photometric grade potassium bromide (KBR). The pellet was placed in the path of infrared ray for a total cumulative 32 scans. Before placing the pellet in the path of infrared ray, the background was collected continuously for every 32 cumulative scans. The collected background was used as reference for sample FTIR analysis.

The range of wave number was kept between  $4000\text{ cm}^{-1} - 400\text{ cm}^{-1}$ . The spectrum was extrapolated between wave number and % transmittance. It became evident from figure 5.1 (j) that the surface of metal unloaded orange waste was quite enriched in peaks obtained between  $4000\text{ cm}^{-1} - 400\text{ cm}^{-1}$ . The spectrum did not indicate any vibration for moisture in the sample, since the curve was smooth and the peaks obtained were sharp. The detailed analysis of orange waste has been shown in table 5.1(j).

Table 5.1 (j): Detailed study of orange waste before adsorption

Wave number ( $\text{cm}^{-1}$ )	Functional group	Reference
3100 – 3700	Free and hydrogen bonded hydroxyl group, Si – OH (Siol group), Primary amide group (-CONH <sub>2</sub> )	Srivastava et al., 2007, Nuhoglu and Malkoc 2009
~ 2925	CH <sub>3</sub> – OH stretching	Basha et al., 2009
1450.17-1728.04	C= C aromatic ring and C= H stretching	Mishra et al., 2011



1600 -1800	-CH stretching	Srivastava et al., 2007
1300 - 1400	conjugated hydrocarbon groups, aromatic CH, carboxyl groups, carboxyl and carbonate structure	Srivastava et al., 2007
1000 -1400	C= C aromatic ring and C-O stretching	Mishra et al., 2011
~1630-1700	C=O stretching from lactones and amide I band	Basha et al., 2009
1050 - 590	C=O stretching, aromatic -CH stretching, -C-C group, amine group (-NH <sub>2</sub> ) group	Nuhoglu and Malkoc 2009

It is clear from figure 5.1 (j) and table 5.1 (j) that the negatively charged groups such as carbonyl, aromatic ring stretching, amide, hydroxyl and carboxyl stretching are present on the surface of orange waste. These groups contribute significantly to the binding of metal ion surface on biomass surface.

In the extrapolation of the curve, no smoothing factor was used. The lines of spectrum were drawn at regular interval of 500 cm<sup>-1</sup> wave number. The lines of the spectrum were interpreted as the function of their respective wave numbers.

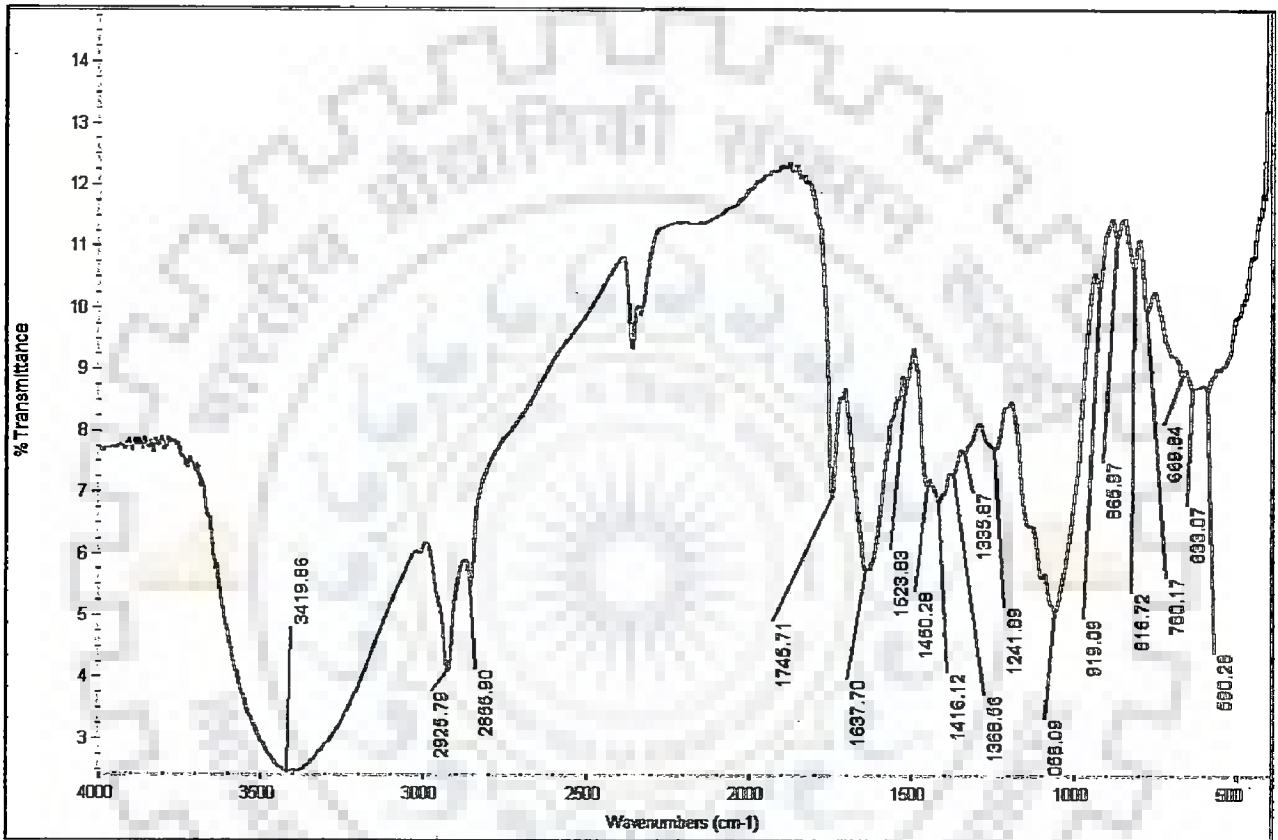


Figure 5.1 (j): FTIR spectrum of orange waste before adsorption

Figure 5.1(k) and table 5.1 (k) represent the detailed study of pineapple peel powder. The samples for FTIR analysis of pineapple peel was prepared by making 1% pellet of sample with photometric grade potassium bromide (KBR). The pellet was placed in the path of infrared ray for a total cumulative 32 scans. The range of wave number was kept between  $4000\text{ cm}^{-1} - 400\text{ cm}^{-1}$ . The spectrum was extrapolated between wave number and % transmittance.

It became evident from figure 5.1 (k) that the surface of metal unloaded pineapple peel was quite enriched in peaks obtained between  $4000\text{ cm}^{-1} - 400\text{ cm}^{-1}$ . The spectrum did not indicate any vibration for moisture in the sample, since the curve was smooth and the peaks obtained were sharp. The detailed analysis of orange waste has been shown in table 5.1(k).

Table 5.1 (k): Detailed study of pineapple fruit peel powder before adsorption

Wave number ( $\text{cm}^{-1}$ )	Functional group	Reference
3100 – 3500	Free and hydrogen bonded hydroxyl group, Si – OH (Siol group), Primary amide group (-CONH <sub>2</sub> )	Srivastava et al., 2007, Nuhoglu and Malkoc 2009
1450.17-1728.04	C= C aromatic ring and C= H stretching	Mishra et al., 2011
1000 -1400	C= C aromatic ring and C-O stretching	Mishra et al., 2011
~1630-1700	C=O stretching from lactones and amide I band	Basha et al., 2009
1050 - 460	C=O stretching, aromatic –CH stretching, -C-C group, amine group (-NH <sub>2</sub> ) group	Nuhoglu and Malkoc 2009

It is clear from figure 5.1 (k) and table 5.1 (k) that the negatively charged groups such as carbonyl, aromatic ring stretching, amide, hydroxyl and carboxyl stretching are present on the surface of pineapple fruit peel powder. These groups contribute significantly to the binding of metal ion surface on biomass surface.

In the extrapolation of the curve, no smoothing factor was used. The lines of spectrum were drawn at regular interval of  $500 \text{ cm}^{-1}$  wave number. The lines of the spectrum were interpreted as the function of their respective wave numbers.

Figure 5.1(l) and table 5.1.1 (l) represent the detailed study of eucalyptus leaf powder. The samples for FTIR analysis of eucalyptus leaf powder was prepared by making 1% pellet of sample with photometric grade potassium bromide (KBR). The pellet was placed in the path of infrared ray for a total cumulative 32 scans. The range of wave number was kept between  $4000 \text{ cm}^{-1} - 400 \text{ cm}^{-1}$ . The spectrum was extrapolated between wave number and % transmittance.

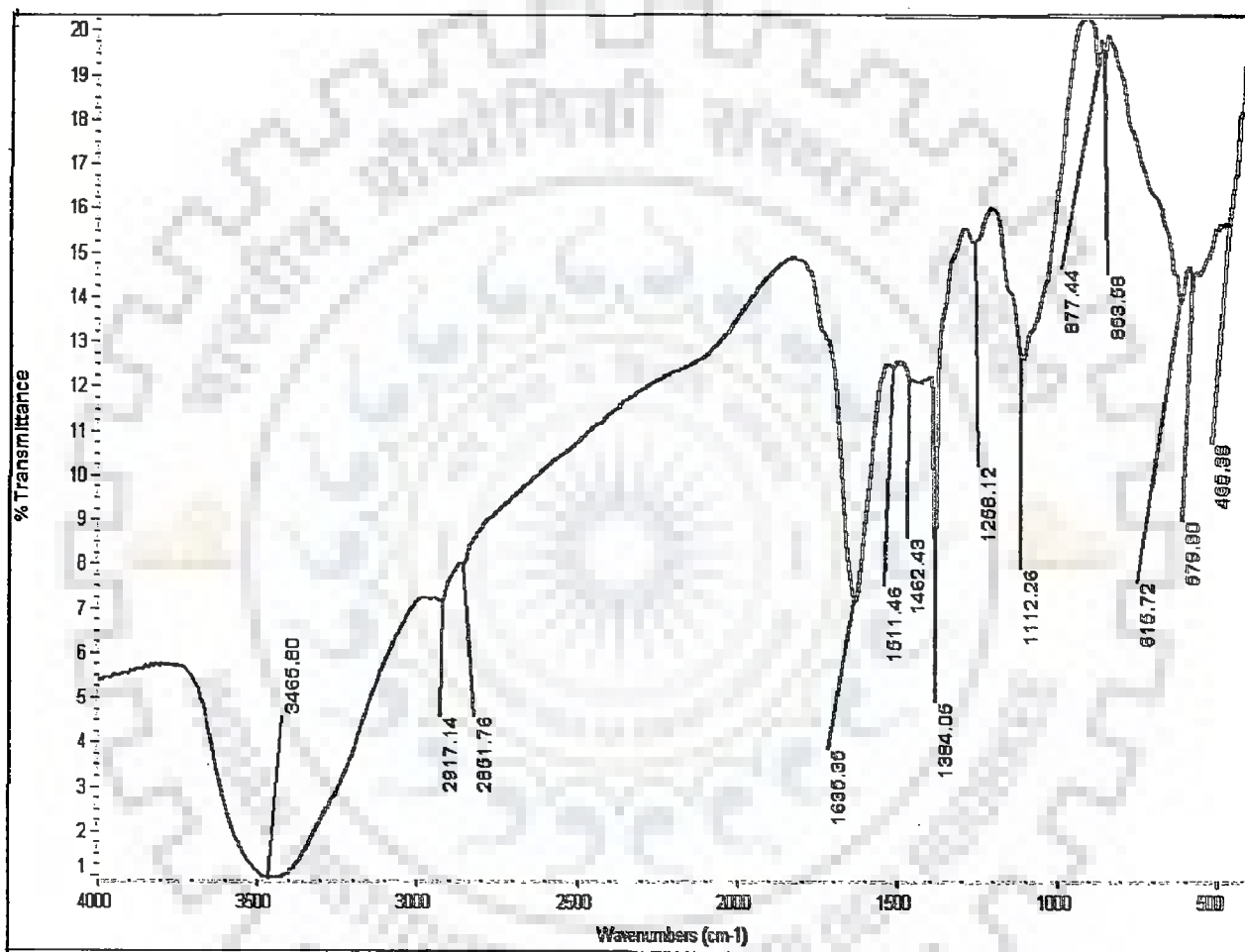


Figure 5.1 (k): FTIR spectrum of pineapple fruit peel powder before adsorption

It became evident from figure 5.1 (1) that the surface of metal unloaded eucalyptus leaf powder was quite enriched in peaks obtained between  $4000\text{ cm}^{-1}$  –  $400\text{ cm}^{-1}$ . The spectrum did not indicate any vibration for moisture in the sample, since the curve was smooth and the peaks obtained were sharp. The detailed analysis of orange waste has been shown in table 5.1(I).

Table 5.1 (I): Detailed study of eucalyptus leaf powder before adsorption

Wave number ( $\text{cm}^{-1}$ )	Functional group	Reference
3100 – 3500	Free and hydrogen bonded hydroxyl group, Si – OH (Siol group), Primary amide group (-CONH <sub>2</sub> )	Srivastava et al. 2007, Nuhoglu and Malkoc 2009
~ 2925	CH <sub>3</sub> – OH stretching	Basha et al., 2009
~1600	-CH stretching	Srivastava et al., 2007
1100	CO group	Srivastava et al., 2007
1300 – 1400	conjugated hydrocarbon groups, aromatic CH, carboxyl groups, carboxyl and carbonate structure	Srivastava et al., 2007
~1700 - 1630	C=O stretching from lactones and amide I band	Basha et al., 2009
1050 - 518	C=O stretching, aromatic –CH stretching, -C-C group, amine group (-NH <sub>2</sub> ) group	Nuhoglu and Malkoc 2009

It is clear from figure 5.1 (1) and table 5.1 (I) that the negatively charged groups such as carbonyl, aromatic ring stretching, amide, hydroxyl and carboxyl stretching are present on the surface of pineapple fruit peel powder. These groups contribute significantly to the binding of metal ion surface on biomass surface. In the extrapolation of the curve, no smoothing factor was used. The lines of spectrum were drawn at regular interval of  $500\text{ cm}^{-1}$  wave number. The lines of the spectrum were interpreted as the function of their respective wave numbers.

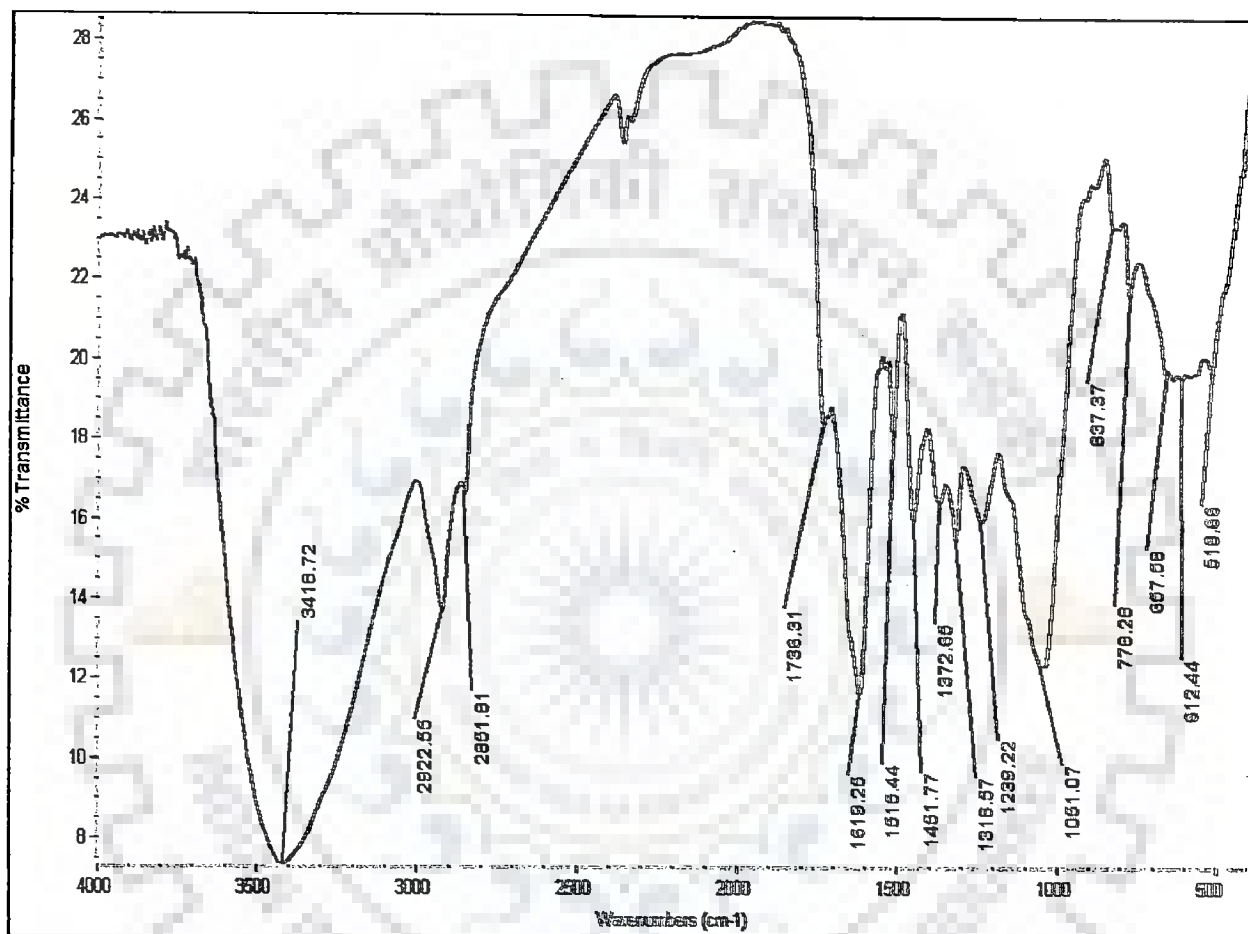


Figure 5.1 (I): FTIR spectrum of eucalyptus leaf powder before adsorption

Figure 5.1(m) and table 5.1 (m) represent the detailed study of mango bark powder. The samples for FTIR analysis of mango bark powder was prepared by making 1% pellet of sample with photometric grade potassium bromide (KBR). The pellet was placed in the path of infrared ray for a total cumulative 32 scans. The range of wave number was kept between  $4000\text{ cm}^{-1} - 400\text{ cm}^{-1}$ . The spectrum was extrapolated between wave number and % transmittance.

It became evident from figure 5.1 (m) that the surface of metal unloaded mango bark powder was quite enriched in peaks obtained between  $4000\text{ cm}^{-1} - 400\text{ cm}^{-1}$ . The spectrum did not indicate any vibration for moisture in the sample, since the curve was smooth and the peaks obtained were sharp. The detailed analysis of mango bark powder has been shown in table 5.1(m).

Table 5.1.1 (m): Detailed study of mango bark powder before adsorption

Wave number ( $\text{cm}^{-1}$ )	Functional group	Reference
3100 – 3500	Free and hydrogen bonded hydroxyl group, Si – OH (Siol group), Primary amide group (-CONH <sub>2</sub> )	Srivastava et al., 2007, Nuhoglu and Malkoc 2009
~ 2925	CH <sub>3</sub> – OH stretching	Basha et al., 2009
1600 -1800	-CH stretching	Srivastava et al., 2007
1300 – 1400	conjugated hydrocarbon groups, aromatic CH, carboxyl groups, carboxyl and carbonate structure	Srivastava et al., 2007
~1700 - 1630	C=O stretching from lactones and amide I band	Basha et al., 2009
1050 – 559.8	C=O stretching, aromatic –CH stretching, -C-C group, amine group (-NH <sub>2</sub> ) group	Nuhoglu and Malkoc 2009



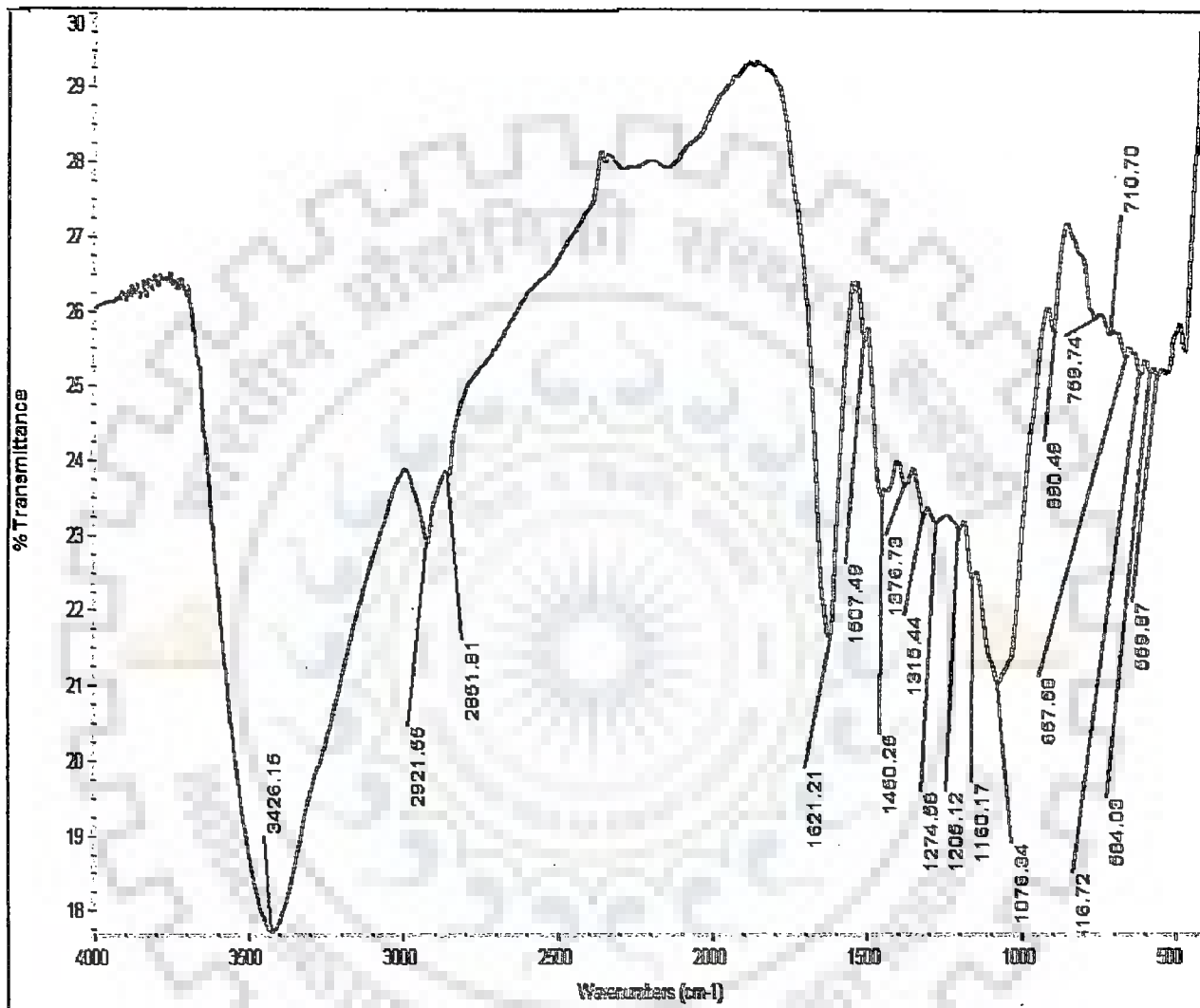


Figure 5.1 (m): FTIR spectrum of mango bark powder before adsorption

It is clear from figure 5.1 (m) and table 5.1 (m) that the negatively charged groups such as carbonyl, aromatic ring stretching, amide, hydroxyl and carboxyl stretching are present on the surface of mango bark powder. These groups contribute significantly to the binding of metal ion surface on biomass surface.

In the extrapolation of the curve, no smoothing factor was used. The lines of spectrum were drawn at regular interval of  $500\text{ cm}^{-1}$  wave number. The lines of the spectrum were interpreted as the function of their respective wave numbers.

Figure 5.1(n) and table 5.1 (n) represent the detailed study of eggshell powder. The samples for FTIR analysis of eggshell powder was prepared by making 1% pellet of sample with photometric grade potassium bromide (KBR). The pellet was placed in the path of infrared ray for a total cumulative 32 scans. The range of wave number was kept between  $4000\text{ cm}^{-1} - 400\text{ cm}^{-1}$ . The spectrum was extrapolated between wave number and % transmittance.

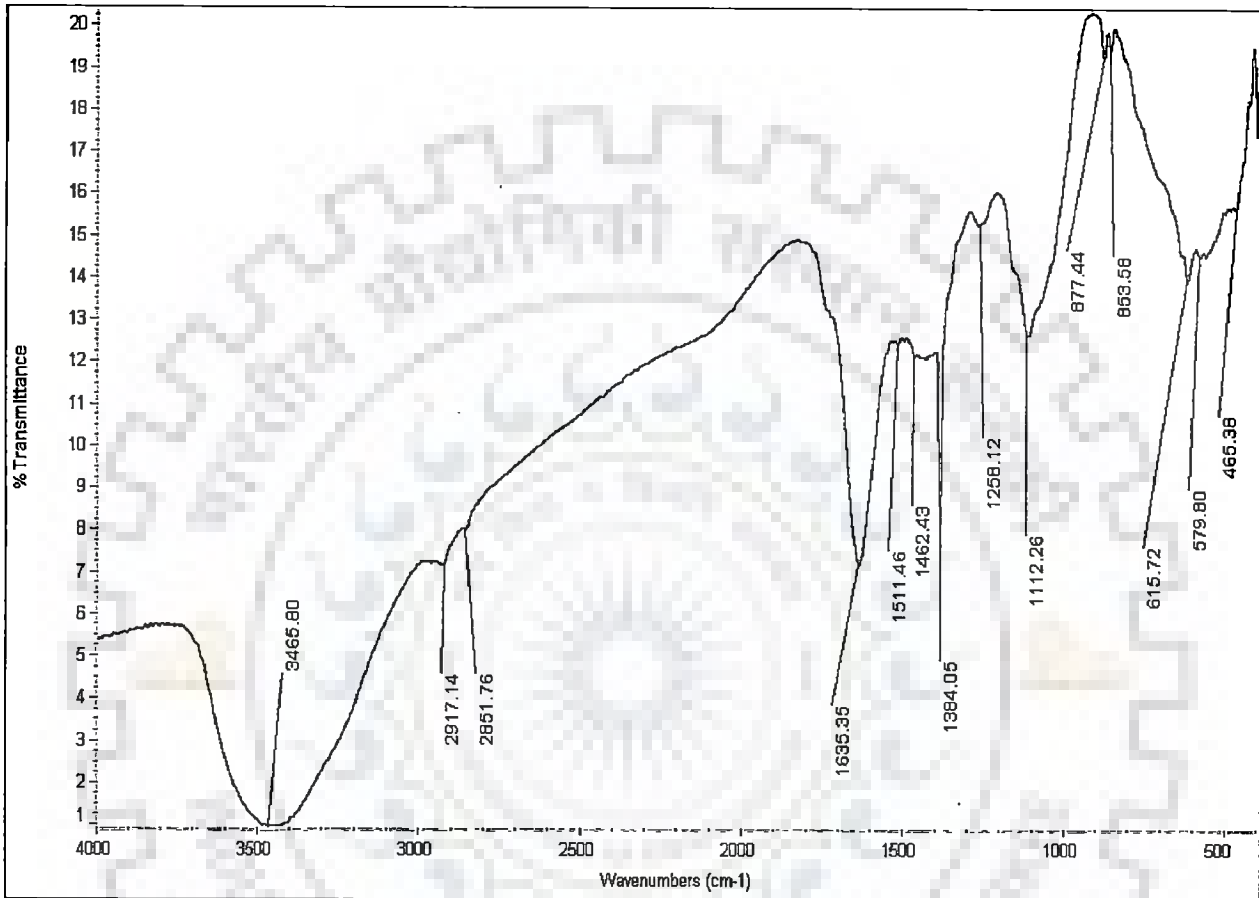


Figure 5.1 (n): FTIR spectrum eggshell powder before adsorption

It became evident from figure 5.1 (n) that the surface of metal unloaded eggshell powder was quite enriched in peaks obtained between  $4000\text{ cm}^{-1} - 400\text{ cm}^{-1}$ . The spectrum did not indicate any vibration for moisture in the sample, since the curve was smooth and the peaks obtained were sharp. The detailed analysis of eggshell powder has been shown in table 5.1(n). The samples for FTIR analysis of orange waste was prepared by making 1% pellet of sample with photometric grade potassium bromide (KBR). The pellet was placed in the path of infrared ray for a total cumulative 32 scans. The range of wave number was kept between  $4000\text{ cm}^{-1} - 400\text{ cm}^{-1}$ . The spectrum was extrapolated between wave number and % transmittance.

Table 5.1 (n): Detailed study of eggshell powder before adsorption

Wave number ( $\text{cm}^{-1}$ )	Functional group	Reference
3100 – 3500	Free and hydrogen bonded hydroxyl group, Si – OH (Siol group), Primary amide group (-CONH <sub>2</sub> )	Srivastava et al., 2007, Nuhoglu and Malkoc 2009
~1600	-CH stretching	Srivastava et al., 2007
1300 – 1400	conjugated hydrocarbon groups, aromatic CH, carboxyl groups, carboxyl and carbonate structure	Srivastava et al., 2007
1100	CO group	Srivastava et al., 2007
1050 - 460	C=O stretching, aromatic -CH stretching, -C-C group, amine group (-NH <sub>2</sub> ) group	Nuhoglu and Malkoc 2009

It is clear from figure 5.1 (n) and table 5.1 (n) that the negatively charged groups such as carbonyl, aromatic ring stretching, amide, hydroxyl and carboxyl stretching are present on

the surface of eggshell powder. These groups contribute significantly to the binding of metal ion surface on biomass surface.

In the extrapolation of the curve, no smoothing factor was used. The lines of spectrum were drawn at regular interval of  $500\text{ cm}^{-1}$  wave number. The lines of the spectrum were interpreted as the function of their respective wave numbers.

Figure 5.1(o) and table 5.1 (o) represent the detailed study of eucalyptus bark powder. The samples for FTIR analysis of eucalyptus bark powder was prepared by making 1% pellet of sample with photometric grade potassium bromide (KBR). The pellet was placed in the path of infrared ray for a total cumulative 32 scans. The range of wave number was kept between  $4000\text{ cm}^{-1} - 400\text{ cm}^{-1}$ . The spectrum was extrapolated between wave number and % transmittance.



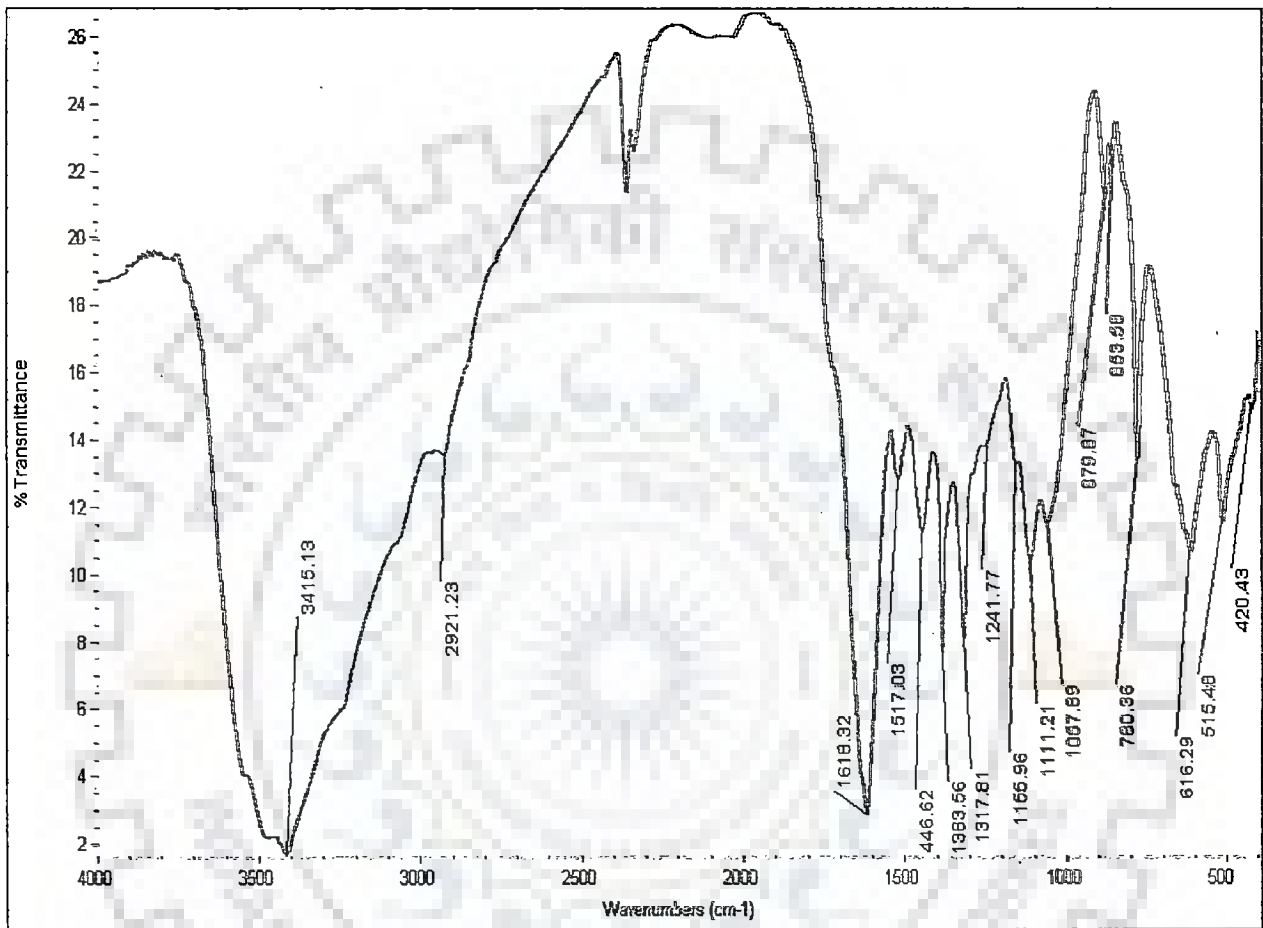


Figure 5.1 (o): FTIR spectrum of Eucalyptus bark sawdust before adsorption

It became evident from figure 5.1 (o) that the surface of metal unloaded Eucalyptus bark sawdust was quite enriched in peaks obtained between  $4000\text{ cm}^{-1} - 400\text{ cm}^{-1}$ . The spectrum did not indicate any vibration for moisture in the sample, since the curve was smooth and the peaks obtained were sharp. The detailed analysis of Eucalyptus bark sawdust has been shown in table 5.1(o).

The samples for FTIR analysis of Eucalyptus bark sawdust was prepared by making 1% pellet of sample with photometric grade potassium bromide (KBR). The pellet was placed in the path of infrared ray for a total cumulative 32 scans. The range of wave number was kept between  $4000\text{ cm}^{-1} - 400\text{ cm}^{-1}$ . The spectrum was extrapolated between wave number and % transmittance.

Table 5.1 (o): Detailed study of Eucalyptus bark sawdust before adsorption

Wave number ( $\text{cm}^{-1}$ )	Functional group	Reference
3100 – 3500	Free and hydrogen bonded hydroxyl group, Si – OH (Siol group), Primary amide group (-CONH <sub>2</sub> )	Srivastava et al., 2007, Nuhoglu and Malkoc 2009
~1600	-CH stretching	Srivastava et al., 2007
~1100	CO group	Srivastava et al., 2007
1300 – 1400	conjugated hydrocarbon groups, aromatic CH, carboxyl groups, carboxyl and carbonate structure	Srivastava et al., 2007
~1700 - 1630	C=O stretching from lactones and amide I band	Basha et al., 2009
1050 - 460	C=O stretching, aromatic -CH stretching, -C-C group, amine group (-NH <sub>2</sub> ) group	Nuhoglu and Malkoc 2009

It is clear from figure 5.1 (o) and table 5.1 (o) that the negatively charged groups such as carbonyl, aromatic ring stretching, amide, hydroxyl and carboxyl stretching are present on the surface of eucalyptus bark sawdust. These groups contribute significantly to the binding of metal ion surface on biomass surface.

In the extrapolation of the curve, no smoothing factor was used. The lines of spectrum were drawn at regular interval of  $500\text{ cm}^{-1}$  wave number. The lines of the spectrum were interpreted as the function of their respective wave numbers.

Figure 5.1(p) and table 5.1 (p) represent the detailed study of Jackfruit peel powder. The samples for FTIR analysis of Jackfruit peel waste was prepared by making 1% pellet of sample with photometric grade potassium bromide (KBR). The pellet was placed in the path of infrared ray for a total cumulative 32 scans. The range of wave number was kept between  $4000\text{ cm}^{-1} - 400\text{ cm}^{-1}$ . The spectrum was extrapolated between wave number and % transmittance.



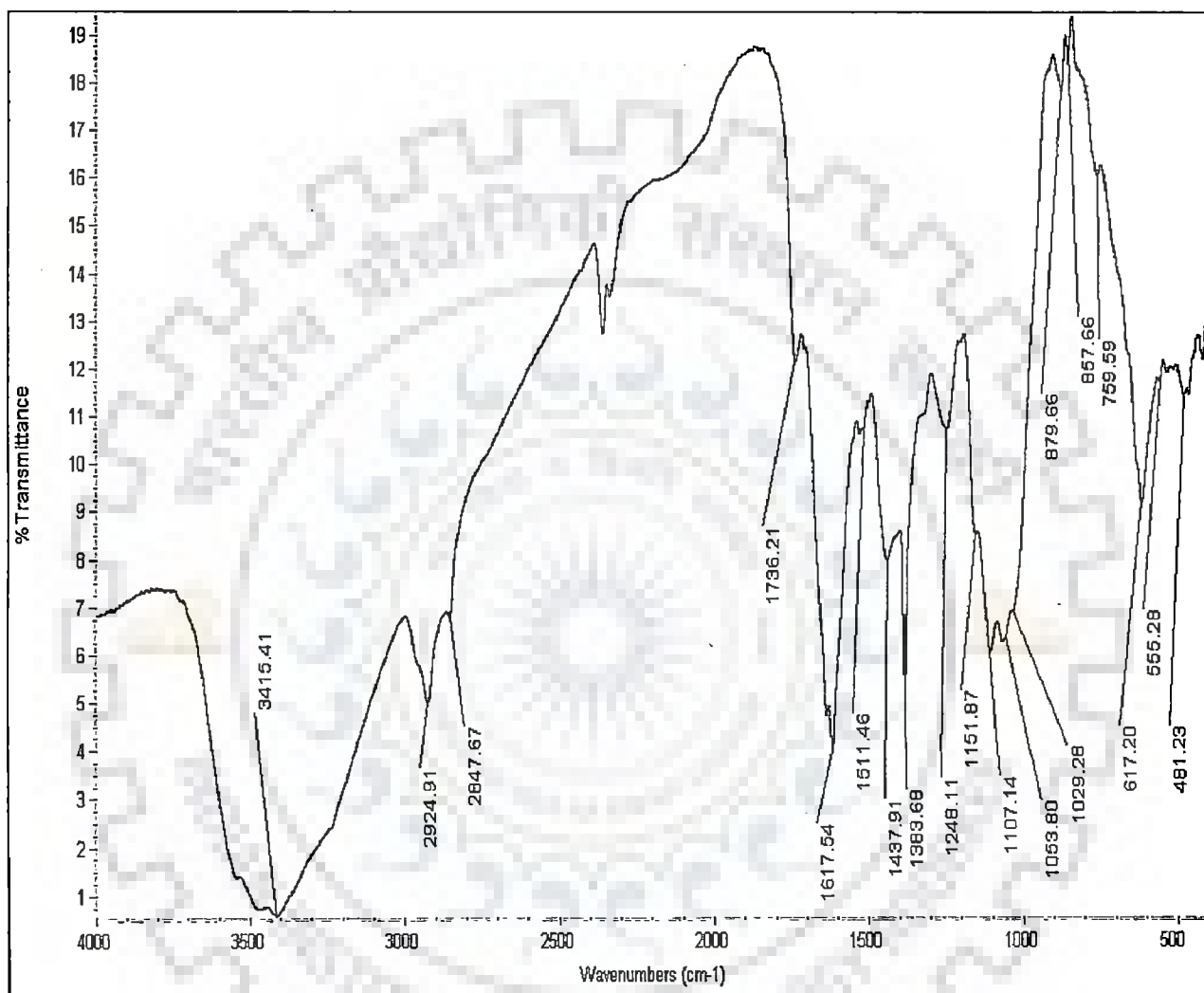


Figure 5.1 (p): FTIR spectrum of Jackfruit peel powder before adsorption

It became evident from figure 5.1 (p) that the surface of metal unloaded Jackfruit peel powder was quite enriched in peaks obtained between  $4000\text{ cm}^{-1} - 400\text{ cm}^{-1}$ . The spectrum did not indicate any vibration for moisture in the sample, since the curve was smooth and the peaks obtained were sharp. The detailed analysis of Jackfruit peel powder sawdust has been shown in table 5.1(p).

The samples for FTIR analysis of Jackfruit peel powder was prepared by making 1% pellet of sample with photometric grade potassium bromide (KBR). The pellet was placed in the path of infrared ray for a total cumulative 32 scans. The range of wave number was kept between  $4000\text{ cm}^{-1} - 400\text{ cm}^{-1}$ . The spectrum was extrapolated between wave number and % transmittance.

Table 5.1 (p): Detailed study of Jackfruit peel powder before adsorption

Wave number ( $\text{cm}^{-1}$ )	Functional group	Reference
3100 – 3500	Free and hydrogen bonded hydroxyl group, Si – OH (Siol group), Primary amide group (-CONH <sub>2</sub> )	Srivastava et al., 2007, Nuhoglu and Malkoc 2009
~ 2925	CH <sub>3</sub> – OH stretching	Basha et al., 2009
1600 -1800	-CH stretching	Srivastava et al., 2007
~1100	CO group	Srivastava et al., 2007
1300 – 1400	conjugated hydrocarbon groups, aromatic CH, carboxyl groups, carboxyl and carbonate structure	Srivastava et al. (2007)
~1700 - 1630	C=O stretching from lactones and amide I band	Basha et al., 2009
1050 - 460	C=O stretching, aromatic –CH stretching, -C-C group, amine group (-NH <sub>2</sub> ) group	Nuhoglu and Malkoc 2009

It is clear from figure 5.1 (p) and table 5.1 (p) that the negatively charged groups such as carbonyl, aromatic ring stretching, amide, hydroxyl and carboxyl stretching are present on the surface of Jackfruit peel powder. These groups contribute significantly to the binding of metal ion surface on biomass surface.

In the extrapolation of the curve, no smoothing factor was used. The lines of spectrum were drawn at regular interval of  $500\text{ cm}^{-1}$  wave number. The lines of the spectrum were interpreted as the function of their respective wave numbers.

#### **Concluding remarks of the section 5.1.1**

The study of surface characterization through scanning electron micrograph of the biosorbents revealed the fact that the surfaces of biosorbents were quite porous and heterogeneous. Additionally, several protrusions seemed to elongate inside the matrix of biomass (Ahamd et al. 2009). Further, it became evident from the Fourier transformation infrared spectrum analysis of various biomasses that the surfaces of the biosorbents were quite enriched in negatively charged functional groups.

## 5.2 BIOSORPTION OF Zn (II) ION alone and ALSO IN PRESENCE OF TOTAL Fe (II, III), Cu (II) IN BATCH STUDIES

In this section, optimization of various parameters for the biosorption of Zn (II) ion has been done in batch reactor using synthetic wastewater and real wastewater. The biosorbents used in the present work were *Cedrus deodara* sawdust (CDS), Eucalyptus leaf powder, Eucalyptus bark sawdust, Pine apple peel powder, Mango bark sawdust, Jack fruit peel powder, Egg shell with egg shell membrane, Orange peel and dead cells of *Zinc sequestering bacterium VMSDCM* Accession no. HQ108109. Optimization of various parameters like pH, temperature, biosorbent dose, initial concentration of zinc, contact time and agitation rates for the biosorption of Zn (II) ion alone and also in presence of total Fe (II, III) and Cu (II) ions have been studied in detail in section 5.2.1 to 5.2.8.

The basic conditions for all the batch experiments were pH 5, temperature  $303 \pm 1$  K, biosorbent dose  $1 \text{ g l}^{-1}$ , particle size 0.05 mm, initial concentrations of Zn (II), Cu (II) and total Fe (II, III) was  $150 \text{ mg l}^{-1}$ , contact time 8 hours, 500 rpm. All the basic conditions of the experiments were kept unchanged in all the batch experiments unless mentioned otherwise. Eight round bottom flasks of 500 ml capacity containing  $150 \text{ mg l}^{-1}$  of metal ions solution each with 1 g of biomass were agitated at  $303 \pm 1$  K. The whole set up of the batch reactor has been shown in figure 4.1 of chapter 4. The system of ions studied in the present work were pure zinc, Zn (II)- Cu (II), Zn (II)- Fe (II, III) and Zn (II) – Fe (II, III)- Cu (II). The metal ions Zn (II), Cu (II) and Fe (II, III) are referred as Zn, Cu and Fe in various figures.

### 5.2.1 Optimization of pH

The pH of the system significantly affects the biosorption of adsorbent (Dash et al., 2009). This section analyses the data on the biosorption of Zn (II) ion in liquid phase. In this section, pH was varied in between 1-8. Figures 5.2.1 (a) and 5.2.1 (b) represent the influence of pH on biosorption of Zn (II), Fe (II, III) and Cu (II) ion on the surface of Mango bark sawdust. The

It is evident from figure 5.2.1 (a) that the peaks have been obtained for all the curves at pH 5. Moreover, the maximum 84.88 % removal of Zn (II) ion was obtained in case of

pure zinc pH 5. The presence of other ions hindered the biosorption of Zn (II) ion in liquid phase.

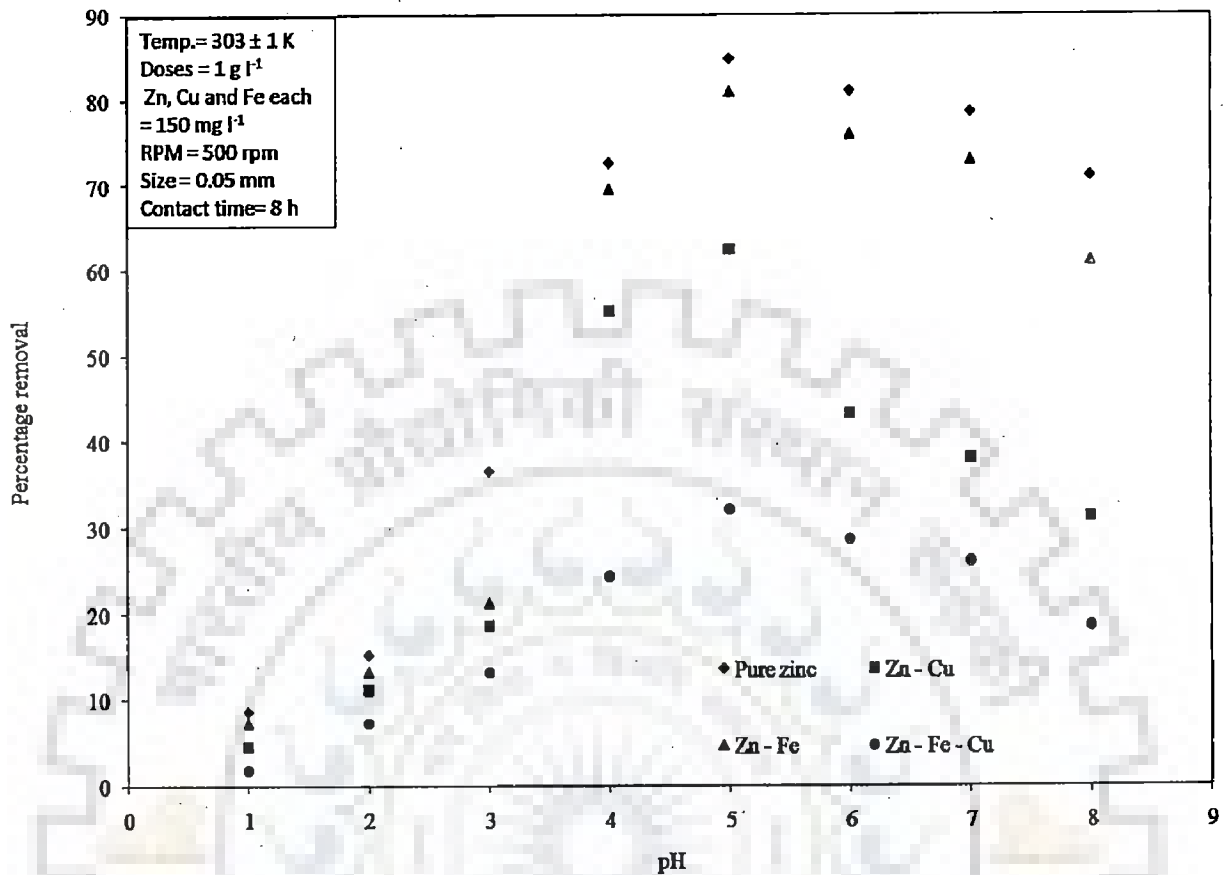


Figure 5.2.1 (a): Effect of pH on biosorption of Zn on Mango bark sawdust

In the presence of Cu (II) ions, the removal of Zn (II) ion decreased to 62.36 %. Furthermore, the presence of total Fe (II, III) also decreased the removal of Zn (II) ion from liquid phase. The maximum removal of Zn (II) ion in presence of total Fe (II, III) was 81.12 %. 32.11% of Zn (II) ion was removed in case of Zn (II) – Cu (II) – total Fe (II, III). However, in all cases, the maximum removal was obtained at pH 5.

The maximum removal of Zn (II) ion was obtained in pure zinc environment followed by Zn (II) – Fe (II, II), Zn (II) – Cu (II) and Zn (II) – Cu (II) - Fe (II, III) combination of ions. The biosorption of metal ions in all the metal ion systems considered was quite low at pH 3.

In case of pure zinc environment, the removal of Zn (II) ion was 36.61% at pH 3 (fig. 5.2.1 a).

In other combination of heavy metals (Zn (II) –Cu (II), Zn (II) – Fe (II, III) and Zn – Cu Fe (II, III)- Cu (II)), the removal of Zn (II) ion was 18.66 %, 21.31% and 13.21%, respectively. The lower percentage removal of Zn (II) ions or any other metal ion was due to extreme competition between hydrogen and metal ions present in the liquid phase (Mishra et al. 2011).

The active binding sites got protonated at low pH resulting in the generation of repulsive forces between metal ions and active adsorption sites leading to underprivileged biosorption of metal ions. With the increase in pH from 3 to 5, the metal ion removal increased from 36.31% to 84.88%, 18.66% to 62.36%, 21.31% to 81.12% and 13.21 % to 32.11% for pure zinc, Zn (II) –Cu (II), Zn (II) – Fe (II, III) and Zn – Cu (II)-Fe (II, III), respectively.

The increase in pH leads to decrease in repulsive forces and generation of attractive forces between active sites of biosorbent and metal ions (Mishra et al. 2011). Further, with the increase in pH from 5 to 8, the percentage removal of Zn (II) ion in all types of metal ion systems was found to be decreasing. The decrease in percentage removal of Zn (II) removal above pH 5 was due to the fact that at higher pH values the active sites of biosorbent became denatured which resulted in decrease in percentage removal of Zn (II) ion in all types of metal ion system (Sari and Tuzen 2008). Figure 5.2.1 (b) represents the percentage removal of Cu (II) and Fe (II, III) ion in presence of zinc. The maximum removal of Cu(II) ions was obtained in Zn (II) - Cu (II) ion system at pH 5. Moreover, the lowest percentage removal of total Fe (II, III) was obtained in case of Zn (II)- Cu (II) – total Fe (II, III) ions.

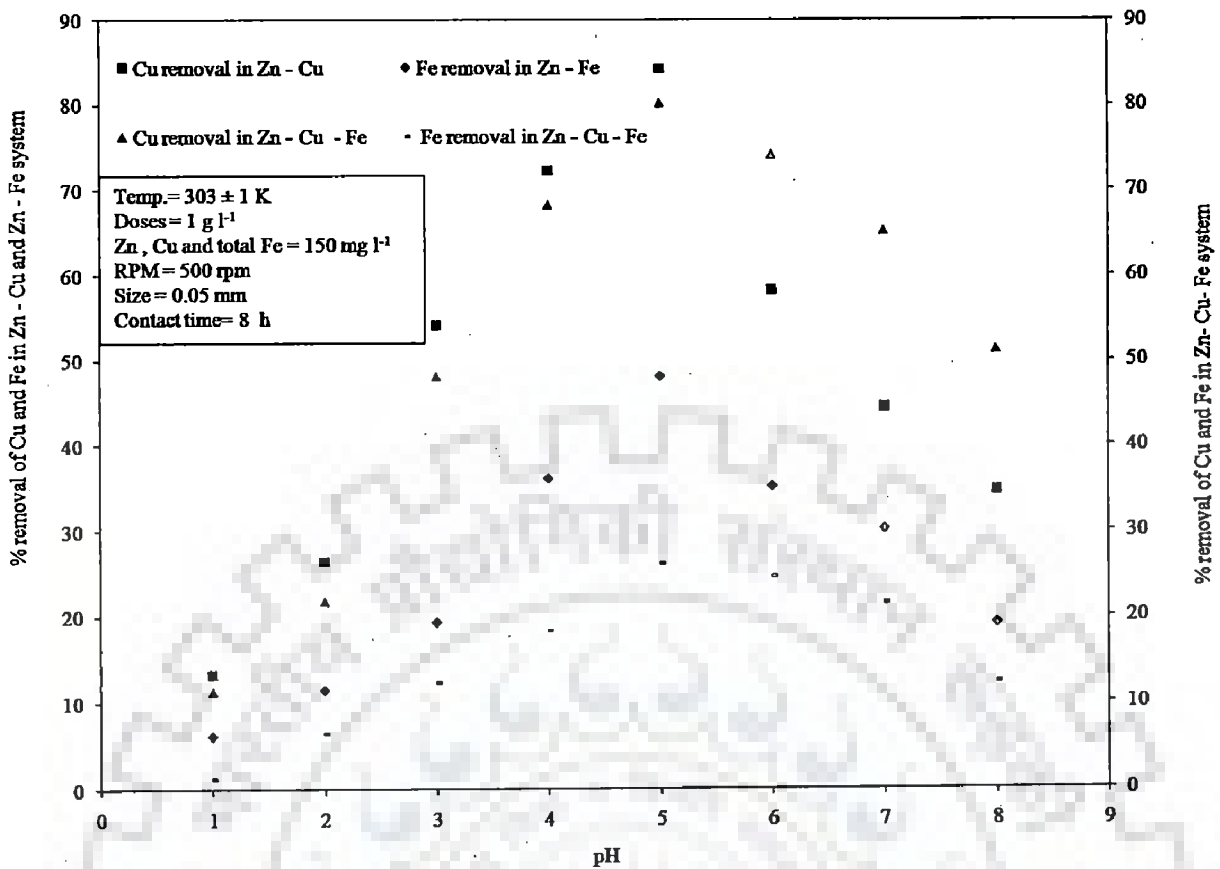


Figure 5.2.1 (b): Effect of pH on biosorption of Cu and Fe in presence of Zn on Mango bark sawdust

However, maximum removal has been obtained in all the cases at pH 5. The order of removal obtained for metal ions were Cu (II) > Zn (II) > Fe (II, III). The maximum removal of Cu (II) and total Fe (II, III) obtained in case of Zn (II) – Cu (II) and Zn (II)- total Fe (II, III) was 84.16% and 36.11%, respectively. However, 84.16% and 26.11% removal of Cu (II) and total Fe (II, III) was obtained in Zn (II) – Cu (II) – total Fe (II, III), respectively.

Figure 5.2.1 (c) and figure 5.2.1 (d) represent the influence of pH on biosorption of Zn (II), Cu (II) and Fe (II, III) ion on the surface of Orange peel. It is evident from figure 5.2.1 (c) that the peaks have been obtained for all the curves at pH 5. Moreover, the maximum 80.21% removal of Zn (II) ion was obtained in case of pure zinc at pH 5.

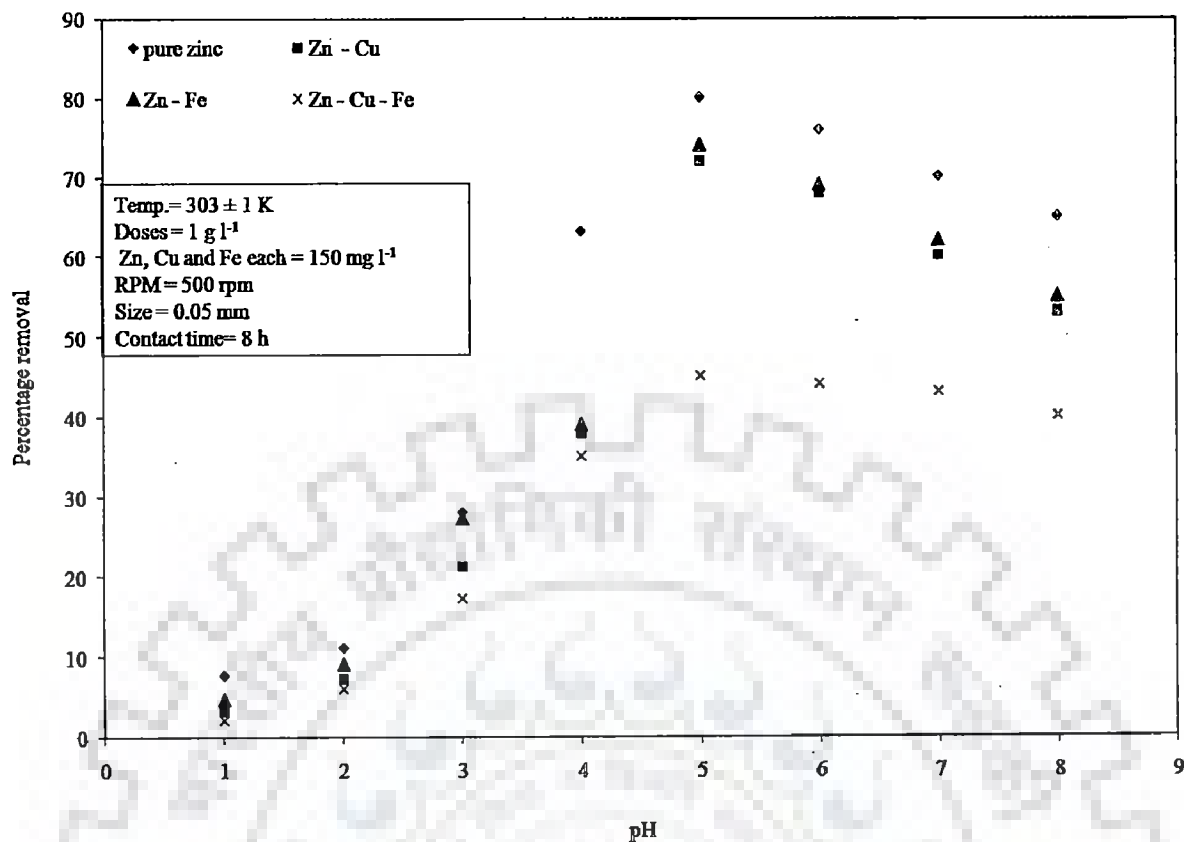


Figure 5.2.1 (c): Effect of pH on biosorption of Zn on orange peel

The presence of other ions hindered the biosorption of Zn (II) ion in liquid phase. In the presence of Cu (II) ions, the removal of Zn (II) ion decreased to 72.11%. Furthermore, presence of total Fe (II, III) also decreased the removal of Zn (II) ion from liquid phase. The maximum removal of Zn (II) ion in presence of total Fe (II, III) was 74.16%. In the complex system of Zn – Cu – Fe, removal was almost 45.11%.

However, in all the cases, the maximum removal was obtained at pH 5. The maximum removal of Zn (II) ion was obtained in pure zinc environment followed by Zn (II) – Fe (II, III), Zn (II) – Cu (II) and Zn (II) – Fe (II, III)- Cu (II) combination of ions. The biosorption of metal ions in all the metal ion systems considered was quite low at pH 3. In case of pure zinc environment, at pH 3, the removal of Zn (II) ion was 28.11%.



In other combination of heavy metals (Zn (II) –Cu (II), Zn (II) – Fe (II, III) and Zn – Fe (II, III)-Cu (II)), the removal of Zn (II) ion was 21.31 %, 27.34% and 17.31%, respectively. The lower percentage removal of Zn (II) ions or any other metal ion was due to extreme competition between hydrogen and metal ions present in the liquid phase (Mishra et al 2011). The active binding sites got protonated at low pH resulting in the generation of repulsive forces between metal ions and active adsorption sites, which led to underprivileged biosorption of metal ions.

With the increase in pH from 3 to 5, the metal ion removal increased from 28.11% to 80.21%, 21.31% to 72.11%, 27.34% to 74.16% and 17.31 % to 45.11% for pure zinc, Zn (II) –Cu (II), Zn (II) – Fe (II, III) and Zn – Cu (II)-Fe (II, III), respectively. The increase in pH leads to decrease in repulsive forces and generation of attractive forces between active sites of biosorbent and metal ions.

Further increase in pH from 5 to 8, the percentage removal of Zn (II) ion in all types of metal ion systems was found to be decreasing. The decrease in percentage removal of Zn (II) removal above pH 5 was due to the fact that at higher pH values the active sites of biosorbent became denatured resulting in decrease in percentage removal of Zn (II) ion in all types of metal ion systems. pH values beyond 8 were not considered in the present work, since zinc ion changes its speciation from its ionic form to hydroxide form above pH 8.

Figure 5.2.1 (d) presents data regarding the percentage removal of Cu (II) and Fe (II, III) ion in presence of zinc. The maximum removal of Cu(II) ions was obtained in Zn (II) - Cu (II) ion system and Zn (II) – Cu (II) – Fe (II, III) metal ion system at pH 5. In Zn (II)- Cu (II), Zn (II)- total Fe (II, III) and Zn (II)- Cu (II) – Fe (II, III) metal ion systems the maximum removal of Cu (II) and total Fe (II, III) ion was obtained at pH 5.

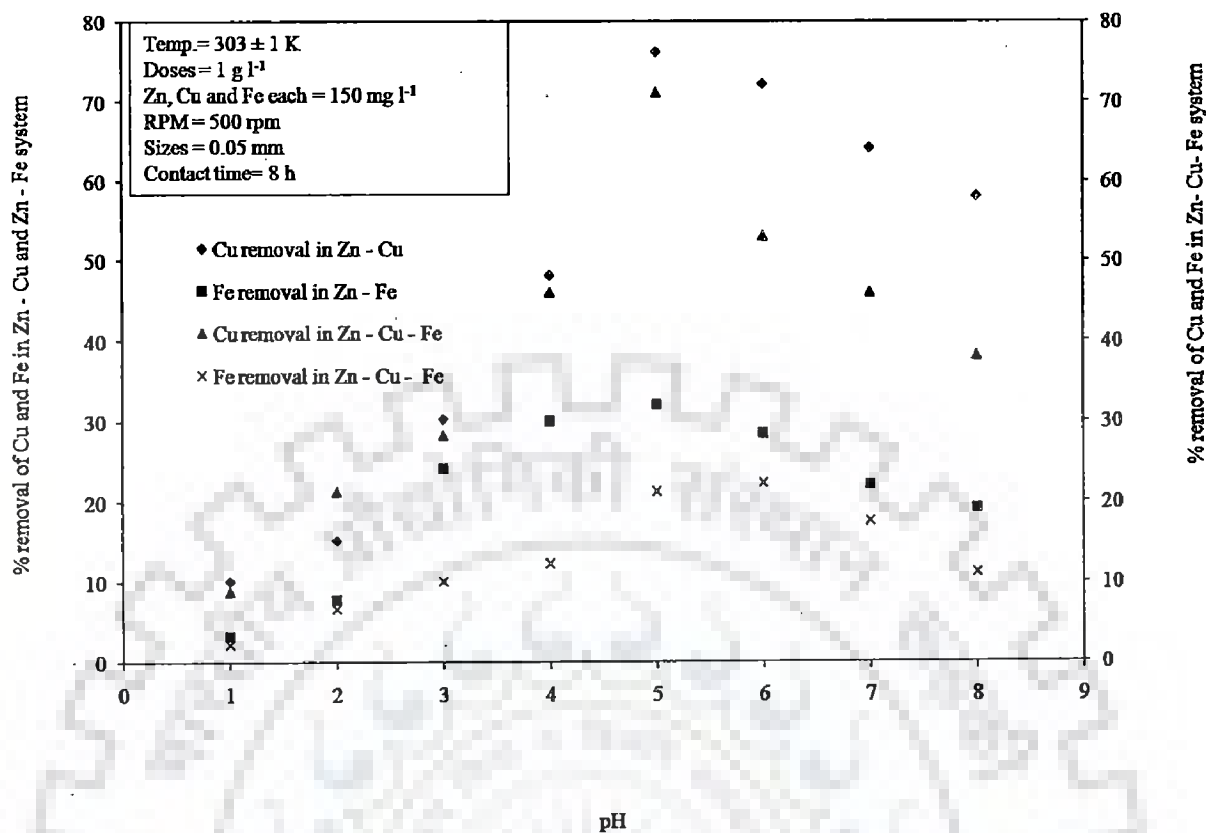


Figure 5.2.1 (d): Effect of pH on biosorption of Cu and Fe in presence of Zn on orange peel

Moreover, the lowest percentage removal was obtained in case of Zn (II) – Cu (II) – Fe (II, III). However, maximum removal has been obtained in all the cases at pH 5. The order of removal obtained for metal ions was Cu (II) > Zn (II) > Fe (II, III). The maximum removal of Cu (II) and total Fe (II, III) obtained in case of Zn (II) – Cu (II) and Zn (II)- total Fe (II, III) was 76.18% and 32.11%, respectively. However, 71.16% and 21.31% removal of Cu (II) and total Fe (II, III) was obtained in Zn (II) – Cu (II) – total Fe (II, III), respectively.

Figure 5.2.1 (e) and figure 5.2.1 (f) represent the influence of pH on biosorption of Zn (II), Cu (II) and Fe (II, III) ion on the surface of Pineapple peel powder. It is evident from figure 5.2.1 (e) that the peaks have been obtained for all the curves at pH 6. Moreover, the maximum 66.2% removal of Zn (II) ion was obtained in case of pure zinc at pH 6. The presence of other ions hindered the biosorption of Zn (II) ion in liquid phase. In the presence

of Cu (II) ions, the removal of Zn (II) ion decreased to 26.25%. Furthermore, presence of total Fe (II, III) also decreased the removal of Zn (II) ion from liquid phase.

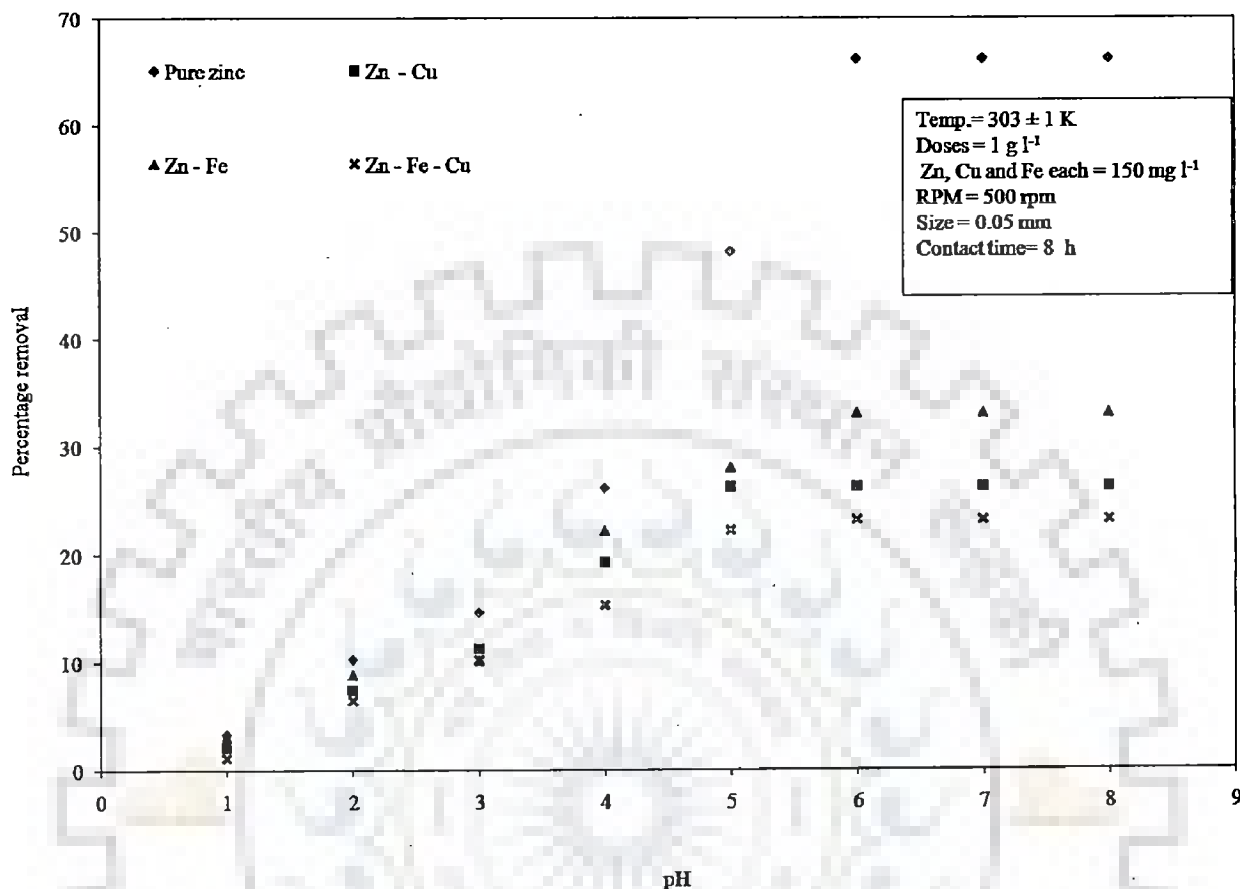


Figure 5.2.1 (e): Effect of pH on biosorption of Zn on pineapple peel

The maximum removal of Zn (II) ion in presence of total Fe (II, III) was 33.17 %. 23.18% Zn (II) ion was removed in case of Zn (II)- Cu (II)- total Fe (II, III). 23.18% Zn (II) ion was removed in case of Zn (II)- Cu (II) – Fe (II, III) system. However, in all the cases, the maximum removal was obtained at pH 6. The maximum removal of Zn (II) ion was obtained in pure zinc environment followed by Zn (II) – Fe (II, II), Zn (II) – Cu (II) and Zn (II) – Fe (II, III)- Cu (II) combination of ions.

The biosorption of metal ions in all the metal ion systems considered was quite low at pH 3. In case of pure zinc environment, the removal of Zn (II) ion was 14.64% at pH 3. In other combination of heavy metals (Zn (II) –Cu (II), Zn (II) – Fe (II, III) and Zn – Cu (II)-Fe (II, III)), the removal of Zn (II) ion was 11.24 %, 10.21% and 10.19%, respectively. The

lower percentage removal of Zn (II) ions or any other metal ion was due to extreme competition between hydrogen and metal ions present in the liquid phase.

The active binding sites got protonated at low pH resulting in the generation of repulsive forces between metal ions and active adsorption sites, which led to underprivileged biosorption of metal ions (Mishra et al., 2011). With the increase in pH from 3 to 7, the metal ion removal increased from 14.64% to 66.2%, 11.24% to 26.25%, 10.28% to 33.17% and 10.19 % to 23.18% for pure zinc, Zn (II) –Cu (II), Zn (II) – Fe (II, III) and Zn – Cu (II)-Fe (II, III), respectively. The increase in pH leads to decrease in repulsive forces and generation of attractive forces between active sites of biosorbent and metal ions.

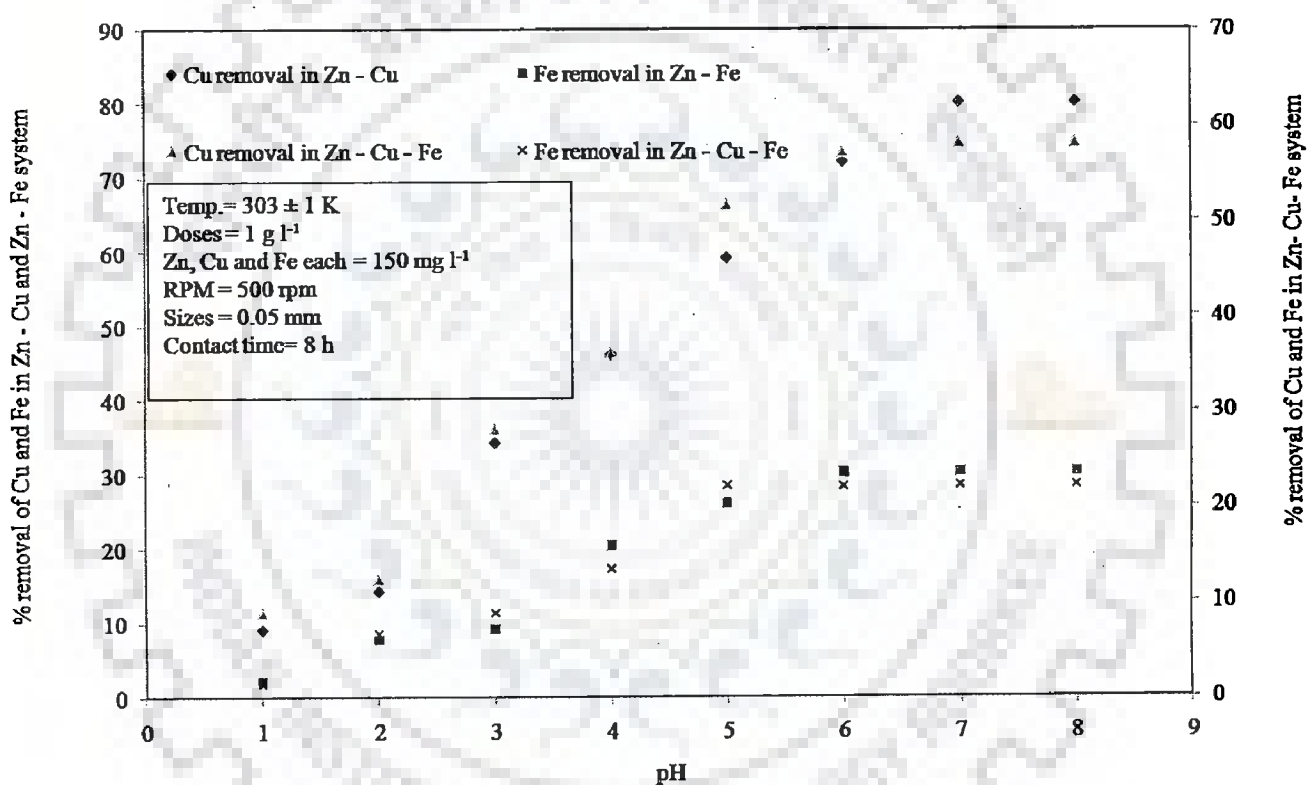


Figure 5.2.1 (f): Effect of pH on biosorption of Cu and Fe in presence of Zn on Pineapple peel powder

Figure 5.2.1 (f) embodies data regarding the percentage removal of Cu (II) and Fe (II, III) ion in presence of zinc. The maximum removal of Cu(II) ions was obtained in Zn (II) - Cu (II) ion system at pH 6. Moreover, the lowest percentage removal was obtained in case of

Zn (II)-Cu (II)- total Fe (II, III) ions. However, maximum removal has been obtained in all the cases at pH 6. The order of removal obtained for metal ions was Cu (II) > Zn (II) > Fe (II, III). In Zn (II)- Cu (II), Zn (II)- total Fe (II, III) and Zn (II)- Cu (II) – Fe (II, III) metal ion systems the maximum removal of Cu (II) and total Fe (II, III) ion was obtained at pH 6. The maximum removal of Cu (II) and total Fe (II, III) obtained in case of Zn (II) – Cu (II) and Zn (II)- total Fe (II, III) was 72.15% and 30.28%, respectively. However, 57.18% and 22.1% removal of Cu (II) and total Fe (II, III) was obtained in Zn (II) – Cu (II) – total Fe (II, III), respectively.

Figure 5.2.1 (g) and figure 5.2.1 (h) represent the influence of pH on biosorption of Zn (II), Fe (II, III) and Cu (II) ion on the surface of Jackfruit peel powder. It became evident from figure 5.2.1 (g) that the peaks have been obtained for all the curves at pH 5. Moreover, the maximum 42.11% removal of Zn (II) ion was obtained in case of pure zinc at pH 5.

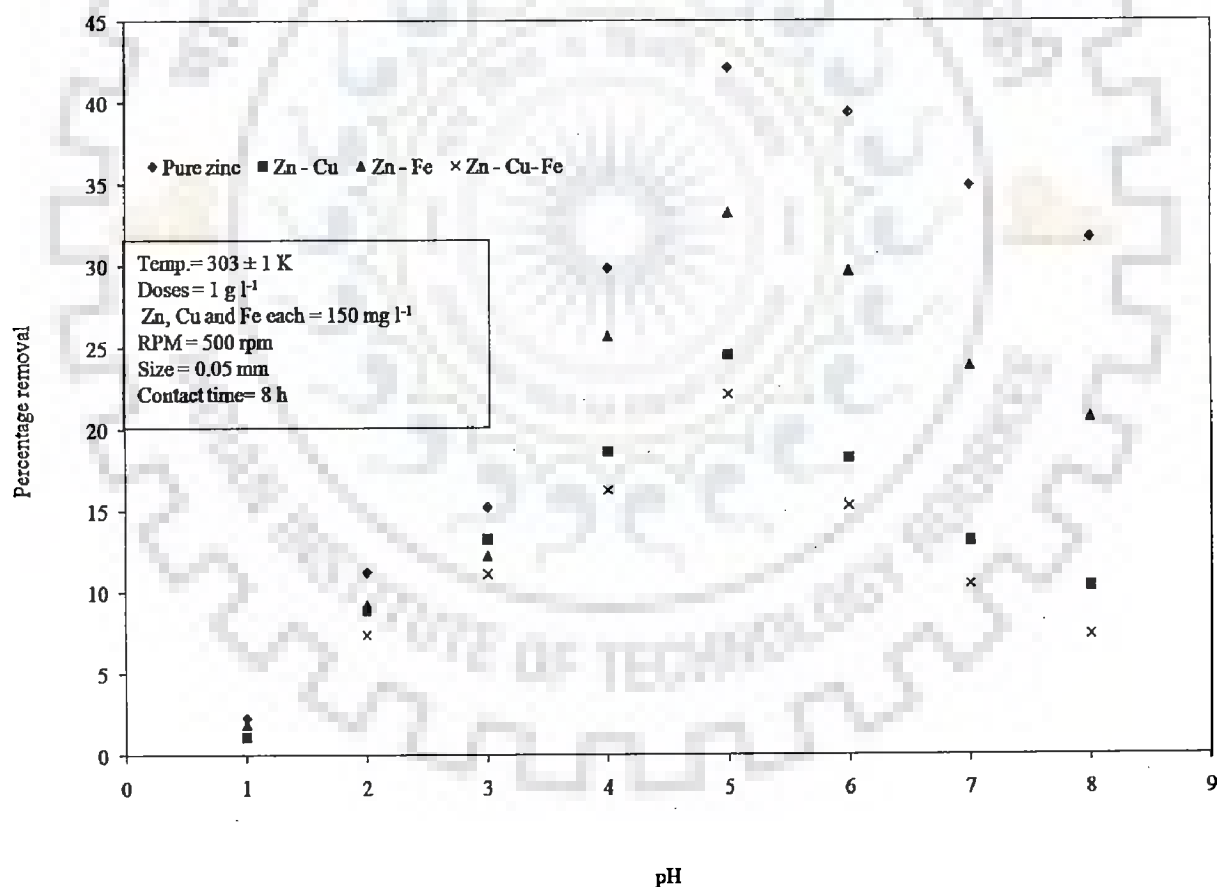


Figure 5.2.1 (g): Effect of pH on biosorption of Zn on jackfruit peel powder

The presence of other ions hindered the biosorption of Zn (II) ion in liquid phase. In the presence of Cu (II) ions, the removal of Zn (II) ion decreased to 24.51%. Furthermore, presence of total Fe (II, III) also decreased the removal of Zn (II) ion from liquid phase. The maximum removal of Zn (II) ion in presence of total Fe (II, III) was 33.18%. 22.11% Zn (II) ion was removed in case of Zn (II)- Cu (II)- total Fe (II, III) system. However, in all the cases, maximum removal was obtained at pH 5.

The maximum removal of Zn (II) ion was obtained in pure zinc environment followed by Zn (II) – Fe (II, II), Zn (II) – Cu (II) and Zn (II) – Fe (II, III)- Cu (II) combination of ions. The biosorption of metal ions in all the metal ion systems considered was quite low at pH 3. In case of pure zinc environment, the removal of Zn (II) ion was 15.21% at pH 3. In combination of heavy metals (Zn (II) –Cu (II), Zn (II) – Fe (II, III) and Zn – Cu (II)-Fe (II, III)), the removal of Zn (II) ion was 13.26 %, 12.21% and 11.1%, respectively.

The lower percentage removal of Zn (II) ions or any metal ion was due to extreme competition between hydrogen and metal ions present in the liquid phase (Mishra et al., 2011). The active binding sites became protonated at low pH resulting in the generation of repulsive forces between metal ions and active adsorption sites, which led to underprivileged biosorption of metal ions (Mishra et al., 2010). With the increase in pH from 3 to 5, the metal ion removal increased from 15.21% to 42.11%, 13.26% to 24.51%, 12.21% to 33.18% and 11.11 % to 22.11% for pure zinc, Zn (II) –Cu (II), Zn (II) – Fe (II, III) and Zn)-Fe (II, III)– Cu (II),, respectively. The increase in pH leads to decrease in repulsive forces and generation of attractive forces between active sites of biosorbent and metal ions. Further, with the increase in pH from 5 to 8, the percentage removal of Zn (II) ion in all types of metal ion systems was found to be decreasing.

The decrease in percentage removal of Zn (II) above pH 5 was due to the fact that at higher pH values the active sites of biosorbent became denatured resulting in decrease in

percentage removal of Zn (II) ion in all types of metal ion system. pH values beyond 8 were not considered in the present work, since zinc ion changes its speciation completely from its ionic form to hydroxide form above pH 8.

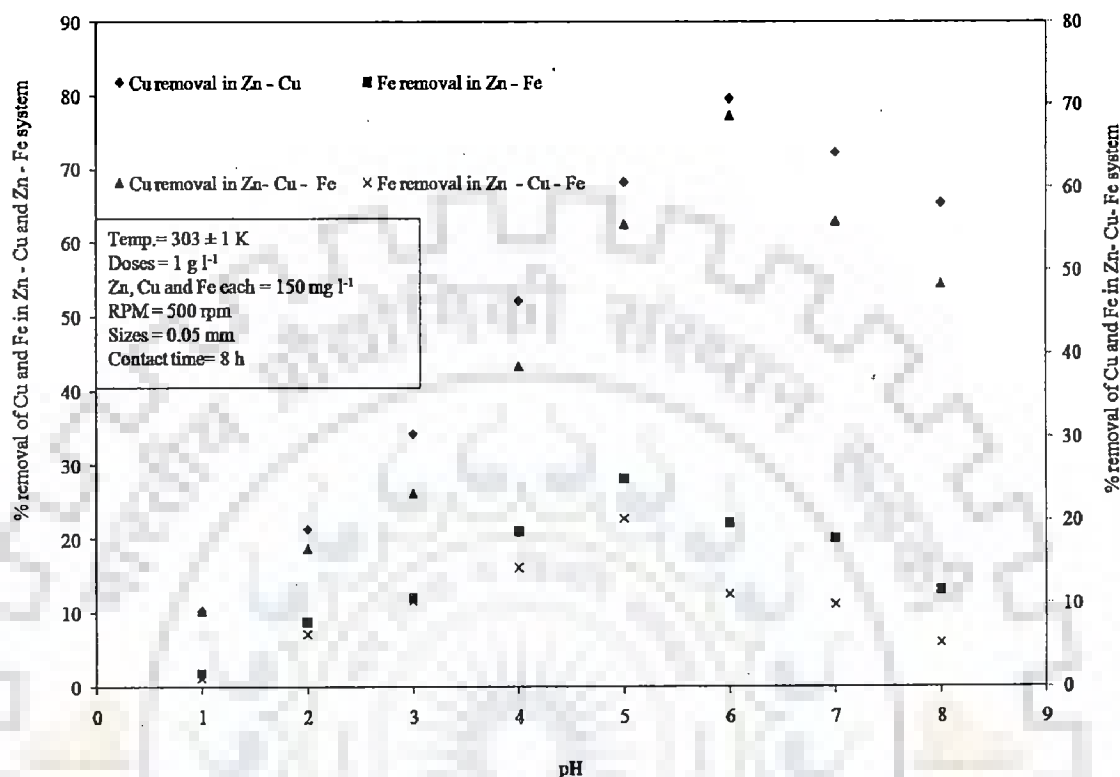


Figure 5.2.1 (h): Effect of pH on biosorption of Cu and Fe in presence of Zn on Jackfruit peel powder

Figure 5.2.1 (h) embodies data regarding the percentage removal of Cu (II) and Fe (II, III) ion in presence of zinc. The maximum removal of Cu(II) ions was obtained in Zn (II) - Cu (II) ion system at pH 5. Moreover, the lowest percentage removal was obtained in case of Zn (II)- Cu (II) – Fe (II, III). In Zn (II)- Cu (II), Zn (II)- total Fe (II, III) and Zn (II)- Cu (II) – Fe (II, III) metal ion systems the maximum removal of Cu (II) and total Fe (II, III) ion was obtained at pH 5 and at pH 6.

The order of removal obtained for metal ions was Cu (II) > Zn (II) > Fe (II, III). The maximum removal of Cu (II) and total Fe (II, III) obtained in case of Zn (II) – Cu (II) and Zn (II)- total Fe (II, III) was 79.56% and 28.16%, respectively. However, 68.61% and 20.24%

removal of Cu (II) and total Fe (II, III) was obtained in Zn (II) – Cu (II) – total Fe (II, III), respectively.

Figure 5.2.1 (i) and figure 5.2.1 (j) represent the influence of pH on biosorption of Zn (II), Fe (II, III) and Cu (II) ion on the surface of *Cedrus deodara* sawdust. It is evident from figure 5.2.1 (i) that the peaks have been obtained for all the curves at pH 5. Moreover, the maximum 89.19% removal of Zn (II) ion was obtained in case of pure zinc at pH 5.

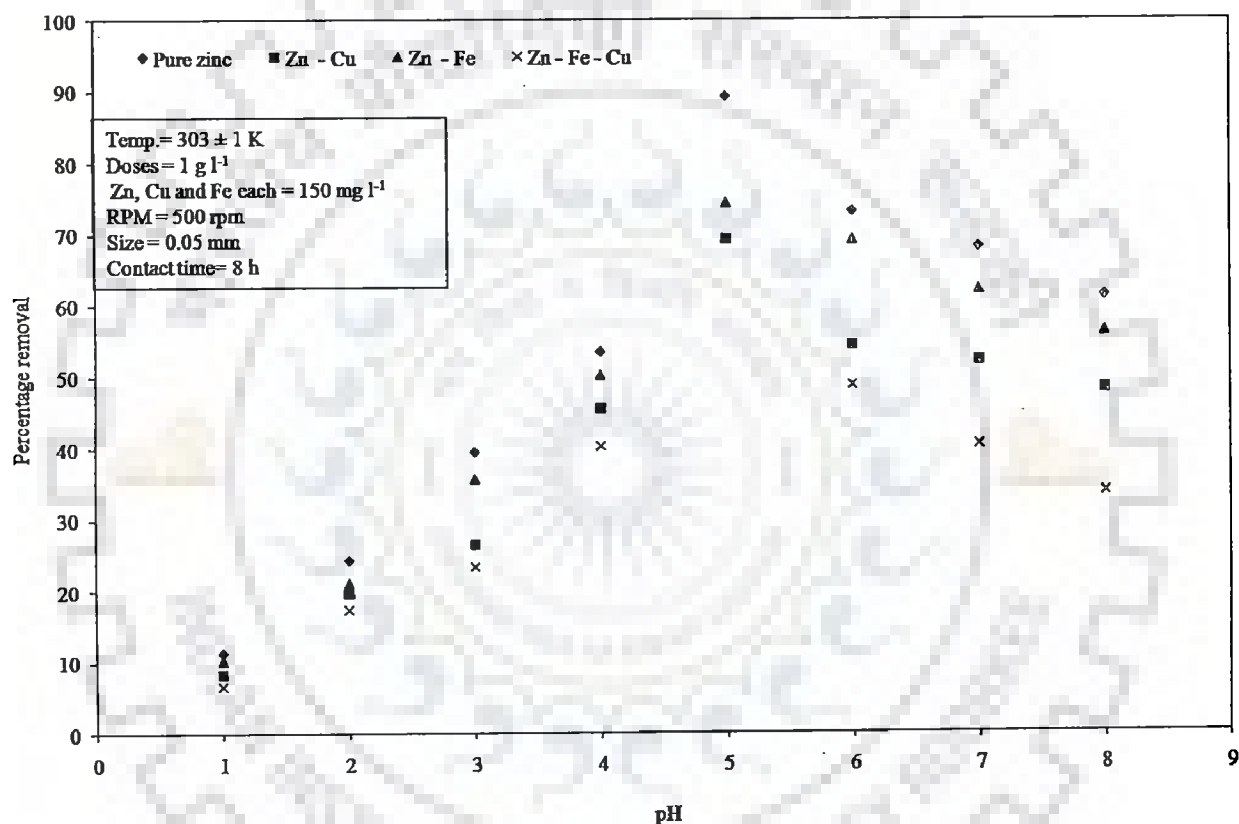


Figure 5.2.1 (i): Effect of pH on biosorption of Zn on *Cedrus deodara* sawdust

The presence of other ions hindered the biosorption of Zn (II) ion in liquid phase. In the presence of Cu (II) ions, the removal of Zn (II) ion decreased to 69.11%. Furthermore, presence of total Fe (II, III) also decreased the removal of Zn (II) ion from liquid phase. The maximum removal of Zn (II) ion in presence of total Fe (II, III) was 74.31%. 69.11% Zn (II)



ion was removed in case of Zn (II) – Cu (II)- total Fe (II, III). However, in all the cases, the maximum removal was obtained at pH 5. The maximum removal of Zn (II) ion was obtained in pure zinc environment followed by Zn (II) – Fe (II, II), Zn (II) – Cu (II) and Zn (II) – Cu (II) - Fe (II, III) combination of ions. The biosorption of metal ions in all the metal ion systems was quite low at pH 3. In case of pure zinc environment, at pH 3, the removal of Zn (II) ion was 39.45%. In other combination of heavy metals (Zn (II) –Cu (II), Zn (II) – Fe (II, III) and Zn – Cu (II)-Fe (II, III)), the removal of Zn (II) ion was 26.38 %, 35.66% and 23.31%, respectively at pH 3. The lower percentage removal of Zn (II) ions or any other type of metal ion systems was due to extreme competition between hydrogen and metal ions present in the liquid phase.

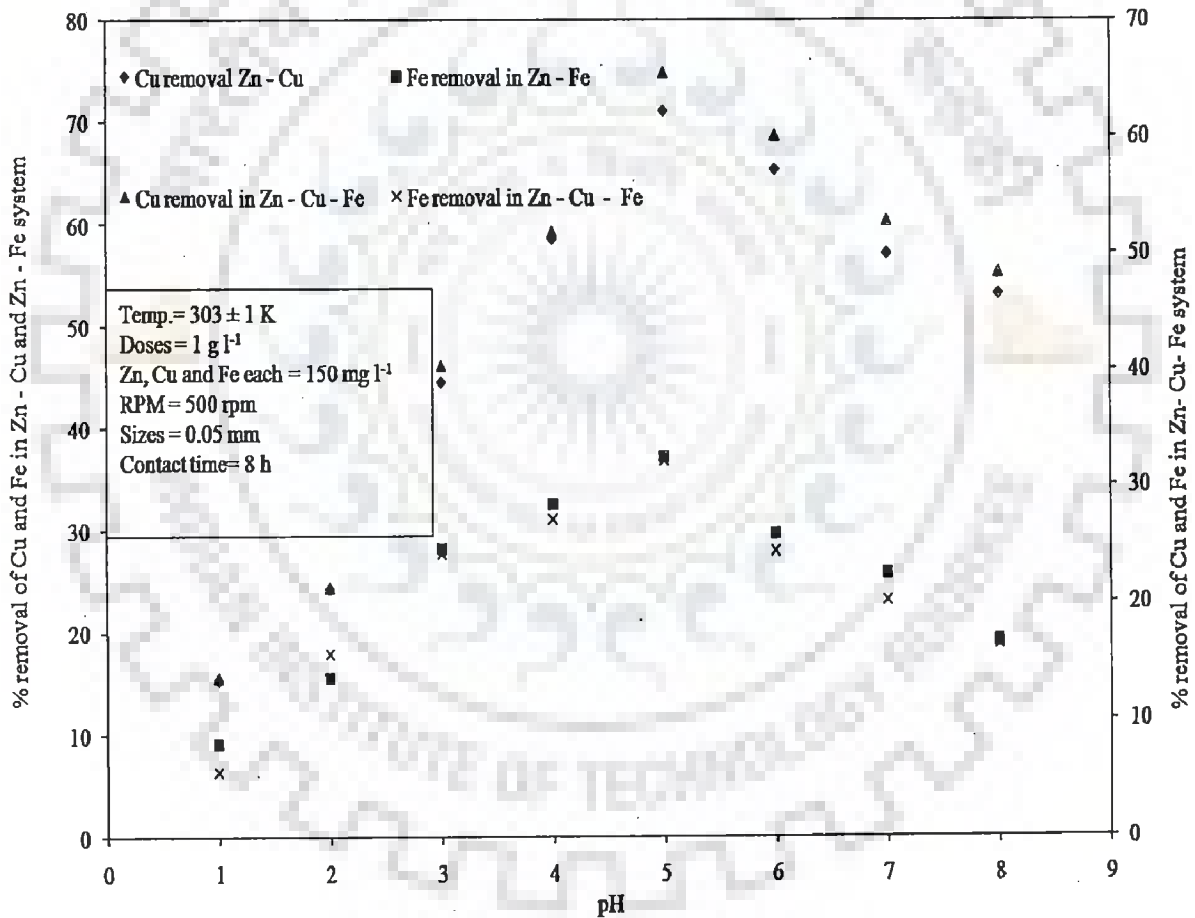


Figure 5.2.1 (j): Effect of pH on biosorption of Cu and Fe in presence of Zn *Cedrus deodara* sawdust

The active binding sites got protonated at low pH resulting in the generation of repulsive forces between metal ions and active adsorption sites, which led to underprivileged biosorption of metal ions (Mishra et al., 2010). With the increase of pH from 3 to 5, the metal ion removal increased from 39.45% to 89.19%, 26.38% to 69.12%, 34.66% to 74.31% and 23.31% to 69.11% for pure zinc, Zn (II) – Cu (II), Zn (II) – Fe (II, III) and Zn – Cu (II)-Fe (II, III), respectively. The increase in pH leads to decrease in repulsive forces and generation of attractive forces between active sites of biosorbent and metal ions. Further increase in pH from 5 to 8, the percentage removal of Zn (II) ion in all types of metal ion systems was found to be decreasing. The decrease in percentage removal of Zn (II) removal above pH 5 was due to the fact that at higher pH values the active sites of biosorbent were denatured resulting in decrease in percentage removal of Zn (II) ion in all types of metal ion system (Sari and Tuzen, 2008).

Figure 5.2 (j) embodies data regarding the percentage removal of Cu (II) and Fe (II, III) ion in presence of zinc. The maximum removal of Cu(II) ions was obtained in Zn (II) - Cu (II) ion system at pH 5. Moreover, the lowest percentage removal was obtained in case of Zn (II) - Cu (II) – Fe (II, III) systems. However, maximum removal has been obtained in all the cases at pH 5. The order of removal obtained for metal ions was Cu (II) > Zn (II) > Fe (II, III). The maximum removal of Cu (II) and total Fe (II, III) obtained in case of Zn (II) – Cu (II) and Zn (II)- total Fe (II, III) was 71.11% and 37.19%, respectively. However, 65.5% and 32.14% removal of Cu (II) and total Fe (II, III) was obtained in Zn (II) – Cu (II) – total Fe (II, III), respectively.

Figure 5.2.1 (k) and Figure 5.2.1 (l) represent the influence of pH on biosorption of Zn (II), Cu (II) and Fe (II, III). It became evident from figure 5.2.1 (k) that the peaks have been obtained for all the curves at pH 5. Moreover, the maximum 71.33% removal of zinc was obtained in case of pure zinc at pH 5. The presence of other ions hindered the biosorption of Zn (II) ion in liquid phase. In the presence of Cu (II) ions, the removal of Zn (II) ion decreased to 49.41% at pH 5.

Furthermore, presence of total Fe (II, III) also decreased the removal of Zn (II) ion from liquid phase. The maximum removal of Zn (II) ion in presence of total Fe (II, III) was 52.18% at pH 5. 27.36% Zn (II) ion was removed in case of Zn (II)- Cu (II)- Fe (II, III). However, in all the cases, the maximum removal was obtained at pH5. The maximum removal of Zn (II) ion was obtained in pure zinc environment followed by Zn (II) – Fe (II, II), Zn (II) – Cu (II) and Zn (II) – Fe (II, III)- Cu (II) combination of ions.

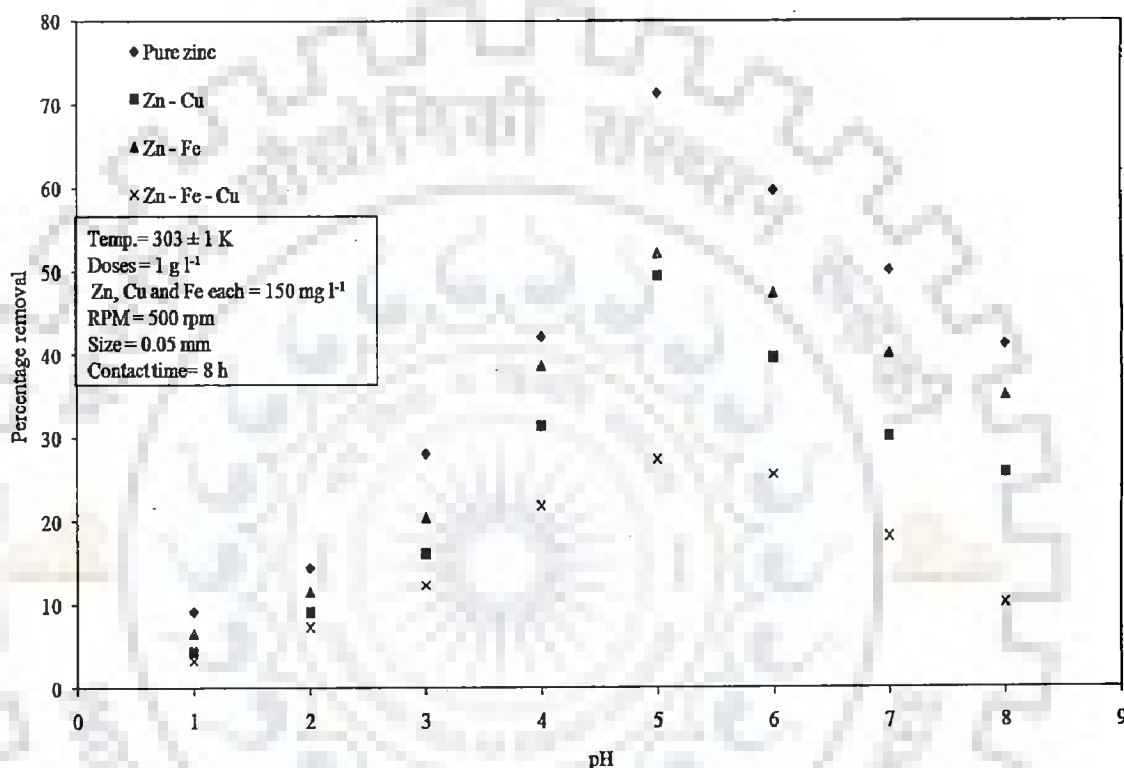


Figure 5.2.1 (k): Effect of pH on biosorption of Zn on Eucalyptus bark sawdust

The biosorption of metal ions in all the metal ion systems was quite low at pH 3. In case of pure zinc environment, the removal of Zn (II) ion was 28.16% at pH 3. In combination of heavy metals (Zn (II) –Cu (II), Zn (II) – Fe (II, III) and Zn – Cu (II)-Fe (II, III)), the removal of Zn (II) ion was 16.23 %, 20.48% and 12.36%, respectively at pH 3. The lower percentage removal of Zn (II) ions or any other type of metal ion systems was due to extreme competition between hydrogen and metal ions present in the liquid phase (Mishra et

al., 2011). The active binding sites gets protonated at low pH resulting in the generation of repulsive forces between metal ions and active adsorption sites, which led to underprivileged biosorption of metal ions (Sari et al., 2008). With the increase in pH from 3 to 5, the metal ion removal increased from 28.16% to 71.33%, 16.23% to 49.41%, 20.48% to 52.18% and 12.36 % to 27.36% for pure zinc, Zn (II) –Cu (II), Zn (II) – Fe (II, III) and Zn – Cu (II)-Fe (II, III), respectively. The increase in pH leads to decrease in repulsive forces and generation of attractive forces between active sites of biosorbent and metal ions. Further increase in pH from 5 to 8, the percentage removal of Zn (II) ion in all types of metal ion systems was found to be decreasing. The decrease in percentage removal of Zn (II) above pH 5 was due to the fact that at higher pH values the active sites of biosorbent got denatured resulting in decrease in percentage removal of Zn (II) ion in all types of metal ion system.

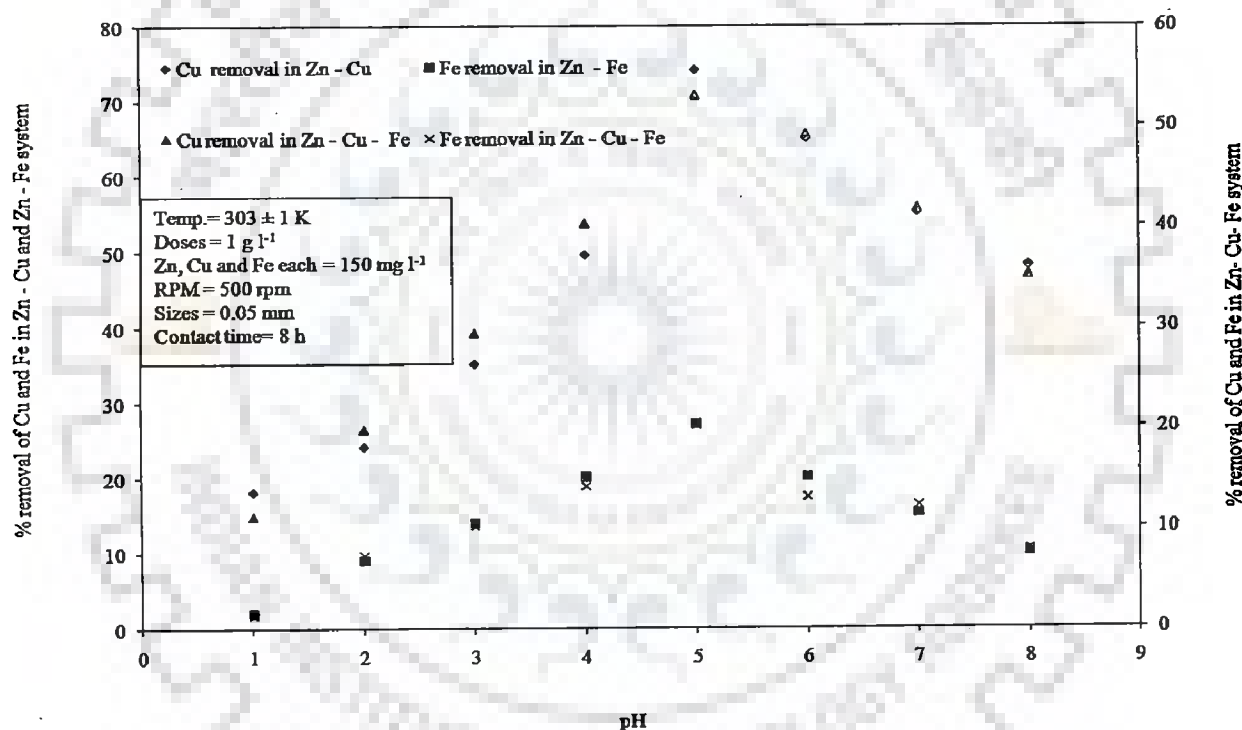


Figure 5.2.1 (l): Effect of pH on biosorption of Cu and Fe in presence of Zn on Eucalyptus bark sawdust

Figure 5.2.1 (l) presents data regarding the percentage removal of Cu (II) and Fe (II, III) ions in presence of zinc. The maximum removal of Cu(II) ions was obtained in Zn (II) - Cu (II) ion system at pH 5. Moreover, the lowest percentage removal was obtained in case of Zn (II)- Cu (II)-Fe (II, III) system. However, maximum removal has been obtained in

all the cases at pH 5. The order of removal obtained for metal ions was Cu (II) > Zn (II) > Fe (II, III). The maximum removal of Cu (II) and total Fe (II, III) obtained in case of Zn (II) – Cu (II) and Zn (II)- total Fe (II, III) was 74.19% and 27.19%, respectively. However, 53.12% and 20.22% removal of Cu (II) and total Fe (II, III) was obtained in Zn (II) – Cu (II) – total Fe (II, III), respectively.

Figure 5.2.1 (m) and figure 5.2.1 (n) represent the influence of pH on biosorption of Zn (II), Fe (II, III) and Cu (II) ion on the surface of Eucalyptus leaf powder. It is evident from figure 5.2.1 (m) that the peaks have been obtained for all the curves at pH 5. Moreover, the maximum 72.18% removal of Zn (II) ion was obtained in case of pure zinc at pH 5. The presence of other ions hindered the biosorption of Zn (II) ion in liquid phase. In the presence of Cu (II) ions, the removal of Zn (II) ion decreased to 62.16% at pH 5.

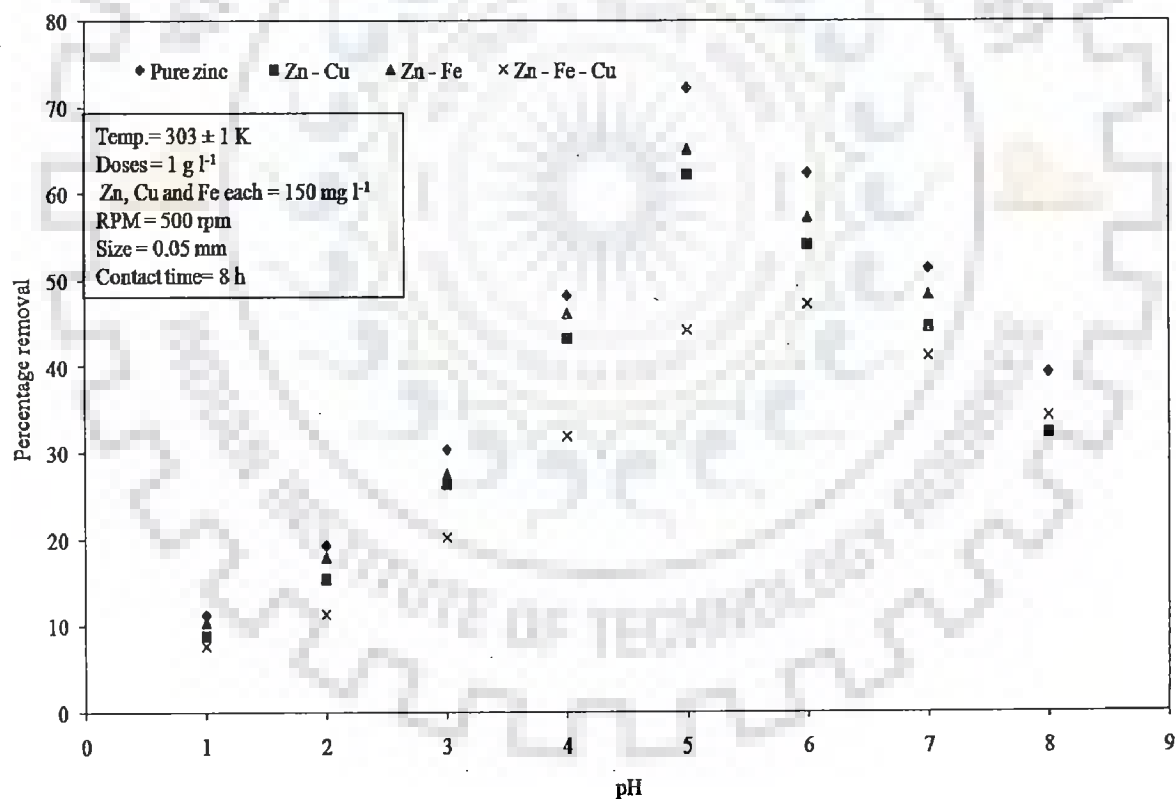


Figure 5.2.1 (m): Effect of pH on biosorption of Zn on Eucalyptus leaf powder

Furthermore, presence of total Fe (II, III) also decreased the removal of Zn (II) ion from liquid phase. The maximum removal of Zn (II) ion in presence of total Fe (II, III) was 65.13%. 44.16% Zn (II) ion was removed in case of Zn (II)- Cu (II)- Fe (II, III) system. However, in all cases, the maximum removal was obtained at pH 5. The maximum removal of Zn (II) ion was obtained in pure zinc environment followed by Zn (II) – Fe (II, II), Zn (II) – Cu (II) and Zn (II) – Fe (II, III)- Cu (II) combination of ions.

The biosorption of metal ions in all the metal ion systems was quite low at pH 3. In case of pure zinc environment, the removal of Zn (II) ion was 30.34% at pH 3. In combination of heavy metals (Zn (II) –Cu (II), Zn (II) – Fe (II, III) and Zn – Cu (II)-Fe (II, III)), the removal of Zn (II) ion was 26.31%, 27.56% and 20.18%, respectively at pH 3. The lower percentage removal of Zn (II) ions or any other type of metal ion systems was due to extreme competition between hydrogen and metal ions present in the liquid phase.

The active binding sites are protonated at low pH resulting in the generation of repulsive forces between metal ions and active adsorption sites, which leads to underprivileged biosorption of metal ions (Mishra et al., 2011; Mishra et al., 2010). With the increase in pH from 3 to 5, the metal ion removal increased from 30.34% to 72.18%, 26.31% to 62.16%, 27.56% to 65.13% and 20.18 % to 44.16% for pure zinc, Zn (II) –Cu (II), Zn (II) – Fe (II, III) and Zn – Cu (II)-Fe (II, III), respectively.

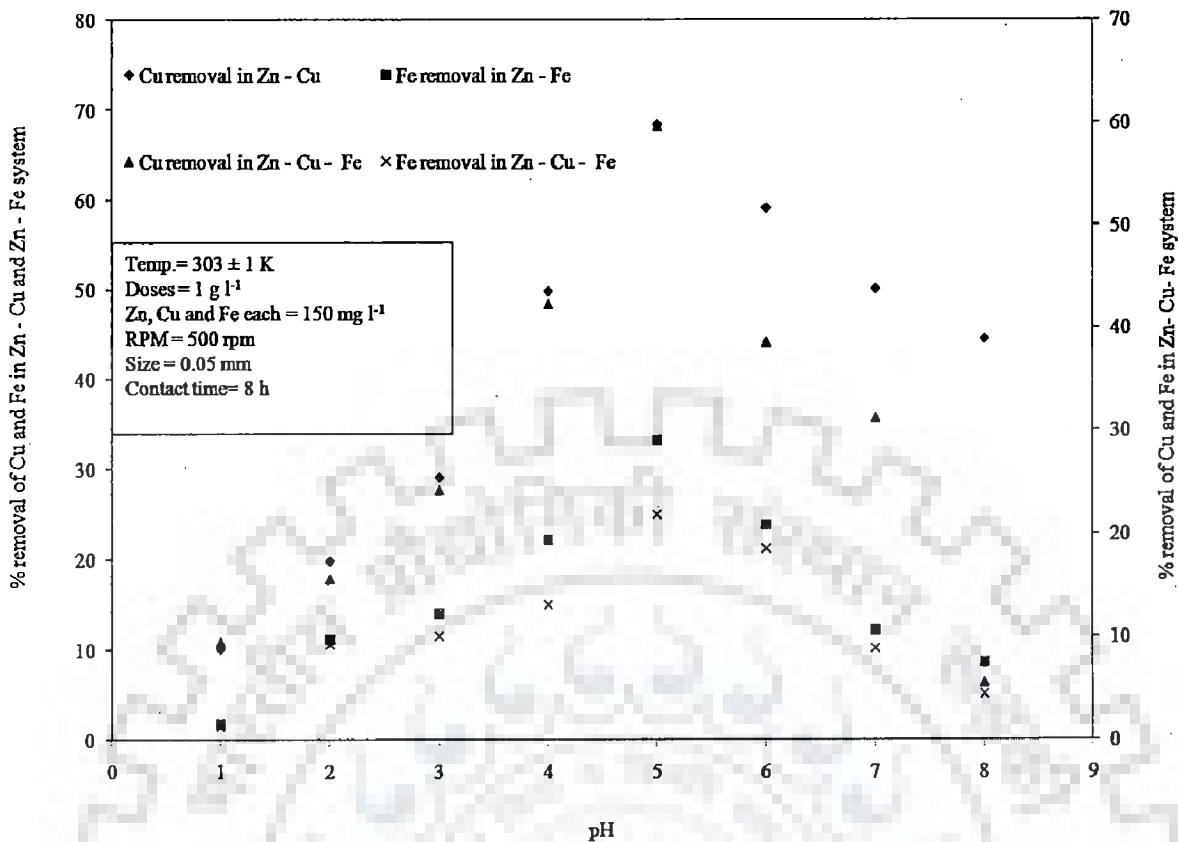


Figure 5.2.1 (n): Effect of pH on biosorption of Cu and Fe in presence of Zn on Eucalyptus leaf powder

The increase in pH leads to decrease in repulsive forces and generation of attractive forces between active sites of biosorbent and metal ions. Further increase in pH from 5 to 8, the percentage removal of Zn (II) ion in all types of metal ion systems was found to be decreasing. The decrease in percentage removal of Zn (II) above pH 5 was due to the fact that at higher pH values the active sites of biosorbent are denatured resulting in decrease in percentage removal of Zn (II) ion in all types of metal ion system (Sari and Tuzen 2008). Figure 5.2.1 (n) embodies data regarding the percentage removal of Cu (II) and Fe (II, III) ion in presence of zinc. The maximum removal of Cu(II) ions was obtained in Zn (II) - Cu (II) ion system at pH 5. Moreover, the lowest percentage removal was obtained in case of Zn(II) - Cu (II)- Fe (II, III) system. However, the maximum removal has been obtained in all the cases at pH 5. The order of removal obtained for metal ions was Cu (II) > Zn (II) > Fe (II, III). The maximum removal of Cu (II) and total Fe (II, III) obtained in case of Zn (II) - Cu (II) and Zn (II)- total Fe (II, III) was 68.38% and 33.18%, respectively. However, 59.64% and

21.86% removal of Cu (II) and total Fe (II, III) was obtained in Zn (II) – Cu (II) – total Fe (II, III), respectively.

Figure 5.2.1 (o) and Figure 5.2.1 (p) represent the influence of pH on biosorption of Zn (II), Cu (II) and Fe (II, III) ion on the surface of Eggshell and membrane powder. It is evident from figure 5.2.1 (o) that the peaks have been obtained for all the curves at pH 5. Moreover, the maximum 42.59% removal of Zn (II) ion was obtained in case of pure zinc at pH 5. The presence of other ions hindered the biosorption of Zn (II) ion in liquid phase. In the presence of Cu (II) ions, the removal of Zn (II) ion decreased to 39.36% at pH 5. Furthermore, presence of total Fe (II, III) also decreased the removal of Zn (II) ion from liquid phase.

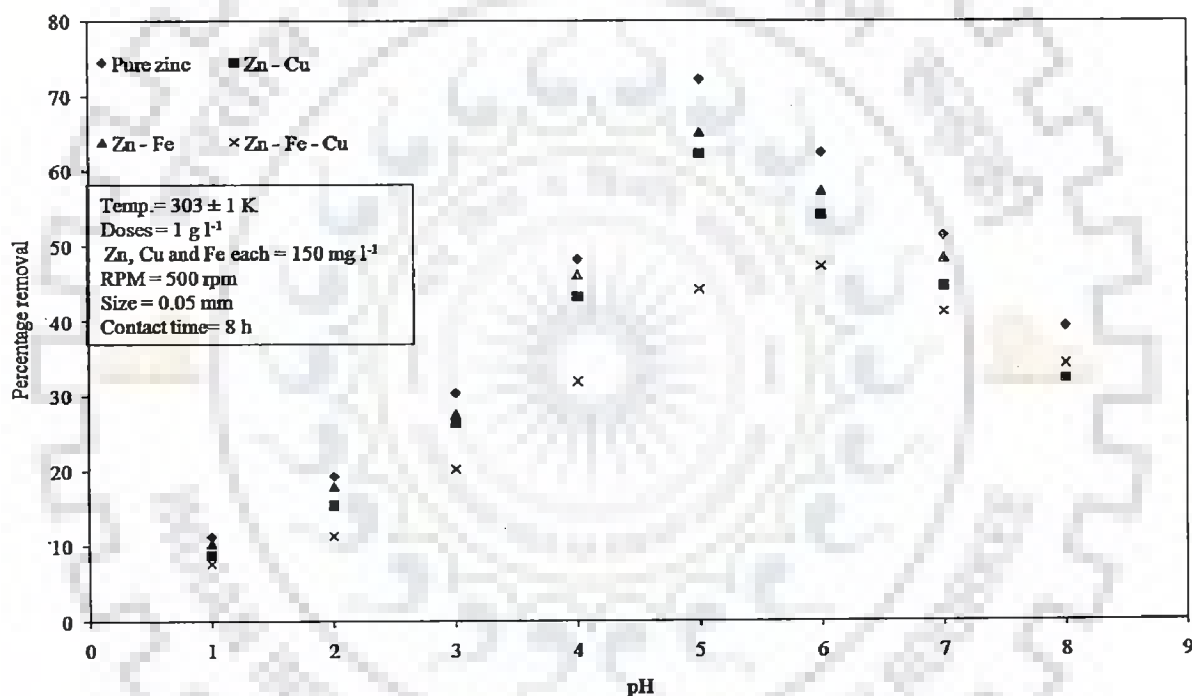


Figure 5.2.1 (o): Effect of pH on biosorption of Zn on Eggshell and membrane powder

The maximum removal of Zn (II) ion in presence of total Fe (II, III) was 42.18%. 35.11% Zn (II) ion was removed in case of Zn (II)- Cu(II)- Fe (II, III) system. However, in all cases, the maximum removal was obtained at pH 5. The maximum removal of Zn (II) ion was obtained in pure zinc environment followed by Zn (II) – Fe (II, II), Zn (II) – Cu (II) and Zn (II) – Fe (II, III)- Cu (II) combination of ions.



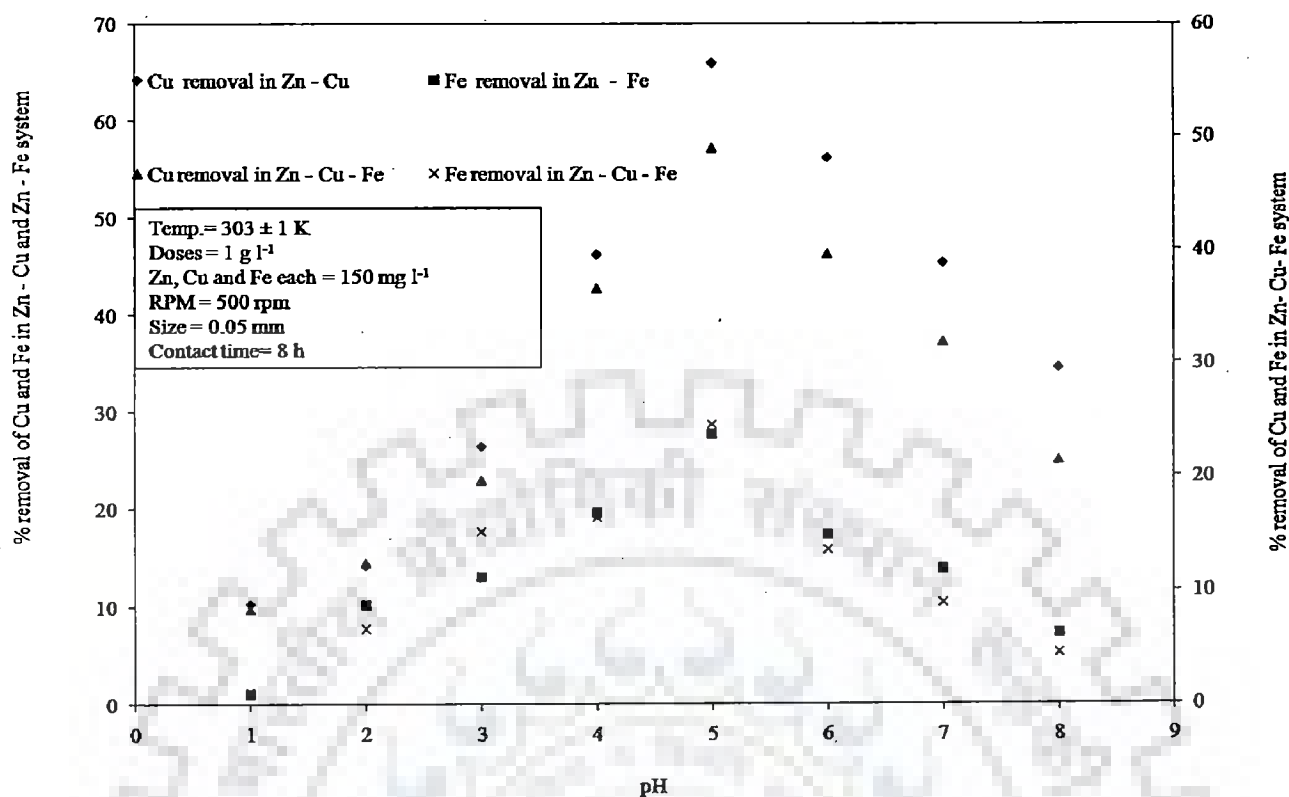


Figure 5.2.1 (p): Effect of pH on biosorption of Cu and Fe in presence of Zn on Eggshell and membrane powder

The biosorption of metal ions in all the metal ion systems was quite low at pH 3. In case of pure zinc environment, the removal of Zn (II) ion was 30.34% at pH 3. In combination of heavy metals (Zn (II) –Cu (II), Zn (II) – Fe (II, III) and Zn – Cu (II)-Fe (II, III)), the removal of Zn (II) ion was 16.36%, 12.31% and 10.36%, respectively at pH 3. The lower percentage removal of Zn (II) ions or any other type of metal ion systems was due to extreme competition between hydrogen and metal ions present in the liquid phase. The active binding sites are protonated at low pH resulting in the generation of repulsive forces between metal ions and active adsorption sites, which led to underprivileged biosorption of metal ions (Mishra et al., 2011, Mishra et al., 2010). With the increase of pH from 3 to 5, the metal ion removal increased from 16.36 to 42.59%, 12.31% to 29.36%, 14.21% to 42.18% and 10.36 % to 35.31% for pure zinc, Zn (II) –Cu (II), Zn (II) – Fe (II, III) and Zn – Cu (II)-Fe (II, III), respectively. The increase in pH leads to decrease in repulsive forces and generation of attractive forces between active sites of biosorbent and metal ions. Further increase in pH

from 5 to 8, the percentage removal of Zn (II) ion in all types of metal ion systems was found to be decreasing.

The decrease in percentage removal of Zn (II) above pH 5 was due to the fact that at higher pH values the active sites of biosorbent got denatured resulting in decrease in percentage removal of Zn (II) ion in all types of metal ion systems. Figure 5.2.1 (p) embodies data regarding the percentage removal of Cu (II) and Fe (II, III) ion removal in presence of zinc.

The maximum removal of Cu(II) ions was obtained in Zn (II) - Cu (II) ion system at pH 5. Moreover, the lowest percentage removal was obtained in case of Zn (II) - Cu (II) - Fe(II, III) system. However, the maximum removal has been obtained in all the cases at pH 5. The order of removal obtained for metal ions was Cu (II) > Zn (II) > Fe (II, III). The maximum removal of Cu (II) and total Fe (II, III) obtained in case of Zn (II) - Cu (II) and Zn (II) - total Fe (II, III) was 65.91% and 27.57%, respectively. However, 48.97% and 24.51% removal of Cu (II) and total Fe (II, III) was obtained in Zn (II) - Cu (II) - total Fe (II, III), respectively.

Figure 5.2.1 (q) and Figure 5.2.1 (r) represent the influence of pH on biosorption of Zn (II), Fe (II, III) and Cu (II) ion on the surface of *Zinc sequestering bacterium VMSDCM* accession no. HQ 108109 (dead cells). It is evident from figure 5.2.1 (q) that the peaks were obtained for all the curves at pH 5.

Moreover, the maximum 100% removal of Zn (II) ion was obtained in case of pure zinc at pH 7. The presence of other ions hindered the biosorption of Zn (II) ion in liquid phase. In the presence of Cu (II) ions, the removal of Zn (II) ion decreased to 86.66% at pH 7. Furthermore, presence of total Fe (II, III) also decreased the removal of Zn (II) ion from liquid phase.

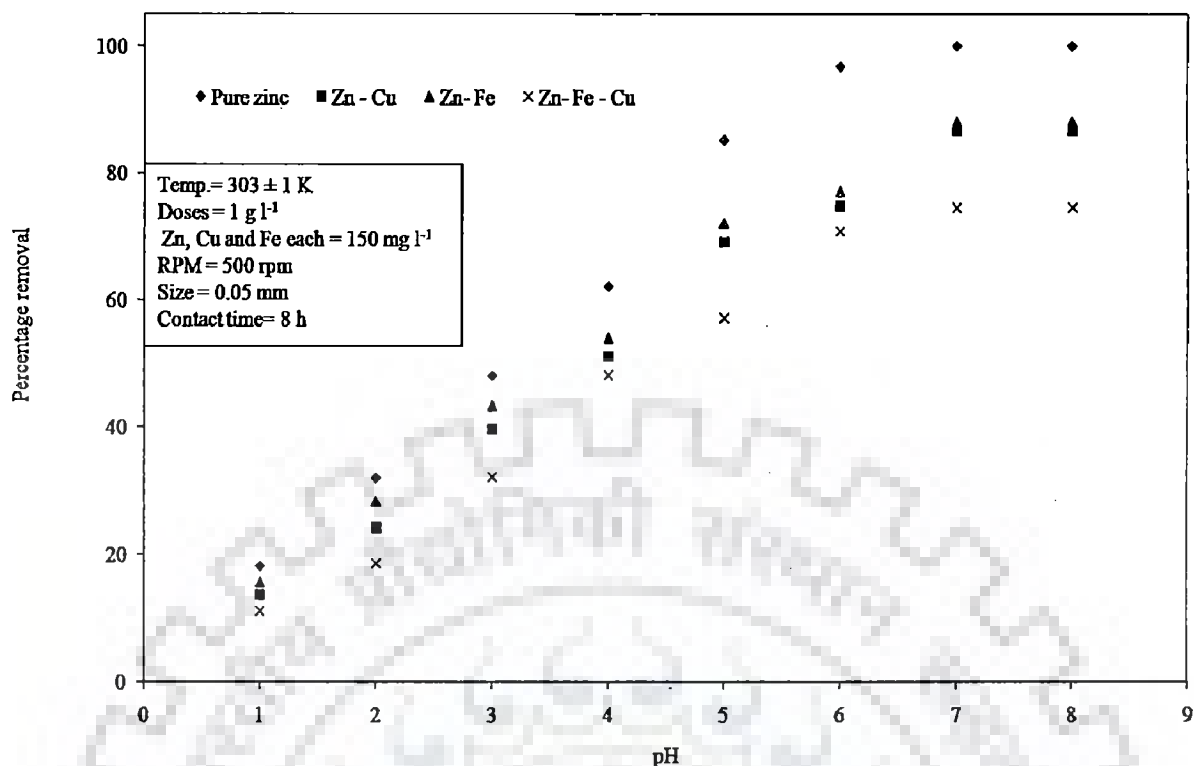


Figure 5.2.1 (q): Effect of pH on biosorption of Zn on dead cells of *Zinc sequestering bacterium VMSDCM* accession no. HQ108109

It is evident from figure 5.2.1 (q) that the peaks were obtained for all the curves at pH 7. Moreover, the maximum 100% removal of Zn (II) ion was obtained in case of pure zinc at pH 7. The presence of other ions hindered the biosorption of Zn (II) ion in liquid phase.

In the presence of Cu (II) ions, the removal of Zn (II) ion decreased to 86.66% at pH 7. Furthermore, presence of total Fe (II, III) also decreased the removal of Zn (II) ion from liquid phase. The maximum removal of Zn (II) ion in presence of total Fe (II, III) was 88.19% . 74.61% Zn (II) ion was removed in case of Zn (II)- Cu (II)- Fe (II, III).

However, in all the cases, the maximum removal was obtained at pH 7. The maximum removal of Zn (II) ion was obtained in pure zinc environment followed by Zn (II) – Fe (II, II), Zn (II) – Cu (II) and Zn (II) – Fe (II, III)- Cu (II) combination of ions. The biosorption of metal ions in all the metal ion systems was quite low at pH 3. In case of pure zinc environment, the removal of Zn (II) ion was 48.09% at pH 3. In other combination of heavy

metals (Zn (II) –Cu (II), Zn (II) – Fe (II, III) and Zn – Cu (II)-Fe (II, III)), the removal of Zn (II) ion was 39.64%, 43.19% and 32.16%, respectively at pH 3.

The lower percentage removal of Zn (II) ions or any other type of metal ion systems was due to extreme competition between hydrogen and metal ions present in the liquid phase. The active binding sites got protonated at low pH resulting in the generation of repulsive forces between metal ions and active adsorption sites, which led to underprivileged biosorption of metal ions (Mishra et al., 2011, Mishra et al., 2010).

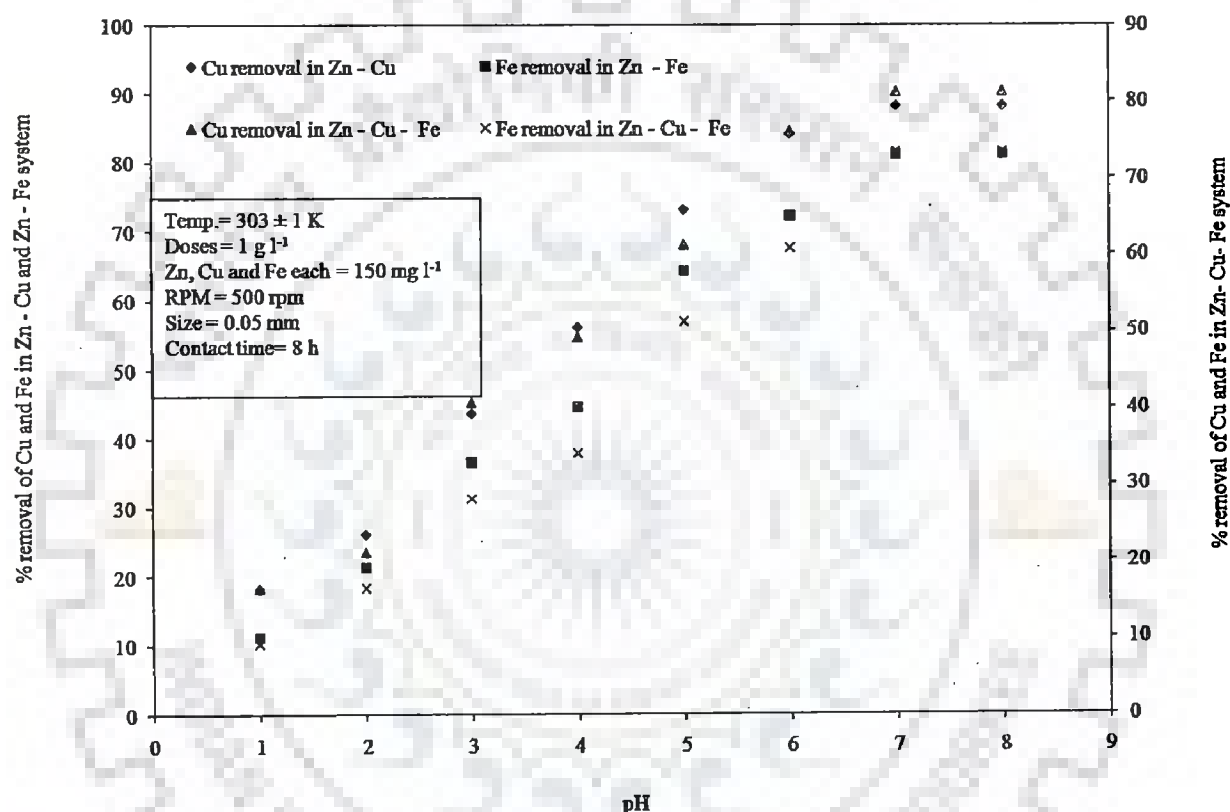


Figure 5.2.1 (r): Effect of pH on biosorption of Cu and Fe in presence of Zn on dead cells of *Zinc sequestering bacterium VMSDCM* accession no. HQ108109

With the increase in pH from 3 to 7, the metal ion removal increased from 48.09% to 100%, 39.64% to 89.66%, 43.19% to 88.19% and 32.16% to 74.61% for pure zinc, Zn (II) – Cu (II), Zn (II) – Fe (II, III) and Zn – Cu (II)-Fe (II, III), respectively. The increase in pH leads to decrease in repulsive forces and generation of attractive forces between active sites of biosorbent and metal ions. Figure 5.2.1 (r) embodies data regarding the percentage removal of

Cu (II) and Fe (II, III) ion in presence of zinc. The maximum removal of Cu(II) ions was obtained in Zn (II) - Cu (II) ion system at pH 7. Moreover, the lowest percentage removal was obtained in case of Zn (II) - Cu (II) - Fe (II, III) system. However, maximum removal has been obtained in all the cases at pH 7. The order of removal obtained for metal ions was Cu (II) > Zn (II) > Fe (II, III). The maximum removal of Cu (II) and total Fe (II, III) obtained in case of Zn (II) – Cu (II) and Zn (II)– total Fe (II, III) was 84.19% and 81.1%, respectively. However, 81.23% and 73.34% removal of Cu (II) and total Fe (II, III) was obtained in Zn (II) – Cu (II) – total Fe (II, III), respectively. Table 5.2.1 represents the comparison between the uptake capacities various sorts of living and non-living biomasses in various experimental conditions.

Table 5. 2. 1: Uptake capacities of zinc by various living and non-living microorganism

Name of biomass	Physiological stage	Initial metal ion conc. (mg l <sup>-1</sup> )	pH	Temp. (°C)	Uptake capacity (mg g <sup>-1</sup> )	Percent. removal	Reference
<i>Pseudomonas putida</i>	Inactive	1000	7.0-7.5	N. D	6.9	80	Pardo et al., 2003
<i>Sterptomyces rimosus</i>	Inactive	100	7.5	20	30	N.D	Mameri et al., 1999
<i>Bacillus firmus</i>	Polysaccharide (Inactive)	0-500	6	25	418	61.8	Salehizadeh and Shojaosadati, 2003
<i>Bacillus firmus</i>	Polysaccharide (Inactive)	0-2000	6	25	722	61.8	Salehizadeh and Shojaosadati, 2003
<i>Pseudomonas veronii</i> 2E	Living	32690	7.5	32	N.D	50	Vullo et al., 2008
Biological sludge	Aerobic (Living)	450	5-6, uncontrolled	20±1	138.30	18.1	Artola and Rigola, 1992

	Thickened (Living)	313.20	5-6, uncontrolled	20±1	28.39	32.7	Artola and Rigola, 1992
	Anaerobic (Living)	455.50	5-6, uncontrolled	20±1	38.38	27.5	Artola and Rigola, 1992
	Dewatered (Inactive)	312.50	5-6, uncontrolled	20±1	33.87	43.4	Artola and Rigola, 1992
	Dehydrated (Inactive)	312.50	5-6, uncontrolled	20±1	12.15	16.6	Artola and Rigola, 1992
<i>Pseudomonas putida</i> CZ1	Living	6.5 - 279.4	5	30	24.4±0.5	N.D	Chen et al., 2005
<i>Pseudomonas putida</i> CZ1	Inactive	6.5 - 279.4	5	30	14.4 ± 0.81	N. D	Chen et al., 2005
<i>Pseudomonas putida</i> strain B14	Living	65380	7	5	N.D	80	Andreoni, et al., 2003
<i>Bacillus circulans</i> strain EB 1	Living	N.D	7	37	22 (mg/l)	68	Yilmaz et al., 2003
Bacterial strain W-6	Living	100	6	40	27.63 (mg/l)	81.68	Yaman and Zia, 2010
<i>Brevibacterium</i> sp. strain HZM-1	Living	0-653800	3	30	42	N. D	Taniguchi et al., 2000
<i>Aphanothece halophytica</i>	Living	0-47.9	6.5	30	133	-	Incharoenakdi and Kitjaharn, 2002

<i>Streptoverticillium cinnamoneum</i>	Living	65.38 - 114415	6.5	28±3	22.7±0.9	100	Puranik and Panikar, 1999
<i>Streptoverticillium cinnamoneum</i>	Chemically or physically pretreated cell (Inactive)	65.38 - 114415	6.5	28±3	6.9 -24.8	reduced by 22 – 78%	Puranik and Panikar, 1999
<i>Sterptomyces rimosus</i>	Chemically pretreated (Inactive)	100	7.5	20	80	N. D	Mameri et al.,1999
<i>Thiobacillus ferrooxidans</i>	Inactive	100	6	25	82.61	N. D	Celaya et al., 2000
<i>Thiobacillus ferrooxidans</i>	Chemically pretreated (Living)	25-150	6	40	172.4	N. D	Liu et al., 2004
<i>Pseudomonas syringae</i>	Living	0-13	N. D	22	8	N. D	Cabral, 1992
<i>Streptomyces noursei</i>	Living	0.6-65	5.8	30	1.6	N. D	Mattuschka and Straube 1993
<i>Geobacillus thermoleovorans</i> sub.sp. <i>strombolien sis</i> (G2)	Inactive	10 - 300	4	70	29	N. D	Ozdermir et al., 2009
<i>Geobacillus toebii</i> sub.sp. <i>decanicus</i> (G1)	Inactive	10 - 300	5	80	21.1	N. D	Ozdermir et al., 2009
<i>Geobacillus thermodentrificans</i>	Inactive	88	5	65±1	42.9	9.02 – 55.14	Charterje et al., 2010

<i>Pseudomonas aeruginosa</i>	Living	70	7	30	77.5	87.7	Silva et al., 2009
AT 18							
<i>Sphaerotilus natans</i>	Living	3.6 - 901.4	6.0-7.5	30	3.4-741.4	N. D	Lodi et al., 1998
<b>Zinc sequestering bacterium VMSDCM</b> Accession no. HQ108109 (dead cells)	<b>Inactive</b>	<b>150</b>	<b>7</b>	<b>30 ± 0.5</b>	<b>150</b>	<b>100</b>	<b>Present study</b>
<i>Cedrus deodara</i> sawdust (CDS)	<b>Inactive</b>	<b>150</b>	<b>5</b>	<b>30 ± 0.5</b>	<b>133.5</b>	<b>89.19</b>	<b>Present study</b>

It is clear from table 5.2.1 that the uptake capacity of dead cells of *Zinc sequestering bacterium VMSDCM* accession no. HQ108109 has tremendous potential of up taking zinc from liquid phase. However, these uptake capacities cited in table 5.2.1 have been derived in various types of experimental condition. However, the analysis of the data cited in table 5.2.1 presents the valuable comparative analysis of various sorts of biomasses with the present study.

#### **Concluding remarks of the section 5.2.1**

Among all the biosorbents selected, the two most suitable biosorbent for the biosorption of Zn (II) ion in liquid phase were *Cedrus deodara* sawdust and dead cells of *Zinc sequestering bacterium VMSDCM* accession no. HQ108109 (dead cells). The maximum removal of Zn (II) ion obtained in case of *Cedrus deodara* sawdust and dead biomass of *Zinc sequestering bacterium VMSDCM* accession no. HQ108109 were at pH 5 and pH 7, respectively. The rationale behind the order of the removal of metal ions, i.e., Cu (II) > Zn (II) > Fe (II, III) ion was due to the difference in the molecular weights of Cu (II) and Zn (II) ion.



The molecular weight of Zn (II) ion is  $65.41 \text{ g mol}^{-1}$  and the molecular weight of Cu (II) ion is  $63.55 \text{ g mol}^{-1}$ . The mobility of heavier metal ion from liquid to solid phase is quite less compared to the mobility of heavier metal ion (Dang et al. 2009). Sengil and Ozacar (2009) reported that greater the atomic weight, electronegativity, electrode potential and ionic size, greater is the affinity of metal ions towards sorption. Contrary to this, Chatterjee et al., 2010 reported that the metal ions with smaller ionic radii adsorb quickly on active sites of adsorbents. The ionic radii of total Fe (II, III) are 73.8 pm and 77 pm. The ionic radii of Cu (II) and Zn (II) are 87 pm and 88 pm, respectively. In the present investigation, the biosorption of Fe (II, III) ion was the lowest. The difference between the ionic radii of Cu (II) and Zn (II) was quite small however the difference between the electronegativities of Cu (II) ion (1.90 in Pauling scale) and Zn (II) (1.65 in Pauling scale) is quite significant. Hence, the present study revealed that the more pronounced biosorption of Cu (II) ion over Zn (II) was due to large electronegativity and low molecular weight and the lowest sorption of Fe (II, III) ion among all the three metals was due to its smallest ionic size.

### 5.2.2 Optimization of temperature

This section embodies the results of influence of temperature on biosorption of Zn (II) ion in liquid phase. The experiments were conducted from 298 K to 318 K. The metal ion combinations used were pure zinc, Zn (II) – Cu(II), Zn (II) – Fe (II, III) and Zn (II) – Fe (II, III)- Cu (II). The system of ions studied in the present work were pure zinc, Zn (II)- Cu (II), Zn (II)- Fe (II, III) and Zn (II) – Fe (II, III)- Cu (II). The metal ions Zn (II), Cu (II) and Fe (II, III) are referred as Zn, Cu and Fe in various figures. Results of influence of temperature have been shown in figures 5.2.2 (a) to 5.2.2 (r).

Figure 5.2.2 (a) and figure 5.2.2 (b) represent the influence of temperature on biosorption of Zn (II), Fe (II, III) and Cu (II) ion in liquid phase on the surface of Mango bark sawdust. It is evident from figure 5.2.2 (a) that the maximum removal of Zn (II) ion was obtained in pure zinc phase. The maximum removal of Zn (II) ion was 84.88% at 303 K. The presence of other metal ions hindered the biosorption of Zn (II) ion. The maximum removal

of total Fe (II, III) and Cu (II) ion in Zn (II) – Cu (II), Zn – Fe (II) and Zn (II)- Cu (II)- Fe (II, III) were also obtained at 303 K (Figure 5.2.2 b).

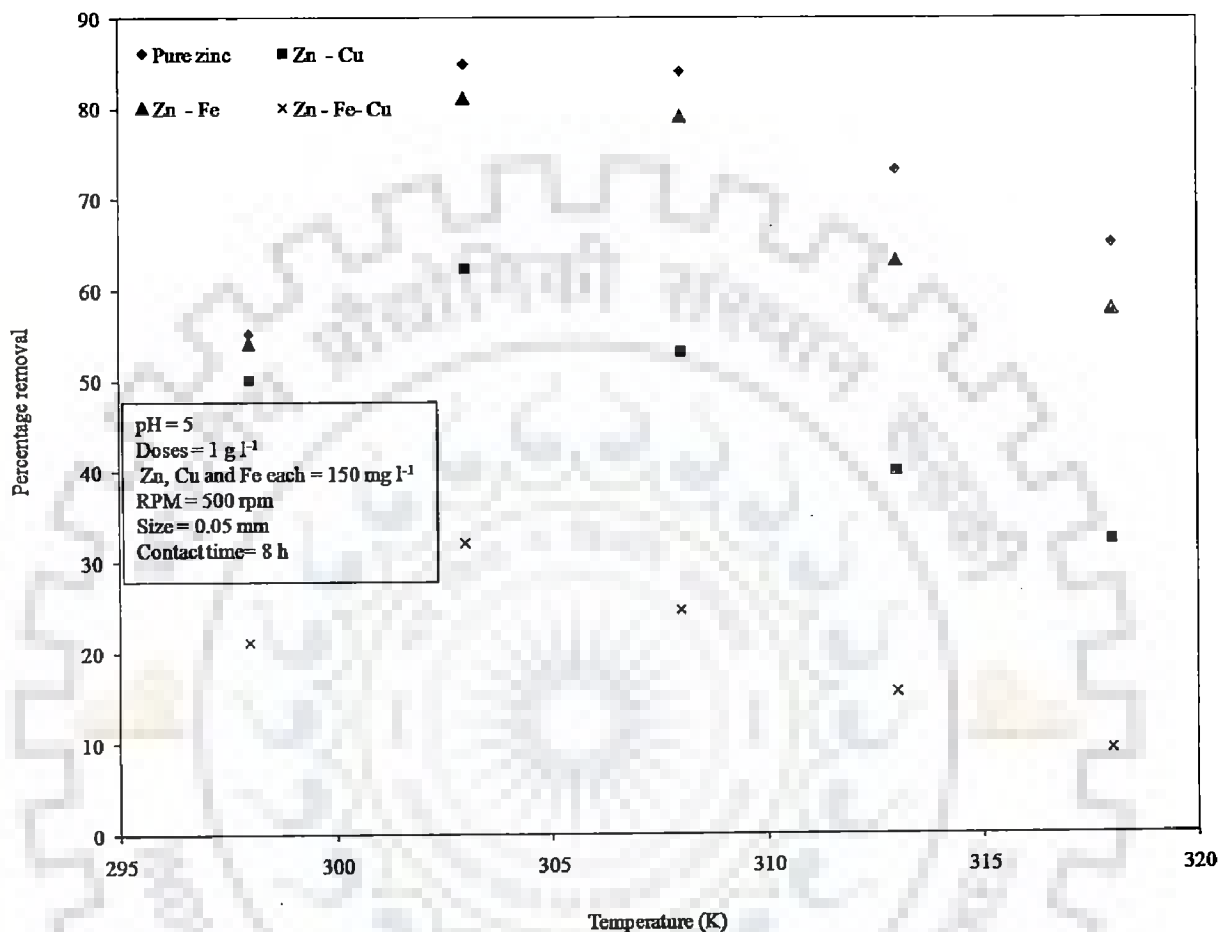


Figure 5.2.2 (a): Effect of temperature on biosorption of Zn on mango bark sawdust

The rise in temperature from 298 K to 303 K favoured the biosorption of Zn (II), Fe (II, III) and Cu (II) in all types of metal ion systems.

Further, the rise in temperature from 303 K to 318 K did not favour the biosorption of Zn (II), Fe (II, III) and Cu (II) ion in liquid phase. The decrease in biosorption of Zn (II), Fe (II, III) and Cu (II) in liquid phase in all the types of metal ion system at the rise of temperature from 303 K to 318 K was due to fact that the rise in temperature changed or

deformed the texture of biosorbent (Areco et al., 2010). The change in texture of biosorbent resulted in loss of biosorption capacity. The preferential order of removal of heavy metal ions was Cu (II) > Zn (II) > Fe (II, III).

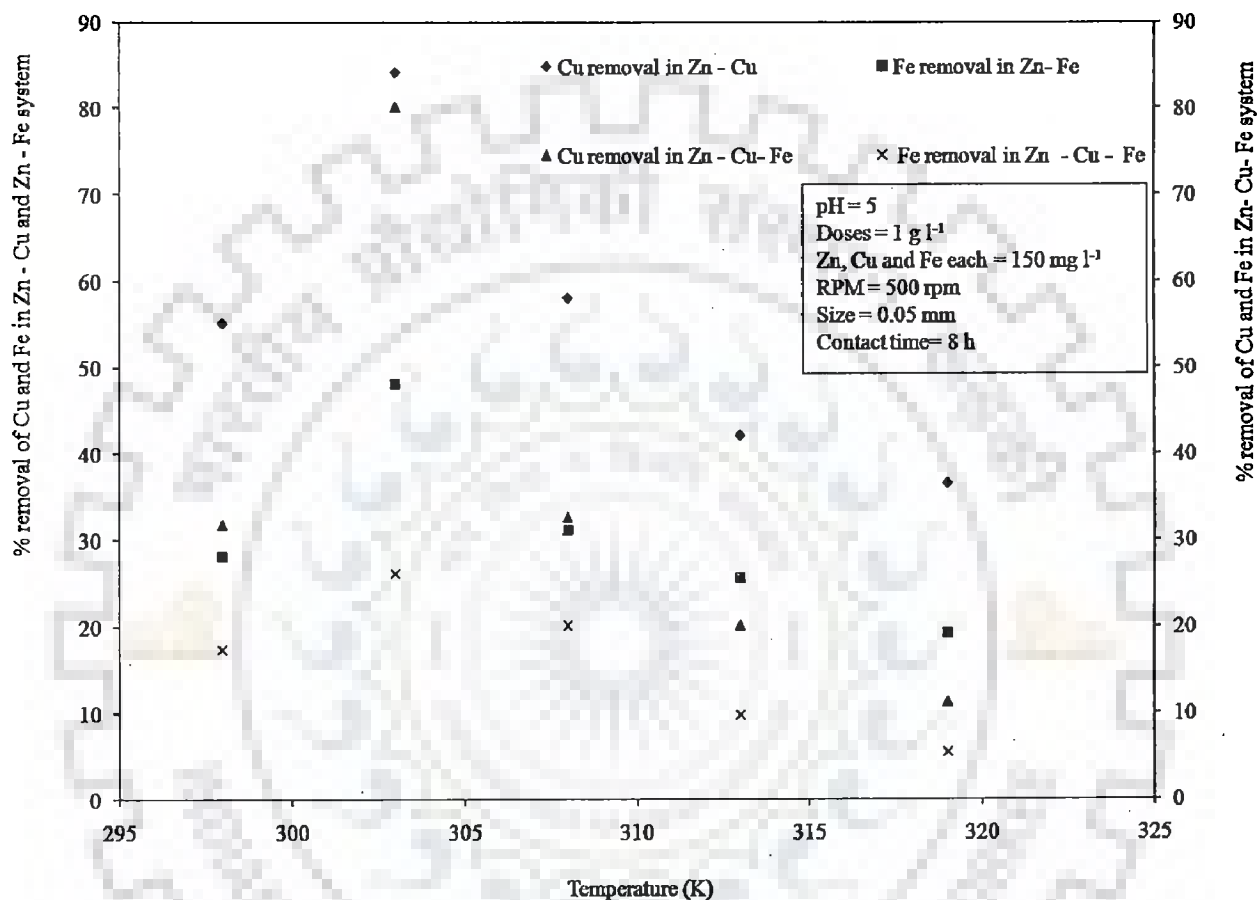


Figure 5.2.2 (b): Effect of temperature on biosorption of Cu and Fe in presence of Zn on mango bark sawdust

Figure 5.2.2 (c) and figure 5.2.2 (d) represent the influence of temperature on biosorption of Zn (II), total Fe (II, III) and Cu (II) on Orange peel in liquid phase. It is evident from figure 5.2.2 (c) that the maximum removal of Zn (II) ion was obtained in pure zinc phase. The maximum removal of Zn (II) ion were also 80.21% at 303 K.

The maximum removal of total Fe (II, III) and Cu (II) ion in Zn (II) – Cu (II), Zn – Fe (II) and Zn (II)- Cu (II)- Fe (II, III) was obtained at 303 K (Figure 5.2.2 (d)). The presence of other metal ions hindered the biosorption of Zn (II) ion. The rise in temperature from 298 K to 303 K favoured the biosorption of Zn (II), Cu (II) and Fe (II, III) in all types of metal ion systems.

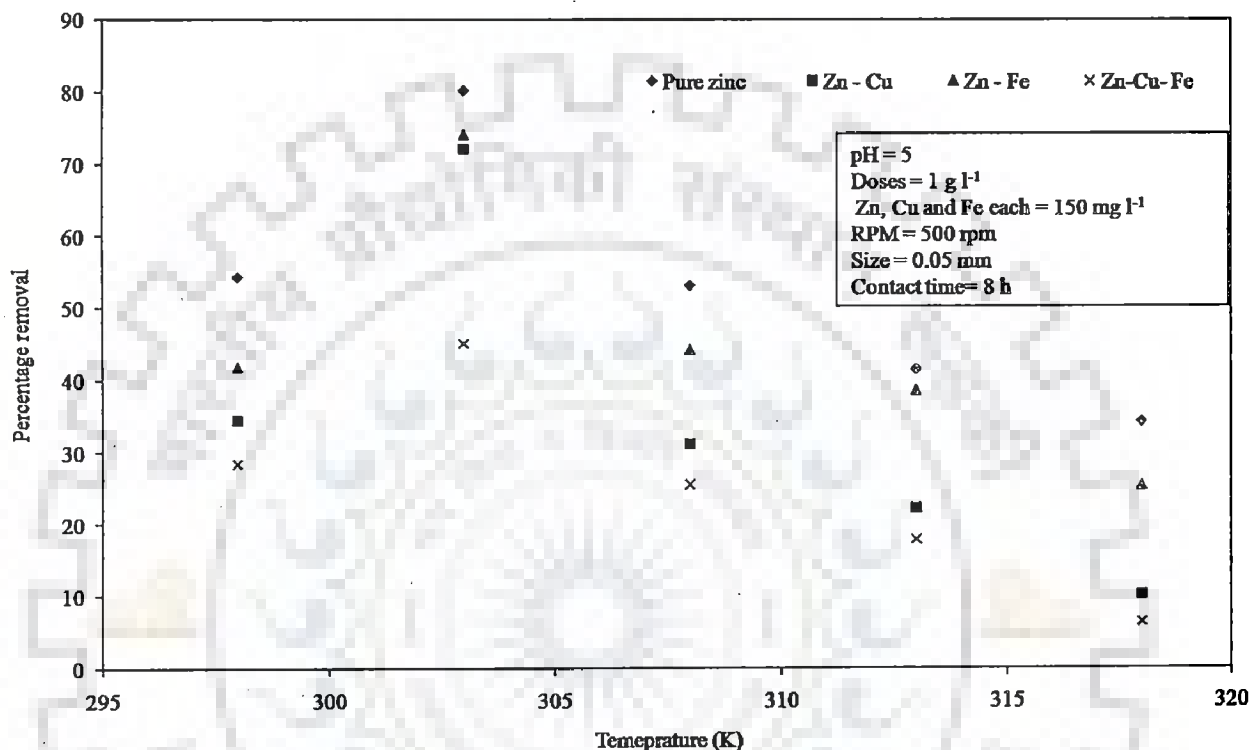


Figure 5.2.2 (c): Effect of temperature on biosorption of Zn on orange peel

Further, the rise in temperature from 303 K to 318 K did not favour the biosorption of Zn (II), Fe (II, III) and Cu (II) ion in liquid phase. The decrease in biosorption of Zn (II), Fe (II, III) and Cu (II) in liquid phase in all the types of metal ion system with the rise of temperature from 303 K to 318 K was due to fact that the rise in temperature changed or deformed the texture of biosorbent (Areco et al., 2010). The change in texture of biosorbent resulted in loss of biosorption capacity. The preferential order of removal of heavy metal ions was Cu (II) > Zn (II) > Fe (II, III).

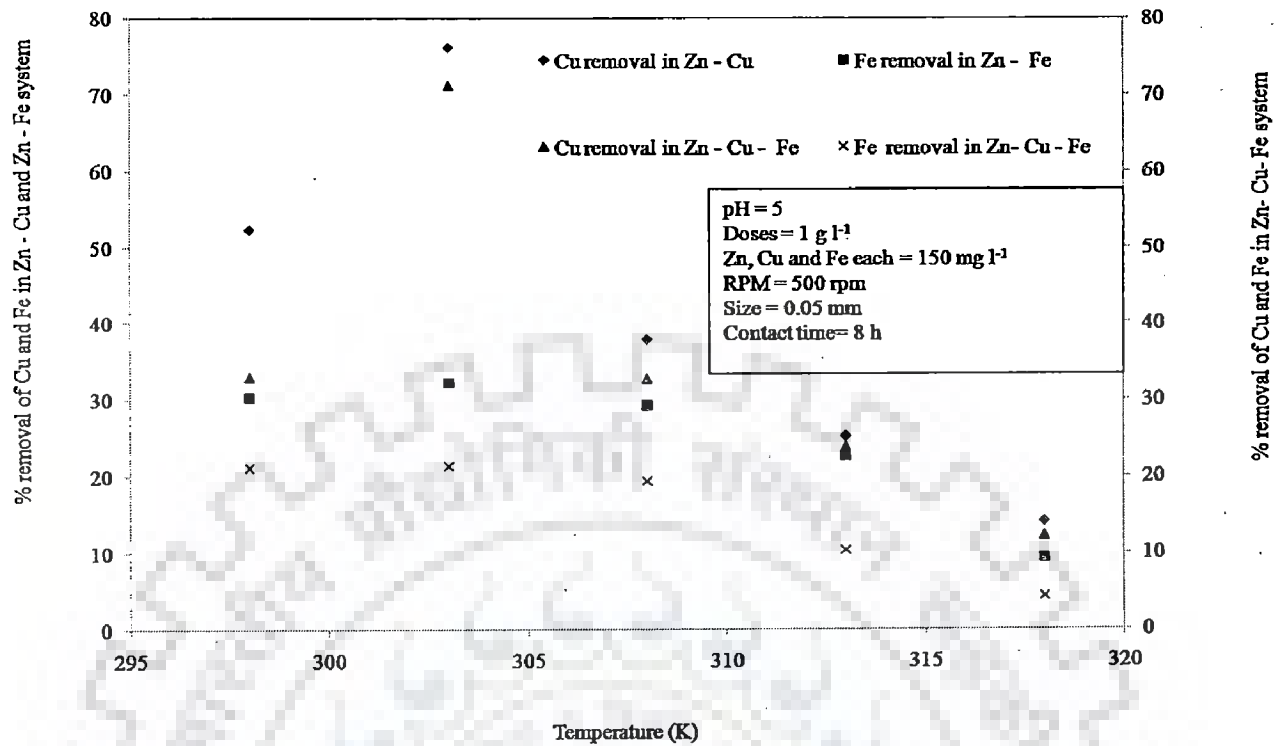


Figure 5.2.2 (d): Effect of temperature on biosorption of Cu and Fe in presence of Zn on Orange peel

Figure 5.2.2 (e) and figure 5.2.2 (f) represent the influence of temperature on biosorption of Zn (II), total Fe (II, III) and Cu (II) on Pineapple peel in liquid phase. It became evident from figure 5.2.2 (e) that the maximum removal of Zn (II) ion was obtained in pure zinc phase. The maximum removal of Zn (II) ion was 66.2% at 303 K. The presence of other metal ions hindered the biosorption of Zn (II) ion.

The rise in temperature from 298 K to 303 K favoured the biosorption of Zn (II), Fe (II, III) and Cu (II) in all the types of metal ion systems. The maximum removal of total Fe (II, III) and Cu (II) ion in Zn (II) – Cu (II), Zn – Fe (II) and Zn (II)- Cu (II)- Fe (II, III) were also obtained at 303 K (Figure 5.2.2 (f)). Further, the rise in temperature from 303 K to 318 K did not favour the biosorption of Zn (II), Fe (II, III) and Cu (II) ion in liquid phase.

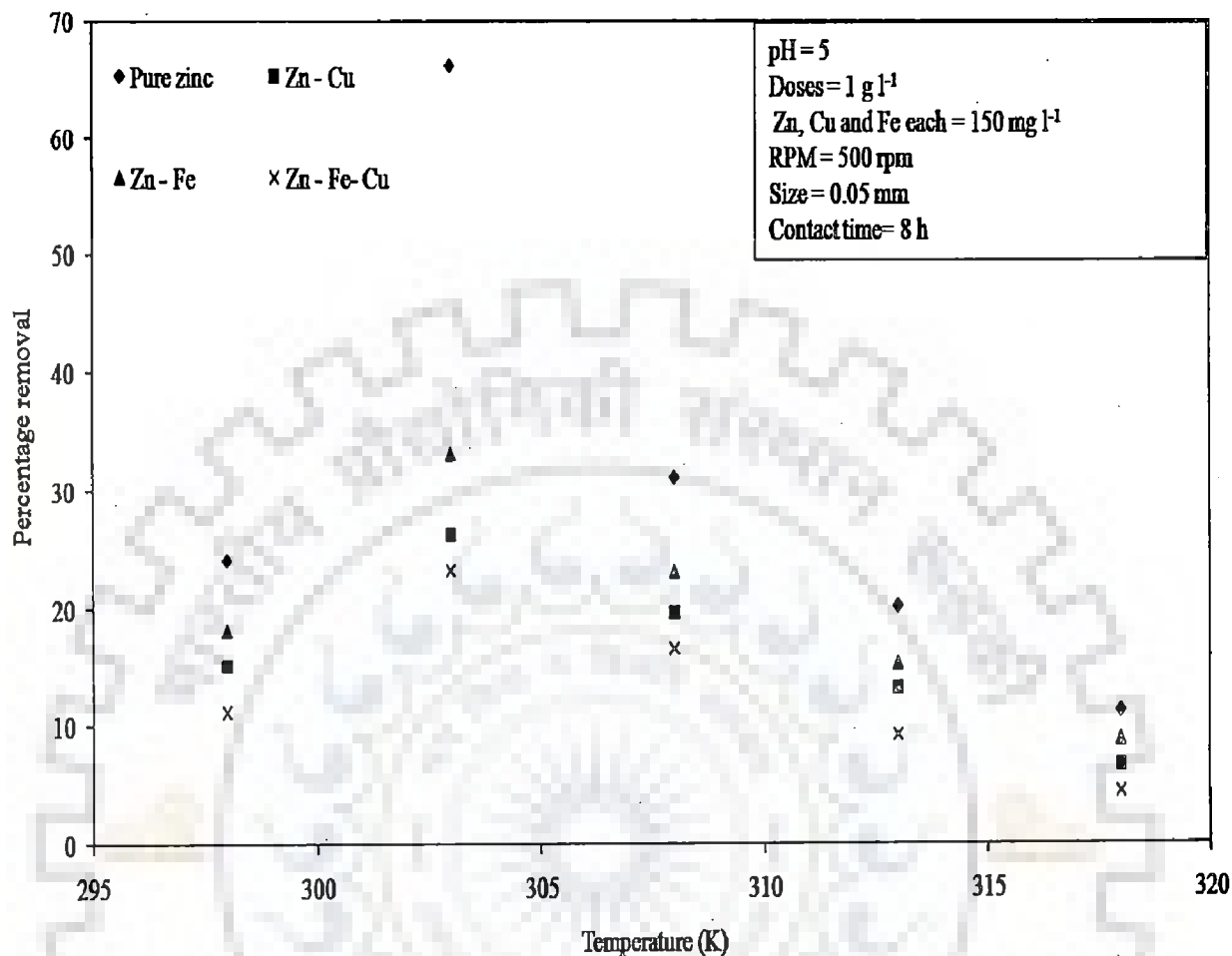


Figure 5.2.2 (e): Effect of temperature on biosorption of Zn on Pineapple peel

The decrease in biosorption of Zn (II), Fe (II, III) and Cu (II) in liquid phase in all the types of metal ion system with the rise of temperature from 303 K to 318 K was due to the fact that the rise in temperature changed or deformed the texture of biosorbent (Areco et al., 2010). The change in texture of biosorbent resulted in loss of biosorption capacity. The preferential order of removal of heavy metal ions was Cu (II) > Zn (II) > Fe (II, III).

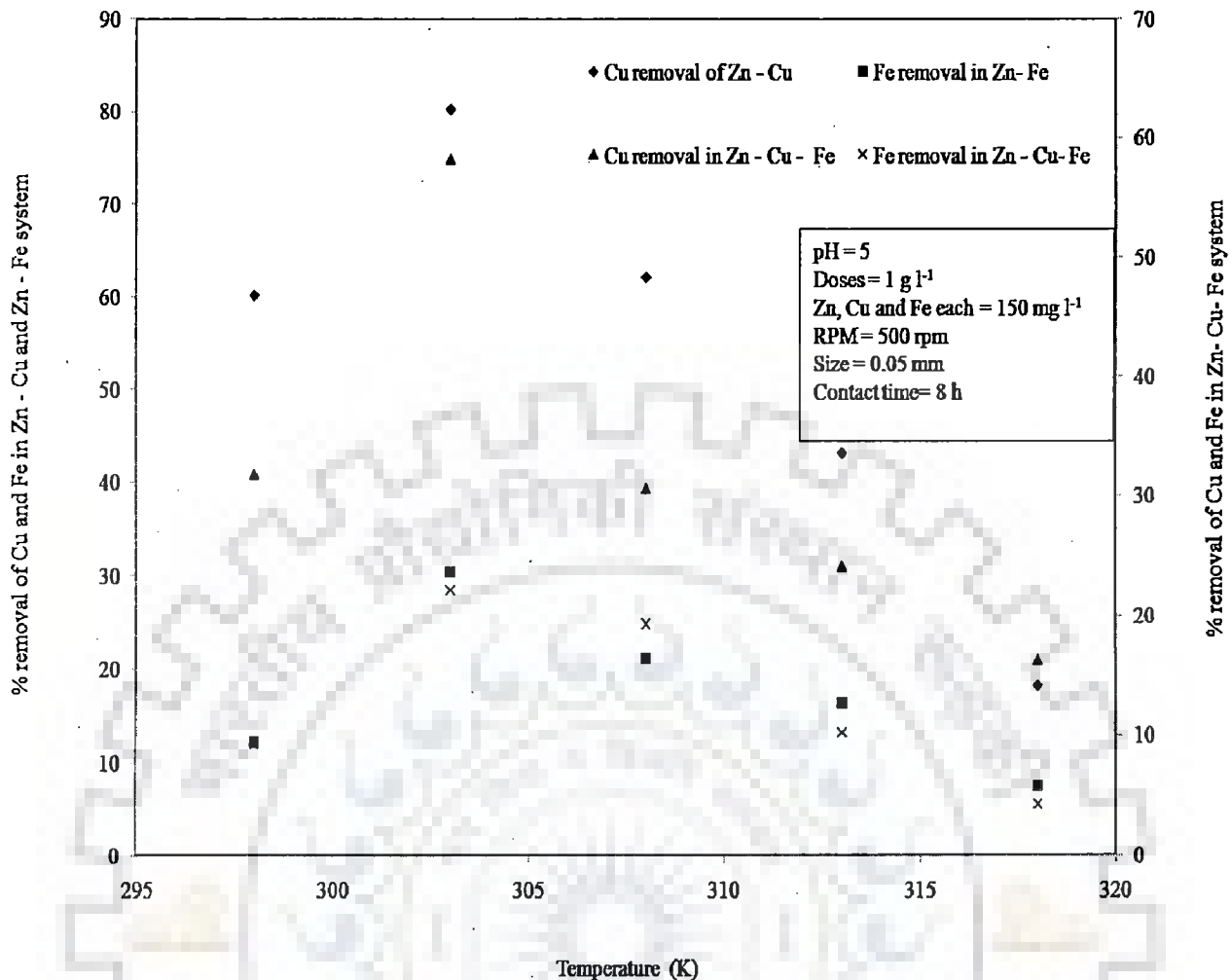


Figure 5.2.2 (f): Effect of temperature on biosorption of Cu and Fe in presence of Zn on Pineapple peel

Figure 5.2.2 (g) and figure 5.2.2 (h) represent the influence of temperature on biosorption of Zn (II), total Fe (II, III) and Cu (II) on Jackfruit peel in liquid phase. It is evident from figure 5.2.2 (g) that the maximum removal of Zn (II) ion was obtained in pure zinc phase. The maximum removal of Zn (II) ion was 42.1% at 303 K. The presence of other metal ions hindered the biosorption of Zn (II) ion. The rise in temperature from 298 K to 303 K favoured the biosorption of Zn (II), Fe (II, III) and Cu (II) in all the types of metal ion systems. The maximum removal of total Fe (II, III) and Cu (II) ion in Zn (II) – Cu (II), Zn – Fe (II) and Zn (II)- Cu (II)- Fe (II, III) was obtained also at 303 K (figure 5.2.2 (h)).

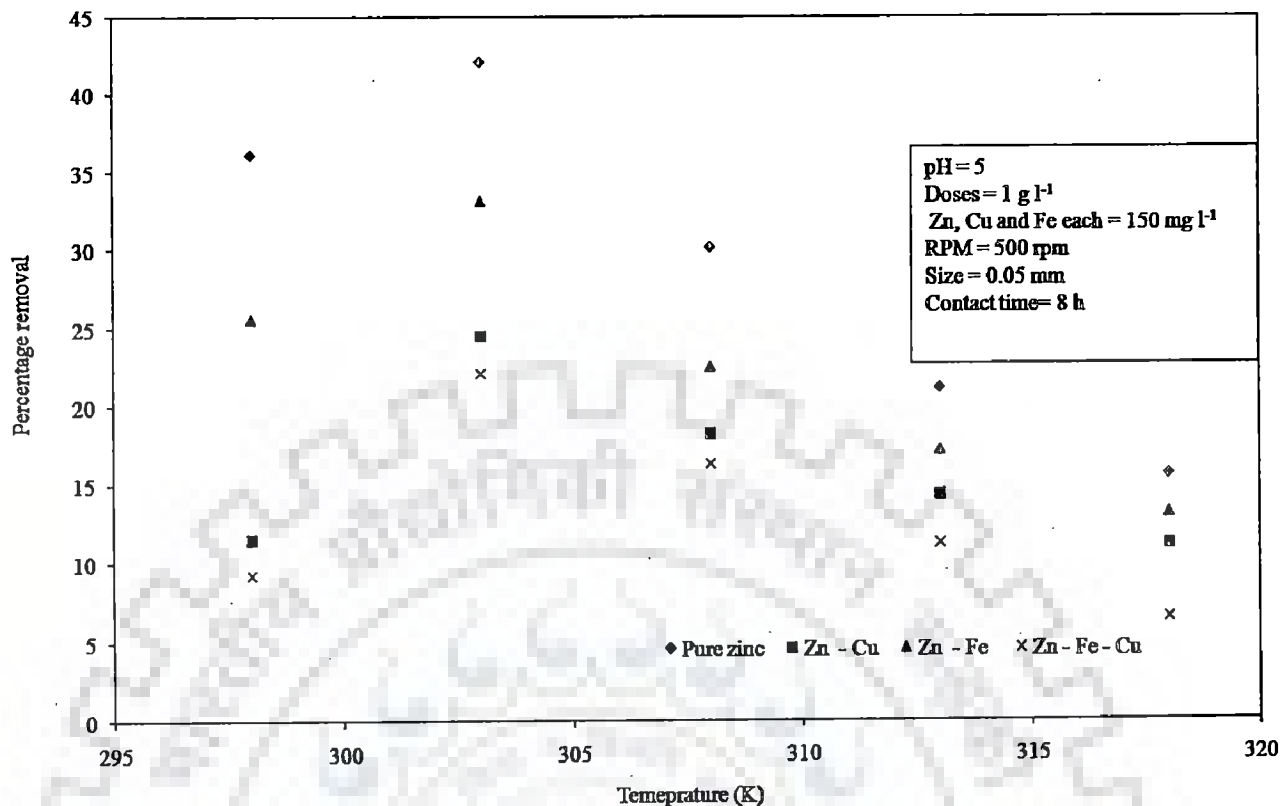


Figure 5.2.2 (g): Effect of temperature on biosorption of Zn on Jackfruit peel powder

Further, the rise in temperature from 303 K to 318 K did not favour the biosorption of Zn (II), Fe (II, III) and Cu (II) ion in liquid phase. The decrease in biosorption of Zn (II), Fe (II, III) and Cu (II) in liquid phase in all the types of metal ion system at the rise of temperature from 303 K to 318 K was due to fact that the rise in temperature changed or deformed the texture of biosorbent (Areco et al. 2010). The change in texture of biosorbent resulted in loss of biosorption capacity. The preferential order of removal of heavy metal ions was Cu (II) > Zn (II) > Fe (II, III) at 303 K.



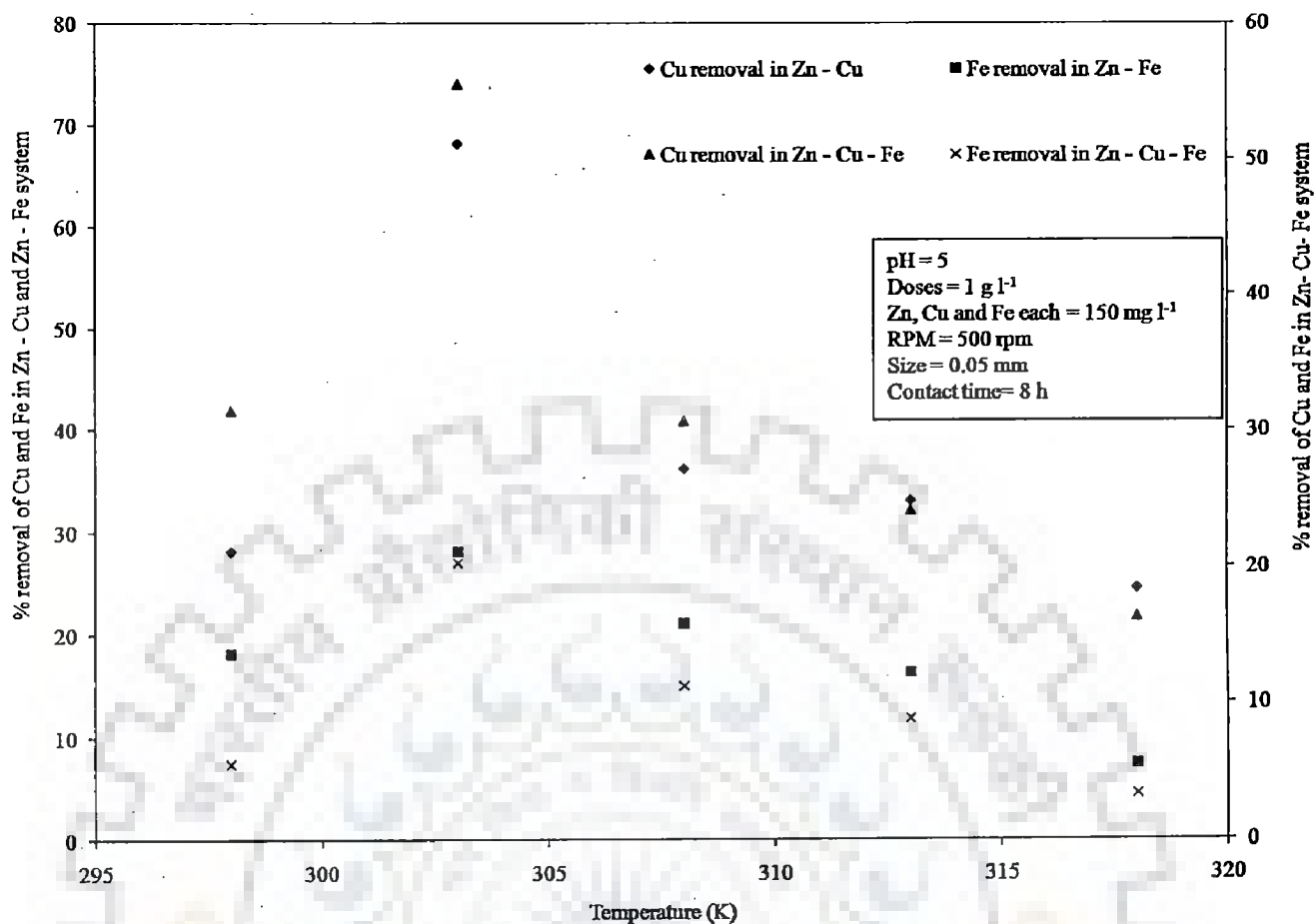


Figure 5.2.2 (h): Influence of temperature on biosorption of Cu and Fe in presence of Zn on Jackfruit peel powder

Figure 5.2.2 (i) and figure 5.2.2 (j) represent the influence of temperature on biosorption of Zn (II), total Fe (II, III) and Cu (II) on *Cedrus deodara* sawdust in liquid phase. It is evident from figure 5.2.2 (i) that the maximum removal of Zn (II) ion was obtained in pure zinc phase. The maximum removal of Zn (II) ion was 95.29% at 318 K. The presence of other metal ions hindered the biosorption of Zn (II) ion. The rise in temperature from 298 K to 318 K favoured the biosorption of Zn (II) in all the types of metal ion systems. The maximum removal of total Fe (II, III) and Cu (II) ion in Zn (II) – Cu (II), Zn – Fe (II) and Zn (II)- Cu (II)- Fe (II, III) was also obtained at 303 K (figure 5.2.2 (j)). In various types of other metal ion systems, the biosorption of Zn (II) ion between 303 K to 318 K did not increase significantly.

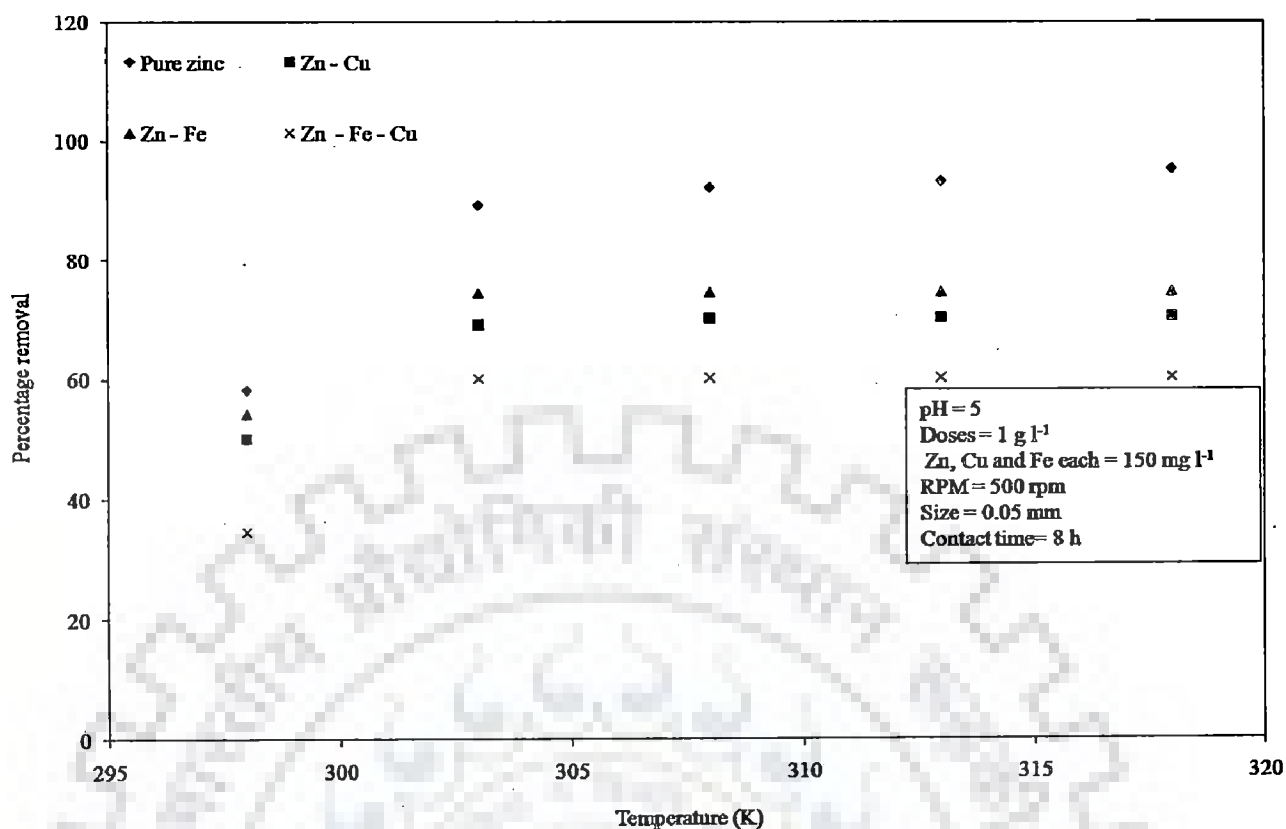


Figure 5.2.2 (i): Effect of temperature on biosorption of Zn on *Cedrus deodara* sawdust

However, the decrease in biosorption of Fe (II, III) and Cu (II) in liquid phase in all types of metal ion system at the rise of temperature from 303 K to 318 K was due to the fact that the rise in temperature changed or deformed the texture of biosorbent (Areco et al., 2010).

The preferential order of removal of heavy metal ions was Cu (II) > Zn (II) > Fe (II, III). Since the increase in the biosorption of Zn (II) ion was not significant above temperature 303 K. Hence, the optimum temperature for the biosorption of Zn (II) was considered as 303 K.

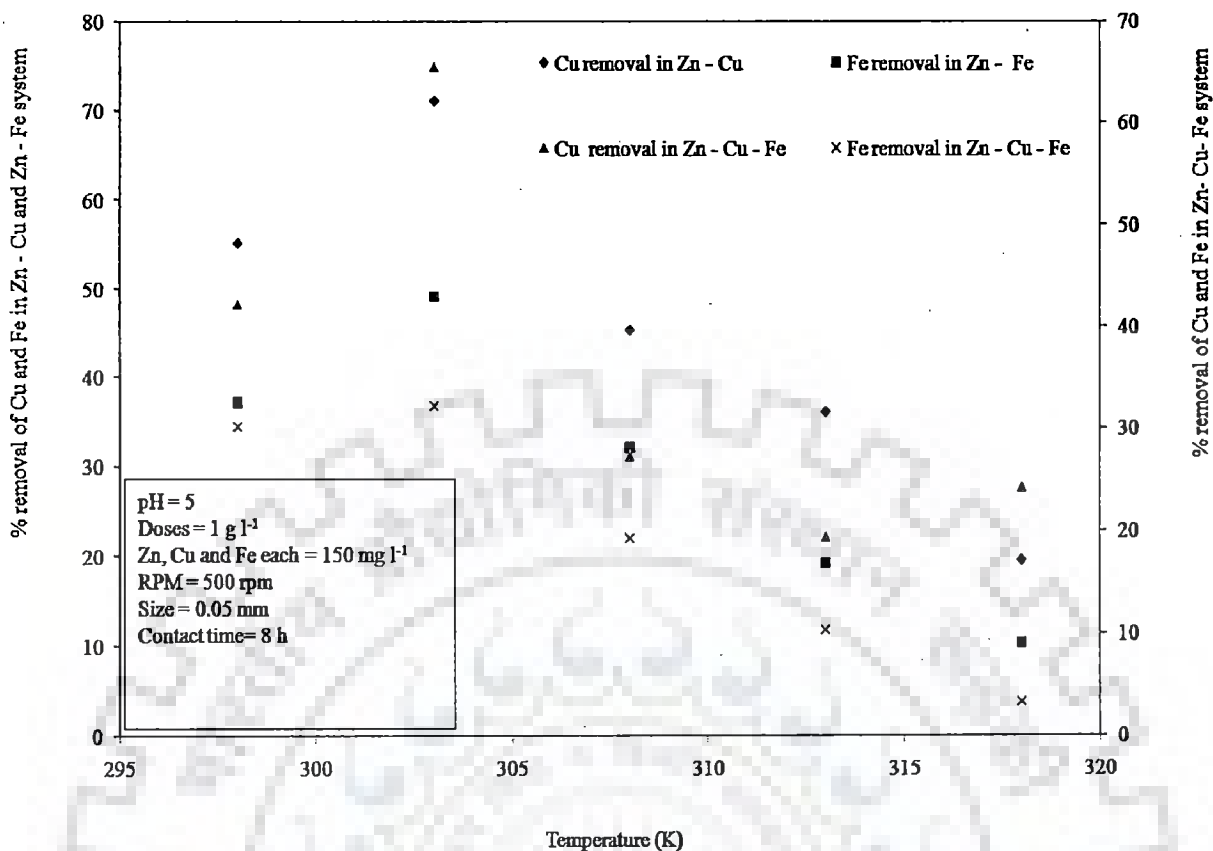


Figure 5.2.2 (j): Effect of temperature on biosorption of Cu and Fe in presence of Zn on *Cedrus deodara* sawdust

Figure 5.2.2 (k) and figure 5.2.2 (l) represent the influence of temperature on biosorption of Zn (II), total Fe (II, III) and Cu (II) on Eucalyptus bark sawdust in liquid phase. It is evident from figure 5.2.2 (k) that the maximum removal of Zn (II) ion was obtained in pure zinc phase. The maximum removal of Zn (II) ion was 71.33% at 303 K.

The presence of other metal ions hindered the biosorption of Zn (II) ion. The rise in temperature from 298 K to 303 K favoured the biosorption of Zn (II), Fe (II, III) and Cu (II) in all types of metal ion systems (figure 5.2.2 (l)). Further, the rise in temperature from 303 K to 318 K did not favour the biosorption of Zn (II), Fe (II, III) and Cu (II) ion in liquid phase. The maximum removal of total Fe (II, III) and Cu (II) ion in Zn (II) – Cu (II), Zn – Fe (II) and Zn (II)- Cu (II)- Fe (II, III) was also obtained at 303 K.

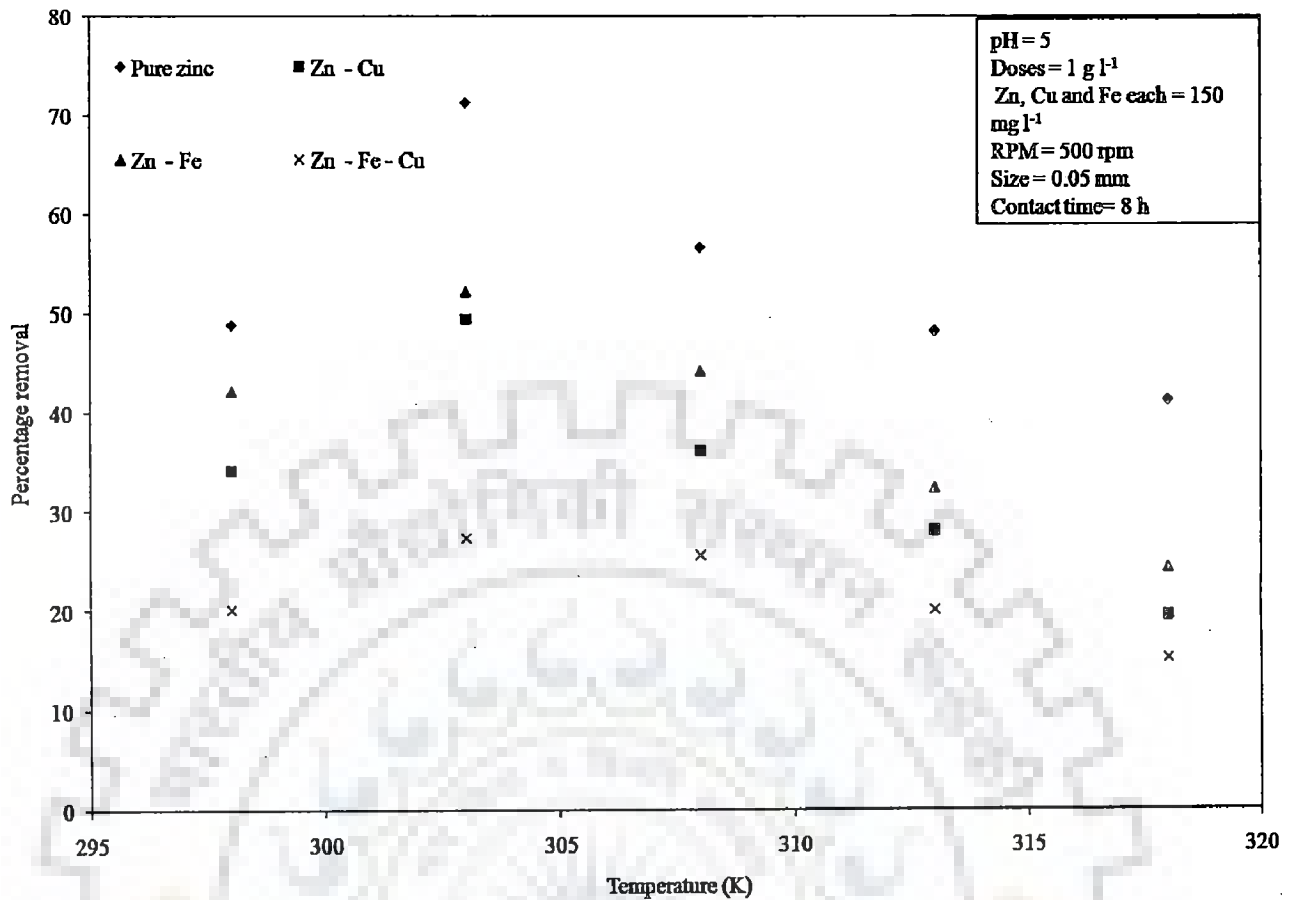


Figure 5.2.2 (k): Effect of temperature on biosorption of Zn on Eucalyptus bark sawdust

The decrease in biosorption of Zn (II), Fe (II, III) and Cu (II) in liquid phase in all the types of metal ion system with the rise of temperature from 303 K to 318 K was due to the fact that the rise in temperature changed or deformed the texture of biosorbent (Areco et al., 2010). The change in texture of biosorbent resulted in loss of biosorption capacity. The preferential order of removal of heavy metal ions was Cu (II) > Zn (II) > Fe (II, III).

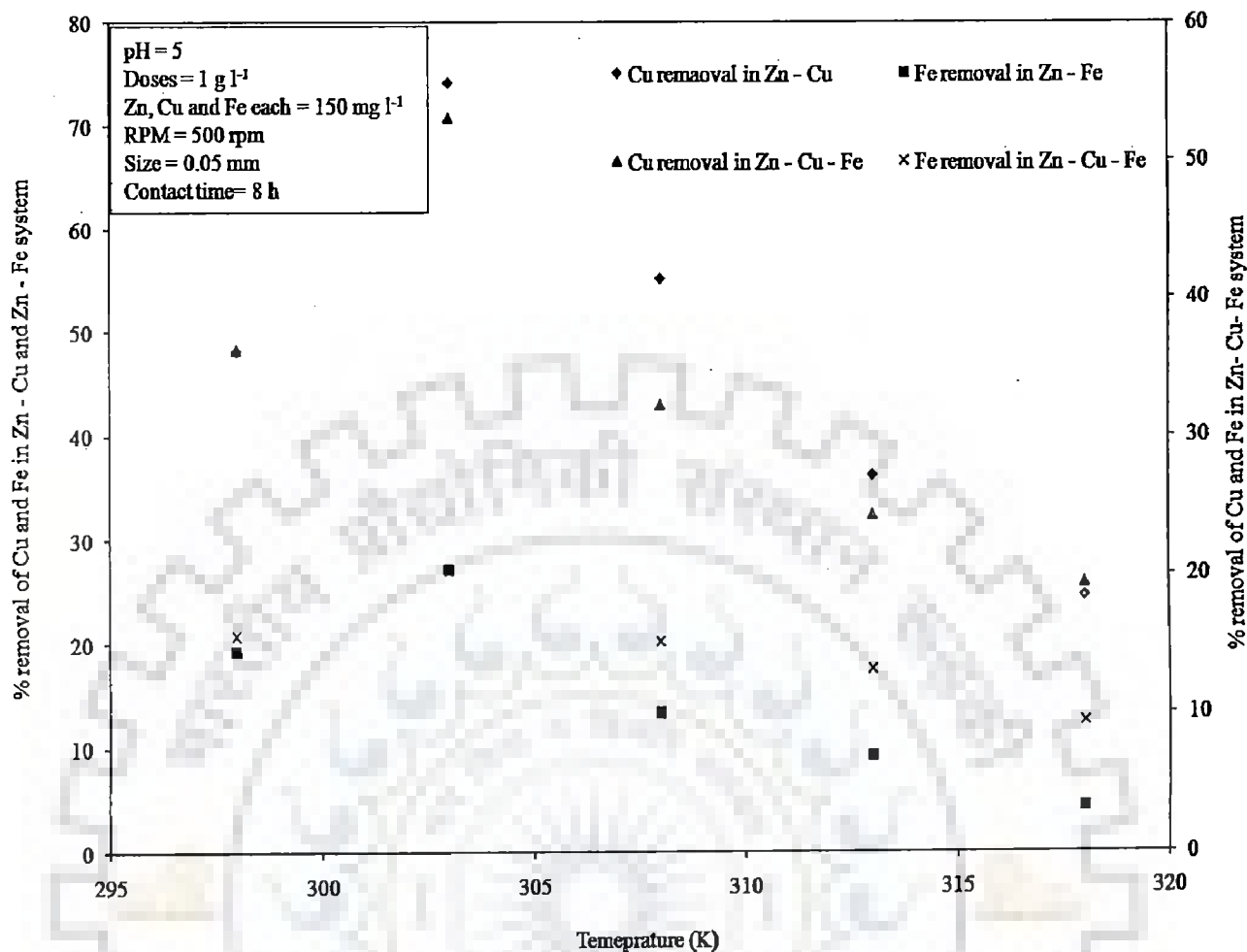


Figure 5.2.2 (l): Effect of temperature on biosorption of Cu and Fe in presence of Zn on Eucalyptus bark sawdust

Figure 5.2.2 (m) and figure 5.2.2 (n) represent the influence of temperature on biosorption of Zn (II), total Fe (II, III) and Cu (II) on Eucalyptus leaf powder in liquid phase. It is evident from figure 5.2.2 (m) that the maximum removal of Zn (II) ion was obtained in pure zinc phase. The maximum removal of Zn (II) ion was 72.18% at 303 K.

The presence of other metal ions hindered the biosorption of Zn (II) ion. The rise in temperature from 298 K to 303 K favoured the biosorption of Zn (II), Fe (II, III) and Cu (II) in all types of metal ion systems (figure 5.2.2 (n)). Further, the rise in temperature from 303 K to 318 K did not favour the biosorption of Zn (II), Fe (II, III) and Cu (II) ion in liquid

phase. The maximum removal of total Fe (II, III) and Cu (II) ion in Zn (II) – Cu (II), Zn – Fe (II) and Zn (II)- Cu (II)- Fe (II, III) was also obtained at 303 K.

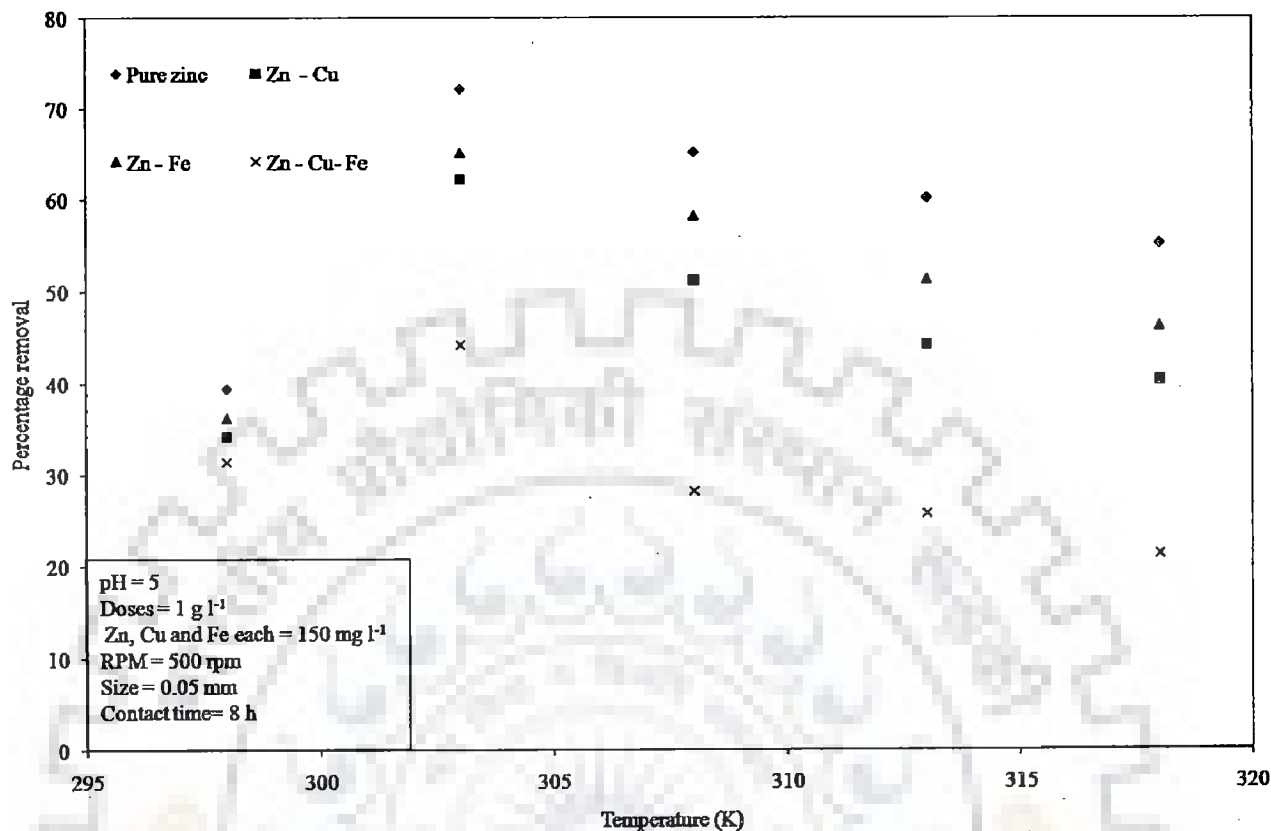


Figure 5.2.2 (m): Effect of temperature on biosorption of Zn in presence of on Eucalyptus leaf powder

The decrease in biosorption of Zn (II), Fe (II, III) and Cu (II) in liquid phase in all types of metal ion system with the rise of temperature from 303 K to 318 K was due to the fact that the rise in temperature changed or deformed the texture of biosorbent (Areco et al., 2010). The change in texture of biosorbent resulted in loss of biosorption capacity. The preferential order of removal of heavy metal ions was Cu (II) > Zn (II) > Fe (II, III).

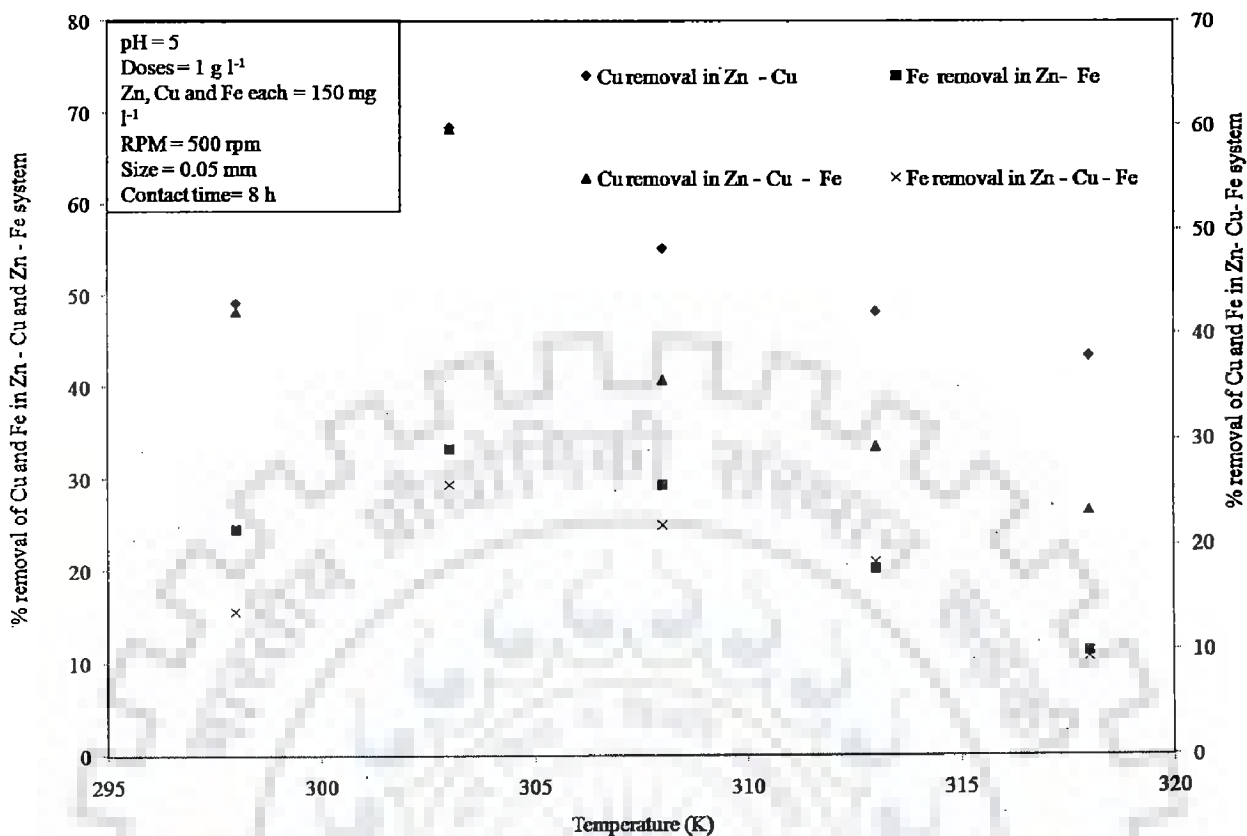


Figure 5.2.2 (n): Effect of temperature on biosorption of Cu and Fe in presence of Zn on Eucalyptus leaf powder

Figure 5.2.2 (o) and figure 5.2.2 (p) represent the influence of temperature on biosorption of Zn (II), total Fe (II, III) and Cu (II) on Eggshell and membrane in liquid phase. It is evident from figure 5.2.2 (o) that the maximum removal of Zn (II) ion was obtained in pure zinc phase. The maximum removal of Zn (II) ion was 42.59% at 303 K.

The presence of other metal ions hindered the biosorption of Zn (II) ion. The rise in temperature from 298 K to 303 K favoured the biosorption of Zn (II), Fe (II, III) and Cu (II) in all types of metal ion systems (figure 5.2.2 (p)). The maximum removal of total Fe (II, III) and Cu (II) ion in Zn (II) – Cu (II), Zn – Fe (II) and Zn (II)- Cu (II)- Fe (II, III) was also obtained at 303 K . Further, the rise in temperature from 303 K to 318 K did not favour the biosorption of Zn (II), Fe (II, III) and Cu (II) ion in liquid phase.

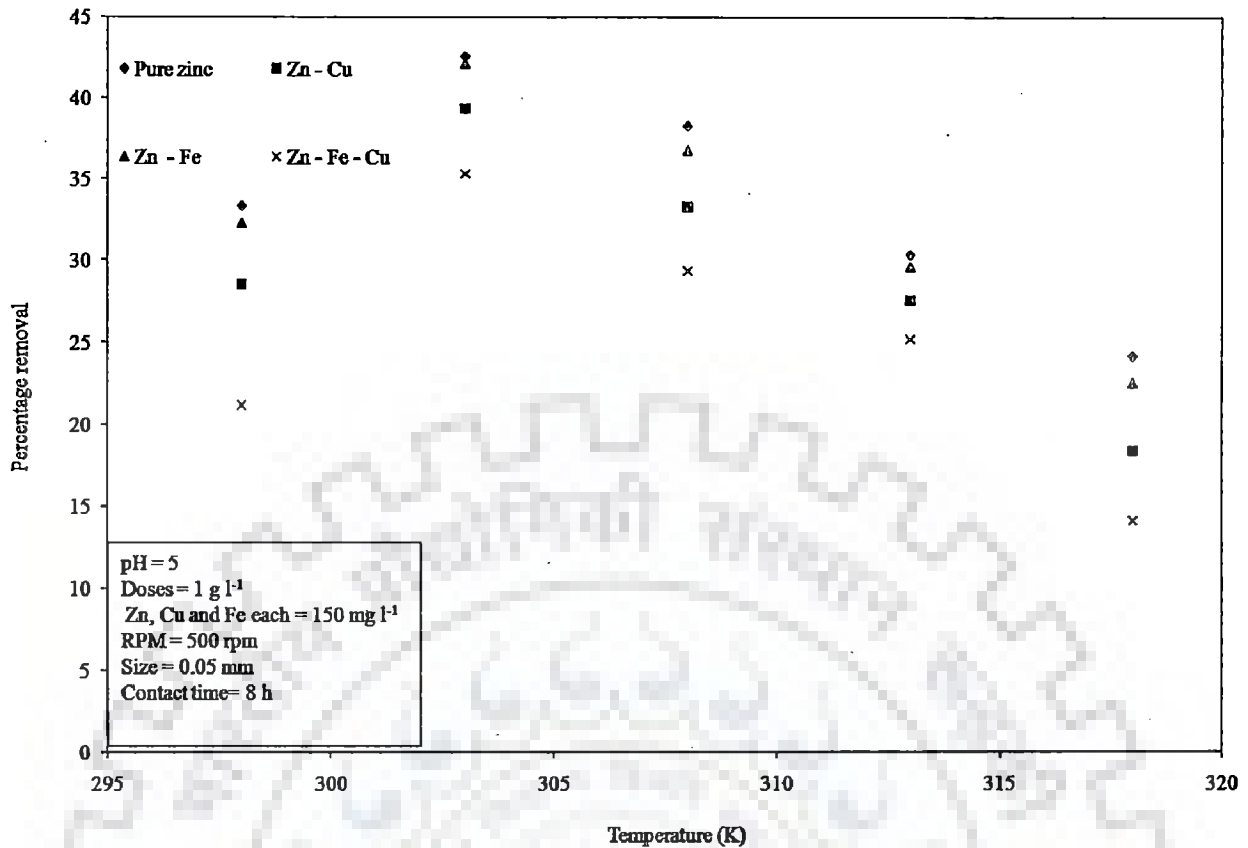


Figure 5.2.2 (o): Effect of temperature on biosorption of Zn on Eggshell and membrane

The decrease in biosorption of Zn (II), Fe (II, III) and Cu (II) in liquid phase in all types of metal ion system with the rise of temperature from 303 K to 318 K was due to the fact that the rise in temperature changed or deformed the texture of biosorbent (Areco et al. 2010). The change in texture of biosorbent resulted in loss of biosorption capacity. The preferential order of removal of heavy metal ions was Cu (II) > Zn (II) > Fe (II, III).



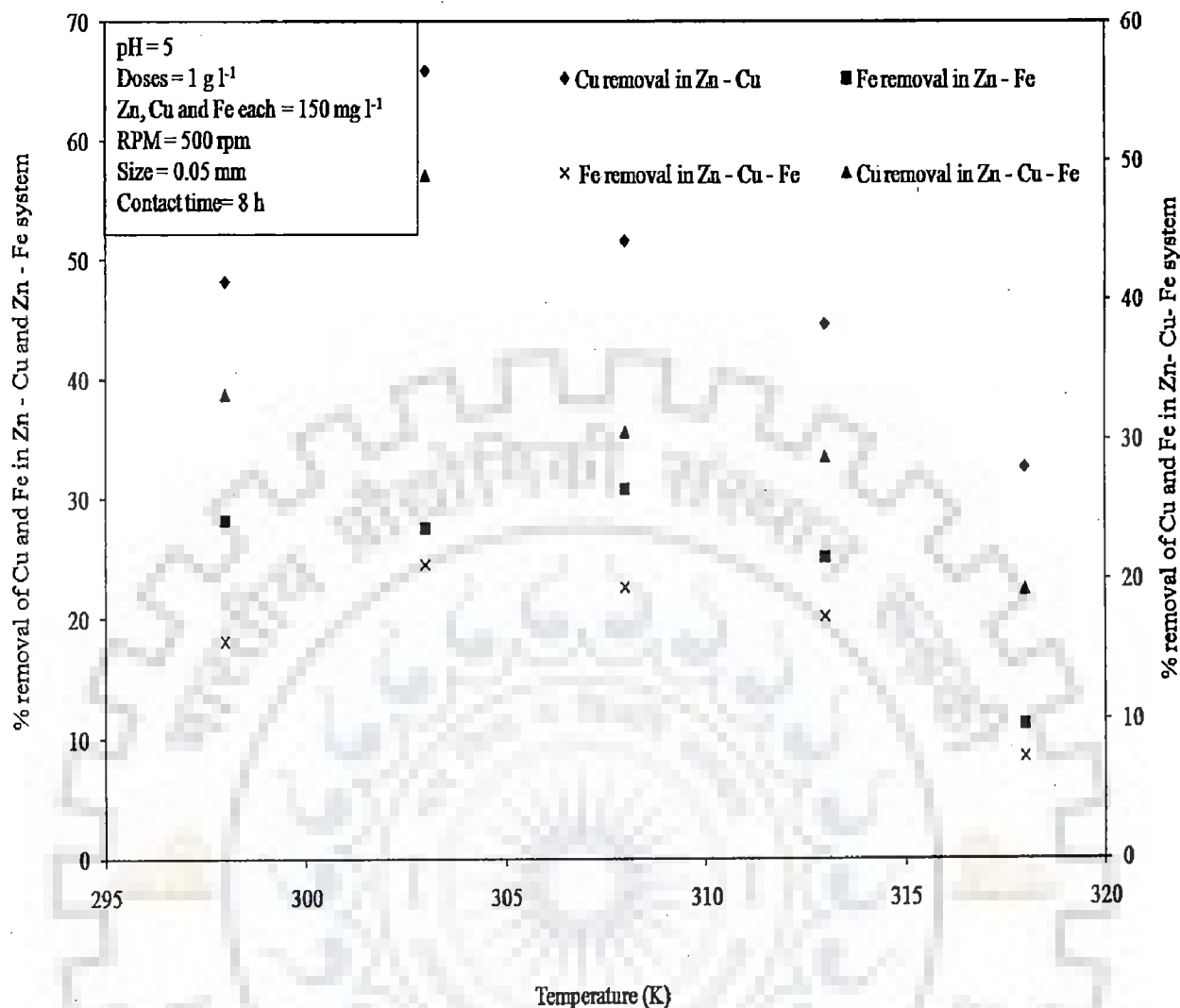


Figure 5.2.2 (p): Effect of temperature on biosorption of Cu and Fe in presence of Zn on Eggshell and membrane in liquid phase

Figure 5.2.2 (q) and figure 5.2.2 (r) represent the influence of temperature on biosorption of Zn (II), total Fe (II, III) and Cu (II) on dead cells of *Zinc sequestering bacterium VMSDCM* accession no. HQ108109 in liquid phase. It is evident from figure 5.2.2 (q) that the maximum removal of Zn (II) ion was obtained in pure zinc phase. The maximum removal of Zn (II) ion was 100% at 303 K and 308 K. The presence of other metal ions hindered the biosorption of Zn (II) ion. The rise in temperature from 298 K to 303 K favoured the biosorption of Zn (II), Fe (II, III) and Cu (II) in all types of metal ion systems.

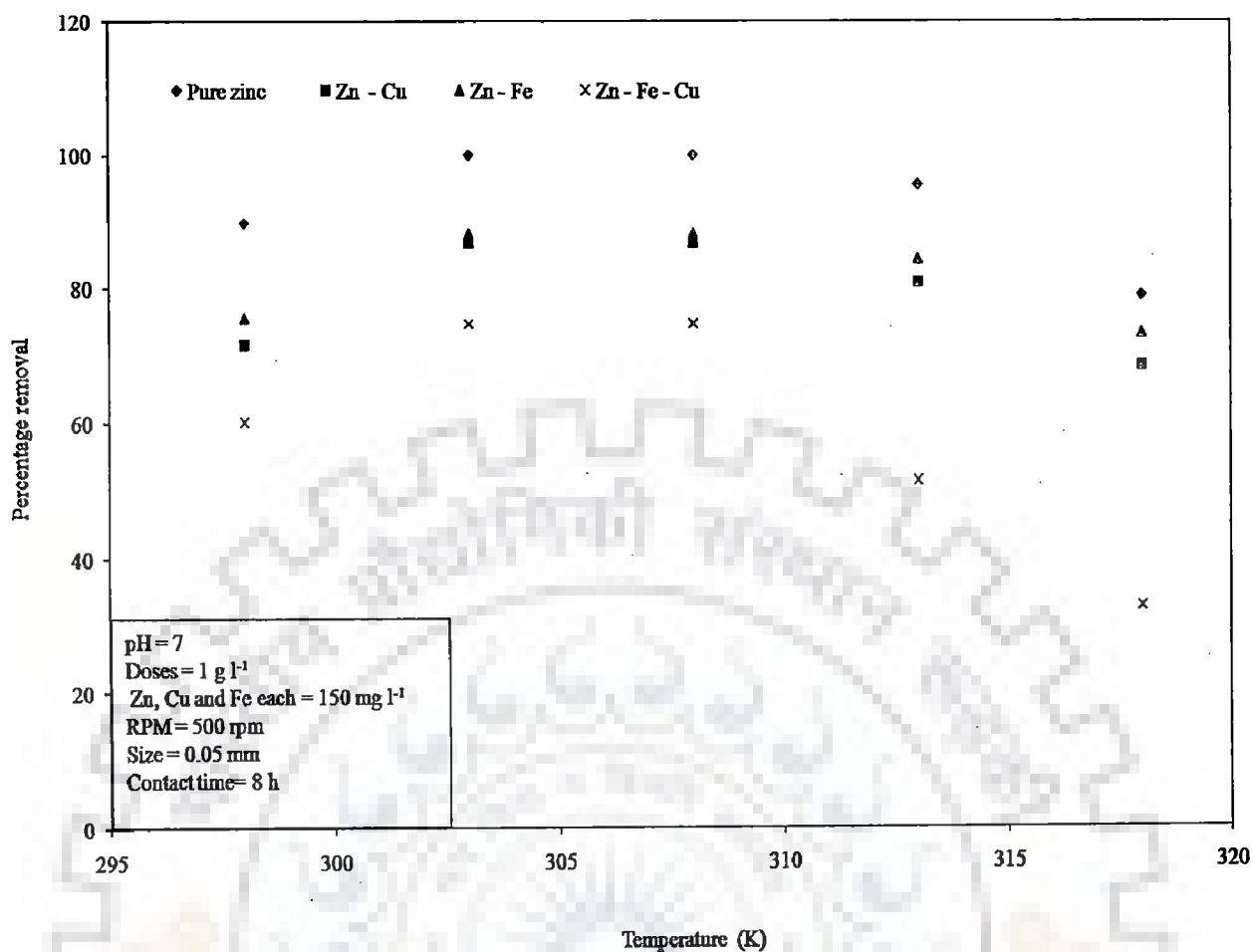


Figure 5.2.2 (q): Effect of temperature on biosorption of Zn on dead cells of *Zinc sequestering bacterium VMSDCM* accession no. HQ108109

The removal of Zn (II) ion was constant during rise in temperature from 303 K to 308 K. The maximum removal of total Fe (II, III) and Cu (II) ion in Zn (II) – Cu (II), Zn – Fe (II) and Zn (II)- Cu (II)- Fe (II, III) was also obtained at 303 K and 308 K (figure 5.2.2 (r)). Further rise in temperature from 308 K to 313 K did not favour the biosorption of Zn (II), Fe (II, III) and Cu (II) ion in liquid phase.

The decrease in biosorption of Zn (II), Fe (II, III) and Cu (II) in liquid phase in all types of metal ion system at the rise of temperature from 308 K to 318 K was due to the fact that the rise in temperature changed or deformed the texture of biosorbent (Areco et al.,

2010). The change in texture of biosorbent resulted in loss of biosorption capacity. The preferential order of removal of heavy metal ions was Cu (II) > Zn (II) > Fe (II, III).

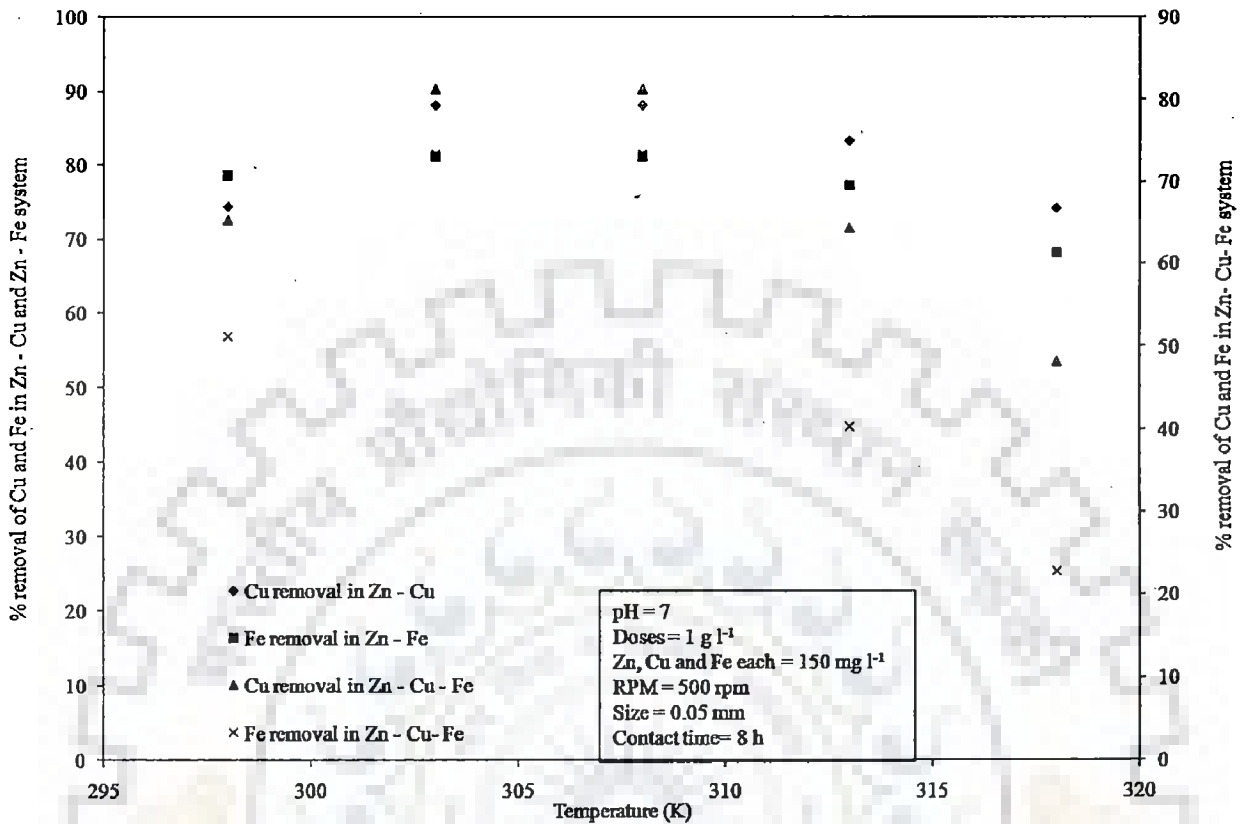


Figure 5.2.2 (r): Effect of temperature on biosorption of Cu and Fe in presence of Zn on dead cells of *Zinc sequestering bacterium VMSDCM*

Table 5.2.2 and table 5.2.3 represent the the comparison between the uptake capacities various sorts of living and non-living biomasses in various experimental conditions.

Table 5. 2. 2: Uptake capacities of Zn (II) ion by various algae

Name of biomass	Physiological stage	Initial metal ion conc. (mg l <sup>-1</sup> )	pH	Temp. (°C)	Uptake capacity (mg g <sup>-1</sup> )	Percent. removal	Reference
<i>Chlorella vulgaris</i>	Inactive	100	4	R. T	24190.6	N. D	Klimmek and Stan, 2001
<i>L. taylorii</i>	Inactive	100	4-6	R. T	32036.2	N. D	Klimmek and Stan, 2001
<i>L. taylorii</i> phos.	Inactive	100	4-6	R. T	169988	N. D	Klimmek and Stan, 2001
<i>Ankistodes mus densus</i>	Inactive	100	4-6	R. T	15037.4	N. D	Klimmek and Stan, 2001
<i>Vaucheria dichotoma</i>	Inactive	100	4-6	R. T	27459.6	N. D	Klimmek and Stan, 2001
<i>Dunaliella bioculata</i>	Inactive	100	4-6	R. T	2615.2	N. D	Klimmek and Stan, 2001
<i>Fucus spiralis</i> , <i>Laminaria hyperborea</i>	Inactive	75 -100	4.5	25 °C	18.6–32.0	N. D	Freitas et al., 2008
<i>Bifurcaria bifurcata</i> , <i>Sargassum muticum</i> <i>Sargassum</i>	Inactive	65380-653800	5	N. D	N.D	N. D	Figueira et al., 2000
<i>Sargassum</i>	Inactive	0 - 196.	5	30	41.84	N. D	Fagundes

<i>filipendula</i>			14					et al., 2007
<i>Caulepra lentiferra</i>	Inactive	10		1.0	21±2	1372.98	N. D	Pavasant et al., 2006
				7.5		2680.58		
<i>Codium vermilara</i>	Inactive	10 - 150	6	N. D	23.8		N. D	Romera et al., 2007
<i>Spirogyra insignis</i>	Inactive	10 - 150	6	N. D	21.1		N. D	Romera et al., 2007
<i>Asparagopsis armata</i>	Inactive	10 - 150	6	N. D	21.6		N. D	Romera et al., (2007)
<i>Chondrous crispus</i>	Inactive	10 - 150	6	N. D	45.7		N. D	Romera et al., 2007
<i>Ascophyllum nodosum</i>	Inactive	10 - 150	6	N. D	42.0		N. D	Romera et al., 2007
<i>Fucas spiralis</i>	Inactive	10 - 150	6	N. D	53.2		N. D	Romera et al., 2007
<i>Laminaria japonica</i>	Inactive	326900	4.5	R. T	91532		N. D	Fourest and Volesky 1997
<i>Sargassum fluitans</i>	Inactive	326900	4.5	R. T	77148.4		N. D	Fourest and Volesky 1997
<i>Fucus vesiculosos</i>	Inactive	326900	4.5	R. T	52304		N. D	Fourest and Volesky 1997
<i>Cedrus deodara sawdust</i>	Inactive	150	5	45±0.5 °C	61.21	59.19		This study

Table 5.2.3: Uptake capacities of Zn (II) ion by various fungal biomasses

Name of Biomass	Physiological stage	Initial metal ion conc. (mg l <sup>-1</sup> )	pH	Temp. (°C)	Uptake capacity (mg g <sup>-1</sup> )	Percent. removal	Reference
<i>Streptomyces remosus</i>	Inactive	100	7.5	20	30	N. D	Mameri et al., 1999
<i>Streptomyces remosus</i>	Inactive	100	6.5	20	80	N. D	Mameri et al., 1999
<i>Penicillium spinulosum</i> (Non growing cell)	Living	2.5	N. D	N. D	1.3	N. D	Karpoor and Viraraghavan 1995
<i>Penicillium spinulosum</i> (Growing cell)	Living	2.5	N. D	N. D	0.2	N. D	Karpoor and Viraraghavan 1995
<i>Penicillium notatum</i>	Living	N. D	7	25	23	2.3 ±1.6	Siegel et al., 1983
<i>Rhizopus arrhizus</i>	Inactive	N. D	4	25	20	N. D	Tobin et al., 1984
<i>Saccharomyces cerevisiae</i> (Portuguese origin)	Inactive	40.8	5.5	N. D	3.45	9	Bakkaloglu et al., 1998
<i>Saccharomyces cerevisiae</i> (United kingdom)	Inactive	40.8	5.5	N. D	1.95	5	Bakkaloglu et al., 1998
<i>Penicillium chrysogenum</i>	Inactive	45.5	5.5	N. D	19.2	42	Bakkaloglu et al., 1998
<i>Saccharomyces cerevisiae</i>	Living Free cells	N. D	5	25	23.41±0.13	N. D	Al-Saraj et al., 1999
<i>Phanerochaete chrysogenum</i>	Living (immobilized cells)	100	6	20±2	41.9	N. D	Iqbal and Edyvean, 2004
<i>Phanerochaete chrysogenum</i>	Living (Free cells)	100	6	20±2	34.13±1.84	N. D	Iqbal and Edyvean, 2004
<i>Aspergillus niger</i>	Living	64.8	6.5	30	2.82	N. D	Yang et al., 2009
<i>Trametes</i>	Living	400	4-6	15-45	86955.4	N. D	Bayramoglu

<i>versicolor</i> (Immobilized)							et al., 2003
<i>Trametes versicolor</i>	Inactive	400	4-6	15-45	109184.6	N. D	Bayramoglu et al., 2003
<i>Phanerochaete chrysosporium</i> (Immobilized cells)	Living	30 - 600	6	15 - 45	37	N. D	Arica et al., 2003
<i>Phanerochaete chrysosporium</i>	Inactive	30 - 600	6	15 - 45	48	N. D	Arica et al., 2003
<i>Mucor rouxii</i>	Living	10	5	N. D	7.75	N. D	Yan and Viraraghavan, 2003)
<i>Mucor rouxii</i>	Inactive	10	6	N. D	53.85	N. D	Yan and Viraraghavan, 2003
<i>Penicillium chrysogenum</i> PE-10/94	Inactive	65.38 - 65380	7	21±1	13	32	Skowronski et al., 2001
<i>Saprolegnia delica</i>	Living	0.003	8	20	N. D	44	Ali and Hashem, 2007
<i>Trichoderma viride</i>	Living	0.003	6	25	N. D	61.7	Ali and Hashem, 2007
Fungal Biomass Isolated from Industrial Wastewater	Living	500	4.5	30	77	N. D	Sharma et al., 2002
<i>Streptomyces ciscaucasicus</i>	Living	1 - 150	5.0	28	42.75	N. D	Li et al., 2010
<i>Streptomyces ciscaucasicus</i>	Inactive	1 - 150	5.0	28	54	N. D	Li et al., 2010

It is clear from table 5.2.2 and table 5.2.3 that the uptake capacity of dead cells of *Zinc sequestering bacterium VMSDCM* Accession no. HQ108109 has tremendous potential of up taking zinc from liquid phase. However, these uptake capacities cited in table 5.2.2 and table 5.2.3 have been derived in various types of experimental condition. Though the analysis of the data cited in table 5.2.2 and table 5.2.3 present the valuable comparative analysis of various sorts of biomasses with the present study.

#### **Concluding remark of the section 5.2.2**

Among all the biosorbents selected for the present work, the maximum removal of Zn (II) ion was obtained with *Cedrus deodara* sawdust and dead cells of *Zinc sequestering bacterium VMSDCM* accession no HQ108109. The maximum removal of Zn (II) ion obtained in case of *Cedrus deodara* sawdust and *Zinc sequestering bacterium VMSDCM* accession no. HQ108109 were 89.19 % and 100%, respectively in pure zinc environment. In presence of Cu (II) ion, the removal of Zn (II) was less in comparison to the pure zinc environment. The removal of zinc in presence of Cu (II) in case of *Cedrus deodara* sawdust and dead cells of *Zinc sequestering bacterium VMSDCM* accession no HQ108109 was 69.12% and 86.6%, respectively. Similarly, the presence of total Fe (II, III) the percentage removal of Zn (II) ion was quite diminished. The removal of zinc in presence of total Fe (II, III) in case of *Cedrus deodara* sawdust and dead cells of *Zinc sequestering bacterium VMSDCM* accession no HQ108109 was 74.31% and 88.19%, respectively. In ternary metal ion complex system the removal of Zn (II) ion was 69.11% and 74.61% in case of *Cedrus deodara* sawdust and dead cells of *Zinc sequestering bacterium VMSDCM* accession no HQ108109,, respectively. 303 K and 308 K temperature for *Cedrus deodara* sawdust and dead cells of *Zinc sequestering bacterium VMSDCM* accession no. HQ108109 were established as optimum temperature for the maximum removal of Zn (II) from liquid phase.



### 5.2.3 Optimization of adsorbent dose

This section describes the optimization of adsorbent dose for biosorption of Zn (II) ion in liquid phase. The doses of biomass used in present work were  $0.1 \text{ g l}^{-1}$ ,  $0.5 \text{ g l}^{-1}$ ,  $1 \text{ g l}^{-1}$ ,  $2 \text{ g l}^{-1}$ ,  $3 \text{ g l}^{-1}$ ,  $4 \text{ g l}^{-1}$  and  $5 \text{ g l}^{-1}$ . The system of ions studied in the present work were pure zinc, Zn (II)- Cu (II), Zn (II)- Fe (II, III) and Zn (II) – Fe (II, III)- Cu (II). The metal ions Zn (II), Cu (II) and Fe (II, III) are referred as Zn, Cu and Fe in various figures.

Figure 5.2.3 (a) and figure 5.2.3 (b) represent the influence of biosorbent dose on biosorption of Zn (II), total Fe (II, III) and Cu (II) on Mango bark sawdust.

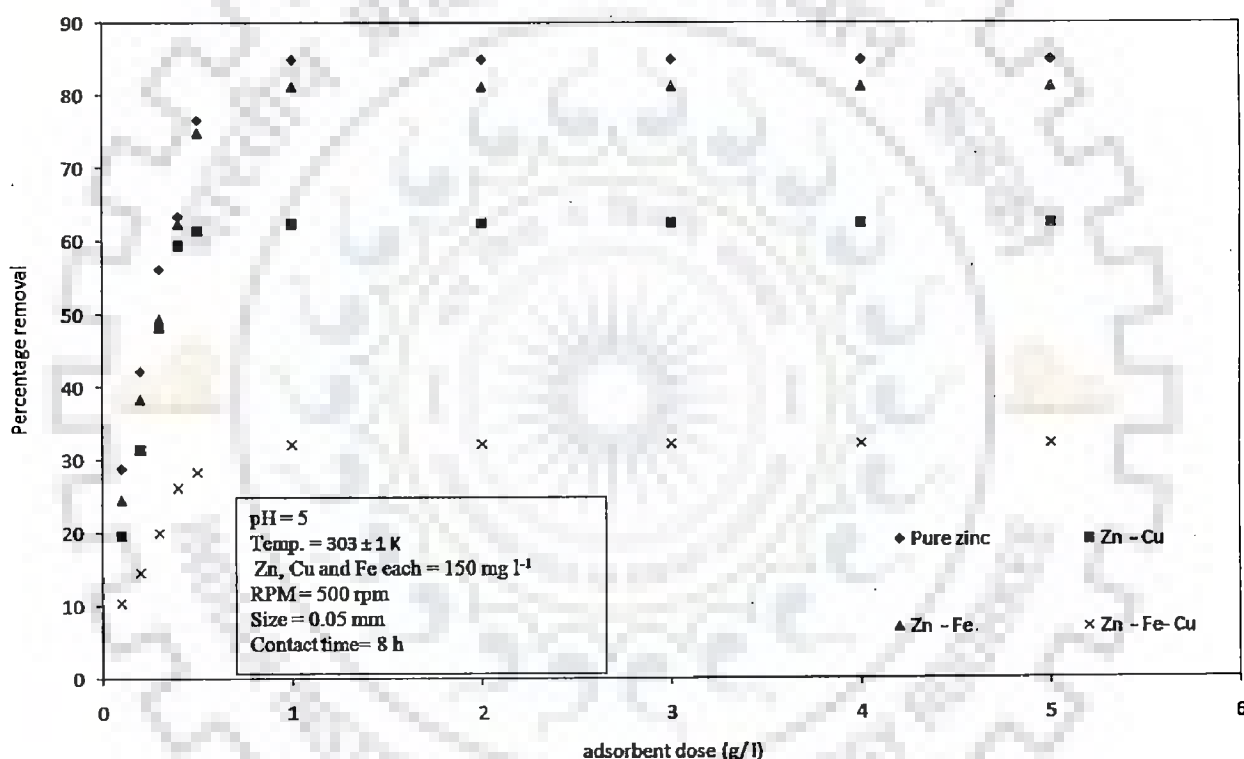


Figure 5.2.3 (a): Effect of adsorbent dose on biosorption of Zn on Mango bark sawdust

It is evident from figure 5.2.3 (a) that the maximum removal of Zn (II) ion was obtained in pure zinc phase at  $1 \text{ g l}^{-1}$  dose. The maximum removal of total Fe (II, III) and Cu (II) ion in Zn (II) – Cu (II), Zn – Fe (II) and Zn (II)- Cu (II)- Fe (II, III) was obtained also at  $1 \text{ g l}^{-1}$  of adsorbent dose in fig. 5.2.3 (b).

The maximum removal of Zn (II) ion was 84.88% at  $1 \text{ g l}^{-1}$  of Mango bark sawdust. The presence of other metal ions hindered the biosorption of Zn (II) ion. The increase in biosorbent dose from  $0.1 \text{ g l}^{-1}$  to  $1 \text{ g l}^{-1}$  favoured the biosorption of Zn (II), Fe (II, III) and Cu (II) in all types of metal ion systems. Further, the rise in biosorbent dose from  $1 \text{ g l}^{-1}$  to  $5 \text{ g l}^{-1}$  did not increase significantly the removal of Zn (II), total Fe (II, III) and Cu (II) ion.

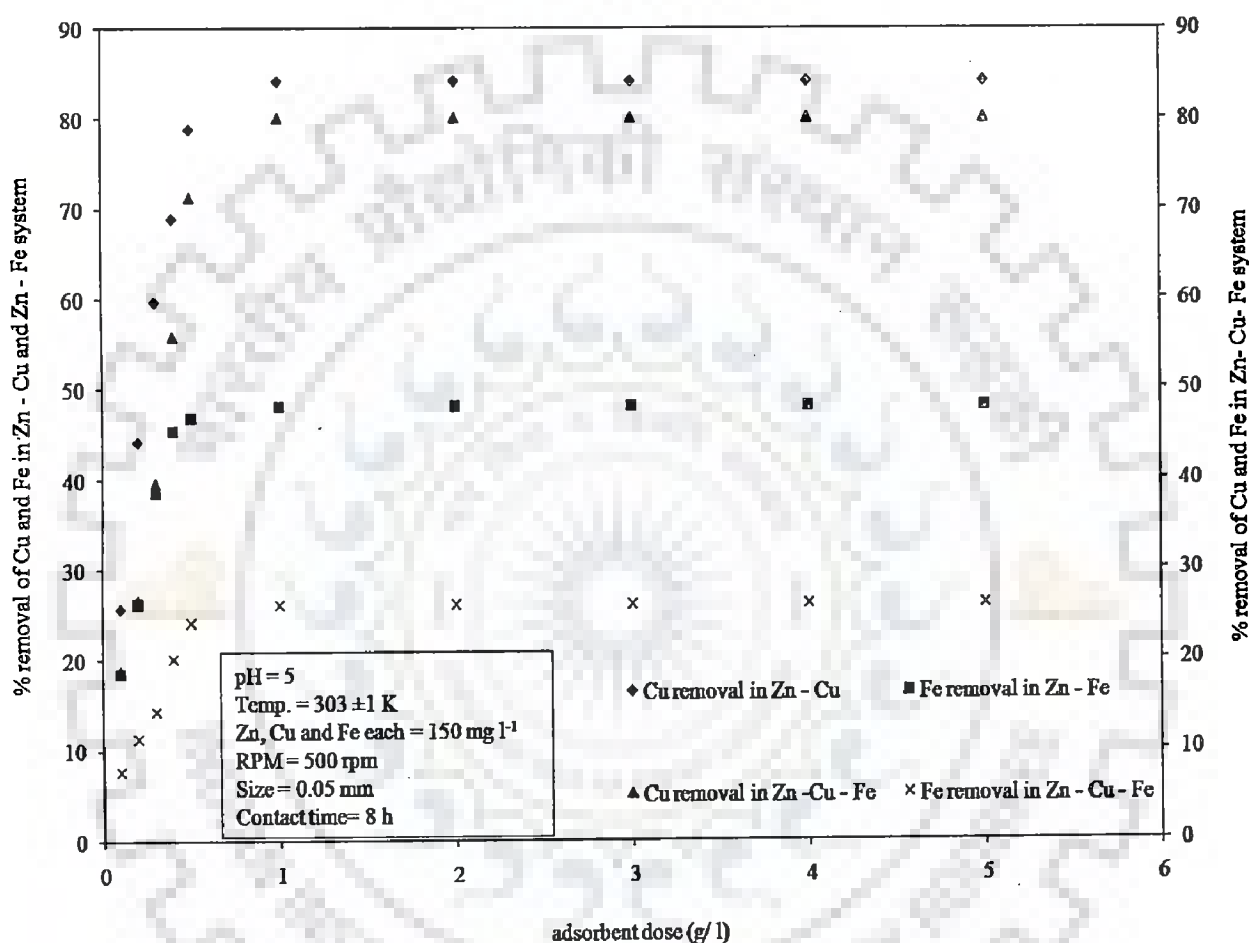


Figure 5.2.3 (b): Effect of adsorbent dose on biosorption of Cu and Fe in presence of Zn on Mango bark sawdust

The increase in biosorption of Zn (II), Fe (II, III) and Cu (II) with the increase in biosorbent dose from  $0.1 \text{ g l}^{-1}$  to  $1 \text{ g l}^{-1}$  was due to the availability of higher number of binding sites after every increment in biosorbent dose. However, the reason behind the insignificant change in biosorption of Zn (II), total Fe (II, III) and Cu (II) at higher concentration of biosorbent ranging between  $1 \text{ g l}^{-1}$  to  $5 \text{ g l}^{-1}$  was the agglomeration and clumping of biosorbent particles

which led to the decrease in effective surface area of biosorbent (Ahmad et al., 2009, Ucun et al., 2009). The preferential order of removal of heavy metal ions was Cu (II) > Zn (II) > Fe (II, III).

Figure 5.2.3 (c) and figure 5.2.2 (d) represent the influence of biosorbent dose on biosorption of Zn (II), total Fe (II, III) and Cu (II) on Orange peel.

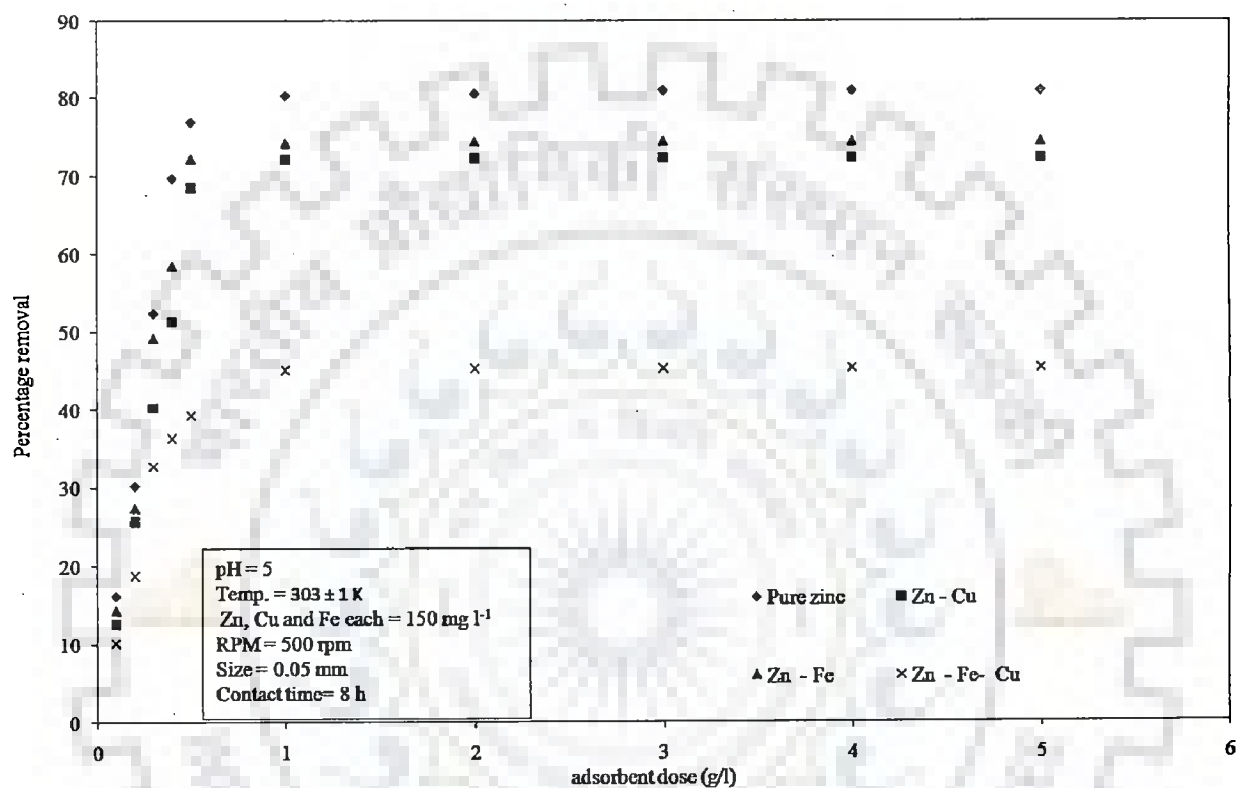


Figure 5.2.3 (c): Effect of adsorbent dose on biosorption of Zn in presence of Cu and Fe on Orange peel

It is evident from figure 5.2.3 (c) that the maximum removal of Zn (II) ion was obtained in pure zinc phase at  $1 \text{ g l}^{-1}$  dose. The maximum removal of Zn (II) ion was 80.21% at  $1 \text{ g l}^{-1}$  of Orange peel. The maximum removal of total Fe (II, III) and Cu (II) ion in Zn (II) – Cu (II), Zn – Fe (II) and Zn (II)- Cu (II)- Fe (II, III) was obtained also at  $1 \text{ g l}^{-1}$  of adsorbent dose in figure 5.2.3 (d). The presence of other metal ions hindered the biosorption of Zn (II) ion. The increase in biosorbent dose from  $0.1 \text{ g l}^{-1}$  to  $1 \text{ g l}^{-1}$  favoured the biosorption of Zn (II), Fe (II, III) and Cu (II) in all types of metal ion systems. Further, the rise in biosorbent

dose from 1  $\text{gl}^{-1}$  to 5  $\text{gl}^{-1}$  did not increase significantly the removal of Zn (II), total Fe (II, III) and Cu (II) ion.

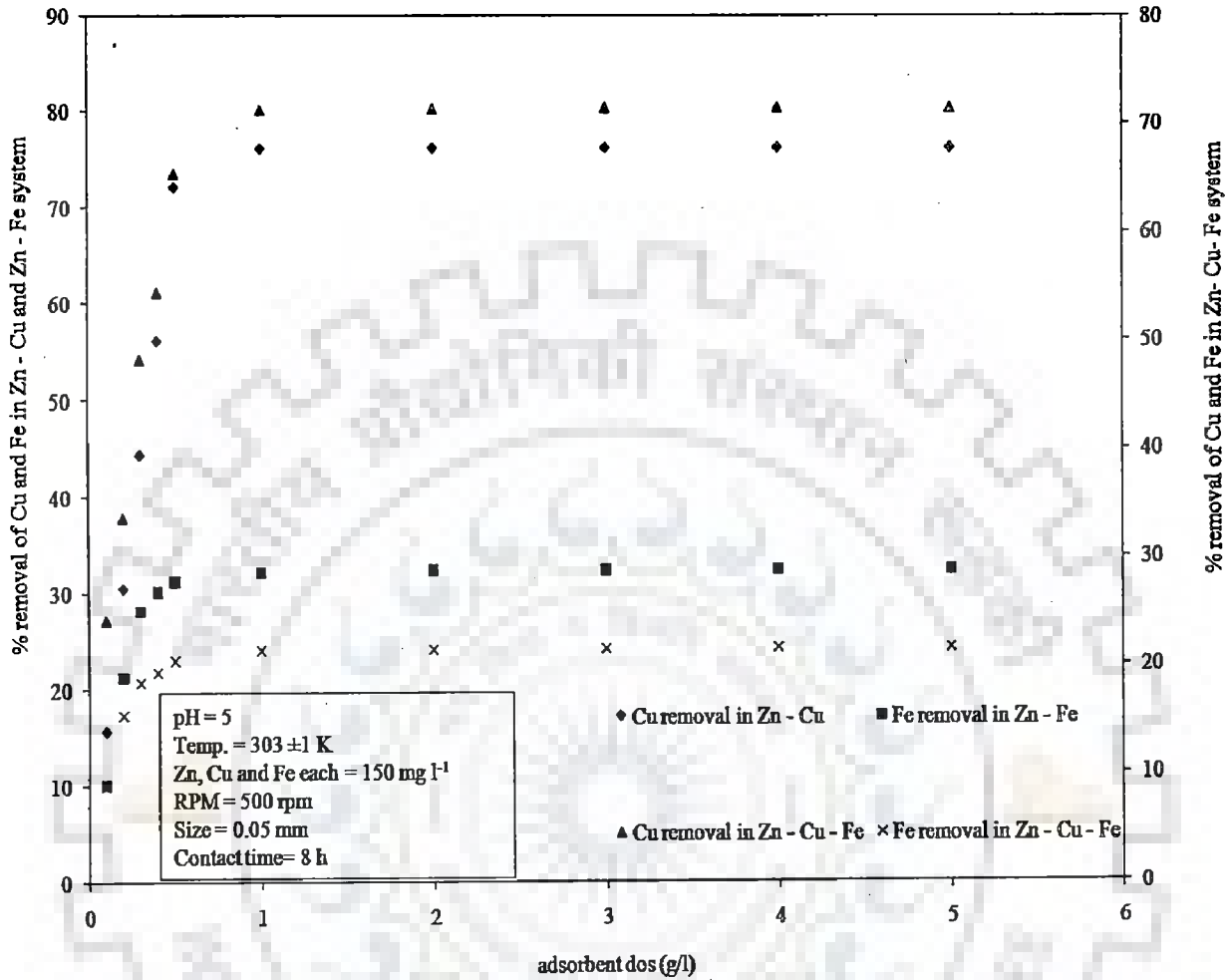


Figure 5.2.3 (d): Effect of adsorbent dose on biosorption of Cu and Fe in presence of Zn on Orange peel

The increase in biosorption of Zn (II), Fe (II, III) and Cu (II) with the increase in biosorbent dose from 0.1  $\text{gl}^{-1}$  to 1  $\text{gl}^{-1}$  was due to the availability of higher number of binding sites after every increment in biosorbent dose. However, the reason behind the insignificant change in biosorption of Zn (II), total Fe (II, III) and Cu (II) at higher concentration of biosorbent ranging between 1  $\text{gl}^{-1}$  to 5  $\text{gl}^{-1}$  was the agglomeration and clumping of biosorbent particles which led to the decrease in effective surface area of biosorbent (Ahmad et al., 2009, Uzun et

al., 2009). The preferential order of removal of heavy metal ions was Cu (II) > Zn (II) > Fe (II, III).

Figure 5.2.3 (e) and figure 5.2.2 (f) represent the influence of biosorbent dose on biosorption of Zn (II), total Fe (II, III) and Cu (II) on Pineapple peel.

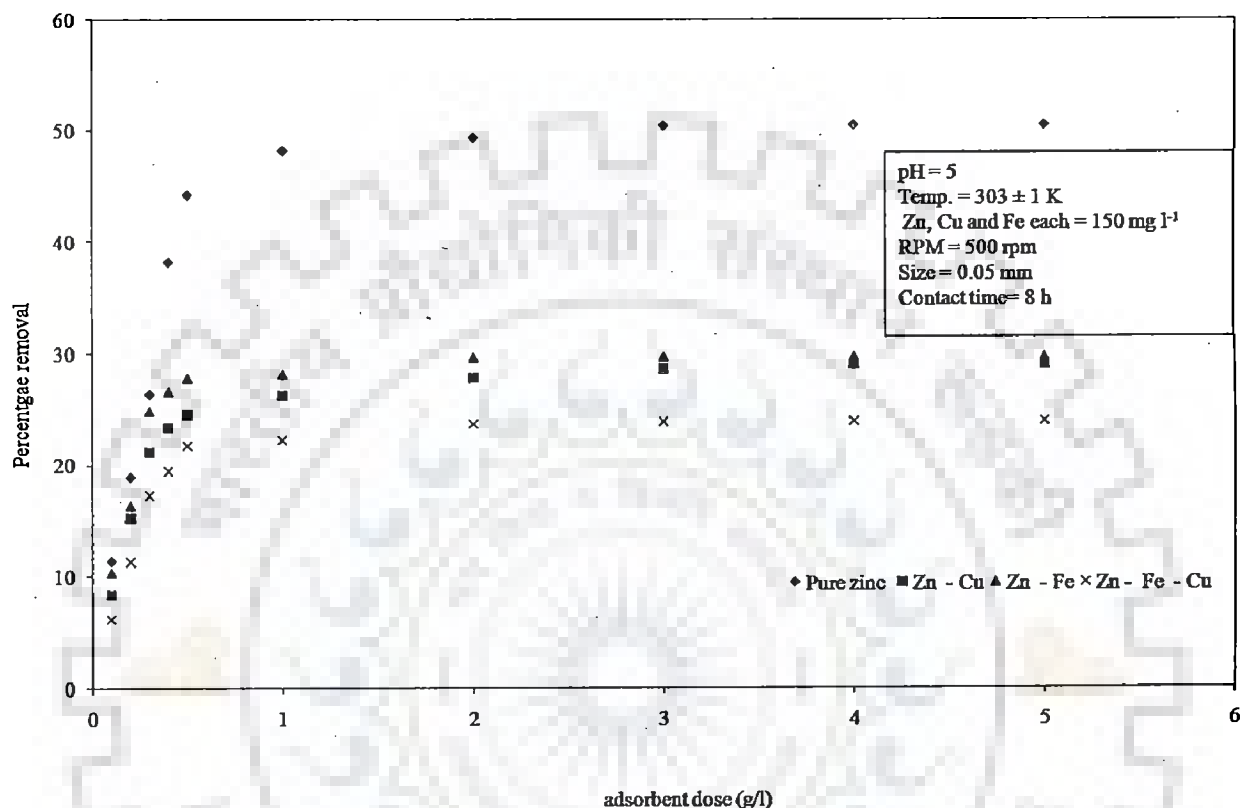


Figure 5.2.3 (e): Effect of adsorbent dose on biosorption of Zn on Pineapple peel

It is evident from figure 5.2.3 (e) that the maximum removal of Zn (II) ion was obtained in pure zinc phase. The maximum removal of Zn (II) ion was 49.32% at  $2 \text{ g l}^{-1}$  of Pineapple peel. The maximum removal of total Fe (II, III) and Cu (II) ion in Zn (II) – Cu (II), Zn – Fe (II) and Zn (II)- Cu (II)- Fe (II, III) was obtained also at  $2 \text{ g l}^{-1}$  of adsorbent dose in figure 5.2.3 (f). The presence of other metal ions hindered the biosorption of Zn (II) ion. The increase in biosorbent dose from  $0.1 \text{ g l}^{-1}$  to  $2 \text{ g l}^{-1}$  favoured the biosorption of Zn (II), Fe (II, III) and Cu (II) in all types of metal ion systems. Further, the rise in biosorbent dose from  $2 \text{ g l}^{-1}$  to  $5 \text{ g l}^{-1}$ , did not increase significantly the removal of Zn (II), total Fe (II, III) and Cu (II)

ion. The increase in biosorption of Zn (II), Fe (II, III) and Cu (II) with the increase of biosorbent dose from 0.1  $\text{g l}^{-1}$  to 2  $\text{g l}^{-1}$  was due to the availability of higher number of binding sites after every increment in biosorbent dose.

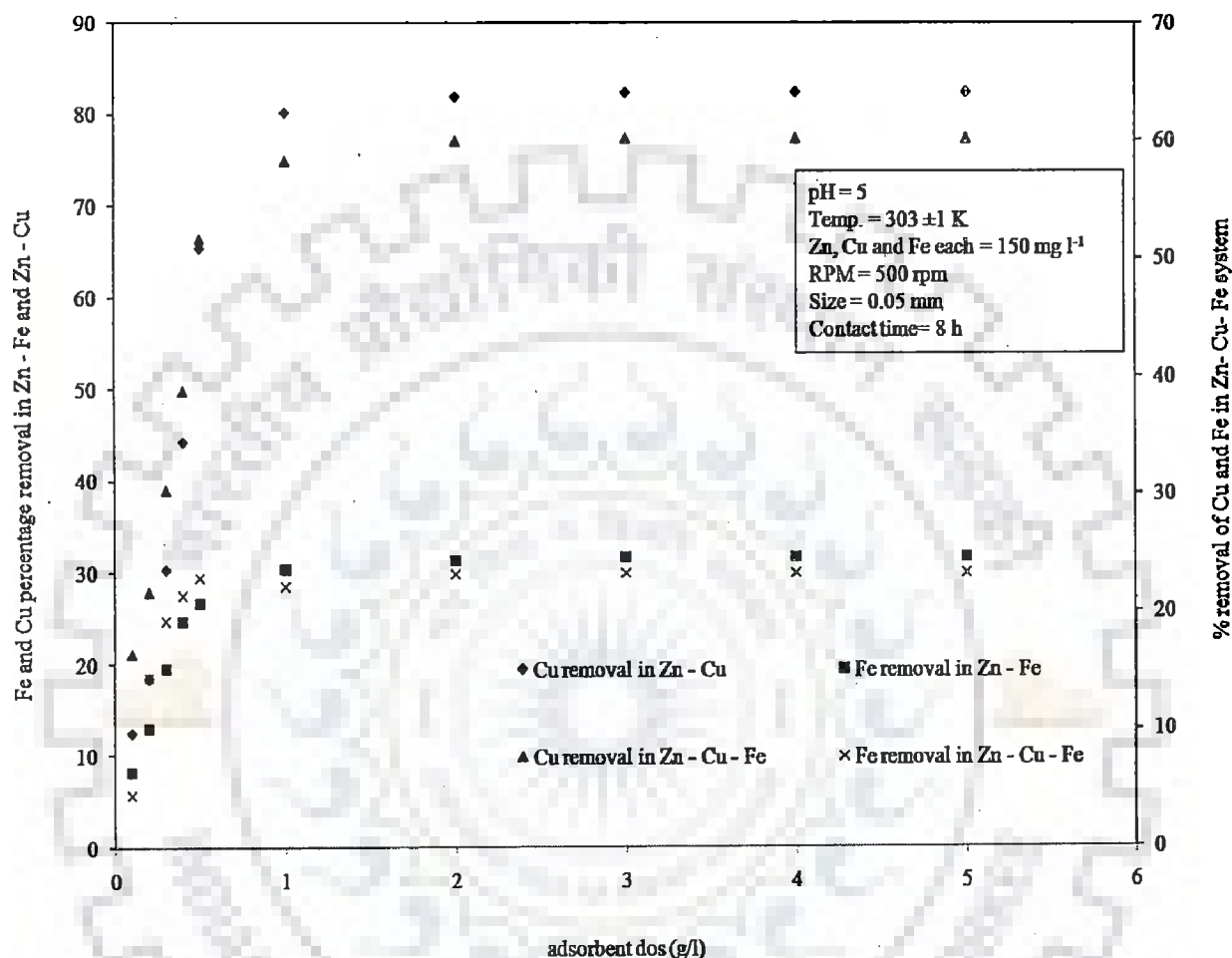


Figure 5.2.3 (f): Effect of biosorbent dose on biosorption of Cu and Fe in presence of Zn on Pineapple peel

However, the reason behind the insignificant change in biosorption of Zn (II), total Fe (II, III) and Cu (II) at higher concentration of biosorbent ranging between 2  $\text{g l}^{-1}$  to 5  $\text{g l}^{-1}$  was the agglomeration and clumping of biosorbent particles which led to the decrease in effective surface area of biosorbent (Ahmad et al., 2009, Uzun et al., 2009). The preferential order of removal of heavy metal ions was Cu (II) > Zn (II) > Fe (II, III).

Figure 5.2.3 (g) and figure 5.2.2 (h) represent the influence of biosorbent dose on biosorption of Zn (II), total Fe (II, III) and Cu (II) on Jackfruit peel.

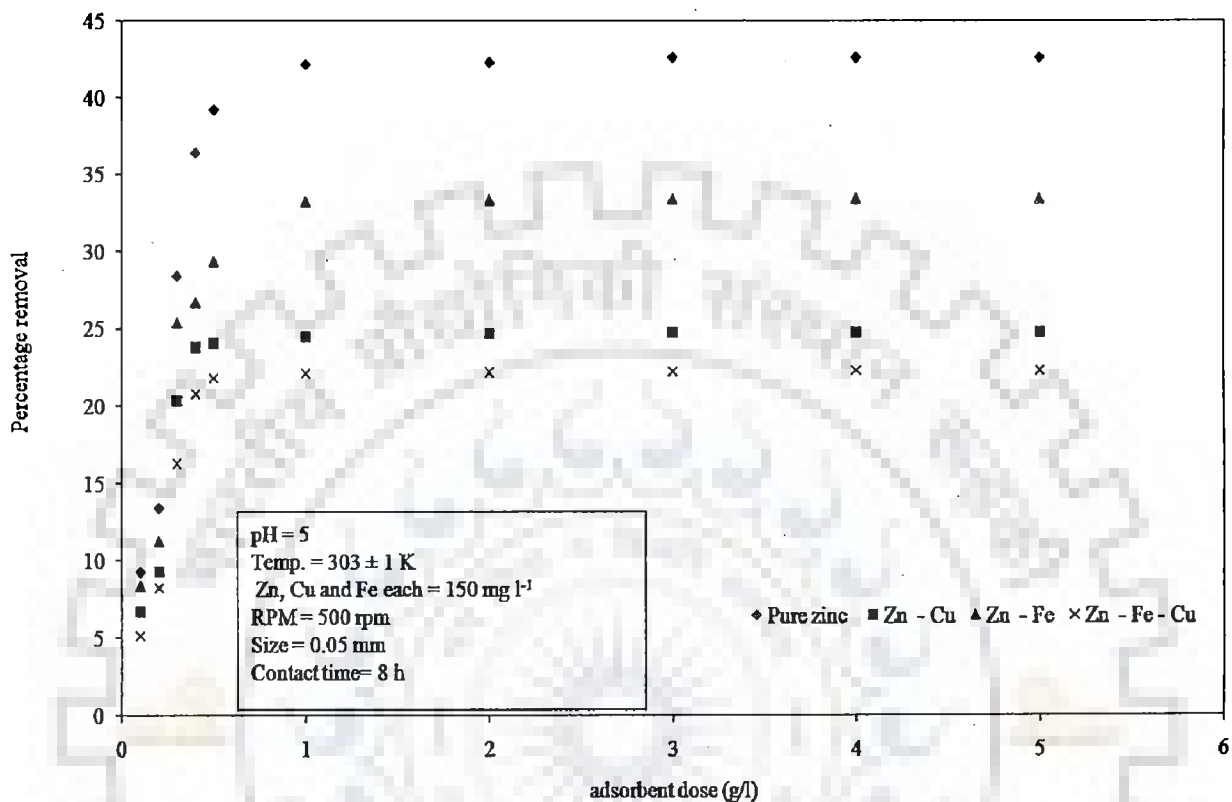


Figure 5.2.3 (g): Effect of adsorbent dose on biosorption of Zn on Jackfruit peel

It is evident from figure 5.2.3 (g) that the maximum removal of Zn (II) ion was obtained in pure zinc phase. The maximum removal of Zn (II) ion was 42.11% at 1 g l<sup>-1</sup> of Jackfruit peel. The maximum removal of total Fe (II, III) and Cu (II) ion in Zn (II) – Cu (II), Zn – Fe (II) and Zn (II)- Cu (II)- Fe (II, III) were obtained also at 1 g l<sup>-1</sup> of adsorbent dose in figure 5.2.3 (f). The presence of other metal ions hindered the biosorption of Zn (II) ion.

The increase in biosorbent dose from 0.1 g l<sup>-1</sup> to 1 g l<sup>-1</sup> favoured the biosorption of Zn (II), Fe (II, III) and Cu (II) in all types of metal ion systems. Further, the rise in biosorbent dose from 1 g l<sup>-1</sup> to 5 g l<sup>-1</sup> did not increase significantly the removal of Zn (II), total Fe (II,

III) and Cu (II) ion. The increase in biosorption of Zn (II), Fe (II, III) and Cu (II) with the increase in biosorbent dose from 0.1 g l<sup>-1</sup> to 1 g l<sup>-1</sup> was due to the availability of higher number of binding sites after every increment in biosorbent dose.

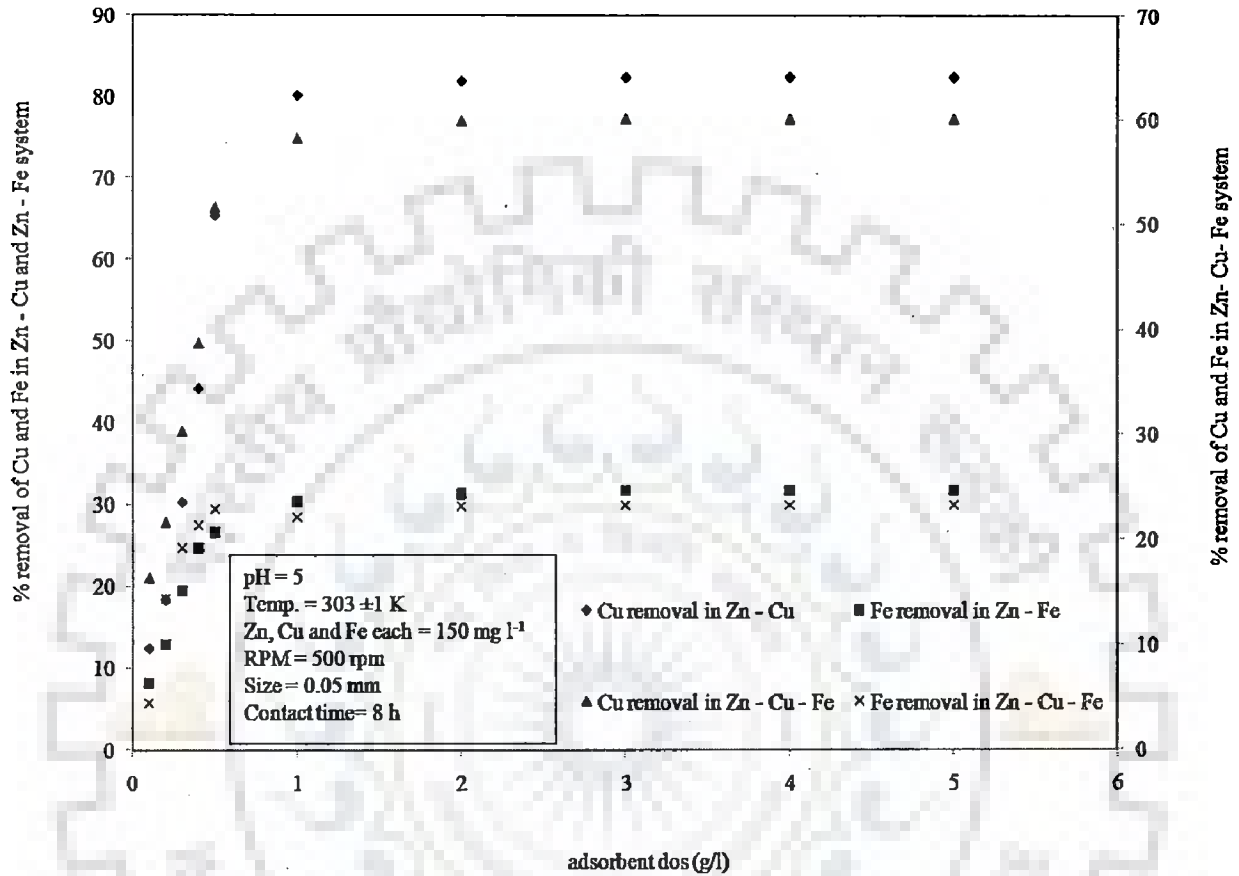


Figure 5.2.3 (h): Effect of adsorbent dose on biosorption of Cu and Fe in presence of Zn on Jackfruit peel

However, the reason behind the insignificant change in biosorption of Zn (II), total Fe (II, III) and Cu (II) at higher concentration of biosorbent ranging between 1 g l<sup>-1</sup> to 5 g l<sup>-1</sup> was the agglomeration and clumping of biosorbent particles which led to the decrease in effective surface area of biosorbent (Ahmad et al., 2009, Ucun et al., 2009). The preferential order of removal of heavy metal ions was Cu (II) > Zn (II) > Fe (II, III).

Figure 5.2.3 (i) and table 5.2.2 (j) represent the influence of biosorbent dose on biosorption of Zn (II), total Fe (II, III) and Cu (II) on *Cedrus deodara* sawdust. It is evident



from figure 5.2.3 (i) that the maximum removal of Zn (II) ion was obtained in pure zinc phase at  $1 \text{ g l}^{-1}$  dose.

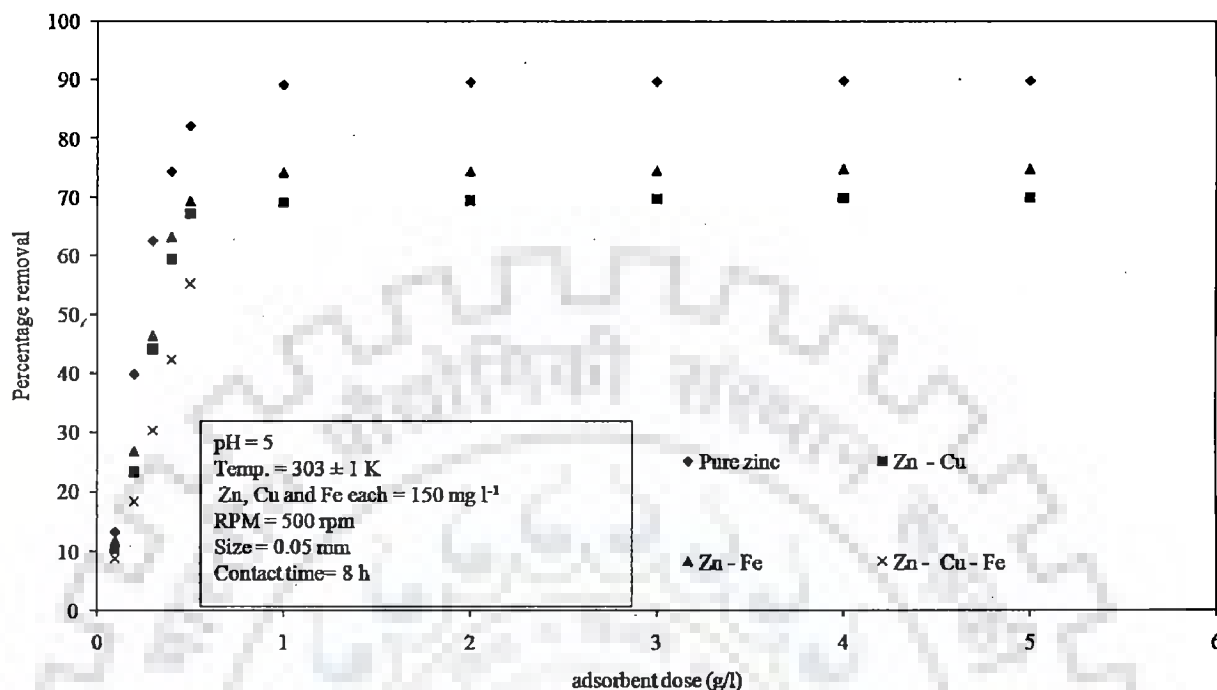


Figure 5.2.3 (i): Effect of adsorbent dose on biosorption of Zn (II) on *Cedrus deodara* sawdust

The maximum removal of Zn (II) ion was 89.19% at  $1 \text{ g l}^{-1}$  of *Cedrus deodara* sawdust. The maximum removal of total Fe (II, III) and Cu (II) ion in Zn (II) – Cu (II), Zn – Fe (II) and Zn (II)- Cu (II)- Fe (II, III) was obtained also at  $1 \text{ g l}^{-1}$  of adsorbent dose in figure 5.2.3 (j). The presence of other metal ions hindered the biosorption of Zn (II) ion. The increase in biosorbent dose from  $0.1 \text{ g l}^{-1}$  to  $1 \text{ g l}^{-1}$  favoured the biosorption of Zn (II), Fe (II, III) and Cu (II) in all the types of metal ion systems.

Further, the rise in biosorbent dose from  $1 \text{ g l}^{-1}$  to  $5 \text{ g l}^{-1}$  did not increase significantly the removal of Zn (II), Cu (II) and total Fe (II, III) ion. The increase in biosorption of Zn (II), Fe (II, III) and Cu (II) with the increase of biosorbent dose from  $0.1 \text{ g l}^{-1}$  to  $1 \text{ g l}^{-1}$  was due to the availability of higher number of binding sites after every increment in biosorbent dose.

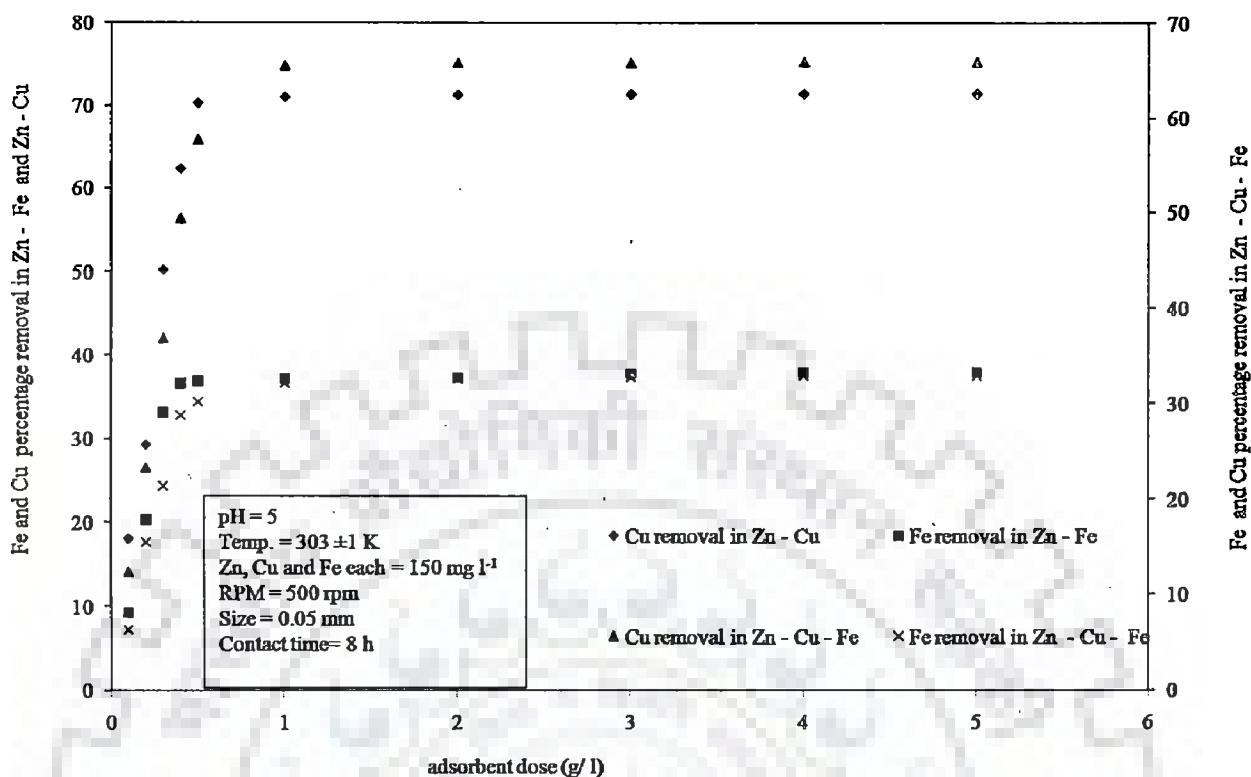


Figure 5.2.3 (j): Effect of adsorbent dose on biosorption of Cu and Fe in presence of Zn on *Cedrus deodara* sawdust

However, the reason behind the insignificant change in biosorption of Zn (II), total Fe (II, III) and Cu (II) at higher concentration of biosorbent ranging between 1  $\text{g l}^{-1}$  to 5  $\text{g l}^{-1}$  was the agglomeration and clumping of biosorbent particles which led to the decrease in effective surface area of biosorbent (Ahmad et al., 2009, Ucun et al., 2009). The preferential order of removal of heavy metal ions was Cu (II) > Zn (II) > Fe (II, III).

Figure 5.2.3 (k) and figure 5.2.2 (l) represent the influence of biosorbent dose on biosorption of Zn (II), total Fe (II, III) and Cu (II) on Eucalyptus bark sawdust. It became evident from figure 5.2.3 (k) that the maximum removal of Zn (II) ion was obtained in pure zinc phase at 1  $\text{g l}^{-1}$ . The maximum removal of Zn (II) ion was 71.33% at 1  $\text{g l}^{-1}$  of Eucalyptus bark sawdust. The maximum removal of total Fe (II, III) and Cu (II) ion in Zn (II) – Cu (II),

Zn – Fe (II) and Zn (II)- Cu (II)- Fe (II, III) was obtained also at 1 g l<sup>-1</sup> of adsorbent dose in figure 5.2.3 (l). The presence of other metal ions hindered the biosorption of Zn (II) ion.

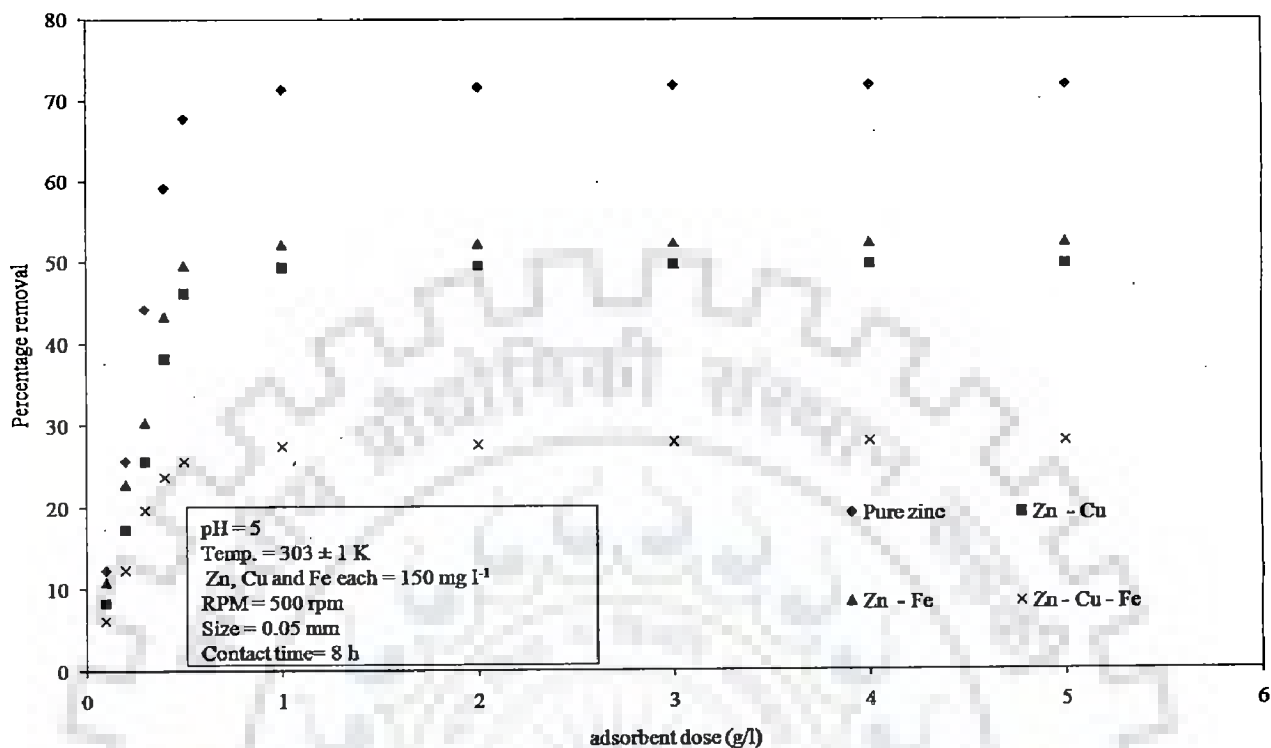


Figure 5.2.3 (k): Effect of adsorbent dose on biosorption of Zn on Eucalyptus bark sawdust

The increase in biosorbent dose from 0.1 g l<sup>-1</sup> to 1 g l<sup>-1</sup> favoured the biosorption of Zn (II), Fe (II, III) and Cu (II) in all the types of metal ion systems. Further, the rise in biosorbent dose from 1 g l<sup>-1</sup> to 5 g l<sup>-1</sup> did not increase significantly the removal of Zn (II), total Fe (II, III) and Cu (II) ion.

The increase in biosorption of Zn (II), Fe (II, III) and Cu (II) with the increase of biosorbent dose from 0.1 g l<sup>-1</sup> to 1 g l<sup>-1</sup> was due to the availability of higher number of binding sites after every increment in biosorbent dose. However, the reason behind the insignificant change in biosorption of Zn (II), total Fe (II, III) and Cu (II) at higher concentration of biosorbent ranging between 1 g l<sup>-1</sup> to 5 g l<sup>-1</sup> was the agglomeration and clumping of biosorbent particles which led to the decrease in effective surface area of biosorbent (Ahmad et al., 2009,

Ucun et al., 2009). The preferential order of removal of heavy metal ions was Cu (II) > Zn (II) > Fe (II, III).

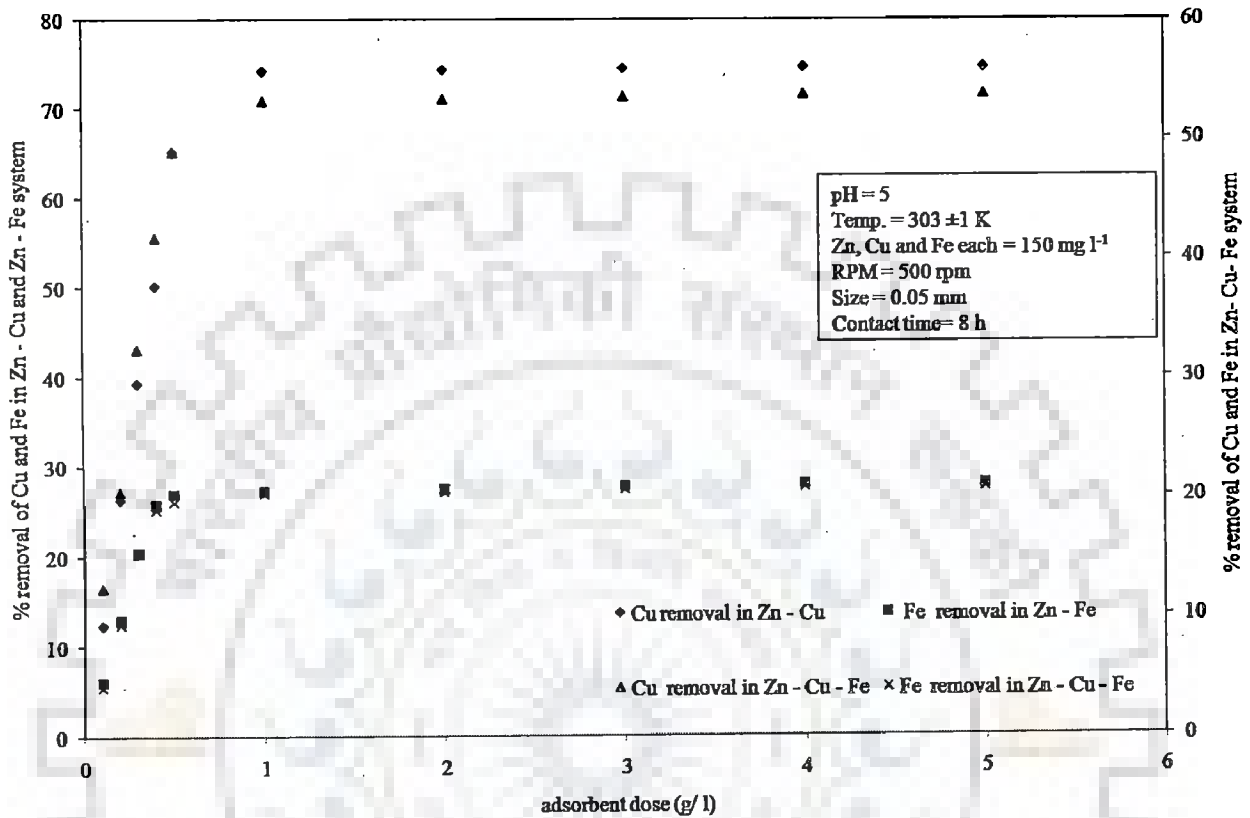


Figure 5.2.3 (l): Effect of adsorbent dose on biosorption of Cu and Fe ions in presence of Zn on Eucalyptus bark sawdust

Figure 5.2.3 (m) and figure 5.2.3 (n) represent the influence of biosorbent dose on biosorption of Zn (II), total Fe (II, III) and Cu (II) on Eucalyptus leaf powder. It became evident from figure 5.2.3 (m) that the maximum removal of Zn (II) ion was obtained in pure zinc phase at 1 g l<sup>-1</sup>. The maximum removal of Zn (II) ion was 72.18% at 1 g l<sup>-1</sup> of Eucalyptus leaf powder. The maximum removal of total Fe (II, III) and Cu (II) ion in Zn (II) – Cu (II), Zn – Fe (II) and Zn (II)- Cu (II)- Fe (II, III) was obtained also at 1 g l<sup>-1</sup> of adsorbent dose in figure 5.2.3 (n). The presence of other metal ions hindered the biosorption of Zn (II) ion. The increase in biosorbent dose from 0.1 g l<sup>-1</sup> to 1 g l<sup>-1</sup> favoured the biosorption of Zn (II), Fe (II,

III) and Cu (II) in all the types of metal ion systems. Further, the rise in biosorbent dose from  $1 \text{ g l}^{-1}$  to  $5 \text{ g l}^{-1}$  did not increase significantly the removal of Zn (II), total Fe (II, III) and Cu (II) ion.

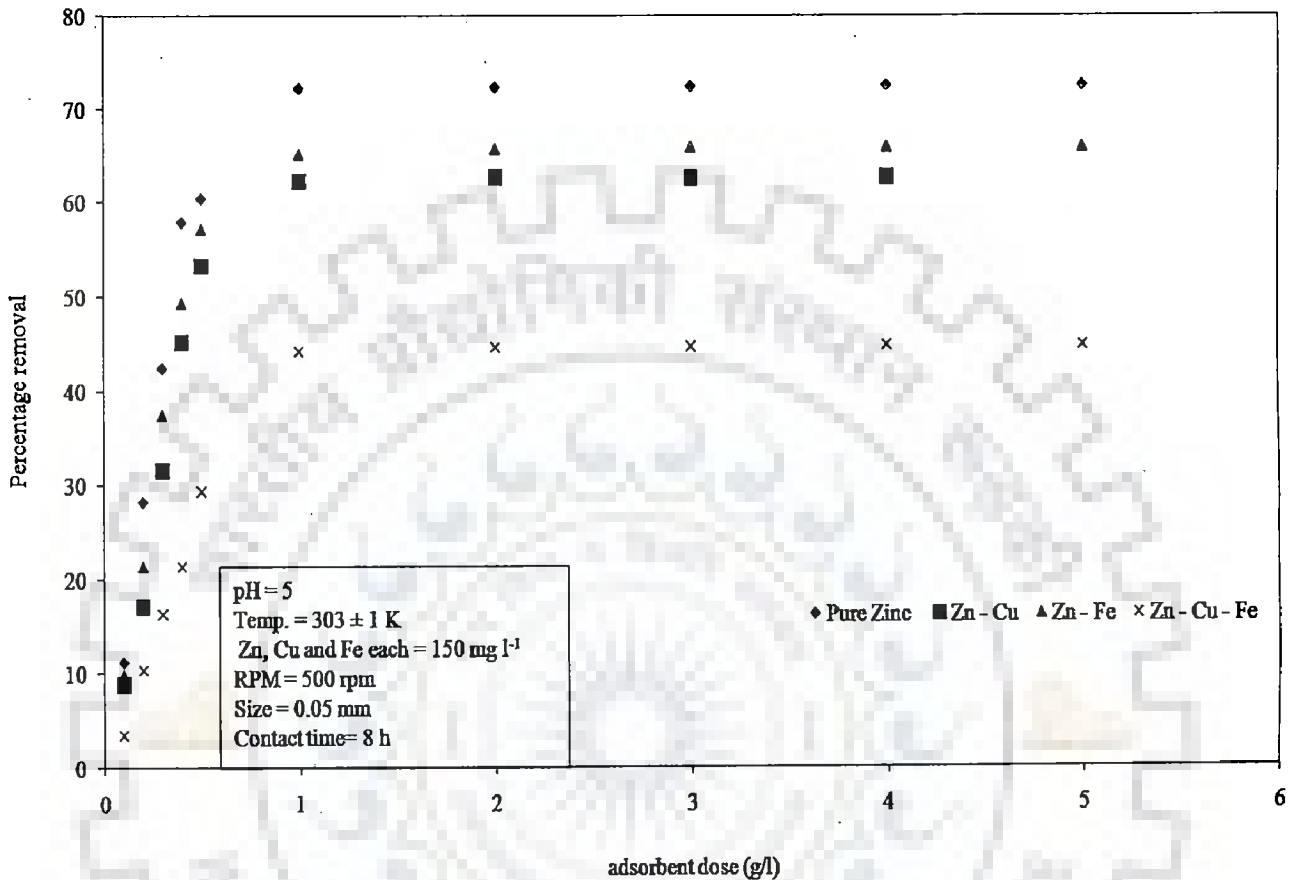


Figure 5.2.3 (m): Effect of adsorbent dose on biosorption of Zn on Eucalyptus leaf powder

The increase in biosorption of Zn (II), Fe (II, III) and Cu (II) with the increase of biosorbent dose from  $0.1 \text{ g l}^{-1}$  to  $1 \text{ g l}^{-1}$  was due to the availability of higher number of binding sites after every increment in biosorbent dose. The maximum removal of total Fe (II, III) and Cu (II) ion in Zn (II) – Cu (II), Zn – Fe (II) and Zn (II)- Cu (II)- Fe (II, III) was obtained at  $1 \text{ g l}^{-1}$  of adsorbent dose.

However, the reason behind the insignificant change in biosorption of Zn (II), total Fe (II, III) and Cu (II) at higher concentration of biosorbent ranging between  $1 \text{ g l}^{-1}$  to  $5 \text{ g l}^{-1}$  was

the agglomeration and clumping of biosorbent particles which led to the decrease in effective surface area of biosorbent (Ahmad et al., 2009, Ucun et al., 2009). The preferential order of removal of heavy metal ions was Cu (II) > Zn (II) > Fe (II, III).

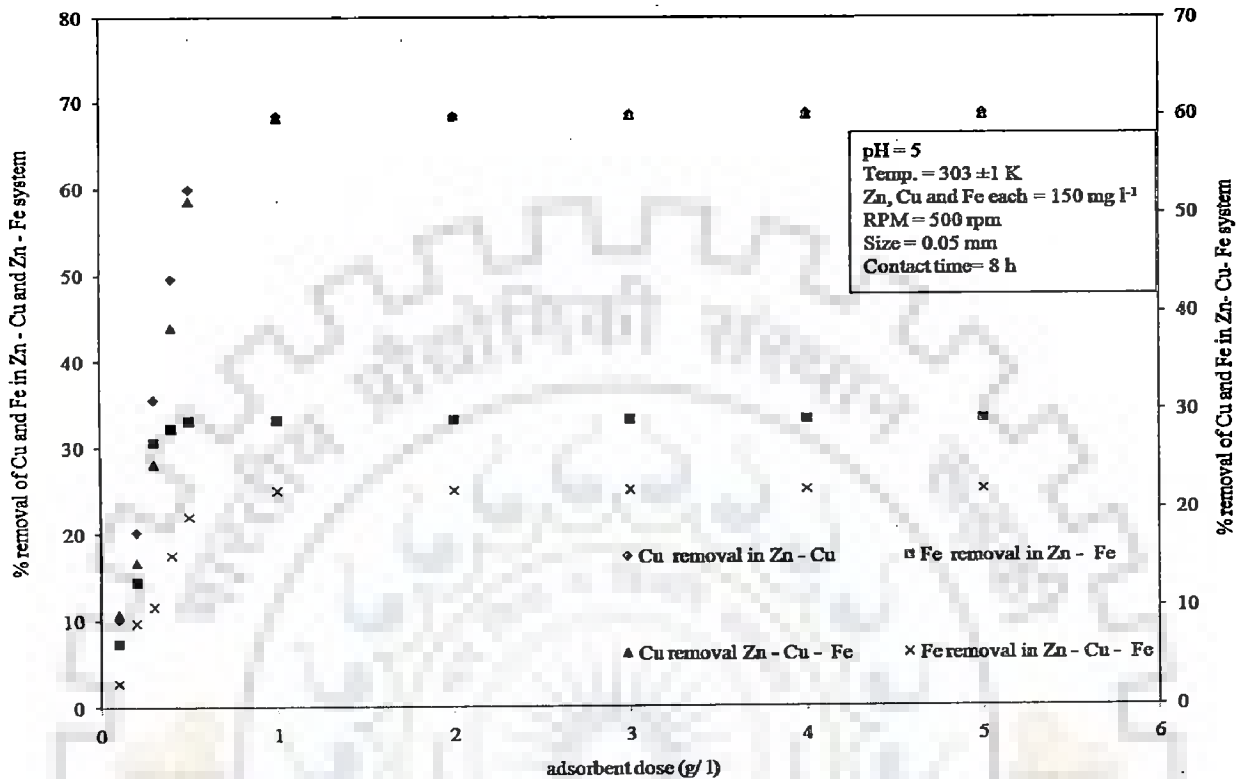


Figure 5.2.3 (n): Effect of adsorbent dose on biosorption of Cu and Fe in presence of Zn on Eucalyptus leaf powder

Figure 5.2.3 (o) and figure 5.2.2 (p) represent the influence of biosorbent dose on biosorption of Zn (II), total Fe (II, III) and Cu (II) on Eggshell and membrane. It became evident from figure 5.2.3 (o) figure 5.2.3 (p) that the maximum removal of Zn (II) ion was obtained in pure zinc phase at 1 g l<sup>-1</sup> dose. The maximum removal of Zn (II) ion was 42.59% at 1 g l<sup>-1</sup> of Eggshell and membrane. The presence of other metal ions hindered the biosorption of Zn (II) ion. The increase in biosorbent dose from 0.1 g l<sup>-1</sup> to 1 g l<sup>-1</sup> favoured the biosorption of Zn (II), Fe (II, III) and Cu (II) in all the types of metal ion systems.

Further, the rise in biosorbent dose from 1 g l<sup>-1</sup> to 5 g l<sup>-1</sup> did not increase significantly the removal of Zn (II), total Fe (II, III) and Cu (II) ion. The increase in biosorption of Zn (II),

Fe (II, III) and Cu (II) with the increase of biosorbent dose from 0.1 g l<sup>-1</sup> to 1 g l<sup>-1</sup> was due to the availability of higher number of binding sites after every increment in biosorbent dose.

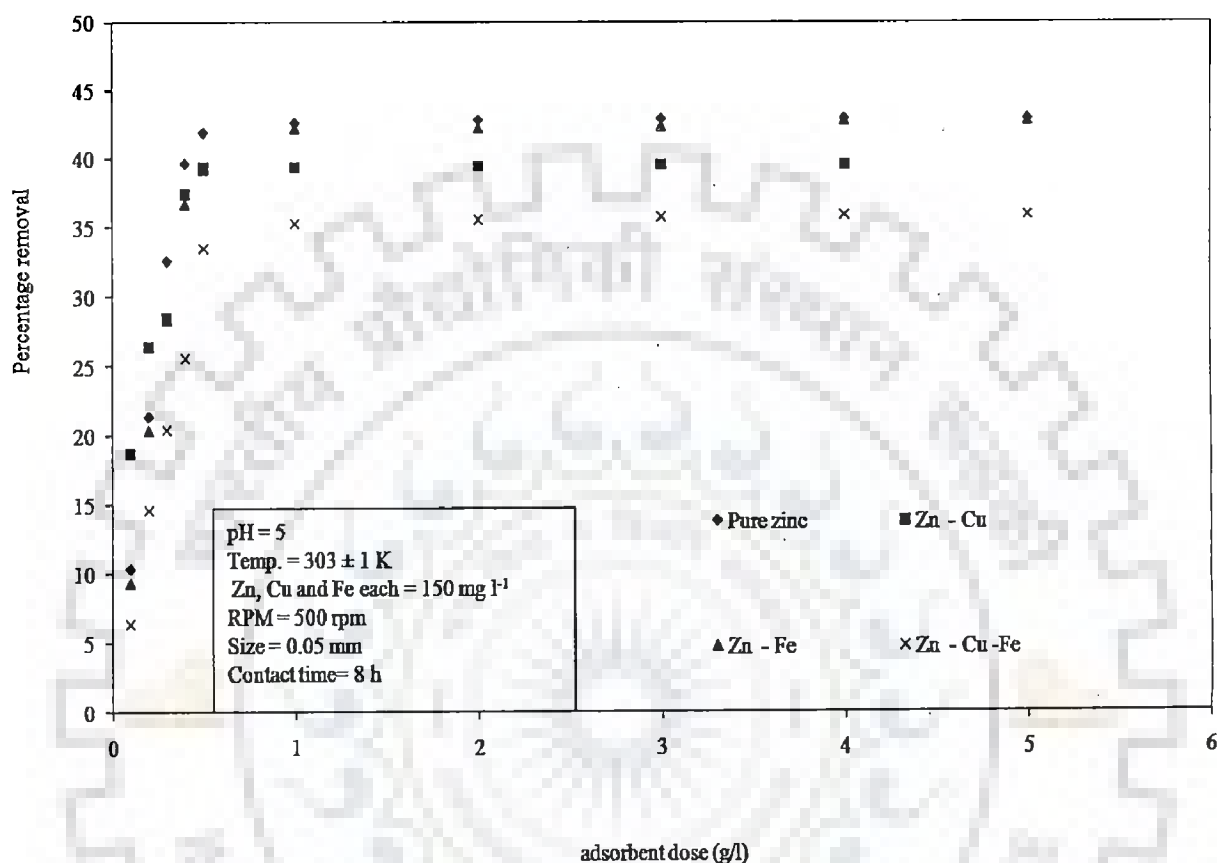


Figure 5.2.3 (o): Effect of adsorbent dose on biosorption of Zn on Eggshell and membrane

The maximum removal of total Fe (II, III) and Cu (II) ion in Zn (II) – Cu (II), Zn – Fe (II) and Zn (II)- Cu (II)- Fe (II, III) was obtained at also 1 g l<sup>-1</sup> of adsorbent dose in figure 5.2.3 (p).

However, the reason behind the insignificant change in biosorption of Zn (II), total Fe (II, III) and Cu (II) at higher concentration of biosorbent ranging between 1 g l<sup>-1</sup> to 5 g l<sup>-1</sup> was the agglomeration and clumping of biosorbent particles which led to the decrease in effective surface area of biosorbent (Ahmad et al., 2009, Ucin et al., 2009). The preferential order of removal of heavy metal ions was Cu (II) > Zn (II) > Fe (II, III).

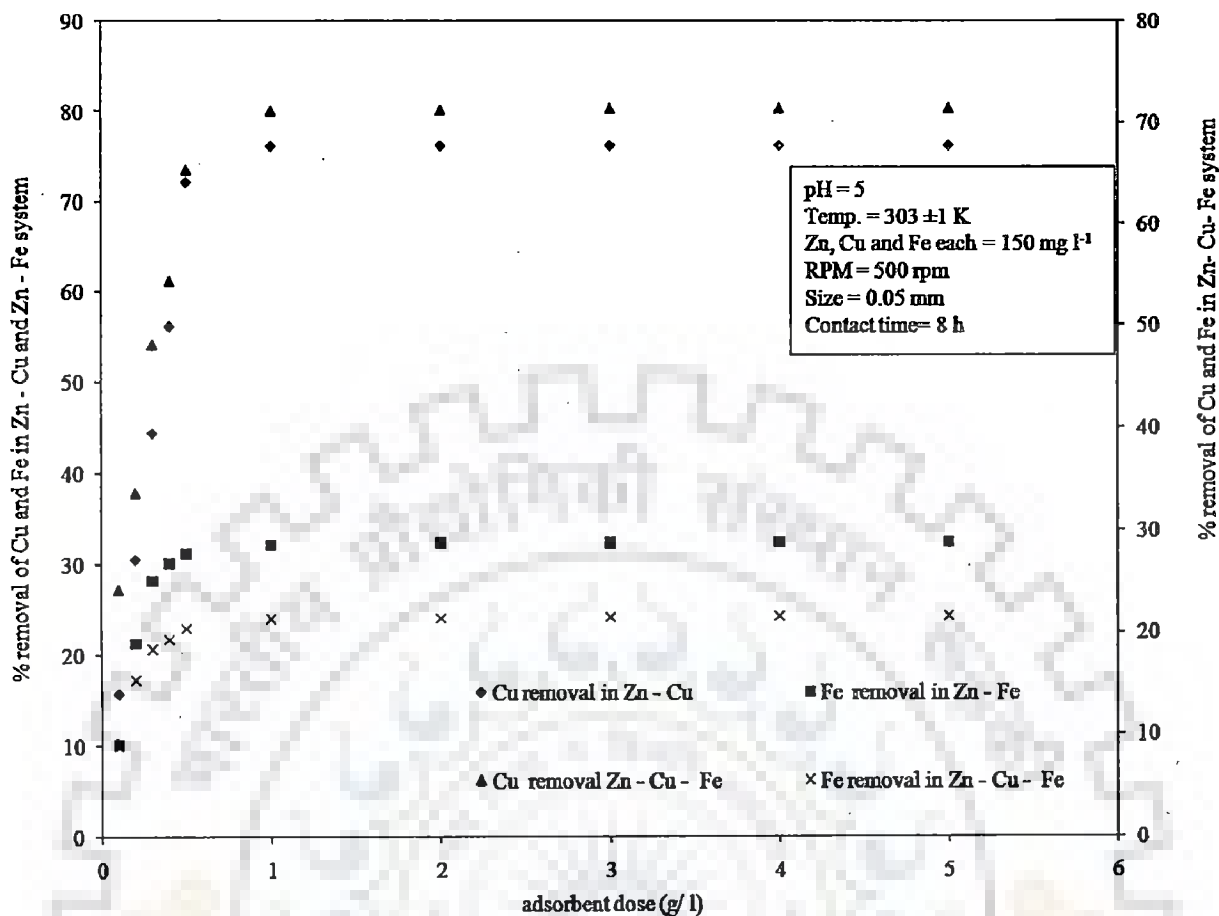


Figure 5.2.3 (p): Effect of adsorbent dose on biosorption of Cu and Fe and ions in presence of Zn on Eggshell and membrane

Figure 5.2.3 (q) and figure 5.2.3 (r) represent the influence of biosorbent dose on biosorption of Zn (II), total Fe (II, III) and Cu (II) on dead cells of *Zinc sequestering bacterium VMSDCM* accession no. HQ108109. It became evident from figure 5.2.3 (q) that the maximum removal of Zn (II) ion was obtained in pure zinc phase at 1 g l<sup>-1</sup> dose. The maximum removal of Zn (II) ion was 100% at 1 g l<sup>-1</sup> of dead cells of *Zinc sequestering bacterium VMSDCM* accession no. HQ108109.

The presence of other metal ions hindered the biosorption of Zn (II) ion. The increase in biosorbent dose from 0.1 g l<sup>-1</sup> to 1 g l<sup>-1</sup> favoured the biosorption of Zn (II), Fe (II, III) and Cu (II) in all the types of metal ion systems. The maximum removal of total Fe (II, III) and



Cu (II) ion in Zn (II) – Cu (II), Zn – Fe (II) and Zn (II)- Cu (II)- Fe (II, III) was obtained also at  $1 \text{ g l}^{-1}$  of adsorbent dose in figure 5.2.3 (r).

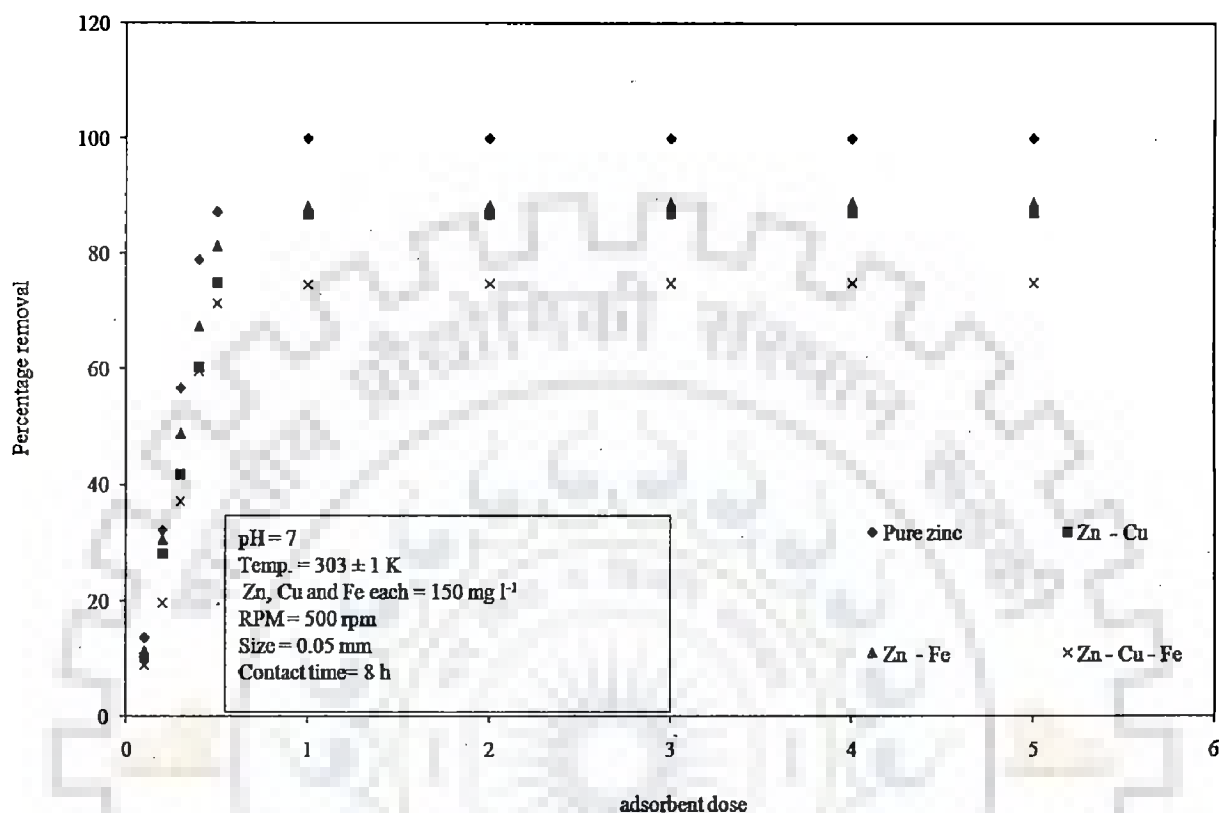


Figure 5.2.3 (q): Effect of adsorbent dose on biosorption of Zn on dead cells of *Zinc sequestering bacterium VMSDCM* accession no. HQ108109

Further, with the rise in biosorbent dose from  $1 \text{ g l}^{-1}$  to  $5 \text{ g l}^{-1}$  the removal of Zn (II), total Fe (II, III) and Cu (II) ion did not increase significantly. The increase in biosorption of Zn (II), Fe (II, III) and Cu (II) with the increase of biosorbent dose from  $0.1 \text{ g l}^{-1}$  to  $1 \text{ g l}^{-1}$  was due to the availability of higher number of binding sites after every increment in biosorbent dose. However, the reason behind the insignificant change in biosorption of Zn (II), total Fe (II, III) and Cu (II) at higher concentration of biosorbent ranging between  $1 \text{ g l}^{-1}$  to  $5 \text{ g l}^{-1}$  was the agglomeration and clumping of biosorbent particles which led to the decrease in effective surface area of biosorbent (Ahmad et al., 2009, Uzun et al., 2009). The preferential order of removal of heavy metal ions was  $\text{Cu (II)} > \text{Zn (II)} > \text{Fe (II, III)}$ .

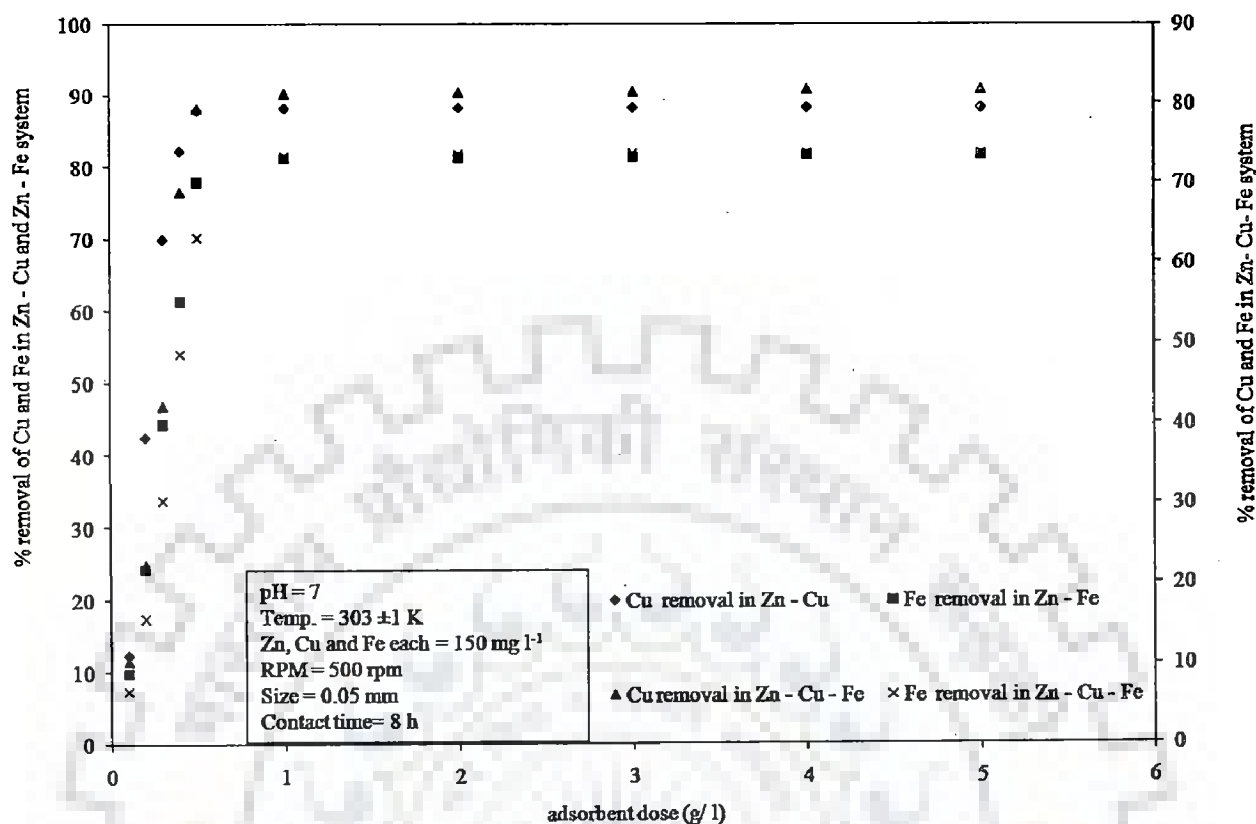


Figure 5.2.3 (r): Effect of adsorbent dose on biosorption of Cu and Fe in presence of Zn on dead cells of *Zinc sequestering bacterium VMSDCM* accession no. HQ108109

### Concluding remarks of section 5.3.3

Among all the biosorbents selected for the present work, the maximum removal of Zn (II) ion was obtained with *Cedrus deodara* sawdust and dead cells of *Zinc sequestering bacterium VMSDCM* accession no HQ108109. The maximum removal of Zn (II) ion obtained in case of *Cedrus deodara* sawdust and dead cells of *Zinc sequestering bacterium VMSDCM* accession no HQ108109 were 89.19 % and 100%, respectively in pure zinc environment. In presence of Cu (II) ion, the removal of Zn (II) was less in comparison to the pure zinc environment. The removal of zinc in presence of Cu (II) in case of *Cedrus deodara* sawdust and dead cells of *Zinc sequestering bacterium VMSDCM* accession no HQ108109 was 69.12% and 86.6%,

respectively. Similarly, in the presence of total Fe (II, III) the percentage removal of Zn (II) ion was quite diminished. The removal of zinc in presence of total Fe (II, III) using *Cedrus deodara* sawdust and dead cells of *Zinc sequestering bacterium VMSDCM* accession no HQ108109 was 74.31% and 88.19%, respectively. In ternary metal ion complex system, the removal of Zn (II) ion was 69.11% and 74.61% in case of *Cedrus deodara* sawdust and dead cells of *Zinc sequestering bacterium VMSDCM* accession no. HQ108109, respectively. The optimum dose for the maximum removal of Zn (II) from liquid phase of both the biosorbents was estimated as  $1 \text{ g l}^{-1}$ .

#### 5.2.4 Optimization of initial concentration of Zn (II) ion

This section embodies the results of influence of initial concentration of Zn (II) ion on biosorption of Zn (II) ion in liquid phase. The experiments were conducted in range of  $1 \text{ mg l}^{-1}$  to  $150 \text{ mg l}^{-1}$ . The experiments were conducted in round bottom flasks of 500 ml capacity containing 1, 2, 4, 8, 10, 20, 40, 80, 100, 120 and  $150 \text{ mg l}^{-1}$  of metal ion solution. The system of ions studied in the present work were pure zinc, Zn (II)- Cu (II), Zn (II)- Fe (II, III) and Zn (II) – Fe (II, III)- Cu (II). The metal ions Zn (II), Cu (II) and Fe (II, III) are referred as Zn, Cu and Fe in various figures.

Results of influence of initial concentration have been shown in figures 5.2.4 (a) to 5.2.4 (r).

Figure 5.2.4 (a) and figure 5.2.4 (b) represent the influence of initial concentration of Zn (II) ion on the biosorption of Zn (II), Cu (II) and total Fe (II, III) on Mango bark sawdust.

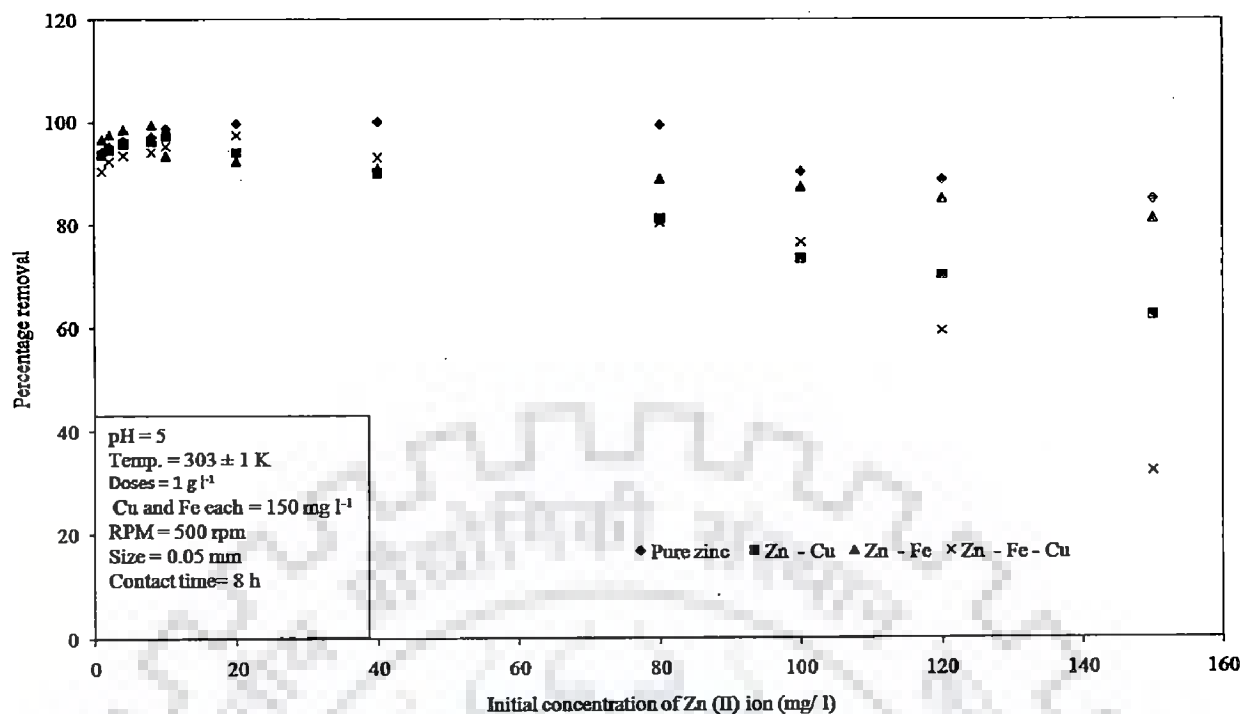


Figure 5.2.4 (a): Effect of initial concentration of Zn on biosorption on Mango bark sawdust

It is evident from figure 5.2.4 (a) that the maximum removal of Zn (II) ion was obtained in pure zinc phase. The maximum removal of Zn (II) ion (100%) was obtained at 80 mg l<sup>-1</sup> of initial concentration of metal ion. In all types of metal ion systems, the increase in metal ion concentration from 1 mg l<sup>-1</sup> to 40 mg l<sup>-1</sup> of Zn (II) ion favoured the percentage removal of Zn (II) ion in liquid phase.

The increase in percentage removal of Zn (II) ion from liquid phase with an increase in Zn (II) ion concentration from 1 mg l<sup>-1</sup> to 40 mg l<sup>-1</sup> was due to the fact that increase in concentration of metal ion led to the increase in driving force or concentration gradient which resulted in higher percentage removal.

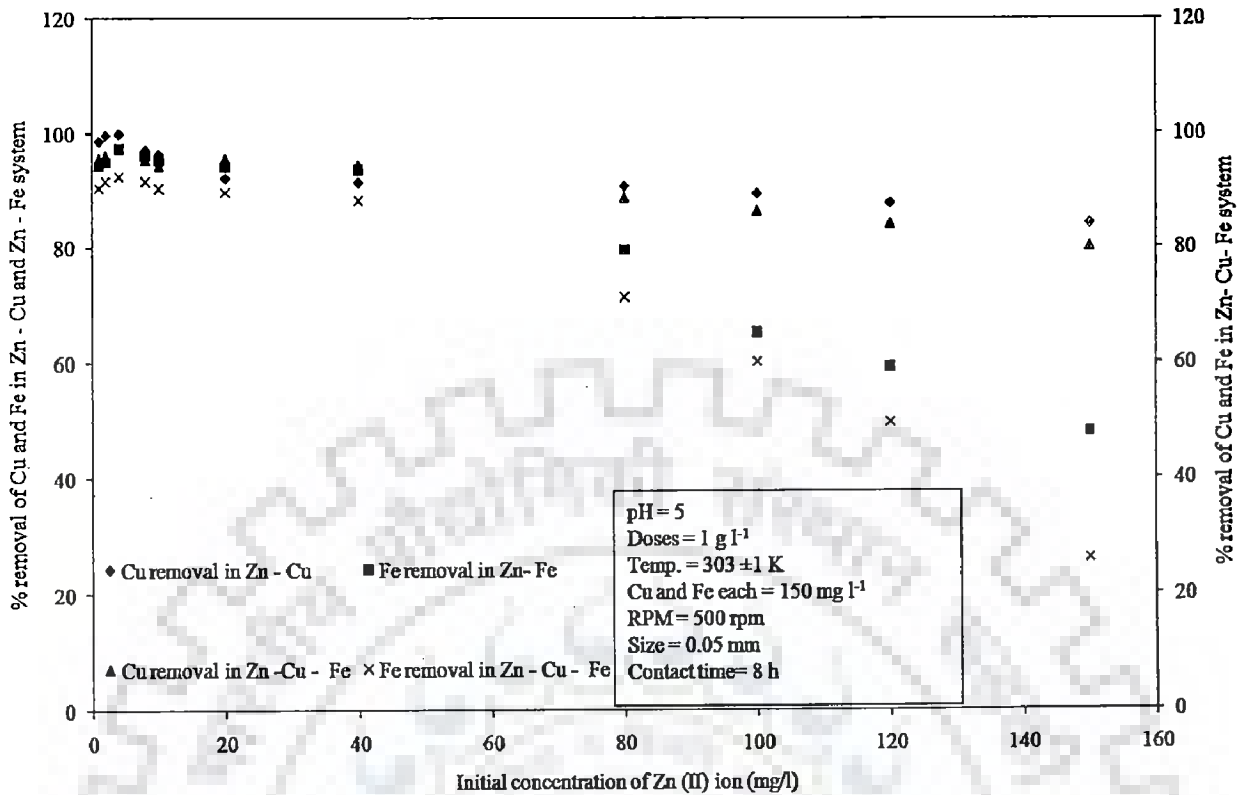


Figure 5.2.4(b): Effect of initial concentration of Zn on biosorption of Cu and Fe on Mango bark

Similarly, the maximum removal of Total Fe (II, III) and Cu (II) ion in Zn (II)- Cu (II), Zn (II)- Total Fe (II, III) and Zn (II)- Cu (II)- Total Fe (II, III) metal ion system was obtained at 40 mg l<sup>-1</sup> of zinc (figure 5.2.4 (b)). However, the increase in initial concentration of Zn (II) ion from 40 to 150 mg l<sup>-1</sup> led to the decrease in removal of Zn (II) ion in all types of the metal ion systems.

The decrease in removal of Zn (II) ion with the increase in initial concentration of Zn (II) ion was due to the saturation of active sites present on the surface of biosorbent (Ozdes et al., 2009, Ozdemir et al., 2009). The presence of other metal ions hindered the biosorption of Zn (II) ion. The preferential order of removal of heavy metal ions was Cu (II) > Zn (II) > Fe (II, III).

Figure 5.2.4 (c) and figure 5.2.4 (d) represent the influence of initial concentration of Zn (II) ion on the Orange peel.

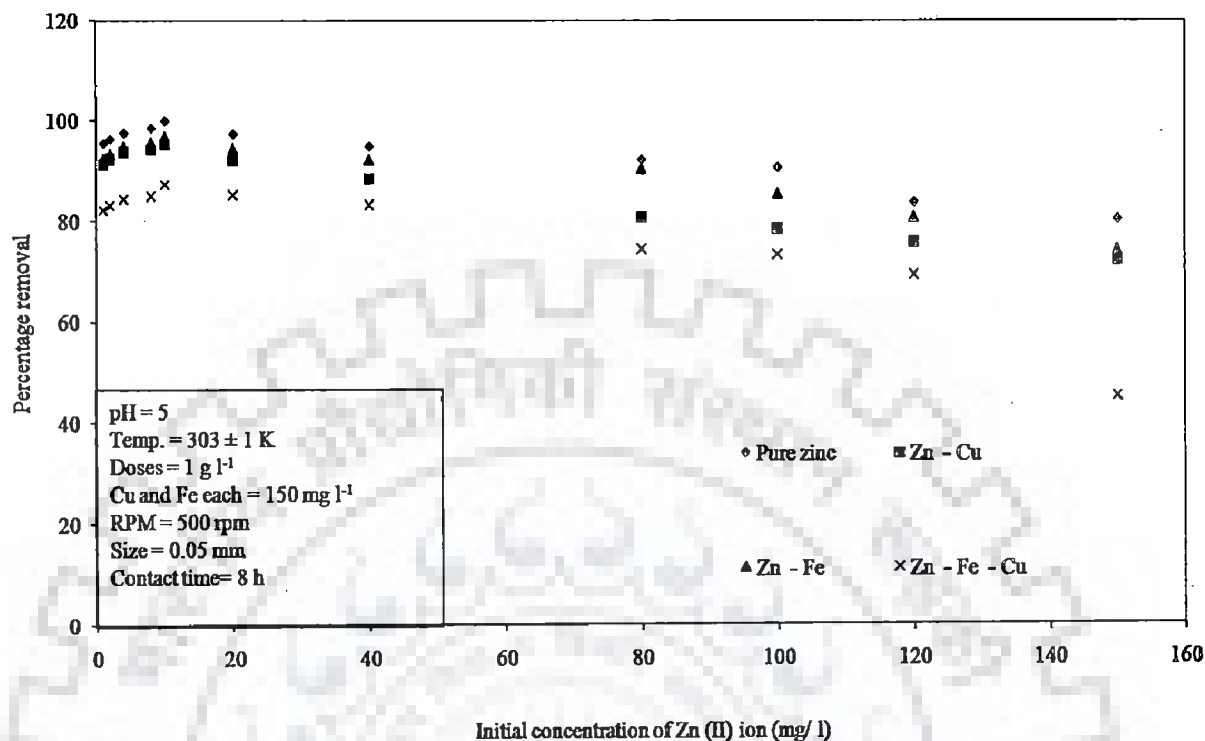


Figure 5.2.4 (c): Effect of initial concentration of Zn on biosorption of Zn on Orange peel

It is evident from figure 5.2.4 (c) that the maximum removal of Zn (II) ion was obtained in pure zinc phase. The maximum removal of Zn (II) ion (100%) was obtained at  $10 \text{ mg l}^{-1}$  of initial concentration of metal ion. In all types of metal ion systems, the increase in metal ion concentration from  $1 \text{ mg l}^{-1}$  to  $10 \text{ mg l}^{-1}$  of Zn (II) ion favoured the percentage removal of Zn (II) ion in liquid phase.

The increase in percentage removal of Zn (II) ion from liquid phase with an increase in Zn (II) ion concentration from  $1 \text{ mg l}^{-1}$  to  $10 \text{ mg l}^{-1}$  was due to the fact that increase in concentration of metal ion led to the increase in driving force or concentration gradient which resulted in higher percentage removal.

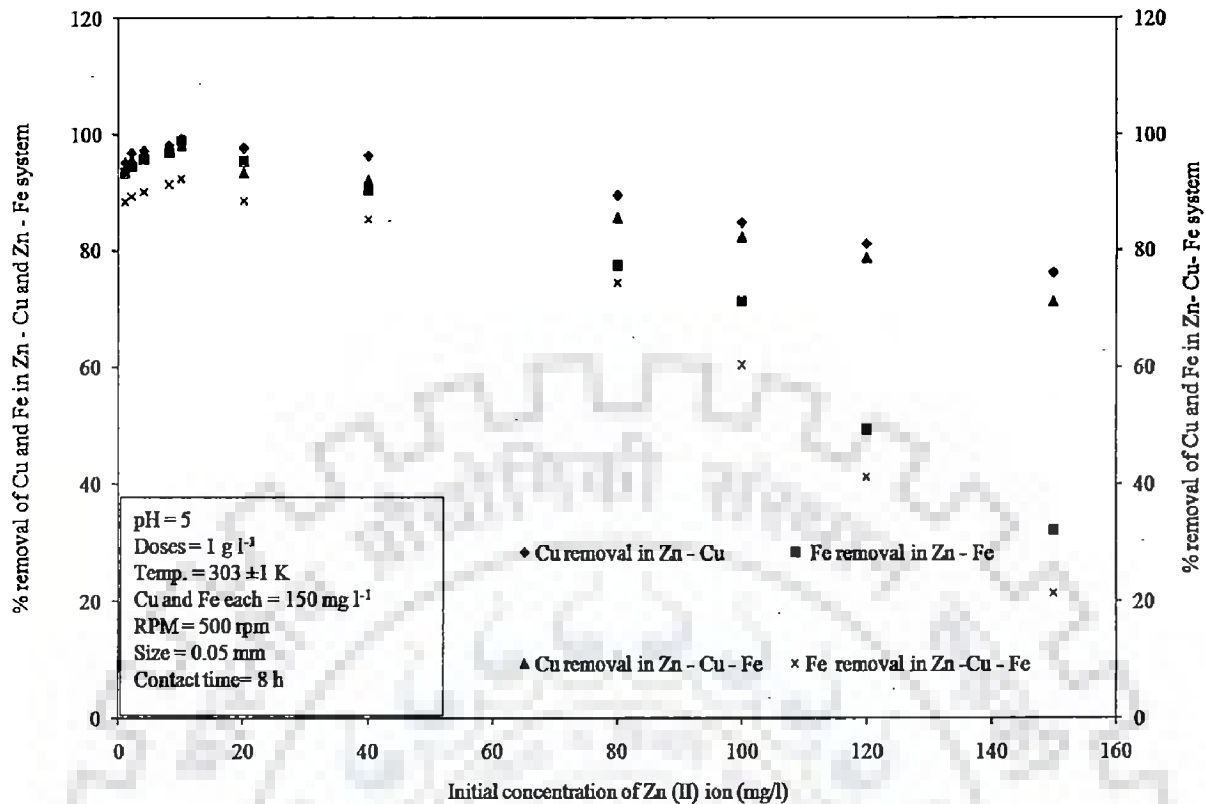


Figure 5.2.4 (d): Effect of initial concentration of Zn on biosorption of Cu and Fe on Orange peel

Similarly, the maximum removal of Total Fe (II, III) and Cu (II) ion in Zn (II)- Cu (II), Zn (II)- Total Fe (II, III) and Zn (II)- Cu (II)- Total Fe (II, III) metal ion system was obtained at 10 mg l<sup>-1</sup> of zinc figure 5.2.4 (d). However, the increase in initial concentration of Zn (II) ion from 10 to 150 mg l<sup>-1</sup> led to the decrease in removal of Zn (II) ion in all types of the metal ion systems.

The decrease in removal of Zn (II) ion with the increase in initial concentration of Zn (II) ion was due to the saturation of active sites present on the surface of biosorbent (Ozdes et al., 2009, Ozdemir et al., 2009). The presence of other metal ions hindered the biosorption of Zn (II) ion. The preferential order of removal of heavy metal ions was Cu (II) > Zn (II) > Fe (II, III).

Figure 5.2.4 (e) and figure 5.2.4 (f) represent the influence of initial concentration of Zn (II) ion on pineapple peel.

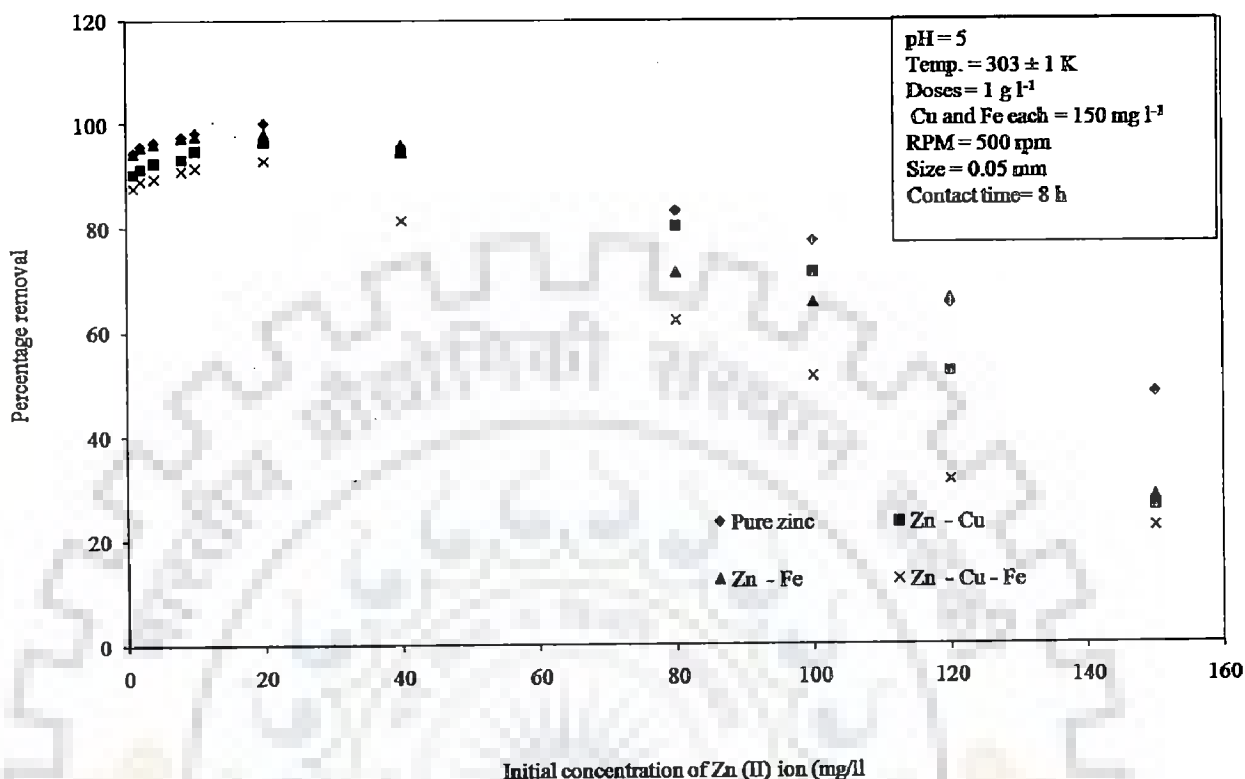


Figure 5.2.4 (e): Effect of initial concentration of Zn on biosorption of Zn on Pineapple peel

It is evident from figure 5.2.4 (e) that the maximum removal of Zn (II) ion was obtained in pure zinc phase. The maximum removal of Zn (II) ion (100%) was obtained at 20 mg l<sup>-1</sup> of initial concentration of metal ion. In all types of metal ion systems, the increase in metal ion concentration from 1 mg l<sup>-1</sup> to 20 mg l<sup>-1</sup> of Zn (II) ion favoured the percentage removal of Zn (II) ion in liquid phase.

The increase in percentage removal of Zn (II) ion from liquid phase with an increase in Zn (II) ion concentration from 1 mg l<sup>-1</sup> to 20 mg l<sup>-1</sup> was due to the fact that increase in concentration of metal ion led to the increase in driving force or concentration gradient which resulted in higher percentage removal. Similarly, the maximum removal of Total Fe (II, III) and Cu (II) ion in Zn (II)- Cu (II), Zn (II)- Total Fe (II, III) and Zn (II)- Cu (II)- Total Fe (II, III) metal ion system was obtained at 20 mg l<sup>-1</sup> of zinc (figure 5.4.2 (f)).



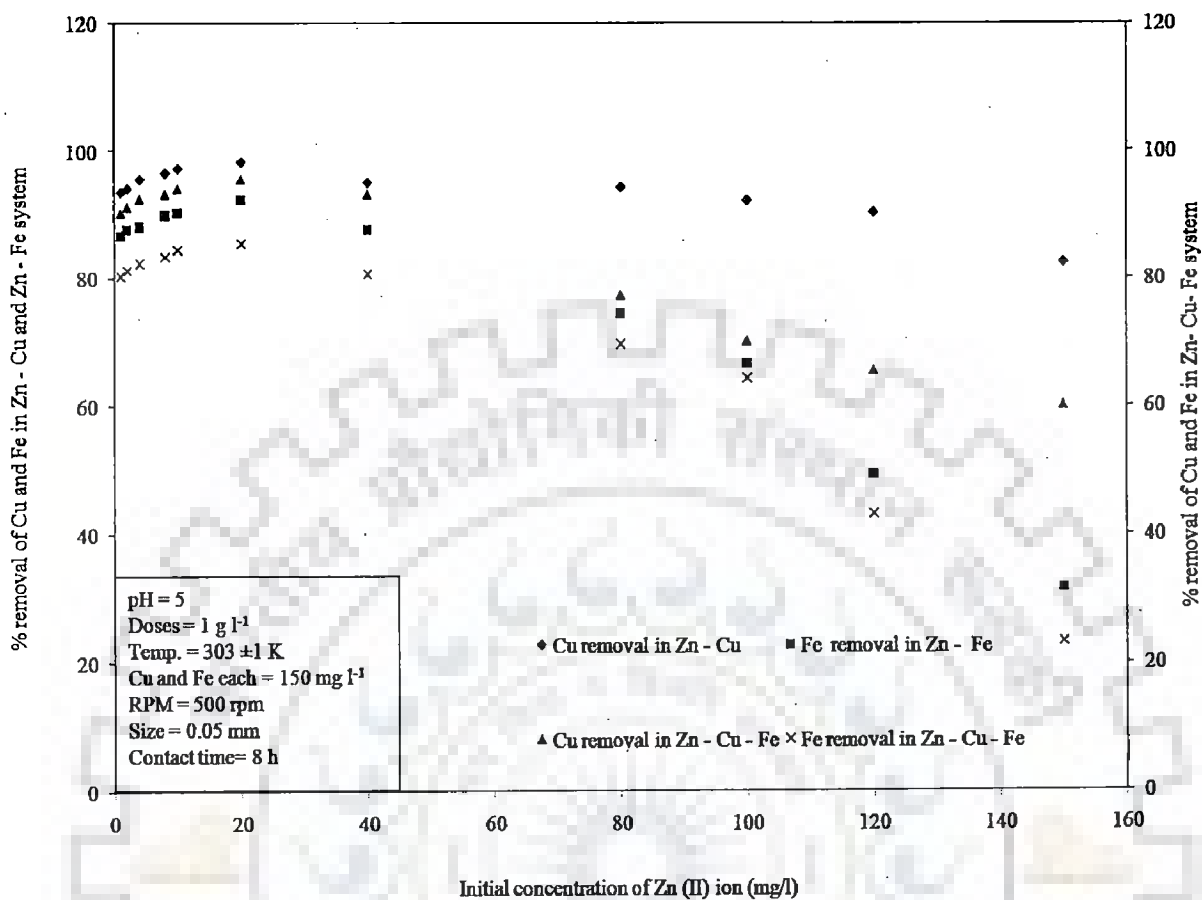


Figure 5.2.4 (f): Effect of initial concentration of Zn on biosorption of Cu and Fe on Pineapple peel

However, the increase in initial concentration of Zn (II) ion above 20 mg l<sup>-1</sup> led to the decrease in removal of Zn (II) ion in all types of the metal ion systems. The decrease in removal of Zn (II) ion with the increase in initial concentration of Zn (II) ion was due to the saturation of active sites present on the surface of biosorbent (Ozdes et al., 2009, Ozdemir et al., 2009).

The presence of other metal ions hindered the biosorption of Zn (II) ion. The preferential order of removal of heavy metal ions was Cu (II) > Zn (II) > Fe (II, III).

Figure 5.2.4 (g) and figure 5.2.4 (h) represent the influence of initial concentration of Zn (II) ion on Jackfruit peel powder.

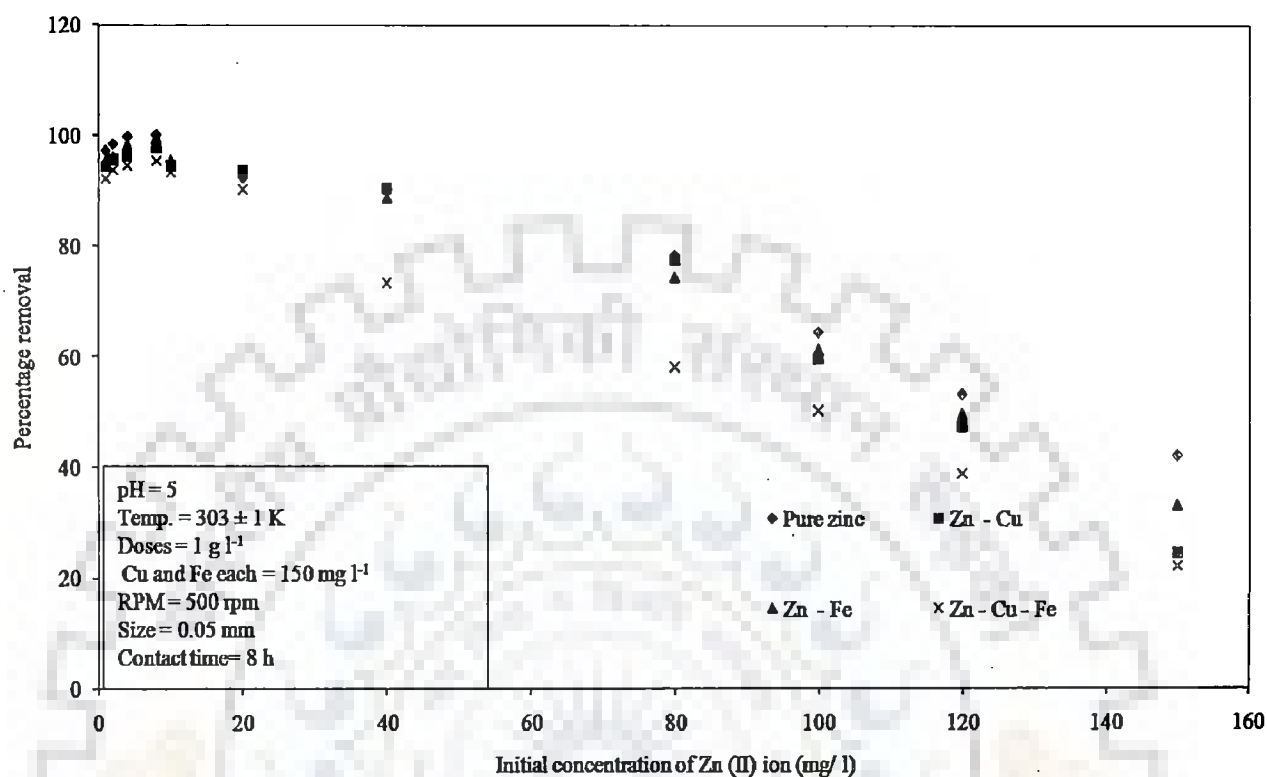


Figure 5.2.4 (g): Effect of initial concentration of Zn on biosorption of Zn on Jackfruit peel powder

It is evident from figure 5.2.4 (g) that the maximum removal of Zn (II) ion was obtained in pure zinc phase. The maximum removal of Zn (II) ion (100%) was obtained at 8 mg l<sup>-1</sup> of initial concentration of metal ion. In all types of metal ion systems, the increase in metal ion concentration from 1 mg l<sup>-1</sup> to 8 mg l<sup>-1</sup> of Zn (II) ion favoured the percentage removal of Zn (II) ion in liquid phase. Similarly, the maximum removal of Total Fe (II, III) and Cu (II) ion in Zn (II)- Cu (II), Zn (II)- Total Fe (II, III) and Zn (II)- Cu (II)- Total Fe (II, III) metal ion system was obtained at 8 mg l<sup>-1</sup> of zinc (figure 5.2.4 (h)).

The increase in percentage removal of Zn (II) ion from liquid phase with an increase in Zn (II) ion concentration from 1 mg l<sup>-1</sup> to 8 mg l<sup>-1</sup> was due to the fact that increase in

concentration of metal ion led to the increase in driving force or concentration gradient which resulted in higher percentage removal.

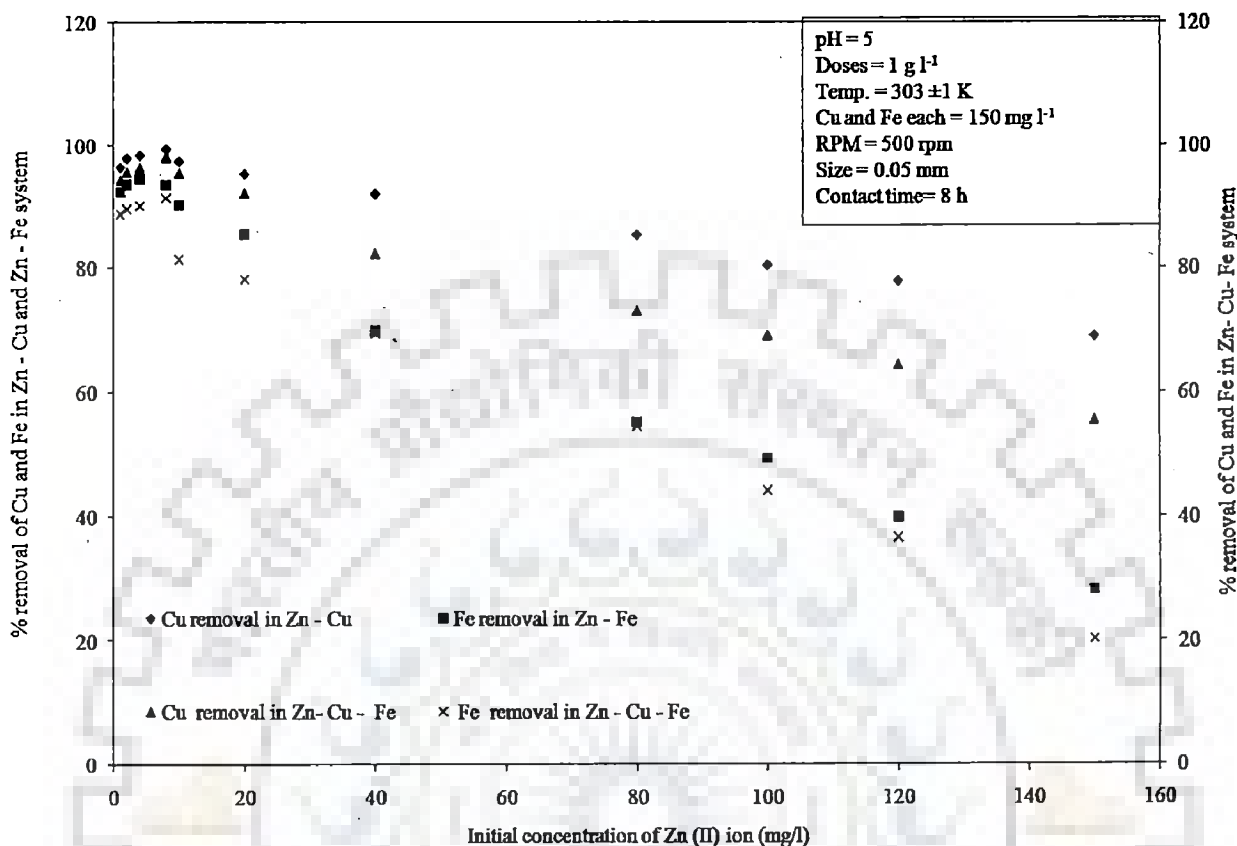


Figure 5.2.4 (h): Effect of initial concentration of Zn on biosorption of Cu and Fe on Jackfruit peel powder

The increase in initial concentration of Zn (II) ion above  $8 \text{ mg l}^{-1}$  saturation of active sites present on the surface of biosorbent (Ozdes et al., 2009, Ozdemir et al., 2009). The presence of other metal ions hindered the biosorption of Zn (II) ion. The preferential order of removal of heavy metal ions was  $\text{Cu (II)} > \text{Zn (II)} > \text{Fe (II, III)}$ .

Figure 5.2.4 (i) and figure 5.2.4 (j) represent the influence of initial concentration of Zn (II) ion on the biosorption of Zn (II), Cu (II) and total Fe (II, III) on *Cedrus deodara* sawdust. It became evident from figure 5.2.4 (i) that the maximum removal of Zn (II) ion was obtained in pure zinc phase. The maximum removal of Zn (II) ion (100%) was obtained at  $100 \text{ mg l}^{-1}$  of

initial concentration of metal ion. In all types of metal ion systems, the increase in metal ion concentration from 1 mg l<sup>-1</sup> to 100 mg l<sup>-1</sup> of Zn (II) ion favoured the percentage removal of Zn (II) ion in liquid phase.

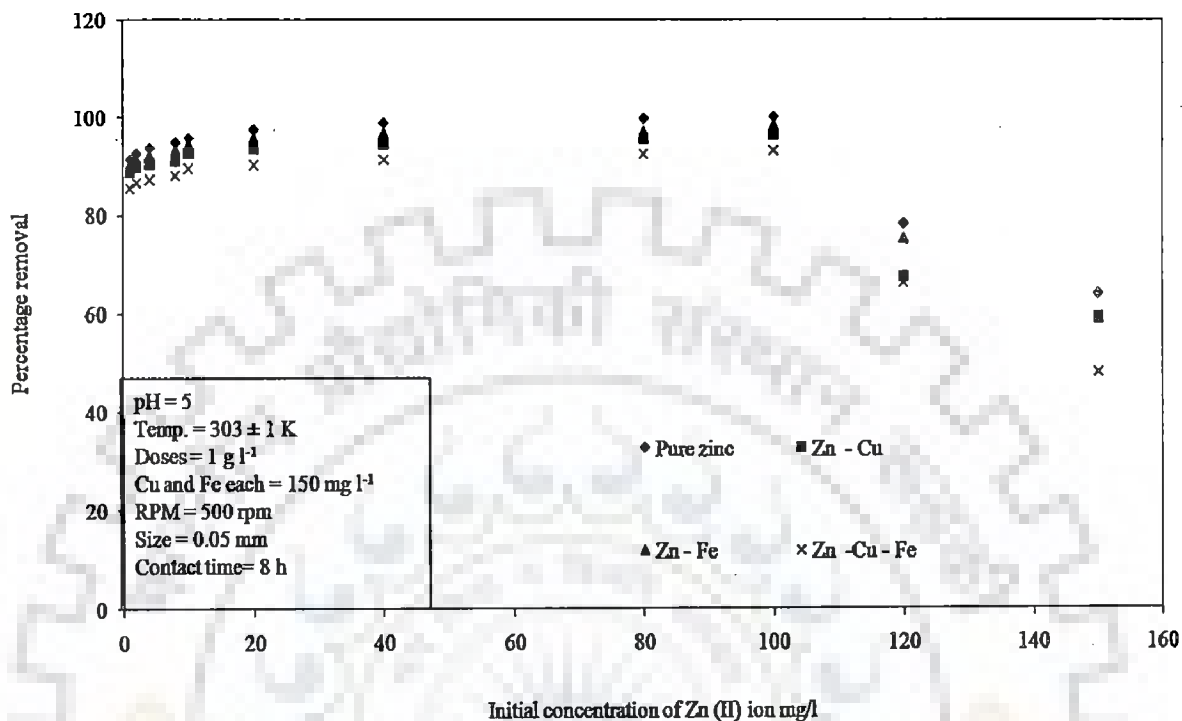


Figure 5.2.4 (i): Effect of initial concentration of Zn on biosorption of Zn on *Cedrus deodara* sawdust

Similarly, the maximum removal of Total Fe (II, III) and Cu (II) ion in Zn (II)- Cu (II), Zn (II)- Total Fe (II, III) and Zn (II)- Cu (II)- Total Fe (II, III) metal ion system was obtained at 100 mg l<sup>-1</sup> of zinc (figure 5.2.4 (j)). The increase in percentage removal of Zn (II) ion from liquid phase with an increase in Zn (II) ion concentration from 1 mg l<sup>-1</sup> to 100 mg l<sup>-1</sup> was due to the fact that increase in concentration of metal ion led to the increase in driving force or concentration gradient which resulted in higher percentage removal.

The increase in initial concentration of Zn (II) ion above 100 mg l<sup>-1</sup> ion led to the decrease in removal of Zn (II) ion in all types of the metal ion systems. The decrease in

removal of Zn (II) ion with the increase in initial concentration of Zn (II) ion was due to the saturation of active sites present on the surface of biosorbent (Ozdes et al., 2009, Ozdemir et al., 2009). The presence of other metal ions hindered the biosorption of Zn (II) ion. The preferential order of removal of heavy metal ions was Cu (II) > Zn (II) > Fe (II, III).

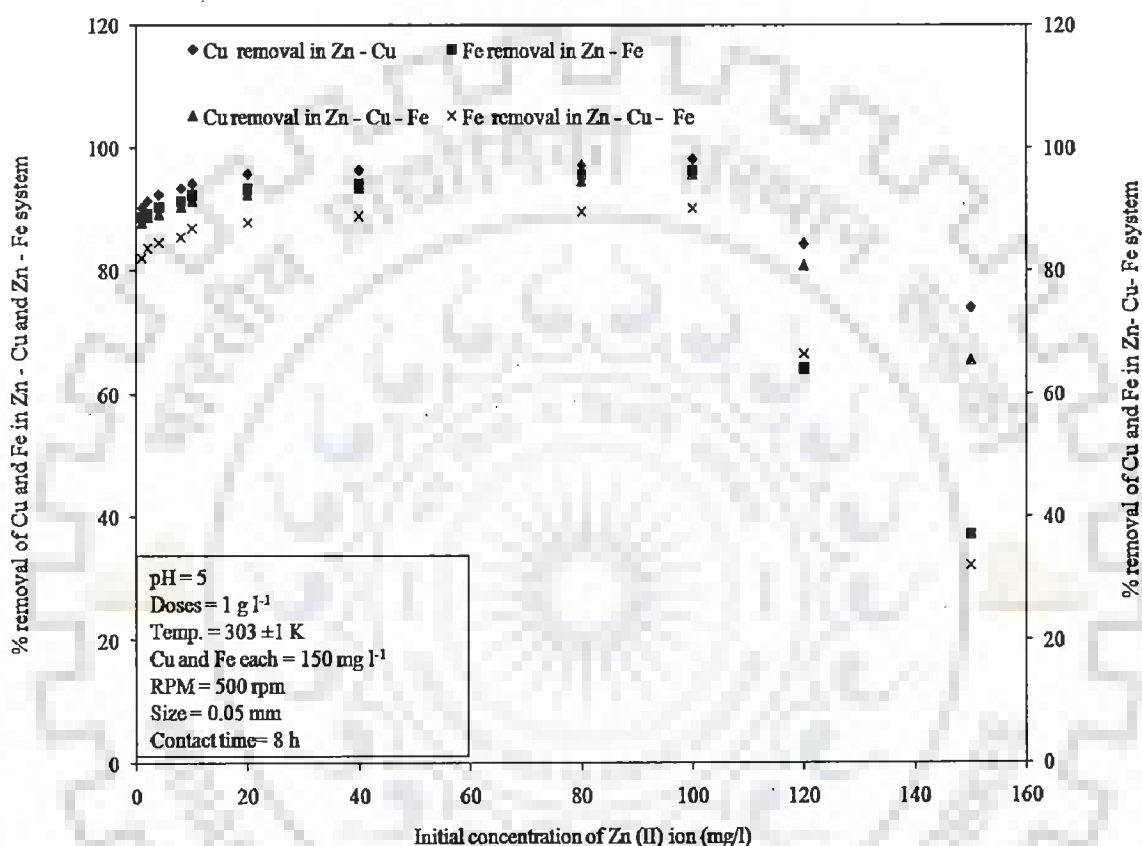


Figure 5.2.4 (j): Effect of initial concentration of Zn on biosorption of Cu and Fe on *Cedrus deodara* sawdust.

Figure 5.2.4 (k) and figure 5.2.4 (l) represent the influence of initial concentration of Zn (II) ion on the biosorption of Zn (II), Cu (II) and total Fe (II, III) and on Eucalyptus bark sawdust. It became evident from figure 5.2.4 (k) that the maximum removal of Zn (II) ion was obtained in pure zinc phase. The maximum removal of Zn (II) ion (100%) was obtained at 80 mg l<sup>-1</sup> of initial concentration of metal ion (figure 5.2.4 (l)). In all types of metal ion

systems, the increase in metal ion concentration from  $1 \text{ mg l}^{-1}$  to  $80 \text{ mg l}^{-1}$  of Zn (II) ion favoured the percentage removal of Zn (II) ion in liquid phase.

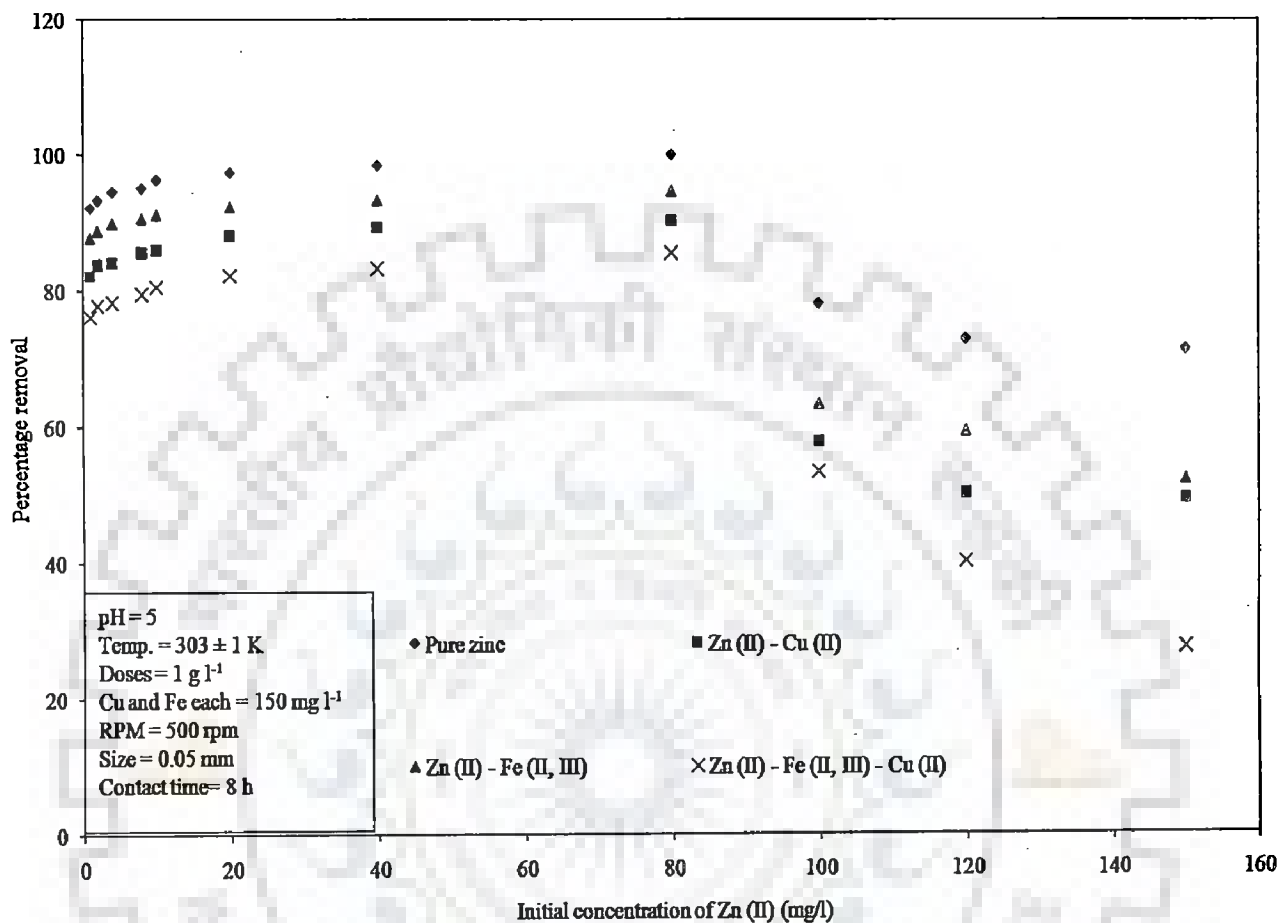


Figure 5.2.4 (k): Effect of initial concentration of Zn on biosorption of Zn on Eucalyptus bark sawdust

Similarly, the maximum removal of Total Fe (II, III) and Cu (II) ion in Zn (II)- Cu (II), Zn (II)- Total Fe (II, III) and Zn (II)- Cu (II)- Total Fe (II, III) metal ion system was obtained at  $80 \text{ mg l}^{-1}$  of zinc. The increase in percentage removal of Zn (II) ion from liquid phase with an increase in Zn (II) ion concentration from  $1 \text{ mg l}^{-1}$  to  $80 \text{ mg l}^{-1}$  was due to the fact that increase in concentration of metal ion led to the increase in driving force or concentration gradient which resulted in higher percentage removal.

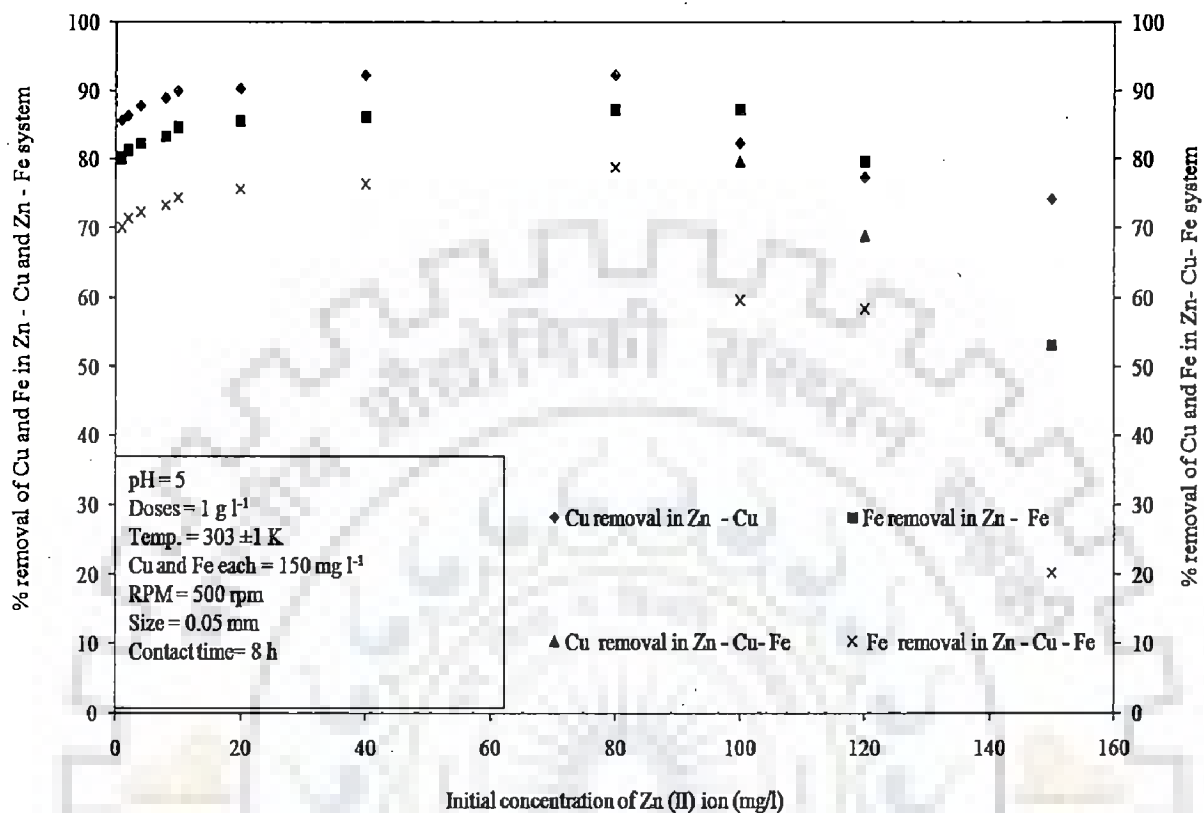


Figure 5.2.4 (l): Effect of initial concentration of Zn on biosorption of Cu and Fe ions on Eucalyptus bark sawdust

The increase in initial concentration of Zn (II) ion above 80 mg l<sup>-1</sup> led to the decrease in removal of Zn (II) ion in all types of the metal ion systems. The decrease in removal of Zn (II) ion with the increase in initial concentration of Zn (II) ion was due to the saturation of active sites present on the surface of biosorbent (Ozdes et al., 2009, Ozdemir et al., 2009). The presence of other metal ions hindered the biosorption of Zn (II) ion. The preferential order of removal of heavy metal ions was Cu (II) > Zn (II) > Fe (II, III).

Figure 5.2.4 (m) and figure 5.2.4 (n) represent the influence of initial concentration of Zn (II) ion on the biosorption of Zn (II), Cu (II) and total Fe (II, III) on Eucalyptus leaf powder. It is evident from figure 5.2.4 (m) that the maximum removal of Zn (II) ion was

obtained in pure zinc phase. The maximum removal of Zn (II) ion (100%) was obtained at 40 mg l<sup>-1</sup> of initial concentration of metal ion. In all types of metal ion systems, the increase in metal ion concentration from 1 mg l<sup>-1</sup> to 40 mg l<sup>-1</sup> of Zn (II) ion favoured the percentage removal of Zn (II) ion in liquid phase.

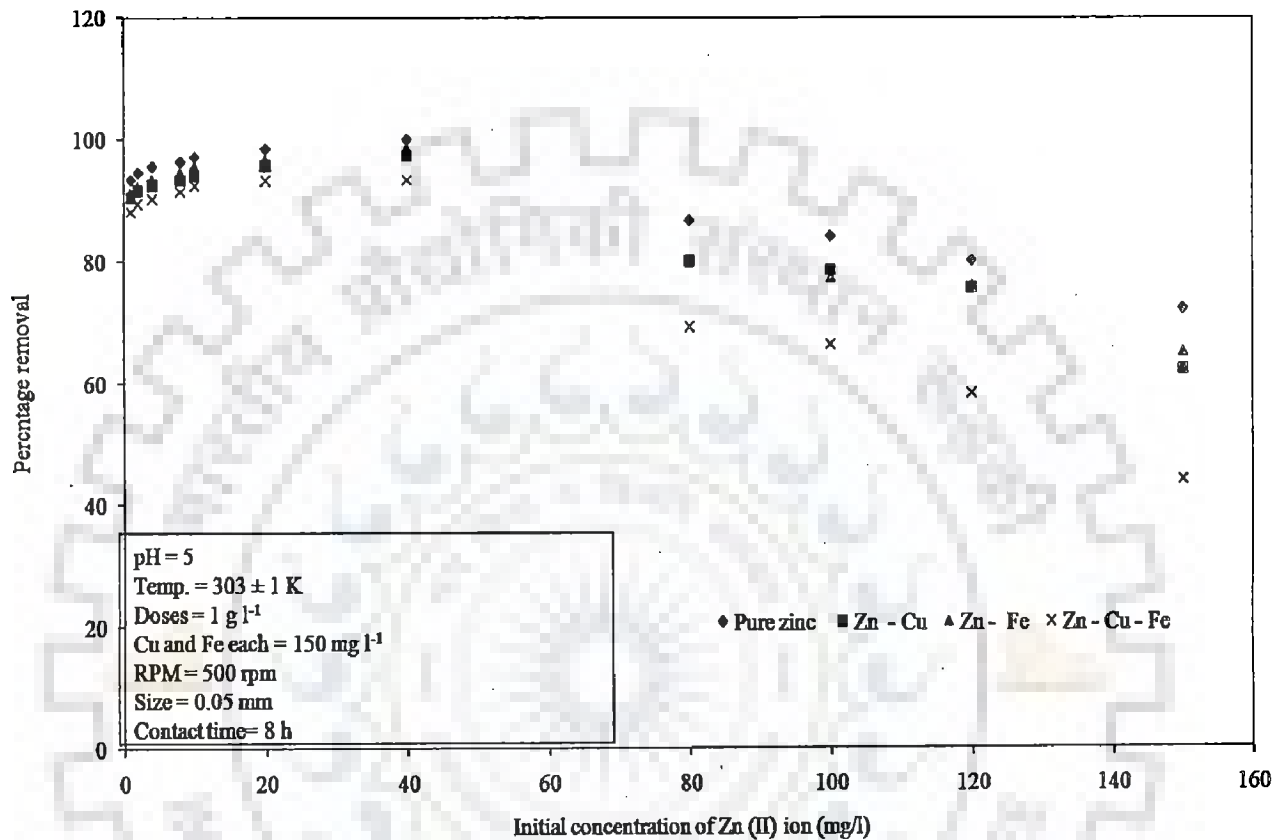


Figure 5.2.4 (m): Effect of initial concentration of Zn on biosorption of Zn on Eucalyptus leaf powder

Similarly, the maximum removal of Total Fe (II, III) and Cu (II) ion in Zn (II)- Cu (II), Zn (II)- Total Fe (II, III) and Zn (II)- Cu (II)- Total Fe (II, III) metal ion system was obtained at 40 mg l<sup>-1</sup> of zinc (figure 5.2.4 (n)). The increase in percentage removal of Zn (II) ion from liquid phase with an increase in Zn (II) ion concentration from 1 mg l<sup>-1</sup> to 40 mg l<sup>-1</sup> was due to the fact that increase in concentration of metal ion led to the increase in driving force or concentration gradient which resulted in higher percentage removal.



The increase in initial concentration of Zn (II) ion led to the decrease in removal of Zn (II) ion in all types of the metal ion systems. The decrease in removal of Zn (II) ion with the increase in initial concentration of Zn (II) ion above 40 mg l<sup>-1</sup> was due to the saturation of active sites present on the surface of biosorbent (Ozdes et al., 2009, Ozdemir et al., 2009). The presence of other metal ions hindered the biosorption of Zn (II) ion. The preferential order of removal of heavy metal ions was Cu (II) > Zn (II) > Fe (II, III).

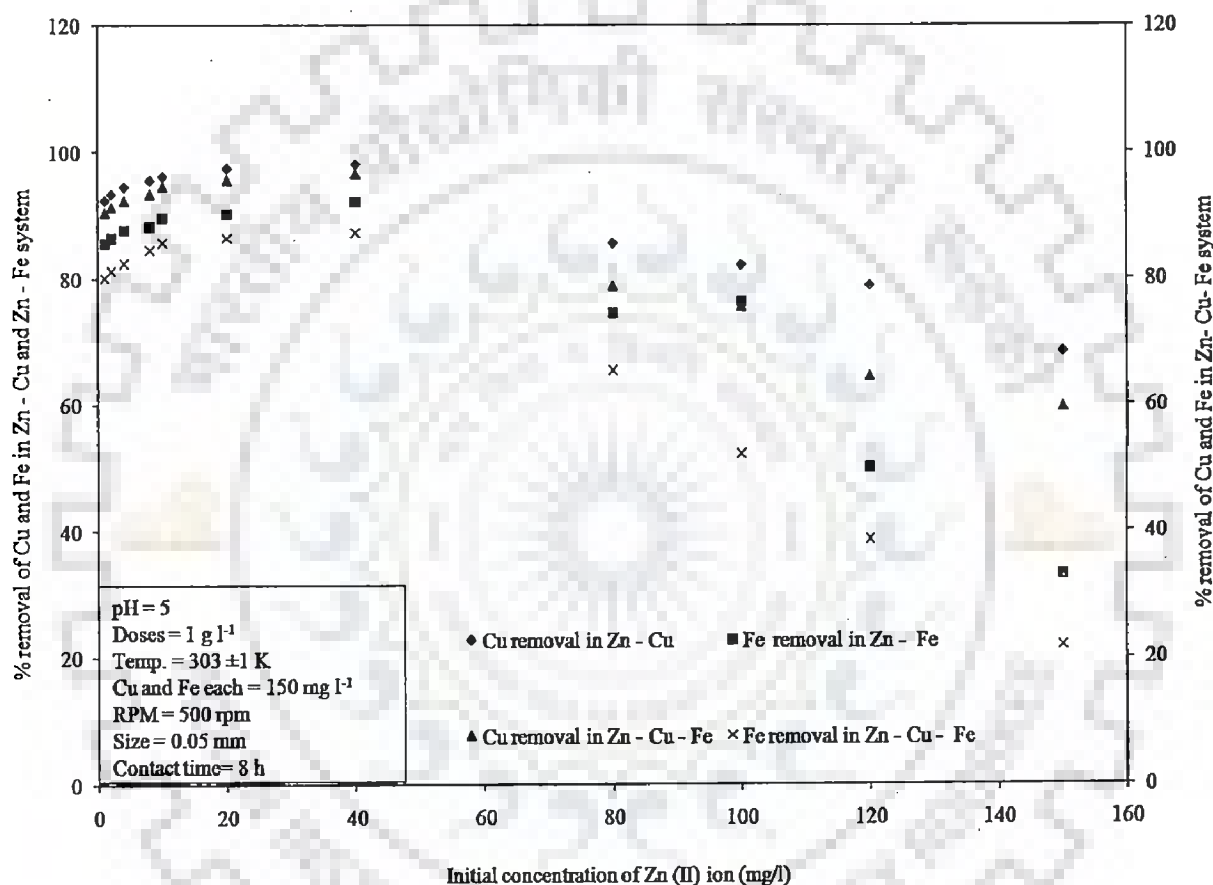


Figure 5.2.4 (n): Effect of initial concentration of Zn biosorption of Cu and Fe and on Eucalyptus leaf powder

Figure 5.2.4 (o) and figure 5.2.4 (p) represent the influence of initial concentration of Zn (II) ion on the biosorption of Zn (II), Cu (II) and total Fe (II, III) and on Eggshell and membrane.

It is evident from figure 5.2.4 (o) that the maximum removal of Zn (II) ion was obtained in pure zinc phase. The maximum removal of Zn (II) ion (99.36%) was obtained at 10 mg l<sup>-1</sup> of initial concentration of metal ion.

In all types of metal ion systems, the increase in metal ion concentration from 1 mg l<sup>-1</sup> to 10 mg l<sup>-1</sup> of Zn (II) ion favoured the percentage removal of Zn (II) ion in liquid phase.

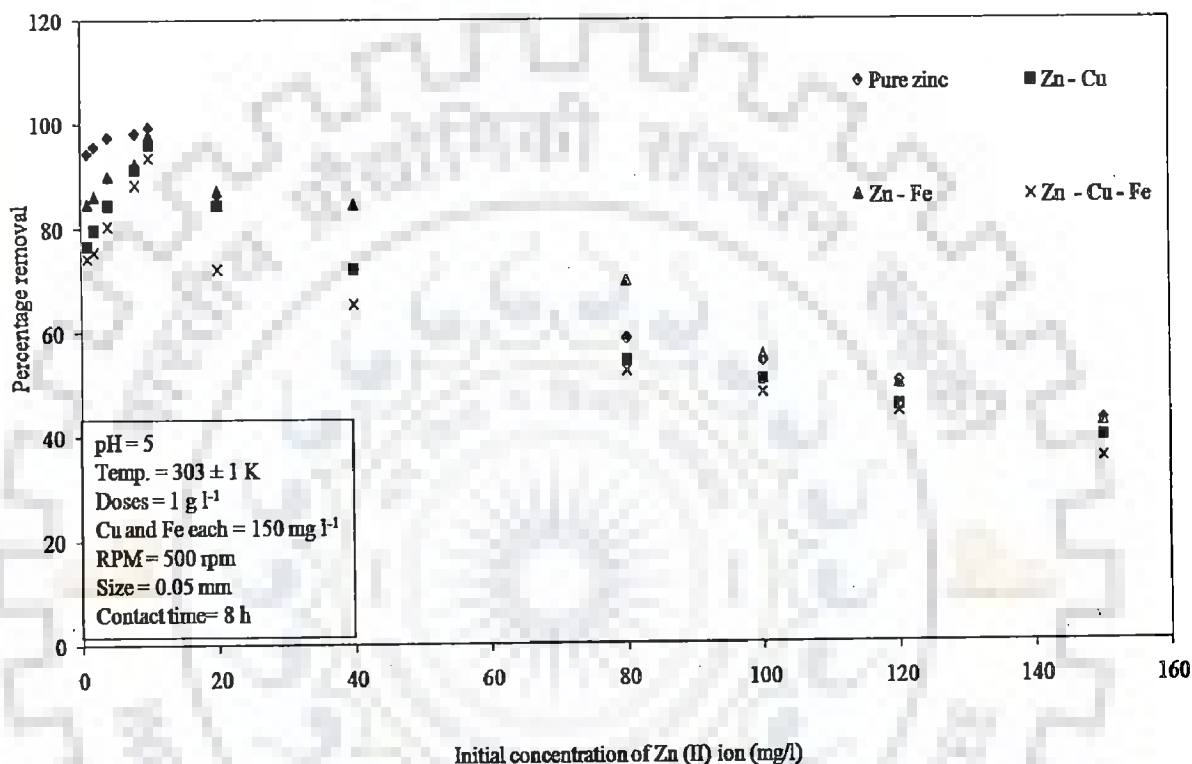


Figure 5.2.4 (o): Effect of initial concentration of Zn on biosorption of Zn on Eggshell and membrane

Similarly, the maximum removal of Total Fe (II, III) and Cu (II) ion in Zn (II)- Cu (II), Zn (II)- Total Fe (II, III) and Zn (II)- Cu (II)- Total Fe (II, III) metal ion system was obtained at 10 mg l<sup>-1</sup> of zinc (figure 5.2.4 (p)). The increase in percentage removal of Zn (II) ion from liquid phase with an increase in Zn (II) ion concentration from 1 mg l<sup>-1</sup> to 10 mg l<sup>-1</sup> was due to the fact that increase in concentration of metal ion led to the increase in driving force or concentration gradient which resulted in higher percentage removal.

The increase in initial concentration of Zn (II) ion above 10 mg l<sup>-1</sup> led to the decrease in removal of Zn (II) ion in all types of the metal ion systems. The decrease in removal of Zn (II) ion with the increase in initial concentration of Zn (II) ion was due to the saturation of active sites present on the surface of biosorbent (Ozdes et al., 2009, Ozdemir et al., 2009). The presence of other metal ions hindered the biosorption of Zn (II) ion. The preferential order of removal of heavy metal ions was Cu (II) > Zn (II) > Fe (II, III).

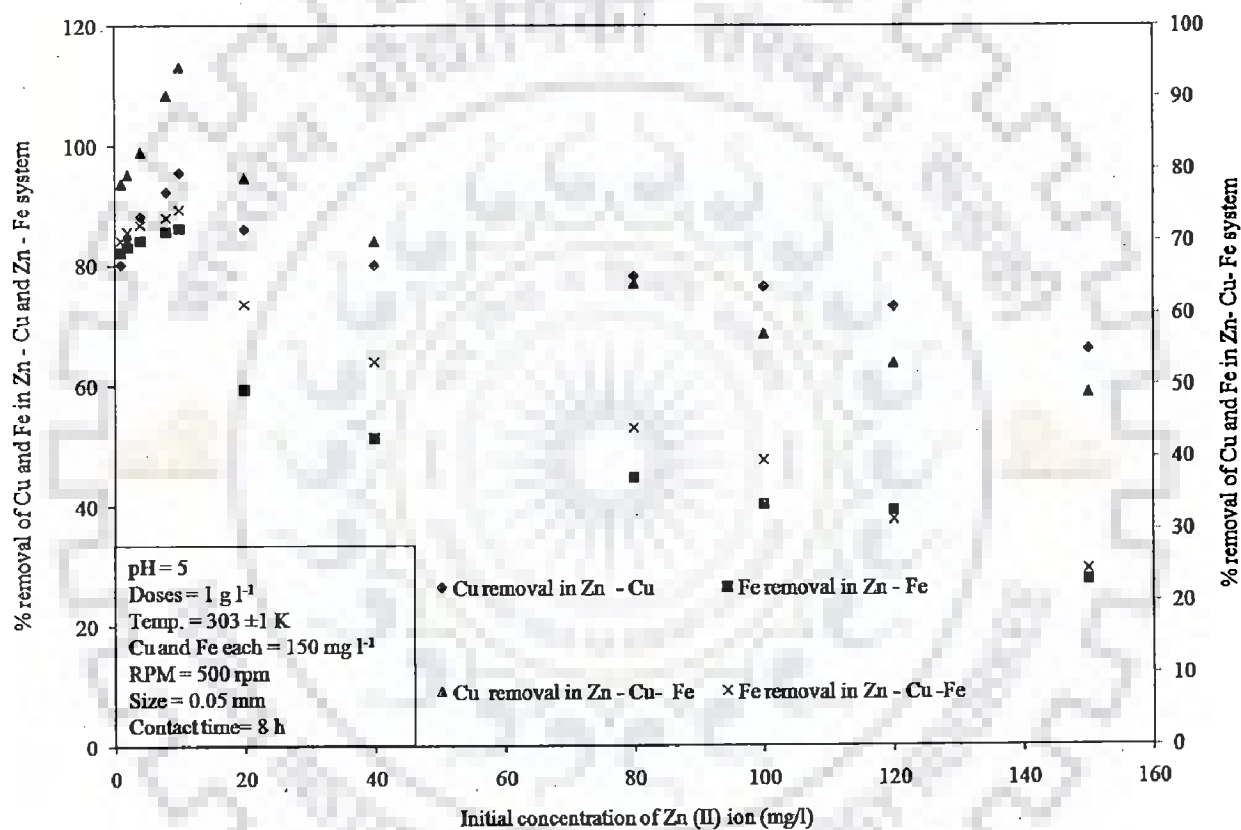


Figure 5.2.4 (p): Effect of initial concentration of Zn on biosorption of Cu and Fe on Eggshell and membrane

Figure 5.2.4 (q) and figure 5.2.4 (r) represent the influence of initial concentration of Zn (II) ion on the biosorption of Zn (II), total Fe (II, III) and Cu (II) on dead cells of *Zinc*

*sequestering bacterium VMSDCM* accession no. HQ108109. It is evident from figure 5.2.4 (q) that the maximum removal of Zn (II) ion was obtained in pure zinc phase.

The maximum removal of Zn (II) ion (100%) was obtained at initial concentration of metal ion ranging between at 150 mg l<sup>-1</sup>. Similarly, the maximum removal of Total Fe (II, III) and Cu (II) ion in Zn (II)- Cu (II), Zn (II)- Total Fe (II, III) and Zn (II)- Cu (II)- Total Fe (II, III) metal ion system was obtained at 150 mg l<sup>-1</sup> of zinc (figure 5.2.4 (r)).

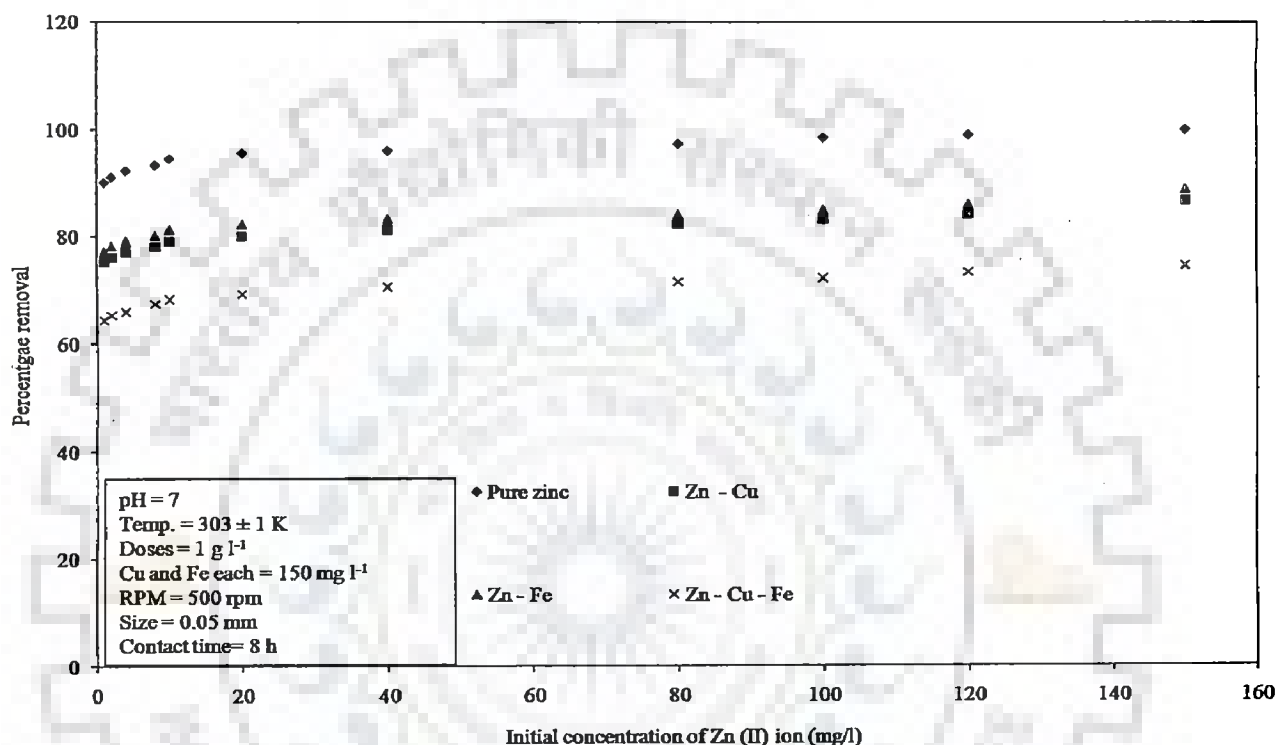


Figure 5.2.4 (q): Effect of initial concentration of Zn on biosorption of Zn on dead cells of *Zinc sequestering bacterium VMSDCM* accession no HQ108109

In all types of metal ion systems, the increase in metal ion concentration from 1 mg l<sup>-1</sup> to 150 mg l<sup>-1</sup> of Zn (II) ion favoured the percentage removal of Zn (II) ion in liquid phase. The increase in percentage removal of Zn (II) ion from liquid phase with an increase in Zn (II) ion concentration from 1 mg l<sup>-1</sup> to 150 mg l<sup>-1</sup> was due to the fact that increase in concentration of metal ion led to the increase in driving force or concentration gradient which resulted in higher percentage removal. The presence of other metal ions hindered the biosorption of Zn

(II) in liquid phase. The preferential order of removal of heavy metal ions was Cu (II) > Zn (II) > Fe (II, III).

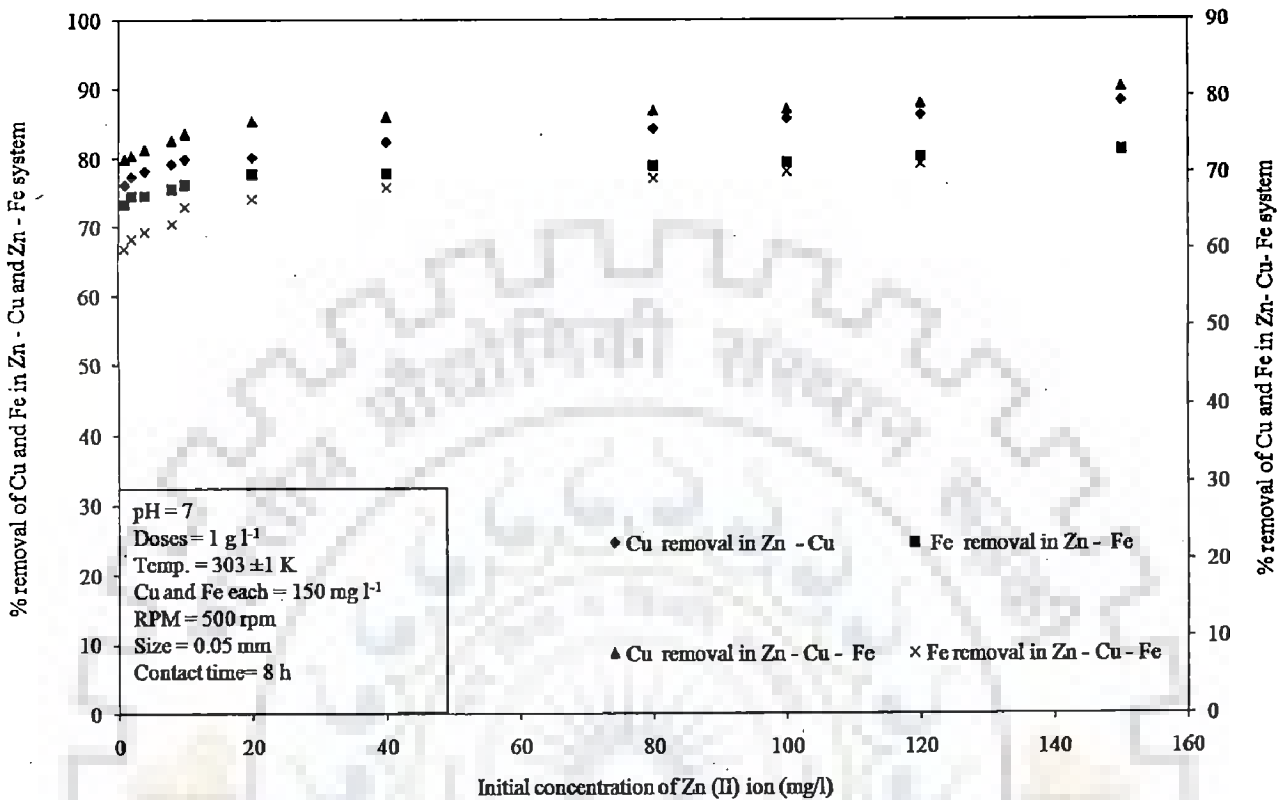


Figure 5.2.4 (r): Effect of initial concentration of Zn on biosorption of Cu and Fe on dead cells of *Zinc sequestering bacterium VMSDCM* accession no. HQ108109

#### Concluding remarks of section 5.2.4

Among all the biosorbents selected for the present work, the maximum removal of Zn (II) ion was obtained with *Cedrus deodara* sawdust and dead cells of *Zinc sequestering bacterium VMSDCM* accession no HQ108109. The maximum removal of Zn (II) ion obtained in case of *Cedrus deodara* sawdust and dead cells of *Zinc sequestering bacterium VMSDCM* accession no HQ108109 were 100 % and 100% at 120 mg l<sup>-1</sup> and 150 mg l<sup>-1</sup> of initial concentration of zinc, respectively in pure zinc environment. In presence of Cu (II) ion, the removal of Zn (II) was less in comparison to the pure zinc environment. The removal of zinc in presence of Cu (II) in case of *Cedrus deodara* sawdust and dead cells of *Zinc sequestering bacterium*

VMSDCM accession no HQ108109 was 67.57% and 86.6%, respectively. Similarly, in the presence of total Fe (II, III) the percentage removal of Zn (II) ion was quite diminished. The removal of zinc in presence of total Fe (II, III) in case of *Cedrus deodara* sawdust and dead cells of *Zinc sequestering bacterium* VMSDCM accession no HQ108109 was 75.33% and 88.19%, respectively. In ternary metal ion complex system, the removal of Zn (II) ion was 66.34% and 74.61% in case of *Cedrus deodara* sawdust and dead cells of *Zinc sequestering bacterium* VMSDCM accession no HQ108109, respectively. The optimum concentration for *Cedrus deodara* sawdust and dead cells of *Zinc sequestering bacterium* VMSDCM accession no. HQ108109 of Zn (II) ion was estimated as 120 mg l<sup>-1</sup> and 150 mg l<sup>-1</sup>, respectively. Table 5.2.4 represents the uptake capacity of zinc (II) ion by various agricultural biosorbents.

Table 5.2.4: Uptake capacities of Zn (II) ion various by agricultural biosorbents

Name of biomass	pH	Temp (°C)	Initial concentration of Zn (II) ion (mg l <sup>-1</sup> )	Contact time (hours)	Uptake capacity (mg g <sup>-1</sup> )	Functional groups	Reference
Bagasse fly ash (BFA)	6	20 - 50	3269000-32690000	5	24190.6 - 25498.2	Si-OH, adsorbed water, OH-CH <sub>2</sub> , C=O, CHO, aromatic CH, carboxyl carbonate structures	Srivastava et al., 2007
Rice husk ash (RHA)	6	20 - 50	3269000-32690000	5	15037.4-16998.8	Free and hydrogen bonded OH group, C=O, CHO, aromatic CH, carboxyl carbonate structures	Srivastava et al., 2007
Modified clay	5	20±1	10 - 2000	6	68322.1	Hydromica, quartz and	Vengris et al., 2001

sorbent						feldspar, iron and aluminum hydroxide	
Valonia tannin resin	5	N. D	5 - 100	N. D	35.51	Phenolic, hydroxyl and oxyl groups	Sengil and ozacar, 2009
Zeolite NAY	4.5	30	3.26-98.07	15	47.40- 53.93	3 D dimensiona l framework of silica and alumina joined by shared oxygen atom	Ostroski et al., 2009
<i>Pinus silvestris</i> L.	6	35	10 – 100	< 1	15.12	Lignin, tannin, rosin, cellulose	Ucun et al., 2009
Ion exchange resin	5.5	25±2	N. D	72	176526	H <sup>+</sup> , Ca <sup>2+</sup> , Na <sup>+</sup>	Shek et al., 2009
Neem leaves	4	25	25 - 800	12	147.08	N. D	Arshad et al., 2008
Neem stem bark	5	25	25 - 800	12	137.67	N. D	Arshad et al., (2008)
Brine sediment	7	25	75	11.5	4.85	Halite, calcite, quartz, iron siliceous, calcium oxide, Ca, Fe	Agouborde and Navia, 2009
Sawdust	7	25	75	11.5	2.58	Calcium, Magnesium , Sodium, Potassium	Agouborde and Navia, 2009
Combinatio n of brine sediment	7	25	75	11.5	5.59	CH, C-O, C-C, alcholoic	Agouborde and Navia, 2009

and sawdust						and phenolic group	
<i>Triticum aestivum</i>	N. D	N. D	N. D	N. D	N. D	N. D	Farooq et al., 2010
<i>Triticum aestivum</i>	6.5	R. T	N. D	N. D	15691.2	N. D	Dupont et al., 2005
Activated carbon, Kaolin, bentonite, blast furnace slag and fly ash	6	25±2	50 - 100	3	3.05 – 11.24	N. D	Mishra and Patel, 2009
Activated from bagasse	4.5	25±1	200	10 - 12	31.11	N. D	Mohan and Singh, 2002
Phosphogypsum	9 - 11	R. T	0.1 - 100	0.66	2.57	N. D	Cesur and Balkaya, 2007
Thermal power plant	4.5 - 5	18	30 - 130	0.25-24	5.75	N. D	Tofan et al., 2008
<i>Tectona grandis</i> L. F	5	30 - 60	20 - 100	3	16.42	N. D	Kumar et al., 2006
Esterified lemon	4.8	25 - 55	65380-1634500	0.5 - 4	5264-62764.8	N. D	Arslanoglu et al., 2008
Amberlite IR -20 synthetic resin	4-8	1.5	N. D	3	50022238	-SO <sub>3</sub> H	Demirbas et al., 2005
Biosolids	4	20±2	4968.8 - 98070	5	36874.32	N. D	Norton et al., 2004
Rice straw	5	25±1	189602-2007166	1.5	8630.16	Hydroxyl, C-H stretching, C=C in aromatic ring, Si-O stretching and Si-O bending	Rocha et al., 2008
Calcium hydroxyapatite	2-8	30±1	60 - 120	3	102.04	OH group, CO <sub>3</sub> <sup>2-</sup> ,	Sheha, 2007



Barium hydroxyapatite	2-8	30±1	60 -120	3	36.62	PO <sub>4</sub> <sup>3-</sup> OH group, CO <sub>3</sub> <sup>2-</sup> , PO <sub>4</sub> <sup>3-</sup>	Sheha, 2007
Short hemp fibers(Chemically modified)	5.5	R. T	3269-13076	0.05 - 2	5099.64	N. D	Pejic et al., 2008
Sawdust	5	30±2	25	3	14.10	Carboxylic, amine, amide, sulphonate, amino	Naiya et al., 2009
Neem bark	5	30±2	25	3	13.29	Carboxylic, amine, amide, sulphonate, amino	Naiya et al., 2009
Eucalyptus leaf powder	5	20±1	100	6	23.5	Carboxylic, amine, amide, hydroxyl, methyl	Mishra et al., 2010
<i>Cedrus deodara</i> sawdust	5	45	100	2.5	97.39	carboxyl, hydroxyl, amine, amide and methyl	Mishra et al., 2011
<i>Cedrus deodara</i> sawdust	5	45	150	8	61.21	carboxyl, hydroxyl, amine, amide methyl	This study

It is clear from table 5.2.4 that the uptake capacity of dead cells of *Zinc sequestering bacterium VMSDCM* accession no. HQ108109 has tremendous potential of up taking zinc from liquid phase. However, these uptake capacities cited in table 5.2.4 have been derived in various types of experimental condition. However, the analysis of the data cited in table 5.2.4 presents the valuable comparative analysis of various sorts of biomasses with the present study.

### 5.2.5 Optimization of initial concentration of total Fe (II, III) and Cu (II)

This section embodies the results of influence of initial concentration of total Fe (II, III) and Cu (II) on biosorption of total Fe (II, III) and Cu (II) ion in liquid phase in presence of Zn (II) ion. The experiments were conducted in range of  $1 \text{ mg l}^{-1}$  to  $150 \text{ mg l}^{-1}$ . The experiments were conducted in round bottom flasks of 500 ml capacity containing 1, 2, 4, 8, 10, 20, 40, 80, 100, 120 and  $150 \text{ mg l}^{-1}$  of total Fe (II, III) and Cu (II) ion and  $150 \text{ mg l}^{-1}$  of Zn (II) ion. Results of influence of initial concentration have been shown in figures 5.2.5 (a) to 5.2.5 (i). The system of ions studied in the present work were pure zinc, Zn (II)- Cu (II), Zn (II)- Fe (II, III) and Zn (II) – Fe (II, III)- Cu (II). The metal ions Zn (II), Cu (II) and Fe (II, III) are referred as Zn, Cu and Fe in various figures.

Figure 5.2.5 (a) represents the influence of initial concentration of Cu (II) and total Fe (II, III) ion on biosorption of Zn (II), total Fe (II, III) and Cu (II) ions in presence of on Mango bark sawdust. It became evident from figure 5.2.5 (a) that the maximum removal of Cu (II) and Fe (II, III) was obtained in binary metal ion system. The maximum percentage removal of Cu (II) and Fe (II, III) ions in Zn (II) – Cu (II) and Zn (II) – Fe (II, III) ion was 98.33% and 85.66% at initial concentration of  $10 \text{ mg l}^{-1}$  of Cu (II) and Fe (II, III), respectively. In ternary metal ion system Zn (II) – Fe (II, III) – Cu (II), the removal of Cu (II) and Fe (II, III) ion was found to be low. Furthermore, with the rise of initial concentration of Cu (II) and Fe (II, III) ions from  $10 \text{ mg l}^{-1}$  to  $150 \text{ mg l}^{-1}$  in all types of metal ion systems, the removal of Zn (II), Fe (II, III) and Cu (II) ions decreased gradually.

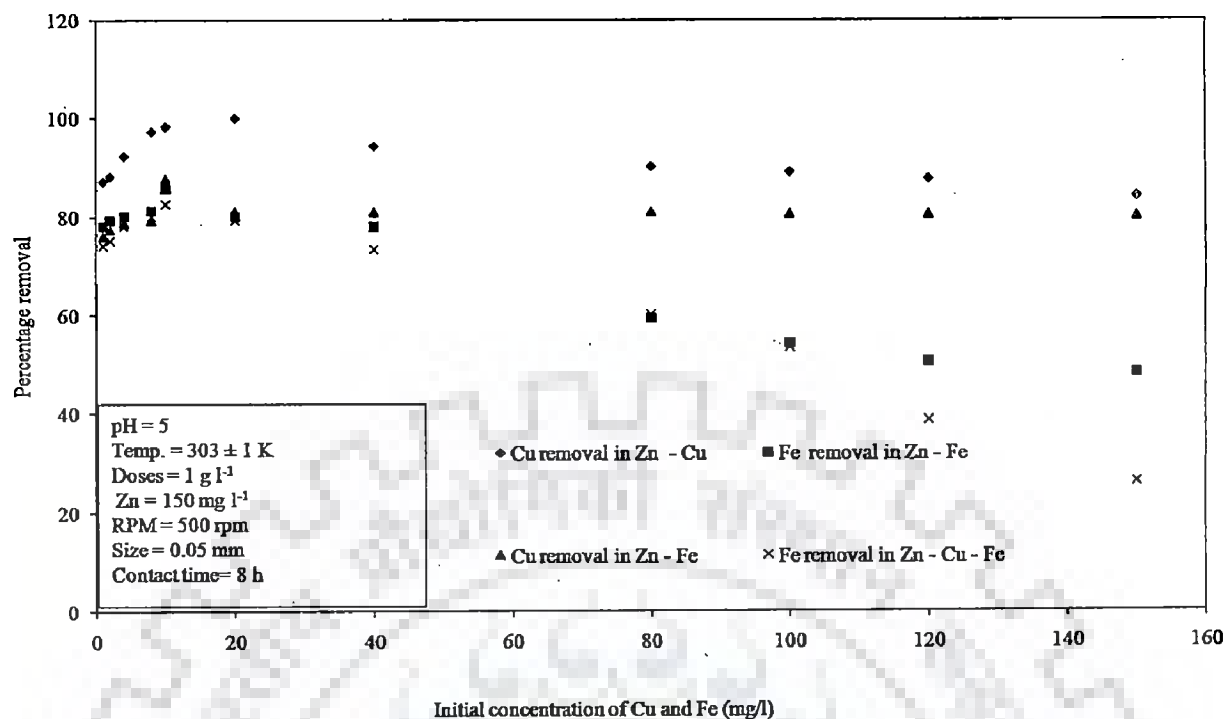


Figure 5.2.5 (a): Effect of initial concentration of Cu and Fe on biosorption of Cu and Fe in presence of Zn on Mango bark sawdust

The reason behind the gradual decrease in biosorption of Zn (II), Fe (II, III) and Cu (II) ions with an increase in initial concentration of total Fe (II, III) and Cu (II) ion from 10 mg l<sup>-1</sup> to 150 mg l<sup>-1</sup> was the steady increase in the saturation of active sites present on the surface of biosorbent. At 10 mg l<sup>-1</sup> of Cu (II) and total Fe (II, III) ions concentration, 98.04% of Zn (II) ion removal was obtained. This value was comparatively higher against the removal reported in figure 5.2.4 (a).

Figure 5.2.5 (b) represents the influence of initial concentration of total Fe (II, III) and Cu (II) ion on biosorption of Zn (II), total Fe (II, III) and Cu (II) Orange peel. It became evident from figure 5.2.5 (b) that the maximum removal of Cu (II) and Fe (II, III) was obtained in binary metal ion system. The percentage removal of Cu (II) and Fe (II, III) ions in Zn (II) – Cu (II) and Zn (II) – Fe (II, III) ion was 88.32% and 82.7%, respectively at 40 mg l<sup>-1</sup> of Cu (II) and Fe (II, III).

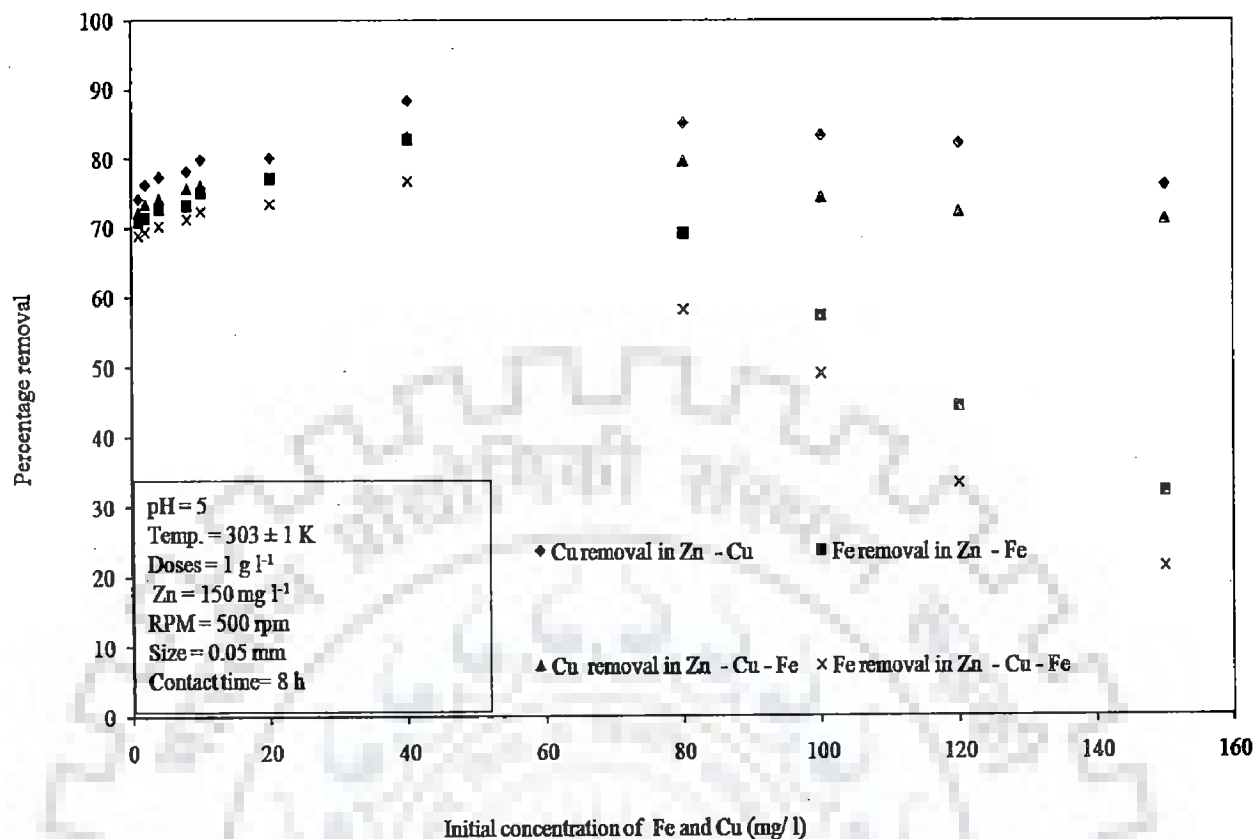


Figure 5.2. 5 (b): Influence of initial concentration of Cu and Fe on biosorption of Cu and Fe in presence of Zn on Orange peel

In ternary metal ion system Zn (II) – Fe (II, III) – Cu (II), the removal of Cu (II) and Fe (II, III) ion was found to be low. Furthermore, with the rise of initial concentration of Cu (II) and Fe (II, III) ions from  $40 \text{ mg l}^{-1}$  to  $150 \text{ mg l}^{-1}$  in all types of metal ion systems, the removal of Zn (II), Fe (II, III) and Cu (II) ions decreased gradually. The reason behind the gradual decrease in biosorption of Zn (II), Fe (II, III) and Cu (II) ions with an increase in initial concentration of total Fe (II, III) and Cu (II) ion from  $40 \text{ mg l}^{-1}$  to  $150 \text{ mg l}^{-1}$  was the steady increase in the saturation of active sites present on the surface of biosorbent. At  $40 \text{ mg l}^{-1}$  of Cu (II) and total Fe (II, III) ions concentration, 87.39% of Zn (II) ion removal was obtained. This value was comparatively higher than the removal reported in figure 5.2.4 (c). Figure 5.2.5 (c) represents the influence of initial concentration of total Fe (II, III) and Cu (II) ion on biosorption of Zn (II), total Fe (II, III) and Cu (II) ions on Pineapple peel.

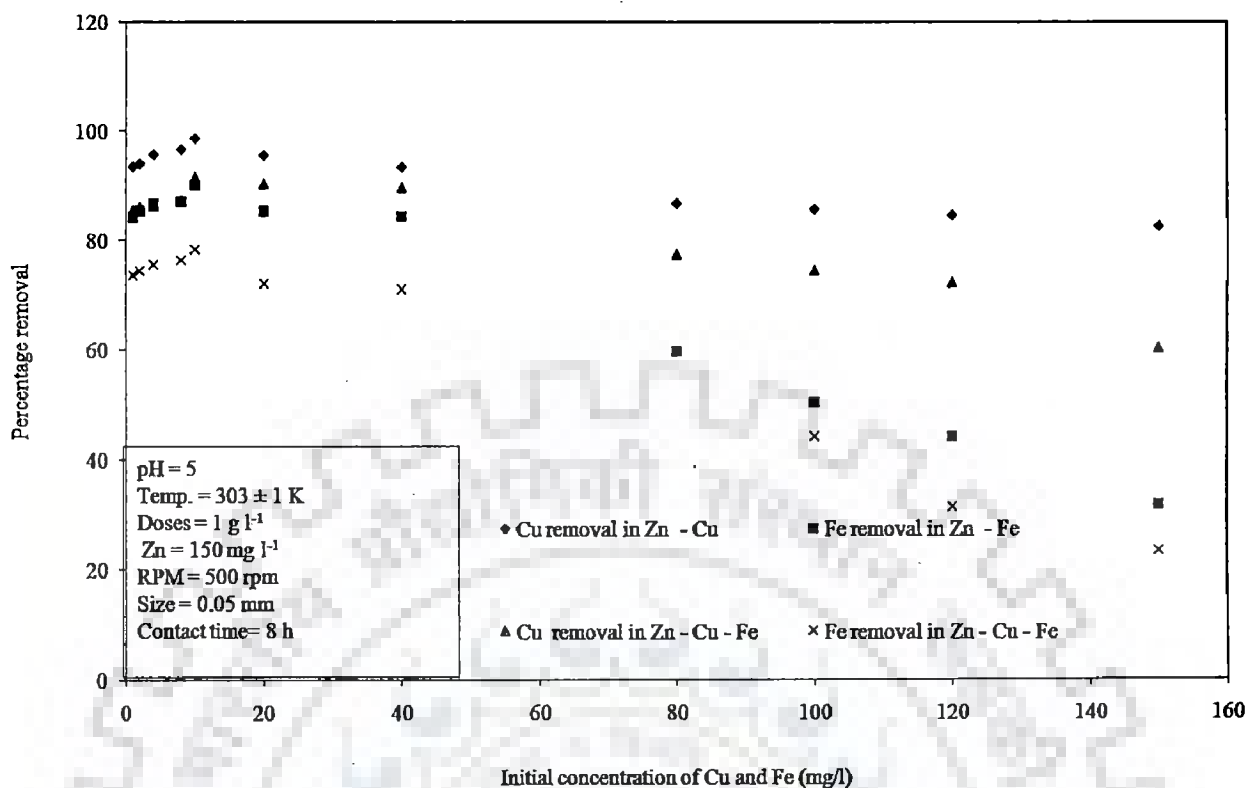


Figure 5.2.5 (c): Effect of initial concentration of Cu and Fe on biosorption of Cu and Fe in presence of Zn on Pineapple peel

It is evident from figure 5.2.5 (c) that the maximum removal of Cu (II) and Fe (II, III) was obtained in binary metal ion system. The percentage removal of Cu (II) and Fe (II, III) ions in Zn (II) – Cu (II) and Zn (II) – Fe (II, III) ion was 98.66% and 90.15%, respectively at  $10 \text{ mg l}^{-1}$  of Cu (II) and total Fe (II, III). In ternary metal ion system Zn (II) – Fe (II, III) – Cu (II), the removal of Cu (II) and Fe (II, III) ion was found to be low. Furthermore, with the rise in initial concentration of Cu (II) and Fe (II, III) ions from  $10 \text{ mg l}^{-1}$  to  $150 \text{ mg l}^{-1}$  in all types of metal ion systems, the removal of Zn (II), Fe (II, III) and Cu (II) ions decreased gradually. The reason behind the gradual decrease in biosorption of Zn (II), Fe (II, III) and Cu (II) ions with an increase in initial concentration of total Fe (II, III) and Cu (II) ion from  $10 \text{ mg l}^{-1}$  to  $150 \text{ mg l}^{-1}$  was the steady increase in the saturation of active sites present on the surface of biosorbent. At  $10 \text{ mg l}^{-1}$  of Cu (II) and total Fe (II, III) ions concentration, 95.39% of Zn (II) ion removal was obtained. This value was comparatively higher than the removal reported in figure 5.2.4 (e) Hence,  $10 \text{ mg l}^{-1}$  of Cu (II) and total Fe (II, III) ion was assessed as an

optimum concentration of Cu (II) and total Fe (II, III) ion for biosorption of Zn (II) ion on the surface of Pineapple peel in liquid phase.

Figure 5.2.5 (d) represents the influence of initial concentration of total Fe (II, III) and Cu (II) ion on biosorption of Zn (II), total Fe (II, III) and Cu (II) ions on Jackfruit peel.

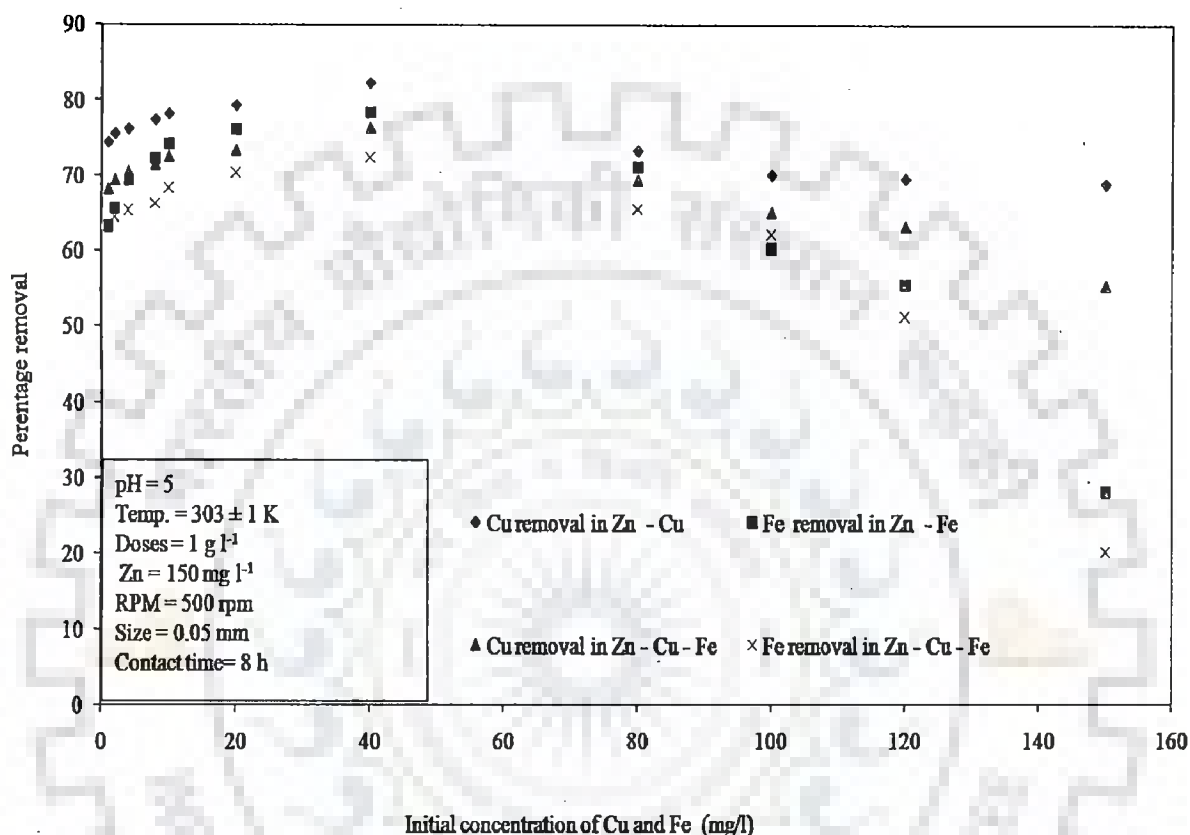


Figure 5.2.5 (d): Effect of initial concentration of Cu and Fe on biosorption of Cu and Fe in presence of Zn on Jackfruit peel

It is evident from figure 5.2.5 (d) that the maximum removal of Cu (II) and Fe (II, III) was obtained in binary metal ion system. The percentage removal of Cu (II) and Fe (II, III) ions in Zn (II) – Cu (II) and Zn (II) – Fe (II, III) ion was 82.33% and 78.33%, respectively, at 40 mg l<sup>-1</sup> of Cu (II) and total Fe (II, III). In ternary metal ion system Zn (II) – Fe (II, III) – Cu (II), the removal of Cu (II) and Fe (II, III) ion was found to be low. Furthermore, with the rise in initial concentration of Cu (II) and Fe (II, III) ions from 40 mg l<sup>-1</sup> to 150 mg l<sup>-1</sup> in all types of metal ion systems, the removal of Zn (II), Fe (II, III) and Cu (II) ions decreased gradually.

The reason behind the gradual decrease in biosorption of Zn (II), Fe (II, III) and Cu (II) ions with an increase in initial concentration of total Fe (II, III) and Cu (II) ion from 40 mg l<sup>-1</sup> to 150 mg l<sup>-1</sup> was the steady increase in the saturation of active sites present on the surface of biosorbent. At 40 mg l<sup>-1</sup> of Cu (II) and total Fe (II, III) ions concentration, 97.84% of Zn (II) ion removal was obtained. This value was comparatively higher than the removal reported in figure 5.2.4 (g).

Figure 5.2.5 (e) represents the influence of initial concentration of total Fe (II, III) and Cu (II) ion on biosorption of Zn (II), total Fe (II, III) and Cu (II) ions on *Cedrus deodara* sawdust.

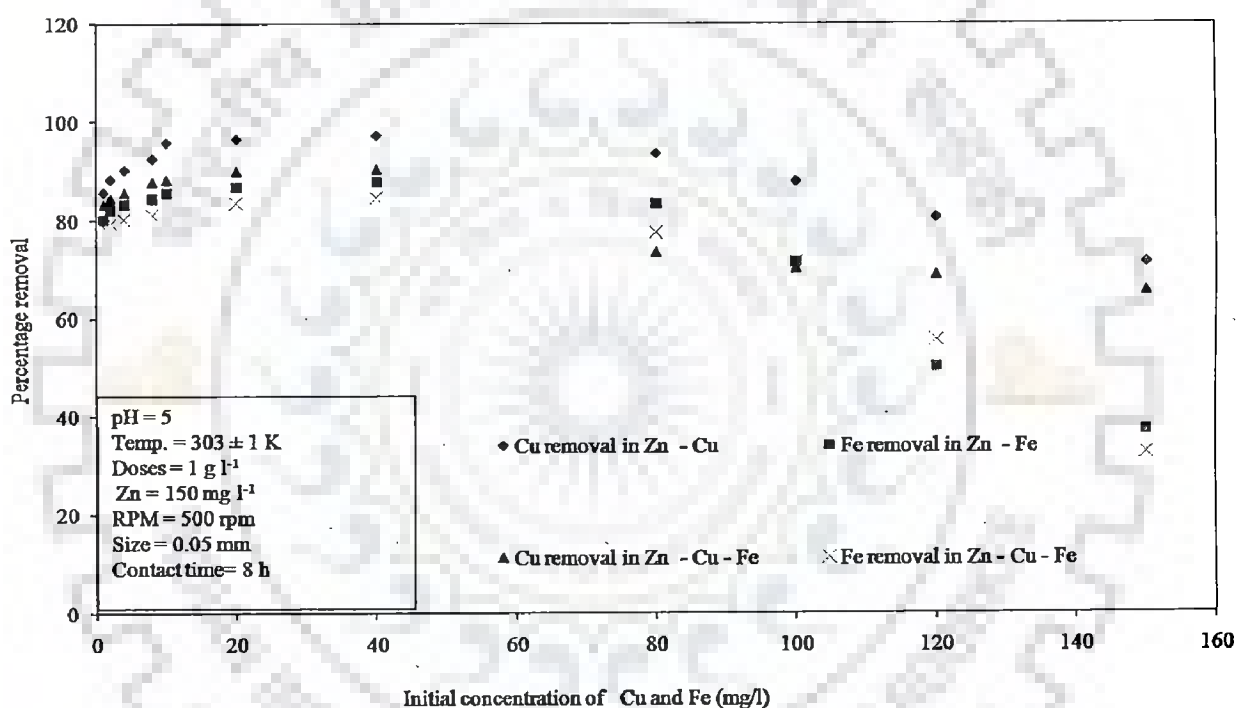


Figure 5.2.5 (e): Effect of initial concentration of Cu and Fe on biosorption of Fe and Cu in presence of zinc on *Cedrus deodara* sawdust

It became evident from figure 5.2.5 (e) that the maximum removal of Cu (II) and Fe (II, III) was obtained in binary metal ion system. The percentage removal of Cu (II) and Fe (II, III) ions in Zn (II) – Cu (II) and Zn (II) – Fe (II, III) ion was 97.14% and 87.74%, respectively at 40 mg l<sup>-1</sup> of total Fe (II, III) and Cu (II). In ternary metal ion system Zn (II) – Fe (II, III) – Cu (II), the removal of Cu (II) and Fe (II, III) ion was found to be low. Furthermore, with the

rise in initial concentration of Cu (II) and Fe (II, III) ions from 40 mg l<sup>-1</sup> to 150 mg l<sup>-1</sup> in all types of metal ion systems, the removal of Zn (II), Fe (II, III) and Cu (II) ions decreased gradually. The reason behind the gradual decrease in biosorption of Zn (II), Fe (II, III) and Cu (II) ions with an increase in initial concentration of total Fe (II, III) and Cu (II) ion from 40 mg l<sup>-1</sup> to 150 mg l<sup>-1</sup> was the steady increase in the saturation of active sites present on the surface of biosorbent. At 40 mg l<sup>-1</sup> of Cu (II) and total Fe (II, III) ions concentration, 99.33% of Zn (II) ion removal was obtained. This value was comparatively higher than the removal reported in figure 5.2.4 (i).

Figure 5.2.5 (f) represents the influence of initial concentration of Cu (II) and total Fe (II, III) ion on biosorption of Zn (II), total Fe (II, III) and Cu (II) ions on Eucalyptus bark sawdust.

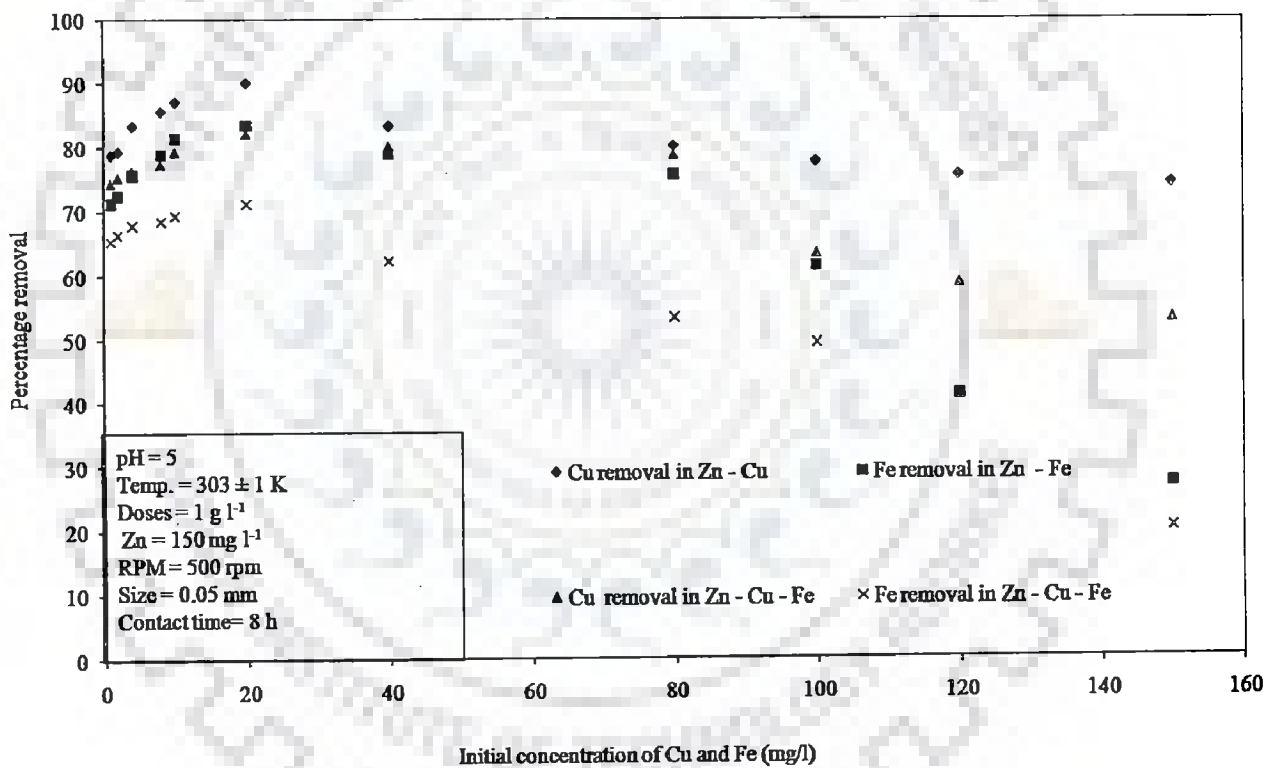


Figure 5.2.5 (f): Effect of initial concentration of Cu and Fe on biosorption of Cu and Fe in presence of Zn on Eucalyptus bark sawdust

It is evident from figure 5.2.5 (f) that the maximum removal of Cu (II) and Fe (II, III) was obtained in binary metal ion system. The maximum percentage removal of Cu (II) and Fe (II,



III) ions in Zn (II) – Cu (II) and Zn (II) – Fe (II, III) ion was 90.19% and 83.36%, respectively at 20 mg l<sup>-1</sup> of Cu (II) and total Fe (II, III). In ternary metal ion system Zn (II) – Fe (II, III) – Cu (II), the removal of Cu (II) and Fe (II, III) ion was found to be low. Furthermore, with the rise in initial concentration of Cu (II) and Fe (II, III) ions from 20 mg l<sup>-1</sup> to 150 mg l<sup>-1</sup> in all types of metal ion systems, the removal of Zn (II), Fe (II, III) and Cu (II) ions decreased gradually. The reason behind the gradual decrease in biosorption of Zn (II), Fe (II, III) and Cu (II) ions with the increase in initial concentration of total Fe (II, III) and Cu (II) ion from 20 mg l<sup>-1</sup> to 150 mg l<sup>-1</sup> was the steady increase in the saturation of active sites present on the surface biosorbent. At 20 mg l<sup>-1</sup> of Cu (II) and total Fe (II, III) ions concentration, 88.92% of Zn (II) ion removal was obtained. This value was comparatively higher against the removal reported in figure 5.2.4 (k). Figure 5.2.5 (g) represents the influence of initial concentration of total Fe (II, III) and Cu (II) ion on biosorption of Zn (II), total Fe (II, III) and Cu (II) ions on Eucalyptus leaf powder.

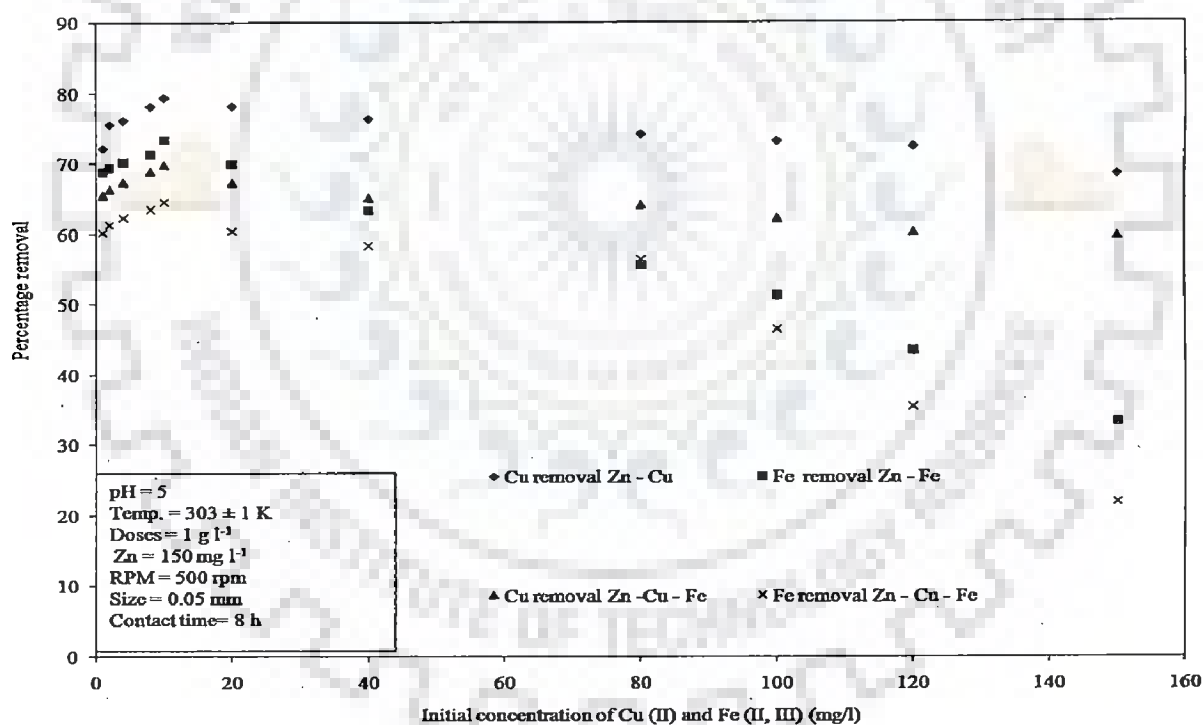


Figure 5.2.5 (g): Effect of initial concentration of Cu and Fe on biosorption of Cu and Fe in presence of Zn on Eucalyptus leaf powder

It is evident from figure 5.2.5 (g) that the maximum removal of Cu (II) and Fe (II, III) was obtained in binary metal ion system. The maximum percentage removal of Cu (II) and Fe (II, III) ions in Zn (II) – Cu (II) and Zn (II) – Fe (II, III) ion was 79.35% and 73.39%, respectively at 10 mg l<sup>-1</sup> of Cu (II) and total Fe (II, III). In ternary metal ion system Zn (II) – Fe (II, III) – Cu (II), the removal of Cu (II) and Fe (II, III) ion was found to be low. Furthermore, with the rise in initial concentration of Cu (II) and Fe (II, III) ions from 10 mg l<sup>-1</sup> to 150 mg l<sup>-1</sup> in all types of metal ion systems, the removal of Zn (II), Fe (II, III) and Cu (II) ions decreased gradually. The reason behind the gradual decrease in biosorption of Zn (II), Fe (II, III) and Cu (II) ions with an increase in initial concentration of total Fe (II, III) and Cu (II) ion from 10 mg l<sup>-1</sup> to 150 mg l<sup>-1</sup> was the steady increase in the saturation of active sites present on the surface of biosorbent. This value was comparatively higher than the removal reported in figure 5.2.4 (m). Figure 5.2.5 (h) represents the influence of initial concentration of total Fe (II, III) and Cu (II) ion on biosorption of Zn (II), total Fe (II, III) and Cu (II) ions on Eggshell and membrane.

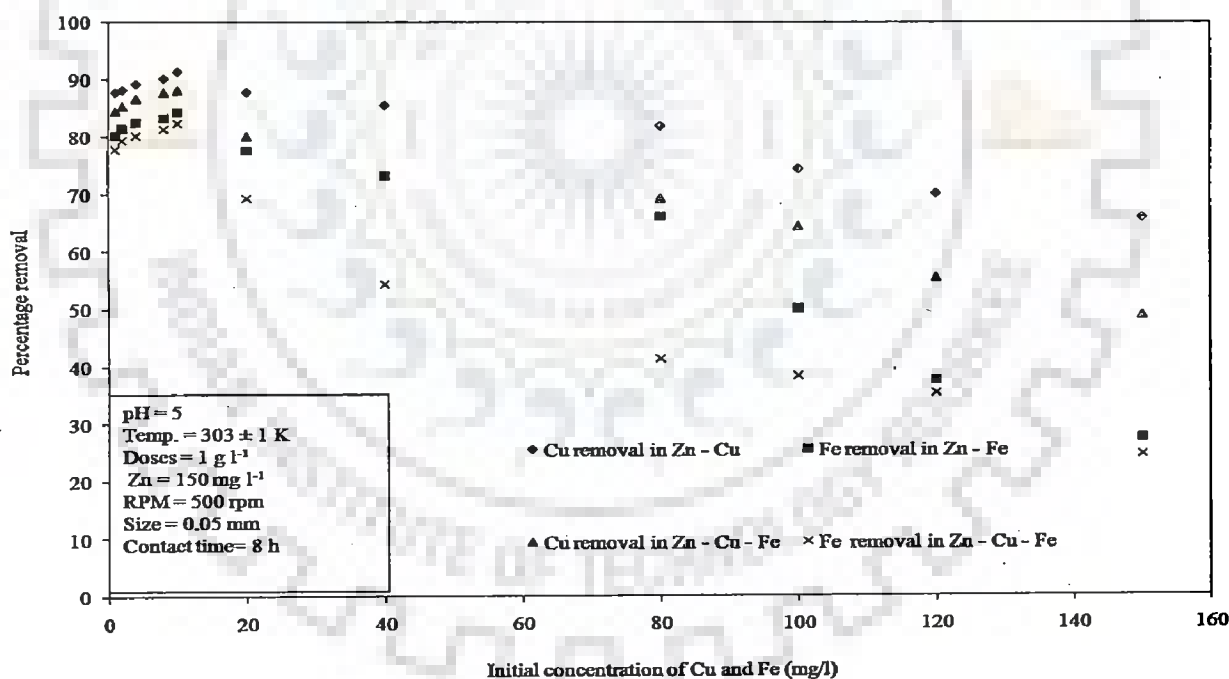


Figure 5.2.5 (h): Effect of initial concentration of Cu and Fe on biosorption of Cu and Fe in presence of Zn on Eggshell and membrane

It is evident from figure 5.2.5 (h) that the maximum removal of Cu (II) and Fe (II, III) was obtained in binary metal ion system. The maximum percentage removal of Cu (II) and Fe (II, III) ions in Zn (II) – Cu (II) and Zn (II) – Fe (II, III) ion was 91.33% and 84.31%, respectively at 10 mg l<sup>-1</sup> of Cu (II) and total Fe (II, III). In ternary metal ion system Zn (II) – Fe (II, III) – Cu (II), the removal of Cu (II) and Fe (II, III) ion was found to be low. Furthermore, with the rise in initial concentration of Cu (II) and Fe (II, III) ions from 10 mg l<sup>-1</sup> to 150 mg l<sup>-1</sup> in all types of metal ion systems, the removal of Zn (II), Fe (II, III) and Cu (II) ions decreased gradually. The reason behind the gradual decrease in biosorption of Zn (II), Fe (II, III) and Cu (II) ions with an increase in initial concentration of total Fe (II, III) and Cu (II) ion from 10 mg l<sup>-1</sup> to 150 mg l<sup>-1</sup> was the steady increase in the saturation of active sites present on the surface of biosorbent. At 10 mg l<sup>-1</sup> of Cu (II) and total Fe (II, III) ions concentration, 98.58% of Zn (II) ion removal was obtained. This value was comparatively higher than the removal reported in figure 5.2.4 (o).

Figure 5.2.5 (i) represents the influence of initial concentration of total Fe (II, III) and Cu (II) ion on biosorption of Zn (II), total Fe (II, III) and Cu (II) ions on *Zinc sequestering bacterium VMSDCM* accession no. HQ108109. It became evident from figure 5.2.5 (i) that the maximum removal of Cu (II) and Fe (II, III) was obtained in binary metal ion system. The maximum percentage removal of Cu (II) and Fe (II, III) ions in Zn (II) – Cu (II) and Zn (II) – Fe (II, III) ion was 95.44% and 85.36%, respectively at 100 mg l<sup>-1</sup> of Cu (II) and total Fe (II, III). In ternary metal ion system Zn (II) – Fe (II, III) – Cu (II), the removal of Cu (II) and Fe (II, III) ion was found to be low. Furthermore, with the rise in initial concentration of Cu (II) and Fe (II, III) ions from 100 mg l<sup>-1</sup> to 150 mg l<sup>-1</sup> in all types of metal ion systems, the removal of Zn (II), Fe (II, III) and Cu (II) ions decreased gradually. The reason behind the gradual decrease in biosorption of Zn (II), Fe (II, III) and Cu (II) ions with an increase in initial concentration of total Fe (II, III) and Cu (II) ion from 100 mg l<sup>-1</sup> to 150 mg l<sup>-1</sup> was the steady increase in the saturation of active sites present on the surface of biosorbent. At 100 mg l<sup>-1</sup> of Cu (II) and total Fe (II, III) ions concentration, 99.58% of Zn (II) ion removal was obtained. This value was comparatively higher against the removal reported in figure 5.2.4 (q).

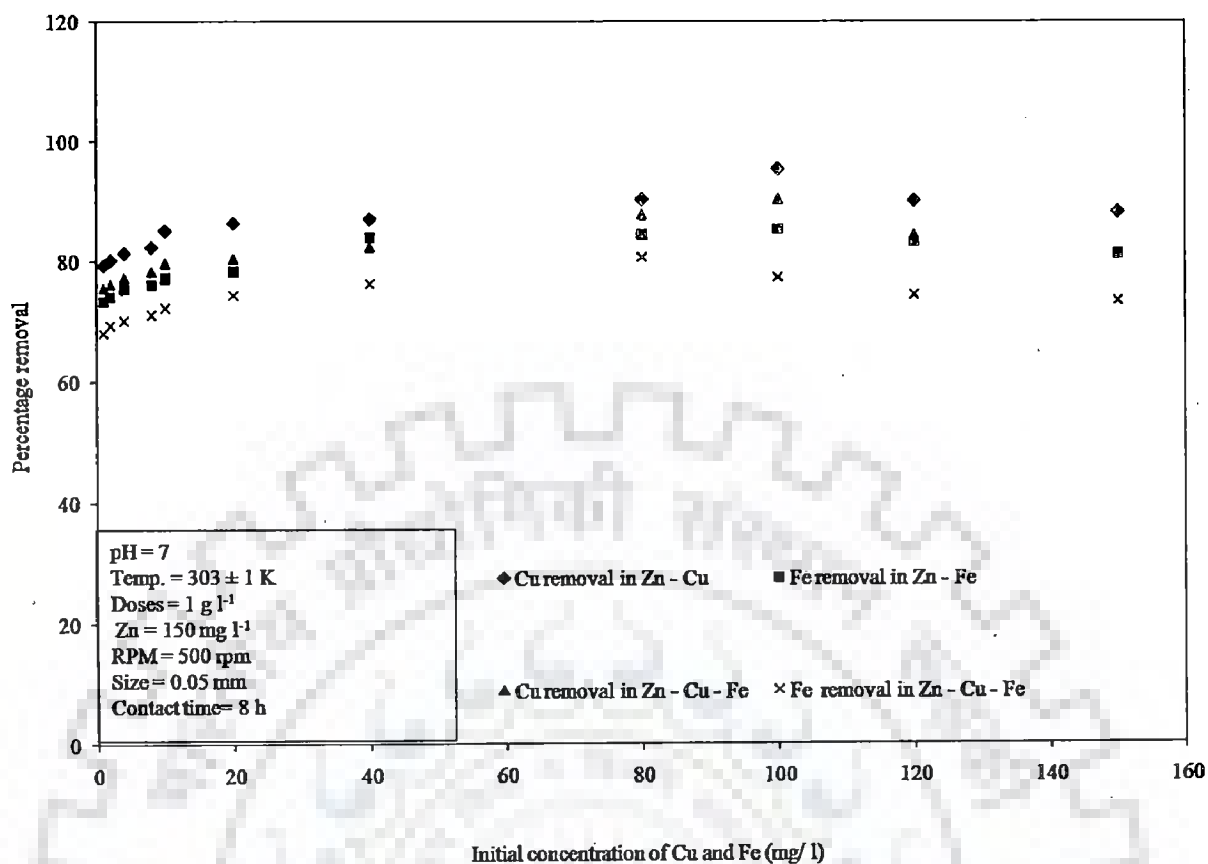


Figure 5.2.5 (i): Effect of initial concentration of Cu and Fe on biosorption of Cu and Fe in presence of Zn on dead cells of *Zinc sequestering bacterium VMSDCM* accession no. HQ108109

### Concluding remarks of the section 5.2.5

Among all the bisorbents selected for the present work, the maximum removal of Zn (II) ion was obtained with *Cedrus deodara* sawdust and dead cells of *Zinc sequestering bacterium VMSDCM* accession no. HQ108109. The maximum removal of Zn (II) ion obtained in case of *Cedrus deodara* sawdust and dead cells of *Zinc sequestering bacterium VMSDCM* accession no. HQ108109 were 99.33% and 99.58% from the solution containing 40 mg l<sup>-1</sup>, 100 mg l<sup>-1</sup> and 150 mg l<sup>-1</sup> of initial concentration of Cu (II), Fe (II, III) and Zn (II), respectively. The maximum removal of Cu (II) and Fe (II) in Zn (II) – Fe (II, III) – Cu (II) metal ion complex, in case of *Cedrus deodara* sawdust, was obtained at 40 mg l<sup>-1</sup> of Fe (II, III) and Cu (II), respectively. The maximum removal of Cu (II) and Fe (II) in Zn (II) – Fe (II, III) – Cu (II) metal ion complex, in case of dead cells of *Zinc sequestering bacterium VMSDCM* accession

no. HQ108109 was obtained at  $100 \text{ mg l}^{-1}$  of Fe (II, III) and Cu (II), respectively. The preferential order of removal of heavy metal ions was  $\text{Cu (II)} > \text{Zn (II)} > \text{Fe (II, III)}$ .

### 5.2.6 Optimization of particle size

This section embodies the results of influence of particle size of adsorbent on biosorption of Zn(II), total Fe (II, III) and Cu (II) in liquid phase. The experiments were conducted in range of 0.05 mm to 4 mm particle size. The metal ion combinations used were pure zinc, Zn (II) – Cu(II), Zn (II) – Fe (II, III) and Zn (II) – Fe (II, III)- Cu (II). Results of influence of particle size have been shown in figures 5.2.6 (a) to 5.2.6 (r). The system of ions studied in the present work were pure zinc, Zn (II)- Cu (II), Zn (II)- Fe (II, III) and Zn (II) – Cu (II) - Fe (II, III). The metal ions Zn (II), Cu (II) and Fe (II, III) are referred as Zn, Cu and Fe in various figures. Figure 5.2.6 (a) and figure 5.2.6 (b) represent the influence of particle size on biosorption of Zn (II), total Fe (II, III) and Cu (II) ions on Mango bark sawdust.

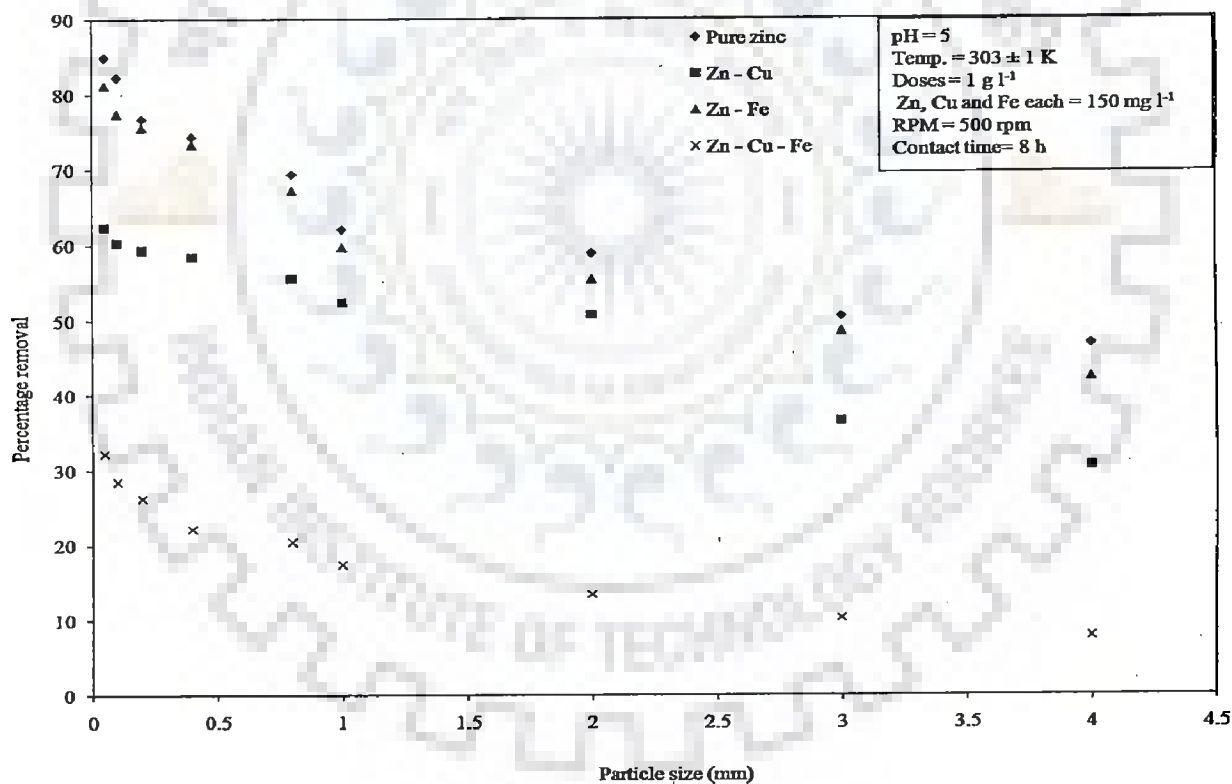


Figure 5.2.6 (a): Effect of particle size on biosorption of Zn on Mango bark sawdust

It is clear from figure 5.2.6 (a) and figure 5.2.6 (b) that lowest particle size (0.05 mm) offered maximum percentage removal of Zn (II), Cu (II) and total Fe (II, III) ion from liquid phase. The maximum removal of Zn (II) was obtained in pure zinc phase. The maximum removal was 84.88% at a particle size of 0.05 mm (figure 5.2.6 (a)). The maximum removal of Zn (II) ion in Zn (II) - Cu (II) and Zn (II) – total Fe (II, III) was 62.36 % and 81.12%, respectively at a particle size of 0.05 mm. The maximum removal of Cu (II) and total Fe (II, III) in Zn (II)- Cu (II) and Zn (II)- total Fe (II, III) were 84.16% and 48.11%, respectively at a particle size of 0.05 mm (figure 5.2.6 (b)).

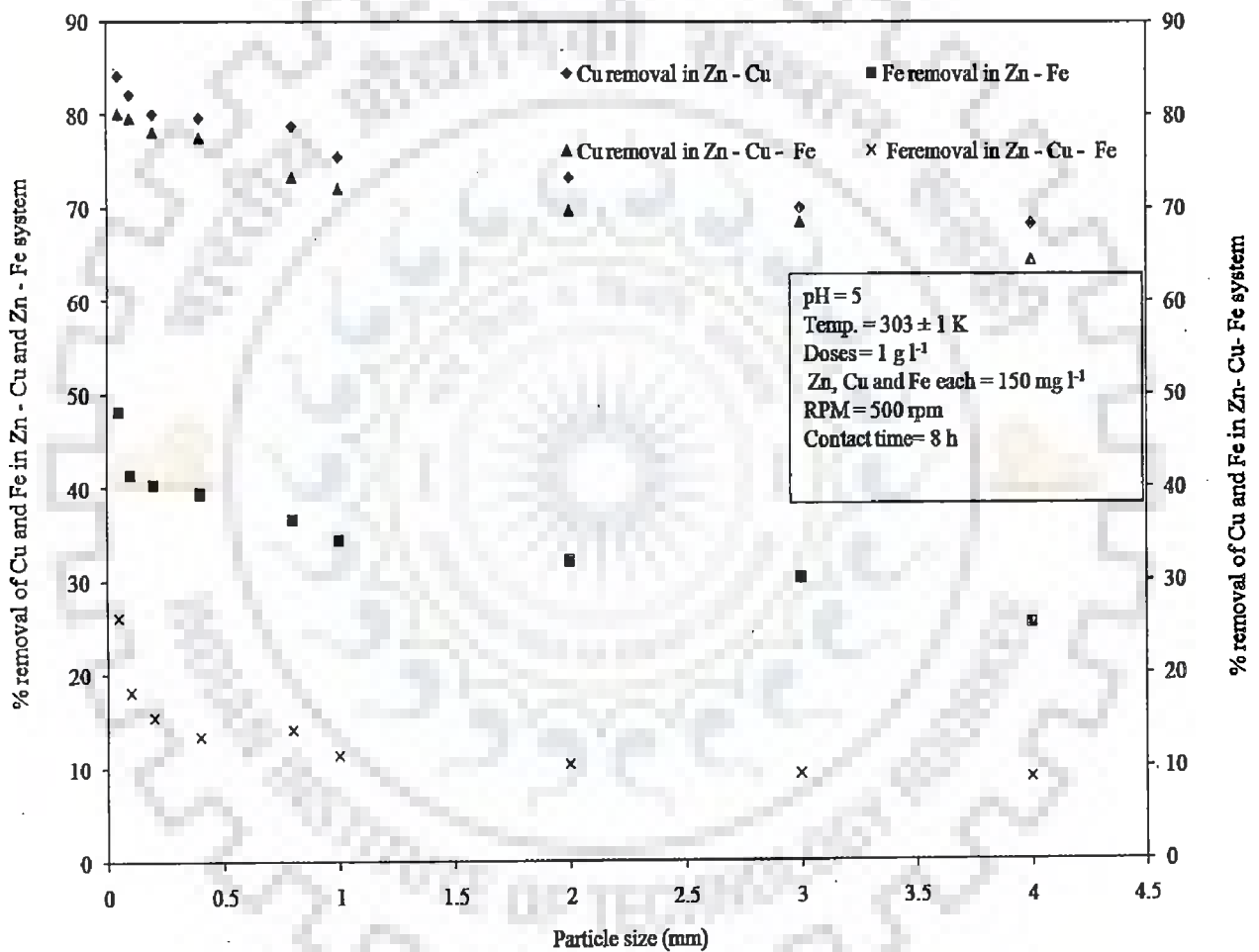


Figure 5.2.6 (b): Effect of particle size on biosorption of Cu and Fe in presence of Zn on Mango bark sawdust

The maximum removal of Zn (II), Cu (II) and total Fe (II, III) ion in Zn (II) - Fe (II, III) – Cu (II) was 32.11%, 80.16% and 26.11%, respectively (figure 5.2.6 (b)). With the increase in particle size from 0.05 mm to 4 mm of biosorbent, the percentage removal of metal ions decreased. The increase in particle size of biosorbent led to the decrease in effective surface area of the biosorbent, which resulted in lowering of removal of metal ions. The smaller is the particle size of biosorbent, larger is the effective surface area for sorption of metal ion on biosorbent particle, which results in higher percentage removal of metal ions (Dang et al., 2009, Mishra et al., 2010). The preferential order of removal of heavy metal ions was Cu (II)> Zn (II)> Fe (II, III). Figure 5.2.6 (c) and figure 5.2.6 (d) represent the influence of particle size on biosorption of Zn (II), total Fe (II, III) and Cu (II) ions on Orange peel. It became obvious from figure 5.2.6 (c) and figure 5.2.6 (d) that the lowest particle size (0.05 mm) offered maximum percentage removal of Zn (II), Cu (II) and total Fe (II, III) ion from liquid phase.

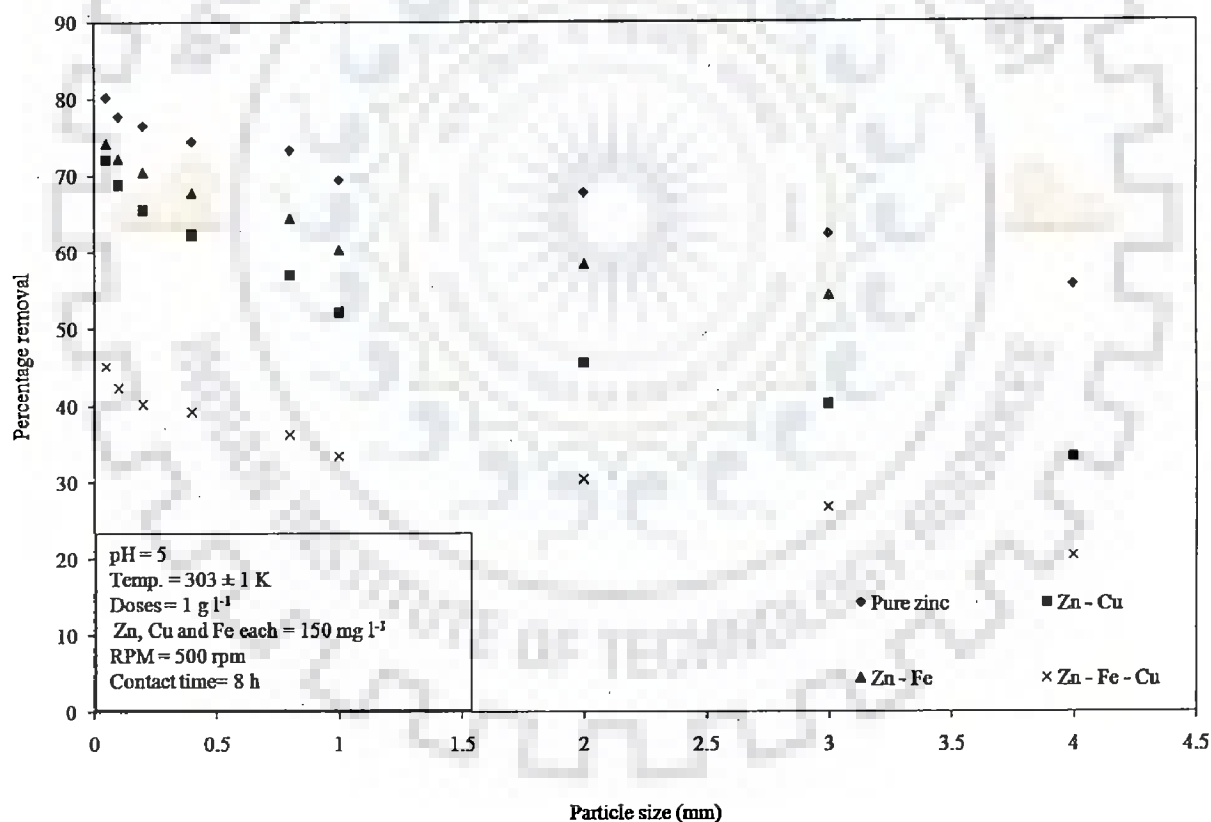


Figure 5.2.6 (c): Effect of particle size on biosorption of Zn on Orange peel

The maximum removal of Zn (II) was obtained in pure zinc phase. The maximum removal was 80.21% at a particle size of 0.05 mm. The maximum removal of Zn (II) ion in Zn (II) - Cu (II) and Zn (II) – total Fe (II, III) was 72.18% and 74.71%, respectively at a particle size of 0.05 mm.

The maximum removal of Cu (II) and total Fe (II, III) in Zn (II)- Cu (II) and Zn (II)-total Fe (II, III) were 76.16% and 32.11%, respectively at a particle size of 0.05 mm (figure 5.2.6 (c)). The maximum removal of Zn (II), Cu (II) and total Fe (II, III) ion in Zn (II) - Fe (II, III) – Cu (II) was 45.11%, 71.16% and 21.31%, respectively at a particle size of 0.05 mm (figure 5.2.6 (d)).

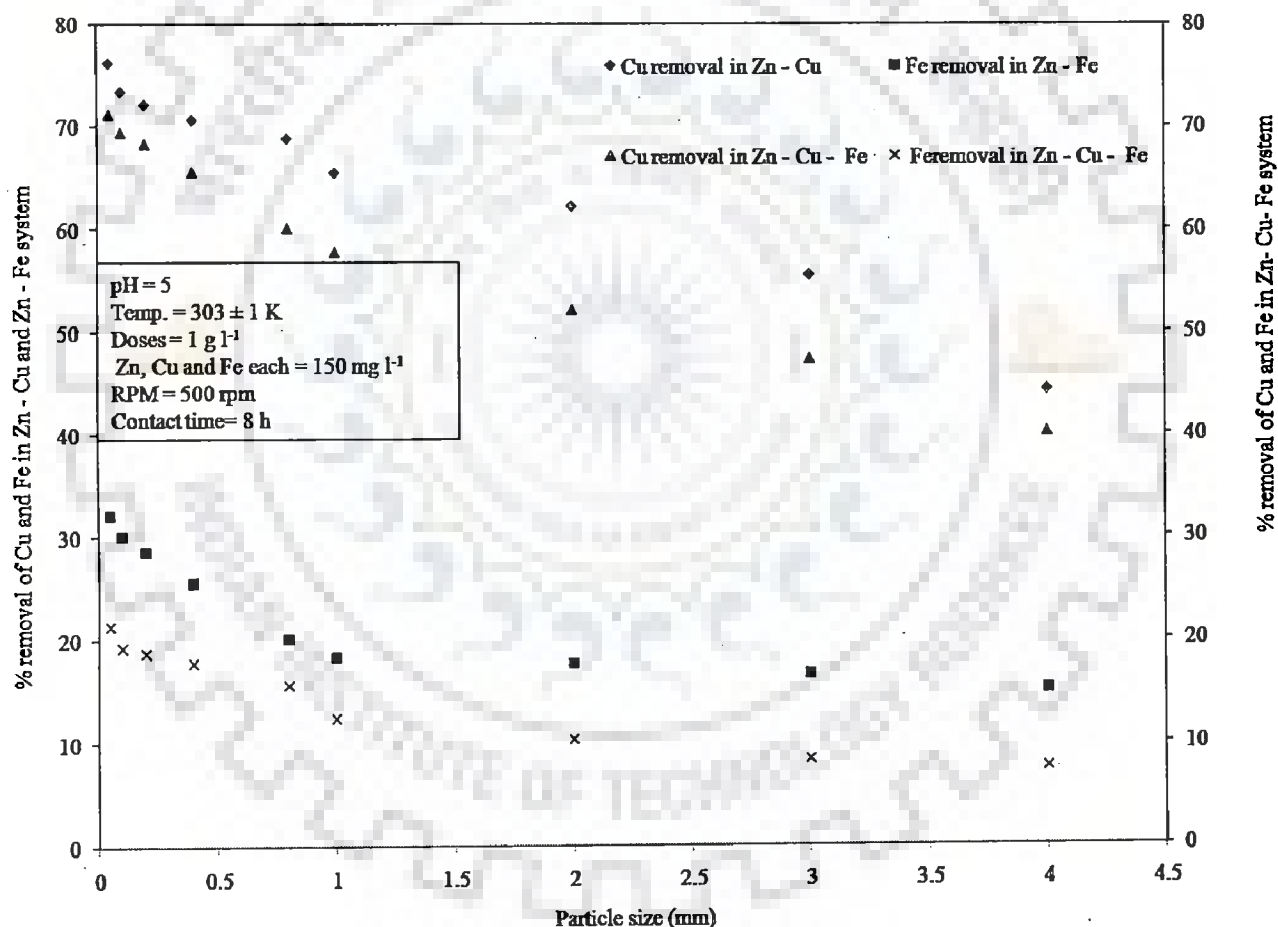


Figure 5.2.6 (d): Effect of particle size on biosorption of Cu and Fe in presence of Zn on Orange peel



With the increase in particle size from 0.05 mm to 4 mm of biosorbent, the percentage removal of metal ions decreased. The increase in particle size of biosorbent led to the decrease in effective surface area of the biosorbent, which resulted in lowering of removal of metal ions. The smaller is the particle size of biosorbent, larger is the effective surface area for sorption of metal ion on biosorbent particle, which results in higher percentage removal of metal ions (Dang et al., 2009, Mishra et al., 2010). The preferential order of removal of heavy metal ions was Cu (II) > Zn (II) > Fe (II, III). Figure 5.2.6 (e) and figure 5.2.6 (f) represent the influence of particle size on biosorption of Zn (II), total Fe (II, III) and Cu (II) ions on Pineapple peel.

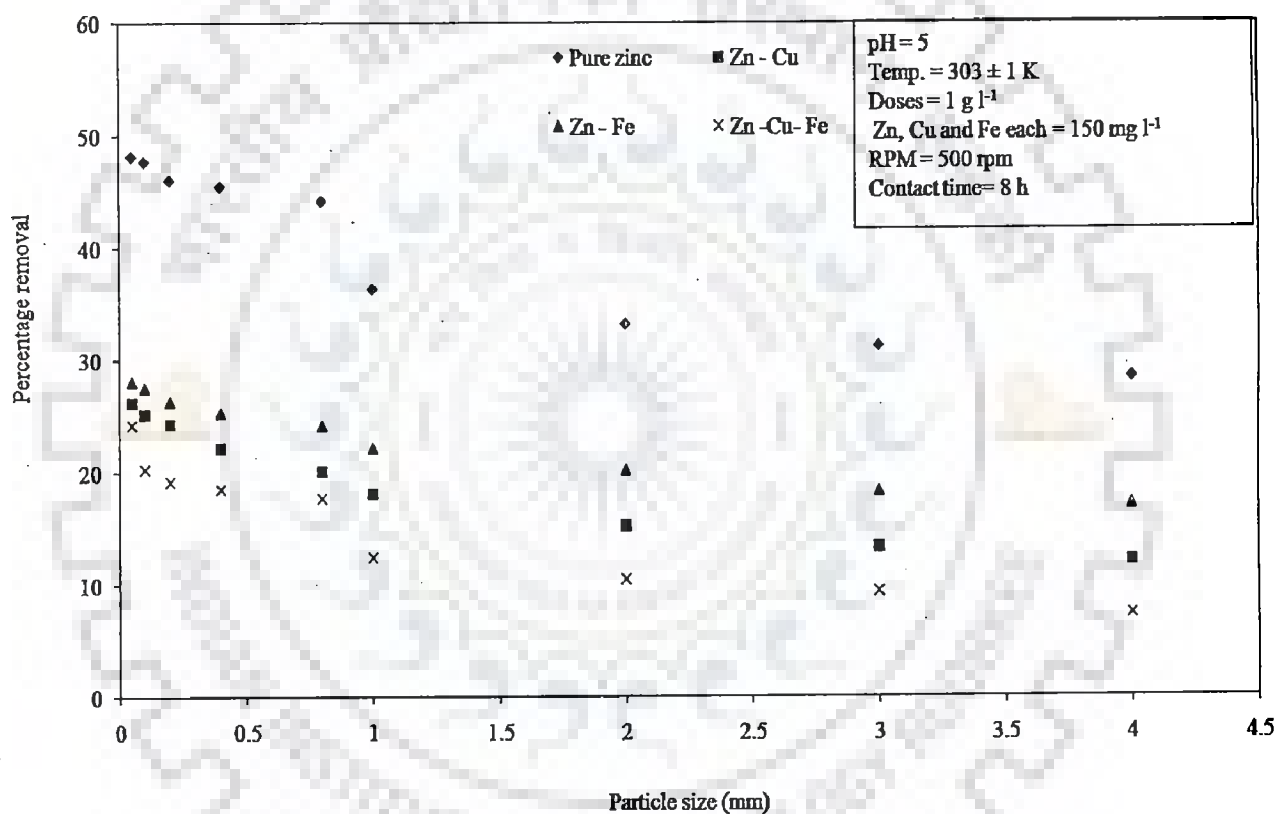


Figure 5.2.6 (e): Effect of particle size on biosorption of Zn on Pineapple peel

It is clear from figure 5.2.6 (e) and figure 5.2.6 (f) that lowest particle size (0.05 mm) offered maximum percentage removal of Zn (II), Cu (II) and total Fe (II, III) ion from liquid phase. The maximum removal of Zn (II) was obtained in pure zinc phase. The maximum removal was 48.16% at a particle size of 0.05 mm. The maximum removal of Zn (II) ion in Zn (II) - Cu (II) and Zn (II) - total Fe (II, III) was 26.22 % and 28.11%, respectively at a

particle size of 0.05 mm (figure 5.2.6 (e)). The maximum removal of Cu (II) and total Fe (II, III) in Zn (II)- Cu (II) and Zn (II)- total Fe (II, III) were 82.43% and 31.65%, respectively, at a particle size of 0.05 mm. The maximum removal of Zn (II), Cu (II) and total Fe (II, III) ion in Zn (II) - Fe (II, III) – Cu (II) was 24.19%, 60.11% and 23.26%, respectively, at a particle size of 0.05 mm (figure 5.2.6 (f)). With the increase in particle size from 0.05 mm to 4 mm of biosorbent, the percentage removal of metal ions decreased.

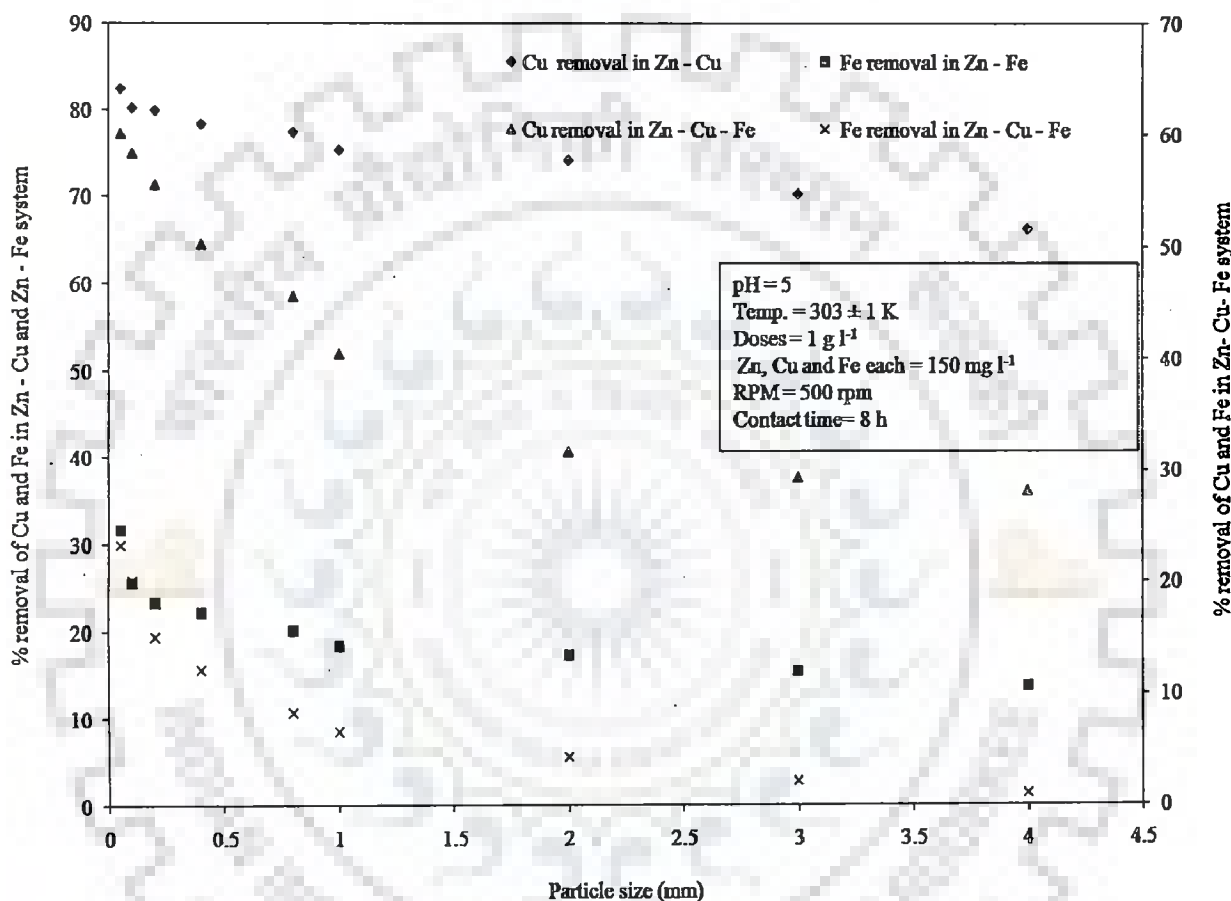


Figure 5.2.6 (f): Effect of particle size on biosorption of Cu and Fe in presence of Zn on Pineapple peel

The increase in particle size of biosorbent led to the decrease in effective surface area of the biosorbent, which resulted in lowering of removal of metal ions. The smaller is the particle size of biosorbent, larger is the effective surface area for sorption of metal ion on biosorbent particle, which results in higher percentage removal of metal ions (Dang et al., 2009, Mishra et al., 2010). The preferential order of removal of heavy metal ions was Cu

(II) > Zn (II) > Fe (II, III). Figure 5.2.6 (g) and figure 5.2.6 (h) represent the influence of particle size on biosorption of Zn (II), total Fe (II, III) and Cu (II) ions on Jackfruit peel powder.

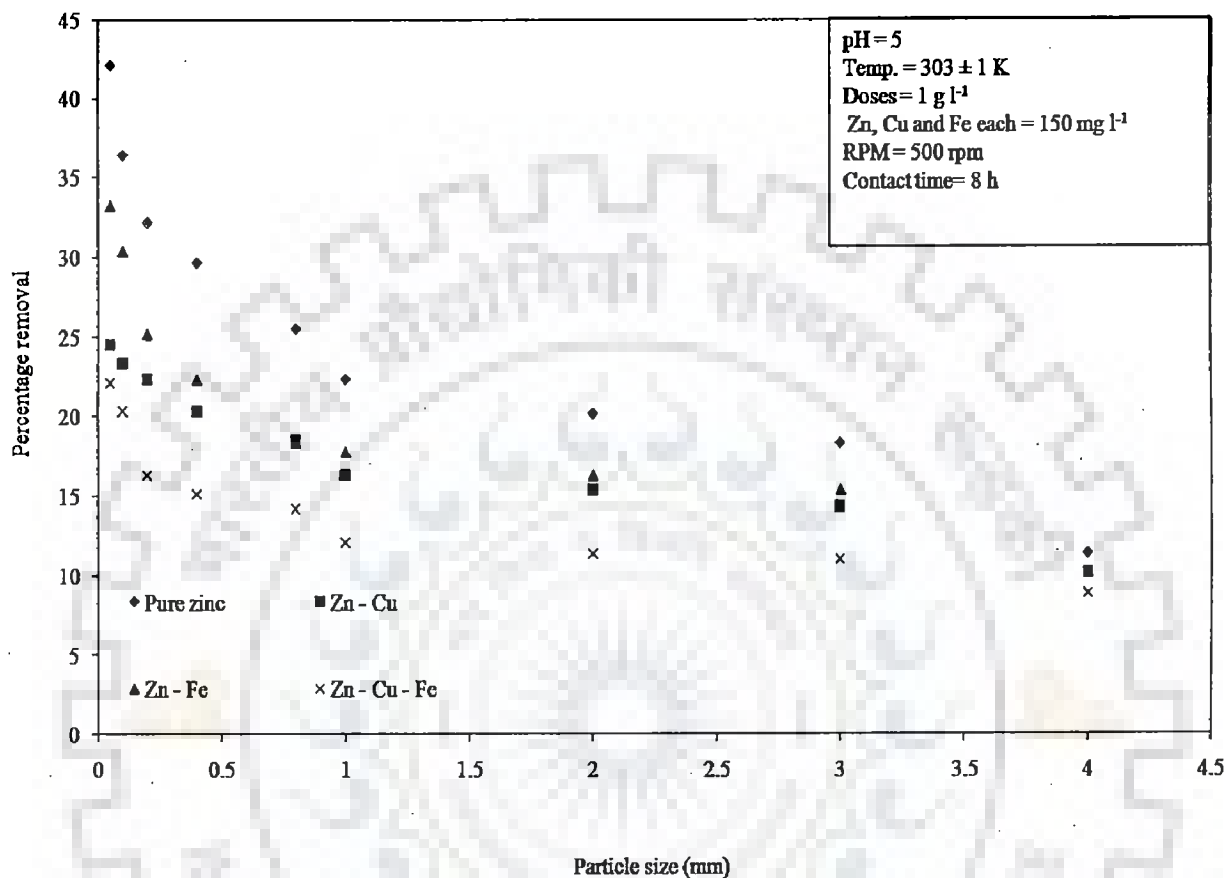


Figure 5.2.6 (g): Effect of particle size on biosorption of Zn on Jackfruit peel powder

It is clear from figure 5.2.6 (g) and figure 5.2.6 (h) that lowest particle size (0.05 mm) offered maximum percentage removal of Zn (II), Cu (II) and total Fe (II, III) ion from liquid phase. The maximum removal of Zn (II) was obtained in pure zinc phase. The maximum removal was 42.11% at a particle size of 0.05 mm. The maximum removal of Zn (II) ion in Zn (II) - Cu (II) and Zn (II) - total Fe (II, III) was 24.51 % and 33.8%, respectively at a particle size of 0.05 mm (figure 5.2.6 (g)). The maximum removal of Cu (II) and total Fe (II, III) in Zn (II)- Cu (II) and Zn (II)- total Fe (II, III) were 68.94% and 28.16%, respectively at a particle size of 0.05 mm. The maximum removal of Zn (II), Cu (II) and total Fe (II, III) ion in

Zn (II) - Fe (II, III) – Cu (II) was 22.11%, 55.51% and 20.24%, respectively (figure 5.2.6 (f)). With the increase in particle size from 0.05 mm to 4 mm of biosorbent, the percentage removal of metal ions decreased.

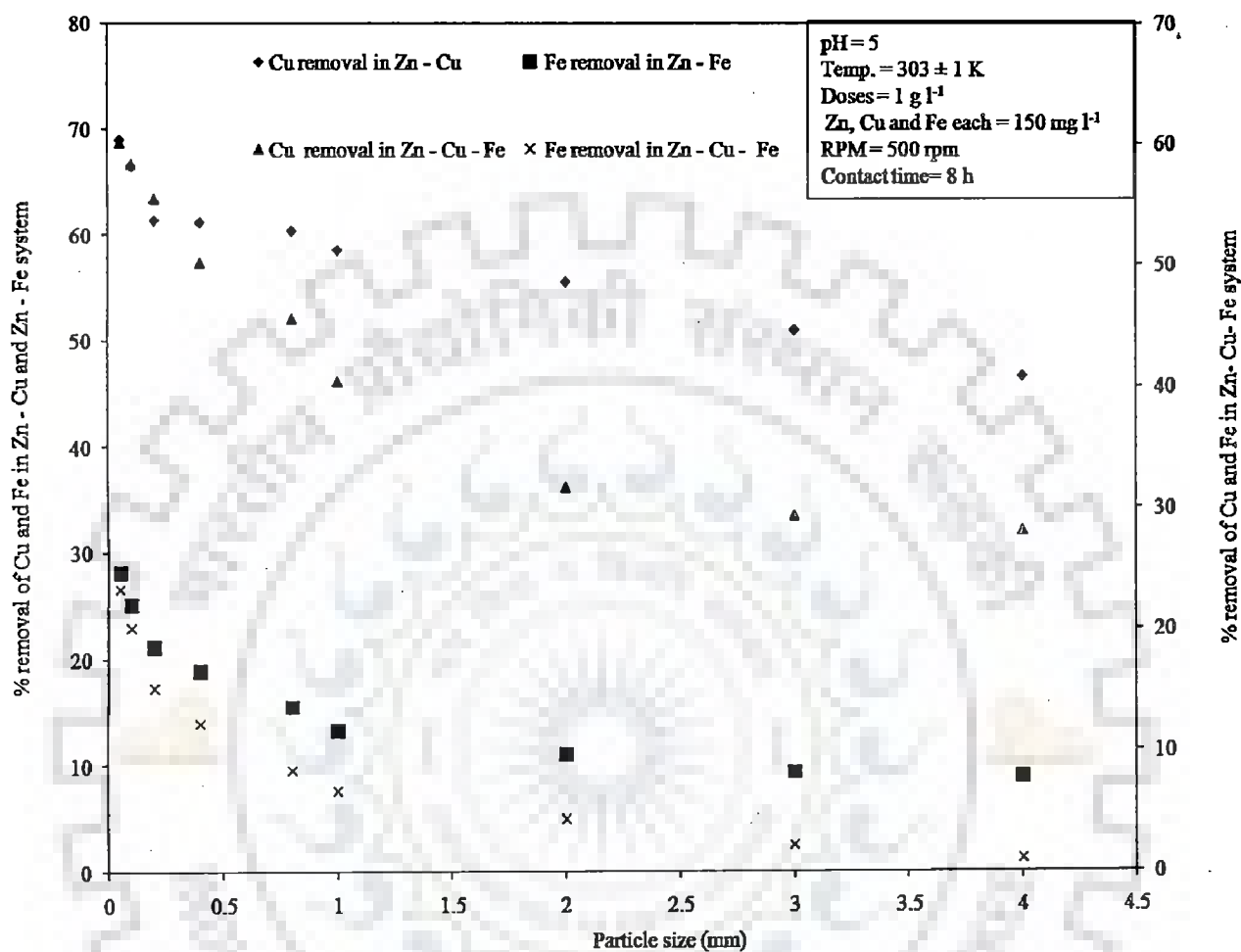


Figure 5.2.6 (h): Effect of particle size on biosorption of Cu and Fe in presence of Zn on Jackfruit peel powder.

The increase in particle size of biosorbent led to the decrease in effective surface area of the biosorbent, which resulted in lowering of removal of metal ions. The smaller is the particle size of biosorbent, larger is the effective surface area for sorption of metal ion on biosorbent particle, which results in higher percentage removal of metal ions (Dang et al., 2009, Mishra et al., 2010). The preferential order of removal of heavy metal ions was Cu (II) > Zn (II) > Fe (II, III).

Figure 5.2.6 (i) and figure 5.2.6 (j) represent the influence of particle size on biosorption of Zn (II), Cu (II) and Fe on *Cedrus deodara* sawdust. It is clear from figure 5.2.6 (i) and figure 5.2.6 (j) that lowest particle size (0.05 mm) offered maximum percentage removal of Zn (II), Cu (II) and total Fe (II, III) ion from liquid phase.

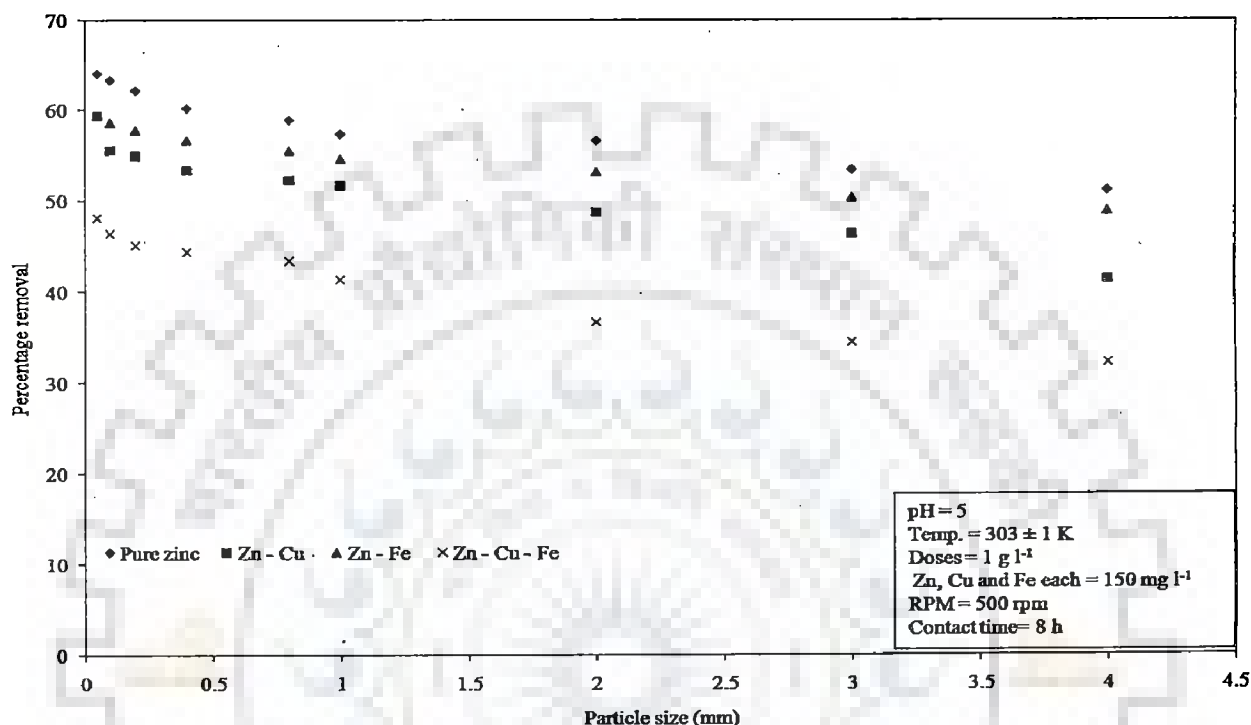


Figure 5.2.6 (i): Effect of particle size on biosorption of Zn on *Cedrus deodara* sawdust

The maximum removal of Zn (II) was obtained in pure zinc phase. The maximum removal was 64.11% at a particle size of 0.05 mm. The maximum removal of Zn (II) ion in Zn (II) - Cu (II) and Zn (II) - total Fe (II, III) was 59.29 % and 59.39%, respectively at a particle size of 0.05 mm (figure 5.2.6 (i)). The maximum removal of Cu (II) and total Fe (II, III) in Zn (II)- Cu (II) and Zn (II)- total Fe (II, III) were 74.11% and 37.19%, respectively at a particle size of 0.05 mm. The maximum removal of Zn (II), Cu (II) and total Fe (II, III) ion in Zn (II) - Fe (II, III) - Cu (II) was 48.13%, 65.5% and 32.14%, respectively at a particle size of 0.05 mm (figure 5.2.6 (j)). With the increase in particle size from 0.05 mm to 4 mm of biosorbent, the percentage removal of metal ions decreased. The increase in particle size of biosorbent led

to the decrease in effective surface area of the biosorbent, which resulted in lowering of removal of metal ions.

The smaller is the particle size of biosorbent, larger is the effective surface area for sorption of metal ion on biosorbent particle, which results in higher percentage removal of metal ions (Dang et al., 2009, Mishra et al., 2010). The preferential order of removal of heavy metal ions was Cu (II) > Zn (II) > Fe (II, III).

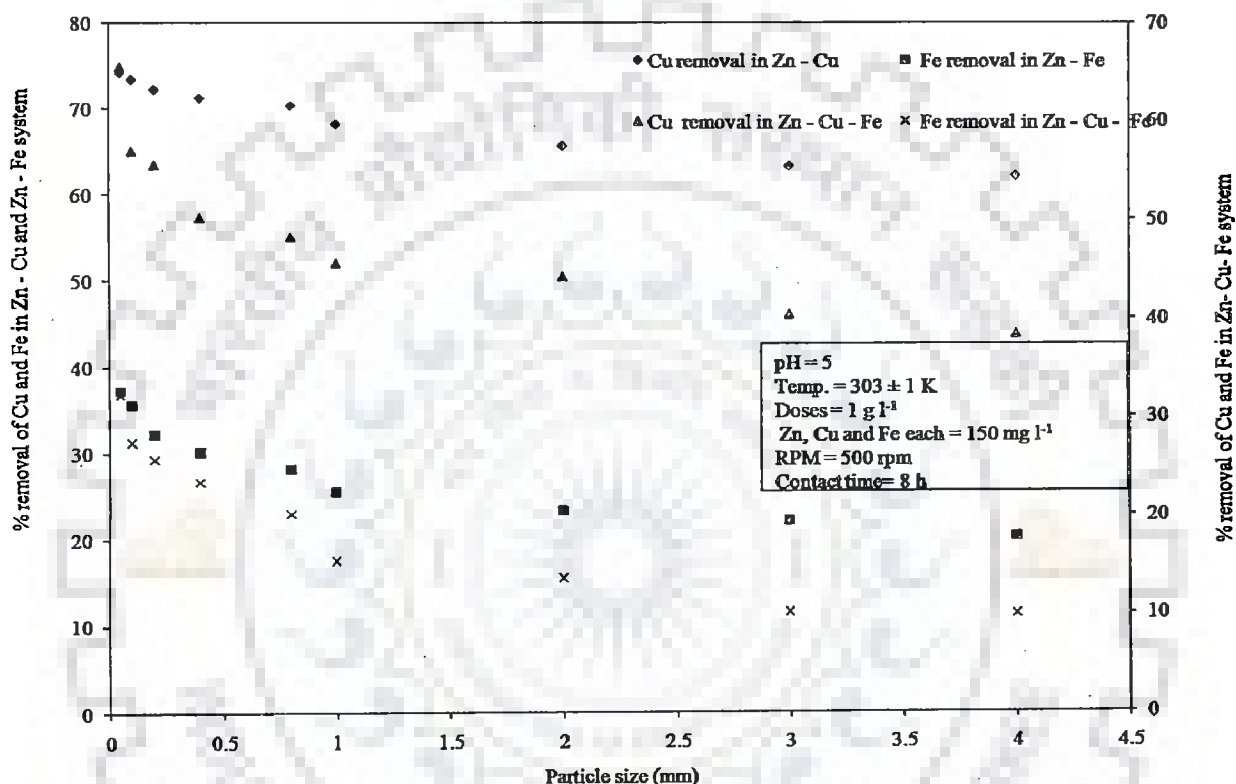


Figure 5.2.6 (j): Effect of particle size on biosorption of Cu and Fe in presence of Zn on *Cedrus deodara* sawdust

Figure 5.2.6 (k) and figure 5.2.6 (l) represent the influence of particle size on biosorption of Zn (II), total Fe (II, III) and Cu (II) ions on Eucalyptus bark sawdust. It is clear from figure 5.2.6 (k) and figure 5.2.6 (l) that lowest particle size (0.05 mm) offered maximum percentage removal of Zn (II), Cu (II) and total Fe (II, III) ion from liquid phase. The maximum removal of Zn (II) was obtained in pure zinc phase. The maximum removal was 71.33% at a particle size of 0.05 mm. The maximum removal of Zn (II) ion in Zn (II) - Cu

(II) and Zn (II) – total Fe (II, III) was 49.41 % and 52.18%, respectively at a particle size of 0.05 mm (figure 5.2.6 (k)).

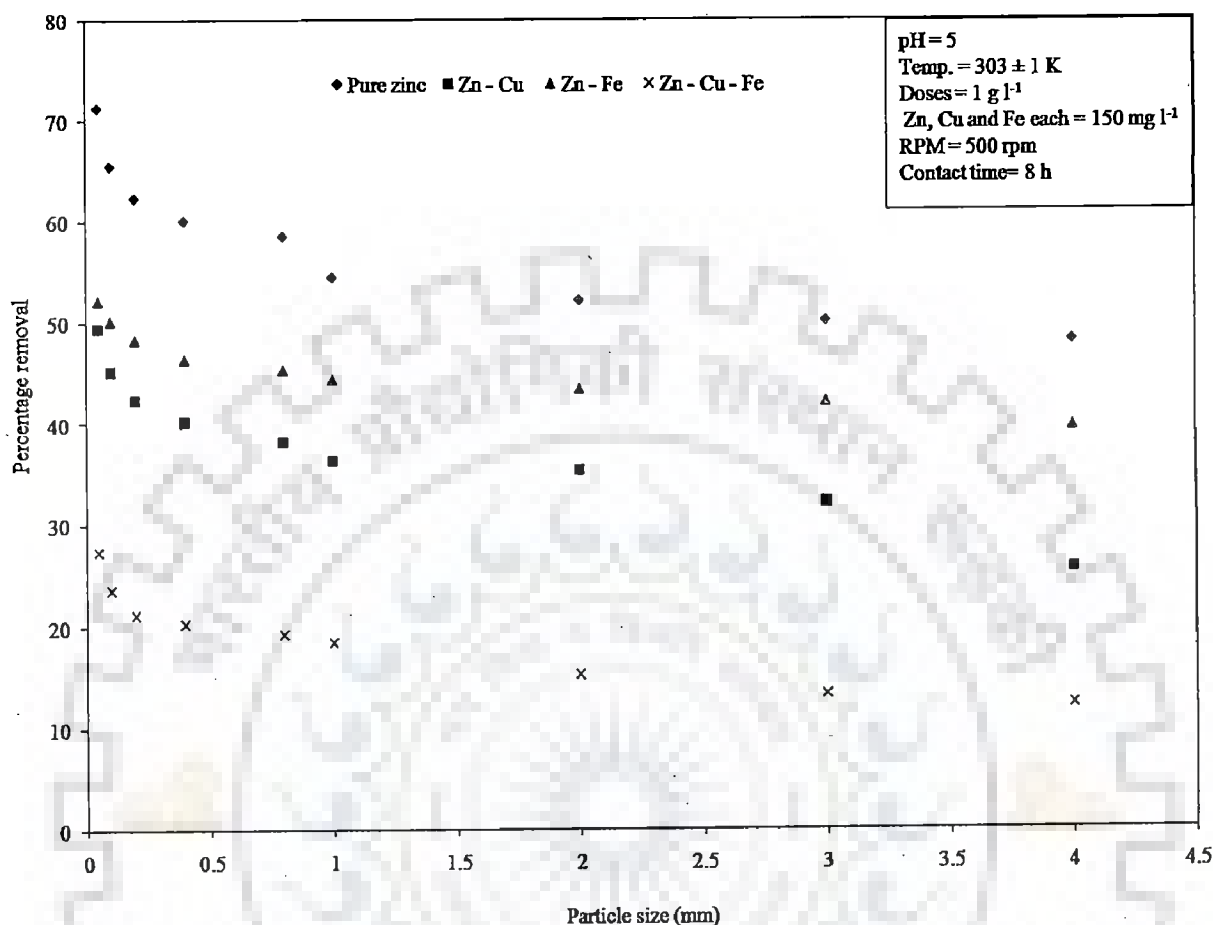


Figure 5.2.6 (k): Effect of particle size on biosorption of Zn on Eucalyptus bark sawdust

The maximum removal of Cu (II) and total Fe (II, III) in Zn (II)- Cu (II) and Zn (II)- total Fe (II, III) were 74.19% and 27.19%, respectively at a particle size of 0.05 mm. The maximum removal of Zn (II), Cu (II) and total Fe (II, III) ion in Zn (II) - Fe (II, III) – Cu (II) was 27.36%, 53.12% and 20.22%, respectively at a particle size of 0.05 mm (figure 5.2.6 (l)). With the increase in particle size from 0.05 mm to 4 mm of biosorbent, the percentage removal of metal ions decreased.

The increase in particle size of biosorbent led to the decrease in effective surface area of the biosorbent, which resulted in lowering of removal of metal ions. The smaller is the

particle size of biosorbent, larger is the effective surface area for sorption of metal ion on biosorbent particle, which results in higher percentage removal of metal ions (Dang et al., 2009, Mishra et al., 2010). The preferential order of removal of heavy metal ions was Cu (II) > Zn (II) > Fe (II, III).

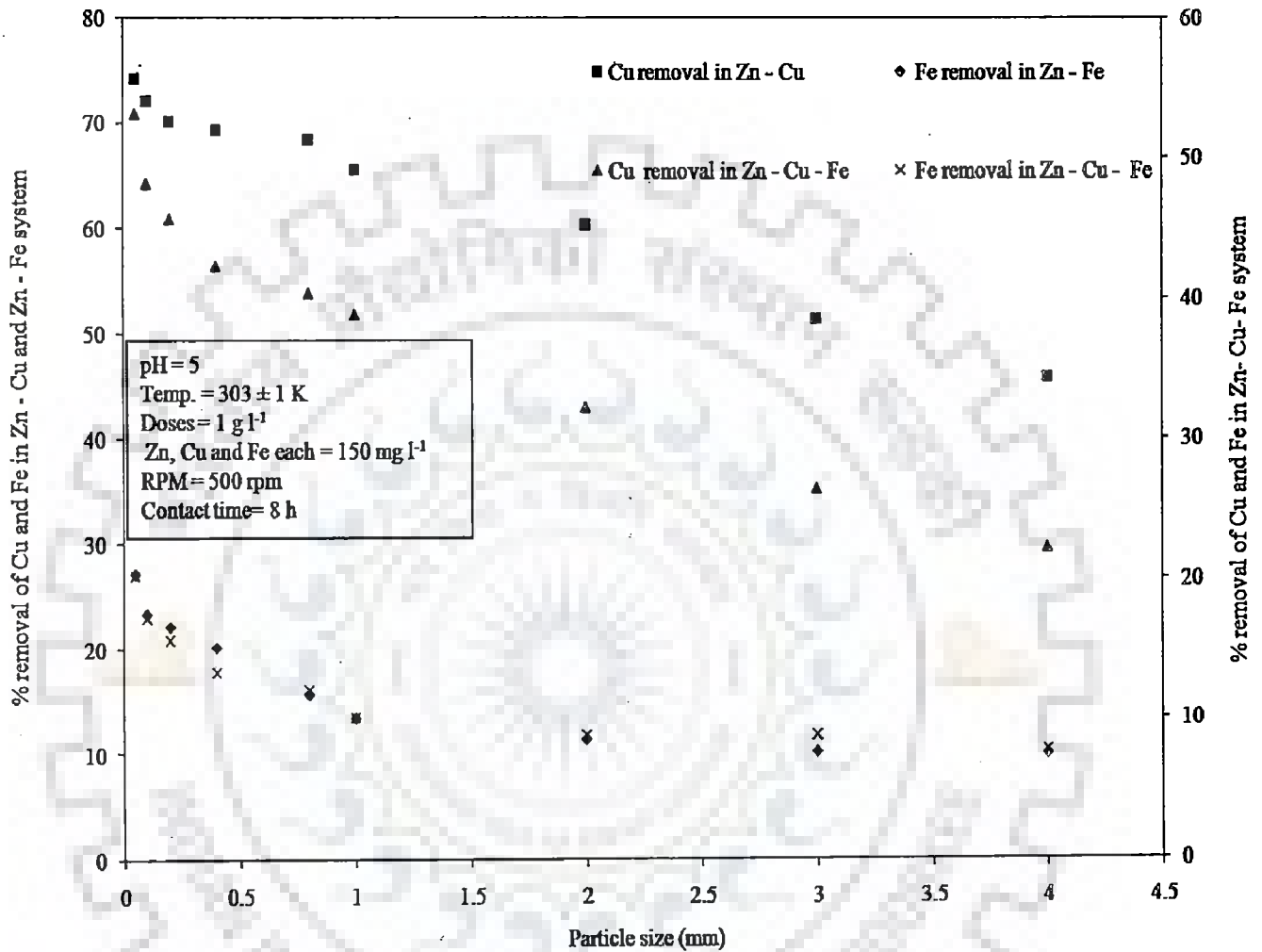


Figure 5.2.6 (l): Effect of particle size on biosorption of Cu and Fe in presence of Zn on Eucalyptus bark sawdust

Figure 5.2.6 (m) and figure 5.2.6 (n) represent the influence of particle size on biosorption of Zn (II), total Fe (II, III) and Cu (II) ions on Eucalyptus Leaf powder. It became obvious from figure 5.2.6 (m) and figure 5.2.6 (n) that lowest particle size (0.05 mm) offered maximum percentage removal of Zn (II), Cu (II) and total Fe (II, III) ion from liquid phase.



The maximum removal of Zn (II) was obtained in pure zinc phase. The maximum removal was 72.18% at a particle size of 0.05 mm. The maximum removal of Zn (II) ion in Zn (II) - Cu (II) and Zn (II) – total Fe (II, III) was 62.16 % and 65.13%, respectively at a particle size of 0.05 mm (figure 5.2.6 (m)). The maximum removal of Cu (II) and total Fe (II, III) in Zn (II)- Cu (II) and Zn (II)- total Fe (II, III) were 68.38% and 33.18%, respectively at a particle size of 0.05 mm.

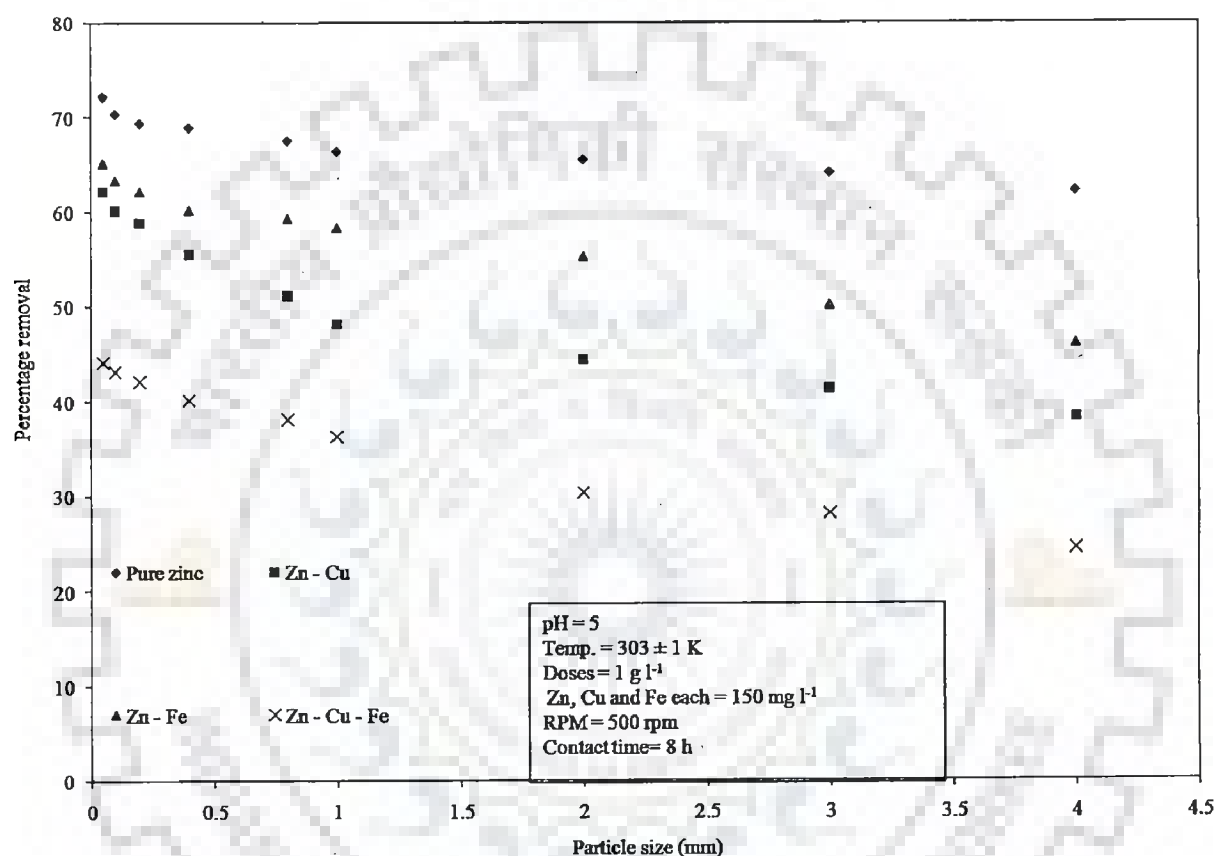


Figure 5.2.6 (m): Effect of particle size on biosorption of Zn on Eucalyptus Leaf powder

The maximum removal of Zn (II), Cu (II) and total Fe (II, III) ion in Zn (II) - Fe (II, III) – Cu (II) was 44.16%, 59.64% and 21.86%, respectively, at a particle size of 0.05 mm (figure 5.2.6 (n)). With the increase in particle size from 0.05 mm to 4 mm of biosorbent, the percentage removal of metal ions decreased.

The increase in particle size of biosorbent led to the decrease in effective surface area of the biosorbent, which resulted in lowering of removal of metal ions. The smaller is the particle size of biosorbent, larger is the effective surface area for sorption of metal ion on biosorbent particle, which results in higher percentage removal of metal ions (Dang et al., (2009), Mishra et al., (2010)). The preferential order of removal of heavy metal ions was Cu (II) > Zn (II) > Fe (II, III).

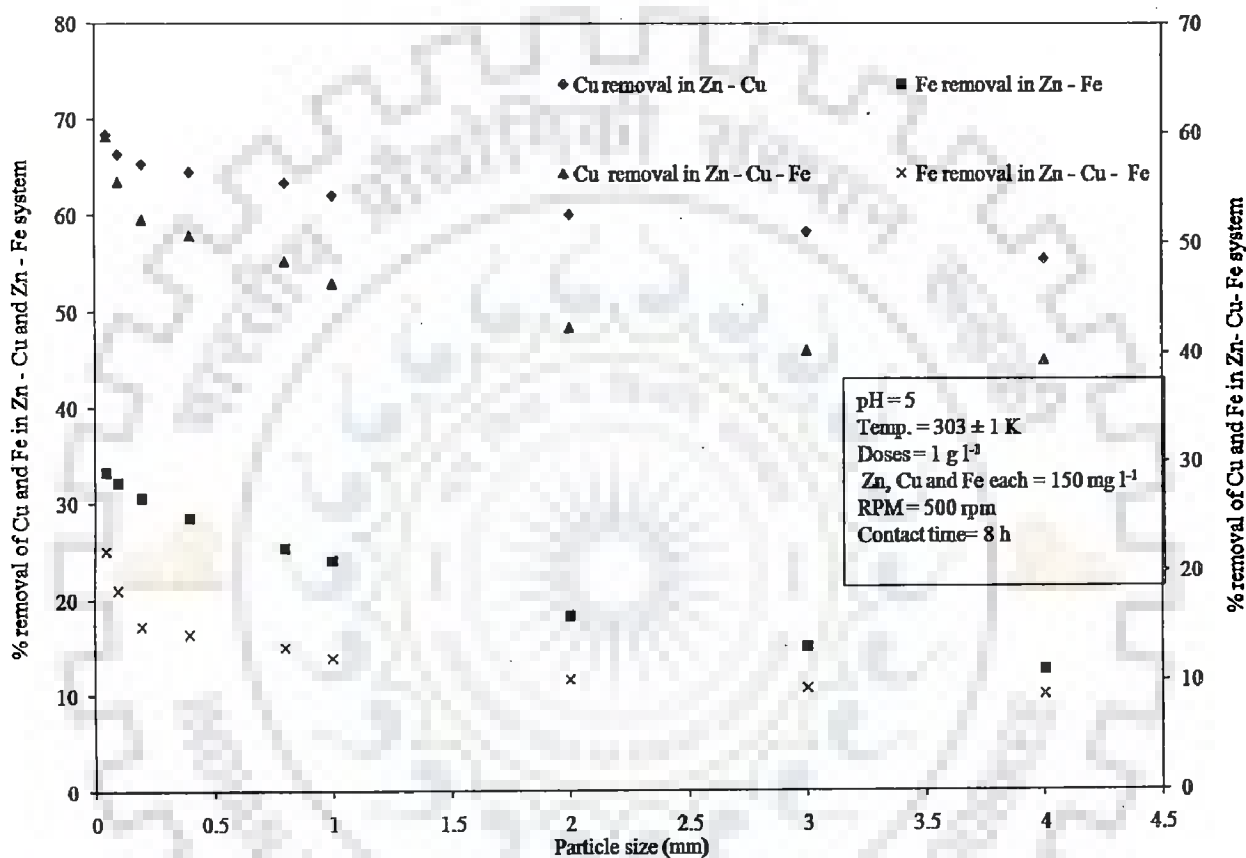


Figure 5.2.6 (n): Effect of particle size on biosorption of Cu and Fe ions in presence of Zn on Eucalyptus Leaf powder

Figure 5.2.6 (o) and figure 5.2.6 (p) represent the influence of particle size on biosorption of Zn (II), total Fe (II, III) and Cu (II) ions on Eggshell and membrane. It is clear from figure 5.2.6 (o) and figure 5.2.6 (p) that lowest particle size (0.05 mm) offered maximum percentage removal of Zn (II), Cu (II) and total Fe (II, III) ion from liquid phase. The maximum removal of Zn (II) was obtained in pure zinc phase. The maximum removal

was 42.59% at a particle size of 0.05 mm. The maximum removal of Zn (II) ion in Zn (II) - Cu (II) and Zn (II) – total Fe (II, III) was 39.36 % and 42.18%, respectively at a particle size of 0.05 mm (figure 5.2.6 (o)). The maximum removal of Cu (II) and total Fe (II, III) in Zn (II)- Cu (II) and Zn (II)- total Fe (II, III) were 65.91% and 27.57%, respectively, at a particle size of 0.05 mm.

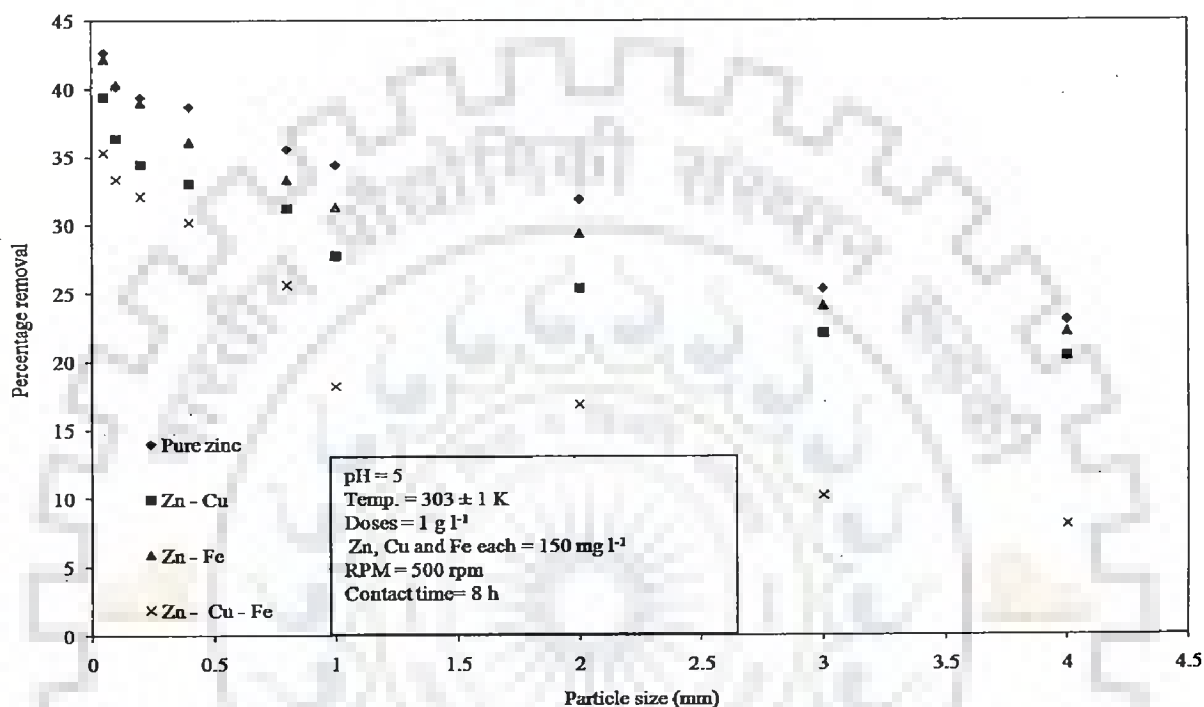


Figure 5.2.6 (o): Effect of particle size on biosorption of Zn on Eggshell and membrane

The maximum removal of Zn (II), Cu (II) and total Fe (II, III) ion in Zn (II) - Fe (II, III) – Cu (II) was 35.31%, 48.97% and 24.51%, respectively, at a particle size of 0.5 mm (figure 5.2.6 (p)). With the increase in particle size from 0.05 mm to 4 mm of biosorbent, the percentage removal of metal ions decreased. The increase in particle size of biosorbent led to the decrease in effective surface area of the biosorbent, which resulted in lowering of removal of metal ions. The smaller is the particle size of biosorbent, larger is the effective surface area for sorption of metal ion on biosorbent particle, which results in higher percentage removal of

metal ions (Dang et al., 2009, Mishra et al., 2010). The preferential order of removal of heavy metal ions was Cu (II) > Zn (II) > Fe (II, III).

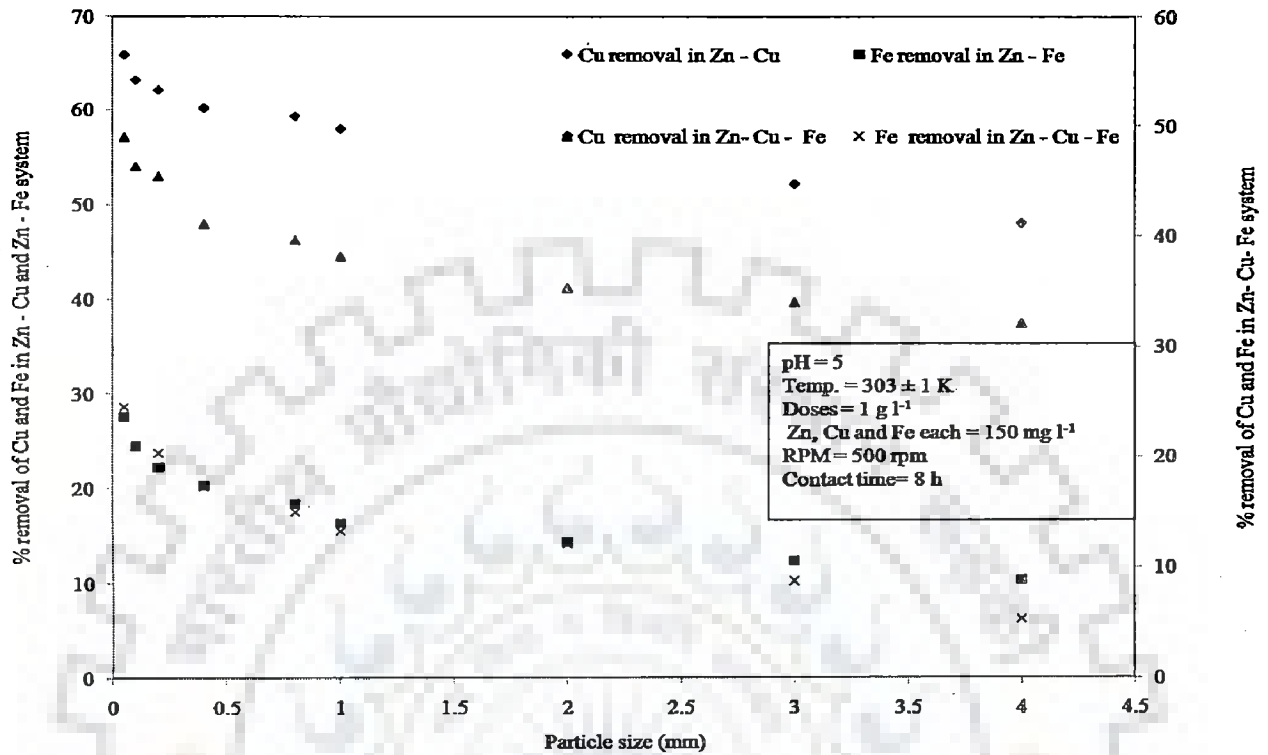


Figure 5.2.6 (p): Effect of particle size on biosorption of total Cu and Fe in presence of Zn on Eggshell and membrane

### Concluding remarks of section 5.2.6

Among all the selected biosorbents in the present investigation, the most suitable biosorbent and particle size were *Cedrus deodara* sawdust and 0.05 mm, respectively. The maximum removal of Zn (II) ion reported in case of Zn (II)- Fe (II, II)- Cu (II) was 48.13%. However, in case of all the biosorbents, the minimum particle size 0.05 mm offered the maximum removal of Zn (II), Cu(II) and Fe (II, III) ions in liquid phase. Hence, 0.05 mm of particle size was assumed as optimum particle size in the present investigation.

### 5.2.7 Optimization of contact time

This section embodies the results of influence of contact time on biosorption of Zn(II), total Fe (II, III) and Cu (II) in liquid phase. The experiments were conducted in the range of 0.5

hour to 40 hours. Results of influence of particle size have been shown in figures 5.2.7 (a) to 5.2.7 (r). The system of ions studied in the present work were pure zinc, Zn (II)- Cu (II), Zn (II)- Fe (II, III) and Zn (II) – Cu (II) - Fe (II, III). The metal ions Zn (II), Cu (II) and Fe (II, III) are referred as Zn, Cu and Fe in various figures.

Figure 5.2.7 (a) and figure 5.2.7 (b) represent the influence of contact time on biosorption of Zn (II), Cu (II) and total Fe (II, III) and ions on Mango bark sawdust.

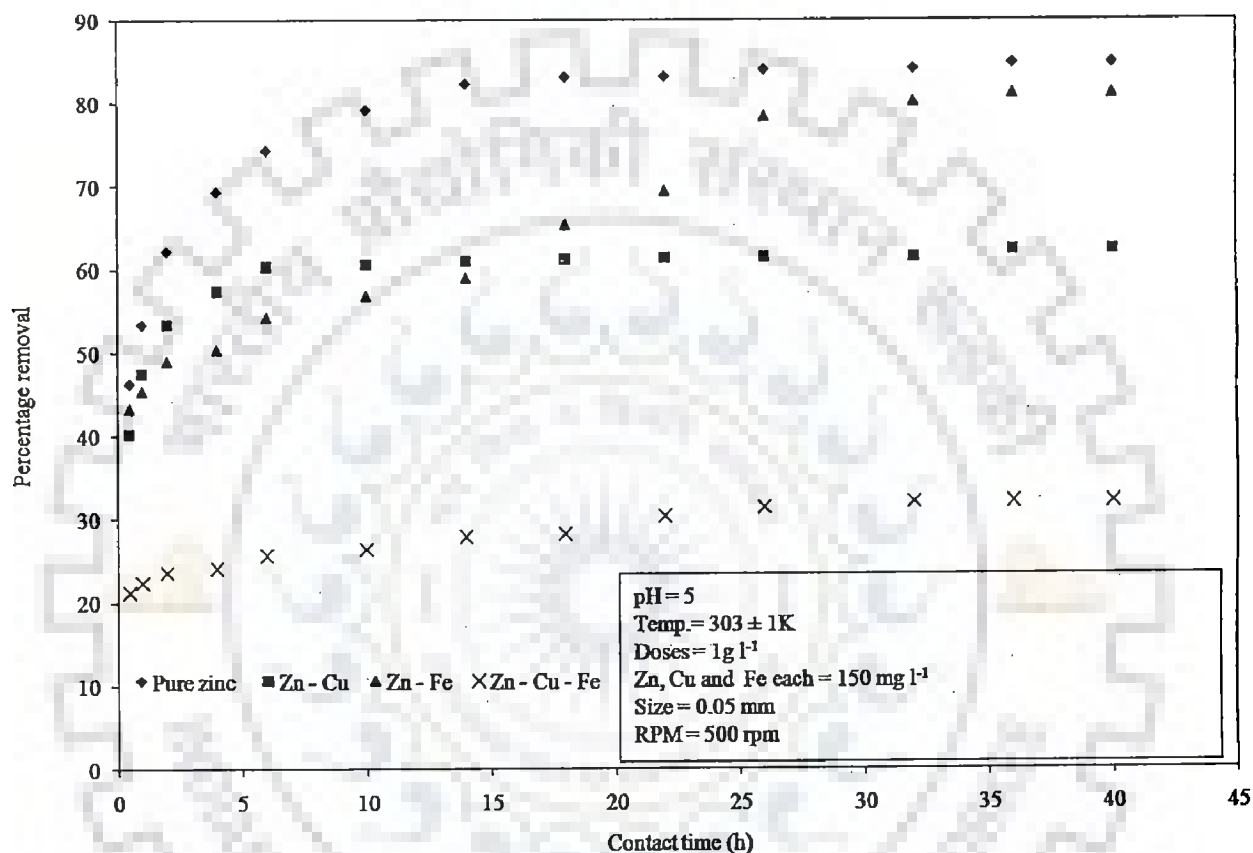


Figure 5.2.7 (a): Effect of contact time on biosorption of Zn on Mango bark sawdust

It is clear from figure 5.2.7 (a) that the maximum removal of zinc was obtained in pure zinc phase. The maximum removal of zinc obtained in pure zinc phase was 84.82%. Initially during first 6 hours the removal zinc ion from pure zinc phase was quite rapid. In Zn (II) - Cu (II), Zn (II)- total Fe (II, III) and Zn (II) – Cu (II) - Fe (II, III) system, initially during 4 hours, 2 hours and 1 hour of contact time, removal of Zn (II) was quite rapid. In another slot of contact time between 4 hours, 2 hours and 1 hour to 36 hours the removal of zinc ion was

quite slow in Zn (II) - Cu (II), Zn (II)- total Fe (II, III) and Zn (II)- Cu (II)-Fe (II, III) systems. Further, the extension in contact time from 36 hours to 40 hours did not yield any change in removal of Zn (II) ion in liquid phase.

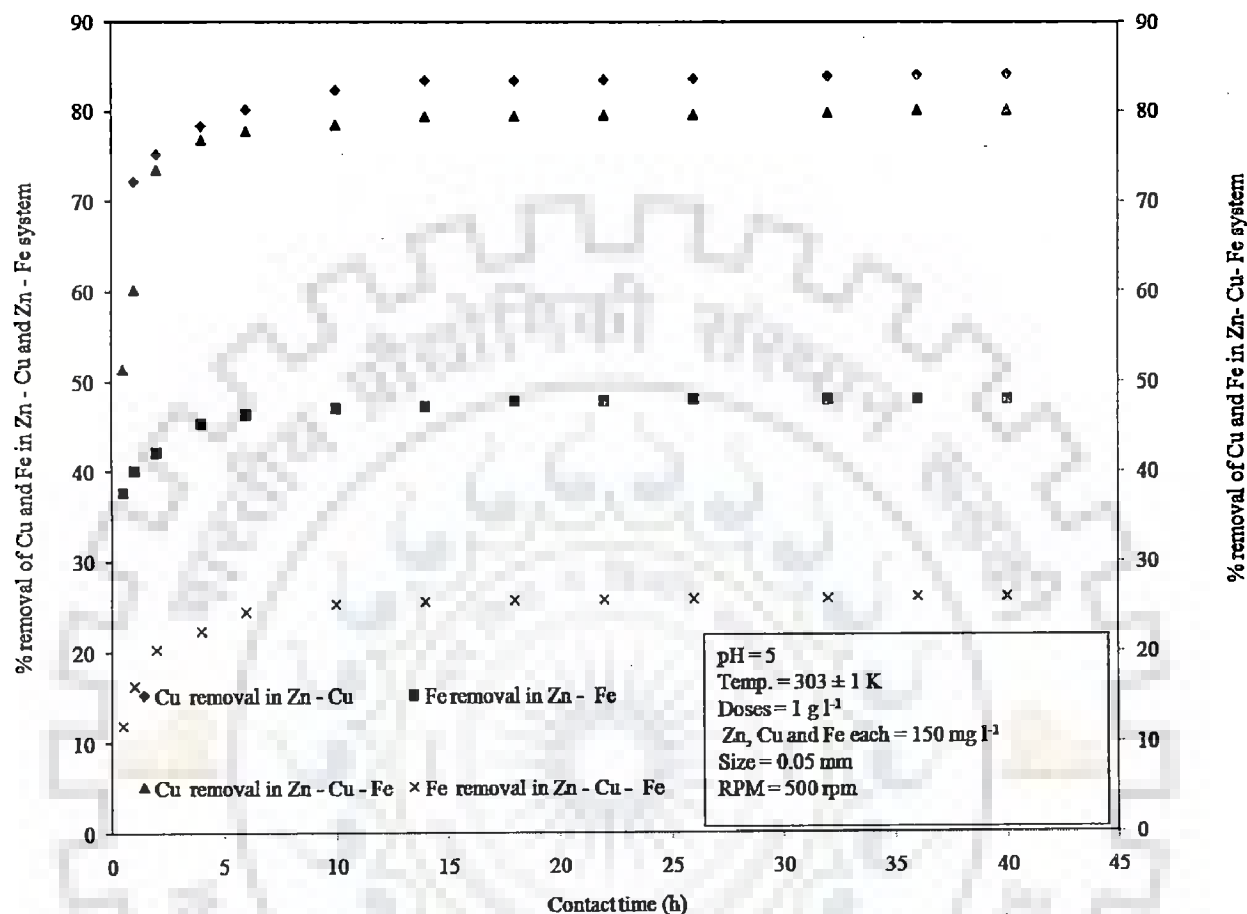


Figure 5.2.7 (b): Effect of contact time on biosorption of Cu and Fe in presence of Zn on Mango bark sawdust

However in figure 5.2.7 (b), the removal of Cu (II) and total Fe (II, III) ion in Zn (II) - Cu (II), Zn (II)- total Fe (II, III) and Zn (II)- Cu (II) - Fe (II, III) metal ion system was quite rapid upto first 4 hours. Further, extension in contact time from 4 hours to 36 hours, the Cu (II) and total Fe (II, III) removal of Cu (II) and total Fe (II, III) ions approached equilibrium. Further, extension in contact time from 36 hours to 40 hours did not yield any increment in removal of Cu (II) and total Fe (II, III) ion in liquid phase. The preferential order of removal of heavy metal ions was Cu (II) > Zn (II) > Fe (II, III).

Figure 5.2.7 (c) and figure 5.2.7 (d) represent the influence of contact time on biosorption of Zn (II), Cu (II) and total Fe (II, III) ions on Orange peel.

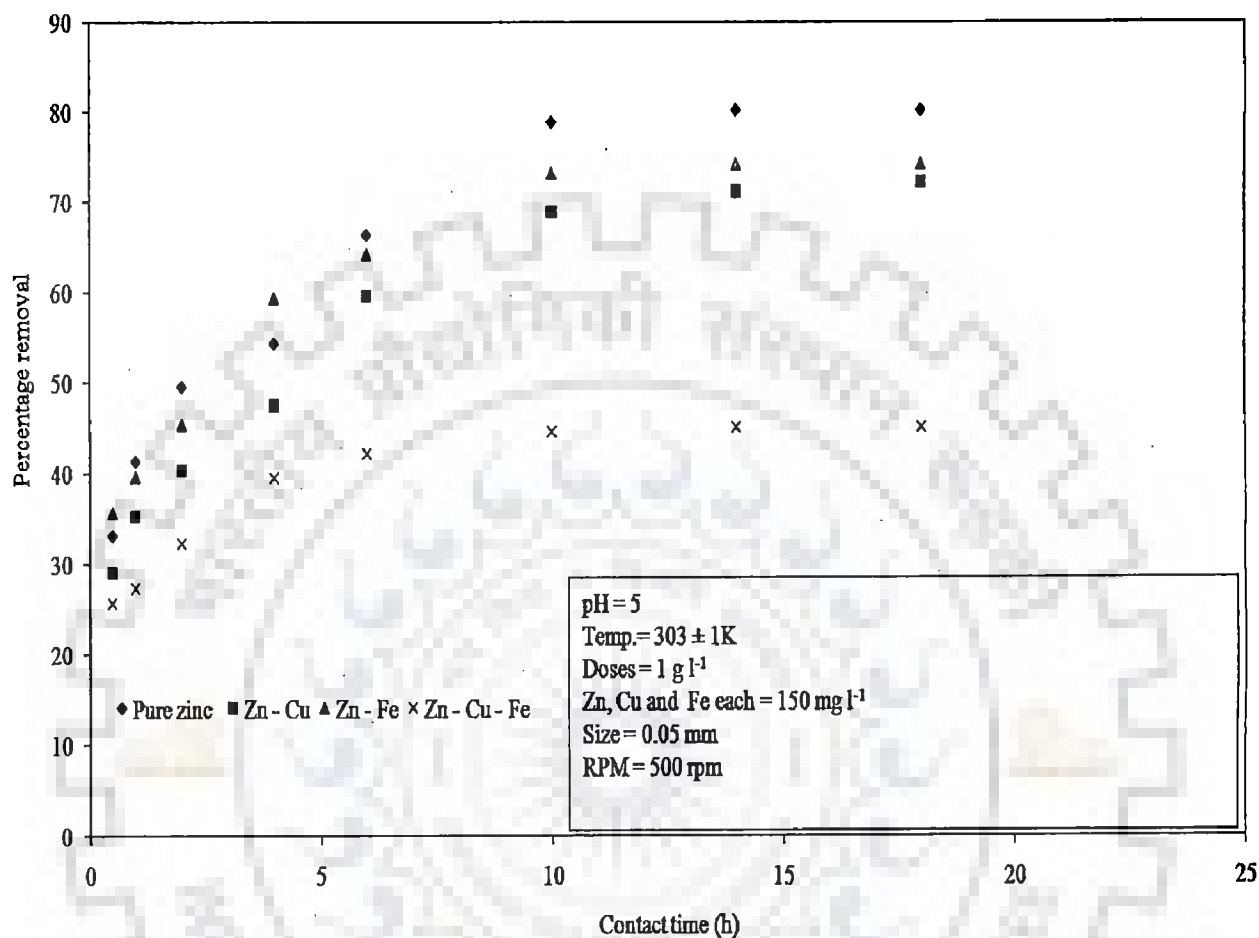


Figure 5.2.7 (c): Effect of contact time on biosorption of Zn on Orange peel.

It is clear from figure 5.2.7 (c) that the maximum removal of zinc obtained in pure zinc phase was 80.21%. Initially during first 10 hours the removal zinc ion from pure zinc phase was quite rapid. In Zn (II) - Cu (II), Zn (II)- total Fe (II, III) and Zn (II)- Cu (II)- Fe (II, III) system, initially during 10 hours, 10 hours and 4 hours of contact time, the removal of Zn (II) was quite rapid. In another slot of contact time between 10 hours, 10 hours and 4 hours to 18 hours the removal of zinc ion was quite slow in Zn (II) - Cu (II), Zn (II)- total Fe (II, III) and Zn (II)- Cu (II) - Fe (II, III) systems. Further, the extension in contact time from 14 hours to 18 hours did not yield any change in removal of Zn (II) ion in liquid phase.

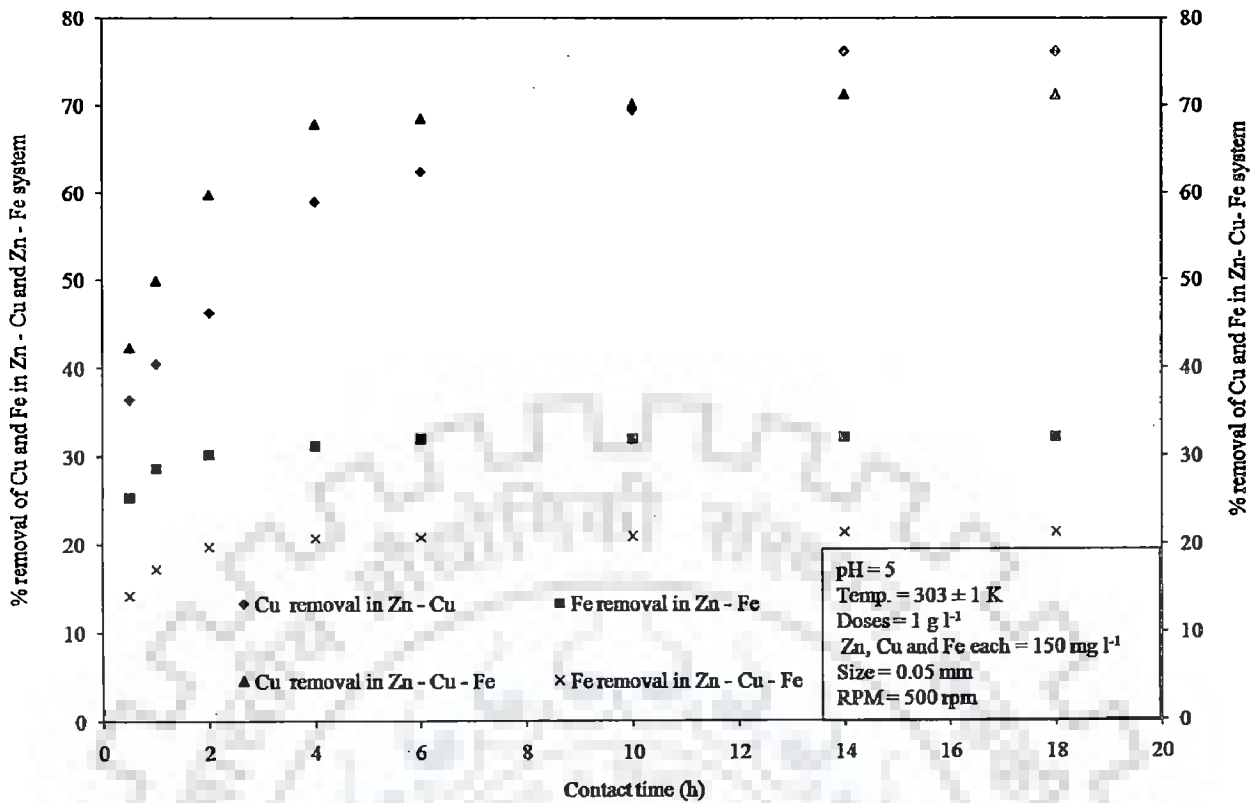


Figure 5.2.7 (d): Effect of contact time on biosorption of Cu and Fe in presence of Zn on Orange peel

However in figure 5.2.7 (d), the removal of Cu (II) and total Fe (II, III) ion in Zn (II) - Cu (II), Zn (II)- total Fe (II, III) and Zn (II)- Cu (II) - Fe (II, III) metal ion systems was quite rapid upto first 4 hours, 1 hour, 6 hours and 1 hour, respectively. Further, extension in contact time from 4 hours, 1 hour, 6 hours and 1 hour to 18 hours, the Cu (II) and total Fe (II, III) removal approached equilibrium. The preferential order of removal of heavy metal ions was Cu (II) > Zn (II) > Fe (II, III).

Figure 5.2.7 (e) and figure 5.2.7 (f) represent the influence of contact time on biosorption of Zn (II), total Fe (II, III) and Cu (II) ions on Pineapple peel.



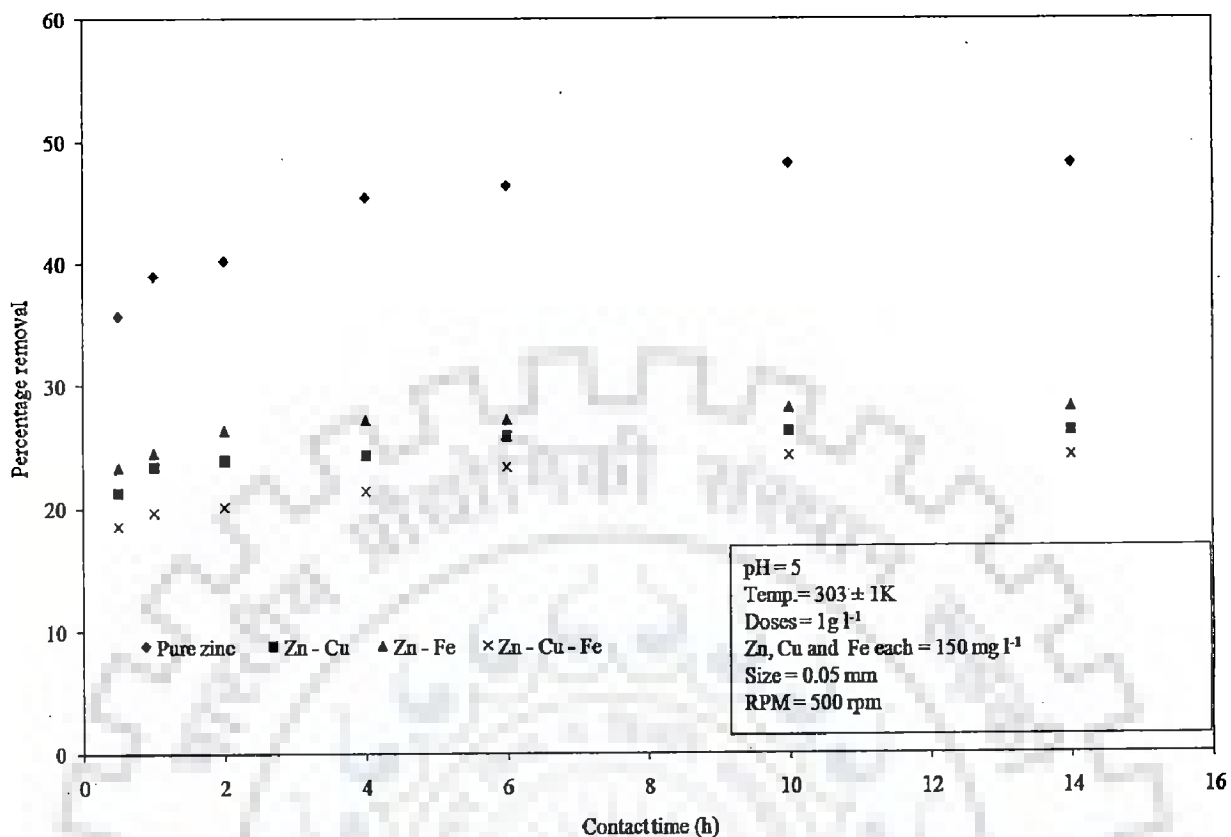


Figure 5.2.7 (e): Effect of contact time on biosorption of Zn on Pineapple peel

It is clear from figure 5.2.7 (e) that the maximum removal of zinc obtained in pure zinc phase was 48.16%. Initially during first 1 hour the removal zinc ion from pure zinc phase was quite rapid. In Zn (II) - Cu (II), Zn (II)- total Fe (II, III) and Zn (II)- Cu (II) - Fe (II, III)-system, initially during 0.5 hou of contact time, the removal of Zn (II) was quite rapid.

In another slot of contact time between 0.5 hours to 10 hours the removal of zinc ion was quite slow. Further, the extension in contact time from 10 hours to 14 hours did not yield any change in removal of Zn (II) ion in liquid phase. However in figure 5.2.7 (f), the removal of Cu (II) and total Fe (II, III) ion in Zn (II) - Cu (II), Zn (II)- total Fe (II, III) and Zn (II)- Cu (II) - Fe (II, III) metal ion system was quite rapid upto first 0.5 hours.

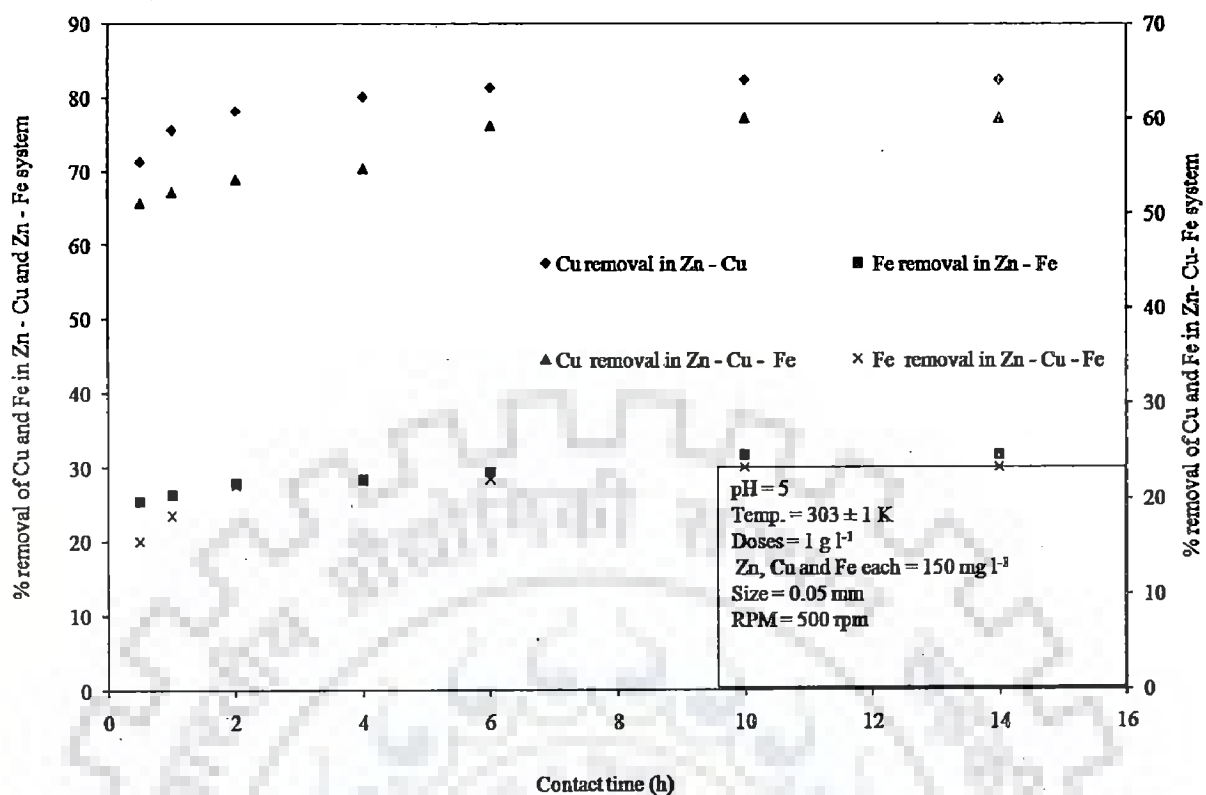


Figure 5.2.7 (f): Effect of contact time on biosorption of Cu and Fe in presence of Zn on Pineapple peel

Further, extension in contact time from 0.5 hours to 14 hours, the Cu (II) and total Fe (II, III) removal approached equilibrium. The preferential order of removal of heavy metal ions was Cu (II) > Zn (II) > Fe (II, III).

Figure 5.2.7 (g) and figure 5.2.7 (h) represent the influence of contact time on biosorption of Zn (II), total Fe (II, III) and Cu (II) ions on Jackfruit peel. It is clear from figure 5.2.7 (g) that the maximum removal of zinc obtained in pure zinc phase was 42.11%. Initially during first 0.5 hours the removal zinc ion from pure zinc phase was quite rapid. In Zn (II) - Cu (II), Zn (II)- total Fe (II, III) and Zn (II)- Cu (II) - Fe (II, III), initially during 0.5 hours of contact time, removal of Zn (II) was quite rapid.

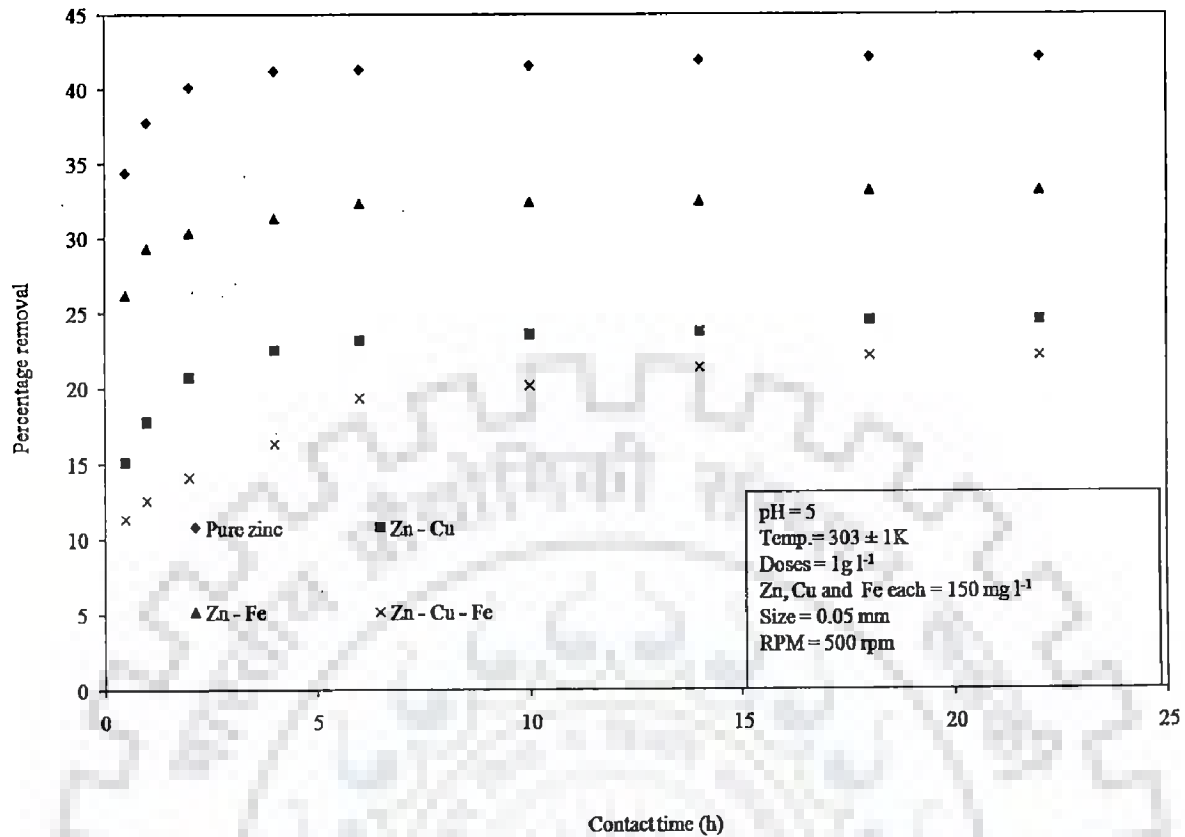


Figure 5.2.7 (g) Influence of contact time on biosorption of Zn on Jackfruit peel

In another slot of contact time between 0.5 hours to 18 hours the removal of zinc ion was quite slow. Further, the extension in contact time from 18 hours to 22 hours did not yield any change in removal of Zn (II) ion in liquid phase. However in figure 5.2.7 (h), the removal of Cu (II) and total Fe (II, III) ion in Zn (II) - Cu (II), Zn (II)- total Fe (II, III) and Zn (II)- Cu (II) - Fe (II, III) metal ion system was quite rapid upto first 0.5 hours.

Further, extension in contact time from 0.5 hours to 22 hours, the Cu (II) and total Fe (II, III) removal approached equilibrium. The preferential order of removal of heavy metal ions was Cu (II) > Zn (II) > Fe (II, III).

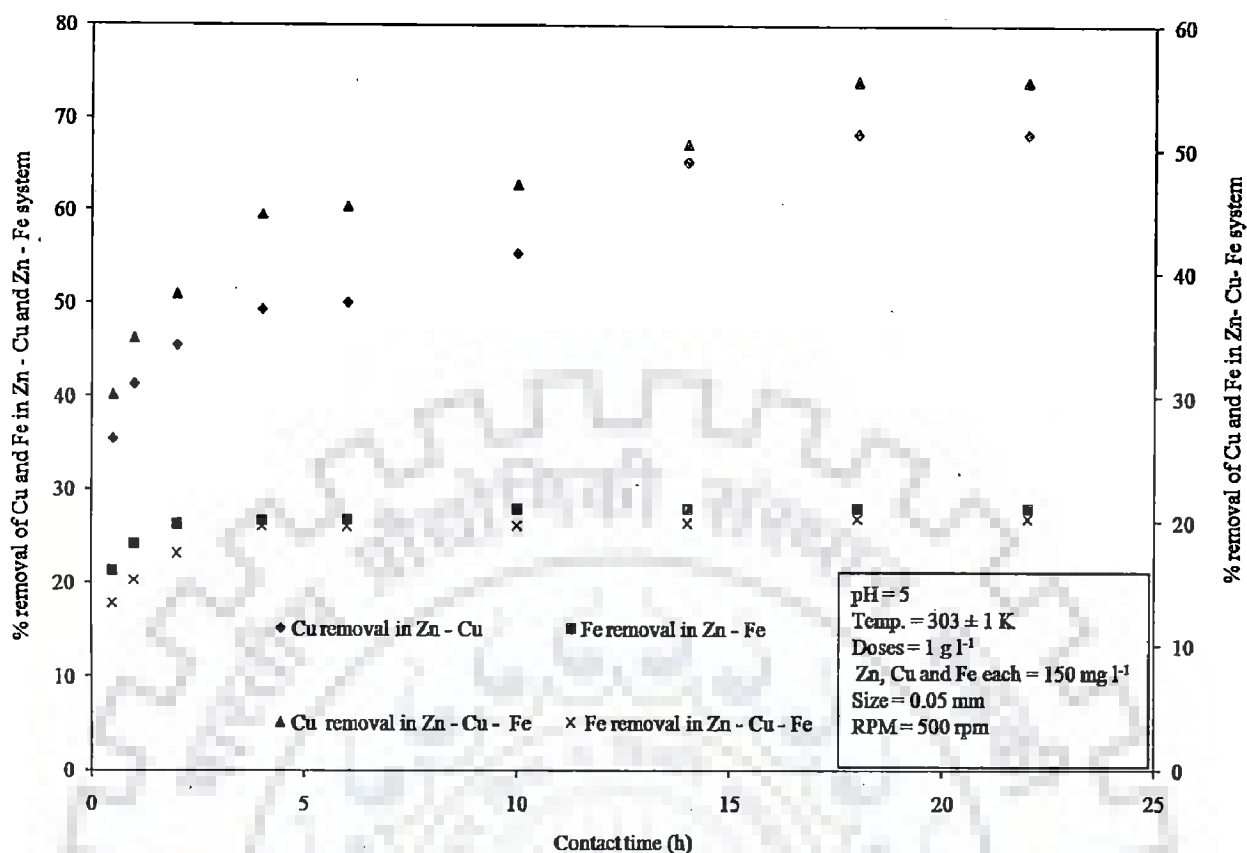


Figure 5.2.7 (h): Effect of contact time on biosorption of Cu and Fe in presence of Zn on Jackfruit peel

Figure 5.2.7 (i) and figure 5.2.7 (j) represent the influence of contact time on biosorption of Zn (II), total Fe (II, III) and Cu (II) ions on *Cedrus deodara* sawdust. It became evident from figure 5.2.7 (i) that the maximum removal of zinc obtained in pure zinc phase was 64.11%. Initially during first 0.5 hours the removal zinc ion from pure zinc phase was quite rapid. In Zn (II) - Cu (II), Zn (II)- total Fe (II, III) and Zn (II) - Cu (II) – Fe (II, III) systems, initially during 1 hour of contact time, removal of Zn (II) was quite rapid.

In another slot of contact time between 1 hours to 4 hours the removal of zinc ion was quite slow in Zn (II) - Cu (II), Zn (II)- total Fe (II, III) and Zn (II) – Cu (II) – Fe (II, III) systems.

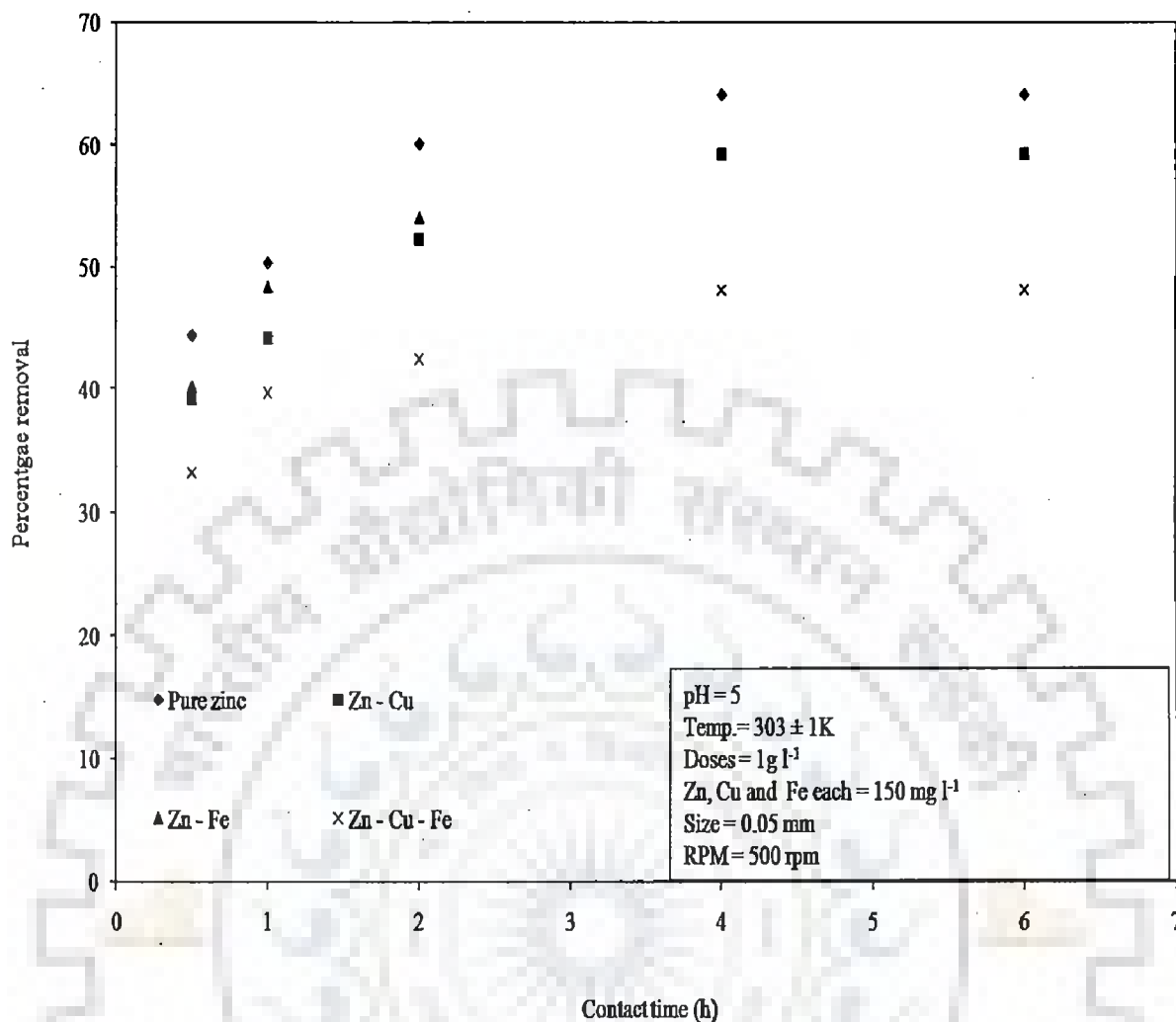


Figure 5.2.7 (i): Effect of contact time on biosorption of Zn on *Cedrus deodara* sawdust

Further, the extension in contact time from 4 hours to 6 hours did not yield any change in removal of Zn (II) ion in liquid phase Zn (II) - Cu (II), Zn (II)- total Fe (II, III) and Zn (II)- Cu (II) - Fe (II, III) systems. However in figure 5.2.7 (j), the removal of Cu (II) and total Fe (II, III) ion in Zn (II) - Cu (II), Zn (II)- total Fe (II, III) and Zn (II)- Cu (II) - Fe (II, III) metal ion system was quite rapid upto first 2 hours, 1 hours, 0.5 hours and 0.5 hours respectively. Further, extension in contact time from 2 hours, 1 hours, 0.5 hours and 0.5 hours to 6 hours, the Cu (II) and total Fe (II, III) removal approached equilibrium. The preferential order of removal of heavy metal ions was Cu (II) > Zn (II) > Fe (II, III).

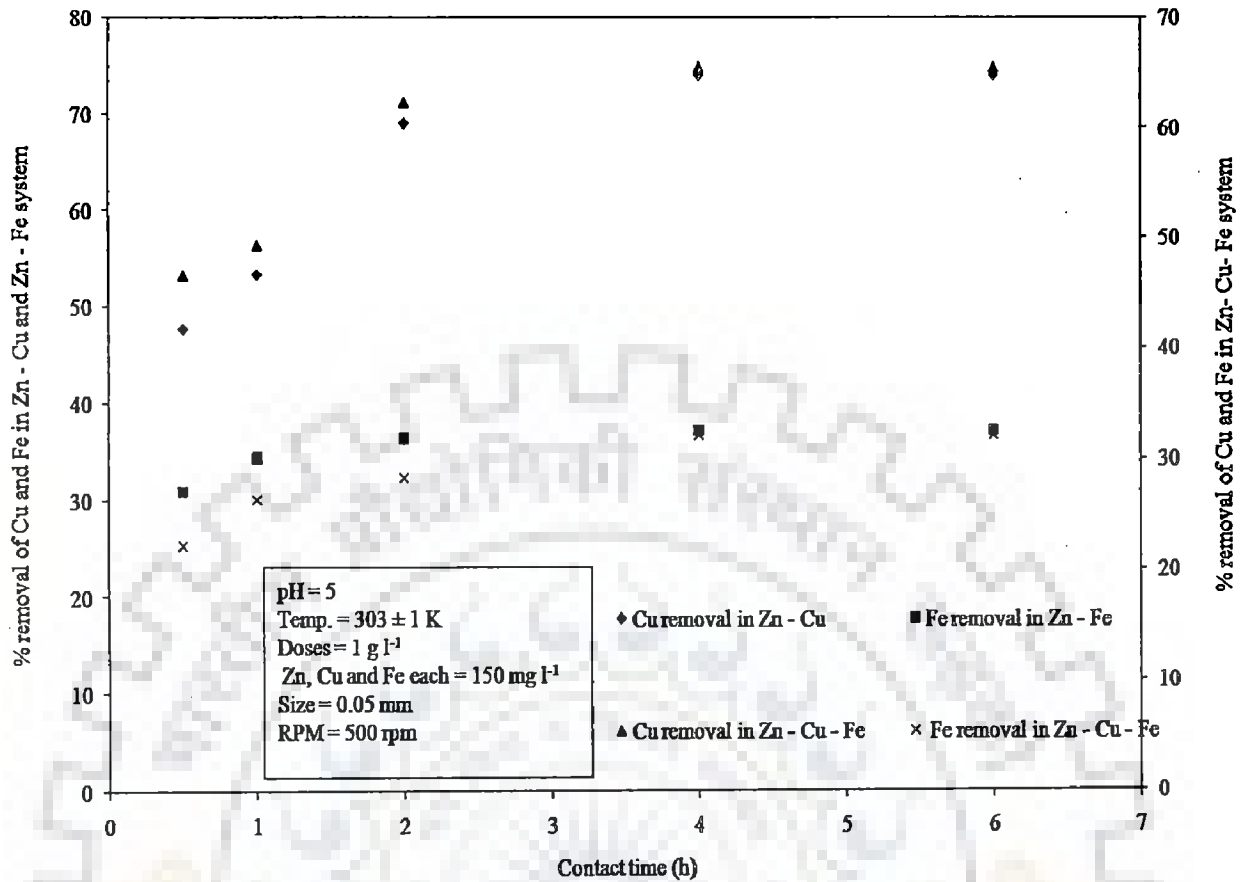


Figure 5.2.7 (j): Effect of contact time on biosorption of Cu and Fe in presence of Zn on *Cedrus deodara* sawdust

Figure 5.2.7 (k) and figure 5.2.7 (l) represent the influence of contact time on biosorption of Zn (II), total Fe (II, III) and Cu (II) ions on Eucalyptus bark sawdust. It is clear from figure 5.2.7 (k) that the maximum removal of zinc obtained in pure zinc phase was 71.33%. Initially during first 0.5 hours the removal zinc ion from pure zinc phase was quite rapid. In Zn (II) - Cu (II), Zn (II)- total Fe (II, III) and Zn (II)- Cu (II) - Fe (II, III) systems, initially during 0.5 hours of contact time, removal of Zn (II) was quite rapid. In another slot of contact time between 0.5 hours to 22 hours the removal of zinc ion was quite slow Zn (II) - Cu (II), Zn (II)- total Fe (II, III) and Zn (II)- Cu (II) - Fe (II, III) systems.

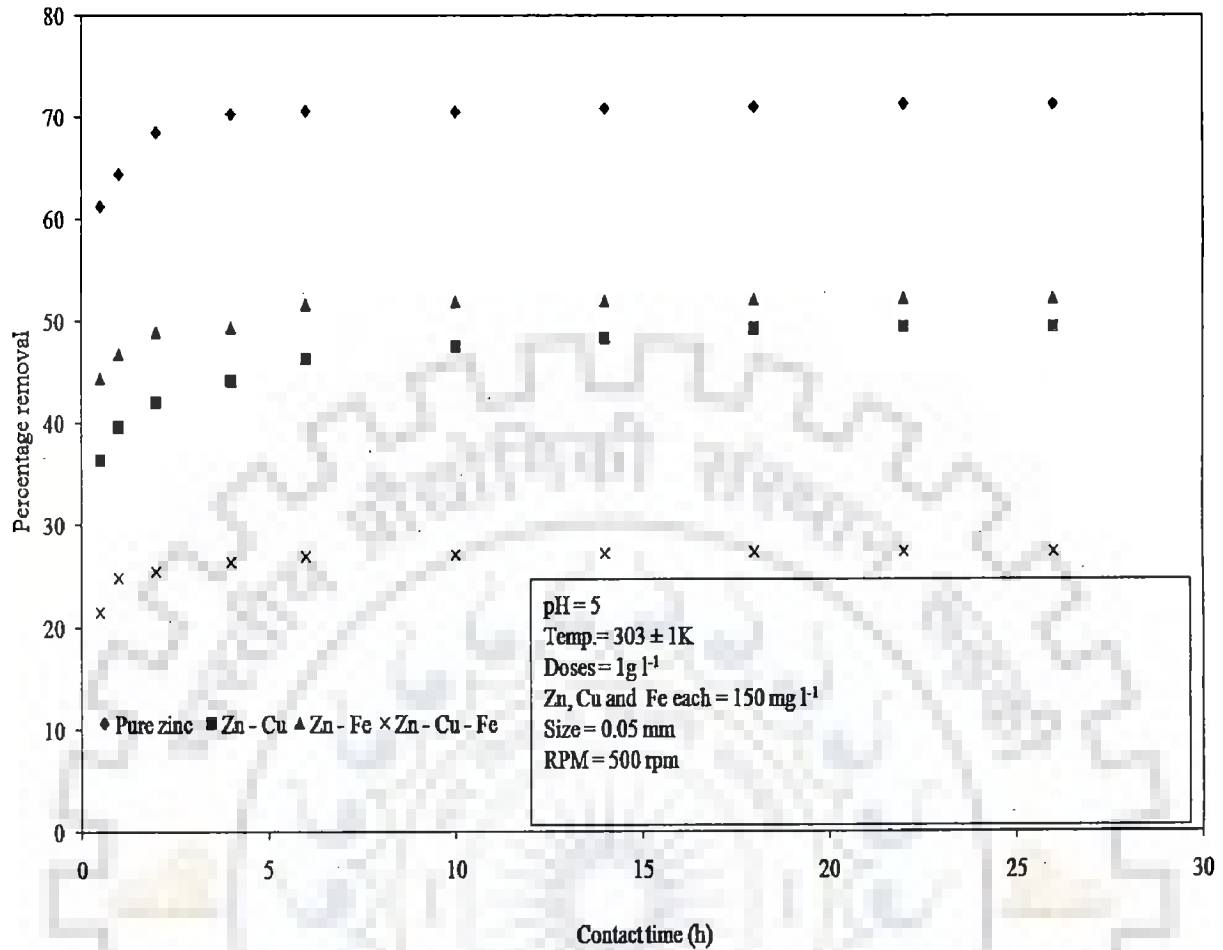


Figure 5.2.7 (k): Effect of contact time on biosorption of Zn on Eucalyptus bark sawdust

Further, the extension in contact time from 22 hours to 26 hours did not yield any change in removal of Zn (II) ion in liquid phase. However in figure 5.2.7 (l), the removal of Cu (II) and total Fe (II, III) ion in Zn (II) - Cu (II), Zn (II)- total Fe (II, III) and Zn (II)- Cu (II) - Fe (II, III) metal ion systems was quite rapid upto first 0.5 hours.

Further, extension in contact time from 0.5 hours to 26 hours, the Cu (II) and total Fe (II, III) removal approached equilibrium. The preferential order of removal of heavy metal ions was Cu (II) > Zn (II) > Fe (II, III).

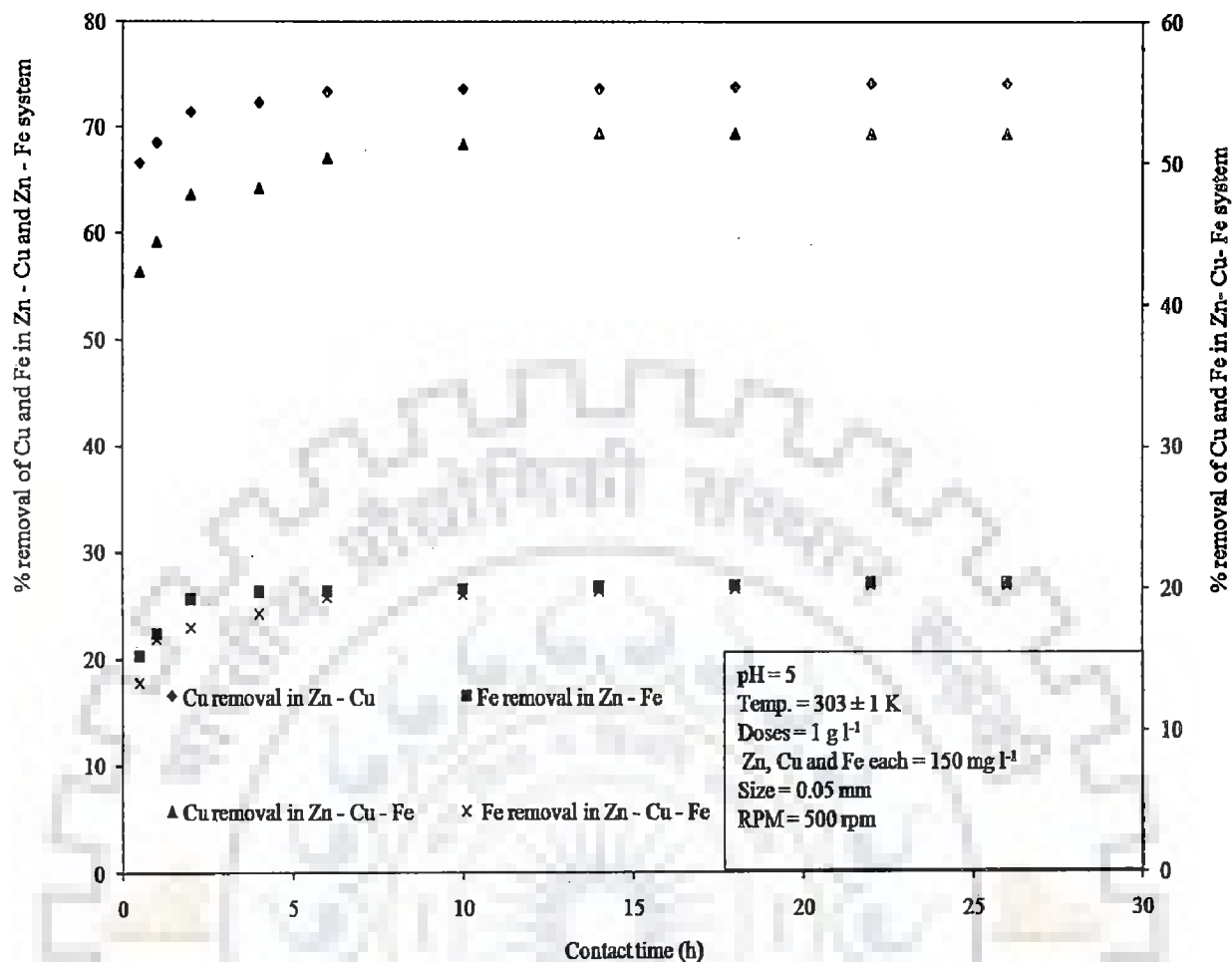


Figure 5.2.7 (l): Effect of contact time on biosorption of Cu and Fe in presence of Zn on Eucalyptus bark sawdust

Figure 5.2.7 (m) and figure 5.2.7 (n) represent the influence of contact time on biosorption of Zn (II), total Fe (II, III) and Cu (II) ions on Eucalyptus leaf powder. It became evident from figure 5.2.7 (m) that the maximum removal of zinc obtained in pure zinc phase was 72.18%. Initially during first 2 hours the removal zinc ion from pure zinc phase was quite rapid. In Zn (II) - Cu (II), Zn (II)- total Fe (II, III) and Zn (II)- Cu (II) - Fe (II, III) systems, initially during 2 hours of contact time, removal of Zn (II) was quite rapid.



In another slot of contact time between 2 hours to 14 hours the removal of zinc ion was quite slow in Zn (II) - Cu (II), Zn (II)- total Fe (II, III) and Zn (II)- Cu (II) - Fe (II, III) systems.

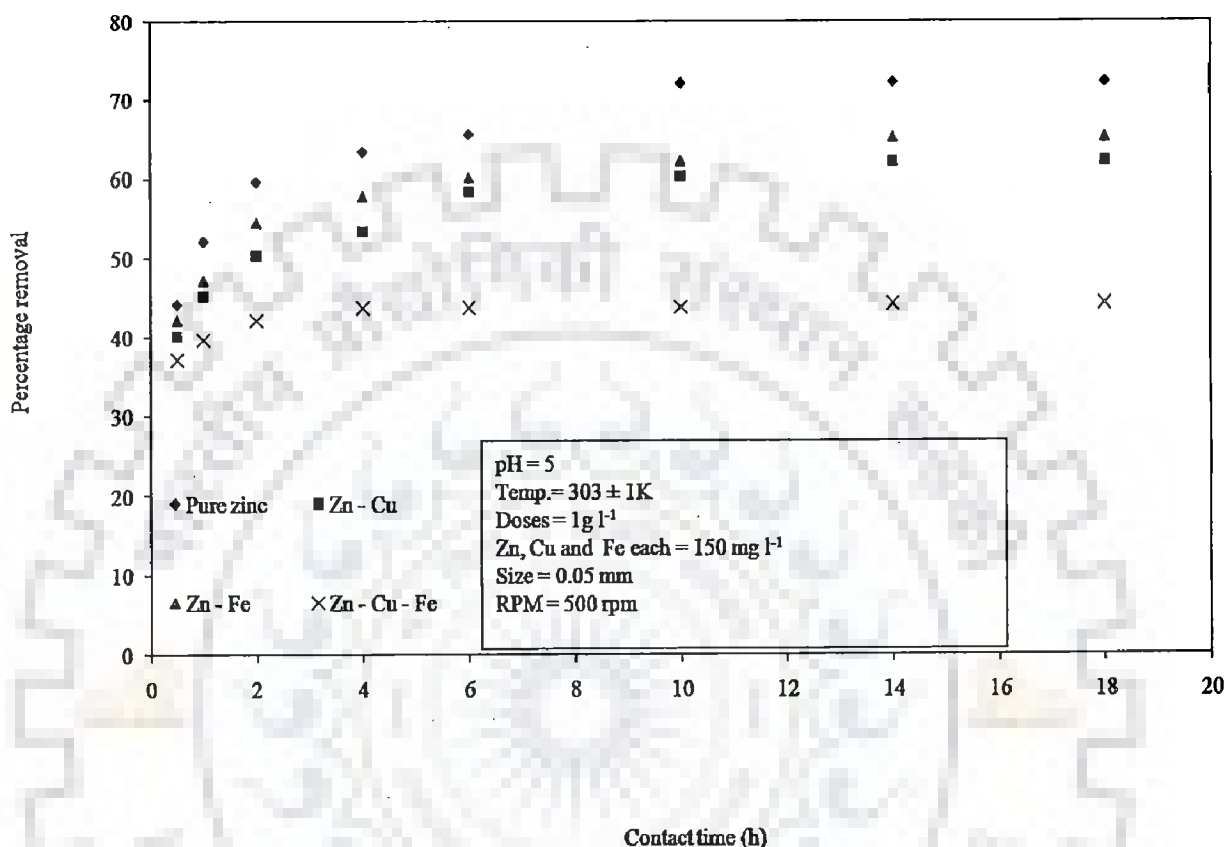


Figure 5.2.7 (m): Effect of contact time on biosorption of Zn on Eucalyptus leaf powder

Further, the extension in contact time from 14 hours to 18 hours did not yield any change in removal of Zn (II) ion in liquid phase. However in figure 5.2.7 (n), the removal of Cu (II) and total Fe (II, III) ion in Zn (II) - Cu (II), Zn (II)- total Fe (II, III) and Zn (II)- Cu (II)- Fe (II, III) metal ion systems was quite rapid upto first 0.5 hours.

Further, extension in contact time from 0.5 hours to 18 hours, the Cu (II) and total Fe (II, III) removal approached equilibrium. The preferential order of removal of heavy metal ions was Cu (II) > Zn (II) > Fe (II, III).

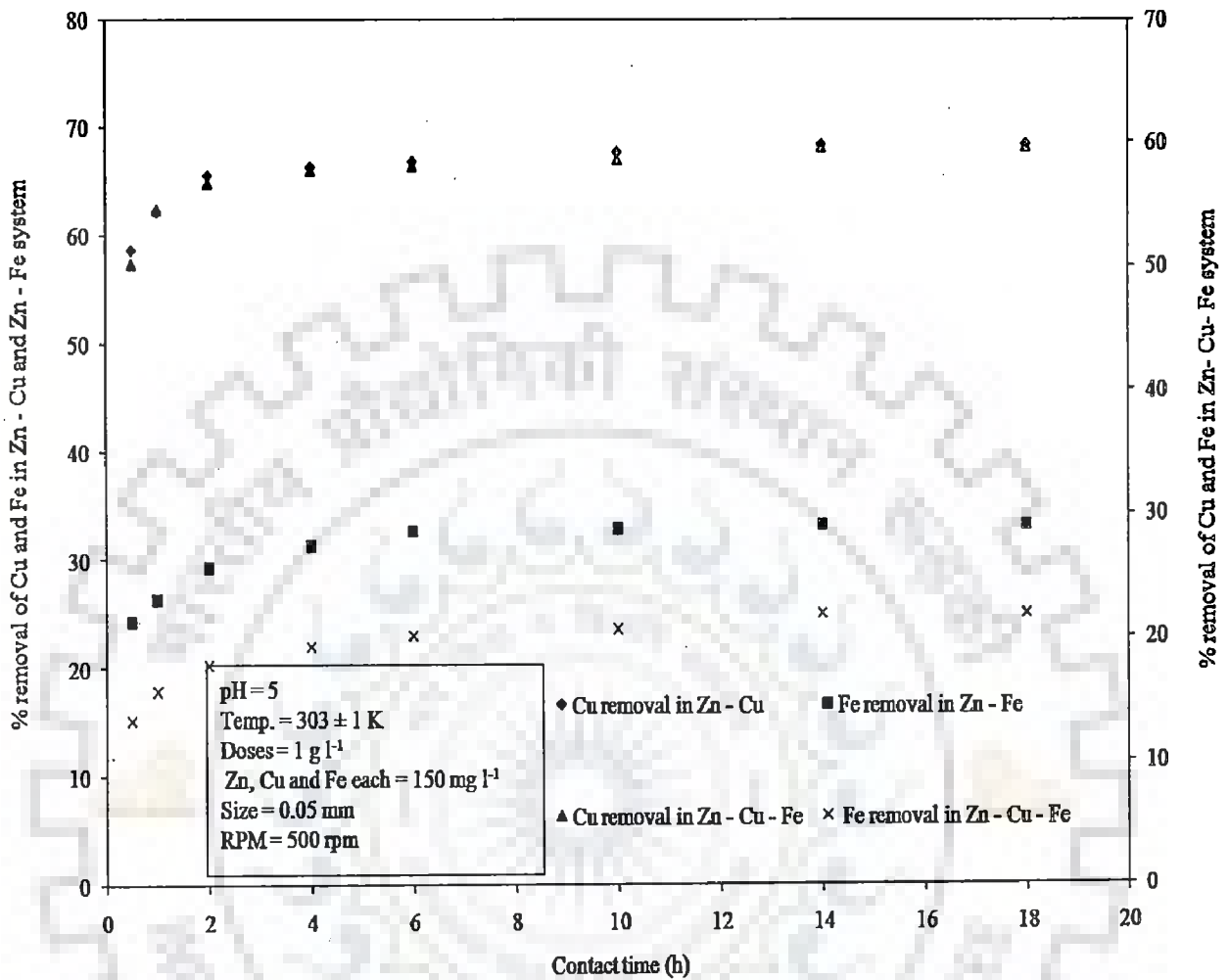


Figure 5.2.7 (n): Effect of contact time on biosorption of Cu and Fe on Eucalyptus leaf powder

Figure 5.2.7 (o) and figure 5.2.7 (p) represent the influence of contact time on biosorption of Zn (II), total Fe (II, III) and Cu (II) ions on Eggshell and membrane. It is clear from figure 5.2.7 (o) that the maximum removal of zinc obtained in pure zinc phase was 42.59%. Initially during first 1 hour the removal zinc ion from pure zinc phase was quite rapid.

In Zn (II) - Cu (II), Zn (II)- total Fe (II, III) and Zn (II)- Cu (II) - Fe (II, III)- systems, initially during 0.5 hours of contact time, removal of Zn (II) was quite rapid.

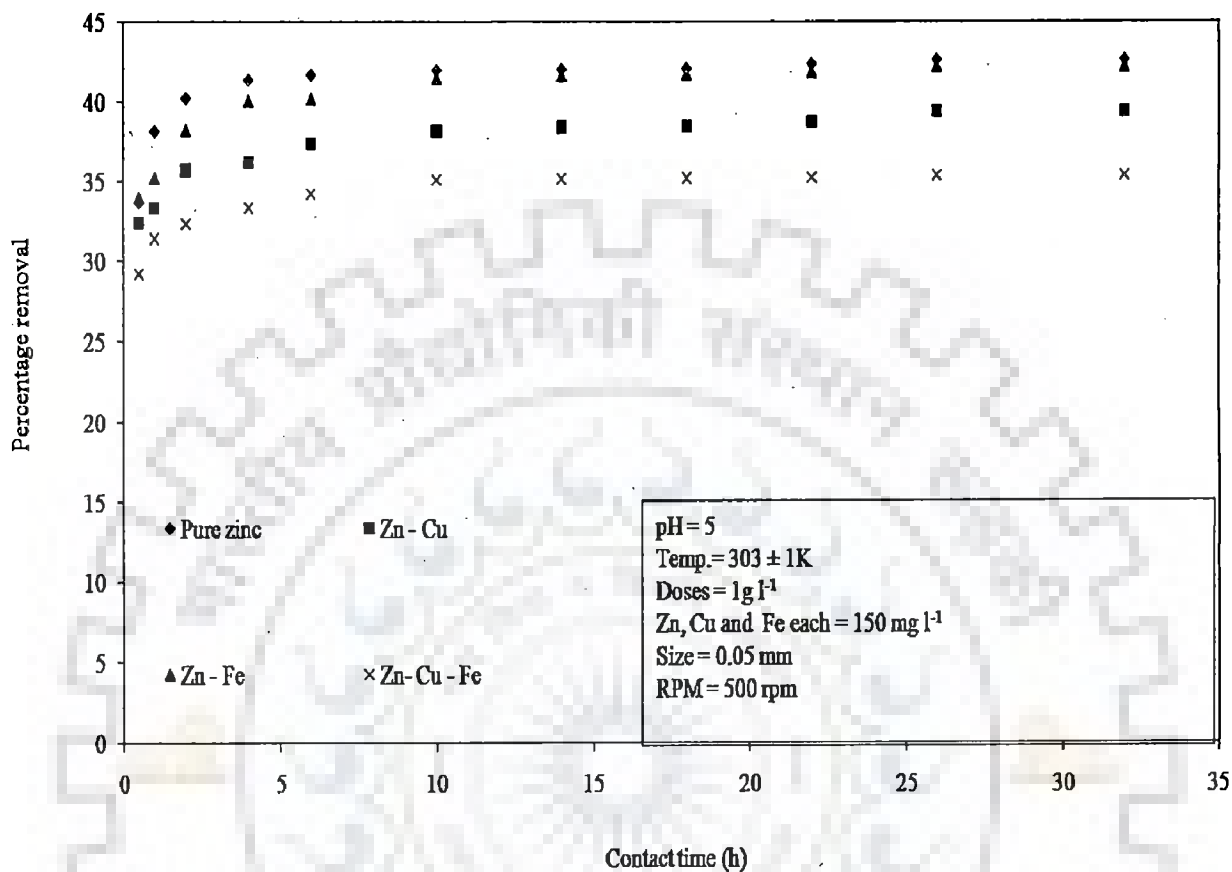


Figure 5.2.7 (o): Effect of contact time on biosorption of Zn on Eggshell and membrane

In another slot of contact time between 0.5 hours to 26 hours the removal of zinc ion was quite slow in Zn (II) - Cu (II), Zn (II)- total Fe (II, III) and Zn (II)- Cu (II) - Fe (II, III) systems. Further, the extension in contact time from 26 hours to 32 hours did not yield any change in removal of Zn (II) ion in liquid phase. However in figure 5.2.7 (p), the removal of Cu (II) and total Fe (II, III) ion in Zn (II) - Cu (II), Zn (II)- total Fe (II, III) and Zn (II)- Cu (II) - Fe (II, III)- metal ion systems was quite rapid upto first 0.5 hours.

Further, extension in contact time from 0.5 hours to 32 hours, the Cu (II) and total Fe (II, III) removal approached equilibrium. The preferential order of removal of heavy metal ions was Cu (II) > Zn (II) > Fe (II, III).

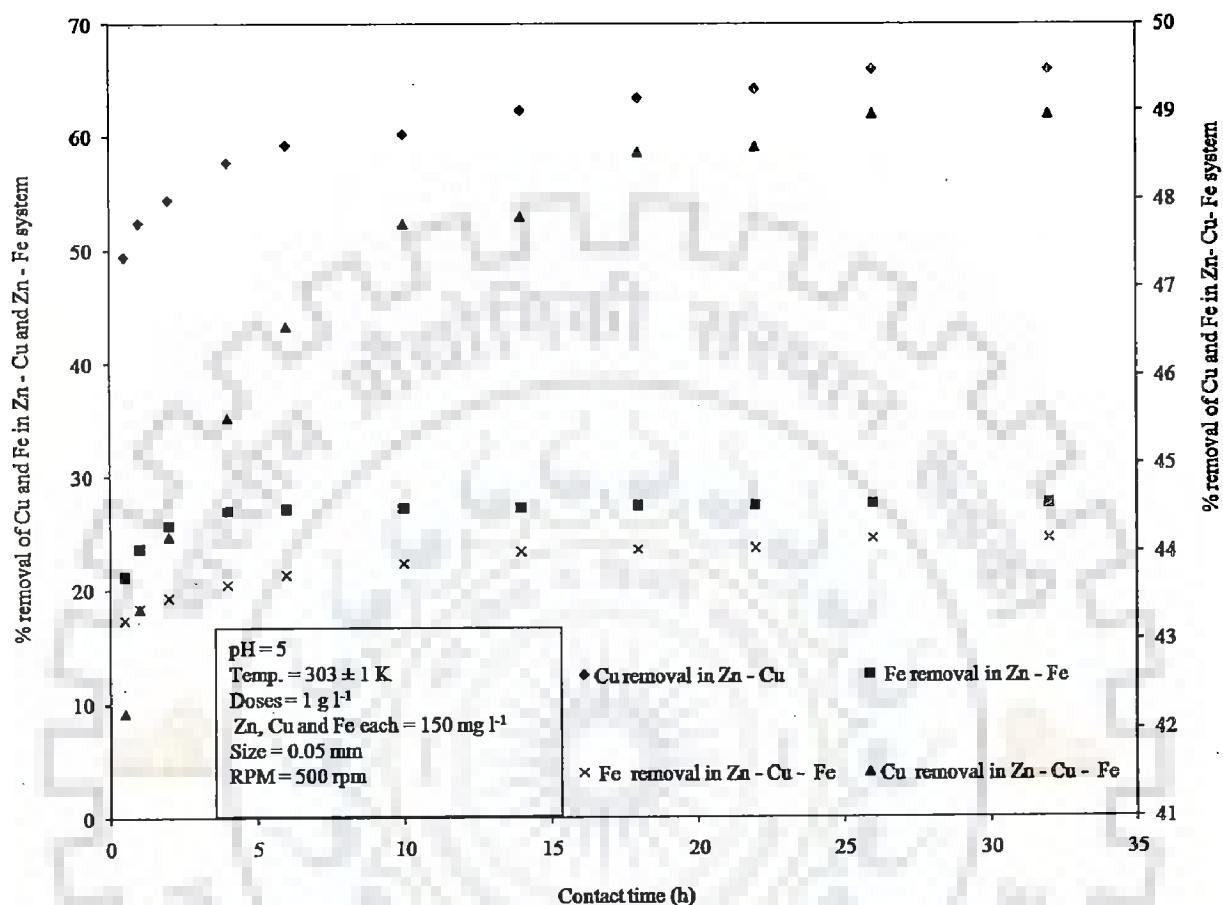


Figure 5.2.7 (p): Effect of contact time on biosorption of Cu and Fe in presence of Zn on Eggshell and membrane

Figure 5.2.7 (q) and figure 5.2.7 (r) represent the influence of contact time on biosorption of Zn (II), Cu (II) and total Fe (II, III) ions on dead cells of *Zinc sequestering bacterium VMSDCM* accession no. HQ108109. It is clear from figure 5.2.7 (q) that the maximum removal of zinc obtained in pure zinc phase was 100%. Initially during first 0.5 hour the removal zinc ion from pure zinc phase was quite rapid. In Zn (II) - Cu (II), Zn (II)-total Fe (II, III) and Zn (II)- Cu (II) - Fe (II, III) systems, initially during 0.5 hours of contact time, removal of Zn (II) was quite rapid. Zn (II)- Cu (II) - Fe (II, III) systems.

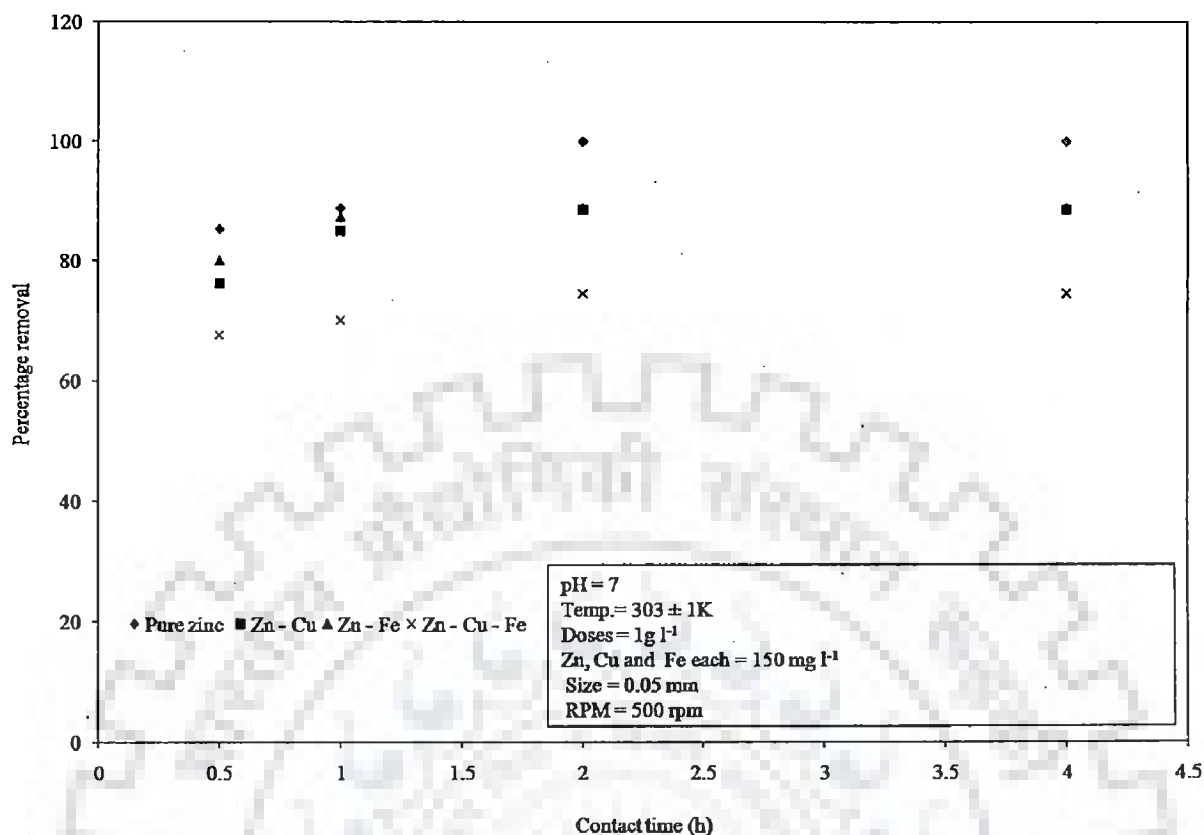


Figure 5.2.7 (q): Effect of contact time on biosorption of Zn on dead cells of *Zinc sequestering bacterium VMSDCM* accession no. HQ108109

In another slot of contact time between 0.5 hours to 2 hours the removal of zinc ion was quite slow. Further, the extension in contact time from 2 hours to 4 hours did not yield any change in removal of Zn (II) ion in liquid phase. However in figure 5.2.7 (r), the removal of Cu (II) and total Fe (II, III) ion in Zn (II) - Cu (II), Zn (II)- total Fe (II, III) and Zn (II)- Cu (II) - Fe (II, III) metal ion system was quite rapid upto first 0.5 hours.

Further, extension in contact time from 0.5 hours to 4 hours, the Cu (II) and total Fe (II, III) removal approached equilibrium. The preferential order of removal of heavy metal ions was Cu (II) > Zn (II) > Fe (II, III).

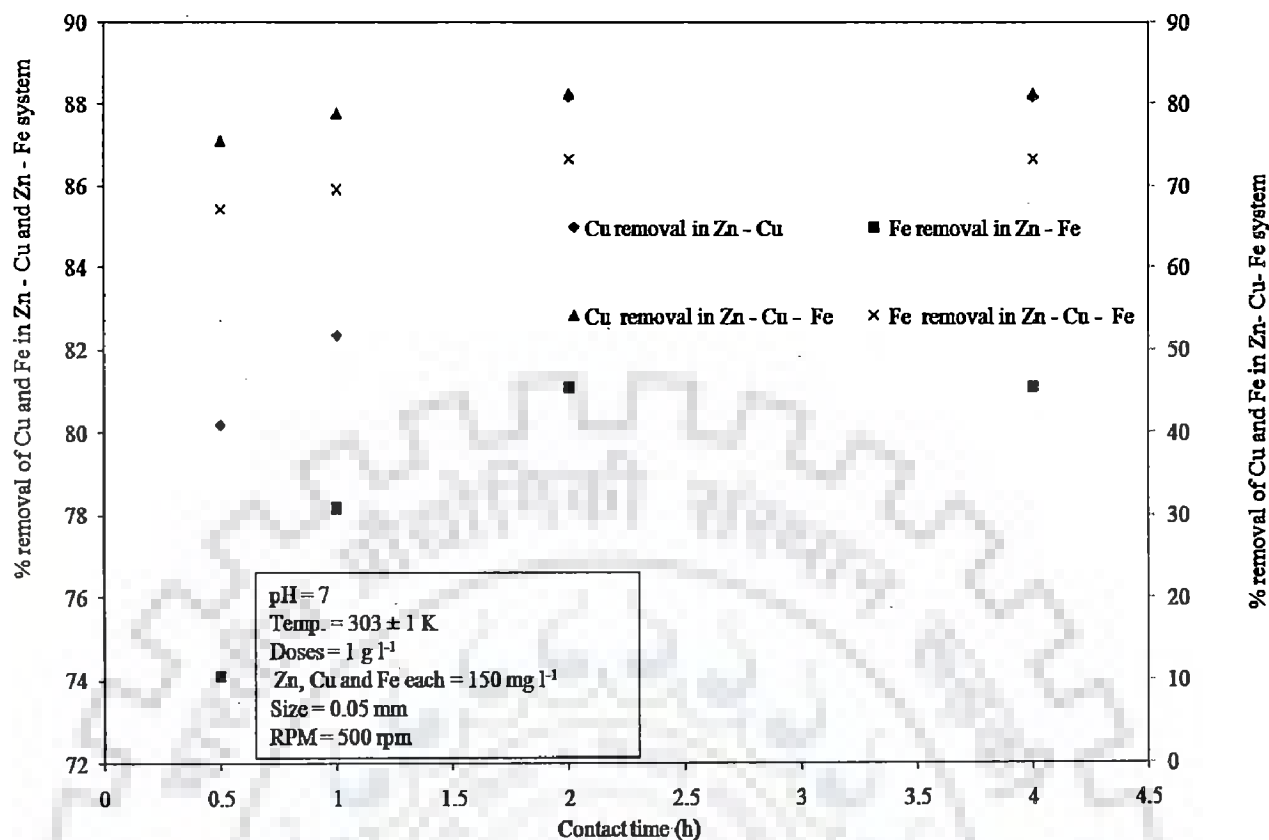


Figure 5.2.7 (r): Effect of contact time on biosorption of Cu and Fe in presence of Zn on dead cells of *Zinc sequestering bacterium VMSDCM* accession no. HQ108109

#### Concluding remark of the section 5.2.7

Among all the selected biosorbents in the present investigation, the most suitable biosorbent were *Cedrus deodara* sawdust and *Zinc sequestering bacterium VMSDCM* accession no. HQ108109. The maximum removal of Zn (II) ion reported in case of Zn (II)- Cu (II) - Fe (II, II) was obtained in 4 hours and 2 hours of contact time. This was the lowest time taken by the *Cedrus deodara* sawdust and *Zinc sequestering bacterium VMSDCM* accession no. HQ108109 among all the selected biosorbents.

The percentage removal of Zn (II) ion by *Cedrus deodara* sawdust and dead cells of *Zinc sequestering bacterium VMSDCM* accession no. HQ108109 in case of Zn (II)-Cu (II) - Fe (II, II) were 48.13% and 74.16%, respectively. These values of percentage removal of Zn

(II) ion were quite higher compared to the values reported by other biosorbents used in the present work.

### 5.2.8 Optimization of agitation rate

This section describes the results of influence of contact time on biosorption of Zn(II), total Fe (II, III) and Cu (II) in liquid phase. The experiments were conducted in range of 25 to 800 revolutions per minute. The metal ion combinations used were pure zinc, Zn (II) – Cu(II), Zn (II) – Fe (II, III) and Zn (II) – Fe (II, III)- Cu (II). Results of influence of agitation rate have been shown in figures 5.2.8 (a) to 5.2.8 (r).

Figure 5.2.8 (a) and figure 5.2.8 (b) represent the influence of agitation rate on biosorption of Zn (II), total Fe (II, III) and Cu (II) ions on Mango bark sawdust.

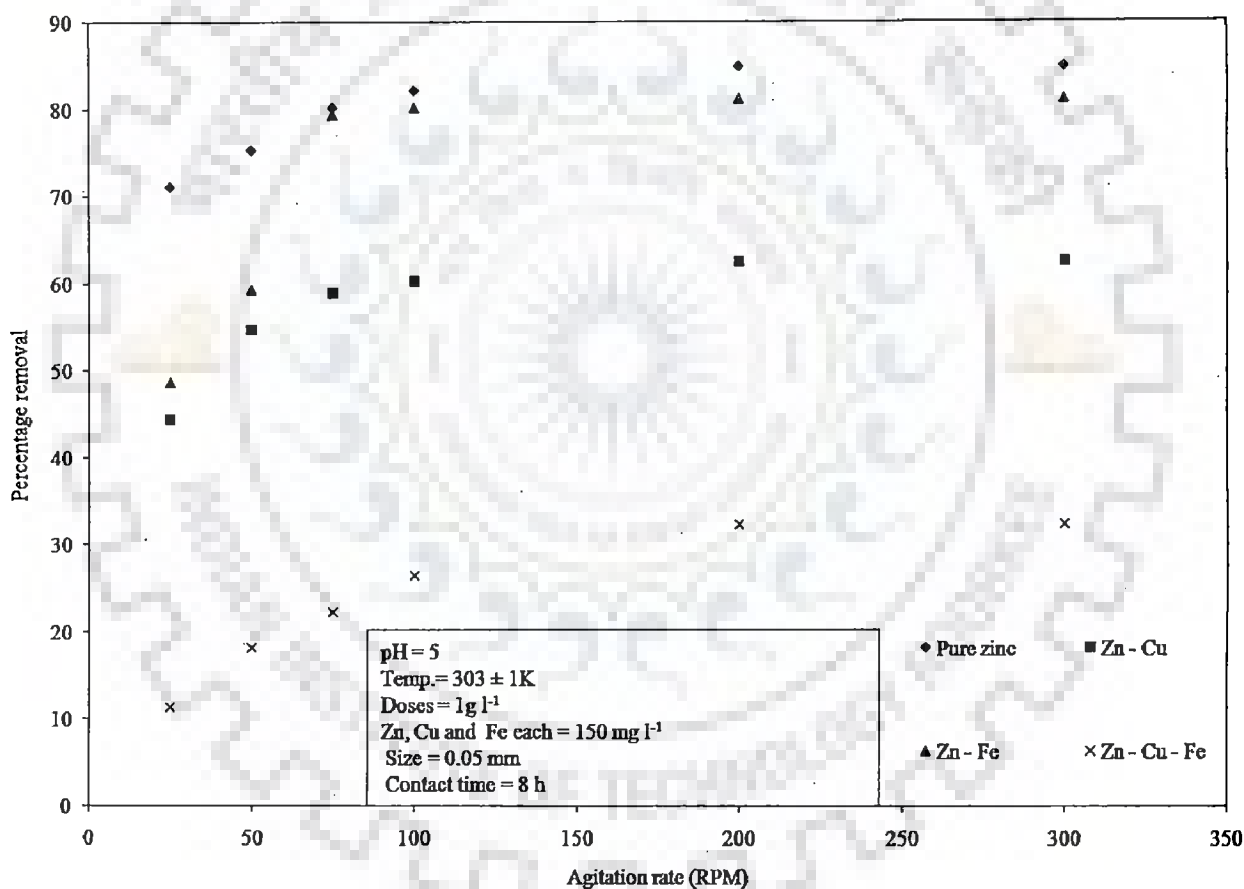


Figure 5.2.8 (a): Effect of agitation rate on biosorption of Zn on Mango bark sawdust

It is clear from figure 5.2.8 (a) that the maximum removal of zinc was obtained in pure zinc phase at 200 rpm. The maximum removal of zinc in Zn (II)- Cu (II), Zn (II) – total Fe (II, III) and Zn (II)- Cu (II)- total Fe (II, III) metal ion systems was obtained 200 rpm.

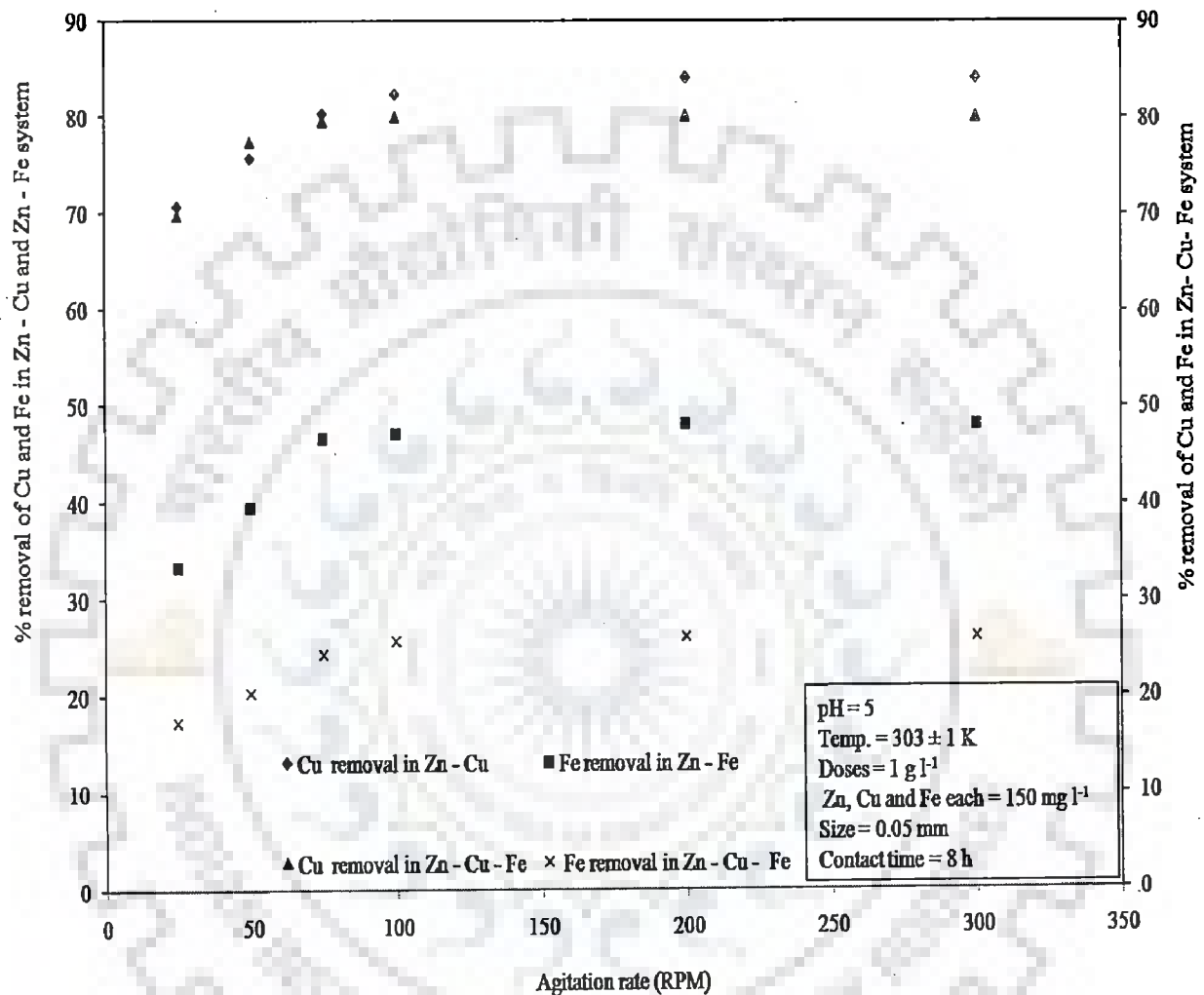


Figure 5.2.8 (b): Effect of agitation rate on biosorption of Cu and Fe in presence of Zn on Mango bark sawdust

However in figure 5.2.8 (b), the removal of Cu (II) and total Fe (II, III) ion in Zn (II)- Cu (II), Zn (II) – total Fe (II, III) and Zn (II)- Cu (II)- Fe (II, III) metal ion system was quite rapid upto 25 rpm. Between 25 rpm to 200 rpm, the removal of Zn (II) ion was quite slow. Further,



extension in agitation rate from 200 rpm to 300 rpm, the Cu (II) and total Fe (II, III) removal approached equilibrium. The maximum removal of Cu (II) and total Fe (II, III) in all the types of metal ion system was obtained at 200 rpm. Initial quite rapid removal of Zn (II), Cu (II) and total Fe (II, III) ion in liquid phase in Zn (II)- Cu (II), Zn (II) – total Fe (II, III) and Zn (II)- Cu (II)- Fe (II, III) system was due to film diffusion of Zn (II), Cu (II) and total Fe (II, III) ion at the surface of Mango bark sawdust in liquid phase at the onset of the process. However, the slowness in the removal of Zn (II), Cu (II) and total Fe (II, III) ion from liquid phase above 25 rpm was due to the rationale that at the higher agitation rate 25 rpm the intraparticle diffusion was rate governing step (Mishra et al., 2010). Figure 5.2.8 (c) and figure 5.2.8 (d) represent the influence of agitation rate on biosorption of Zn (II), total Fe (II, III) and Cu (II) ions on Orange peel.

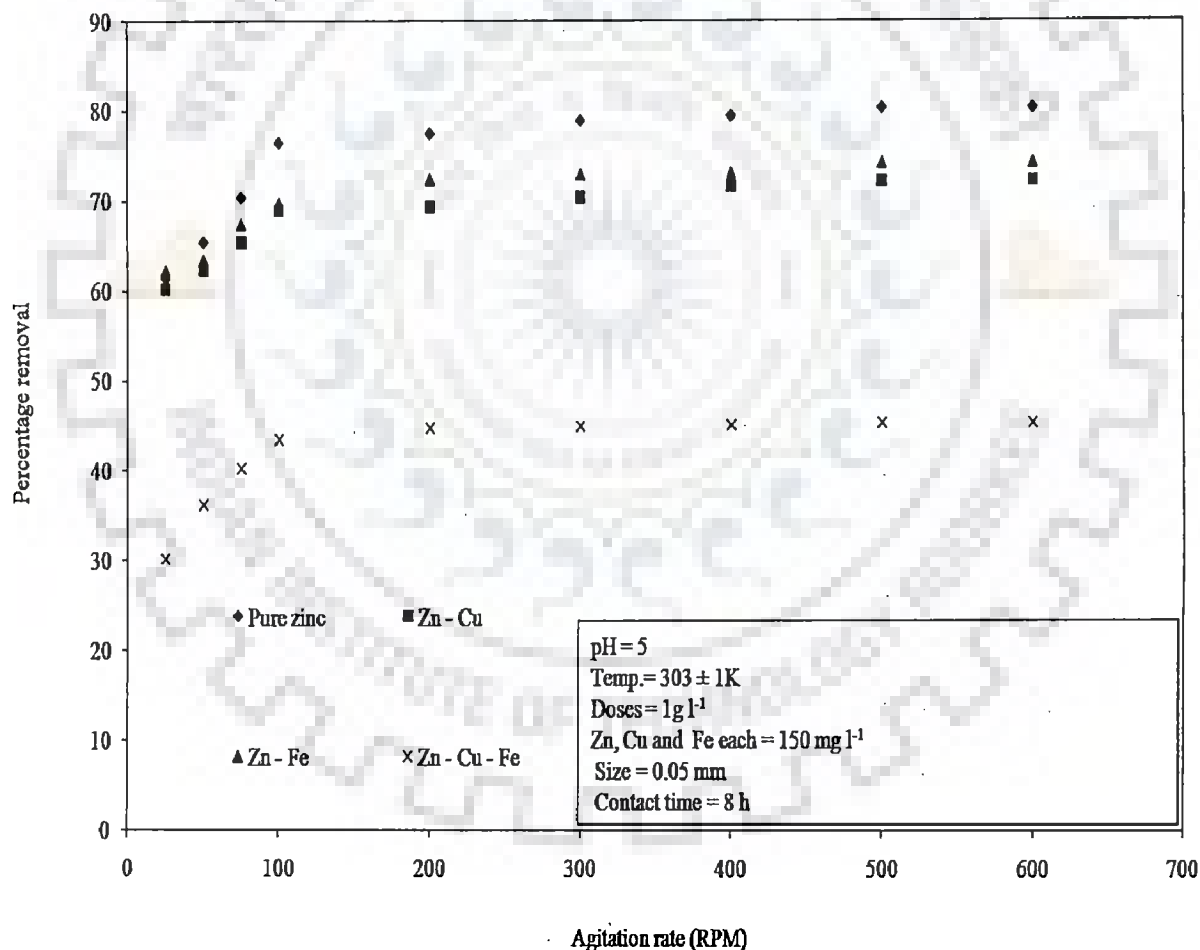


Figure 5.2.8 (c): Effect of agitation rate on biosorption of Zn on Orange peel

It is clear from figure 5.2.8 (c) that the maximum removal of zinc was obtained in pure zinc phase at 100 rpm. The maximum removal of zinc in Zn (II)- Cu (II), Zn (II) – total Fe (II, III) and Zn (II)- Cu (II)- total Fe (II, III) metal ion systems was obtained at 100 rpm. Between 100 rpm to 600 rpm, the removal of Zn (II) ion was quite slow in Zn (II)- Cu (II), Zn (II) – total Fe (II, III) and Zn (II)- Cu (II)- total Fe (II, III).

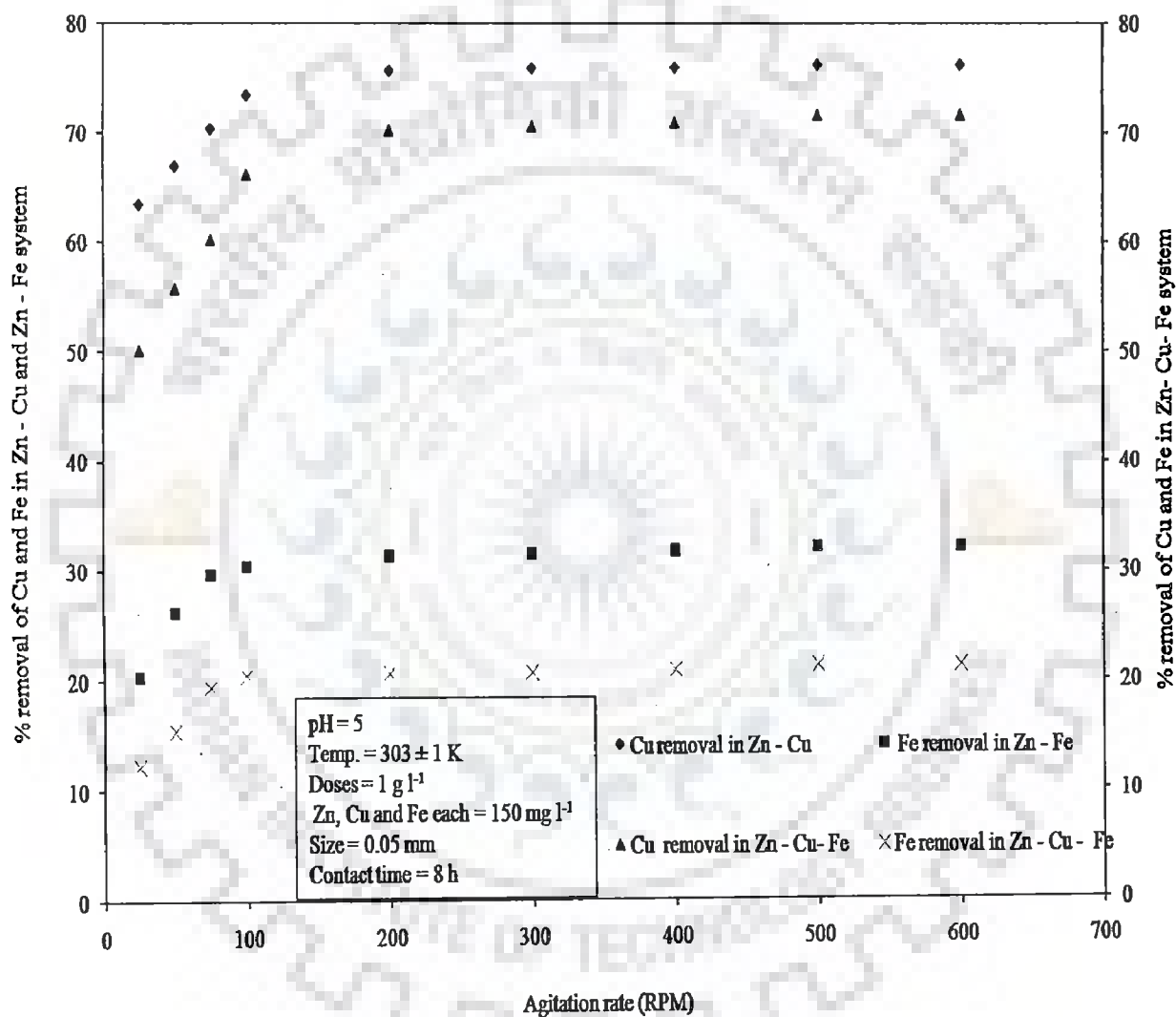


Figure 5.2.8 (d): Effect of agitation rate on biosorption of Cu and Fe in presence of Zn on Orange peel

However in figure 5.2.8 (d), the maximum removal of Cu (II) and total Fe (II, III) ion in Zn (II)- Cu (II), Zn (II) – total Fe (II, III) and Zn (II)- Cu (II)- Fe (II, III) metal ion systems was quite rapid upto 75 rpm. Further, extension in agitation rate from 75 rpm to 600 rpm, the removal of Cu (II) and total Fe (II, III) approached equilibrium. The preferential order of removal of heavy metal ions was Cu (II)> Zn (II)> Fe (II, III). Initial quite rapid removal of Zn (II), Cu (II) and total Fe (II, III) ion in liquid phase in system was due to film diffusion at the surface of Orange peel in liquid phase. However, at the later stage of the process the slowness in the removal of Zn (II), Cu (II) and total Fe (II, III) ion from liquid phase above 100 rpm was due to the rationale that at the higher agitation rate above 100 rpm the intraparticle diffusion was rate governing step (Mishra et al.,2010).

Figure 5.2.8 (e) and figure 5.2.8 (f) represent the influence of agitation rate on biosorption of Zn (II), total Fe (II, III) and Cu (II) ions on Pineapple peel.

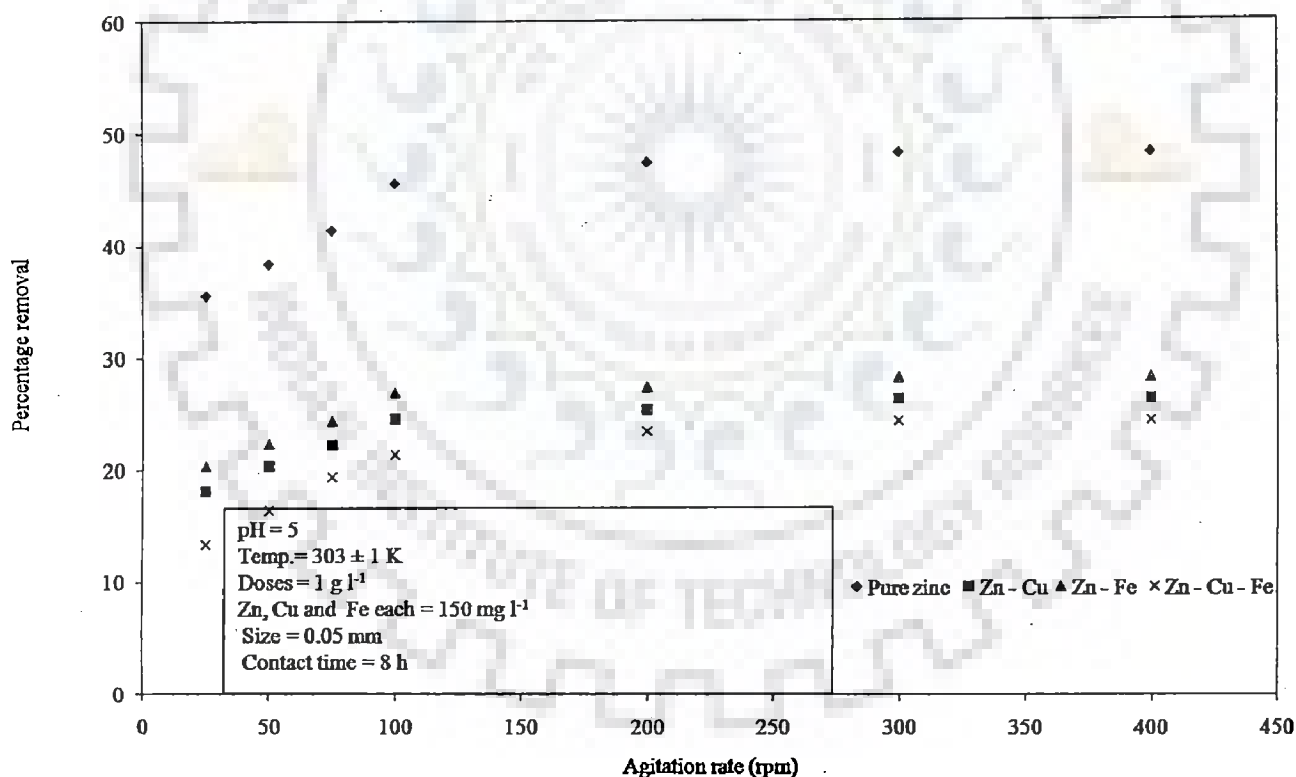


Figure 5.2.8 (e): Effect of agitation rate on biosorption of Zn on Pineapple peel

It is clear from figure 5.2.8 (e) that the maximum removal of zinc was obtained in pure zinc phase at 25 rpm. The maximum removal of zinc in Zn (II)- Cu (II), Zn (II) – total Fe (II, III) and Zn (II)- Cu (II)- total Fe (II, III) metal ion systems was obtained at 50 rpm, 25 rpm and 25 rpm,, respectively. Between 50 rpm, 25 rpm and 25 rpm to 400 rpm, the removal of Zn (II) ion was quite slow in Zn (II)- Cu (II), Zn (II) – total Fe (II, III) and Zn (II)- Cu (II)- total Fe (II, III).

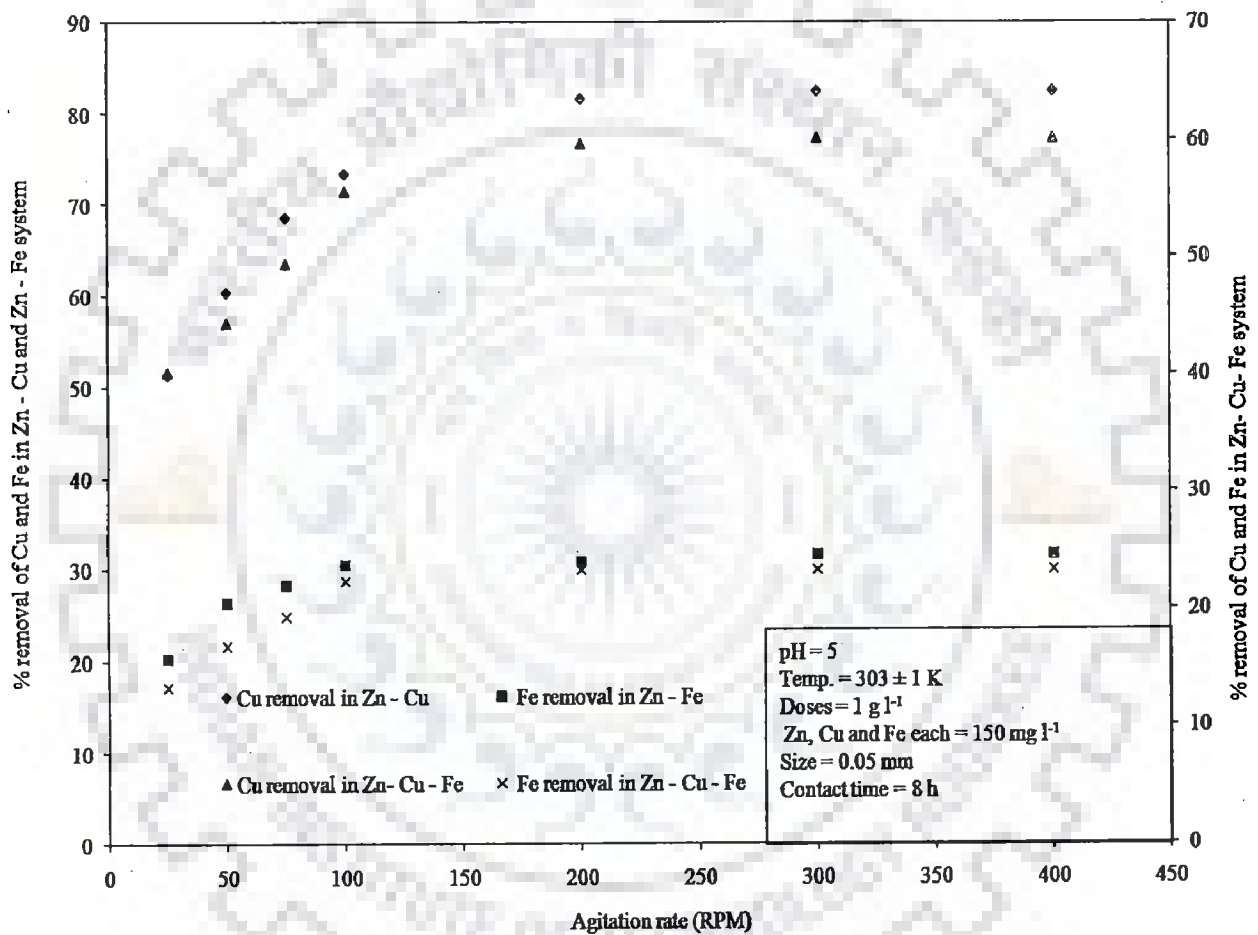


Figure 5.2.8 (f): Effect of agitation rate on biosorption of Cu and Fe in presence of Zn on Pineapple peel

However in figure 5.2.8 (f), the removal of Cu (II) and total Fe (II, III) ion in Zn (II)- Cu (II), Zn (II) – total Fe (II, III) and Zn (II)- Cu (II) - Fe (II, III) metal ion system was quite rapid

upto 50 rpm, 50 rpm, 25 rpm and 25 rpm, respectively. Further, extension in agitation rate from 50 rpm, 50 rpm, 25 rpm and 25 rpm to 400 rpm, the Cu (II) and total Fe (II, III) removal approached equilibrium in Zn (II)- Cu (II), Zn (II) – total Fe (II, III) and Zn (II)- Cu (II) - Fe (II, III). The preferential order of removal of heavy metal ions was Cu (II)> Zn (II)> Fe (II, III). Initial quite rapid removal of Zn (II), Fe (II, III) and Cu (II) ion in liquid phase in Zn (II)- Cu (II), Zn (II) – total Fe (II, III) and Zn (II) - Cu (II) Fe (II, III) system was due to film diffusion of Zn (II), Fe (II, III) and Cu (II) ion at the surface of Pineapple peel in liquid phase. However, the slowness in the removal of Zn (II), Cu (II), and total Fe (II, III) ion from liquid phase above 25 rpm, 50 rpm, 50 rpm, 25 rpm and 25 rpm in pure zinc, Zn (II)- Cu (II), Zn (II) – total Fe (II, III) and Zn (II)- Cu (II) - Fe (II, III) was due to the rationale that at the higher agitation rate above 25 rpm, 50 rpm, 50 rpm, 25 rpm and 25 rpm the intraparticle diffusion was prominent (Mishra et al., 2010).

Figure 5.2.8 (g) and figure 5.2.8 (h) represent the influence of agitation rate on biosorption of Zn (II), total Fe (II, III) and Cu (II) ions on Jackfruit peel.

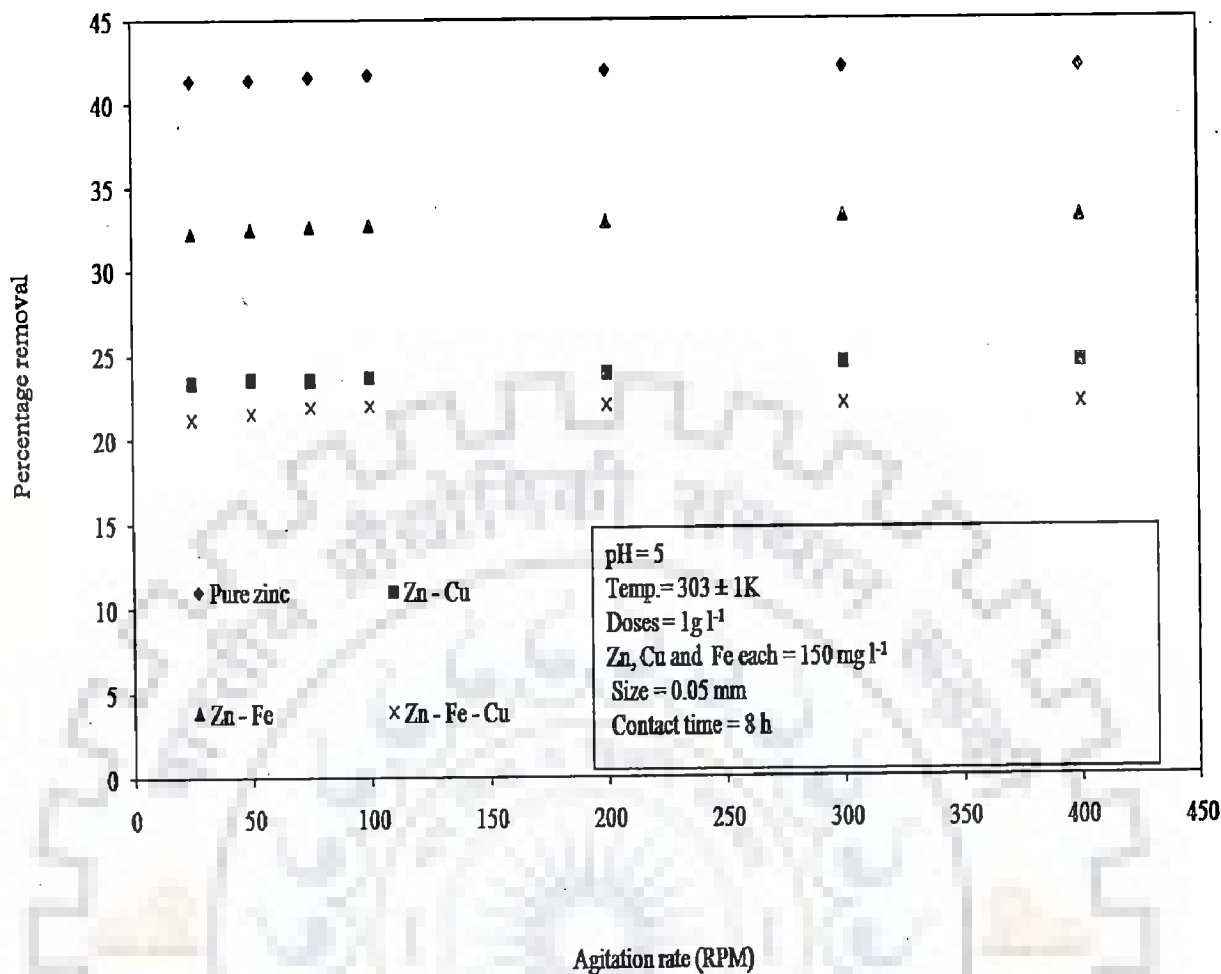


Figure 5.2.8 (g): Influence of agitation rate on biosorption of Zn on Jackfruit peel

It is clear from figure 5.2.8 (g) that the maximum removal of zinc was obtained in pure zinc phase at 25 rpm. The maximum removal of zinc in Zn (II)- Cu (II), Zn (II) – total Fe (II, III) and Zn (II)- Cu (II)- total Fe (II, III) metal ion systems was obtained at 25 rpm, respectively. Between 25 rpm to 400 rpm, the removal of Zn (II), total Fe (II, III) and Cu (II) ion was quite slow in Zn (II)- Cu (II), Zn (II) – total Fe (II, III) and Zn (II)- Cu (II)- total Fe (II, III).

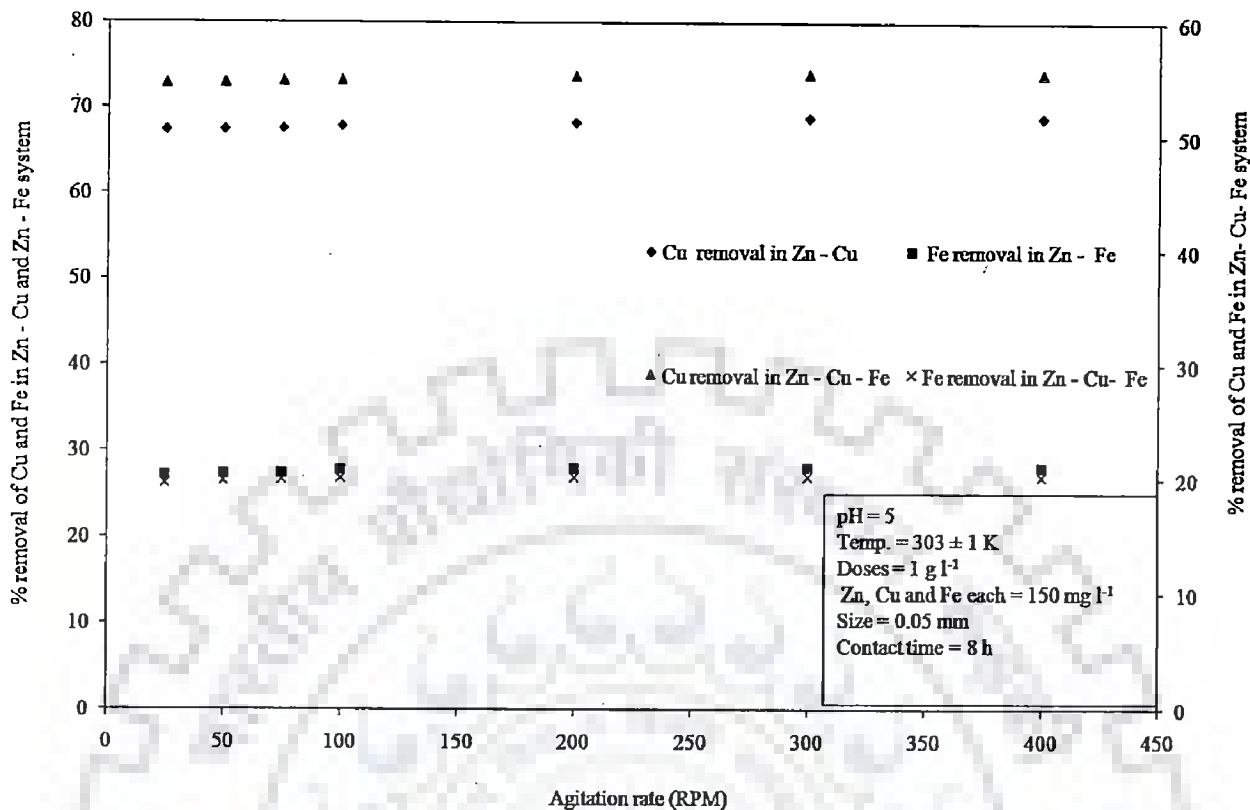


Figure 5.2.8 (h): Effect of agitation rate on biosorption of Cu and Fe in presence of Zn on Jackfruit peel

However in figure 5.2.8 (h), the removal of Cu (II) and total Fe (II, III) ion in Zn (II)- Cu (II), Zn (II) – total Fe (II, III) and Zn (II)- Cu (II)- Fe (II, III) metal ion system was quite rapid upto 25 rpm, respectively. With the increase in agitation rate from 25 rpm to 400 rpm led to the attainment of the equilibrium in Zn (II)- Cu (II), Zn (II) – total Fe (II, III) and Zn (II)- Cu (II)- Fe (II, III) metal ion. The insignificant removal of Zn (II), Fe (II, III) and Cu (II) ion from liquid phase with an increase in 25 rpm to 400 rpm was due to the intraparticle diffusion of metal ions inside the pores of biosorbent (Mishra et al., 2010). The preferential order of removal of heavy metal ions was Cu (II) > Zn (II) > Fe (II, III).

Figure 5.2.8 (i) and figure 5.2.8 (j) represent the influence of agitation rate on biosorption of Zn (II), total Fe (II, III) and Cu (II) ions on *Cedrus deodara* sawdust. It is clear from figure 5.2.8 (i) that the maximum removal of zinc was obtained in pure zinc phase at

100 rpm. The maximum removal of zinc in Zn (II)- Cu (II), Zn (II) – total Fe (II, III) and Zn (II)- Cu (II)- total Fe (II, III) metal ion systems was obtained at 100 rpm, respectively.

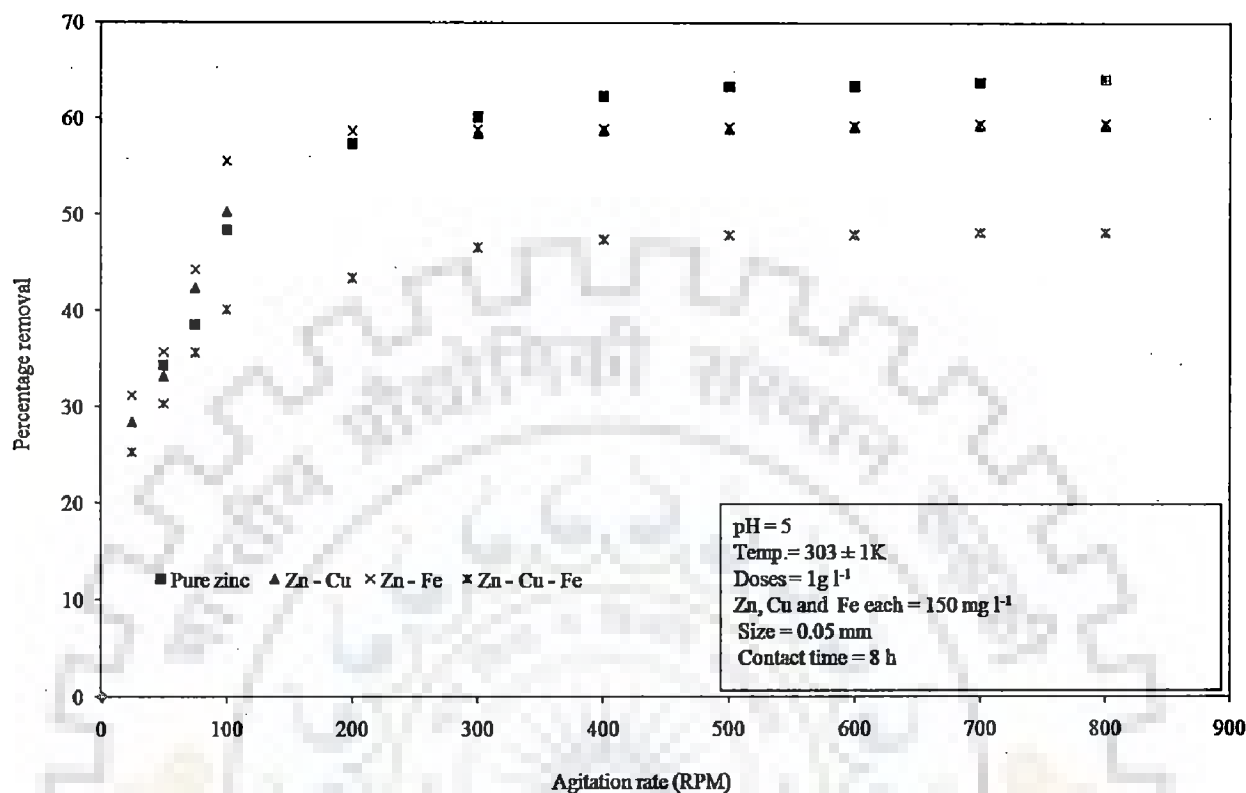


Figure 5.2.8 (i): Effect of agitation rate on biosorption of Zn on *Cedrus deodara* sawdust

Between 100 rpm to 800 rpm, the removal of Zn (II), Cu (II), total Fe (II, III) ion was quite slow. However in figure 5.2.8 (j), the removal of Cu (II) and total Fe (II, III) ion in Zn (II)- Cu (II), Zn (II) – total Fe (II, III) and Zn (II)- Cu (II)- Fe (II, III) metal ion system was quite rapid upto 75 rpm. With the increase in agitation rate from 75 rpm to 800 rpm led to the attainment of the equilibrium. With increase in agitation rate from 25 rpm to 400 rpm the removal of zinc increased substantially. Further extension in agitation rate from 400 rpm to 800 rpm led to the attainment of the equilibrium as well as the removal of Zn (II) ion was quite slow.



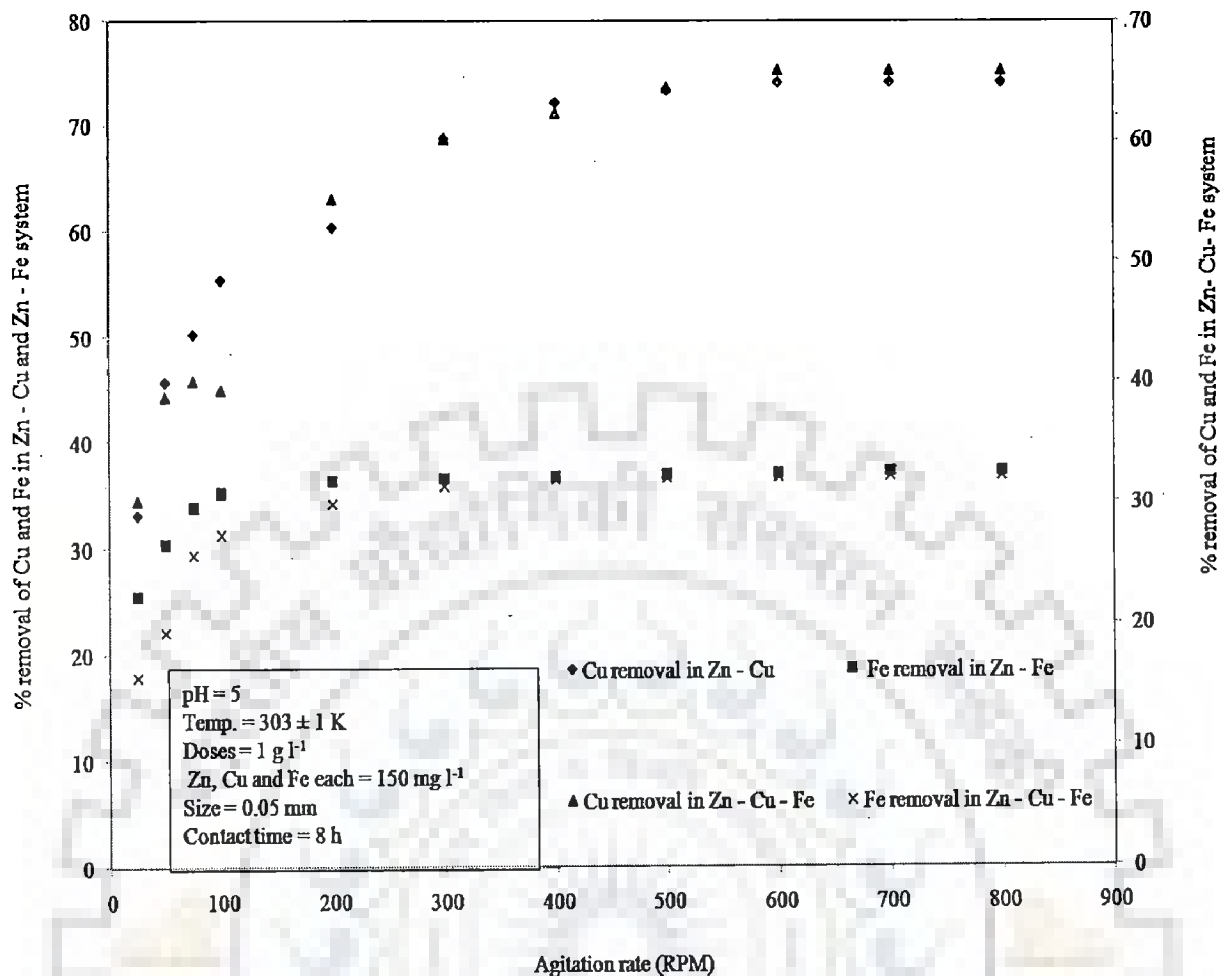


Figure 5.2.8 (j): Effect of agitation rate on biosorption of Cu and Fe in presence of Zn on *Cedrus deodara* sawdust

Further, extension in agitation rate from 500 rpm to 800 rpm and from 400 rpm to 800 rpm, respectively for Cu (II) and Fe (II, III), respectively led to the attainment of the equilibrium. The preferential order of removal of heavy metal ions was Cu (II) > Zn (II) > Fe (II, III). Initial quite rapid removal of Zn (II), Cu (II) and total Fe ions (II, III) ion in liquid phase in Zn (II)-Cu (II), Zn (II) – total Fe (II, III) and Zn (II)- Cu (II)- Fe (II, III) system was due to film diffusion of ions at the surface of *Cedrus deodara* sawdust in liquid phase. However, the slowness in the removal of Zn (II), Cu (II) and total Fe ions (II, III) ion from liquid phase above 100 rpm and 75 rpm was due to the rationale that at the higher agitation rate above 100 rpm and 75 rpm the intraparticle diffusion was prominent (Mishra et al., 2010).

Figure 5.2.8 (k) and figure 5.2.8 (l) represent the influence of agitation rate on biosorption of Zn (II), total Fe (II, III) and Cu (II) ions on Eucalyptus bark sawdust. It is clear from figure 5.2.8 (k) that the maximum removal of zinc was obtained in pure zinc phase at 200 rpm. The maximum removal of zinc in Zn (II)- Cu (II), Zn (II) – total Fe (II, III) and Zn (II)- Cu (II)- total Fe (II, III) metal ion systems was obtained at 100 rpm, respectively.

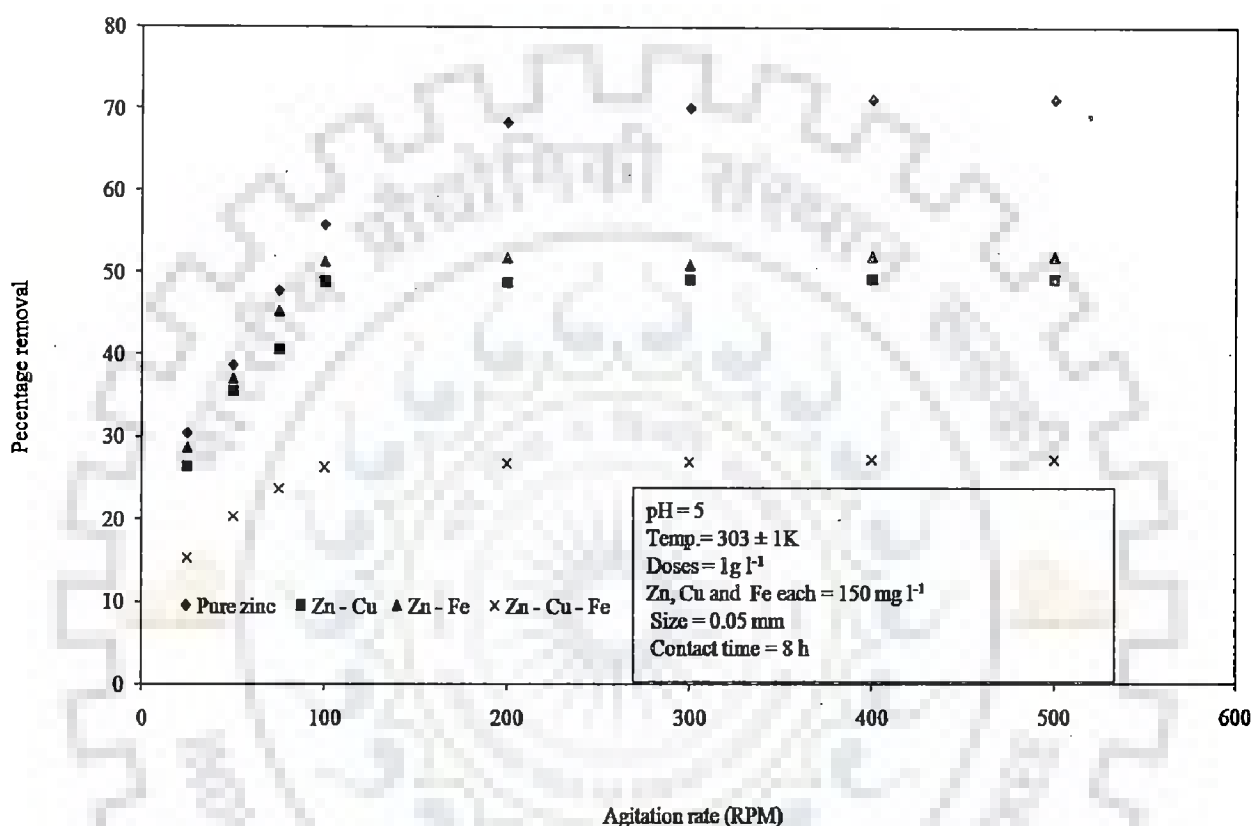


Figure 5.2.8 (k): Effect of agitation rate on biosorption of Zn on Eucalyptus bark sawdust

With increase in agitation rate from 25 rpm to 200 rpm the removal of zinc increased substantially. Further extension in agitation rate from 200 rpm to 500 rpm led to the attainment of the equilibrium as well as the removal of Zn (II) ion was quite slow in Zn (II)- Cu (II), Zn (II) – total Fe (II, III) and Zn (II)- Cu (II)- total Fe (II, III) systems.

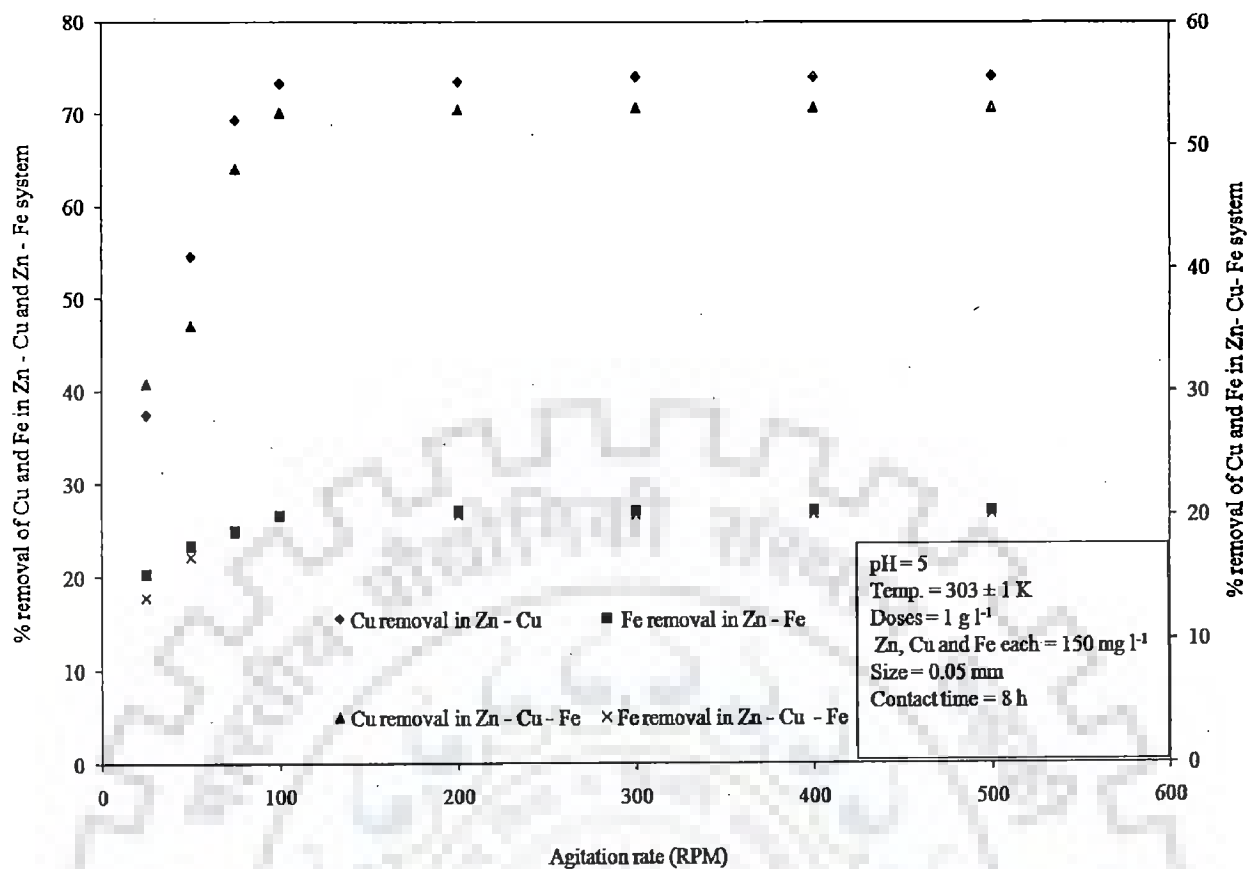


Figure 5.2.8 (I): Effect of agitation rate on biosorption of Cu and Fe in presence of Zn on Eucalyptus bark sawdust

However in figure 5.2.8 (I), the removal of Cu (II) and total Fe (II, III) ion in Zn (II)- Cu (II), Zn (II) – total Fe (II, III) and Zn (II)- Cu (II)- Fe (II, III) metal ion systems was quite rapid upto 50 rpm, 25 rpm, 100 rpm and 25 rpm. Further, extension in agitation rate from 50 rpm, 25 rpm 100 rpm and 25 rpm to 500 rpm for Cu (II) and Fe ions (II, III) in Zn (II)- Cu (II), Zn (II) – total Fe (II, III) and Zn (II)- Cu (II)- total Fe (II, III) systems,, respectively led to the attainment of the equilibrium. The preferential order of removal of heavy metal ions was Cu (II)> Zn (II)> Fe (II, III). Initial quite rapid removal of Zn (II) ion in liquid phase in pure zinc, Zn (II)- Cu (II), Zn (II) – total Fe (II, III) and Zn (II)- Cu (II)- Fe (II, III) systems was due to film diffusion of Zn (II), Cu (II) and Fe ions (II, III) ion on the surface of Eucalyptus bark sawdust in liquid phase. However, the slowness in the removal of Zn (II), Cu (II) and Fe ions (II, III) ion from liquid phase above 200, 50 rpm, 25 rpm, 100 rpm and 25 rpm,, respectively for pure zinc, Zn (II)- Cu (II), Zn (II) – total Fe (II, III) and Zn (II)- Cu (II)- total Fe (II, III)

was due to the rationale that at the higher agitation rate above 200, 50 rpm, 25 rpm, 100 rpm and 25 rpm the intraparticle diffusion was the rate governing step (Mishra et al., 2010).

Figure 5.2.8 (m) and figure 5.2.8 (n) represent the influence of agitation rate on biosorption of Zn (II), total Fe (II, III) and Cu (II) ions on Eucalyptus leaf powder. It is clear from figure 5.2.8 (m) that the maximum removal of Zn (II) in pure zinc, Zn (II)- Cu (II), Zn (II)- total Fe (II, III), Zn (II)- Cu (II)- Fe (II, III) system was obtained at 25 rpm.

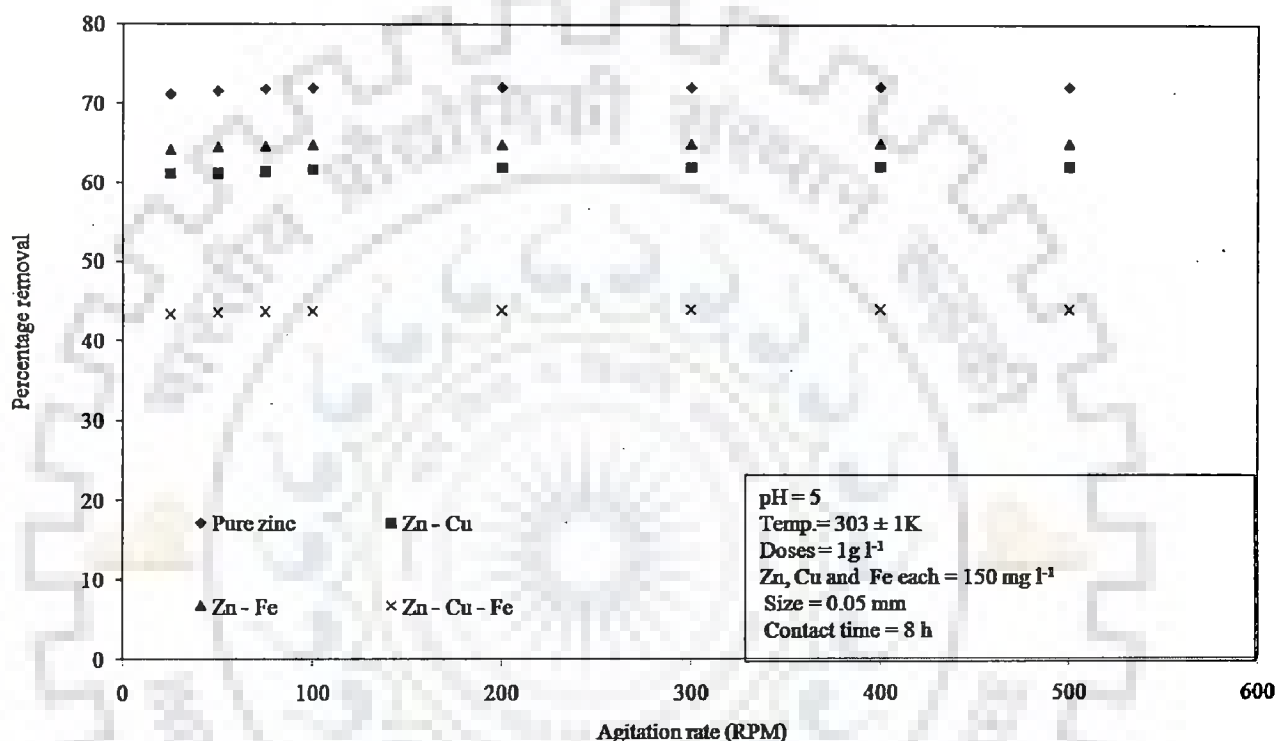


Figure 5.2.8 (m): Effect of agitation rate on biosorption of Zn on Eucalyptus leaf powder

The maximum removal of Cu (II) and total Fe (II, III) in Zn (II)- Cu (II), Zn (II)- total Fe (II, III), Zn (II)- Cu (II)- Fe (II, III) systems was also obtained at 25 rpm (figure 5.2.8 (n)). Between 25 rpm to 500 rpm, the removal of Zn (II), Cu (II), total Fe (II, III) ion was almost constant in pure zinc, Zn (II)- Cu (II), Zn (II)- total Fe (II, III), Zn (II)- Cu (II)- Fe (II, III) systems. With the increase in agitation rate from 25 rpm to 500 rpm the removal of Zn (II), Fe (II, III) and Cu (II) ion was not significant in pure zinc, Zn (II)- Cu (II), Zn (II)- total Fe (II, III), Zn (II)- Cu (II)- Fe (II, III) system.

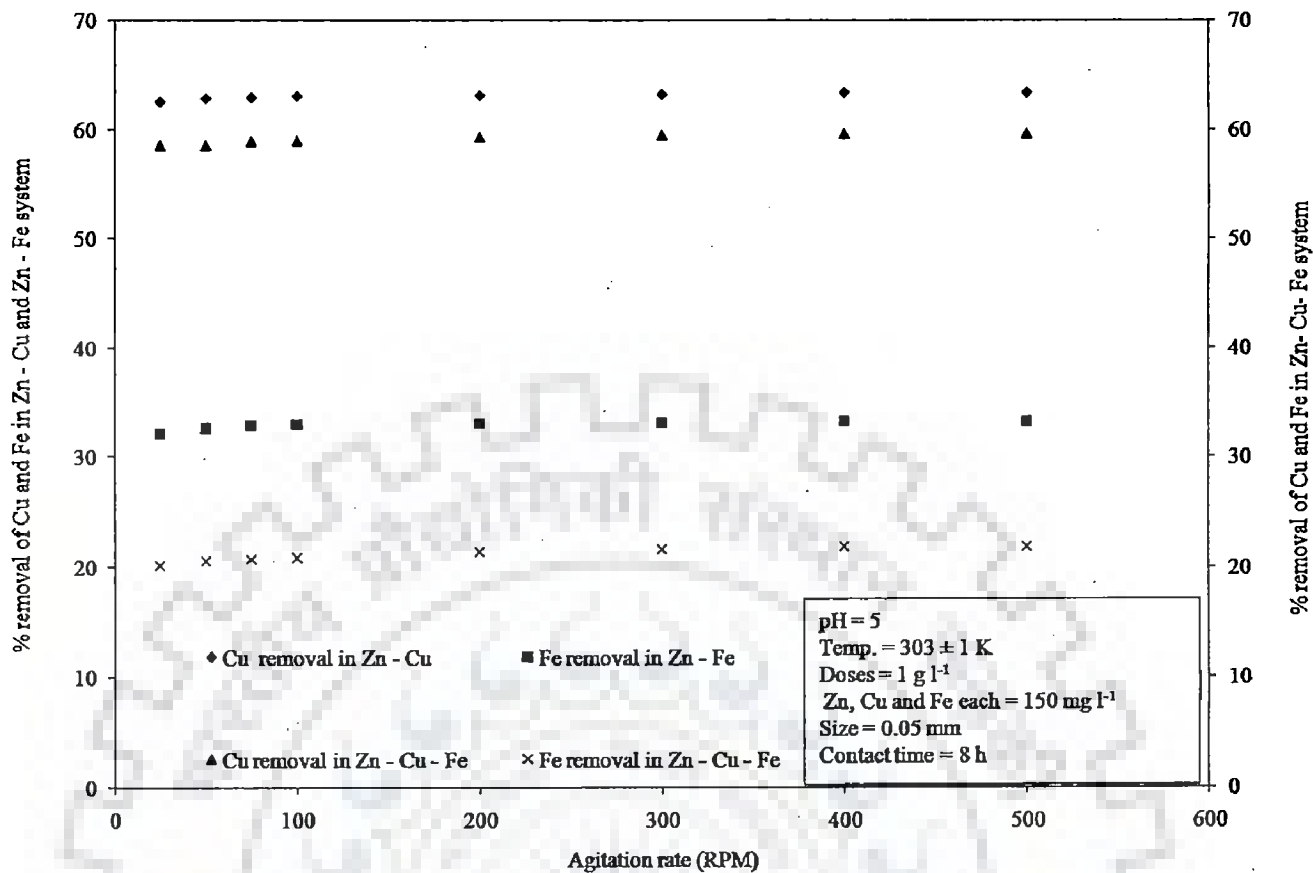


Figure 5.2.8 (n): Effect of agitation rate on biosorption of Cu and Fe in presence of Zn on Eucalyptus leaf powder

The insignificant removal of Zn (II), Fe (II, III) and Cu (II) ion from liquid phase with an increase in 25 rpm to 500 rpm was due to the intraparticle diffusion of metal ions inside the pores of biosorbent (Mishra et al., 2010). The preferential order of removal of heavy metal ions was Cu (II) > Zn (II) > Fe (II, III). Figure 5.2.8 (o) and figure 5.2.8 (p) represent the influence of agitation rate on biosorption of Zn (II), total Fe (II, III) and Cu (II) ions on Eggshell and membrane. It became evident from figure 5.2.8 (o) that the maximum removal of Zn (II) in pure zinc, Zn (II)- Cu (II), Zn (II)- total Fe (II, III), Zn (II)- Cu (II)- Fe (II, III) system was obtained at 75 rpm. With increase in agitation rate from 25 rpm to 75 rpm the removal of zinc increased substantially.

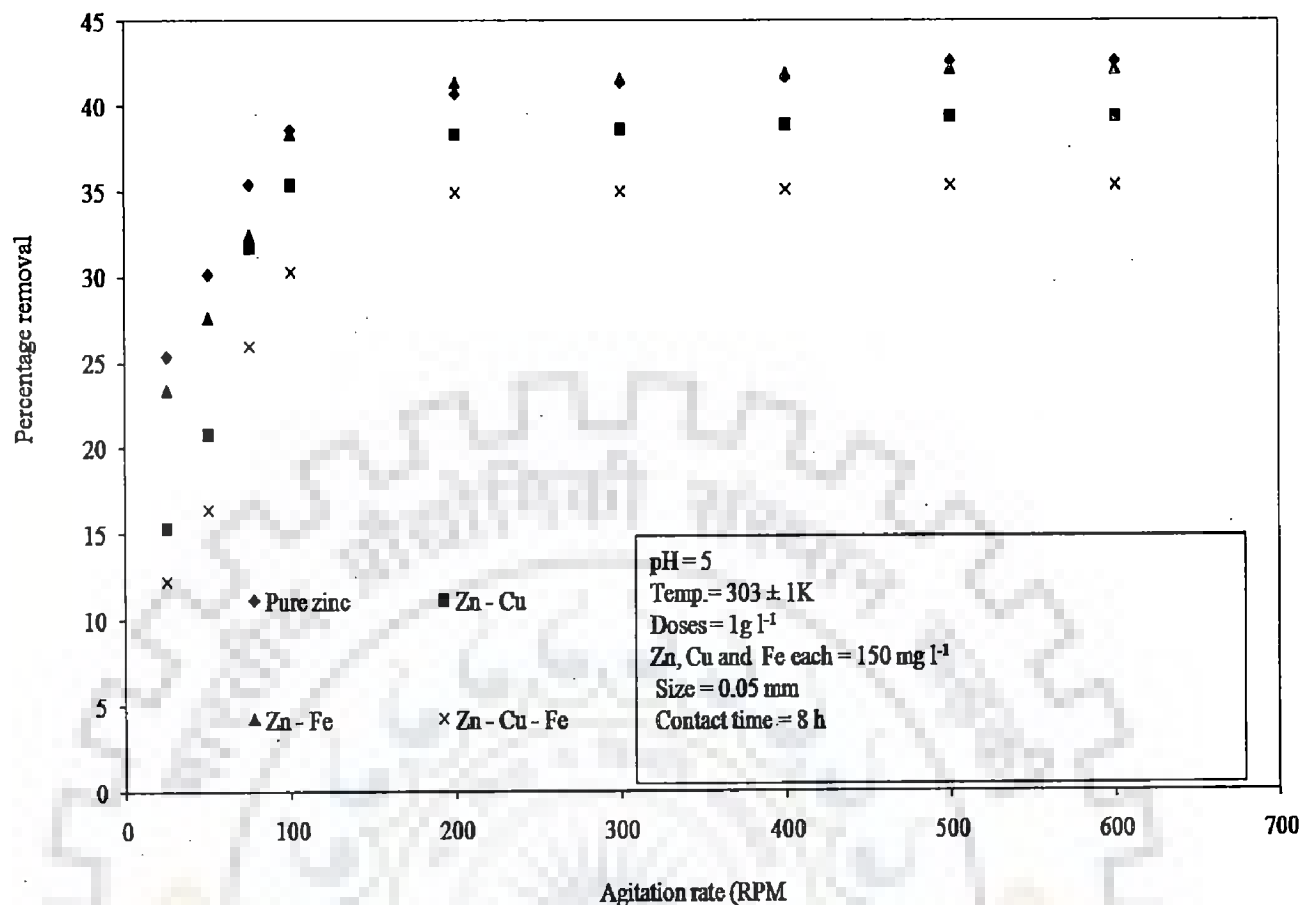


Figure 5.2.8 (o): Effect of agitation rate on biosorption of Zn on Eggshell and membrane

Further extension in agitation rate from 75 rpm to 600 rpm led to the attainment of the equilibrium as well as the removal of Zn (II) ion was quite slow in pure zinc, Zn (II)- Cu (II), Zn (II)- total Fe (II, III), Zn (II)- Cu (II)- Fe (II, III) systems. However in figure 5.2.8 (p), the maximum removal of Cu (II) and total Fe (II, III) ion in Zn (II)- Cu (II), Zn (II)- total Fe (II, III), Zn (II)- Cu (II)- Fe (II, III) metal ion system was quite rapid upto 75 rpm, 25 rpm, 50 rpm and 50 rpm, respectively. Further, extension in agitation rate from 75 rpm, 25 rpm, 50 rpm and 50 rpm to 600 rpm for Cu (II) and Fe ions (II, III) in Zn (II)- Cu (II), Zn (II)- total Fe (II, III), Zn (II)- Cu (II)- Fe (II, III) led to the attainment of the equilibrium. The preferential order of removal of heavy metal ions was Cu (II) > Zn (II) > Fe (II, III). Initial quite rapid removal of Zn (II), Cu (II) and total Fe (II, III) ion in liquid phase in pure zinc, Zn (II)- Cu

(II), Zn (II)- total Fe (II, III) and Zn (II)- Cu (II)- Fe (II, III) system was due to film diffusion of Zn (II) ion on the surface of Eggshell and membrane in liquid phase.

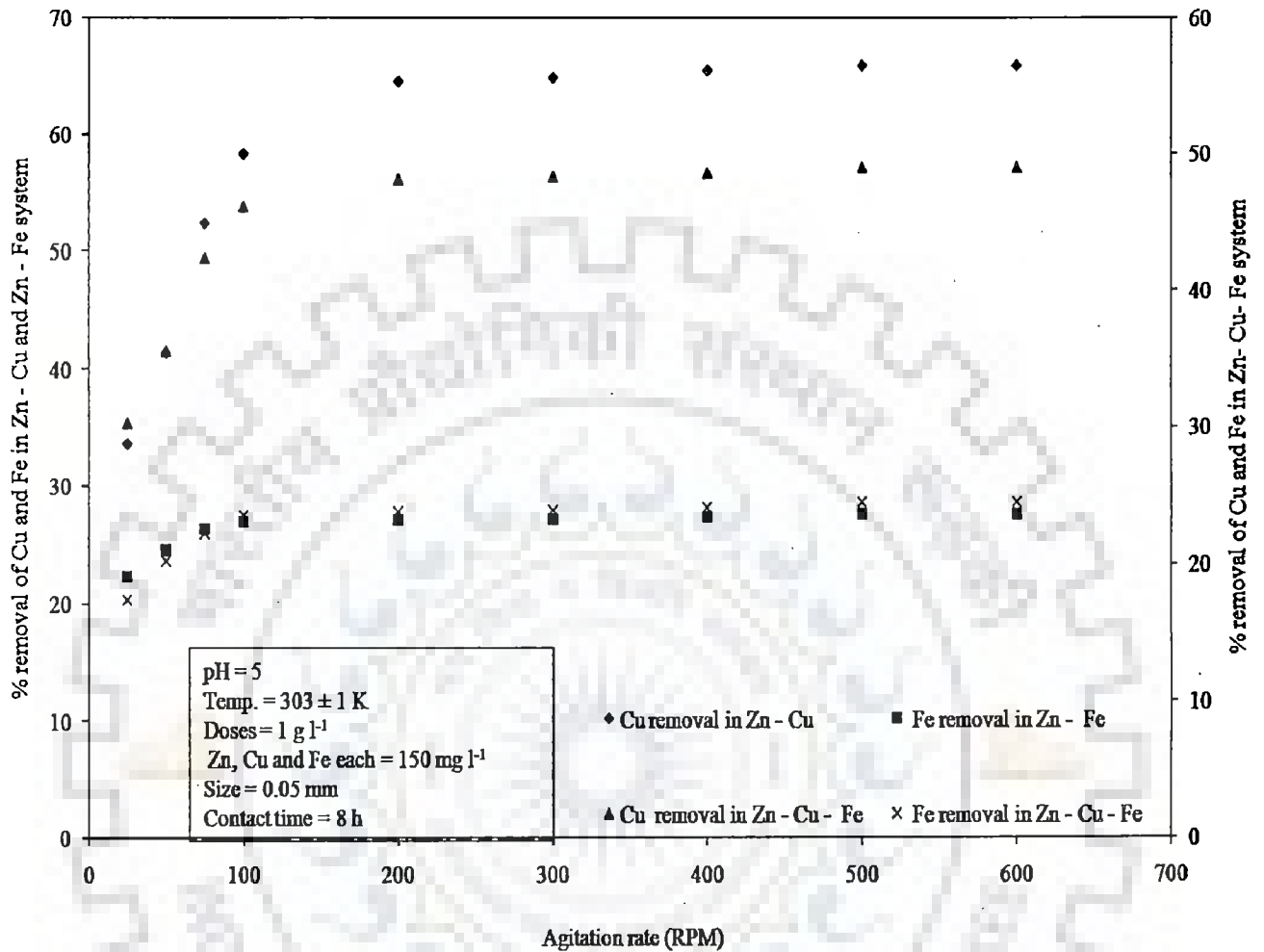


Figure 5.2.8 (p): Effect of agitation rate on biosorption of Cu and Fe in presence of Zn on Eggshell and membrane

However in figure 5.2.8 (p), the slowness in the removal of Zn (II), Cu (II) and total Fe (II, III) ion from liquid phase above 75 rpm, 75 rpm, 25 rpm, 50 rpm and 50 rpm, respectively for pure zinc, Zn (II)- Cu (II), Zn (II)- total Fe (II, III) and Zn (II)- Cu (II)- Fe (II, III) system was due to the rationale that at the higher agitation rate above 75 rpm, 75 rpm, 25 rpm, 50 rpm and 50 rpm rpm the intraparticle diffusion was prominent (Mishra et al., 2010). Figure 5.2.8 (q) and figure 5.2.8 (r) represent the influence of agitation rate on biosorption of Zn (II), Cu

(II) and total Fe (II, III) ions on dead cells of *Zinc sequestering bacterium VMSDCM* accession no. HQ108109.

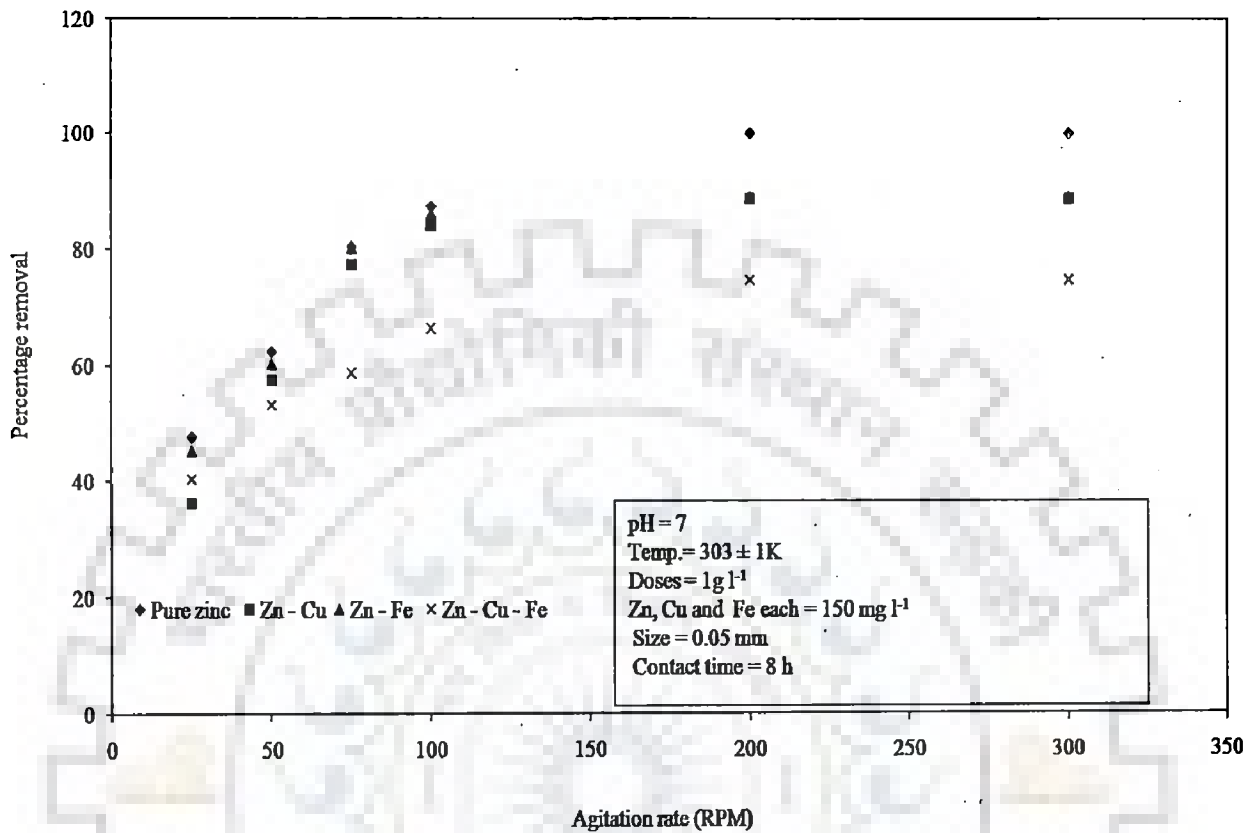


Figure 5.2.8 (q): Effect of agitation rate on biosorption of Zn on dead cells of *Zinc sequestering bacterium VMSDCM* accession no. HQ108109

It became evident from figure 5.2.8 (q) that that the maximum removal of Zn (II) in pure zinc, Zn (II)- Cu (II), Zn (II)- total Fe (II, III) and Zn (II)- Cu (II)- Fe (II, III) system was obtained at 75 rpm. With increase in agitation rate from 25 rpm to 75 rpm the removal of zinc increased substantially. Further extension in agitation rate from 75 rpm to 300 rpm led to the attainment of the equilibrium as well as the removal of Zn (II) ion was quite slow in pure zinc, Zn (II)- Cu (II), Zn (II)- total Fe (II, III), Zn (II)- Cu (II)- Fe (II, III) systems.



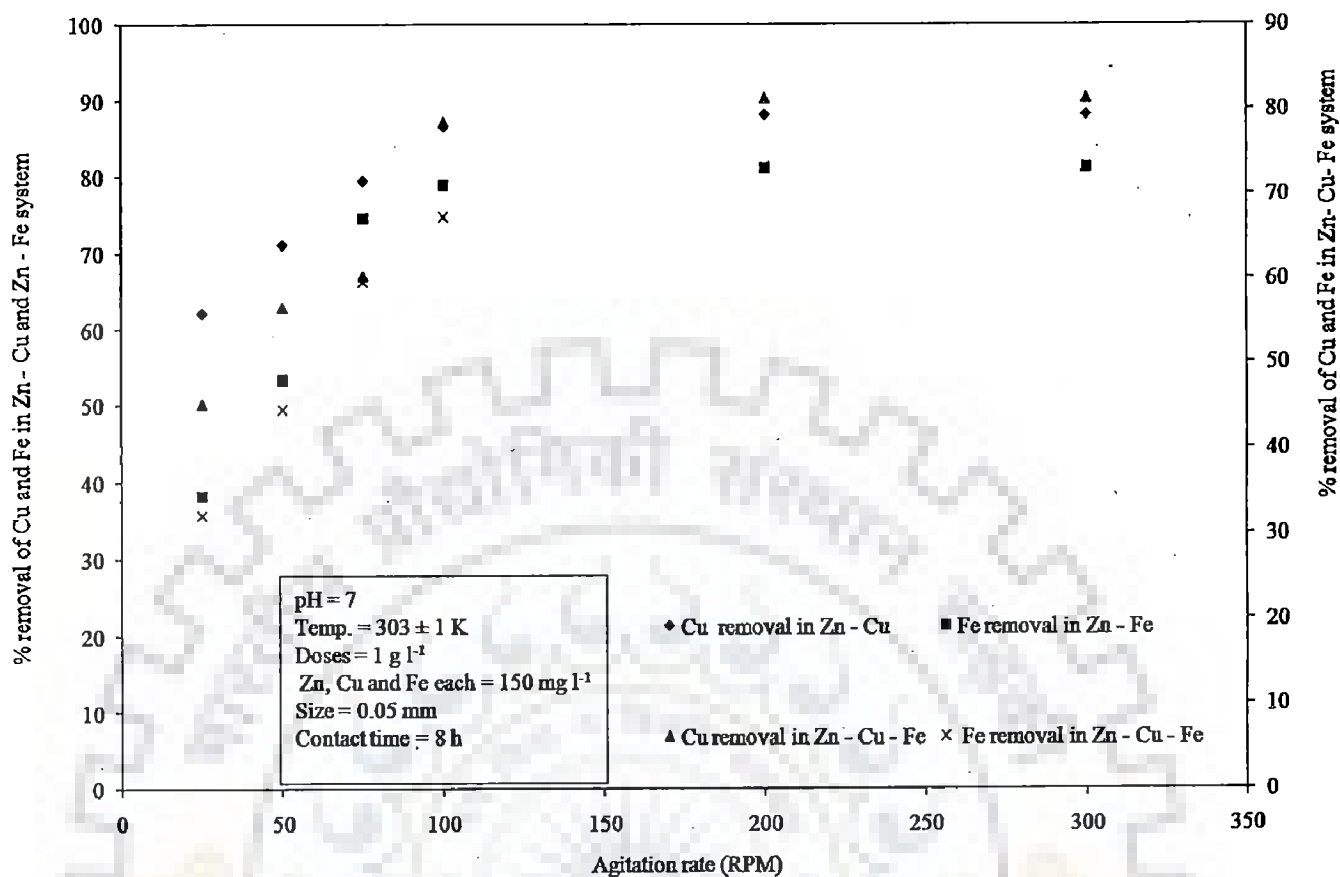


Figure 5.2.8 (r): Effect of agitation rate on biosorption of Cu and Fe in presence of Zn on dead cells of *Zinc sequestering bacterium VMSDCM* accession no. HQ108109

However in figure 5.2.8 (r), the maximum removal of Cu (II) and total Fe (II, III) ion in Zn (II)- Cu (II), Zn (II)- total Fe (II, III) and Zn (II)- Cu (II)- Fe (II, III) metal ion systems was quite rapid upto 75 rpm. Further, extension in agitation rate from 75 rpm to 300 rpm for Cu (II) and Fe ions (II, III) led to the attainment of the equilibrium. The preferential order of removal of heavy metal ions was Cu (II) > Zn (II) > Fe (II, III). Initial quite rapid removal of Zn (II) ion in liquid phase in Zn (II)- Cu (II), Zn (II)- total Fe (II, III) and Zn (II)- Cu (II)- Fe (II, III) systems was due to film diffusion of Zn (II) ion at the surface of dead cells of *Zinc sequestering bacterium VMSDCM* accession no. HQ108109 in liquid phase. However, the slowness in the removal of Zn (II) ion from liquid phase above 75 rpm was due to the

rationale that at the higher agitation rate above 75 rpm the intraparticle diffusion was rate controlling step (Mishra et al., 2010).

### **Concluding remark of the section 5.2.8**

Among all the selected biosorbents *Cedrus deodara* sawdust and dead cells of *Zinc sequestering bacterium VMSDCM* accession no. HQ108109 yielded the maximum percentage removal of Zn (II) ion in liquid phase in ternary metal ion system. The optimum agitation rate for the maximum removal of Zn (II) ion in liquid phase for *Cedrus deodara* sawdust and *Zinc sequestering bacterium VMSDCM* accession no. HQ108109 were 800 rpm and 300 rpm, respectively.

Among all the selected biosorbents *Cedrus deodara* sawdust and dead cells of *Zinc sequestering bacterium VMSDCM* accession no. HQ108109 proved relatively better to comparative over the other selected biosorbents to remove zinc from liquid in ternary metal ion system consisting of Zn (II) - total Fe (II, III) - Cu (II) ion. Hence, in further investigation only these two biosorbents were considered. Section 5.3 includes the applications of these two biosorbents on removal of Zn (II), total Fe (II, III) and Cu (II) ion from synthetic simulated wastewater.

### **Conclusion of the section 5.2**

Among all the biosorbents selected for the present investigation, the *Cedrus deodara* sawdust (CDS) and dead cells of *Zinc sequestering bacterium VMSDCM* accession no. HQ108109 yielded the maximum percentage removal of Zn (II), Cu (II) and total Fe (II, III) in all types of metal ion systems. In case of *Cedrus deodara* sawdust (CDS), the maximum removal of Zn (II), Cu (II) and total Fe (II, III) was obtained at pH 5, 318 K, 1 g l<sup>-1</sup> of biomass, 150 mg l<sup>-1</sup> of Zn (II), Cu (II) and total Fe (II, III), 0.05 mm of particle size, 6 hours of contact time and agitation rate of 800 rpm. In case of dead cells of *Zinc sequestering bacterium VMSDCM* accession no. HQ108109, the maximum removal of Zn (II), Cu (II) and total Fe (II, III) in all the cases of metal ion systems was obtained at pH 7, 303 ± 1 K, 1 g l<sup>-1</sup> of biomass, 150 mg l<sup>-1</sup> of Zn (II), Cu (II) and total Fe (II, III), 4 hours of contact time and 300 rpm of agitation rate.

## 5.2.9 Modeling Using Selected Adsorbents

This section embodies the data regarding the isotherm, kinetic, mechanistic, thermodynamic modeling of the data obtained at equilibrium in case of *Cedrus deodara* sawdust, and dead cells of *Zinc sequestering bacterium VMSDCM* accession no. HQ108109.

### 5.2.9.1 Isotherm, Kinetic, Mechanistic and Thermodynamic Modeling of Sorption of Zn (II) Ion in Liquid Phase on the Surface of *Cedrus deodara* Sawdust

This section embodies the modeling of the data obtained at equilibrium of biosorption of Zn (II) ion in liquid phase on the surface of *Cedrus deodara* sawdust in liquid phase. Various types of the models used in the present investigation have been shown in chapter 2, section 2.2.7 and in appendix (A -1). Initial concentration of Zn (II), total Fe (II, III) and Cu (II) ion was taken as 150 mg l<sup>-1</sup> each. Various temperatures used in the present study were 298 , 308 and 318.

#### 5.2.9.1.1 Isotherm modeling of sorption of Zn (II) on *Cedrus deodara* sawdust

This section embodies the isotherm modeling of the data obtained at equilibrium. Various isotherm models used in the present investigation were Langmuir, Freundlich, and Temkin model. The statistical analysis of the data was performed through, linear regression coefficient (R<sup>2</sup>) an in built function in MS office 2007.

Results of various isotherms such as Langmuir, Freundlich, and Temkin model have been shown in figures 5.2.9.1 (a), 5.2.9.1(a) and 5.2.9.1 (c). The detailed analysis of the model constants have been shown in table 5.2.9.1 (a).

Figure 5.2.9.1(a) represents Langmuir isotherm for the sorption of Zn (II) ion on the surface of *Cedrus deodara* sawdust. Langmuir model was drawn at three temperature levels 298 , 308, and 318 K. With the elevation of temperature from 298 K to 318 K the model constant K<sub>L</sub>(lmg<sup>-1</sup>) increased from 0.72 to 1.14.

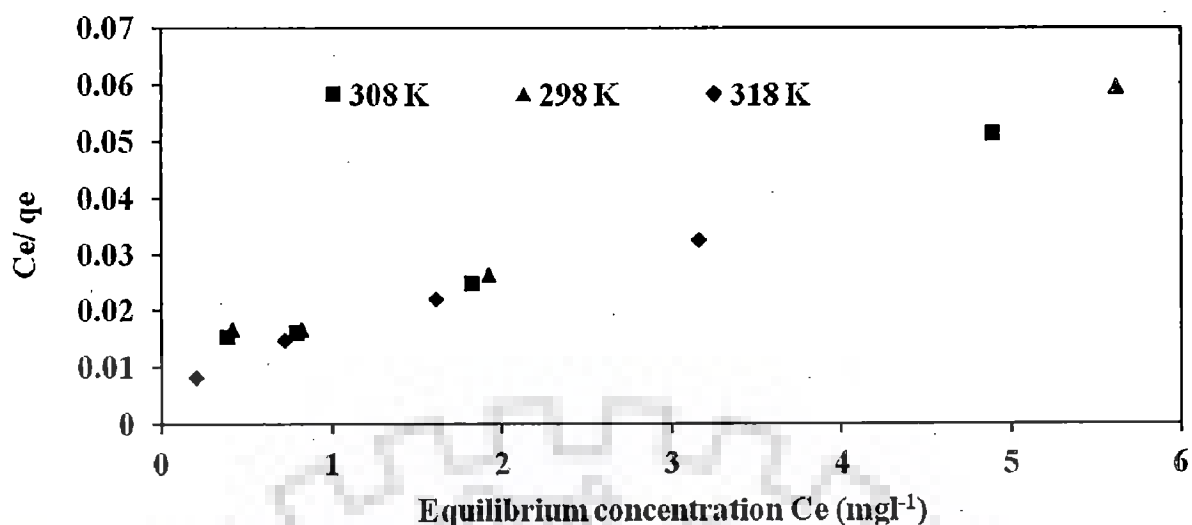


Figure 5.2.9.1 (a): Langmuir isotherm for the biosorption of Zn (II) ion on the surface of *Cedrus deodara* sawdust

Furthermore, the statistical error function analysis leads (table 5.2.9.1(a)) to the conclusion that both  $\chi^2$  and SSE are significantly higher for the Langmuir model at various temperature levels. Significantly higher values of error functions ruled out all the possibilities of langmuir model suitability in the present investigation.

Figure 5.2.9.1 (b) and table 5. 9.2.1 (a) represents Freundlich isotherm model study of sorption of Zn (II) ion on the surface of *Cedrus deodara* sawdust. It became evident from figure 5.2.9.2 that value of  $1/n$  (affinity constant, slope of isotherm, equation no. 7, appendix 4) was less than one at various temperature ranges.

Additionally, the values of SSE and  $\chi^2$  were almost negligible together with higher values of linear regression coefficient ( $R^2$ ). With above mentioned facts, Freundlich isotherm was concluded as more suitable to explain the biosorption of Zn (II) ion across liquid phase. (Mishra et al., 2011)

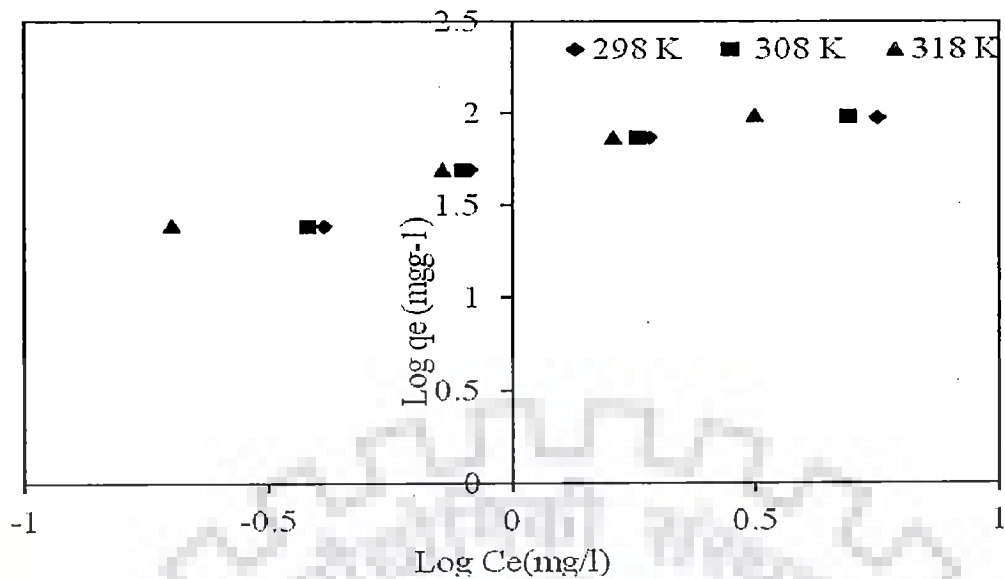


Figure 5.2.9.1 (b): Study of Freundlich model for the biosorption of Zn (II) ion on the surface of *Cedrus deodara* sawdust

Figure 5.2.9.1 (c) represents Temkin isotherm model study of sorption of Zn (II) ion on the surface of *Cedrus deodara* sawdust. It became evident from figure 5.2.9.1 (c) that the Temkin model was quite suitable at 298 K and 308 K.

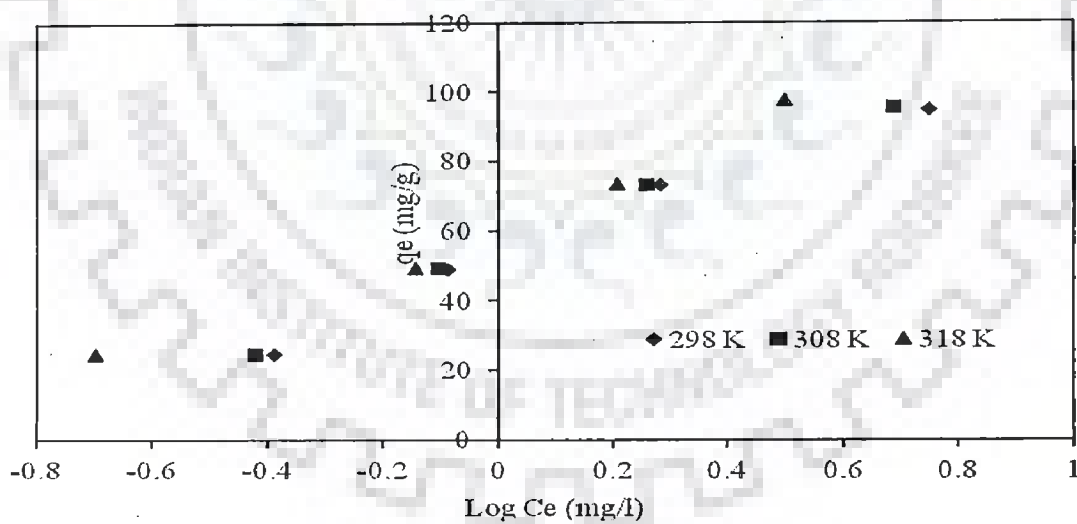


Figure 5.2.9.1 (c): Study of Temkin model for the biosorption of Zn on the surface of *Cedrus deodara* sawdust

The values of statistical parameters (table 5.2.9.1 (a)) also indicate that the values of statistical error function  $\chi^2$  and SSE were quite low. These facts indicated the suitability of Temkin model at 298 K and 308 K.

Table 5.2.9.1 (a) represents the detailed analysis of isotherms and their regression coefficient.

Model	Temp. (K)	R <sup>2</sup>	q <sub>e</sub> (Th)	q <sub>e</sub> (exp)	q <sub>max</sub> (mg g <sup>-1</sup> )	K <sub>L</sub> (l mg <sup>-1</sup> )	χ <sup>2</sup>	SSE	Reference
Langmuir	298	0.99	248.65	241.23	1298	0.727	0.22	55.05	This study
	308	0.99	2981.23	242.12	1298	0.8	0.33	82.99	
	318	0.98	2988.84	244.86	1298	1.142	0.72	187.14	
Freundlich	Temp. (K)	R <sup>2</sup>	q <sub>e</sub> (Th)	q <sub>e</sub> (exp)	1/n	K <sub>f</sub> (lg <sup>-1</sup> )	χ <sup>2</sup>	SSE	This study
	298	0.90	243.77	241.23	0.493	41.30	0.02	6.31	
	308	0.92	242.86	242.12	0.513	47.42	0.00	0.55	
Temkin	Temp. (K)	R <sup>2</sup>	q <sub>e</sub> (Th)	q <sub>e</sub> (exp)	B <sub>t</sub>	K <sub>t</sub>	χ <sup>2</sup>	SSE	This study
	298	0.98	241.15	241.23	60.92	7.07	0.00	0.00	
	308	0.99	242.08	242.12	63.38	7.08	0.00	0.00	
Langmuir	Temp. (K)	R <sup>2</sup>	q <sub>e</sub> (Th)	q <sub>e</sub> (exp)	q <sub>max</sub> (mg g <sup>-1</sup> )	K (l mg <sup>-1</sup> )	χ <sup>2</sup>	SSE	Ong et al.,
	298	0.99	29	N.D	N.D	1.008	N.D	N.D	
	318	0.97	244.81	244.86	59.92	11.30	0.00	0.00	

Freundlich	Temp. (K)	R <sup>2</sup>	q <sub>e</sub> (Th)	q <sub>e</sub> (exp)	1/n	K <sub>f</sub> (lg <sup>-1</sup> )	χ <sup>2</sup>	SSE	
	298	0.99	18	N.D	N.D	0.337	N.D	N.D	Ong et al., 2005
	353	0.99	21	N.D	N.D	0.013	N.D	N.D	Ozdemi r et al., 2009
	343	0.99	29	N.D	N.D	0.014	N.D	N.D	Ozdemi r et al., 2009
	353	0.90	N. D	N. D	0.32	4.3			Ozdemi r et al., 2009
	343	0.91	N.D	N.D	0.34	5.5	N.D	N.D	Ozdemi r et al., 2009

The analysis of data tabulated in tables 5.2.9.1 and in figures 5. 2.9.1 (a), 5.2.9.1(b) and 5.2.9.1(c) revealed that Temkin model was more suitable to predict the Zn (II) ion sorption on surface of CDS across liquid phase. Further, the Temkin model constant (K<sub>t</sub>) increased with the increase in temperature. The linear relation between model constant K<sub>t</sub> and temperature deciphered out the fact that the Zn (II) ion onto surface of CDS was endothermic. The regression coefficient (R<sup>2</sup>) for Temkin model was quite higher with the lowest possible values of χ<sup>2</sup> and SSE in comparison to Langmuir and Freundlich model at 298 K and 308 K, respectively. Moreover, at 318 K, both Freundlich and Temkin isotherm yield a better understanding of Zn (II) sorption across liquid phase, indeed.

### Concluding remark of the section 5.2.9.1

The perusal of isotherm modeling on biosorption of Zn (II) ion uncovered the fact that at the higher temperature level (318 K) Freundlich and Temkin isotherm ( $R^2 = 0.99$  and  $0.97$ , respectively) provide a better understanding of Zn (II) ion adsorption on to surface of CDS biomass against Langmuir isotherm model ( $R^2 = 0.98$ ) and Temkin model was found to be dominant in terms of Zn (II) ion biosorption isotherm modeling on CDS surface at temperature level less than 318 K.

#### 5.2.9.1.2 Kinetic modeling

The results of pseudo first order and pseudo second order models have been represented in table 5.2.9.1. 2 (a) and figures 5.2.9.1.2 (a) and 5.2.9.1.2 (b). The equation of the pseudo first order and pseudo second order has been shown in appendix (A-1). It is evident from figure 5.2.9.1.2 (a) that pseudo first order model yielded a lower linear regression coefficient ( $R^2$ ) of in range of  $0.68 - 0.72$  with higher values of statistical error functions like  $\chi^2$  and SSE in range of  $98.05$  to  $363.81$  and  $420.66$  to  $6377.36$ .

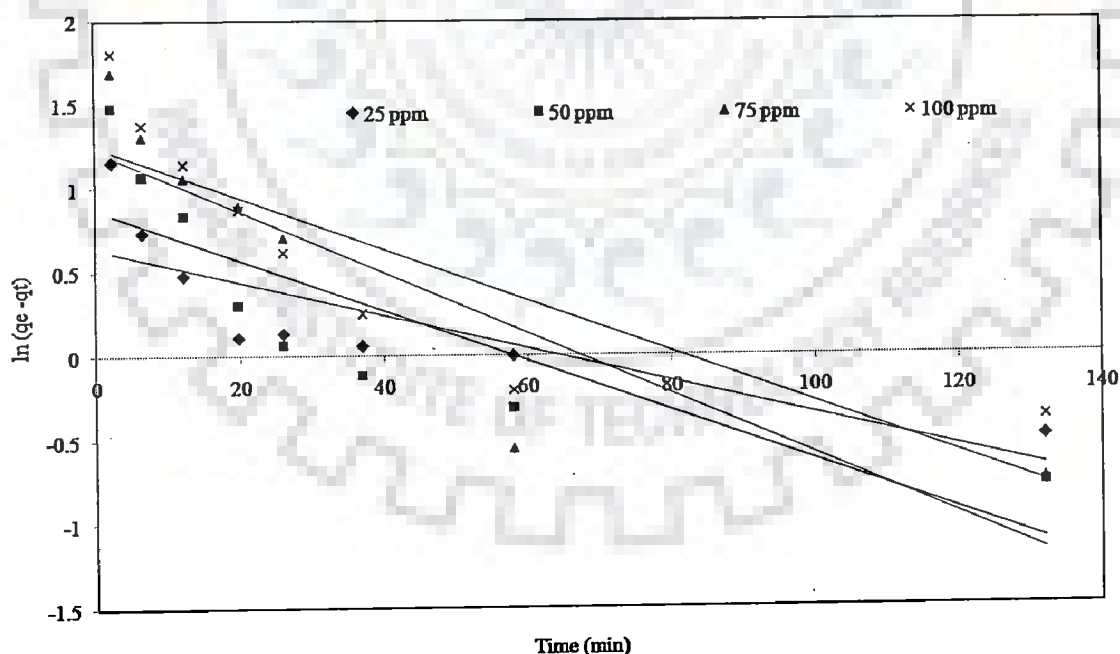


Figure 5.2.9.1.2 (a): Study of pseudo first order reaction model on CDS



Pseudo second order model (figure 5.2.9.1.2 (b) and table 5.2.9.2 (a)) with significant linear correlation coefficients ( $R^2$ ) 0.99 and lower  $\chi^2$  and SSE seemed to be a more appropriate model to describe Zn (II) ion biosorption on sawdust surface. Experimental reading ( $q_e$ ,  $\text{mgg}^{-1}$ ) derived through batch studies is in close relation to the theoretical reading derived from pseudo second order reaction model.

Contrary to this, pseudo first order reaction model together with low linear correlation coefficients in range of coupled with far-reaching differences between calculated and experimental uptake capacity ( $q_e$ ,  $\text{mgg}^{-1}$ ) resulting in higher values of error function ( $\chi^2$  and SSE) proved incompetent to describe lucratively the biosorption of Zn (II) ion on biomass surface across liquid phase in batch studies.

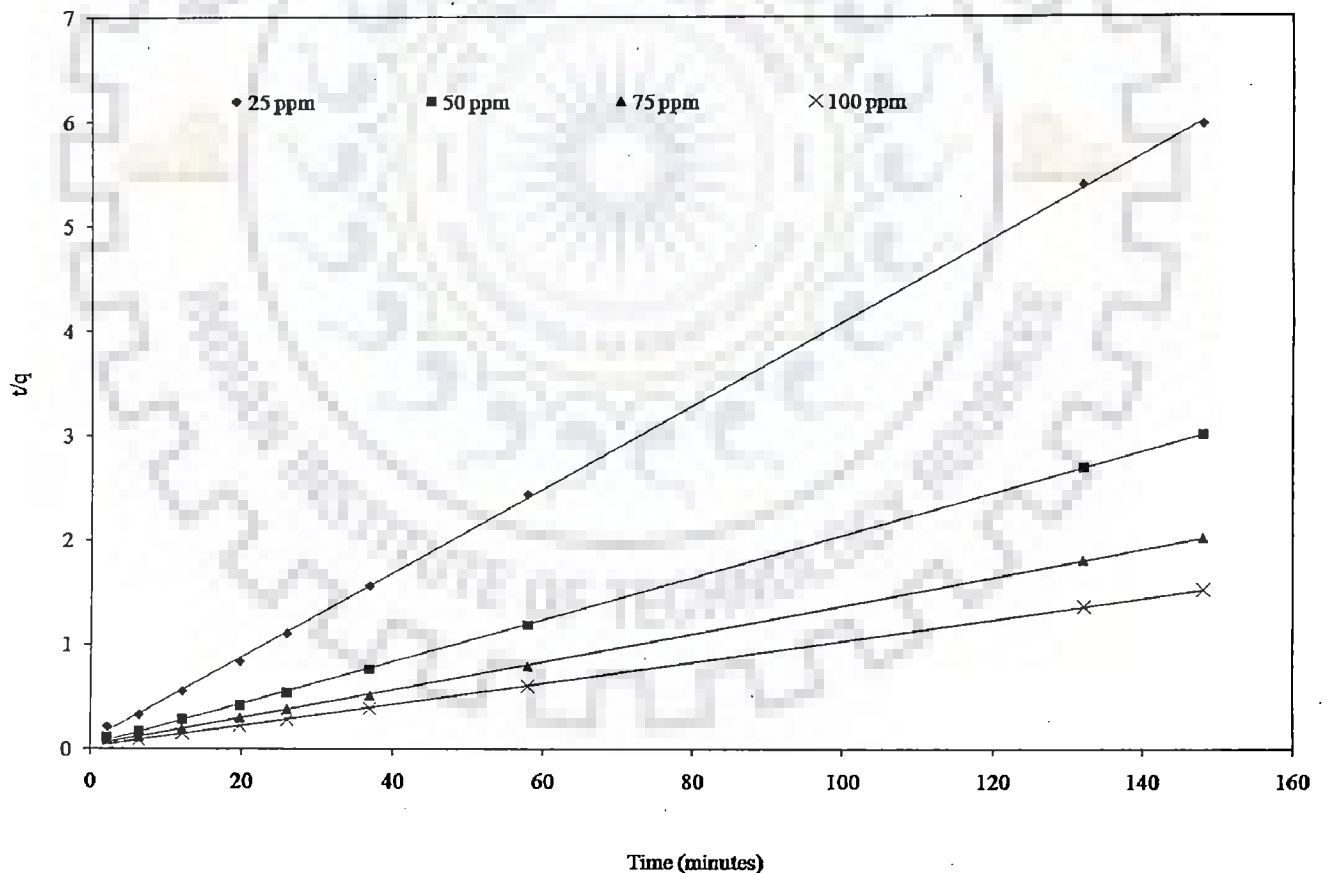


Figure 5.2.9.1.2 (b): Study of pseudo second order reaction model on CDS

To support the above mentioned result of reaction kinetics, a more deep insight study was pursued by extrapolating the graph between the sorption rate constant ( $K_2$ ,  $\text{mg}^{-1}\text{g}^{-1}\text{min}^{-1}$ ) and initial sorption rate ( $h$ ,  $\text{mg}^{-1}\text{g}^{-1}\text{min}^{-1}$ ) against initial concentration of Zn (II) ion. Equation [5.1] and equation [5.2] represent the relation of initial sorption rate ( $h$ ) and rate constant ( $K_2$ ) with initial metal ion concentration, respectively.

$$h = 0.410C_0 + 2.545 \quad R^2 = 0.924 \quad [5.1]$$

$$K_2 = -0.021C_0 + 2.518 \quad R^2 = 0.739 \quad [5.2]$$

The results indicated a linear increase in trend line plotted between initial metal ion concentration ( $C_0$ ) and initial sorption rate ( $h$ ). Contrary to this, the trend line between reaction constant  $K_2$  and initial concentration of metal ion ( $C_0$ ) showed a decreasing trend. Kumar et al., 2005 and Ho and Mc Kay derived a negative trend line in extrapolation of both  $h$  and  $K_2$  against initial metal ion concentration.

On the other hand, Basha et al. 2009 reported a linear and increasing trend line of Hg (II) ion sorption onto surface of *Carica papaya*. The analysis of all the results obtained in case of pseudo second order modeling in the present work were found to be parallel with biosorption of Cr (VI) onto surface of pomegranate husk (Nemr, 2009).

The suitability of pseudo second order model in the present work proved that the sorption of Zn (II) ion on the surface of CDs sawdust was chemisorption rather than adsorption mediated by physical forces of attraction indeed.



$K_1$ (-) ( $\text{min}^{-1}$ )	$R^2$	$\chi^2$	$K_2 \times 10^{-3}$ ( $\frac{\text{gm}}{\text{min}}$ )	$R^2$	$\chi^2$	
0.02	0.98	7.95	0.0447	0.99	0.12	Naiya et al., 2009
0.02	0.98	8.9	0.05	0.99	0.014	Naiya et al., 2009
0.46	0.13	N.D	87.83	0.99	N.D	Areco et al., 2010

### 5.2.9.1.3 Mechanistic and thermodynamic modeling

Figure 5.2.9.1.3 (a) represents the intra particle modeling of biosorption of Zn (II) on the surface of *Cedrus deodra* sawdust. It became evident from figure 5.2.9.1.3 (a) that intra particle model represents the multi linear curve. Such types of curves have been reported in previous studies.

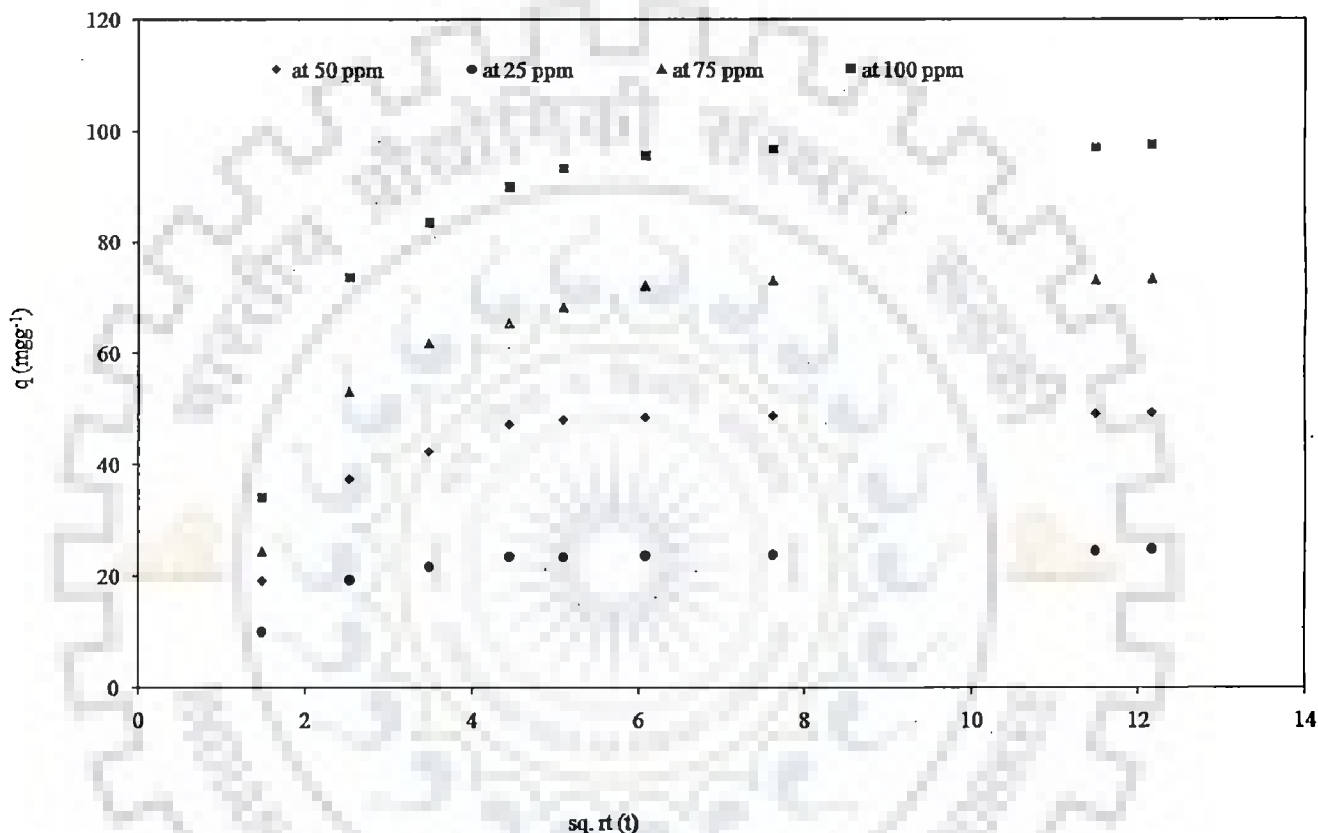


Figure 5.2.9.1.3 (a): Study of intra particle model on CDS

Curve having intercept I with multi – linear nature indicates the involvement of both film mass transfer coupled with intra particle metal ion diffusion inside the pores filled with liquid as rate determining steps. The value of intercept I indicates the thickness of boundary layer around the solid adsorbent particle. The data tabulated in table 5.2.9.1.3 (a) clarified that intra particle model was not proficient (in terms of linear correlation coefficients,  $R^2$ ) model to explain Zn (II) ion biosorption on the CDS biomass surface resulting in no proper clarification of rate determining step

Figure 5.2.9.1.3 (b): represents the Bangham's model study of modeling of biosorption of Zn (II) on the surface of *Cedrus deodra* sawdust. Figure 5.2.9.1.3 (b) and table 5.2.9.1.3 (a) noticeably indicate the higher value of linear correlation coefficient ( $R^2$ ) of Bangham's model over intra particle model resulting in the dominance of film diffusion over pore diffusion mechanism at equilibrium.

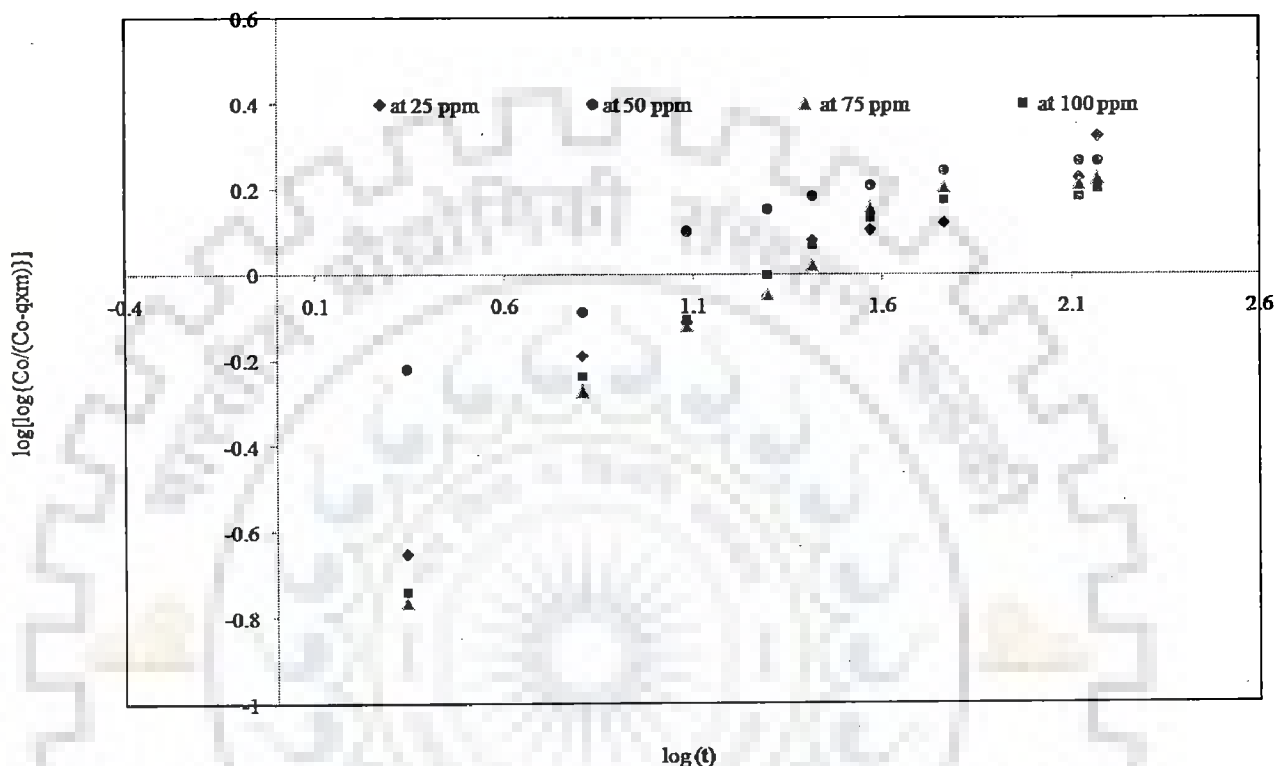


Figure 5.2.9.1.3 (b): Study of Bangham's model on CDS

Though the goodness of fit of Bangham's mechanistic model is significantly higher than the intra particle model but the value of correlation coefficients are not very satisfactory itself, lying between range of 0.84 – 0.91. Hence, now, it is difficult to mention the exact rate-controlling step of Zn (II) ion adsorption on the CDS surface. For this reason, next conformity test consisting of film and pore diffusivity coefficient estimation, rate controlling step was determined.

Table 5.2.9.1.3 (a): Study of intra particle and Bangham's model

Initial concentration of Zn (II) (mg l <sup>-1</sup> )	Intra particle model		Bangham's model	
	K <sub>id</sub> (mgg <sup>-1</sup> )min <sup>0.5</sup>	R <sup>2</sup>	K <sub>0</sub>	R <sup>2</sup>
25	0.832	0.45	4.57	0.91
50	1.761	0.44	1.77	0.88
75	3.011	0.507	5.55	0.881
100	3.719	0.465	4.84	0.846

Assuming the adsorbent particle shape as spherical in dimensions, equations [5.3] and [5.4] (Chabani et al., 2006, Mohan et al., 2008) were used to chalk out rate limiting step.

$$D_f = 0.23 \left[ \frac{R_p \varepsilon}{t^{1/2}} \right] \times \left[ \frac{q_e}{C_0} \right] \quad [5.3]$$

$$D_p = 0.03 \left[ \frac{R_p^2}{t^{1/2}} \right] \quad [5.4]$$

where  $D_f$  is film diffusion coefficient,  $D_p$  is particle diffusion coefficient,  $R_p$  is radius of adsorbent particle = 0.0025 cm,  $\varepsilon$  is thickness of liquid film is  $10^{-3}$  cm,  $t^{1/2}$  is half of the total time required for half biosorption of metal ion and  $q_e$  is metal uptake capacity (mgg<sup>-1</sup>) at equilibrium. If the Zn (II) biosorption onto CDS biomass was controlled by film diffusion, the value of film diffusion coefficient ( $D_f$ ) lies in range of  $10^{-6} - 10^{-8}$  cm<sup>2</sup>s<sup>-1</sup>, if the pore diffusion is the slowest and hence rate determining step, the value of pore diffusion coefficient ( $D_p$ ) should come in the range of  $10^{-11} - 10^{-13}$  cm<sup>2</sup>s<sup>-1</sup>. Taking into account the data of Zn (II) ion biosorption and kinetic model constants, both diffusion coefficients were

evaluated and the results indicated an overwhelming response of diffusion coefficients in range the of film diffusion from  $10^{-6}$  to  $10^{-8}$   $\text{cm}^2\text{s}^{-1}$  ( $D_f = 8.45 \times 10^{-8}$   $\text{cm}^2\text{s}^{-1}$ ). Through complete mechanistic modeling, diffusion coefficient and contact time study, it became clear that the binding of Zn (II) ions on the surface of CDS was governed by two different mechanisms. The first stage of the intra particle curve (figure 5.2.9.1.3 (a))) was quite rapid due the metal ion transfer by film diffusion mediated from liquid phase to the end of solid liquid interface. The second stage of the intra particle curve (figure 5.2.9.1.3(b)) indicates the transition of film diffusion to intra particle diffusion, i.e., the beginning of movement of metal ion inside the pores of CDS and subsequently third stage resembles to the complete intra particle diffusion of metal ions. At the onset of the process, the sorption was quite rapid and about 94% of the metal ion removal was obtained in first 40 minutes. This indicates that the film diffusion was rate controlling step at the onset of the process but with the passage of time, the sorption of zinc ions became slow. The slow sorption of metal ions at the later stage of the process was an indicator of pore or intra particle diffusion indeed. Thermodynamic feasibility of the reaction is very important parameter to delineate the spontaneity and feasibility of the biosorption process. In the present investigation, thermodynamic feasibility of metal ion adsorption was calculated in terms of Gibb's free energy  $\Delta G$  ( $\text{kJmol}^{-1}$ ), enthalpy  $\Delta H$  ( $\text{kJmol}^{-1}$ ) and entropy  $\Delta S$  ( $\text{kJmol}^{-1}\text{K}^{-1}$ ). Equations [5.5], [5.6] and [5.7] were used to calculate thermodynamic parameters.

$$\Delta G = -RT \ln K_c \quad [5.5]$$

$$\ln K_c = \frac{\Delta S}{R} - \frac{\Delta H}{RT} \quad [5.6]$$

$$\text{Hence, } K_c = \frac{C_a}{C_e} \quad [5.7]$$

$C_a$  = Zn (II) ion adsorbed per liter ( $\text{mg l}^{-1}$ ),  $C_e$  = equilibrium concentration of Zn (II) ion ( $\text{mg l}^{-1}$ ),  $R$  = gas constant ( $8.314 \text{ Jmol}^{-1}\text{K}^{-1}$ ),  $T$  = Temperature (K)



The intercept and slope of plot extrapolated between  $\ln K_c$  and  $1/T$  yields the value of  $\Delta S$  ( $\text{kJmol}^{-1}\text{K}^{-1}$ ) and  $\Delta H$  ( $\text{kJmol}^{-1}$ ), respectively. Thermodynamic parametric study and process feasibility has been represented in figure 5.2.9.1.3 (c) and table 5.2.9.1.3 (b).

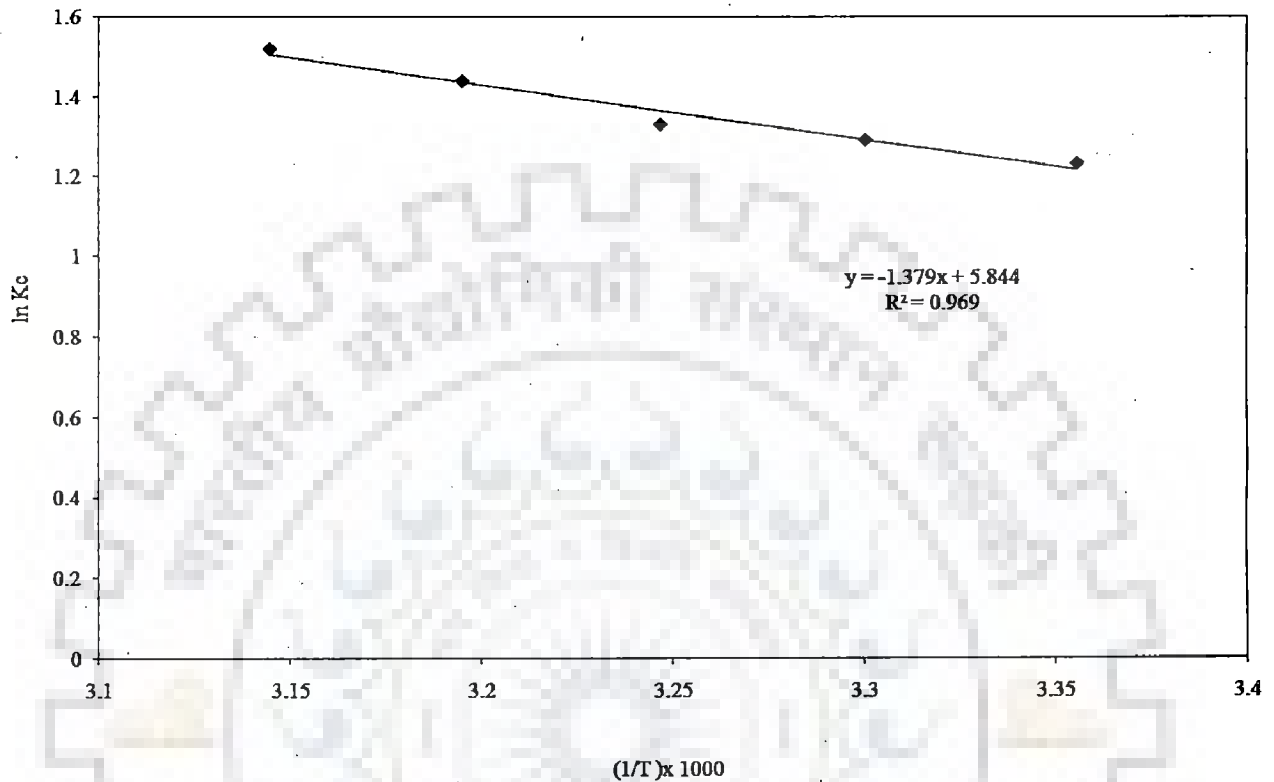


Figure 5.2.9.1.3 (c): Plot of  $\ln K_c$  versus  $1/T$  of CDS

The value of  $\Delta H$ ,  $\Delta S$  and linear regression coefficient ( $R^2$ ) obtained from figure 5.2.9.1.3 (c) were  $+ 10.3176 \text{ kJ mol}^{-1}$ ,  $+ 44.546 \text{ kJ mol}^{-1}\text{K}^{-1}$  and 0.910. The demarcated positive sign for biosorption  $\Delta H$  and  $\Delta S$  indicated that the binding of Zn (II) ion at biomass surface is endothermic coupled with increase in randomness at solid liquid interface during metal ion adsorption with mounting of temperature. The increase in randomness at the solid solution interface was might have been due to the exchange of Zn (II) ions with more transportable ions present on the surface of CDS or due to the liberation of water molecules from the surface of CDS biomass at the time of adsorption.

Table 5.2.9.1.3 (b): Study of Gibb's free energy at three different temperature gradients

Temperature (K)	$\Delta G$ (Gibb's free energy, $\text{kJmol}^{-1}$ )
298	- 3109.353
303	-3149.69
308	- 3191.113
313	-3547.28
318	- 3686.627

Gibbs free energy was negative ( $\Delta G$ ) at every temperature level and was found to be decreasing with the rise of temperature which ruled in every possibility of biosorption of Zn (II) ion on the biomass as spontaneous, feasible and the spontaneous nature of the sorption of Zn (II) over surface of CDS increases with the elevation of temperature (Ahmad et al., 2009).

#### Concluding remarks of the section 5.2.9.1.3

Kinetic and mechanistic modeling of Zn (II) ion adsorption across liquid phase analysis reproduced the fact that the pseudo second order ( $R^2 = 0.99$ ) and Bangham's model ( $R^2 = 0.84 - 0.91$ ) were more suitable to clarify the kinetics and mechanism of metal ion sorption against pseudo first order ( $R^2 = 0.68 - 0.77$ ) and intra particle ( $R^2 = 0.45 - 0.50$ ) diffusion model.

The study of Bangham's model, intra particle model, agitation rate, film and pore diffusion coefficient ( $D_f$  and  $D_p$ ) chalked out the involvement of film and pore diffusion across the boundary layer and inside the pores of CDS, respectively indicated both film and pore diffusion as rate controlling step. Negative value of  $\Delta G$  ( $\text{kJmol}^{-1}$ ), positive value of  $\Delta H$  ( $\text{kJmol}^{-1}$ ) and  $\Delta S$  ( $\text{kJmol}^{-1}\text{K}^{-1}$ ) concluded the overall biosorption of Zn (II) ion on the surface

of CDS biomass as spontaneous, endothermic together with increased randomness at liquid solid interface during the sorption of Zn (II) ion in batch studies.

### 5.2.9.2 Isotherm, Kinetic, Mechanistic and Thermodynamic Modeling on the Surface of Dead Cells of *Zinc sequestering bacterium VMSDCM* accession No. HQ108109

This section embodies the isotherm, kinetic, mechanistic and thermodynamic modeling of the data obtained at biosorption of Zn (II) ion on the surface of *Zinc sequestering bacterium VMSDCM* accession no. HQ108109. Various isotherm, kinetic and mechanistic models used in the present investigation were Langmuir, Freundlich, Temkin and Dubinin-Radushkevich equation (D-R) model, intra particle and Bangham,s model. The statistical analysis of the models was performed through SSE,  $\chi^2$  and linear regression coefficient ( $R^2$ ).

#### 5.2.9.2.1 Isotherm modeling

This section embodies the modeling of data obtained at equilibrium at 298 K, 303 K and 308 K. The statistical analysis of the isotherms was performed through linear regression coefficient ( $R^2$ ),  $\chi^2$  and SSE.

Figures 5.2.9.2.1 (a), 5.2.9.2.1 (b), 5.2.9.2.1 (c) and 5.2.9.2.1 (d) represent the study of various isotherms such as Langmuir, Freundlich, Temkin and Dubinin- Radushkevich equation (D-R) model.

Figure 5.2.9.2.1 (a) represents the study of Langmuir model. The model Langmuir isotherm model was studied between 298 K to 308 K. The results of the Langmuir model study presented in figure 5.2.9.2.1 (a), indicate that at none of the temperature levels, ideal model equation has any agreement with equation derived from equilibrium data obtained in batch experiments.

Furthermore, at 308 K and at the attainment of equilibrium, the concentration of metal ion in liquid phase became 0 mmole<sup>-1</sup>. At this point, the slope and intercept of curve between  $C_e/q_e$  and  $C_e$  became infinity and zero rendering all model constants and error evaluation

functions undefined resulting in unsuitability of the Langmuir model at this temperature. The equations of Langmuir isotherm model with corresponding linear regression coefficient at various temperatures have been tabulated in table 5.2.9.2.1 (a).

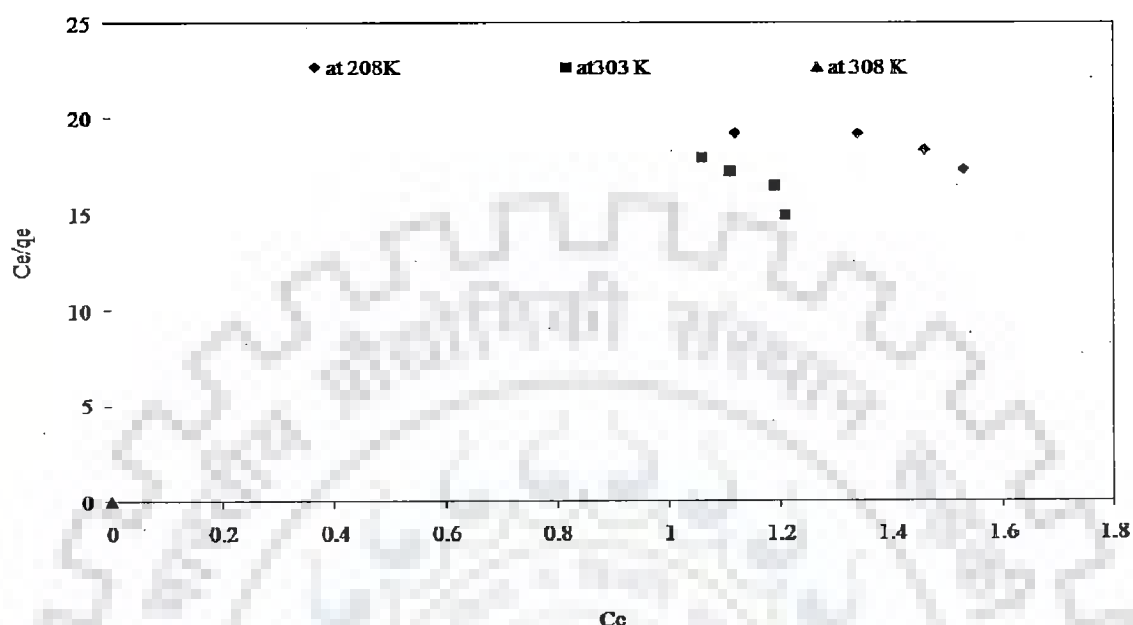


Figure 5.2.9.2.1 (a): Study of langmuir isotherm model between 298 Kto 308 K.

Langmuir isotherm model was found undefined to explain the sorption of Zn (II) ion on the surface of VMSDCM bacterium in the above-mentioned range. Figure 5.2.9.2.1 (b) represents the Freundlich isotherm model study.

The model Freundlich isotherm model was studied between 298 K to 308 K. It became evident from figure 5.2.9.2.1 (b) that Freundlich model at various temperature levels did not posses sufficient throughput to describe proficiently the sorption of Zn (II) ion on the surface of *Zinc sequestering bacterium VMSDCM*. At 298 K and 303 K, the curving fitting of the batch equilibrium data in the Freundlich model yielded the equation of straight line with negative intercept which is not superimposable on the ideal Freundlich isotherm model.

Additionally, at 308 K there was complete removal of zinc from liquid phase at the end of 8 hours. Thus,  $K_f$  and  $1/n$  cannot be calculated from the curve between  $\ln q_e$  and  $\ln C_e$  as the intercept and slope is zero and infinity at the attainment of equilibrium, respectively.

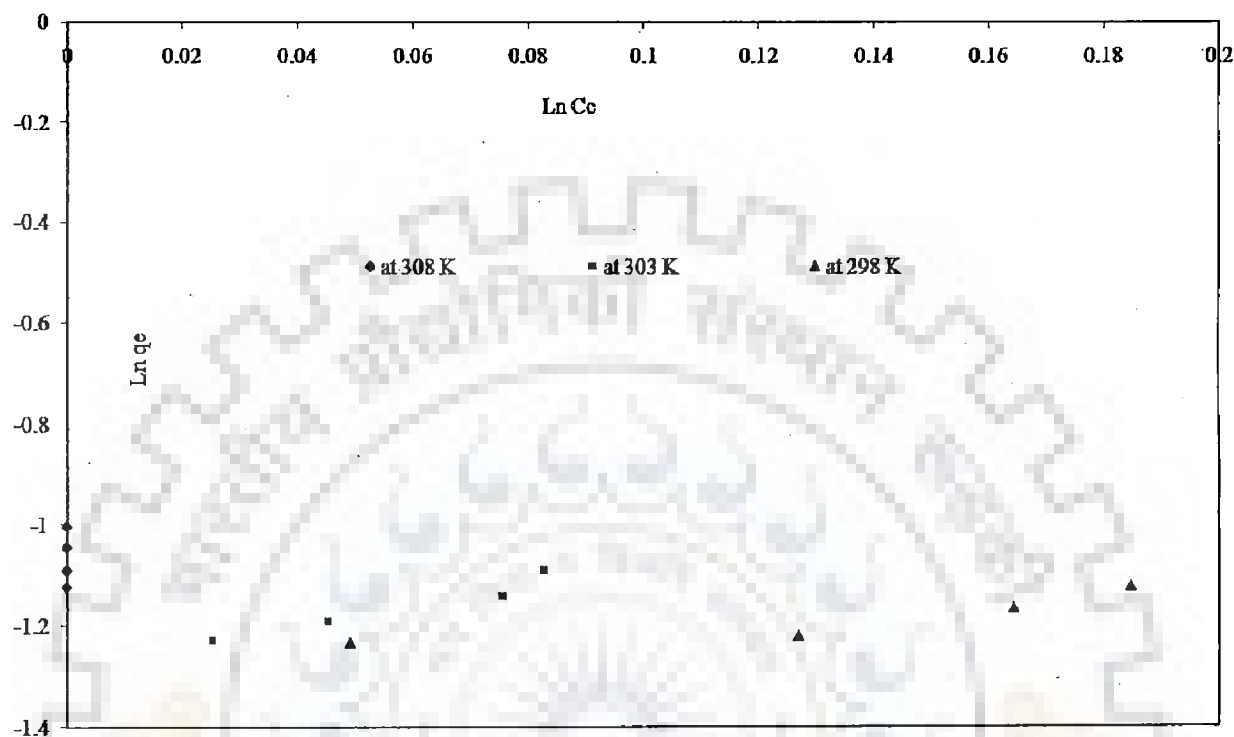


Figure 5.2.9.2.1 (b): Study of Freundlich isotherm model between 298 K to 308 K

The results of Freundlich model with respective equations,  $R^2$  and error reporting functions have been tabulated in table 5.2.9.2.1 (a). The non-defining characteristics of Freundlich isotherm model rendered the isotherm model incapable to explain the sorption of Zn (II) ion on the surface of *VMSDCM* bacterium. Figure 5.2.9.2.1 (c) represents the Temkin isotherm model study. The model Temkin isotherm model was studied between 298 K to 308 K. The results of Temkin model have been shown in figure 5.2.9.3.1 (c). It became obvious from figure 5.2.9.2.1 (c) that at the two temperatures ranges namely 298 K and 303 K Temkin isotherm provided relatively better explanation of sorption of Zn (II) ion on the surface of bacterium *VMSDCM*.

The values of error functions are comparatively lower for this model together with relatively higher value of linear regression coefficient ( $R^2$ ). Additionally, the reported linear equation is completely superimposable on the ideal model equation having positive slope and intercept. The results of the concerned model with respective constants have been shown in table 5.2.9.2.1 (a).

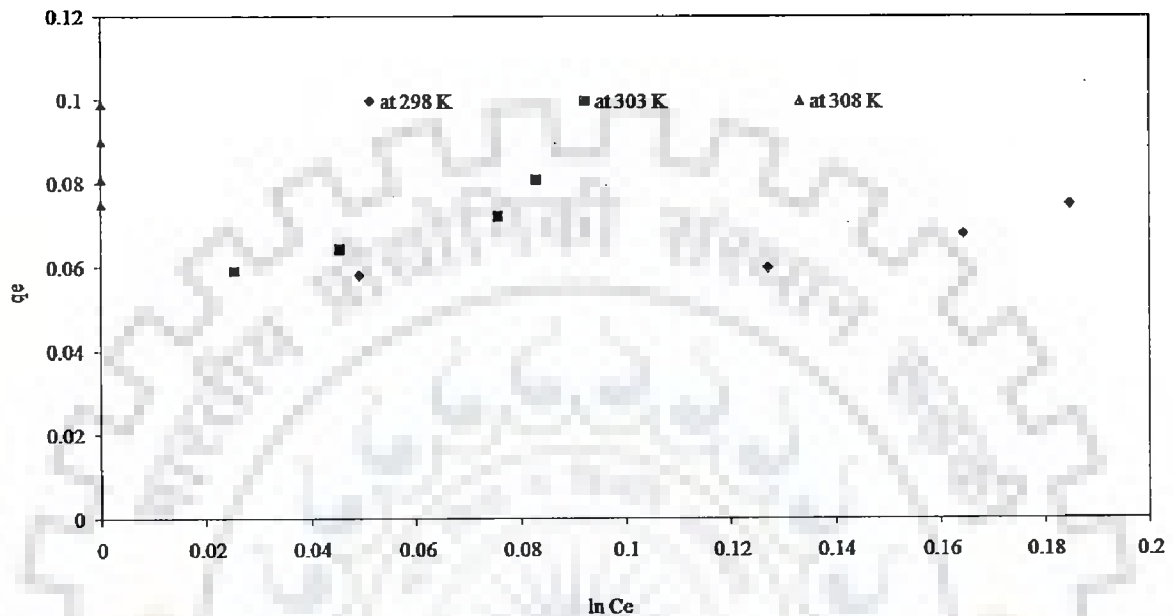


Figure 5.2.9.2.1 (c): Study of Temkin isotherm model between 298 K to 308 K

The slope and intercept of the curve between  $q_e$  and  $\ln C_e$  is infinity and zero, respectively at 308 K. The model constants  $B_t$  and  $K_t$  became undefined at the attainment of equilibrium.

Figure 5.2.9.2 (d) represents the Dubinin- Radushkevich equation (D-R) model study. The model Dubinin- Radushkevich equation (D-R) model was studied between 298 K to 308 K.

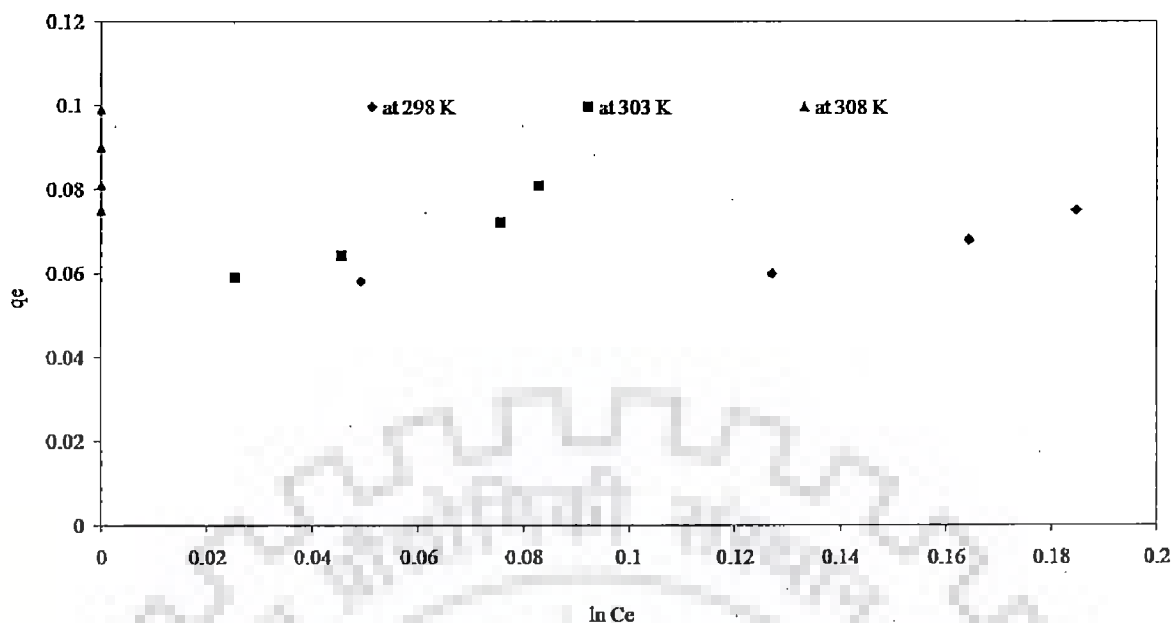


Figure 5.2.9.2.1 (d): Study of D-R model between 298 K to 308 K

The results of D-R model have been represented in figure 5.2.9.2 (d) and in table 5.2.9.2 (a). The values of intercept and slope obtained from D-R model were negative. Furthermore, at 308 K it became evident that slope and intercept of curve extrapolated between  $\ln q_e$  and  $\varepsilon^2$  is infinite and zero rendering all model constants undefined. Thus, it ruled out all the possibilities of D-R isotherm model fitting suitable to explain the binding of Zn (II) ion on the bacterium surface.

Table 5.2.9.2.1 (a): Study of various isotherm models between 298 to 308 K

Name of model	Equations	Temperature (K)	R <sup>2</sup>
Langmuir isotherm	$y = -4.173x + 24.22$	298	0.69
	$y = -16.80x + 35.86$	303	0.85
	$y = \infty x + 00.0$	308	1
Freundlich model	$y = 0.752x - 1.286$	298	0.781
	$y = 2.150x - 1.286$	303	0.943
	$y = \infty x + 00.0$	308	1
Temkin isotherm	$y = 0.113x + 0.050$	298	0.763
	$y = 0.340x + 0.049$	303	0.923

	$y = \infty x + 00.0$	308	1
D-R isotherm	$y = -6E-08x - 0.999$	298	0.943
	$y = -2E-08x - 3.070$	303	0.800
	$y = \infty x + 00.0$	308	1

### 5.2.9.2.2 Isotherm model development

Langmuir, Freundlich, Temkin and D-R isotherm proved incapable to provide better explanation of Zn (II) on the surface of *Zinc sequestering bacterium VMSDCM* accession no. HQ108109. Accordingly, an isotherm model has been developed in the present work to successfully interpret the sorption of Zn (II) onto the surface of bacterium VMSDCM, indeed. It became evident from the studies of various models that none of them is efficient enough to lucratively describe the sorption of Zn (II) ion on the surface of bacterium "VMSDCM". Only Temkin model up to some extent, i.e., at 298 K and 303 K can interpret the binding of metal ion on the surface of "VMSDCM" bacterium. In order to solve the issue of curve fitting cum predicting the goodness of curve and to obtain all the parameters/ constants in defined range from 298 K to 308 K, above mentioned isotherm models have been modified in the present investigation. Equation [5.8] represents the experimental model developed for the temperature 308 K. The principle assumption in this equation was the transition of extreme boundary conditions from  $t = 0$  hours and  $t = 8$  hours to  $t = t'$  and  $t = t''$  where  $t'$  and  $t''$  are the intermittent period of biosorption. The time interval  $t'$  to  $t''$ , virtually in this model signifies the intermittent time interval, between initial equilibrium concentration and final equilibrium concentration in liquid phase, respectively. The time interval kept between two boundary conditions was infinitesimally small, ranging between 2- 4 minutes at initial data point versus final data point. The limiting or saturation condition of model was dependent on the most possible value of equilibrium concentration before the liquid phase concentration of metal ion became zero. The model is based on the assumption that the surface of bacterium VMSDCM is hetrogenous and the sorption of metal ion occurs in multilayers. The first layer of ions gets adsorbed on the surface of the bacterium VMSDCM. Rest all other layers of metal ions are formed one over the another by ionic condensation, i.e., heat of condensation. The model also



assumes that the binding of the metal ion with bacterium surface is endothermic in nature (up to 308 K). The model has been represented in equation [5.8].

$$q_e = \left| \frac{q_m \cdot V_m C_e}{V_m C_e (2 - V_m) - C_{bm}} \right| + Aa' \quad [5.8]$$

where,  $V_m$  is the constant of point function at various temperature gradients. The value of  $V_m$  depends on the various types sorption heats related to heat of formation, isosteric heat of adsorption and heat of condensation. All the heat related functions are to be correlated as function of initial concentration of metal ion in batch liquid phase.  $C_{bm}$  ( $\text{mg l}^{-1}$ ) is adsorbate species concentration in liquid phase, enough to obtain the equilibrium with the residual sufficiently low to create mass transfer gradient at the end of biosorption,  $q_e$  is the equilibrium uptake capacity ( $\text{mg g}^{-1}$ ),  $q_m$  is the maximum uptake capacity ( $\text{mg g}^{-1}$ ) of the bacterium,  $C_e$  is the equilibrium concentration of Zn (II) ion in liquid phase and  $Aa'$  is the model constant. The results of the model have been shown in figure 5.2.9.2.2 (a) and table 5.2.9.2.2 (a).

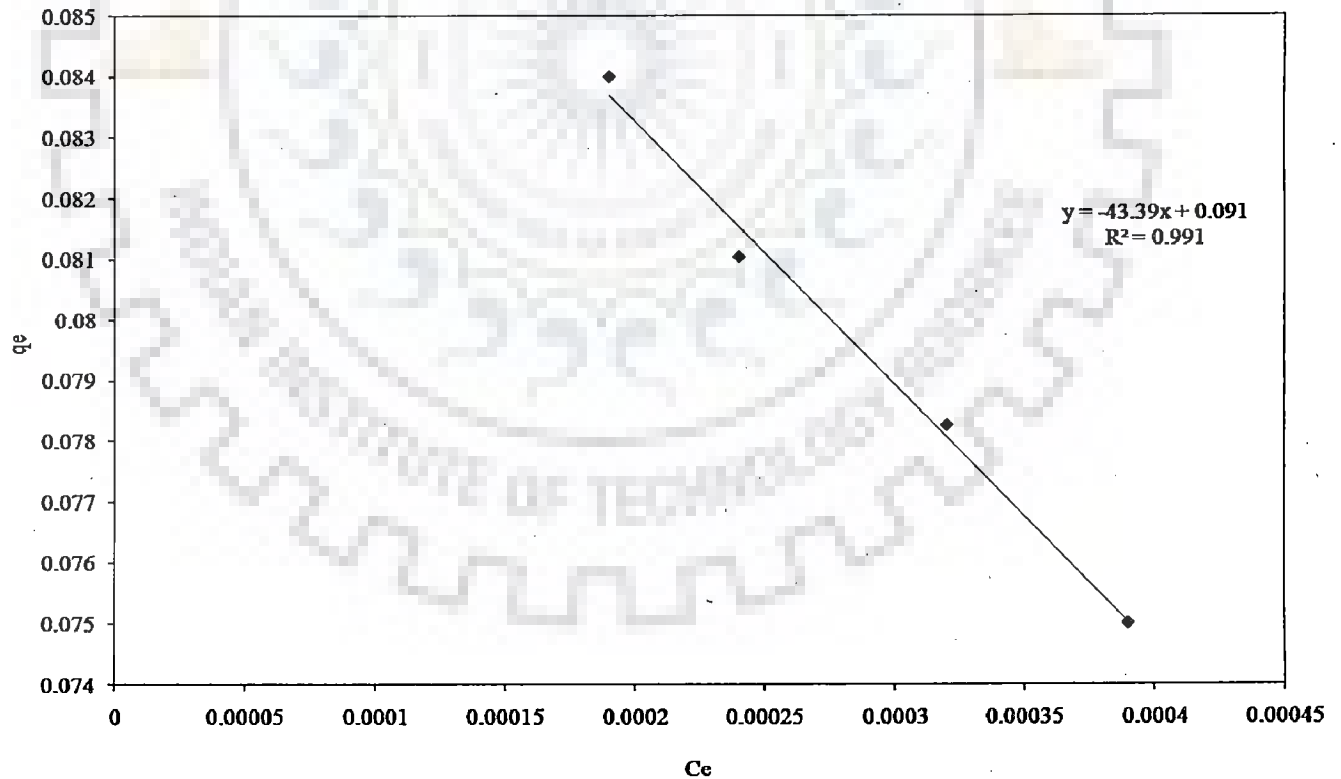


Figure 5.2.9.2.2 (a): Study of the proposed isotherm at 308 K

The linear regression coefficient of this model is quite high together with the very low values of error predicting functions, i.e.,  $\chi^2$  and SSE. Furthermore, the maximum uptake capacity  $q_{\max}$  ( $\text{mg g}^{-1}$ ) at all saturation concentration ranges, predicted by the model, derived from the slope of the curve is ample passable to give reasonable explanation of Zn (II) ion binding on bacterial surface.

Table 5.2.9.2.2 (a): Study of proposed isotherm model study at 308 K.

Equation	$V_m$	$A_a'$	$R^2$	$\chi^2$	SSE
$Y = 14.33X - 0.025$	123.1	0.109	0.99	0.011	0.007
$Y = 13.03X - 0.0160$	124.7	0.109	0.99	0.009	0.006
$Y = 11.55X - 0.010$	125.7	0.109	0.99	0.016	0.010
$Y = 10.73X - 0.0047$	126.1	0.109	0.99	0.777	0.224

The C++ program code was developed for the calculation of model correction constant  $A_a'$ . The model empirical constant cum correction factor ( $A_a'$ ) was calculated by C++ program in Developer Cpp. The code has been represented in annexure A - 3.

The main drawback of this model (equation 21) is its validation only for the temperature 308 K. For this reason and for the generalization of the model (equation 21) the same boundary conditions have also been implemented on conventional isotherm models and the results have been shown in table 5.2.9.2.2 (b).

Table 5.2.9.2.2 (b): Study of various isotherm models at 308K for the boundary condition  $t'$  to  $t''$  towards the attainment of equilibrium.

Isotherm	Temp.	$R^2$	$K_L$ (-)	SSE	$\chi^2$
Langmuir isotherm	308 K	0.99	573.2	0.363	-25.40
		0.99	814.375	0.0002	0.0004
		0.99	1062.55	0.0002	0.0004
		0.99	2283.0	0.0002	0.0003
Freundlich Isotherm	308 K	$R^2$	$1/n$ (-)	SSE	$\chi^2$
		0.52	0.00	0.34	4059145.96
		0.62	-0.00	0.30	6228885.10
		0.67	0.00	0.50	13433426.77
		0.95	0.00	0.58	86439188.06
Temkin Isotherm	308 K	$R^2$	$\ln K_t$	SSE	$\chi^2$
		0.53	0.00	0.00	0.01
		0.63	0.00	0.00	0.00
		0.68	0.00	0.02	0.04
		0.95	0.02	0.02	0.03
D-R Model	308 K	$R^2$	$q_e$ (Th)	$\chi^2$	
		0.08	$2.95 \times 10^{12}$	$2.94 \times 10^{12}$	
		0.19	$4.81 \times 10^{11}$	$4.81 \times 10^{11}$	
		0.17	$2.63 \times 10^9$	$2.63 \times 10^9$	
		0.62	$1.45 \times 10^8$	$1.453 \times 10^8$	

It became evident from table 5.2.9.2.2 (b) that the Langmuir, Freundlich, Temkin and D-R models have not enough adeptness to describe the adhesion of Zn (II) ion on the bacterial surface. All these models have very higher values of error reporting functions and lower linear regression coefficient ( $R^2$ ) except Langmuir isotherm.

In case of Langmuir isotherm, the model has negative value of sorption equilibrium ( $K_L, \text{mg}^{-1}$ ) constant coupled with absurd value of maximum uptake capacity ( $\text{mmoleg}^{-1}$ ) which is not at all feasible according to the model equation since the principle model equation represents the positive intercept of the isotherm extrapolated between  $C_e/q_e$  vs  $C_e$  at constant temperature and at fixed concentration.

The suitability of the equations [5.9] and [5.10] were validated through the linear regression coefficient ( $R^2$ ), statistical error functions like ( $\chi^2$ ) and sum of square errors (SSE). The linear regression coefficient was calculated through the inbuilt function in MS 2007.

Therefore, at the moment it becomes difficult to chalk out any model suitability. However, two derivatives of Langmuir model (type 3 and 4) having negative slope have been validated at the same boundary conditions. The respective model equations have been shown in eq. [5.9] and [5.10].

$$q_e = \frac{[q_m - (1/K_L)q_e]}{C_e} \quad [5.9]$$

$$q_e = K_L q_m - K_L q_e \quad [5.10]$$

The results of type 3 and 4 model validation have been shown in table 5.2.9.2.2 (b). The data represented in table 5.2.9.2.2 (c) shows the validation of Langmuir type 3 and 4 model at 308 K.

Table 5.2.9.2.2 (c): Results of equation [5.9] and [5.10] at boundary conditions.

Type 3	$1/K_L$	$R^2$	SSE	$\chi^2$
$Y = 2 \times 10^{-6} X + 0.073$	$2 \times 10^{-6}$	0.1	$9.33 \times 10^{-06}$	$1.59 \times 10^{-05}$
$Y = 3 \times 10^{-6} X + 0.078$	$3.0 \times 10^{-06}$	0.1	$3.123 \times 10^{-05}$	$9.75 \times 10^{-10}$
$Y = 2 \times 10^{-06} X + 0.088$	$2.00 \times 10^{-06}$	0.2	0.008	0.013
$Y = 4 \times 10^{-06} X + 0.094$	$4.0 \times 10^{-06}$	0.6	0.010	0.016
Type 4	$K_L$	$R^2$	SSE	$\chi^2$
Equation $Y = 42536X - 3025$	42536	0.1	0.084	0.095
$Y = 73147X - 5671$	73147	0.1	0.366	0.134
$Y = 10239 X - 8945$	10239	0.2	39347406.98	-6273.459
$Y = 151221 X - 14285$	15122	0.6	51747284.62	-7194.321

None of them was found suitable to elucidate the sorption of Zn (II) ion on bacterial surface for both the models. Both, type 3 and 4 models have very squat linear regression coefficients ( $R^2$ ) ranging between (0.1 – 0.6). Further, the comparison of equations derived in the present work against the ideal model equations [5.9] and [5.10] does not have any similarity, except representing straight line. The comparison between eq no. [5.9] and the equations derived for type 3 model (table 5.2.9.2.2(c)), indicate that model equation ideally has negative slope but in the present investigation, slope obtained was positive, rendering any further explanation to accept type 3 model as suitable and relevant for present work became nullified. Similarly, the comparison between type 4 model with equations (table 5.2.9.2.2 (c)) indicated the positive slope instead of negative slope values represented in ideal model equation [5.10]. Moreover, for the type 4 model, the value of error functions is significantly high compared to values reported for the isotherm. Here another isotherm model was proposed for the temperature range 298 K to 308 K, shown in equation [5.11]. The model has been divided into two parts. The first part (R. H. S) is from Temkin model coupled with model equation represented in equation [5.8]. The assumptions were similar to the assumptions assumed for equation [5.8].

$$q_e = B_1 \ln(K_1 C_e) + \left. \frac{q_m V_m C_e}{V_m C_e (2 - V_m) - C_{bm}} \right|_{t'}^{t''} + D_{vm} \quad [5.11]$$

where,  $V_m$  is the constant of point function at various temperature gradients,  $q_e$  is the equilibrium uptake capacity ( $\text{mg g}^{-1}$ ),  $q_m$  is the maximum uptake capacity ( $\text{mg g}^{-1}$ ) of the bacterium,  $C_{bm}$  ( $\text{mg l}^{-1}$ ) is adsorbate species concentration in liquid phase,  $C_e$  is the equilibrium concentration of Zn (II) ion in liquid phase and  $D_{VM}$  is the model constant obtained at all the permissible temperature ranges.

Another program was developed on developer C++ interface to calculate the model constant  $D_{vm}$ . The code of the program has been shown in annexure A-3. The results of equation [5.11] and model constants have been represented in table 5.2.9.2.2 (d), table 5.2.9.2.2 (e) and in figure 5.2.9.2.2 (b).

Table 5.2.9.2.2 (d): Results of equation [5.11] at various temperature and concentration ranges between 298 to 308 K, respectively

Equation	Temp. (K)	Chi ( $\chi^2$ ) value	Sum of square Errors (SSE)
$y = 0.053x + 0.007$	0.99 208	$1.1864 \times 10^{-3}$	$3.5344 \times 10^{-4}$
$y = 0.150x + 0.100$	0.99 303	$1.32013 \times 10^{-4}$	$3.7559 \times 10^{-5}$
$Y = -43.39x + 0.091$	0.99 308	$7.5933 \times 10^{-2}$	$1.67728 \times 10^{-1}$

Table 5.2.9.2.2 (e): Value of model constants between 298 to 308 K

Temperature (K)	Equation	$D_{vm}$	$B_t$	$K_t$	$R^2$
298	$y = 0.053x + 0.007$	0.00967263	0.038	1.37	0.99
303	$y = 0.150x + 0.100$	0.0027212	0.130	470.52	0.99
Temperature	Equation	$D_{vm}$	$C_{bm}$ (mmole <sup>-1</sup> )	$V_m$	$R^2$
308	$Y = -43.39x + 0.091$	0.10958825	5, 5.4, 6 and 6.6	123.1, 124.7, 125.7 and 126.1	0.99

Obviously, the data represented in tables 5.2.9.2.2 (a) and 5.2.9.2.2 (b) and in figures 5.2.9.2.2 (a) and 5.2.9.2.2 (b) established that model developed in the present investigation between 298 K to 308 K yields a clear explanation of sorption of Zn (II) ion on to bacterial surface indeed.

The proposed model explicitly involves the higher values of linear regression coefficient ( $R^2 = 0.99$ ) with minor values of error reporting functions, i.e.,  $\chi^2$  and SSE compared to other conventional models.

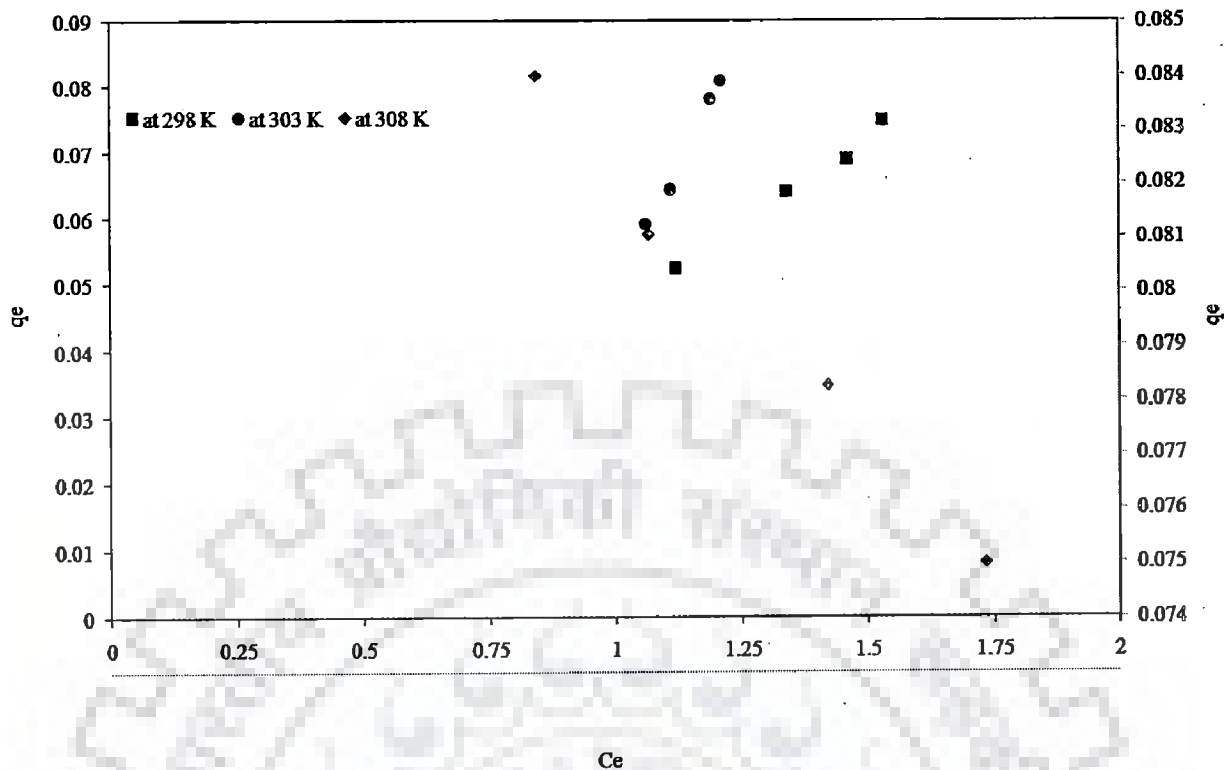


Figure 5.2.9.2.2 (b): Study of proposed model between 298 K– 308 K

#### Concluding remarks of the section 5.2.9.2.2

Various conventional isotherms were tried to validate the batch biosorption data obtained at attainment of equilibrium and at boundary conditions but none of them were found satisfactory to interpret the data obtained at boundary and at equilibrium condition. A new isotherm has been proposed and was found quite satisfactory in terms of higher  $R^2$  (0.99) and lower error functions to resolve this issue.

#### 5.2.9.2.3 Kinetic modeling on dead cells of *Zinc sequestering bacterium VMSDCM* accession no. HQ108109

This section describes the applicability of pseudo first and pseudo second order model for the sorption of Zn (II) ion on the surface of dead cells of *Zinc sequestering bacterium VMSDCM* accession no. HQ108109. The results of pseudo first order and pseudo second order model have been shown in figure 5.2.9.2.3 (a), figure 5.2.9.2.3 (b) , table 5.2.9.2.3 (a) and table 5.2.9.2.3 (b).



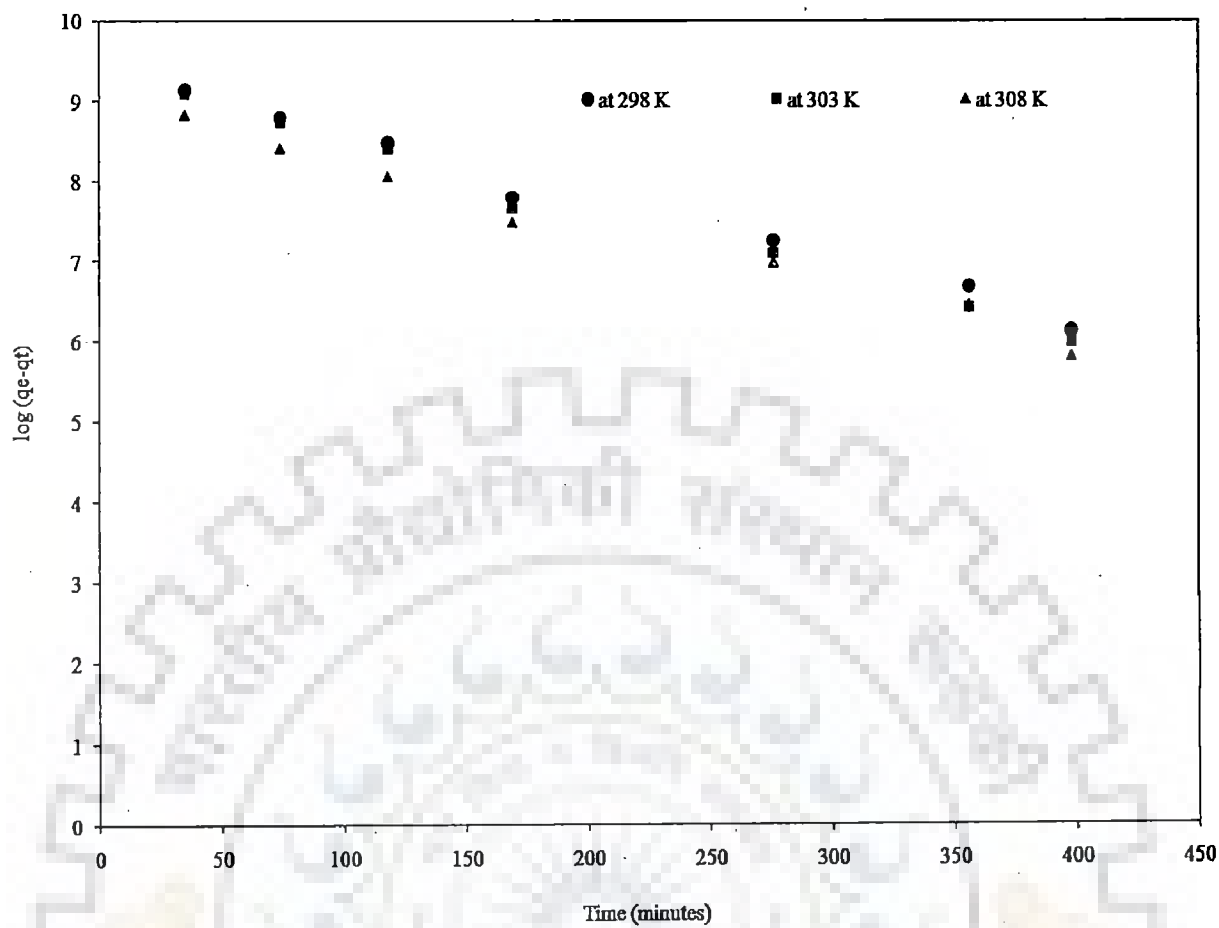


Figure 5.2.9.2.3 (a): Pseudo first order model study of Zn (II) ion biosorption on surface of *zinc sequestering bacterium VMSDCM* accession no. HQ108109

The study of pseudo first order and pseudo second order model indicated that both the models significantly explain the binding of Zn (II) on surface of *zinc sequestering bacterium VMSDCM*. The suitability of both the models for binding of Zn (II) ion on the surface of *zinc sequestering bacterium VMSDCM* accession no. HQ108109 indicated that the both physical adsorption (weak interaction between Zn (II) ion and cell wall moieties) and chemisorptions are involved (Naiya et al., 2008). Pseudo second order model was found superior to the pseudo first order rate kinetics.

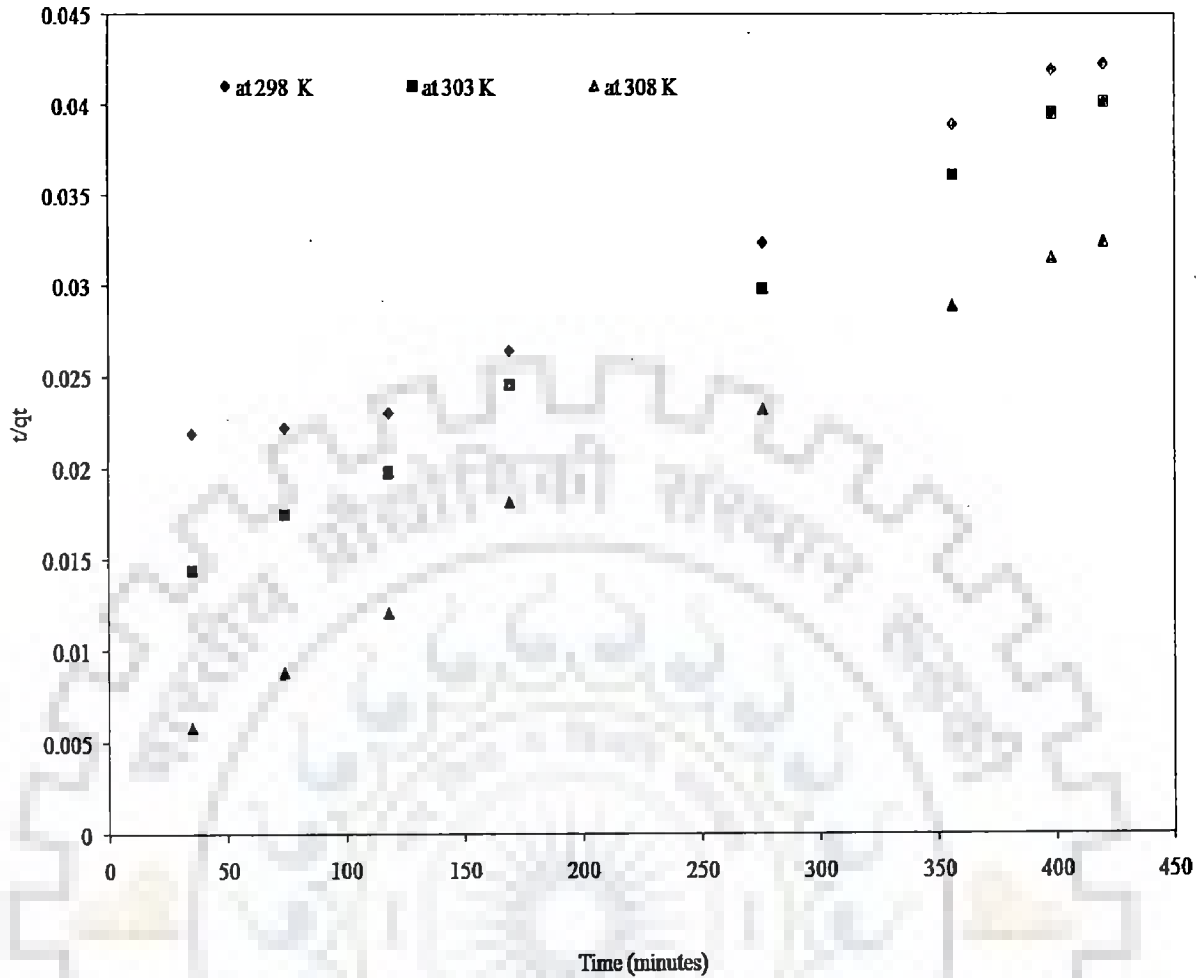


Figure 5.2.9.2.3 (b) : Pseudo second order model study of Zn (II) ion biosorption on surface of *zinc sequestering bacterium VMSDCM* accession no. HQ108109.

Precisely, the rate kinetics of the reaction adopts pseudo first order rate model for short initial time. Usually, this period is only recognized up to the 20% total uptake of the metal (Shek et al., 2009).

After passage of time, the surface of the *zinc sequestering bacterium VMSDCM* Accession no. HQ108109 became heavily loaded with Zn (II) ion and the concentration of zinc in liquid solution changed. Therefore, pseudo first order model was not efficiently applicable to endow a better explanation of rate kinetics.

Table 5.2.9.2.3 (a): Tabulation of kinetic model equations

Name of model	Model equation	Linear regression coefficient ( $R^2$ )	Temperature (K)
Pseudo first order kinetic model	$y = -0.007x + 9.366$	0.988	298
	$y = -0.008x + 9.331$	0.990	303
	$y = -0.007x + 8.999$	0.982	308
Pseudo second order equation	$y = 6 \times 10^{-5} + 0.017$	0.979	298
	$y = 7 \times 10^{-5} x + 0.012$	0.996	303
	$y = 7 \times 10^{-5} x + 0.004$	0.991	308

The values of linear regression coefficient ( $R^2$ ) of pseudo second order kinetic model were compared to pseudo first order kinetic model. Furthermore, the values  $\chi^2$  and SSE represented in table 5.2.9.2.3 (a) and table 5.2.9.2.3 (b) were quite less for pseudo second order rate kinetics against pseudo first order kinetics. Biosorption of Zn (II) ion on the surface of *zinc sequestering bacterium VMSDCM* accession no. HQ108109 with lower values of statistical error functions and with higher values of curve goodness of fit ( $R^2$ ) indicated the supremacy of pseudo second order rate kinetics over pseudo first-rate kinetics.

Table 5.2.9.2.3 (b): Tabulation of kinetic model equations constants

Name of model	Temperature (K)	Model constants ( $K_1, \text{min}^{-1}$ )	$\chi^2$	SSE
Pseudo first order kinetic model	298	$7 \times 10^{-3}$	4.8	28.9
	303	$8 \times 10^{-3}$	3.39	26.3
	308	$7 \times 10^{-3}$	2.89	21.1

Pseudo second order kinetic model	Temperature (K)	Model constants ( $K_2, \text{mgg}^{-1}\text{min}^{-1}$ )	$\chi^2$	SSE
	298	$1.681114 \times 10^6$	0.0021	0.081
	303	$1.312186 \times 10^6$	0.0013	0.052
	308	$6.712493 \times 10^5$	0.009	0.035

#### 5.2.9.2.4 Intra particle diffusion, Bangham's film diffusion model and thermodynamic modeling

The results of Intra particle diffusion and Bangham's film diffusion model have been shown in figure 5.2.9.2.4 (a), figure 5.2.9.2.4(b) and table 5.2.9.2.4 (a) and table 5.2.9.2.4 (b).

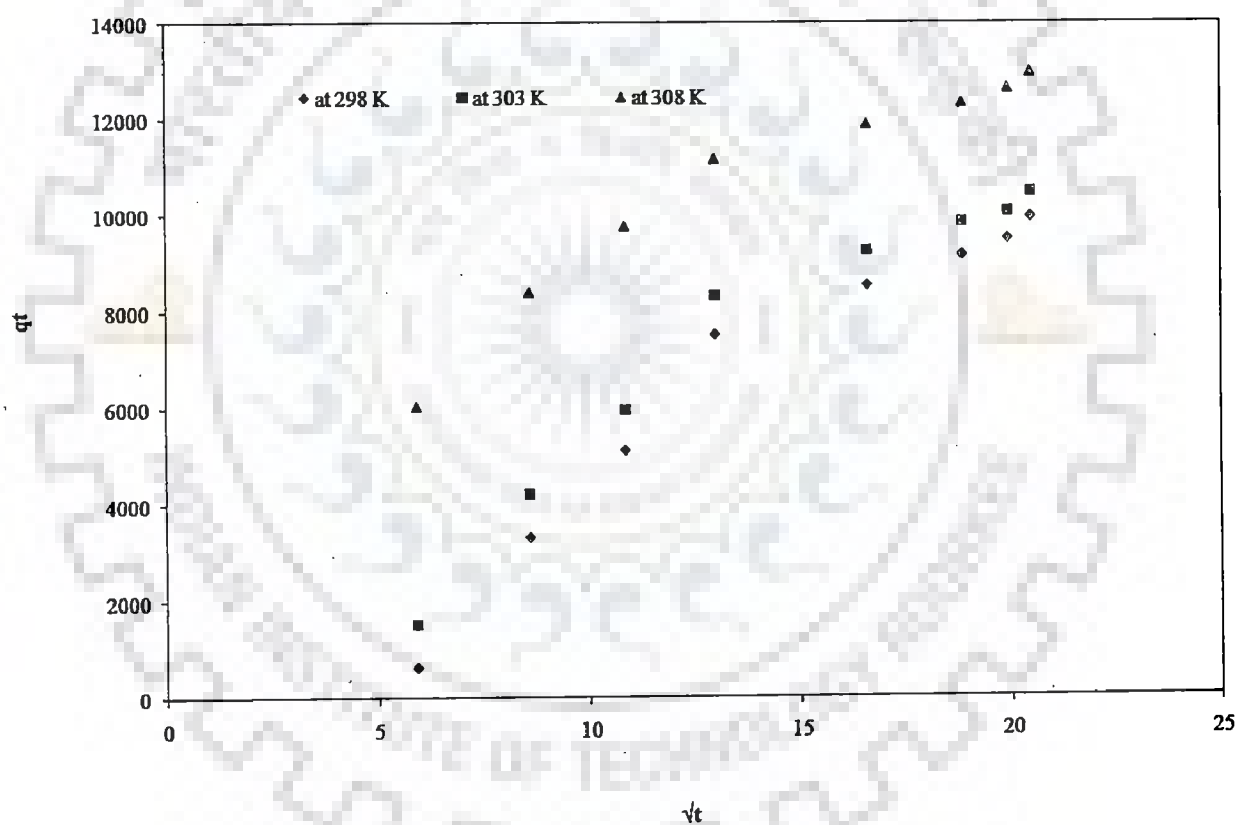


Figure 5.2.9.2.4 (a): Study of Intra particle diffusion model at various temperature ranges

Mass transfer in inter phase system is usually three step diffusion mediated mechanism. The three steps are as follows (i) mass transfer of metal ion from bulk liquid phase to the surface of the solid (the boundary layer) (ii) binding of the ligand or adsorbate with the surface of the

biosorbent, this step is quite fast (iii) Intra particle diffusion (pore diffusion) or solid surface diffusion. The rate of biosorption or adsorption depends on any one of these steps or a combination of steps. Considering the above-mentioned principles, figure 5.2.9.2.4 (a), figure 5.2.9.2.4 (b), table 5.2.9.2.1 (a) and table 5.2.9.2.4 (b) were analyzed.

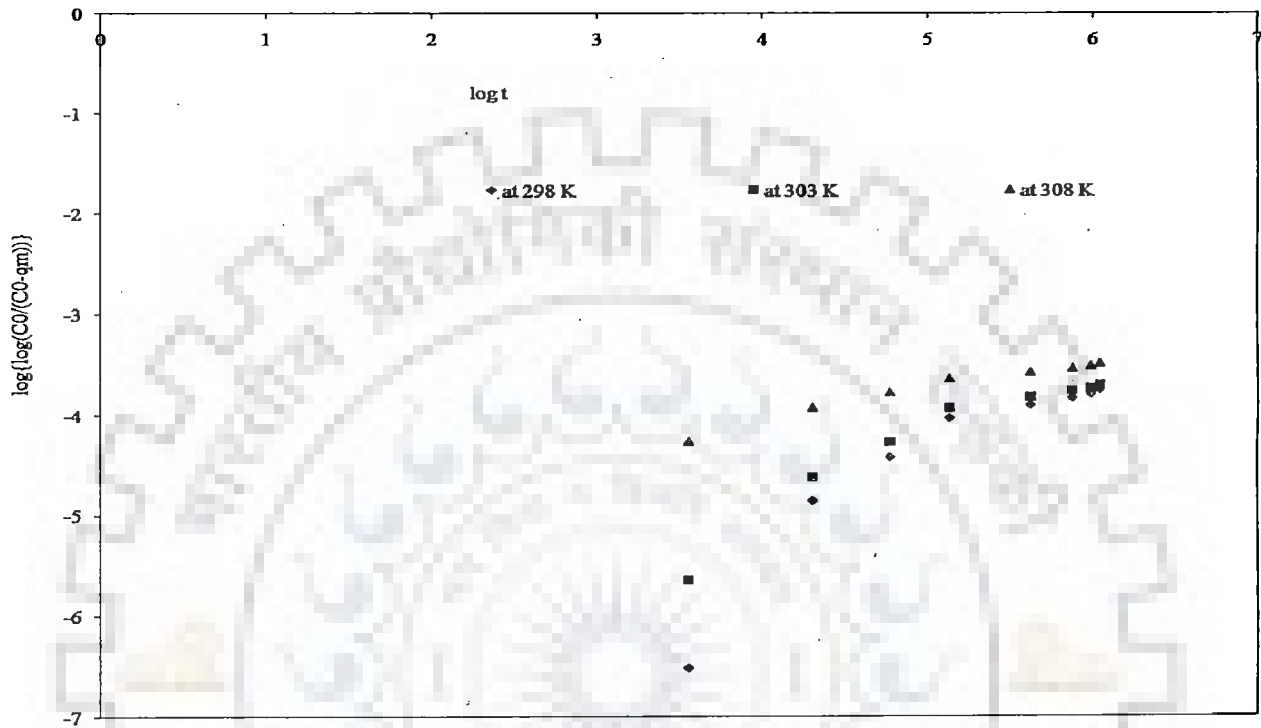


Figure 5.2.9.2.4 (b): Study of Bangham's film diffusion model at various temperature ranges

The curve of the intra particle model (figure 5.2.9.2.4 (a)) was multi linear in nature. The first part of the curve was the indicator of bulk diffusion of Zn (II) ions up to the boundary layer of the fluid over the bacterium VMSDCM. The second phase was dedicated to the slow sorption stage, which was intra particle diffusion.

The first portion was the bulk diffusion and the curve was linear over bulk or boundary layer diffusion portion. This step was quite rapid, therefore, it was concluded that during the onset of the process boundary layer diffusion was rate-controlling step and at the later stages of the metal ion binding, the intra particle diffusion was rate-limiting step.

Table 5.2.9.2.4 (a): Tabulation of mechanistic model equations

Name of model	Model equation	Linear regression coefficient ( $R^2$ )	Temp. (K)
Intra particle modeling	$y = 590.9x - 1726$	0.94	298 K
	$y = 566.2x - 631.6$	0.93	303 K
	$y = 420.9x + 4622$	0.926	308 K
Bangham's equation	$y = 0.970x - 9.402$	0.864	298 K
	$y = 0.705x - 7.832$	0.906	303 K
	$y = 0.288x - 5.207$	0.957	308 K

The curve of the intra particle diffusion did not pass through the origin, this indicated that the intra particle diffusion was not the only rate-limiting step of Zn (II) ion binding on the surface of *Zinc sequestering bacterium VMSDCM* Accession no. HQ108109. The value of constant C (intercept of intra particle diffusion) evaluates the thickness of the boundary layer. Moreover, it became evident from figure 5.2.9.2.4 (b), table 5.2.9.2.4 (a) and table 5.2.9.2.4 (c) that the Bangham's model equation can find its explanation scarcely in elucidating the mechanism of biosorption of Zn (II) ion on *Zinc sequestering bacterium VMSDCM* accession no. HQ108109 surface. The statistical error functions, i.e.,  $\chi^2$  and SSE for the intra particle diffusion were significantly lower compared to the Bangham's model (table 5.2.9.2.4 (b)).

Table 5.2.9.2.4 (b): Tabulation of mechanistic model equation constants

Name of model	Temperature (K)	Model constants (C)	$\chi^2$	SSE
Intra particle	298	1726	3.24	16.33
	303	631.6	2.95	14.65
	308	4622	1.18	9.56

	Temperature (K)	Model constants ( $K_0, l g^{-1}$ )	$\chi^2$	SSE
Bangham's equation	298	$4.77 \times 10^{-05}$	4.11	19.65
	303	$1.13 \times 10^{-07}$	3.04	16.15
	308	$4.77 \times 10^{-05}$	2.18	11.26

Contrary to this, linear correlation coefficient ( $R^2$ ) of intra particle model was higher at all the temperature ranges against Bangham's model (table 5.2.9.2.4 (a)). With these facts, in the present work, the intra particle model was considered more suitable to elucidate the basic mechanism of Zn (II) ion sorption on to the surface of *Zinc sequestering bacterium VMSDCM* Accession no. HQ108109 compared to Bangham's model. The thermodynamic feasibility of the biosorption of Zn (II) ion has been shown in equation [5.12].

$$y = -2 \times 10^{-6} x + 640.6 \quad [5.12]$$

$$R^2 = 0.750$$

The values of entropy ( $\Delta S$ ,  $kJ mol^{-1} K^{-1}$ ) and Enthalpy ( $\Delta H$ ,  $kJ mol^{-1}$ ) calculated from the equation [5.12] were  $5320.90 kJ mol^{-1} K^{-1}$  and  $16.628 \times 10^{-6} kJ mol^{-1}$ . The positive values of  $\Delta H$  and  $\Delta S$  indicated that the biosorption of zinc on *zinc sequestering bacterium VMSDCM* Accession no. HQ108109 surface was endothermic in nature with increased randomness at solid liquid interface.

The values of Gibbs free energy ( $\Delta G$ ,  $kJ mole^{-1}$ ) at various temperature ranges have been tabulated in table 5.2.9.2.4 (c). Negative values of  $\Delta G$  indicated that the biosorption of zinc on the surface of *zinc sequestering bacterium VMSDCM* accession no. HQ108109 was spontaneous in nature (table 5.2.9.2.4 (c)).

Table 5.2.9.2.4 (c): Study of Gibbs free energy and distribution coefficient at various temperature ranges

Temperature (K)	$\Delta G$ , (kJ mole <sup>-1</sup> )	Distribution coefficient ( $D_c$ )
298	-1585628.2	0.71
303	-1612232.7	0.89
308	-1638837.2	0.99

Additionally, the values of distribution coefficient ( $D_c$ ) were quite higher, i.e.,  $D_c > 0.5$  at all the temperature ranges. The values of  $D_c$  delineated the verity that the relatively higher number of Zn (II) ions were adsorbed on the surface of *zinc sequestering bacterium VMSDCM* accession no. HQ108109 against the concentration of Zn (II) ion in liquid phase. The increase in values of  $D_c$  with the increase of temperature indicated that the biosorption of Zn (II) ion on the surface of *zinc sequestering bacterium VMSDCM* Accession no. HQ108109 was temperature dependent and preferably endothermic in nature.

#### Concluding remarks of the section 5.2.9.2.4

The data obtained at equilibrium were modeled and the results shown that the pseudo second order kinetics and intra particle diffusion model were superior in explaining the mechanism of biosorption of Zn (II) ion on surface of *zinc sequestering bacterium VMSDCM* Accession no. HQ108109. The positive value of  $\Delta H$  and  $\Delta S$  categorized the biosorption of Zn (II) ion on *zinc sequestering bacterium VMSDCM* Accession no. HQ108109 as endothermic in nature with increased randomness at solid liquid interface. The negative values of  $\Delta G$  with  $D_c > 0.5$  classified the biosorption of Zn (II) spontaneous in nature.

### 5.3 BIOSORPTION OF Zn (II), Fe (II, III) AND Cu (II) IN SYNTHETIC SIMULATED WASTEWATER AND REAL WASTEWATER

#### 5.3.1 Studies on Synthetic Simulated Wastewater

This section embodies the results of biosorption of Zn (II), Fe (II, III) and Cu (II) ion from synthetic simulated wastewater from Zinc plating industry and Copper smelting plant. The



effluent from zinc plating industry contains zinc and iron. The effluent from copper smelting plant contains zinc, iron and copper. The experiments were conducted at 800 rpm, temperature 303 K, 0.05 mm particle size, 1 g l<sup>-1</sup> adsorbent dose and 6 hours contact time for *Cedrus deodara* sawdust. The experiments were conducted in round bottom flasks of 500 ml capacity containing synthetic simulated wastewater and real industrial wastewater. The experimental conditions for dead cells of *Zinc sequestering bacterium VMSDCM* accession no. HQ108109 were 300 rpm, temperature 308 K, 4 hours of contact time 1 g l<sup>-1</sup> of biomass dose. Results of biosorption of Zn (II), Fe (II, III) and Cu (II) ion from synthetic simulated waste water has been shown on table 5.3.1 (a) and 5.3.1 (b). The composition of synthetic simulated wastewater has been shown in table 3.5 (a) and table 3.5 (b). The higher values of metal ions were considered in all kinds of effluents. Table 5.3.1 (a) represents the biosorption of Zn (II) and total Fe (II, III) ions in synthetic simulated wastewater (Zinc plating industry). The effluent from Zinc plating industry contains the Zn (II) and total Fe (II, III) ions in various concentrations. It is clear from table 5.3.1(a) that the removal of Zn (II) and total Fe (II, III) ion was quite low as reported in case of pure binary component mixture of metal ions in both the types of biosorbents (Figure 5.2. 4 (j), figure 5.2.4 (r)).

Table 5.3.1 (a): Results of biosorption of Zn (II) and total Fe (II, III) ions in synthetic simulated wastewater (Zinc plating industry, wastewater containing Zn (II) and total Fe (II,III))

Name of biosorbent	pH	Temp. (K)	Initial concentration (mg/l)	Final concentration (mg/l)	% removal of Zn (II) ion	% removal of Fe (II, III) ion
<i>Cedrus deodara</i> sawdust	2.5	303	70200 (Zn)	37908 (Zn)	46.55	-
	2.5	303	20390 (Fe)	14273 (Fe)	-	30.34
<i>Zinc sequestering bacterium VMSDCM</i> accession no. HQ108109 (dead cells)	2.5	308	70200 (Zn)	33458 (Zn)	52.34	-
	2.5	308	20390 (Fe)	11338 (Fe)	-	44.39

The rationale behind the lowering of the removal of Zn (II) and total Fe (II, III) ions was the pH of the synthetic simulated wastewater. The pH being 2.5 hindered the biosorption of Zn (II) and total Fe (II, III) ion from liquid phase by providing extreme competition between hydrogen ion (H<sup>+</sup>) and metal ions (Mishra et al., 2010). Both the types of ions compete for the same active binding sites.

However, the biosorption of Zn (II) and total Fe (II, III) ion was relatively higher in case of *Zinc sequestering bacterium VMSDCM* accession no. HQ108109 than the *Cedrus deodara* sawdust. The higher percentage removal of Zn (II) and total Fe (II, III) in case of *Zinc sequestering bacterium VMSDCM* accession no. HQ108109 may be due to the variation in surface texture and surface chemistry of the biosorbent.

The preferential order of removal of heavy metal ions was Zn (II) > Fe (II, III). Table 5.3.1 (b) represents the biosorption of Zn (II) and total Fe (II, III) ions in synthetic simulated wastewater (Copper smelting plant). Effluent from copper smelting plants contain various amounts of Zn (II), Cu (II) and total Fe (II, III).

Table 5.3.1 (b): Results of biosorption of Zn (II), total Fe (II, III) and Cu (II) ions in synthetic simulated wastewater (Copper smelting plant, wastewater containing Zn (II), Cu (II) and total Fe (II,III))

Name of biosorbent	pH	Temp. (K)	Initial concentration (mg/l)	Final concentration (mg/l)	% removal of Zn (II) ion	% removal of Fe (II, III) ion	% removal of Cu (II) ion
<i>Cedrus deodara</i> sawdust	0.6	303	142 (Zn)	120.7	15.33		
	0.6	303	188 (Fe)	162.88		13.36	
	0.6	303	93 (Cu)	73.4			21.22

biosorbent							
<i>Zinc</i>	0.6	308	142 (Zn)	113.04 (Zn)	20.39		
<i>sequestering</i>	0.6	308	188 (Fe)	156.77 (Fe)		16.61	
<i>bacterium</i>	0.6	308	93 (Cu)	130.97 (Cu)			30.33
<i>VMSDCM</i>							
accession							
no.							
HQ108109							
(dead cells)							

It is clear from table 5.3.1(b) that the removal of Zn (II), total Fe (II, III) and Cu (II) ion was quite low as reported in case of pure ternary component mixture of metal ions in both the types of biosorbents (Figure 5.2. 4 (j), figure 5.2.4 (r)). The rationale behind the lowering of the removal of Zn (II) and total Fe (II, III) ions was the pH of the synthetic simulated wastewater. pH of wastewater being 0.6 hindered the biosorption of Zn (II) and total Fe (II, III) ion from liquid phase by providing extreme competition between hydrogen ion (H<sup>+</sup>) and metal ions. Both the types of ions compete for the same active binding sites. However, the biosorption of Zn (II) and total Fe (II, III) ion was relatively higher in case of *Zinc sequestering bacterium VMSDCM* accession no. HQ108109 than the *Cedrus deodara* sawdust. The higher percentage removal of Zn (II), Cu (II) and total Fe (II, III) in case of *Zinc sequestering bacterium VMSDCM* accession no. HQ108109 was may be due to the variation in surface texture and surface chemistry of the biosorbent. The preferential order of removal of heavy metal ions was Cu (II) > Zn (II) > Fe (II, III).

### 5.3.2 Studies on biosorption using real wastewater

Table 5.3.2 (a) represents the biosorption of Zn (II), total Fe (II, III) and Cu (II) ions in real industrial wastewater. The wastewater from zinc producing industry (real wastewater) contains Zn (II), Cu (II) and total Fe (II, III). The experimental conditions were same as conditions mentioned in section 5.3.1. The wastewater was collected from industry Hindustan Zinc Limited, SIDCUL, HARDWAR.

Table 5.3.2 (a): Results of biosorption of Zn (II), Cu (II) and total Fe (II, III) ions in real industrial wastewater (Zinc manufacturing industry, wastewater containing Zn (II), Cu (II) and total Fe (II,III))

Name of biosorbent	pH	Temp. (K)	Initial concentration (mg/l)	Final concentration (mg/l)	% removal of Zn (II) ion	% removal of Fe (II, III) ion	% removal of Cu (II) ion
<i>Cedrus deodara</i> sawdust	5.28	303	4000 (Zn)	3174.4 (Zn)	20.64		
	5.28	303	2389 (Fe)	887.75 (Fe)		62.84	
	5.28	303	123 (Cu)	105.33(Cu)			14.36
<i>Zinc sequestering bacterium</i> VMSDCM accession no. HQ108109 (dead cells)	5.28	308	4000 (Zn)	2407.6 (Zn)	60.19		
	5.28	308	2389 (Fe)	1449.40 (Fe)		39.33	
	5.28	308	123 (Cu)	2686 (Cu)			78.16

It is clear from table 5.3.2 (a) that the removal of Zn (II), total Fe (II, III) and Cu (II) ion was quite low as reported in case of pure ternary component mixture of metal ions in both the types of biosorbents (Figure 5.2. 4 (j), figure 5.2.4 (r)). The rationale behind the lowering of the removal of Zn (II) and total Fe (II, III) ions was very high concentration of Zn (II) and total Fe (II, III) ion. However, the variation in percentage removal of Cu (II) ion in pure synthetic ternary metal ion solution and real wastewater was very close. The reason behind the very close values of percentage removal of Cu (II) ion was initial concentration of Cu (II) ion in both the types of metal ion systems. However, the biosorption of Zn (II) and total Fe (II, III) ion was relatively higher in case of *Zinc sequestering bacterium* VMSDCM accession no. HQ108109 than the *Cedrus deodara* sawdust. The higher percentage removal of Zn (II), Cu (II) and total Fe (II, III) in case of *Zinc sequestering bacterium* VMSDCM accession no. HQ108109 may be due to the variation in surface texture and surface

chemistry of the biosorbent. The preferential order of removal of heavy metal ions was Cu (II) > Zn (II) > Fe (II, III).

### **Concluding remark of the section 5.3.3**

*Zinc sequestering bacterium VMSDCM* accession no. HQ108109 and *Cedrus deodara* sawdust has tremendous potential of treating synthetic simulated and real wastewater.

## **5. 4 Isolation, Purification and Characterization of Zinc Resistant Microbial Strain**

Hindustan Zinc Limited (HZL), SIDCUL, Hardwar, is involved in the extraction of zinc from its various ores. The wastewater discharging out from industrial unit originates from ore washing unit, smelting, refinement section and final metal finishing unit. The samples of effluent was collected from three different places, i.e., from open tank where the effluent was getting stored, from the tap from where the effluent was discharged, and from the outlet of ion exchange unit where the effluent was discharged after treatment. All the samples were collected in dark amber coated bottles in the month of June 2010 when the atmospheric temperature was approximately 308 K. These samples of effluent were collected in sterilized screw cap bottles and kept in ice packs. They were kept at 277 K until further use. All the samples were collected and preserved as per American Public Health Association (APHA) guidelines. (Mishra et al., 2011)

### **5.4.1 Isolation of microbial strains and purification**

The microbial strains were isolated from the effluent by serial dilutions in autoclaved normal saline (0.8% NaCl). Each dilution was plated separately on 100 mg l<sup>-1</sup> of zinc amended LB agar medium. These plates were incubated at 308 K for 24 hours. The microbial colonies growing on the medium were considered tolerant to zinc. These microbial isolates were cultured on minimal salt agar medium at a temperature of 308 K and at pH 7.0. Various concentrations of zinc ranging between 0.5 mM to 7.0 mM were added to the minimal agar medium plates. One, out of five isolates, was found capable of growing in zinc amended minimal medium. This was considered as zinc tolerant bacteria. Plates of the grown bacterium have been shown in figure 5.4.1 (a)



Figure 5.4.1 (a): Petri plates showing the growth of *Zinc sequestering bacterium VMSDCM* accession no. 108109

#### **5.4.2 Genomic DNA isolation**

Total genomic DNA of the microbial strain was isolated from 5 ml culture grown overnight in Luria Bertani broth (Bangalore Genei DNA isolation kit). Cells were re-suspended in 300 µl of lysis buffer and kept at a temperature of 373 K for about 15 minutes. It was further allowed to cool at room temperature. RNase solution was added to the cell resuspension and kept for incubation at 310 K for 1 hour following addition of 100 µl protein precipitation solution. The whole cell resuspension was incubated for a period of 5 minutes. Centrifugation was done at a temperature of 277 K and 8000 xg for 10 minutes. Supernatant was collected in a tube and DNA was precipitated with 95% of ethanol (v/v). DNA precipitate was washed with 70% ethanol (v/v). The pellet was dissolved in sterile nuclease free water after centrifugation.

#### **5.4.3 Polymerase Chain Reaction (PCR)**

Genomic DNA isolated from isolated microbial strain was subjected to 16S rRNA identification using universal primers F (5'-AGA GTT TGA TCC TGG CTC AG-3') and (5'-ACG GCT ACC TTG TTA CGA CTT-3'). Reaction mixture for PCR consisted of 13.5 µl of master mix, genomic DNA (5µl), 3µl (10 pmol/µl) of forward and reverse primers each and the volume was made up to 29.5 µl by sterile nuclease free water. MJ research thermal cycler was used with a 30-cycle program for PCR. An initial denaturation temperature at 368 K for 2 minutes was followed by denaturation at 368 K for 1 minute, annealing at 321 K for 1 minute, extension at 345 K for 1 minute and final extension at 345 K for 5 minutes. Amplification was confirmed by running the PCR products on 1% agarose gel. A desired length was cut from the gel and purified using Bangalore genei PCR purification kit and after elution, the product was sent to Ocimum biosolutions for sequencing. Similarity searches were conducted using NCBI BLAST program of the PHYLIP package (Phylogeny inference package version 3.5c) (Felsenstein, 1993).

#### **5.4.4 Submission of sequence**

The submission of the sequence of the most efficient bacterial isolate was performed by submitting the sequence through BankIt channel of NCBI website. The sequences were uploaded in the FASTA format. The name of the bacterium strain was proposed during the

submission of the sequences. Other options used during submission were as follows (i) unpublished information (ii) original sequencing (iii) pure culture (iv) universal primers (v) environmental conditions.

#### **5.4.5 Phylogenetic, biochemical and Scanning Electron microscopic characterization of Zinc Resistant Microbial Strain**

The bacterium seemed to cluster up with arsenite oxidizing bacteria when plotted in a maximum likelihood tree. The sequence was submitted to NCBI under the accession number of HQ108109 with the name *Zinc sequestering bacterium VMSDCM*. Figure 5.4.5 (a) illustrates the phylogenetic analyses of the bacterium conducted in MEGA 4 (Tamura et al., 2007).





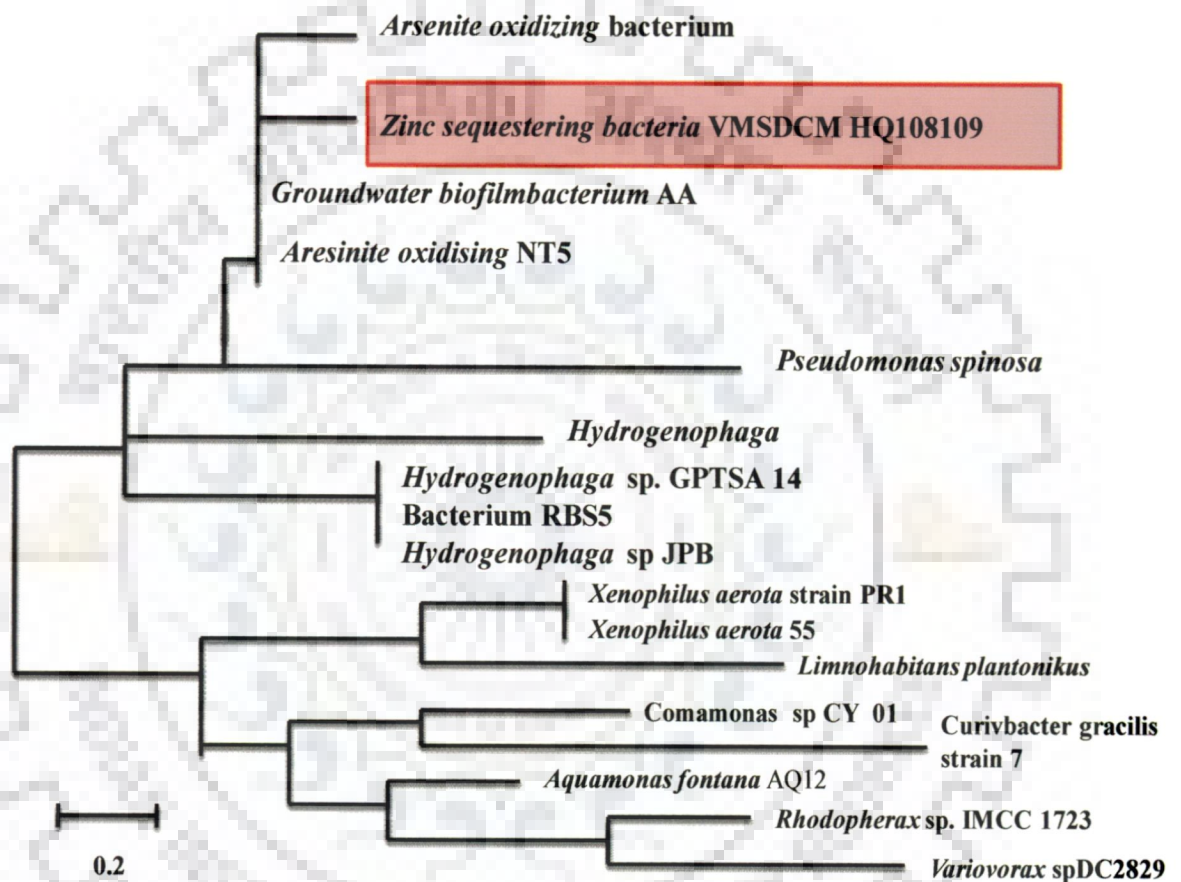


Figure 5.4.5 (a): Phylogenetic tree of 16S rRNA amplified products for Zinc sequestering bacteria. The percentage of replicate trees in which the associated taxa cluster together in the boot strap test (1000 replicates) are shown next to the branches

The evolutionary history was inferred using the Neighbour-Joining method (Saitou and Nei, 1987). The optimal tree with the sum of branch length of 0.09345642 is shown in the figure. The tree is drawn to scale, with branch lengths in the same units as those of the evolutionary distances used to infer the phylogenetic tree. The evolutionary distances were computed using the Jukes-Cantor method (Jukes and Cantor 1969) and were in the units of the number of base substitutions per site. The bacterium seemed to cluster up with arsenite oxidizing bacteria when plotted in a maximum likelihood tree.

#### **5.4.5.1 Biochemical characterization of *Zinc sequestering bacterium VMSDCM* Accession no. HQ108109**

The biochemical characterization of isolated bacterium was performed by gram staining methodology. The shape and cell wall characteristic of *Zinc sequestering bacterium VMSDCM* Accession no. HQ108109 was studied through phase contrast microscopy. Figure 5.4.5.1 (a), figure 5.4.5.1 (b) and figure 5.4.5.1 (c) represent the SEM, gram stain and phase contrast photograph of *Zinc sequestering bacterium VMSDCM* accession no. HQ108109.



Figure 5.4.5.1 (a): Gram stained photograph of bacterium *Zinc sequestering bacterium* VMSDCM accession no. HQ108109



Figure 5.4.5.1 (b): Gram stained (Phase contrast) photograph of bacterium *Zinc sequestering bacterium VMSDCM* accession no. HQ108109

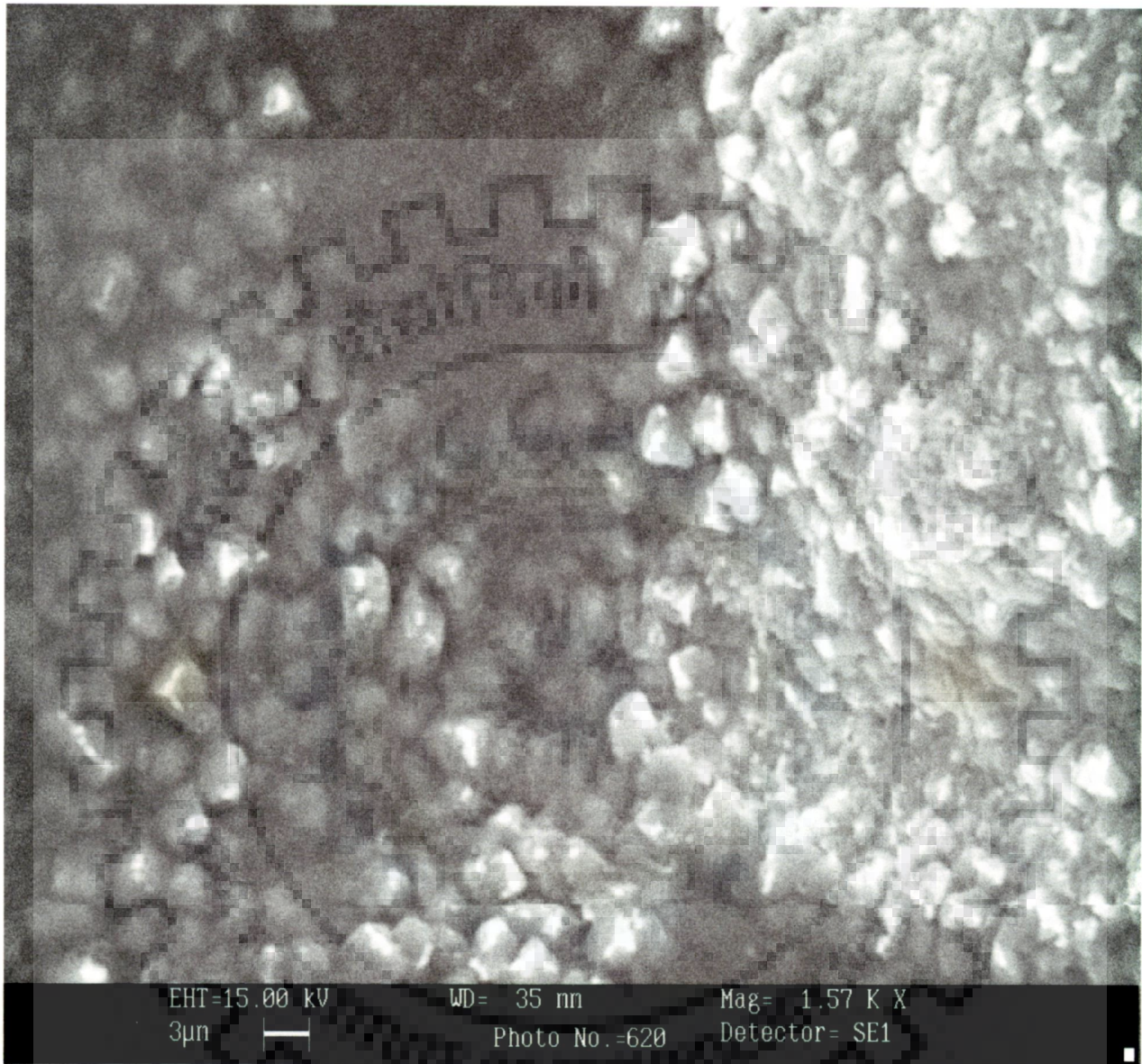


Figure 5.4.5.1 (c): SEM photograph of *Zinc sequestering bacterium VMSDCM* accession no. HQ108109

It is evident from the figures 5.4.5.1 (a), figure 5.4.5.1(b), figure 5.4.5.1 (c) that the cells isolated and used in the present investigation were rod shaped with gram negative cell wall characteristic. The cell wall of gram-negative bacteria consists of lipotechoic acids/lipopolysaccharide (LPS), lipoprotein, porins, peptidoglycan and phospholipids.

Phosphate and carboxyl groups present in LPS and phospholipids render the bacterial cell surface with a net negative charge. Mainly, the phosphate and carboxyl group present in phospholipids and LPS are primary sites of metal ion binding on to surface of the bacterial cell.

Kazy et al., 2009 reported the presence of carboxyl and phosphate groups on the surface of gram negative *Pseudomonas* strain (MTCC 3087). Kazy et al., 2009 reported the significant involvement of these functional groups in binding of uranium and thorium onto bacterium surface. In the present study, the binding of Zn (II) ion onto surface of bacterium *Zinc sequestering bacterium VMSDCM* accession no HQ108109 was probably due to the presence of negatively charged groups present on the surface of this gram-negative bacterium, indeed.

The SEM analysis was made on 15 kV. The biomass surface seemed to be porous and non-crystalline before the sorption of metal ion. Matrix protrusions were also observed in figure 5.4.5.1 (c), running inside the cell mass. Figure 5.4.5.1 (d) represents the SEM photograph of bacterium after the sorption of metal ion.

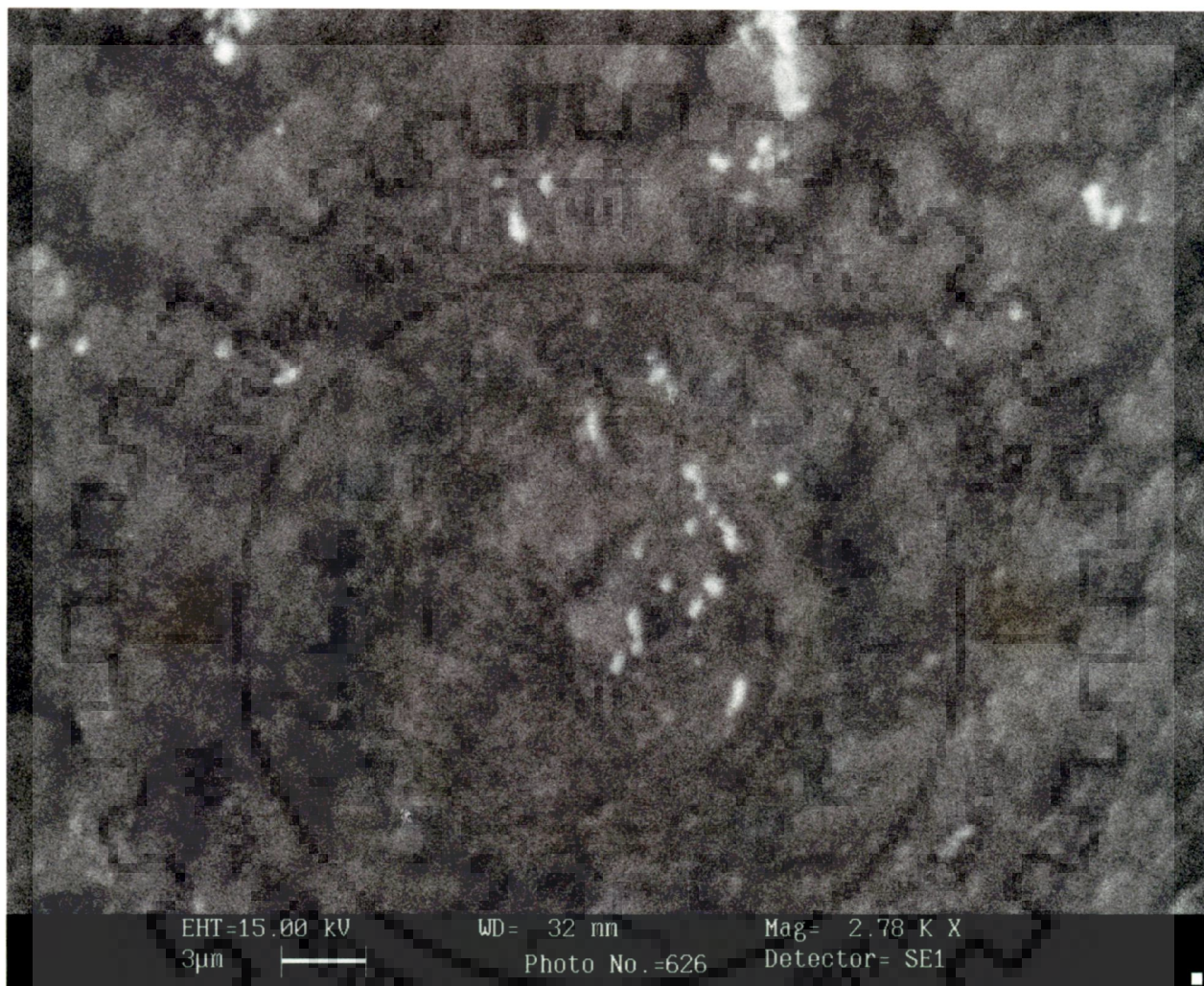


Figure 5.4.5.1 (d): SEM photograph of *Zinc sequestering bacterium VMSDCM* accession no. HQ108109 (after adsorption)

The surface of metal biomass looked smooth and crystalline in nature without surface protrusions, indicating the impregnation of Zn (II) ion on biomass surface.

#### **Concluding remarks of the 5.4.5**

SEM analysis of bacterial surface indicated the presence of non-crystalline surface full of protrusions running into the *Zinc sequestering bacterium VMSDCM* accession no HQ108109. The bacterium *Zinc sequestering bacterium VMSDCM* Accession no HQ108109 were identified as gram negative and rod shaped.

### **5.5 SIMULTANEOUS BIOSORPTION AND BIOACCUMULATION (SBB) OF ZN (II) ION IN LIQUID PHASE IN BATCH STUDY**

#### **5.5.1 Batch study**

The standard growth curve of the *Zinc sequestering bacterium VMSDCM* Accession no. HQ108109 has been shown in figure 5.5.1.1. The standard growth curve of the bacterium was extrapolated in optimized environmental conditions. The Luria Bertaini broth was used to achieve the growth of bacterium. Furthermore, the growth of the bacterium was also analyzed in various environments of zinc, copper and iron.

##### **5.5.1.1 Standard growth curve of bacterium**

The standard growth curve of the bacterium has been shown in figure 5.5.1.1 (a). The growth of the bacterium was observed at 600 nm (Mishra et al., 2011). The standard growth curve of the *Zinc sequestering bacterium VMSDCM* accession no. HQ108109 was drawn at optimized parameters such as pH 7, temperature 303 K and agitation rate of 150 rpm.



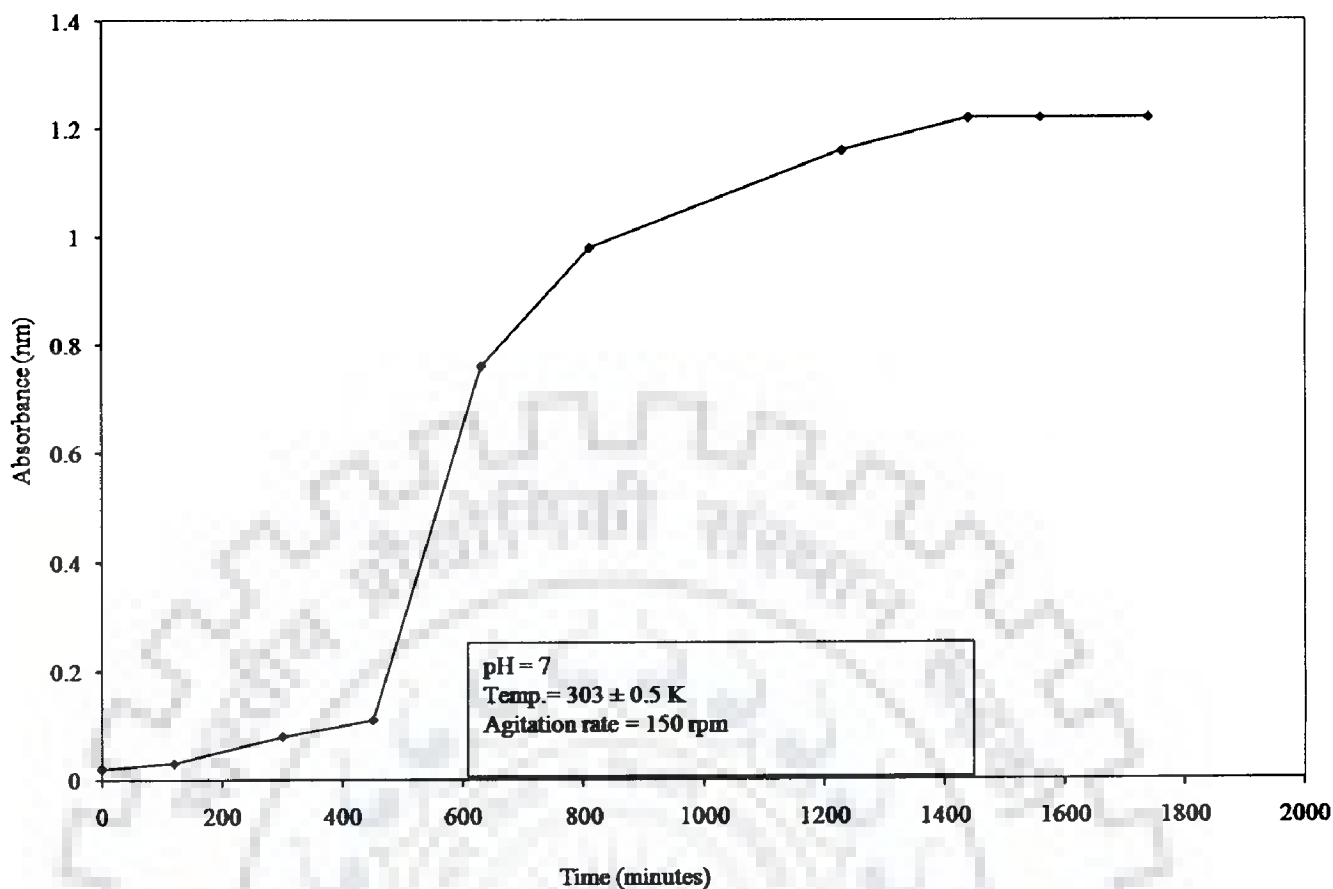


Figure 5.5.1.1 (a): Standard growth curve of *Zinc sequestering bacterium VMSDCM* Accession no. HQ108109

It is clear from figure 5.5.1.1 (a) that the stationary phase of bacterial growth exists between 1440 to 1740 minutes. A initial lag period in the growth of *Zinc sequestering bacterium VMSDCM* accession no. HQ108109 has been observed during 0 minute to 450 minutes. The growth curve of *Zinc sequestering bacterium VMSDCM* accession no. HQ108109 in various environments of Zn (II), total Fe (II, III) and Cu (II) ions has been discussed in section 5.5.2.

#### 5.5.2.1 Growth of *Zinc sequestering bacterium VMSDCM* Accession no. HQ108109 in pure zinc environment

Figure 5.5.2.1 (a) represents the growth curve of bacteria in an environment having variable amount of zinc ranging between 65.37 g/l to 523.04 g l<sup>-1</sup>.

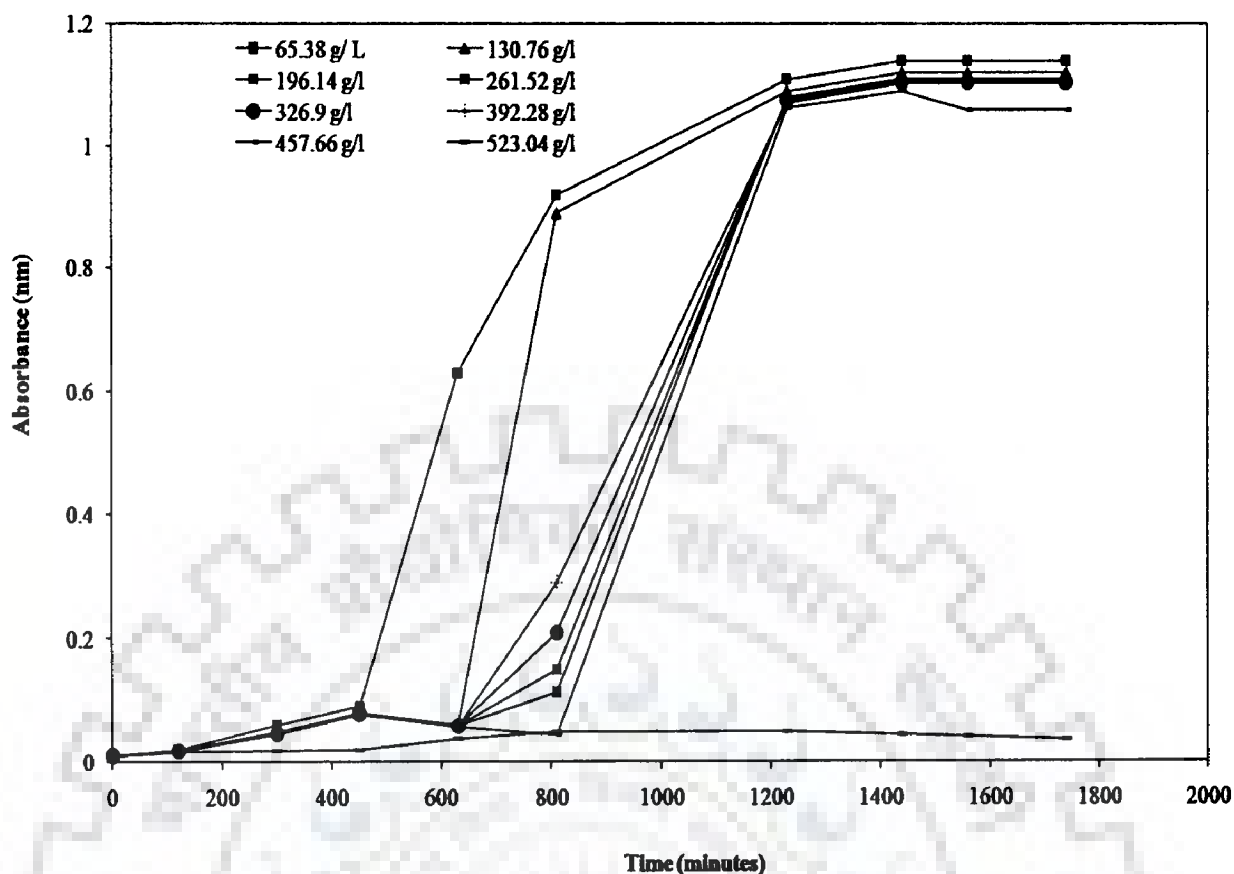


Figure 5.5.2.1 (a): Growth curve of *Zinc sequestering bacterium VMSDCM* accession no. HQ108109

The growth of bacteria was measured at 600 nm at predefined time interval (Mishra et al., 2011). It became evident from figure 5.5.2.1 (a) that the similar type of overall pattern of bacterial growth was observed from 0 to 1740 minutes in various environments of zinc concentration ranging between 65.38 to 457.66 g l<sup>-1</sup>. With the increase in concentration of zinc in liquid phase, the bacterial growth was found to be decreasing. The log and stationary phase of bacterial growth at all the concentrations of zinc, ranging between 65.38 to 457.66 g l<sup>-1</sup> were obtained in range of 450 to 1440 minutes and 1440 to 1740 minutes, respectively. In case of 523.04 g l<sup>-1</sup> of zinc, the growth pattern of microorganism was somewhat different. In an environment of 523.04 g l<sup>-1</sup> of zinc, the bacterium adopted short log phase, followed by stationary phase and finally cells entered the death phase. The rationale behind the short-term growth of bacteria in 523.04 g l<sup>-1</sup> was due to the role of relevant concentration as maximum inhibitory concentration (MIC). The growth of bacteria in absence and in presence of zinc (65.38 -457.66 g l<sup>-1</sup>) was almost same but the pattern of this range was quite different

compared to the bacterium growth in  $523.04 \text{ g l}^{-1}$  of zinc. With the experimental data obtained in growth rate determination experiments,  $457.66 \text{ g l}^{-1}$  of zinc in liquid phase was obtained as optimum zinc concentration in all other batch experimentals. In the higher concentration of zinc like  $523.04 \text{ g l}^{-1}$ , the microbes take longer time than the other zinc concentration for its growth. Ultimately, it produces longer lag phase situation in the growth curve.

**5.5.2.2 Growth of Zinc sequestering bacterium VMSDCM Accession no. HQ108109 in presence of copper and zinc**

Figure 5.5.2.2 (a) represents the growth curve of bacteria in an environment having  $457.66 \text{ g l}^{-1}$  of zinc and copper ranging between  $63.54 \text{ g l}^{-1}$  to  $254.16 \text{ g l}^{-1}$ .

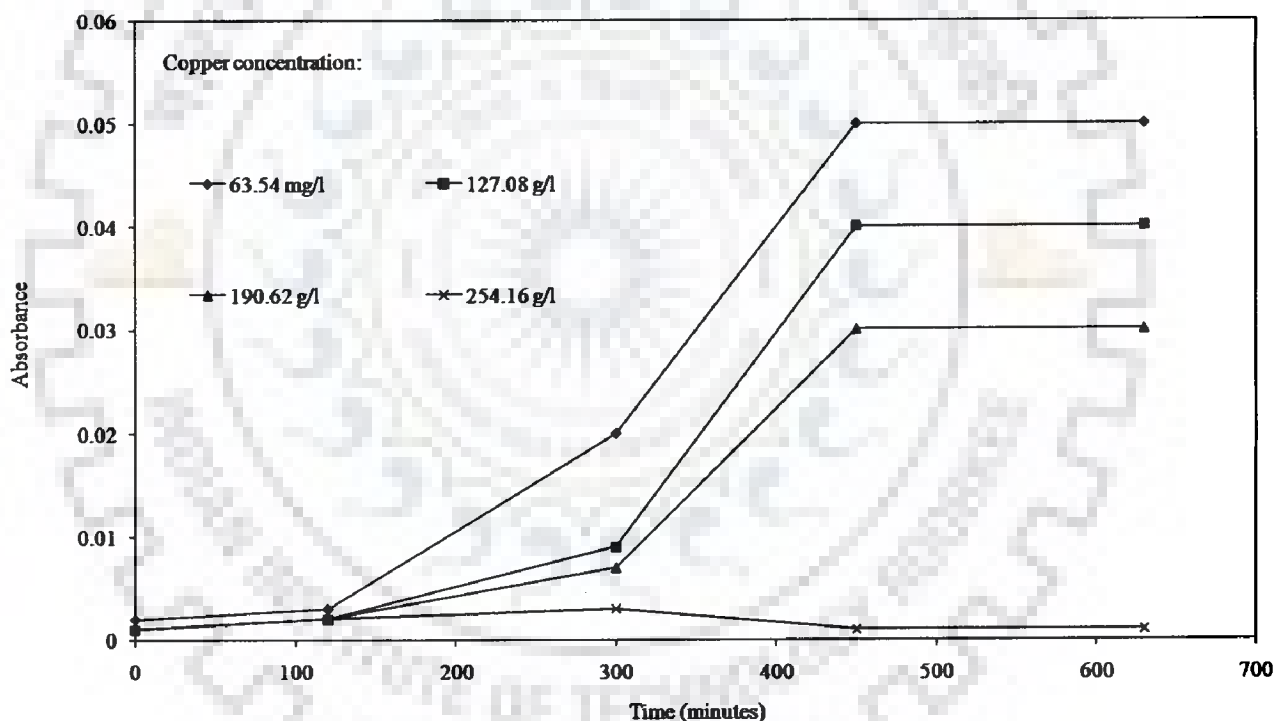


Figure 5.5.2.2 (a): Growth curve of the bacterium in the environment of zinc ( $457.66 \text{ g l}^{-1}$ ) and various copper concentrations

The growth of bacteria was measured at 600 nm at predefined time interval. It became evident from 5.5.2.2 (a) that the similar type of overall pattern of bacterial growth was observed from 0 to 630 minutes in various environments of copper concentration

ranging between  $63.54 \text{ g l}^{-1}$  to  $190.62 \text{ g l}^{-1}$ . With the increase in concentration of copper in liquid phase, the bacterial growth was found to be decreasing. The log and stationary phase of bacterial growth at all the concentrations of copper, ranging between  $63.54$  to  $190.62 \text{ g l}^{-1}$  were obtained in range of 480 to 300 minutes and 480 to 630 minutes, respectively. In case of  $254.16 \text{ g l}^{-1}$  of copper, the growth pattern of microorganism was somewhat different.

In an environment of  $254.16 \text{ g l}^{-1}$  of copper, the bacterium adopted short log phase, followed by stationary phase and finally cells entered the death phase. The rationale behind the short-term growth of bacteria in  $254.16 \text{ g l}^{-1}$  was due to the role of relevant concentration as maximum inhibitory concentration (MIC). The growth of bacteria in presence of copper ( $63.54 - 190.62 \text{ g l}^{-1}$ ) was almost same but the pattern of this range was quite different compared to the bacterium growth in  $254.16 \text{ g l}^{-1}$  of copper, indeed. With the experimental data obtained in growth rate determination experiments,  $190.62 \text{ g l}^{-1}$  of copper in liquid phase was concluded as optimum copper concentration in all other batch experimentals. In the higher concentration of copper like  $254.16 \text{ g l}^{-1}$ , the microbes take longer time than the other zinc concentration for its growth. Ultimately, it produces longer lag phase situation in the growth curve.

### **5.5.2.3 Growth of *Zinc sequestering bacterium VMSDCM* Accession no. HQ108109 in presence of iron and zinc**

Figure 5.5.2.3 (a) represents the growth curve of bacteria in an environment having  $457.66 \text{ g l}^{-1}$  of zinc and total iron ranging between  $54.84 \text{ g l}^{-1}$  to  $329.082 \text{ g l}^{-1}$ .

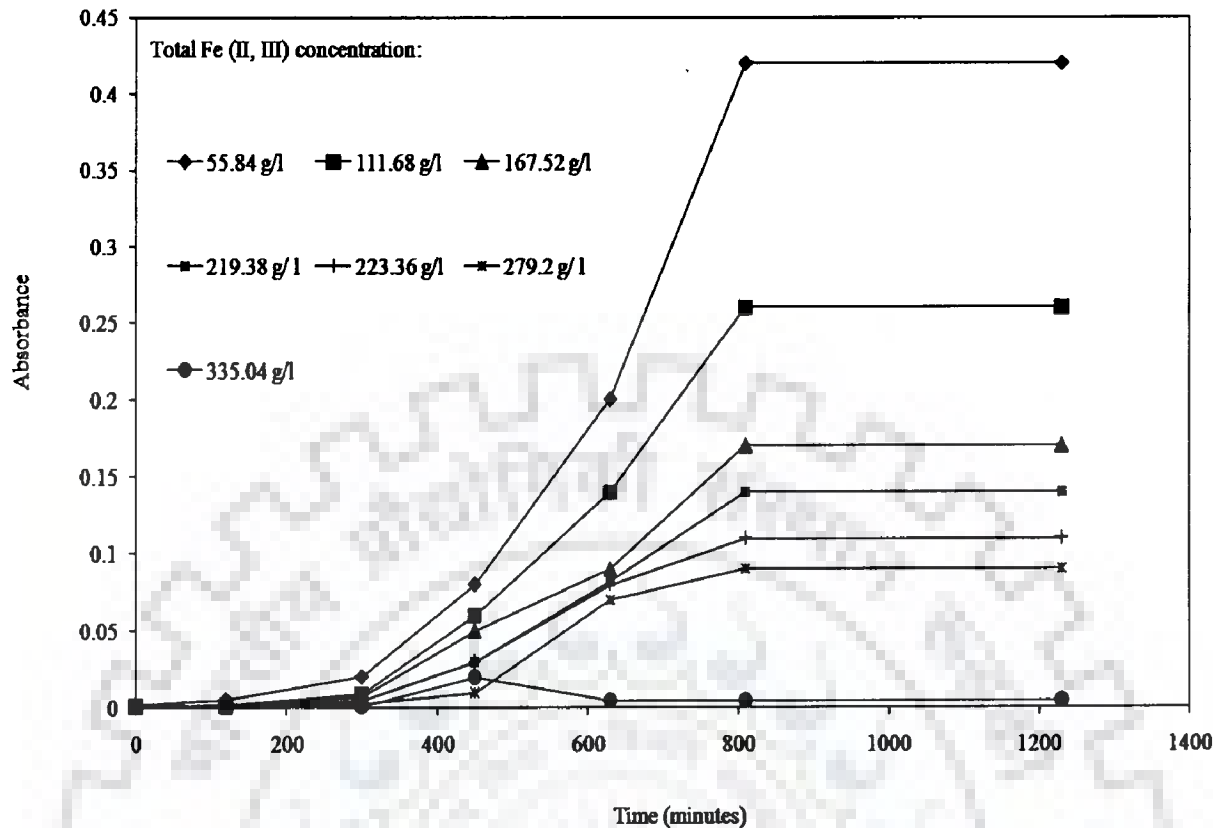


Figure 5.5.2.3 (a): Growth curve of the bacterium in the environment of ( $457.66 \text{ g l}^{-1}$ ) zinc and various iron concentrations

The growth of bacteria was measured at 600 nm at predefined time interval. It became evident from figure 5. 5.2.3 (a) that the similar type of overall pattern of bacterial growth was observed from 0 to 1230 minutes in various environments of total iron concentration ranging between  $55.84 \text{ g l}^{-1}$  to  $335.04 \text{ g l}^{-1}$ . With the increase in concentration of total iron in liquid phase, the bacterial growth was found to be decreasing. The log and stationary phase of bacterial growth at all the concentrations of total iron, ranging between  $55.84 \text{ g l}^{-1}$  to  $279.2 \text{ g l}^{-1}$  were obtained in range of 120 to 300 minutes and 800 to 1200 minutes, respectively. In case of  $335.04 \text{ g l}^{-1}$  of total iron, the growth pattern of microorganism was somewhat different. In an environment of  $335.04 \text{ g l}^{-1}$  of total iron, the bacterium adopted short log phase, followed by stationary phase and finally cells entered the death phase. The rationale behind the short-term growth of bacteria in  $335.04 \text{ g l}^{-1}$  was due to the role of relevant concentration as maximum inhibitory concentration (MIC). The growth of

bacteria in presence of total iron ( $55.84 - 279.2 \text{ g l}^{-1}$ ) was almost same but the pattern of this range was quite different compared to the bacterium growth in  $335.04 \text{ g l}^{-1}$  of total iron, indeed. With the experimental data obtained in growth rate determination experiments,  $272.9 \text{ g l}^{-1}$  of total iron in liquid phase was concluded as optimum total iron concentration in all other batch experimentals. In the higher concentration of total iron like  $335.04 \text{ g l}^{-1}$ , the microbes take longer time than the other total iron concentration for its growth. Ultimately, it produces longer lag phase situation in the growth curve.

#### 5.5.2.4 Growth of Zinc sequestering bacterium VMSDCM Accession no. HQ108109 in presence of iron, zinc and copper

Figure 5.5.2.4 (a) represents the growth curve of bacteria in an environment having  $457.66 \text{ g l}^{-1}$  of zinc, total iron ranging between  $54.84 \text{ g l}^{-1}$  to  $219.38 \text{ g l}^{-1}$  and Cu (II) concentration ranging between  $63.54 \text{ g l}^{-1}$  to  $254.16 \text{ g l}^{-1}$ .

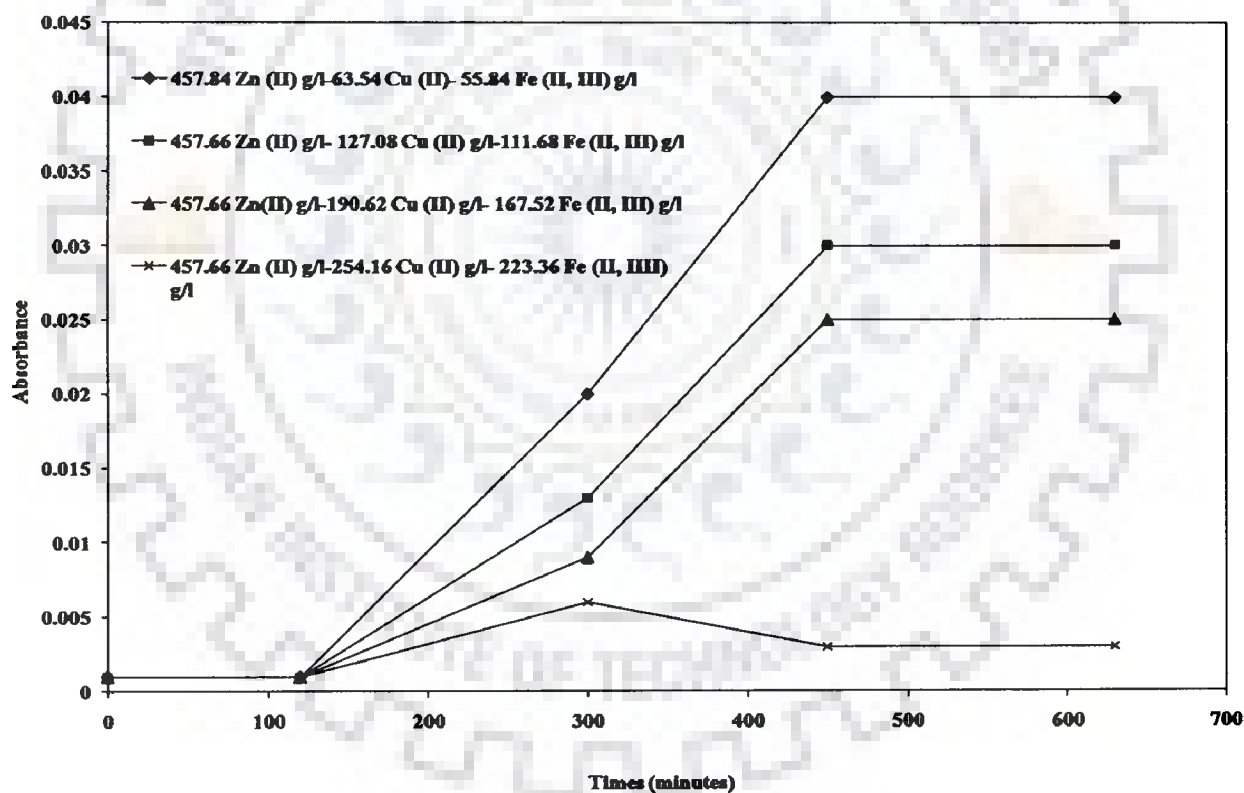


Figure 5.5.2.4 (a): Growth curve of the bacterium in the environment of zinc ( $457.66 \text{ g l}^{-1}$ ), various concentrations of iron and copper

The growth of bacteria was measured at 600 nm at predefined time interval. It became evident from figure 5.5.2.4 (a) that the similar type of overall pattern of bacterial growth was observed from 0 to 630 minutes in various environments of zinc, copper and total iron concentration ranging between 457.66 g l<sup>-1</sup>, 63.54 g l<sup>-1</sup> to 254.16 g l<sup>-1</sup> and 55.84 g l<sup>-1</sup> to 223.36 g l<sup>-1</sup>, respectively. With the increase in concentration of copper and total iron in liquid phase, the bacterial growth was found to be decreasing.

The log and stationary phase of bacterial growth at all the concentrations copper and total iron, ranging between 63.54 g l<sup>-1</sup> to 254.16 g l<sup>-1</sup> and 55.84 g l<sup>-1</sup> to 223.36 g l<sup>-1</sup> were obtained in range of 120 to 450 minutes and 450 to 630 minutes, respectively. In case of 254.16 g l<sup>-1</sup> of copper and 223.36 g l<sup>-1</sup>, the growth pattern of microorganism was somewhat different. In an environment of 254.16 g l<sup>-1</sup> of copper and 223.36 g l<sup>-1</sup>, the bacterium adopted short log phase, followed by stationary phase and finally cells entered the death phase. The rationale behind the short-term growth of bacteria in 254.16 g l<sup>-1</sup> of copper and 223.36 g l<sup>-1</sup> was due to the role of relevant concentration as maximum inhibitory concentration (MIC). The growth of bacteria in presence of copper (63.54 g l<sup>-1</sup> to 190.62 g l<sup>-1</sup>) and total iron (55.84 – 167.52 g l<sup>-1</sup>) was almost same but the pattern of this range was quite different compared to the bacterium growth in 254.16 g l<sup>-1</sup> of copper and 223.36 g l<sup>-1</sup>, indeed.

With the experimental data obtained in growth rate determination experiments, 190.62 g l<sup>-1</sup> of copper and 167.52 g l<sup>-1</sup> of total iron in liquid phase was included as optimum total iron concentration in all other batch experimentals. In the higher concentration, 254.16 g l<sup>-1</sup> of copper and 223.36 g l<sup>-1</sup> of total iron, the microbes take longer time than the other total iron concentration for its growth. Ultimately, it produces longer lag phase situation in the growth curve.

### **Concluding remark of the section 5.5.2**

It became evident from figures 5.5.2.1 (a) to 5.5.2.4 (a) that the maximum growth of *Zinc sequestering bacterium VMSDCM* accession no. HQ108109 was obtained in pure zinc environment. In pure zinc environmental condition, the optimum concentration of Zn (II) assumed as 457.66 g l<sup>-1</sup>. In ternary metal ion system 167.52 g l<sup>-1</sup> of total iron, 190.62 g l<sup>-1</sup> of

copper with  $457.66 \text{ g l}^{-1}$  of Zn (II) ion have been found as optimum concentration for growth of of *Zinc sequestering bacterium VMSDCM* accession no. HQ108109. The Maximum inhibitory concentration (MIC) of Zn (II) ion in pure zinc phase was  $523.04 \text{ g l}^{-1}$  of zinc. In ternary metal ion system, the  $254.16 \text{ g l}^{-1}$  of copper and  $223.36 \text{ g l}^{-1}$  of total iron were as Maximum inhibitory concentration (MIC).

### **5.5.3 Biosorption of Zn (II), Cu (II) and total Fe (II, III) by Immobilized *Zinc sequestering bacterium VMSDCM* accession no. HQ108109**

Immobilization of *Zinc sequestering bacterium VMSDCM* accession no. HQ108109 has been given in chapter 3 section 3.3.2. In section 5.2.8.1, *Cedrus deodara* sawdust was concluded as one of the most promising biomass for the biosorption of Zn (II) ion in liquid phase. Therefore, the *Cedrus deodara* sawdust was used as solid bed to immobilize the *Zinc sequestering bacterium VMSDCM* accession no. HQ108109. The optimized conditions for standard growth curve given in section 5.5.1 were used as optimum conditions in the present section. This section embodied results biosorption of Zn (II) ion in all types metal ion system on the surface of immobilized *Zinc sequestering bacterium VMSDCM* accession no. HQ108109.

Figure 5.5.3 (a) represents the influence of initial concentration of Zn (II) ion on the biosorption of Zn (II) ion in various types of metal ion systems by immobilized *Zinc sequestering bacterium VMSDCM* accession no. HQ108109 on *Cedrus deodara* sawdust. The initial concentration of Cu (II) and total Fe (II, III) was taken as  $254.16 \text{ g l}^{-1}$  and  $223.36 \text{ g l}^{-1}$  in binary and ternary metal ion system.



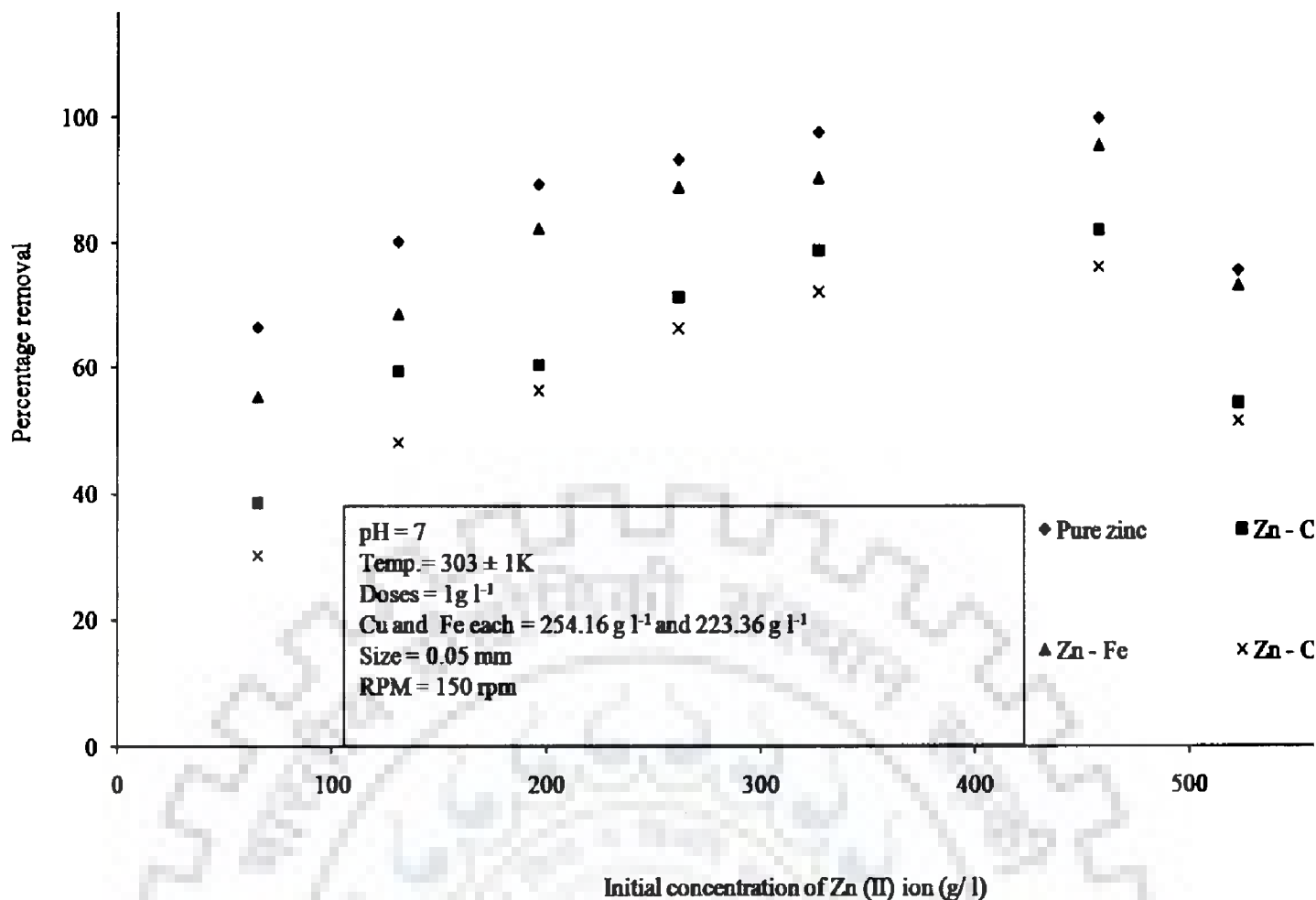


Figure 5.5.3 (a): Effect of initial concentration of Zn on biosorption of Zn on immobilized *Zinc sequestering bacterium VMSDCM* accession no. HQ108109

It became evident from figure 5.5.3 (a) that the maximum removal of zinc was obtained in pure zinc phase. The maximum removal of Zn (II) ion in liquid pure zinc phase was 100%. In case of Zn (II) – Fe (II, III) system, the maximum removal of zinc was 98.34%. In case of Zn (II) - Cu (II), the maximum removals of zinc was 97.44%. In ternary, metal ion, complex system the maximum removal of zinc 82.45%. With the increase in initial concentration of Zn (II) ion in all the types of metal ion systems from 65.38 g l<sup>-1</sup> to 523.04 g l<sup>-1</sup> increased the removal of Zn (II) linearly. However, further increase in initial concentration of Zn (II) from 523.04 g l<sup>-1</sup> to 568.8 g l<sup>-1</sup> led to the decrease in the percentage removal of Zn (II) ion in liquid phase. The rationale behind the increase in percentage removal of Zn (II) ion with elevation in initial metal ion concentration was due to the increase in concentration gradient of metal ions and availability of tremendous number of active sites on the surface of immobilized *Zinc sequestering bacterium VMSDCM* accession no. HQ108109. However,

decrease in biosorption of metal ion with subsequent increase in initial concentration of Zn (II) ion was due to saturation of actives present on the surface of *Zinc sequestering bacterium VMSDCM* accession no. HQ108109.

### **5.6 CONTINUOUS COLUMN STUDY USING REAL WASTEWATER**

The immobilization of isolated *Zinc Sequestering bacterium VMSDCM* accession no: HQ108109 has been discussed in section 3.3.2 and chapter 3. The bacterial cell immobilization was confirmed by observing a small amount of bacterial treated sawdust through Scanning Electron Microscope. The SEM Photograph of immobilized bacterium has been shown in figure 5.6 (a). The living cells were subjected to a voltage beam of 15 kV.





Figure 5.6 (a): SEM Photograph of *zinc sequestering bacterium VMSDCM* accession no. HQ108109 immobilized on surface of sawdust

The design details of the column has been given in chapter 4 and section 4.1.2. The flow rate of the effluent was maintained by peristaltic pump. The range of the flow rate was kept between 109 ml/h to 318 ml/h. Various height of the column used in present investigation were 15.25, 30.5, 45.75, 60 and 75.5 cm. The flow rate and height of the column was correlated with Mass transfer Zone, bed capacity at break point ( $q_{ib}$ ) and at saturation capacity ( $q_s$ ). The break through curves at various flow rates ranging between 109-318 ml/h was extrapolated between the ratio of  $C_e/C_0$  (concentration of metal ions at time t to the initial concentration) and time (in hours) to attain equilibrium.

### 5.6.1 Studies on variation of height of the column and its correlation with mass transfer zone

This section represents the studies on the influence of height of the column on the mass transfer zone of metal ion in solid bed. The flow rates used in present work were 109 ml/h, 160 ml/h, 296 ml/h and 318 ml/h. Table 5.6.1 (a) and figure 5.6.1 (a) represent the influence of the height of column and flow rate on the Mass Transfer Zone (cm) and break through curve of zinc at various flow rates.

Table 5.6.1 (a): Effect of the height of column and flow rate on the Mass Transfer Zone (cm).

Mass Transfer Zone (MTZ) (cm)	Flow rate (ml/ h)	Height of the column (cm)
1.682759	109	15.25
3.365517	109	30.5
5.048276	109	45.75
6.62069	109	60
8.303448	109	75.25
5.49	160	15.25
10.98	160	30.5
16.47	160	45.75
21.6	160	60
27.09	160	75.25
7.334524	296	15.25

14.66905	296	30.5
22.00357	296	45.75
28.85714	296	60
36.19167	296	75.25
7.856061	318	15.25
15.71212	318	30.5
23.56818	318	45.75
30.90909	318	60
38.76515	318	75.25

It is obvious from table 5.6.1 (a) that the increase in flow rate from 109 ml/h to 318 ml/h coupled with height of the column, there was a substantial lengthwise increase in mass transfer zone (MTZ, cm). However, at the 109 ml/h flow rate was maintained in order to obtain the maximum removal of zinc from liquid in column reactor for simultaneous biosorption and bioaccumulation process (SBB).

In one research investigation (Ostroski et al., 2009), the flow rate of the feed did not show any sort of either linear or non-linear pattern of mass transfer zone of zeolite –NaY bed. The disparity in the results was due to the different types of adsorbents used in the investigations.

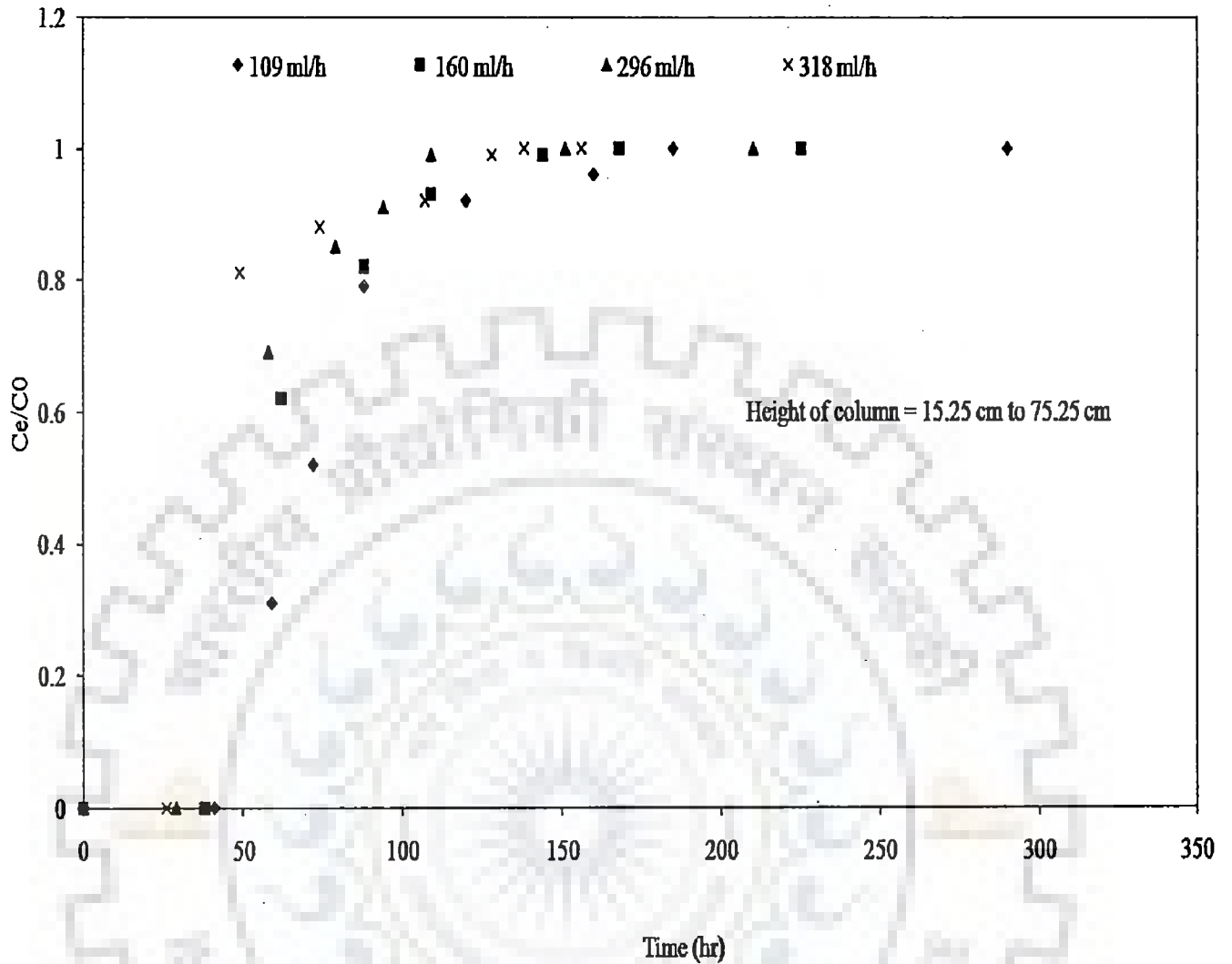


Figure 5.6.1 (a): Influence of flow rate on concentration of zinc (break through curve)

It is evident from figure 5.6.1 (a) that the break through curve of the zinc was obtained at various intervals of time due to various flow rates. By increasing the flow rate of effluent solution from 109 to 318 ml/h, the time to achieve the breakthrough point reduced from 160 hour to 128 hour. Proportionately, the equilibrium was obtained at various intervals of time, depending upon the flow rate (ml/h). At higher flow rates, the break point was obtained at shorter period as compared to lower flow rates. The rationale behind the earlier achievement of break through point in case of higher flow rates was the less contact time of the feed with the adsorbent bed and hence the ratio of concentration of output sample and input feed attained unity sooner.

Figure 5.6.1 (b) represents the break through curve of Cu (II) ions at various flow rates. The range of flow rate was kept between 109 ml/h to 318 ml/h. The curve was extrapolated between the ratio of concentration of metal ion at time t to to initial concentration versus time to attain equilibrium across the column length.

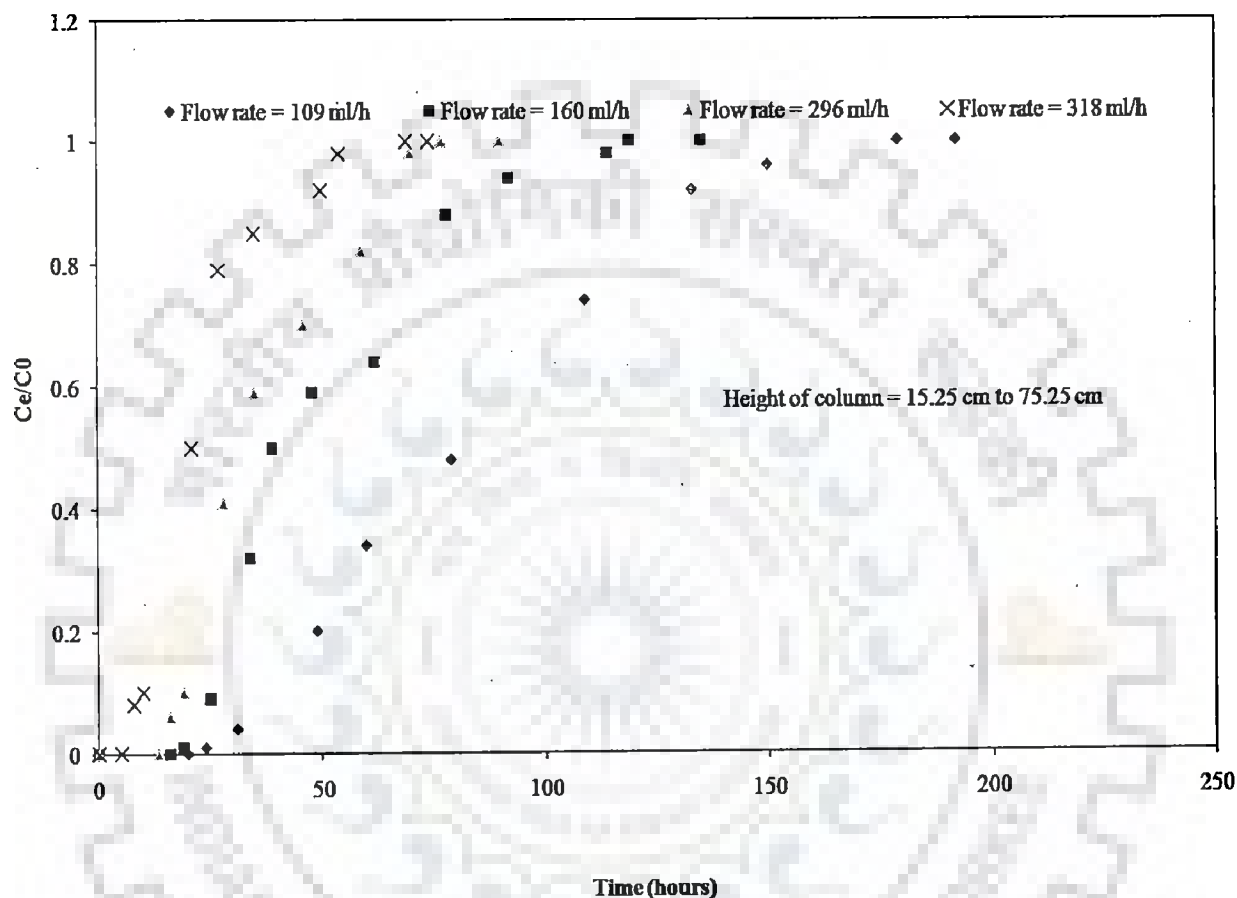


Figure 5.6.1 (b): Influence of flow rate on concentration of copper (break through curve)

It is evident from figure 5.6.1 (b) that the break through curve of the copper was obtained at various intervals of time due to various flow rates. By increasing the flow rate of effluent solution from 109 to 318 ml/h, the time to achieve the breakthrough point reduced from 150 hour to 114 hour. Proportionately, the equilibrium was obtained at various intervals of time, depending upon the flow rate (ml/h). At higher flow rates the break point, was obtained at shorter period relative at lower flow rates. The rationale behind the earlier achievement of break through point in case of higher flow rates was the less contact time of the feed with the adsorbent bed and hence the ratio of concentration of output sample and input feed attained

unity sooner. Moreover, the break point of the Cu (II) ion was attained quite rapidly compared to break point of zinc at all the ranges of flow rate. Figure 5.6.1 (c) represents the break through curve of total Fe (II, III) ions at various flow rates. The curve was extrapolated between the ratio of concentration of metal ion at time t to initial concentration versus time to attain equilibrium across the column length. The range of flow rate was kept between 109 ml/h to 318 ml/h.

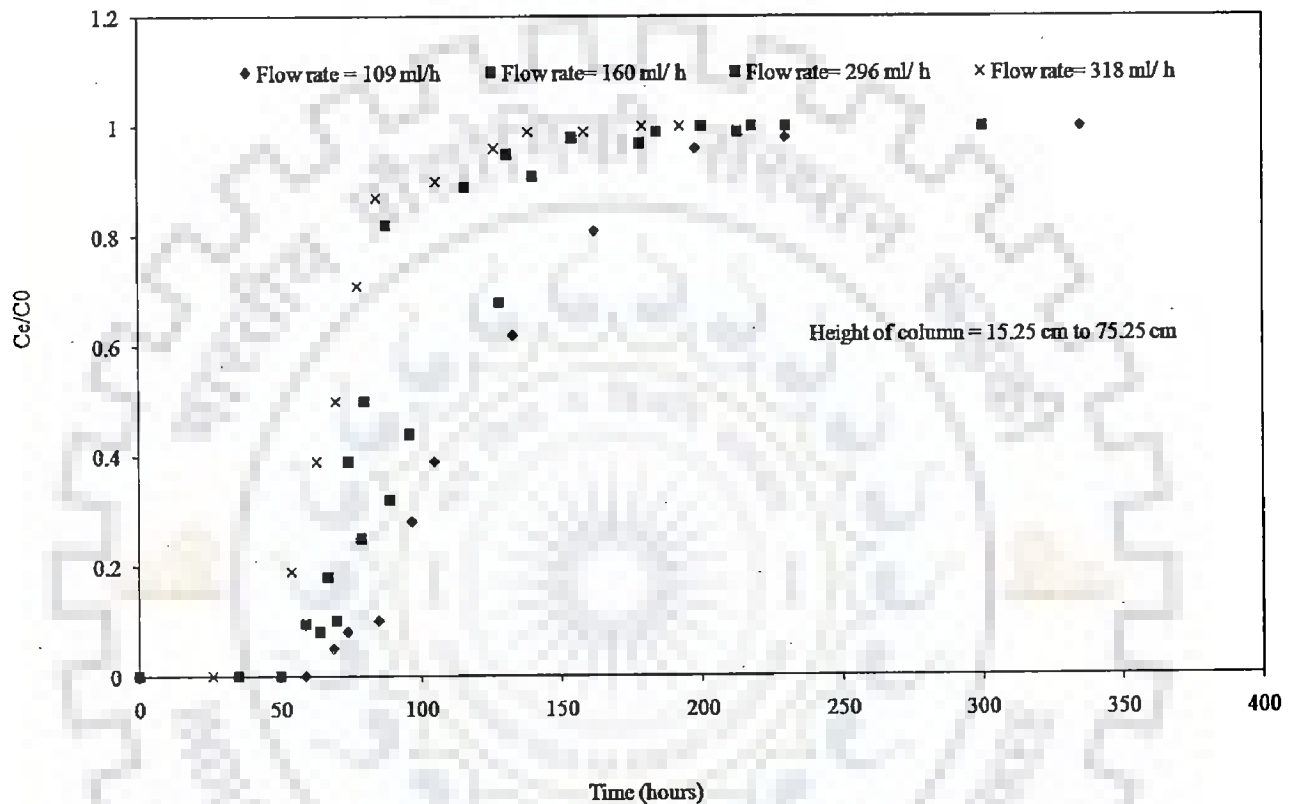


Figure 5.6.1 (c): Influence of flow rate on concentration of total Fe (II, III) (break through curve)

It is evident from figure 5.6.1 (c) that the break through curve of the total Fe (II, III) was obtained at various intervals of time due to various flow rates. By increasing the flow rate of effluent solution from 109 to 318 ml/h, the time to achieve the breakthrough point reduced



from 230 hour to 158 hour. Proportionately, the equilibrium was obtained at various intervals of time, depending upon the flow rate (ml/h). At higher flow rates the break point, was obtained at shorter period relative at lower flow rates. The rationale behind the earlier achievement of break through point in case of higher flow rates was the less contact time of the feed with the adsorbent bed and hence the ratio of concentration of output sample and input feed attained unity sooner. Moreover, the break point of the total Fe (II, III) ion was attained quite slow as compared to break point of zinc and copper at all the ranges of flow rate. The influence of flow rate on biosorption (uptake capacity) of immobilized *Zinc Sequestering Bacterium VMSDCM* accession no. HQ108109 immobilized on CDS has been shown in table 5.6.1 (b).

Table 5.6.1 (b): Influence of height of column and flow rate on mass transfer zone and uptake capacities in continuous system

Flow rate (ml/h)	Height of column (cm)	$q_s$ (mg/g)	$q_{tb}$ (mg/g)	$\chi^2$ ( $q_s$ )	$\chi^2$ ( $q_{tb}$ )	SSE ( $q_s$ )	SSE ( $q_{tb}$ )
109	15.25	3161	281	0.0018	0.0021	0.0021	0.0056
	30.5	1580	140	0.0043	0.0026	0.0059	0.0084
	45.75	1053	937	0.0062	0.0038	0.0079	0.0108
	60	7902	703	0.0091	0.0041	0.0092	0.0121
	75.25	6322	562	0.0013	0.0058	0.0105	0.0159
	160	15.25	5180	330	0.0016	0.0019	0.0028
160	30.5	1300	185	0.0051	0.0041	0.0072	0.0084
	45.75	5760	968	0.0081	0.0092	0.0085	0.0108
	60	3240	776	0.0092	0.0092	0.011	0.0121
	75.25	2073	660	0.0111	0.0194	0.0121	0.0159

296	15.25	6216	322	0.0012	0.0016	0.0124	0.0136
	30.5	3108	161	0.0011	0.0019	0.0134	0.0136
	45.75	2072	107	0.0015	0.0062	0.0136	0.0164
	60	1554	80	0.0018	0.0074	0.145	0.0171
	75.25	12432	64	0.0019	0.0088	0.181	0.0186
318	15.25	4197	20	0.0014	0.0021	0.108	0.0153
	30.5	2098	10	0.0019	0.0019	0.124	0.0266
	45.75	1399	67	0.0024	0.0055	0.165	0.0118
	60	1049	52	0.0036	0.0066	0.232	0.0212
	75.25	8395	43	0.0028	0.0074	0.265	0.0225

It became evident from table 5.6.1 (b) that an increase in flow rate from 109 to 318 ml/h resulted in decrease in both uptake capacities, i.e., ( $q_e$  and  $q_{tb}$ , mg/g). Five observations of both uptake capacities at a fixed flow rate were because the samples of metal were withdrawn at various heights of the column. The rationale behind the decrease in uptake capacity between the two flow rates was the low or less contact time of the liquid phase with the bed resulting in diminished interaction of metal ions ion at higher flow rates. Additionally, the uptake capacities followed a downtrend with the same flow rate, which was due to the variation in volume to mass transfer ratio at various heights of the column. The statistical data analysis indicated that the values of error functions were quite insignificant that further proves the collateral relation between the theoretical values and experimentals. Tiwari et al., (2007) has also reported that change of throughput volume of effluent significantly influences the ratio of final to initial concentration of adsorbate species ( $C_e/C_0$ ) of Cu (II) and Pb (II) ions.

Table 5.6.1 (c) shows the percentage wise removal of heavy metal ions from real industrial wastewater in the column SBB reactor. The flow rate was maintained at 109 ml/h and the height of the column was taken as 75.25 cm.


Table 5.6.1 (c) Results of biosorption of Zn (II), total Fe (II, III) and Cu (II) ions in SBB reactor for real industrial wastewater (Contains zinc, iron and copper)

Name of biosorbent	Flow rate	Initial concentration (mg/l)	Final concentration (mg/l)	% removal of Zn (II) ion	% removal of Fe (II, III) ion	% removal of Cu (II) ion
<i>Zinc sequestering bacterium VMSDCM</i> accession no. HQ108109 (dead cells)	109	4000	472.4	88.19		
	109	2389	736.32		68.09	
	109	123	3.4			97.16

It became evident from table 5.6.1 (c) that the removal of Zn (II), total Fe (II, III) and Cu (II) ion was quite high as reported in case of immobilized *Zinc sequestering bacterium VMSDCM* accession no. HQ108109 in continuous phase. The preferential order of removal of heavy metal ions was Cu (II) > Zn (II) > Fe (II, III).

#### Concluding remarks of the section 5.6.1

With the increase in flow rate, the time to obtain the break point decreased significantly. With the increase in height of the column, the uptake capacity of the bed decreased. However, with the increase in flow rate and height of the column the length of the mass transfer zone increased significantly.



# **CONCLUSIONS AND SCOPE FOR FUTURE WORK**

## CONCLUSIONS AND SCOPE FOR FUTURE WORK

**6.1 Conclusions**

The present work emerged out with the following conclusions.

(i) The removal of Zn (II), Cu (II) and total Fe (II, III) ion was performed through biosorption and bioaccumulation on the surface of nine sorts of adsorbents and isolated microbial strain.

(ii) *Cedrus deodara* sawdust, Eucalyptus leaf powder, Eucalyptus bark sawdust, Pine apple peel powder, Mango bark sawdust, Jack fruit peel powder, Egg shell with egg shell membrane, Orange peel, dead and viable cells of isolated microbial strain of *Zinc sequestering bacterium VMSDCM* accession no. HQ108109 were used as biosorbents for the removal of zinc in liquid phase.

(iii) The characterization of adsorbents revealed the fact that the surfaces of adsorbents were porous and non-crystalline with tremendous number of protrusions. The characterization of isolated living cell of *Zinc sequestering bacterium VMSDCM* accession no. HQ108109 indicated that the bacterial cells were rod shaped and gram negative in nature.

(iv) The phylogenetic analysis of the isolated bacterium revealed the fact that the isolated microbial strain cluster up with arsenite oxidizing bacteria. The 16 S RNA sequencing was performed using universal primers and the sequences were submitted to NCBI under the accession no. HQ108109.

(v) The parameter optimization carried out during the sorption of Zn (II), Cu (II) and total Fe (II, III) ion indicated that *Cedrus deodara* sawdust and dead cells of *Zinc sequestering bacterium VMSDCM* accession no. HQ108109 have tremendous potential for sorption of metal ion.

(vi) The binding of Zn (II) ion on the surface of *Cedrus deodara* sawdust indicated the suitability of Freundlich, Temkin, pseudo second order and Bangham model to interpret the

sorption of Zn (II) ion. Additionally, the sorption of Zn (II) ion on the surface of *Cedrus deodara* sawdust seemed to be endothermic and spontaneous. However, in case of sorption of Zn (II) ion on dead cells of *Zinc sequestering bacterium VMSDCM* accession no. HQ108109, a modified isotherm model has been proposed. The model constant was calculated through code written in C++ language. The modified and proposed isotherm model was validated between 298 K to 308 K. Kinetic, mechanistic and thermodynamic modeling of sorption of Zn (II) ion indicated that the binding of Zn (II) ion on surface of dead cells of *Zinc sequestering bacterium VMSDCM* accession no. HQ108109 followed pseudo second order, intra particle model, spontaneous and endothermic in nature.

(vii) The maximum removal of zinc obtained in case of dead cells of *Zinc sequestering bacterium VMSDCM* accession no. HQ108109 in pure zinc, Zn (II) - Cu (II), Zn (II)- total Fe (II, III) and Zn (II)- Cu (II)- total Fe (II, III) were 89.19%, 69.12%, 74.31% and 69.11%, respectively in case of *Cedrus deodara* sawdust. The removal of total Fe (II, III) and Cu (II) ion obtained in Zn (II) - total Fe (II, III) and Zn (II) - Cu (II) in metal ion systems was 37.19 and 71.11%, respectively. The removal of total Fe (II, III) and Cu (II) removal in Zn (II) - Cu (II) - total Fe (II, III) metal ion system was 32.14% and 65.5%, respectively. In case of dead cells of *Zinc sequestering bacterium VMSDCM* accession no. HQ108109, the maximum removal of Zn (II) ion obtained in pure zinc, Zn (II) - Cu (II), Zn (II)- total Fe (II, III) and Zn (II)- Cu (II)- total Fe (II, III) were 100%, 86.66%, 88.19% and 74.61%, respectively. The removal of total Fe (II, III) and Cu (II) ion in Zn (II) - total Fe (II, III) and Zn (II) - Cu (II) in metal ion systems in case of dead cells of *Zinc sequestering bacterium VMSDCM* accession no. HQ108109 was 81.1% and 88.19% respectively. In case of Zn (II) - Cu (II) - total Fe (II, III) the removal of total Fe (II, III) and Cu (II) by dead cells of *Zinc sequestering bacterium VMSDCM* accession no. HQ108109 was 73.34% and 81.23%, respectively.

(viii) Both the adsorbents were used to treat the real wastewater and simulated synthetic wastewater in batch studies. The results indicated that *Cedrus deodara* sawdust was able to remediate 46.55% and 30.34% of zinc and total Fe (II, III) iron respectively from simulated wastewater discharging from zinc plating industry. Furthermore, results indicated that *Cedrus deodara* sawdust was able to remove 15.33%, 21.22% and 13.36% of Zn (II), Cu (II) and total Fe (II, III) ion from wastewater discharging from copper smelting plant. Similarly, the

dead cells of *Zinc sequestering bacterium VMSDCM* accession no. HQ108109 were able to remove 52.34% and 44.39% of Zn (II) and total Fe (II, III), respectively from simulated wastewater discharging from zinc plating industry. Furthermore, the dead cells *Zinc sequestering bacterium VMSDCM* accession no. HQ108109 was found capable of removing 20.39%, 30.33% and 16.61% of Zn (II), Cu (II) and total Fe (II, III) from simulated wastewater of copper smelting plant.

(ix) Following results were obtained in treatment of real wastewater discharging from zinc producing unit (Hindustan Zinc Limited, SIDCUL HARDWAR). The *Cerdus deodara* sawdust yielded 20.64%, 62.12% and 14.36% removal of Zn (II), Cu (II) and total Fe (II, III) from real wastewater. Similarly, dead cells of *Zinc sequestering bacterium VMSDCM* accession no. HQ108109 yielded 60.19%, 78.16% and 39.33% removal of Zn (II), Cu (II) and total Fe (II, III) from real wastewater. The preferential order of removal of metal ion was Cu (II) > Zn (II) > total Fe (II, III) in liquid phase.

(x) The isolated microbial strain was immobilized on the bed of *Cerdus deodara* sawdust in the lab scale column reactor. The real wastewater was pumped in to the column at various flow rates between 109 ml/h – 318 ml/h. The maximum removal of Zn (II), Cu (II) and total Fe (II, III) ion from real wastewater was obtained at 109 ml/h. The total removal of Zn (II), Cu (II) and total Fe (II, III) ion from real wastewater in column study was reported as 88.19%, 97.16% and 68.09%, respectively.

(xi) In batch simultaneous biosorption and bioaccumulation study, the maximum removal of zinc was 100% in pure zinc phase. In case of Zn (II) – Fe (II, III) system, the maximum removal of zinc was 98.34%. In case of Zn (II)- Cu (II) and Zn (II) – Cu (II) - Fe (II, III) ternary metal ion system, the maximum removals of zinc were 97.44% and 82.45%, respectively. In continuous column studies on treatment of industrial wastewater, the maximum removal of Zn (II), Cu (II) and Fe (II, III) ion from ternary metal ion system was 88.19%, 97.16% and 68.09%, respectively. The preferential order of removal was Cu (II) > Zn (II) > Fe (II, III).

(xii) Present investigation reveals that the treatment, i.e., simultaneous biosorption and bioaccumulation (SBB) gives the best result for the removal of Zn (II), Cu (II), Fe (II, III)

from industrial wastewater. We believe that this can be applied in practice for the successful removal of ternary metal ion complex.





## 6.2 Scope for future work

Scope for the future work has been tabulated below.

- (i) Though, the present work has been performed very extensively, still there remains many more possibilities using various non living biomass and various types of microbial strain to be used as biosorbent for the bioremediation of metal ion in liquid phase.
- (ii) In future, the genetic modification can be attempted to improve the biosorption cum bioaccumulation efficiency of isolated *Zinc sequestering bacterium VMSDCM* Accession no. HQ108109.
- (iii) The isolated resistant and improved strain can be acclimatised in various environmental conditions to facilitate the usage of this bacterium in bioremoval of metal ions from various sorts of industrial effluents.
- (iv) The acclimatised strain of *Zinc sequestering bacterium VMSDCM* Accession no. HQ108109 can be immobilized on various types of biomasses or adsorbents. The immobilized microbial strain can not only be used to remediate heavy metal ions in liquid phase but also the same strain can also be used to remove various organic impurities from industrial effluents.
- (v) The present investigation can also be extended towards the immobilization of *Zinc sequestering bacterium VMSDCM* Accession no HQ108109 on the surface of modified adsorbents for the removal of both metal ions and organic pollutants from industrial effluent. The fluidized bed lab scale reactor can be fabricated and can be used for the bioremoval of pollutants from various industrial effluents.



# **LIST OF PUBLICATIONS**

### Papers published/accepted in referred journal

1. Zn(II) Ion Biosorption onto Surface of Eucalyptus Leaf Biomass: Isotherm, Kinetic, and Mechanistic Modeling, *CLEAN – Soil, Air, Water*, vol 38, pages 1062–1073, 2010.
2. Biosorption of Zn (II) onto the Surface of Non-living Biomasses: A Comparative Study of Adsorbent Particle Size and Removal Capacity of Three Different Biomasses, *Water Air Soil Pollut.*, vol 211, pp. 489–500, 2010.
3. Biosorption of Zn (II) ion onto surface of Cedrus Deodara sawdust: Studies on isotherm modeling and surface characterization, *International Journal of Chemical Sciences and Applications* Vol 2, Issue 3, pp 179-178, 2011.
4. Optimization of physical parameters for batch mode Zn (II) ion removal from liquid phase: A potential biosorption study, *Environmental Progress and Sustainable Energy (AIChE)*, DOI 10.1002/ep.10637
5. Kinetics, mechanistic and thermodynamics of Zn (II) ion sorption: A modeling approach, *CLEAN – Soil, Air, Water* (**Accepted, in press**).
6. Sorption of Zn (II) ion onto surface of activated carbon derived from eucalyptus bark saw dust from industrial wastewater: Isotherm, kinetics, mechanistic modeling and thermodynamics. *Desalination and Water Treatment* (**Accepted, in press**)

**Papers accepted/ published in international conference**

---

1. Biosorption of Zn (II) by activated carbon derived from eucalyptus bark: Effect of pH, temperature and contact time on to the biosorption of the metal ions, *The 7<sup>th</sup> International Symposium on Southeast Asian Water Environment*, University of Tokyo, Japan, 2009.
2. Adsorption of Zn (II), Fe (II), Fe (III) and Cu (II) ion onto activated carbon derived from eucalyptus bark sawdust: surface characterization, isotherm modeling and studies on process parameter optimization, *The Twenty-Seventh International Conference On Solid Waste Technology And Management*, Philadelphia, PA U.S.A, 2012.



# REFERENCES



## REFERENCE

---

Aderhold, D., Williams, C. J., Edyvean, R. G. J., The removal of heavy-metal ions by seaweeds and their derivatives, *Bioresou. Technol.*, vol 58, pp.1-6, 1996.

Agarwal, A., Sahu, K. K., Pandey, B. D., Solid waste management in non ferrous industries in India, *Resource, Conservation and Recycling*, vol 42, pp 99-120, 2004.

Agorboude, L., Navia, R., Heavy metals retention capacity of a non-conventional Sorbent developed from a mixture of industrial and agricultural wastes, *J. Hazard. Mater.*, doi:10.1016/j.jhazmat. 2009 .01.027.

Ahmad, A., Rafatullah, M., Sulaiman, O., Ibrahim, M. H., Chii, Y. Y., Siddque, B. M., Removal of Cu (II) and Pb (II) ions from aqueous solutions by adsorption on sawdust of Meranti Wood, *Desalination*, vol 247, pp. 636 – 646, 2009.

Ajjabi L. C., and Chouba, L., Biosorption of Cu<sup>2+</sup> and Zn<sup>2+</sup> from aqueous solutions by dried marine green macro alga *Chaetomorpha linum*, *J. Environ. Management.*, vol 90, pp. 3485 – 3489, 2009.

Ali, E. H., Hashem, M., Removal efficiency of the heavy metals Zn(II), Pb (II) and Cd(II) by *saprolegnia delica* and *trichoderma viride* at different pH values and temperature degrees, *Microbiol.*, vol – 35, pp. 135-144, 2007.

Al-Saraj, M., Abdel, L. S., El, N. Baraka, R., Bioaccumulation of some hazardous metals by sol-gel entrapped microorganisms, *J. Non crystalline solids*, vol 248, pp. 137 – 140, 1999.

Alvarez, M. T., Crespo, C., Mattiason, B., Precipitation of Zn (II), Cu (II), and Pb (II) at bench scale using biogenic hydrogen sulphide from the utilization of volatile fatty acids, *Chemosphere*, vol 66, pp. 1677 – 1683, 2007.

Anand, P., Etzel, J. E., Friedlaener, F. J., Heavy metals removals by high gradient magnetic separation, *IEEE Trans. Magnet.*, vol 21, pp 2062- 2064, 1985.

Andreoni, V., Colombo, M., Colombo, A., Vecchio, A., Finoli, C., Cadmium and zinc removal by growing cells of *Pseudomonas putida* strain B14 isolated from a metal-impacted soil, *Annals of Microbiol.*, vol 53 , pp. 135-148, 2003.

Arica, Y. M., Arpa, C., Ergene, A., Bayramoglu, G., Genc, O., Ca alginate as support for Pb (II) and Zn (II) biosorption with immobilized *Phanerochaete chrysosporium*, *Carbohydr. Polym.*, vol 52, pp. 167 – 174, 2003.

Arshad, M., Zafar, N. M., Youns, S., Nadeem, R., The use of neem biomass for the biosorption of zinc from aqueous phase, *J. Hazard. Mater.*, vol 157, pp. 534 – 540, 2008.

- Arslanoglu, H., Altundogan, H. S., Tumen, F., Heavy metals binding properties of esterified lemon, *J. Hazard. Mater.*, doi: 10.1016/j.jhazmat.2008.09.054, 2008.
- Artola, A., Rigola, M., Selection of optimum biological sludge for zinc removal from wastewater by a biosorption process, *Biotech. Lett.*, vol 14, pp. 1199 – 1204, 1992.
- Asaf, L., Nativ, R., Shain, D., Hassan, M., Geyer, S., Controls on the chemical and isotopic compositions of urban stormwater in a semiarid zone, *J. Hydrol.*, vol 294, 270–293, 2004.
- Agency for Toxic Substances and Disease Registry (ATSDR), Toxicological Profile for Zinc (Update). Atlanta, GA: U.S. Department of Public Health and Human Services, Public Health Service, 2005.
- Baig, K. S., Doan, H. D., Wu, J., Multicomponent isotherm for biosorption of  $Ni^{2+}$  and  $Zn^{2+}$ , *Desalination*, vol 249, pp 429- 439, 2009.
- Bakkaloglu, I., Butter, T. J., Evison, L. M., Holland, F. S., Hancock, I. C., Screen of various types biomass for removal and recovery of heavy metals (Zn, Cu, Ni) by biosorption, sedimentation and desorption, *Wat. Sci. Technol.*, vol 38, pp. 269 – 277, 1998.
- Basha, S., Murthy, Z. V. P., Jha, B., Sorption of Hg (II) onto *Carica papaya*: Experimental studies and design of batch sorber, *Chem Eng. J.*, vol 147, pp. 226 – 234, 2009.
- Basu, A. K., Swarnkar, S. R., In: proceedings of Hydrometal.-90, 1990.
- Bayramoglu, G., Bektas, S., Arica, Y. M., Biosorption of heavy metal ions on immobilized white-rot fungus *Trametes versicolor*, *J. Hazard. Mater.*, vol B101, pp. 285-300, 2003.
- Berg, U., Donnert, D., Ehbrecht, A., Bumiller, W., Kusche, I., Weidler, I., Nuesch, R., “Active Filtration” for the elimination and recovery of phosphorus from waste water, *Colloids and surface A: Physichem. Eng. Aspects.*, vol 265, pp 141 – 148, 2005.
- Bhatnagar, D., Jancy A., Cobalt recovery from metallurgical waste of zinc industry, Environmental wastage management in non-ferrous metallurgical industries, In: Bandhopadhyay, A., Goswami, N. G., Ramachandra, R. P., Eds, pp 230 – 241, 1998.
- Bhattacharya, A. K., Mandal, S. K., Das, S. K., Adsorption of Zn (II) from aqueous solutions by using different adsorbents, *Chem. Eng. J.*, vol 123, pp 43 – 51, 2006.
- Bold, H. C., Wynne, M. J., Introduction to the algae, Engle-wood Cliff, NJ, Printice- Hall, pp. 516, 1985.
- Cabral, J. P. S., Selective binding of metal ions to *Pseudomonas syringae* cells, *Microbios.*, vol -71, pp. 47 – 53, 1992.

- Cabuk, A., Akar, T., Tunali, S., Gedikili, S., Biosorption of Pb(II) by industrial strain of *Saccharomyces cerevisiae* immobilized on biomatrix of cone biomass of *Pinus nigra*: equilibrium and mechanism analysis, Chem. Eng. J., vol 131, pp. 293 – 300, 2007.
- Carrea, J. A., Bringas, E., Roman, S. M. F., Ortiz, I., Selective membrane alternative to the recovery of zinc from hot dip galvanizing effluents, J. Membr. Sci., doi: 10.1016/j.memsci.2008.11.002, 2008.
- Celaya, R. I., Noriega, J. A., Yeomans, J. H., Ortega, L. J., Ruiz, M. A., Biosorption of Zn (II) by *Thiobacillus ferrooxidans*, Bioprocess Eng., vol 22, pp. 539 – 42, 2000.
- Cesur, H., Balkaya, N., Zinc removal from aqueous solution using an industrial by product phosphogypsum, Chem. Eng. J., vol 131, pp. 203-208, 2007.
- Chang, W. C., Hus, G. S., Chiang, S. M., Su, M. C., Heavy metal removal from aqueous solution by wasted biomass from combined AS-biofilm process, Bioresour. Technol., vol 97, pp. 1503 – 1508, 2006.
- Chatterjee, S. K., Bhattacharya, I., Chandra, G., Biosorption of heavy metals from industrial wastewater by *Geobacillus thermodenitrificans*, J.Hazard. Mater., vol 175, pp. 117-125, 2010.
- Chegrouche, S., Mellah, A., Barkat, M., Removal of strontium from aqueous solutions by adsorption on to activated carbon: kinetic and thermodynamic studies, Desalination, vol 235, pp. 306-318, 2009.
- Chen, X. C., Wang, Y. P., Lin, Q., Shi, J. Y., Wu, W. X., Chen, Y. X., Biosorption of copper and zinc (II) from aqueous solutions by *Pseudomonas putida* CZ1, Colloid Surface B-Biointerface, vol 46, pp. 101 – 107, 2005.
- Choudhary, R., Srivastava, S., Zinc resistance mechanisms in bacteria, Current Sci., vol 81, pp. 768-774, 2001.
- Chojnacka, K., Biosorption and bioaccumulation in practice, Nova Science Publisher, Newyork, 2009.
- Codina, J. C., Cazorla, F. M., Garcia, P. A., Vincente, A. D., Heavy metal toxicity and Genotoxicity in water and sewage determined by microbiological methods, Environmental Toxicology and Chemistry, vol 19, pp 1552-1558, 2000.
- Cooper, G. R., Zinc toxicology following particulate inhalation, Indian Journal of Occupational and Environmental Medicine, col 12, pp. 10 – 13, 2008
- Costely, S. C., Wallis, F. M., Bioremediation of heavy metals in a synthetic wastewater using a rotating biological rotating biological contractor, Wat. Res., vol 35, pp. 3715 – 3723, 2003.



- Crini, G., Recent developments in polysaccharide-based materials used as adsorbents in wastewater treatment, *Progress in Polymer Science*, vol 30, pp 38 -70, 2005.
- Crowell, A. D., Surface forces and solid – gas interaction, In E. Alison Flood (editor), *The solid gas interface*, Marcel Dekker, New York, 1966.
- Csicsovszki, G., Kekesi, T., Torok, T. I., Selective recovery of Zn and Fe from spent pickling solutions by the combination of anion exchange and membrane electrowinning techniques, *Hydrometallurgy*, vol 77, pp 19 -28, 2005.
- Dang, V. B. H., Doan, H. D., Vu- Dang, T., Lohi. A., Equilibrium and kinetics of biosorption of cadmium (II) and copper (II) ions by wheat straw, *Bioresour. Technol.*, vol 100, pp. 211 – 219, 2009.
- Das, T. K., Health and Environmental Risk Assessment and Management Hand Book, American Institute of Chemical Engineers, Newyork, pp.79, 2003.
- Dash, R.R., Balomajumder, C., Kumar, A., Removal of cyanide from water and wastewater using granular activated carbon. *Chem. Eng. J.*, vol 146, pp. 408 –413, 2009.
- Davis, T. A., Volesky, B., Mucci, A., A review of biochemistry of heavy metal biosorption by brown algae, *Wat. Res.*, vol 37, pp. 4311 – 4330, 2003.
- Demirbas, A., Pehlivan, E., Gode, f., Altun, T., Arslan, G., Adsorption of Cu (II), Zn (II), Ni (II), Pb (II), and Cd(II) from aqueous solution on Amberlite IR - @0 synthetic resin, *J. Colloid Interface Sci.*, vol 282, pp. 20 – 25, 2005.
- Diaz, G., Martin, D., Modified zincex process—the clean, safe and profitable solution to the zinc secondaries treatment, *Resource Conservation and Recycling*, vol 10, pp. 43–57, 1994.
- Dilek, F. B., Erbay, A., Yetis, U., Ni (II) biosorption by *Polyporous versicolor*, *Process Biochem.*, vol 37, pp. 723 – 726, 2002.
- Dupont, L., Bouanda, J., Dumaceau, J., Aplincourt, M., Biosorption of Cu (II) and Zn (II) onto a lignocellulosic substrate extracted from wheat bran, *Environ. Chemistry Lett.*, vol 2, pp. 165 – 168, 2005.
- Eccles, H., Treatment of metal contaminated waste: why select a biological process, *Trends Biotech.*, vol 17, pp 462 – 465, 1999.
- Esposito, A., Pagnanelli, F., Lodi, A., Solisio, C., and Veglio, F., Biosorption of heavy metals by *Sphaerotilus natans*: and equilibrium study at different pH and biomass concentration, *Hydrometallurgy*, vol 60, pp. 129 – 141, 2001.

- Fan, T., Liu, Y., Feng, B., Zeng, G., Yang, C., Zhou, M., Zhou, H., Tan, Z., Wang, X., Biosorption of cadmium (II), zinc (II) and lead (II) by *Penicillium simplicissimum*: Isotherm, kinetics and thermodynamics, *J. Hazard. Mater.*, vol 160, pp. 655-661, 2008.
- Fagundes, K. M. R., Ferri, P., Martins, T. D., Tavares, C, R. G., Silva, E. A., Equilibrium study of the binary mixture of cadmium–zinc ions biosorption by the *Sargassum filipendula* species using adsorption isotherms models and neural network, *Biochem. Eng. J.*, vol 34, pp. 136 -146, 2007.
- Farooq, U., Kozinski, J. A., Khan, M. A., Athar, M., Biosorption of heavy metal ions using wheat based biosorbents – A review, *Bioresour. Technol.*, vol 101, pp. 5043 – 5053, 2010.
- Faryal, R., Lodhi, A., Hameed, A., Isolation, characterization and biosorption of Zinc by indigenous fungal strains *aspergillus fumigatus* rh05 and *aspergillus flavus* rh07, *Pak. J. Bot.*, vol 38, pp. 817-832, 2006.
- Febrianto, J., Kosasih, N. A., Sunarso, J., Ju, H. Y., Indraswati, N., Ismadji, S., Equilibrium and kinetic studies in adsorption of heavy metals using biosorbent: A summary of recent studies, *J. Hazard. Mater.*, vol 162, pp. 616– 645, 2009.
- Felsenstein, J., PHYLIP (Phylogeny Inference Package) version 3.5c, Distributed by the author. Department of Genetics, University of Washington, Seattle, 1993.
- Figueira, M . M., Volesky, B., Azarian, K., Ciminelli, V. S. T., Biosorption column performance with a metal mixture, *Environ. Sci. Technol.*, vol 34, pp. 4320-4326, 2000.
- Formigari, A., Irato, P., Santon, A., Zinc anti oxidant systems and metallotheonine in metal mediated apoptosis: Biochemical and cytochemical aspects, *Comparative Biochemistry and physiology (part C)*, vol 146, pp. 443 – 459, 2007.
- Freitas, O. M.M., Martins, R. J. E., Matos, C. M. D., Boaventura, R. A. R., Removal of Cd(II), Zn(II) and Pb(II) from aqueous solutions by brown marine macro algae: Kinetic modeling., *J. Hazard. Mater.*, vol 153, pp. 493–501, 2008.
- Friis, N., Myres, K. P., Biosorption of Uranium and Lead by *Streptomyces longwoodensis*, *Biotechnol, Bioeng.*, vol – 28, pp. 21 – 28, 1986.
- Fourest, E., Volesky, B., Alginate Properties and Heavy Metal Biosorption by Marine Algae, *Applied Biochemistry and Biotechnology*, vol 67, pp. 215– 226, 2007.
- Gavrilescu, M., Removal of heavy metals from environment by biosorption, *Eng. Life sci.*, vol 4, pp 219- 232, 2004.
- Gokhlae, S., Khare, M., Statistical behavior of carbon monoxide from vehicular exhausts in urban environments, *Environment. Modelling & Software.*, Vol 22, pp. 526 -535, 2007.

- Grosse, D. W. G., A review of alternative treatment processes for metal bearing hazardous waste streams, *Air pollut. Control. Assoc.*, vol 36, pp. 3-5, 1986.
- Grzeszczyk, A., Rosocka, M. R., Extraction of zinc (II), iron (II) and iron (III) from chloride media with dibutylbutyl phosphate, *Hydrometallurgy*, vol 86, pp 72 – 79, 2007.
- Hammami, A., Gonzalez, F., Ballester, A., Blazquez, M. L., Munoz, J. A., Simultaneous uptake of metals by activated sludge, *Minerals Eng.*, vol 16, pp 723 – 729, 2003.
- Hanif, M. A., Nadeem, R., Bhatti, H. N., Ahmad, N. R., Ansari, T. M., Ni (II) biosorption by *Cassia Fistula* (Golden Shower) biomass, *J. Hazard. Mater.*, vol B139, pp. 345 – 355, 2007.
- Hirshon, J. M., Shardell, M., Alles, S., Powell, J. L., Squibb, K., Ondov, J., Blaisdell, C. J., Elevated ambient air zinc increases pediatric asthma morbidity, *Research Children's Health*, vol 116, pp 826 – 831, 2008.
- Ho, Y., Ofomaja, A. E., Biosorption thermodynamics of cadmium on coconut copra meal as biosorbent, *Biochem. Eng. J.*, vol 30, pp. 117 -123, 2006.
- Holan, Z. R., Volesky, B., Prasetyo, I., Biosorption of cadmium by biomass of marine algae, *Biotech. Bioeng.*, vol 41, pp. 819 – 825, 1993.
- Holan, Z. R., Volesky, B., Biosorption of lead and nickel by biomass of marine algae, *Biotech. Bioeng.*, vol 43, pp. 1001-1009, 1994.
- Gekeler, W., Grill, E., Winacker, E. L., Zenek, M. H., Algae sequester heavy metals via synthesis of photochelatin complex, *Arch. Microbiol.*, vol - 50, pp. 197 – 202, 1988.
- Husiman, J. L., Schouten, G., Schultz, C., Biologically produced sulphide for purification of process streams, effluent treatment and recovery of metals in the metal and mining industries, *Hydrometallurgy*, vol 83, pp 106 – 113, 2006.
- Igwe, J. C., Abia, A. A., equilibrium sorption isotherm studies of Cd (II), Pb(II) and Zn (II) ions detoxification from wastewater using unmodified and EDTA modified maize husk, *Electronic J. Biotechnol.*, vol 10, pp. 536 – 548, 2007.
- Incharoensakdi, A., Kitjahan, P., Zinc Biosorption from Aqueous Solution by a Halotolerant Cyanobacterium *Aphanothece halophytica*, *Current Microbiol.*, vol 45, pp 261 – 264, 2002.
- Iqbal, M., Edyvean, R.G.J., Biosorption of lead, copper and zinc ions on loofa sponge immobilized biomass of *Phanerochaete chrysosporium*, *Miner. Eng.*, vol 144, pp. 181 – 187, 2004.

Jain, A. K., Hudgins, R. R., Silveston, P. L., Adsorption/desorption models: How useful for predicting reaction rate under cyclic operations, *The Canadian J. of Chem. Eng.*, Vol 61, pp. 46-49, 1983

Jaju, N., Sunrise zinc, Personal Communication, Goa, 1998.

Jha, M. K., Kumar, V., Singh, R. J., Review of hydrometallurgical recovery of zinc from industrial wastes, *Resource, Conservation and Recycling*, vol 33, pp 1-22, 2001.

Jhonson, C. E., Kenson, R. E., Tucker, L. H., Treatment of heavy metals in wastewaters, *Environ. Progress.*, vol 1, pp 212 – 216, 1982.

Jukes, T.H., Cantor, C. R., Evolution of protein molecules. In Munro HN, editor, *Mammalian Protein Metabolism*, pp. 21-132, Academic Press, New York, 1969.

Kadukova, J., Vircikova, E., Comparison of differences between copper bioaccumulation and biosorption, *Environment International*, vol – 31, pp. 227 -332, 2005.

Kambahty, Y., Mody, K., Basha, S., Jha, B., Kinetics, equilibrium and thermodynamic studies on biosorption of hexavalent chromium by dead fungal biomass of marine *Aspergillus niger*, *Chem. Eng. J.*, vol 145, pp. 489-495, 2009.

Kapoor, A., Viraraghavan, T., Fungal biosorption – An alternative treatment option for heavy metal bearing wastewater: A Review, *Bioresour. Technol.*, vol 53, pp. 195 – 206, 1995.

Kerney, U., Treatment of spent pickling acids from hot-dip galvanizing, *Resource Conservation and Recycling*, vol- 10, pp 145–151, 1994 a.

Kerney, U., New recycling technologies for Fe/Zn waste acids from hot dip galvanizing, Edited Proceedings: 17th International Galvanizing Conference Paris, European General Galvanizers Association (EGGA), GE2/1–3, 1994 b.

Kazy, S. K., D'Souza, S. F., Sar, P., Uranium and thorium sequestration by a *Pseudomonas sp.*: mechanism and chemical characterization, *J. Hazard. Mater.*, vol 163, pp. 65 – 72, 2009.

Kerney, U., Treatment of zinc-containing spent pickle acids, Edited Proceedings: 18th International galvanizing Conference Birmingham, European General Galvanizers Association (EGGA) (1997).

Klein, C. J., Zinc supplementation, *J. Am. Diet. Assoc.*, vol 100, pp 1137–1138, 2000.

Klimmek, S., Stan, H. J., Comparative analysis of the biosorption of cadmium, lead, nickel and zinc by algae, *Environ. Sci. Technol.*, vol 35, pp. 4283 – 4288, 2001.

- Kongsricharoern, N., Polprasert, C., Electrochemical precipitation of chromium Cr (VI) from an electroplating wastewater, *Water Science and Technology*, vol 31, pp 109 – 117, 1995.
- Kongsricharoern, N., Polprasert, C., Chromium removal by a bipolar electro-chemical precipitation process, *Water Science and Technology*, vol 34, pp 109 – 116, 1996.
- Kumar, Y. P., King, P., Prasad, V. R. S. K., Zinc biosorption on *Tectona grandis* L. f. leaves biomass: Equilibrium and kinetics, *Chem. Eng. J.*, vol 124, pp 63 – 70, 2006.
- Kuyucak, N., Volesky, B., Biosorbents for recovery of metals from industrial solutions, *Biotechnol. Lett.*, vol 10, pp. 137-142.
- Lee, T., Park, J.W., Lee, J. H., Waste green sands as reactive media for the removal of zinc from water, *Chemosphere*, vol 24, pp 571- 581, 2004.
- Lesmana, S. O., Febriana, N., Setaredjo, N., Sunarso, J., Ismadji, S., Studies on potential applications of biomass for the separation of heavy metals from water and wastewater, *Biochem. Eng. J.*, vol 44, pp 19- 41, 2009.
- Li, H., Lin, Y., Guan, W., Chang, J., Xu, L., Guo, J., Wei, G., Biosorption of Zn(II) by live and dead cells of *Streptomyces ciscaucasicus* strain CCNWHX 72-14, *J. Hazard. Mater.*, vol - 179, pp. 151 – 159, 2010.
- Liesegang, H., Lemke, K., Siddiqui, R.A., Schlegel, H.G., Characterization of the inducible nickel and cobalt resistance determinant *cnr* from pMOL28 of *Alcaligenes eutrophus* CH34. *J. Bacteriol.*, vol - 175, pp. 767–778, 1993.
- Liu, H. L., Chen, B. Y., Lan, Y. W., Cheng, Y. C., Biosorption of Zn (II) and Cu (II) by the indigenous *Thiobacillus thiooxidans*, *Chem. Eng. J.*, vol 94, pp. 195 – 201, 2004.
- Liu, Y., Liu, Y. J., Biosorption isotherms, kinetics and thermodynamics, *Sep. Purif. Technol.*, vol 61, pp. 229- 242, 2008.
- Lodi, A., Solisio, C., Converti, A., Borghi, M. D., Cadmium, Zinc, Copper, Silver and Chromium (III) removal from wastewaters by *Sphaerotilus natans*, *Bioprocess Eng.*, vol 19, pp. 197 – 203, 1998.
- Mackenzie, J., The application of imperial smelting process in India, In *Proceedings of international symposium on Pb-Zn-Cd, Retrospect and prospect*, New Delhi, pp C11 – 34, 1981.
- Madaeni, S. S., Mansourpanah, Y., COD removal from concentrated wastewater using membranes, *Filtrations and Separation*, vol 40 (6), pp 40 – 46, 2003.
- Madigan, M. T., Martinko, J. M., Parker, J., *Brock biology of microorganism*, Upper Saddle River, NJ, Pearson Printice Hall, 2000.

- Mameri, N., Boudries, N., Addour, L., Belhocine, D., Lounici, H., Grib, H., et al. Batch zinc biosorption by a bacterial non living *Streptomyces rimosus* biomass, *Wat. Res.*, vol 33, pp. 1347–1354, 1999.
- Malik, A., Metal bioremediation through growing cells, *Environ. Int.*, vol 30, pp. 261 – 278, 2004.
- Mann, H., Removal and recovery of heavy metals by biosorption, In Volesky, B., editor, *Biosorption of heavy metals*, Boca, Rezon., CRC Press, pp. 93 – 137, 1990.
- Mansur, M. B., Rocha, S. D. F., Magalhaes, F. S., Benedetto, J. S., Selective extraction of zinc (II) over iron (II) from spent hydrochloric acid effluents by liquid liquid extraction, *J. Hazard. Mater.*, vol 150, pp 669 – 678, 2008.
- Maranon, E., Fernandez, Y., Suarez, F.J., Alonso, F. J., Sastre, H., Treatment of acid pickling baths by means of anionic resins, *Ind. Eng. Chem. Res.*, vol 39, pp 3370–3376, 2000.
- Marin, A. B. P., Ortuno, J. F., Aguilar, M. I., Meseguer, V. F., Saez, J., Llorens, M., Use of chemical modification to determine the binding of Cd(II), Zn(II) and Cr(III) ions by orange waste, *Biochem. Eng. J.*, doi:10.1016/j.bej.2008.12.010.
- Miretzky, P., Saralegui, A., Cirelli, A. F., Simultaneous heavy metal removal mechanism by dead microphytes, *Chemosphere*, vol 62, pp 247 – 254.
- Masel, I. R., Principles of adsorption and reaction on solid surfaces, John Wiley Publications, Newyork, 1952.
- Matheickal, J. T., Yu, Q., Biosorption of lead (II) and copper (II) from aqueous solutions by pre treated biomass of Australian marine algae, *Bioresour. Technol.*, vol 69, pp. 223 – 229, 1999.
- Mattuschka, B., Straube, G., Biosorption of metals by a waste biomass, *J. Chem. Technol. Biotechnol.*, vol 58, pp. 57 – 3, 1993.
- Mergeay, M., Monchy, S., Vallaey, T., Auquier, V., Benotmane, A., Bertin, P., Taghavi, S., Dunn, J., van der Lelie, D., Wattiez, R., *Ralstonia metallidurans*, a bacterium specifically adapted to toxic metals: towards a catalogue of metal-responsive genes, *FEMS Microbiol.*, vol 9, pp. 1181–1191, 2003.
- Mishra, P. C., Patel, R. K., Removal of lead and zinc ions from by low cost adsorbents, *J. Hazard. Mater.*, vol 168, pp 319-325, 2009.
- Mishra, V., Balomajumder, C., Agarwal, V. K., Zn (II) ion biosorption on to surface of eucalyptus leaf biomass: isotherm, kinetic and mechanistic modeling, *CLEAN – Soil Air Water*, vol 38, pp 1062–1073, 2010.

Mishra, V., Balomajumder, C., Agarwal, V. K., Biosorption of Zn (II) ion onto surface of *cedrus deodara* sawdust: studies on isotherm modeling and surface characterization, Int. J. Chem. Sci. Applications, vol 2, pp. 179- 185, 2011.

Mishra, V., Balomajumder, C., Agarwal, V. K., Optimization of physical parameters for batch mode Zn (II) ion removal from liquid phase: A potential biosorption study, Environmental Progress and Sustainable Energy (AIChE), DOI 10.1002/ep.10637.

Mishra, V., Balomajumder, C., Agarwal, V. K., Kinetics, mechanistic and thermodynamics of Zn (II) ion sorption: A modeling approach, Clean Soil Air Water (Accepted, in press).

Moat, A. G., Foster, J. W., In: Spector, M. P., Microbial Physiology, Wiley – Liss, Newyork, 2002.

Mohan, D., Singh, K. P., Single- and multi-component adsorption of cadmium and zinc using activated carbon deprived from bagasse-an agricultural waste, Wat. Res., vol 36, pp 2304-2318, 2002.

Mohanty, K., Das, D., Biswas, M.N., Adsorption of phenol from aqueous solutions using activated carbons prepared from *Tectona grandis* sawdust by ZnCl<sub>2</sub> activation, Chem. Eng. J., Vol 115, pp. 121–131, 2005.

Mukherjee, P., Environmental Management Plan For Wallarah Coal Mine”, Parsons Brinckerhoff Australia Pty Limited, 2007.

Mulligan, C. N., Yong, R N., Gibbs, B. F., Heavy metal removal from sediments by Biosurfactants, J. Hazard. Mater., vol 81, pp 111-125, 2001.

Muraleedharan, T. R., Venkobachar, C., mechanism of biosorption of copper (II) by *Ganoderma Lucidum*, Biotechnol. Bioeng., vol – 35, pp. 320 – 325, 1990.

Naiya, T. K., Chowdhury, P., Bhattacharya, A. K., Das, S. K., Sawdust and neem bark as low cost natural biosorbent for adsorptive removal of Zn (II) and Cd (II) ions from aqueous solutions, Chem. Eng. J., vol 148, pp 68-79, 2009.

Nemr, A. E., Potential of pomegranate husk carbon for Cr (VI) removal from wastewater kinetic and isotherm studies, J. Hazard. Mater., vol 161, pp. 132- 141, 2009.

Norton, L., Baskaran, K., Mckenzie, T., Biosorption of zinc from aqueous solutions using biosolids, Adv. Environ. Res., vol 8, pp. 629 – 635, 2004.

Nuhoglu, Y., Malkac, E., Thermodynamic and kinetic studies for environmentally friendly Ni (II) biosorption using waste pomace of olive oil factory, *Bioresour. Technol.*, vol 100, pp. 2375 – 2380, 2009.

Nuttall, C. A., Younger, P. L., Zinc removal from hard, circum-neutral mine waters using a novel closed bed limestone reactor, *Wat. Res.*, vol 34, pp 1262- 1268.

O'Connell, D. W., Birkinshaw, C., O' Dwyer, T. F., Heavy metal adsorbents prepared from modification of cellulose: A review, *Bioresour. Technol.*, vol 99, pp 6709 – 6724, 2008.

Ong, S. A., Toorisaka, E., Hirata, M., Hano, T., The behavior of Ni (II), Cr(III), and Zn (II) in biological wastewater treatment process, *Acta hydrochim. Hydrobiol.*, vol 33, pp. 95 -103, 2005.

Ostroski, I. C., Barros, M. A. S. D., Silva, E. A., Dantas, J. H., Arroyo, P. A., Lima, O. C.M., A comparative study for the ion exchange of Fe (III) and Zn (II) on zeolite NaY, *J. Hazard. Mater.*, vol 161, pp 1404-1412, 2009.

Ozdemir, S., Kilinc, E., Poli, A., Nicolus, B., Guen, K., Biosorption of Cd, Cu, Ni, Mn and Zn from aqueous solutions by thermophilic bacteria, *Geobacillus toebii sub.sp. decanicus* and *Geobacillus thermoleovorans sub.sp. strombolensis*: Equilibrium, kinetic and thermodynamic studies, *Chem. Eng. J.*, vol 152, pp. 195-206, 2009.

Ozdes, D., Gundogdu, A., Kemer, B., Duran, C., Senturk, H. B., Soylak, M., Removal of Pb(II) ions from aqueous solution by a waste mud copper mine industry Equilibrium, kinetic and thermodynamic study, *J. Hazard. Mater.*, doi: 10.1016/j.jhazmat.2008.12.073.

Padmavati, V., Biosorption of nickel (II) ions by bakers's yeast: kinetic, thermodynamic and desorption studies, *Bioresour. Technol.*, vol 99, pp. 3100 – 3109, 2008.

Pamukoglu, M. Y., Kargi, F., Effects of operating parameter on kinetics of copper (II) ion non pre-treated powdered waste sludge (PWS), *Enzyme and microbial technol.*, vol 42, pp. 76 – 82, 2007.

Pardo, R., Herguedas, M., Barrado, E., Vega, M., Biosorption of cadmium, copper, lead and zinc by inactive biomass of *Pseudomonas putida*, *Anal. Bioanal. Chem.*, vol 376, pp. 26 – 32, 2003.

Pavasant, P., Apiratikul, R., Sungkhum, V., Suthiparinyanont, P., Wattanachira, S., Marhaba, T. F., Biosorption of  $\text{Cu}^{2+}$ ,  $\text{Cd}^{2+}$ ,  $\text{Pb}^{2+}$  and  $\text{Zn}^{2+}$  using dried marine green microalga *caulerpa lentillifera*, *Bioresour. Technol.*, vol 97, pp. 2321 – 2329, 2006.

Pejic, B., Vukeevic, M., Kostic, M., Skundric, P., Biosorption of heavy metal ions from aqueous solutions by short hemp fibers: Effect of chemical composition, *J. Hazard. Mater.*, doi 10.1016/j.jhazmat.2008.07.139.



- Prescott, L. M., Harley, J. P., Klein, D. A., Microbiology, McGrawhill-Science, 2002.
- Preetha, B., Viruthagiri, T., Batch and continuous biosorption of Cr (VI) by *Rhizopus arrhizus*, Sep. Purif. Technol., vol 57, pp. 126 – 133, 2007.
- Qin J. J., Wai, M. N., Oo, M. H., Wong, F. S., A feasibility study on the treatment and recycling of a waste water from metal plating, J. Membr. Sci., vol 208, pp. 213 – 221, 2002.
- Rocha, C. G., Zaia, D. A. M., Alfaya, R. V. S., Alfaya, A. A. S., Use of rice straw as biosorbent for removal of Cu (II), Zn (II), Cd (II) and Hg (II) ions in industrial effluent, J. hazard. Mater., doi: 10.1016/j.jhazmat.2008..11.074, 2008.
- Reddy, K. R., Ashraf, A. L. H., Prasanth, A., Enhanced Soil Flushing for Simultaneous Removal of PAHs and Heavy Metals from Industrial Contaminated Soil, *Practice Periodical of Hazard., Toxic, and Radioactive Waste Management*, vol 15, pp. 166 – 174, 2011.
- Remacle, J., The cell wall and metal binding, In: Volesky, B., Editor, Biosorption of heavy metals, Boca Raton, CRC Press, pp. 83 – 92, 1990.
- Romera, E., Gonzalez, F., Ballester, A., Blazquez, M. L., Munoz, J. A., Comparative study of biosorption of heavy metals using different types of algae, Bioresour. Technol., vol 98, pp. 3344 – 3353, 2007.
- Ruiz, C. G., Tirado, V. R., Gil, G. B., Cadmium and zinc removal from aqueous solution by *Bacillus jeotgali*: pH, salinity and temperature effects, Bioresour. Technol., vol 99, pp. 3864 – 3874, 2008.
- Rubio, J., Souza, M. L., Smith, R. W., Overview of flotation as a wastewater treatment Technique, Minerals Eng., vol 15, pp 139 – 155, 2002.
- Ruiz, C. G., Tirado, V. R., Gil, B. G., Cadmium and zinc removal from aqueous solutions by *Bacillus jeotgali*: pH, salinity and temperature effects, Bioresour. Technol., vol 99, pp 3864–3870, 2008.
- Sag, Y., Kutsal, Determination of the biosorption of heavy metal ions on *Zoogloea ramigera* and *Rhizopus arrhizus*, Biochem. Eng. J., vol 6, pp. 145 – 151, 2000.
- Salehideh, H., Shojaosadati, S. A., Removal of metal ions from aqueous solution by polysaccharide produced from *Bacillus firmus*, Wat. Res., vol 37, pp. 4231 – 4235, 2003.
- Sari, A., Tuzen, M., Kinetic and equilibrium studies of biosorption of Pb (II) and Cd (II) from aqueous solution by macrofungus (*Amanita rubescens*) biomass, J. Hazard. Mater. Vol 164, pp. 1004 -1011, 2009.
- Saitou, N., Nei, M., The neighbor-joining method: A new method for reconstructing phylogenetic trees, Mol. Biol. Evol., 4, pp. 406-425, 1987.

Sengil, I. A., Ozacar, M., Competitive biosorption of  $Pb^{2+}$ ,  $Cu^{2+}$ , and  $Zn^{2+}$  ions from aqueous solutions onto valonia tannin resin, *J. Hazard. Mater.*, doi10.1016/j.jhazmat.2008.12.071, 2009.

Siegel, S. M., Siegel, B. Z., Clark, K. E., Bio-corrosion: solubilization and accumulation of metals by fungi, *Water, Air, Soil Pollut.*, vol 19, pp. 229 – 236, 1983.

Silva, R. M. P., Rodriguez, A. A., Oca, J. M. G. M. D., Moreno, D. C., Biosorption of chromium, copper, manganese and zinc by *Pseudomonas aeruginosa* AT18 isolated from a site contaminated with petroleum, *Bioresour. Technol.*, vol 100, pp. 1533-1538, 2009.

Shaker, M. A., Thermodynamic profile of some heavy metal ions adsorption onto biomaterial surface, *Am. J. Appl. Sci.*, vol 4, pp. 605 – 612, 2007.

Sharma, K., Personnel Communication, Birla copper, 1998.

Sharma, S., Dastidar, M. G., Sreekrishnan, T. R., Zinc uptake by fungal biomass isolated from industrial wastewater, pp. 256 – 261, 2002.

Sharma, S. K., In: proceedings of the conference on Base Metal Technology, pp 8 -10, 1989.

Shek, T. Z., Ma, A., Lee, V. K. C., McKay, G., Kinetics of zinc ions removal effluents using ion exchange resin, *Chem. Eng. J.*, vol 146, pp. 63 – 70, 2009.

Sheha, R. R., Sorption behavior of Zn (II) ions on synthesized hydroxyapatites, *J. Colloid and Interface Sci.*, vol 310, pp. 18-26, 2007.

Sherif, S. A., Stock, D. E., Michaelides, E. E., Davis, L. R., Celik, I., Khaligi, B., and Kumar, R., Measurement and modeling of environmental Flows- FED-Vol. 143/HTD.232, Book. No. G00772 (ISBN 0-7918-1128-X), 251, 1992.

Siddiqui, R.A., Benthin, K., Schlegel, H.G., Cloning of pMOL28-encoded nickel resistance genes and expression of the genes in *Alcaligenes eutrophus* and *Pseudomonas* spp, *J. Bacteriol.*, vol 171, pp. 5071–5078, 1989.

Silva, R.M.P., Rodriguez, A.A., Gomez, J.M.D.O., Moreno, D.C., Biosorption of chromium, copper, manganese, and zinc by *Pseudomonas aeruginosa* AT 18 isolated from a site contaminated with petroleum, *Bioresour. Technol.*, vol 100, pp. 1533 – 1536, 2009.

Solanki, S., Singh, V., The electrolytic zinc plant of HZL at Debari and its development, In: proceedings of international symposium on Pb – Zn – Cd, Retrospect and Prospect, New Delhi, E 92-112, 1981.

Skowronski, T., Pirszel, J., Skowronska, B. P., Heavy Metal Removal by the Waste Biomass of *Penicillium chrysogenum*, *Water Qual. Res. J. Canada*, Vol 36, pp. 793–803, 2001.

Sprynskyy, M., Solid-liquid extraction of heavy metals (Cr, Cu, Cd, Ni and Pb) in aqueous systems of zeolite – sewage sludge, *J. Hazard. Mater.*, vol 161, pp 1377 – 1383, 2009.

Srinivasan, K., Hema, M., Nickel removal from waste water by using activated carbon prepared from agro industrial wastes, *Res. J. Chem. Environ.*, 2009, 13, pp. 54 – 65, 2009.

Srivastava, S., Srivastava, A. K., Biological phosphate removal by model based fed-batch cultivation of *Acinetobacter calcoaceticus*, *Biochem. Eng. J.*, 2008, vol 40, pp. 227 - 232.

Srivastava, V.C., Swamy, M.M., Mall, I.D., Prasad, B., Mishra, I.M., Adsorptive removal of phenol by bagasse fly ash and activated carbon: Equilibrium, kinetics and thermodynamics. *Colloids and Surface A: Physicochem. Eng. Aspects.*, vol 272, pp. 89 – 104, 2006.

Srivastava, V. C., Mall, I. D., Mishra, I. M., Adsorption thermodynamics and isosteric heat of adsorption of toxic metals into bagasse fly ash (BFA) and rice ash husk (RHA), *Chem. Eng. J.*, vol 132, pp 267-278, 2007.

Stocks, C., Wood, J., Guy, S., minimization of recycling of spent acid waste from galvanizing plant, *Resource, Conservation and Recycling*, vol 44, pp 153 – 166, 2005.

Tamura, K., Dudley, J., Nei, M., Kumar, S. (2007). MEGA4: Molecular Evolutionary Genetics Analysis (MEGA) software version 4.0, *Molecular Biology and Evolution.*, vol 24, pp.1596-1599.

Taniguchi, J., Hemmi, H., Tanahashi, K., Amano, N., Nakayama, T., Nishino, T., zinc biosorption by zinc resistant bacterium *Brevibacterium* sp. HZM-1, *Appl. Microbiol. Biotechnol.*, vol 54, pp. 581 – 588, 2000.

Tiwari, D., Kin, H. U., Lee, S. K., Removal behavior of sericite for Cu (II) and Pb (II) from aqueous solutions: Batch and column studies, *Separation and Purification Technol.*, vol 57, pp. 11 – 16, 2007.

Tobin, J. M., Cooper, D. G., Neufeld, R. J., Uptake of metal ions by *Rhizopus arrhizus* biomass, *Appl. Environ. Microbiol.*, vol 47, pp. 821-824, 1984.

Tofan, L., Paduraru, C., Bilba, D., Rotariu, M., Thermal power plant ash as sorbent for the removal of Cu (II) and Zn (II) ions from wastewaters, *J. Hazard. Mater.*, vol 156, pp 1 – 8, 2008.

Thomas, G., Bianani Zinc Ltd. Personal communication, Kerala, 1998.

Tsezos, M., Volesky, B., Biosorption of uranium and thorium, *Biotechnology and Bioengineering*, vol – 23, pp. 583 -604, 1981.

- Tsezos, M., Volesky, B., The mechanism of uranium biosorption, *Biotechnology and Bioengineering*, vol – 23, pp. 385 -401, 1982.
- Tuppurainen, K. O., Vaisanan, A. O., Rintala, J. A., Zinc removal in anaerobic sulphate reducing liquid substrate process, *Minerals Eng.*, vol 15, pp 847 – 852.
- Ucun, H., Aksakal, O., Yildiz, E., Copper (II) and zinc (II) biosorption on *Pinus sylvestris* L., *J. Hazard. Mater.*, vol 161, pp 1040-1045, 2009.
- Urrutia, M. M., General bacterium sorption process, in Wase, J., Froster, C., editors, *Biosorbents for metal ions*, London, UK, CRC Press, pp. 39 – 66, 1997.
- Vaghetti, C. J. P., Lima, E. C., Royer, B., Brasil, L. J., Cunha, B. M., Simon, N. M., F.N. Cardosos, F. N., Norena, Z. P. C., Application of Brazilian fruit coat as a biosorbent to remove of Cr (VI) from aqueous solution- kinetic and equilibrium study, *Biochem. Eng. J.*, vol 42, pp. 67 – 76, 2008.
- Velaquez, L., Dussan, J., Biosorption and bioaccumulation of heavy metals on dead and living biomass of *Bacillus sphaericus*, *J. Hazard. Mater.*, doi. 10.1016/j.jhazmat.2009.01.044, 2009.
- Veglio, F., Beolchini, F., Removal of metals by biosorption: a review, *Hydrometallurgy*, vol – 44, pp. 301 – 316, 1997.
- Vijayaraghavan, K., Teo, T. T., Balasubramanian, R., Joshi, U. M., Application of *Sargassum* biomass to remove heavy metal ions from synthetic multi-metal solutions and urban storm water runoff, *J. Hazard. Mater.*, doi:10.1016/j.jhazmat.2008.08.105.
- Vilar, V. J. P., Botelho, C. M. S., Boaventura, R. A. R., Chromium and zinc uptake by algae *Gelidium* and agar extraction algal waste: Kinetics and equilibrium, *J. Hazard. Mater.*, vol 149, pp. 643 – 649, 2007.
- Vilar, V. J. P., Botelho, C. M. S., Boaventura, R. A. R., Chromium and zinc uptake by algae *Gelidium* and agar extraction algal waste: Kinetics and equilibrium, *Bioresour. Technol.*, vol 99, pp. 750- 762, 2008.
- Volesky, B., in: B. Volesky (Ed.), *Sorption and biosorption*, BV Sorbex Inc., Montreal, St. Lambert, Que, Canada, 2003.
- Volesky, B., Holan, Z. R., Biosorption of heavy metals, *Biotechnol. Prog.*, vol 11, pp. 235 – 250, 1995.
- Velaquez, L., Dussan, J., Biosorption and bioaccumulation of heavy metals on dead and living biomass of *Bacillus sphaericus*, doi: 1016./j.jhazmat.2009.01.044, 2009.

- Vengris, T., Binkiene, R., Sveikauskaite, A., Nickle, copper and zinc from waste water by a modified clay, *Applied clay science*, vol 18, pp. 183 – 190, 2001.
- Vullo, D. L., Ceretti, H. M., Daniel, M. A., Ramirez, S. A. M., Zalts, A., Cadmium, zinc and copper biosorption mediated by *Pseudomonas veronii* 2E, *Bioresour. Technol.*, vol 99, pp. 5574 – 5581, 2008.
- Walker, W. J., McNutt, R. P., Maslanka, C. A. K., The potential contribution of urban runoff to surface sediments of the Passaic river: sources and chemical characteristics, *Chemosphere*, vol 38, pp 363–377, 1999.
- Wallenborn, J. G., Evansky, P., Shannahan, J. H., Vallanat, B., Ledbetter, A. D., Schlader, C. M., Richards, J. H., Gottipolu, R. R., Nyska, A., Kodavanti, U. P., Subchronic inhalation of zinc sulphate induces cardiac changes in healthy rats, *Toxicology and applied pharmacology*, vol 232, pp 69 – 77, 2008.
- Wallenborn, J. G., Kovalick, K. D., McGee, K. J., Landis, M. S., Kodavanti, U. P., Systemic translocation of <sup>70</sup> zinc: Kinetics following intratracheal instillation in rats, *Toxicology and Applied pharmacology*, vol 234, pp 25 – 32, 2009.
- Wang, J., Chen, C., Biosorbents for heavy metals removal and their future, *Biotechnol. Adv.*, vol 27, pp 195- 226, 2009.
- Wang, S. W., Li, Y. F., He, W., Miao, H. N., Hg (II) removal from aqueous solutions by bacillus subtilis biomass, *Clean Soil Air Water*, vol 38, pp. 44- 48, 2010.
- Wakatsuki, T., Metal oxidoreduction by microbial cells, *J. Industrial Microbiology.*, vol 14, pp. 169 -177, 1995.
- Wilson, M. R., Foucaud, L., barlow, P. G., Hutchison, G. R., Sales, J., Simson, J. R., Stone, V., Nanoparticle interactions with zinc and iron: Implications for toxicology and inflammation, *Toxicology and applied pharmacy*, vol 255, pp 80 – 89, 2007.
- Wu, Q. T., Hei, L., Wong, J. W. C., Schwartz, C., Morel, J. L., Co-cropping for phyto separation of zinc and potassium from sewage sludge, *Chemosphere*, vol-68, pp 1954- 1960, 2007.
- Yaman, L. H. X., Xia, C. H. L., Isolation and biosorption characteristics of zinc resistant bacterium, *IEEE*, 2010.
- Yan, G., Viraraghavan, T., Heavy-metal removal from aqueous solution by fungus *Mucor rouxii*, *Water Res.*, vol 37, pp. 4486–4496, 2003.

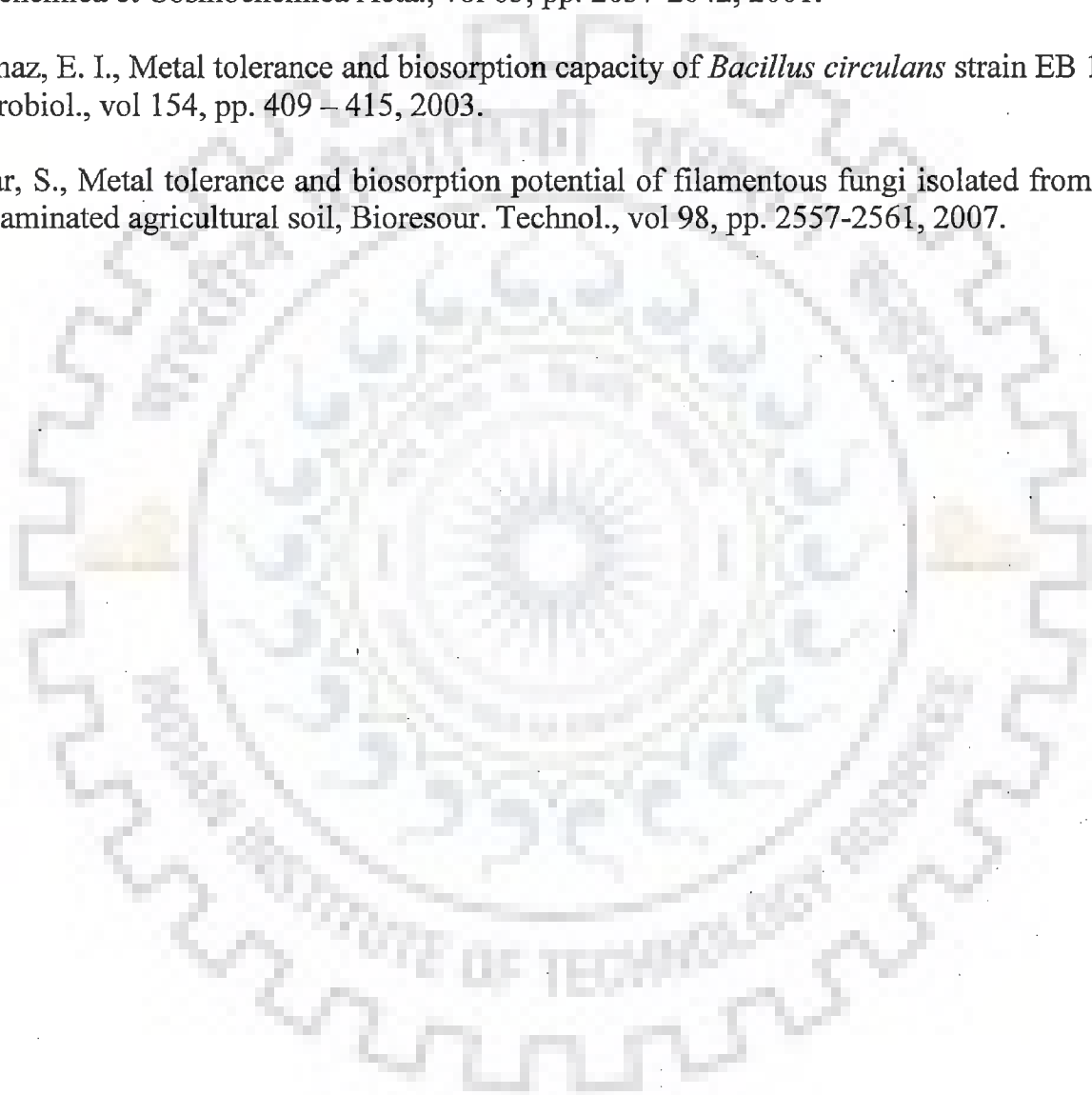
Yang, J., Wang, Q., Luo, Q., Wang, Q., Wu, T., Biosorption behavior of heavy metals in bioleaching, process of MSWI fly ash by *Aspergillus niger*, *Biochem. Eng. J.*, vol 46, pp. 294 – 299, 2009.

Yeddou, N., Bensmaili, A., Equilibrium and kinetic modeling of iron adsorption by eggshell in a batch system: effect of temperature, *Deslination*, vol 206, pp. 127 -134, 2007.

Yee, N., Fein, J., Cd adsorption onto bacterial surfaces: A universal adsorption edge?, *Geochimica et Cosmochimica Acta.*, vol 65, pp. 2037-2042, 2001.

Yilmaz, E. I., Metal tolerance and biosorption capacity of *Bacillus circulans* strain EB 1, *Res. Microbiol.*, vol 154, pp. 409 – 415, 2003.

Zafar, S., Metal tolerance and biosorption potential of filamentous fungi isolated from metal contaminated agricultural soil, *Bioresour. Technol.*, vol 98, pp. 2557-2561, 2007.





# **ANNEXURE AND APPENDIX**

## ANNEXURE (A-1)

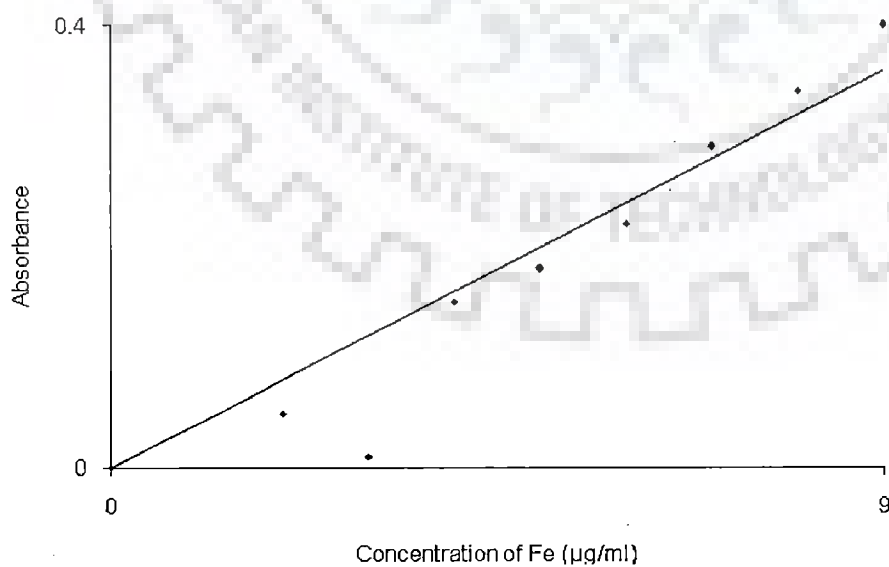
### Analysis

Filename C:\Program Files\GBC Avanta Ver 1.31\Analysis 1 .ani  
Element Fe,  
Date Fri Jul 16 12:54:19 2010

### Full Calibration

Calibration mode Linear LS Through Zero Max Error: 0.055 R<sup>2</sup>: 0.997

Sample Lable	Conc µg/ml	%RSD	Mean Abs
Cal Blank	---	0.05	0
Standard 1	2	3.36	0.05
Standard 2	3	2.12	0.01
Standard 3	4	3.11	0.15
Standard 4	5	3.33	0.18
Standard 5	6	3.18	0.22
Standard 6	7	2.29	0.29
Standard 7	8	2.08	0.34
Standard 8	9	1.93	0.4





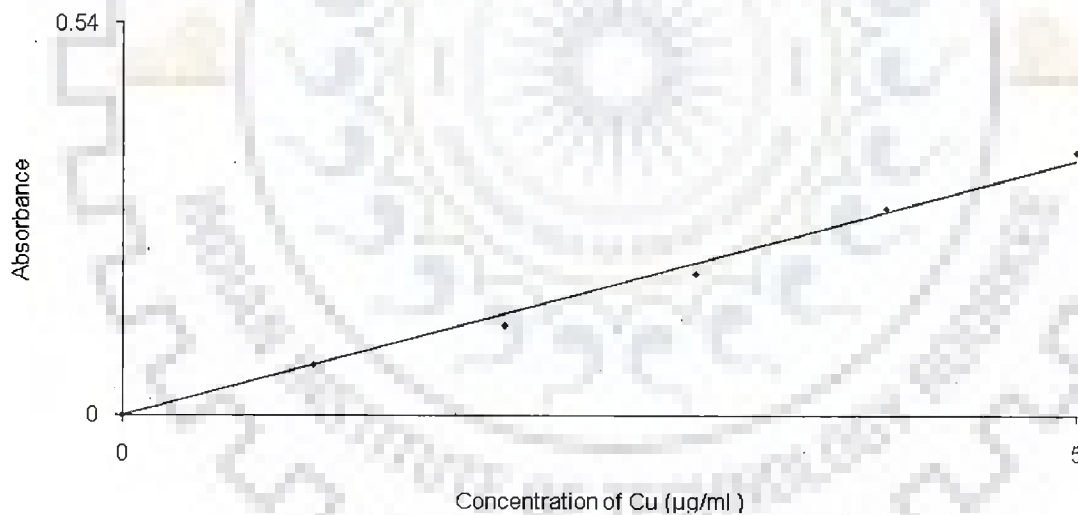
Analysis

Filename C:\Program Files\GBC Avanta Ver 1.31\Analysis 1 .ani  
Element Cu,  
Date Fri Jul 16 14:58:27 2010

Full Calibration

Calibration mode Linear LS Through Zero Max Error: 0.042 R<sup>2</sup>: 0.991

Sample Lable	Conc µg/ml	%RSD	Mean Abs
Cal Blank	---	0.069	0
Standard 1	1	4.28	0.07
Standard 2	2	2.18	0.124
Standard 3	3	3.11	0.196
Standard 4	4	3.33	0.285
Standard 5	5	3.18	0.362



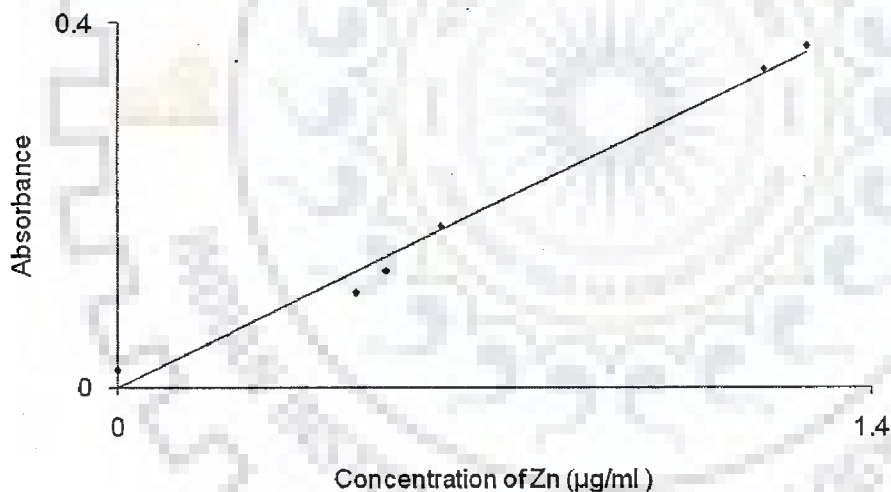
Analysis

Filename C:\Program Files\GBC Avanta Ver 1.31\Analysis 1 .ani  
Element Zn,  
Date Fri Jul 16 16:50:27 2010

Full Calibration

Calibration mode Linear LS Through Zero Max Error: 0.042 R<sup>2</sup>: 0.998

Sample Lable	Conc µg/ml	%RSD	Mean Abs
Cal Blank	-----	3.59	0.0187
Standard 1	0.442	1.28	0.1031
Standard 2	0.5	2.39	0.1285
Standard 3	0.6	0.68	0.1767
Standard 4	1.2	2.58	0.3494
Standard 5	1.28	3.5	0.3743



## ANNEXURE (A-2)

Table 5.2.1 (a) Influence of pH on biosorption of Fe (II, III) and Cu (II) ions in presence of Zn (II) on the surface of Mango bark sawdust

pH	1	2	3	4	5	6	7	8
Metal ion system	Zn (II) – Cu (II)							
% removal (Cu)	13.28	26.39	54.14	72.21	84.16	58.12	44.36	34.66
Metal ion system	Zn (II) – total Fe (II, III)							
% removal (Fe II, III)	6.21	11.5	19.36	36.11	48.11	35.18	30.21	19.21
Metal ion system	Zn (II) – total Fe (II, III) – Cu (II)							
% removal (Cu)	11.36	21.18	48.14	68.24	80.16	74.11	65.16	51.26
% removal (Fe II, III)	1.28	6.51	12.36	18.31	26.11	24.55	30.42	12.31

Table 5.2.1 (b): Influence of pH on biosorption of Fe (II, III) and Cu (II) ions in presence of Zn (II) on the surface of Orange peel

pH	1	2	3	4	5	6	7	8
Metal ion system	Zn (II) – Cu (II)							
% removal (Cu)	10.14	15.24	30.31	48.16	76.18	72.16	64.16	58.12
Metal ion system	Zn (II) – total Fe (II, III)							
% removal (Fe II, III)	3.36	7.88	24.21	30.11	32.11	28.58	22.18	19.28
Metal ion system	Zn (II) – total Fe (II, III) – Cu (II)							

% removal (Cu)	8.84	21.18	28.31	46.1	71.16	53.12	46.11	38.21
% removal (Fe II, III)	2.21	6.6	10.11	12.31	21.31	22.32	17.61	11.21

Table 5.2.1 (c) Influence of pH on biosorption of Fe (II, III) and Cu (II) ions in presence of Zn (II) on the surface of Pineapple peel powder

pH	1	2	3	4	5	6	7	8
Metal ion system Zn (II) – Cu (II)								
% removal (Cu)	9.06	14.21	34.24	46.15	59.18	72.15	80.18	80.18
Metal ion system Zn (II) – total Fe (II, III)								
% removal (Fe II, III)	2.24	7.78	9.24	20.44	26.11	30.28	30.33	30.33
Metal ion system Zn (II) – total Fe (II, III) – Cu (II)								
% removal (Cu)	8.86	12.34	28.11	36.13	51.66	57.18	58.21	58.21
% removal (Fe II, III)	1.38	6.61	8.81	13.44	22.15	22.10	22.14	22.14

Table 5.2.1 (d) Influence of pH on biosorption of Fe (II, III) and Cu (II) ions in presence of Zn (II) on the surface of Jackfruit peel powder

pH	1	2	3	4	5	6	7	8
Metal ion system Zn (II) – Cu (II)								
% removal (Cu)	10.33	21.36	34.24	52.16	68.16	79.56	72.21	65.36
Metal ion system Zn (II) – total Fe (II, III)								
% removal (Fe II, III)	1.88	8.81	12.11	21.11	28.16	22.18	20.11	13.12

Metal ion system	Zn (II) – total Fe (II, III) – Cu (II)								
% removal (Cu)		9.18	16.64	23.31	38.54	55.51	68.61	55.91	48.36
% removal (Fe II, III)		1.11	6.38	10.36	14.36	20.24	11.18	9.91	5.28

Table 5.2.1 (e) Influence of on biosorption of Fe (II, III) and Cu (II) ions in presence of Zn (II) on the surface of *Cedrus deodara* sawdust

pH		1	2	3	4	5	6	7	8
Metal ion system	Zn (II) – Cu (II)								
% removal (Cu)		15.36	24.31	44.51	58.6	71.11	65.36	57.11	53.11
Metal ion system	Zn (II) – total Fe (II, III)								
% removal (Fe II, III)		9.15	15.57	28.56	32.64	37.19	29.66	25.81	19.14
Metal ion system	Zn (II) – total Fe (II, III) – Cu (II)								
% removal (Cu)		13.6	21.34	40.36	51.88	65.5	60.14	52.82	48.36
% removal (Fe II, III)		5.55	15.61	24.21	27.16	32.14	24.41	20.16	16.41

Table 5.2.1 (f) Influence of pH on biosorption of Fe (II, III) and Cu (II) ions in presence of Zn (II) on the surface of *Eucalyptus* bark sawdust

pH		1	2	3	4	5	6	7	8
Metal ion system	Zn (II) – Cu (II)								
% removal (Cu)		18.17	24.18	35.19	49.61	74.19	65.13	55.16	48.11

Metal ion system	Zn (II) – total Fe (II, III)								
% removal (Fe II, III)		2.06	9.04	14.04	20.18	27.19	20.14	15.19	10.12
Metal ion system	Zn (II) – total Fe (II, III) – Cu (II)								
% removal (Cu)		11.18	19.86	29.44	40.31	53.12	49.14	41.82	35.18
% removal (Fe II, III)		1.29	7.21	10.21	14.11	20.22	13.01	12.18	7.76

Table 5.2.1 (g) Influence of pH biosorption of Fe (II, III) and Cu (II) ions in presence of Zn (II) on the surface of Eucalyptus leaf powder

pH		1	2	3	4	5	6	7	8
Metal ion system	Zn (II) – Cu (II)								
% removal (Cu)		10.11	19.86	29.11	49.84	68.38	59.11	50.11	44.51
Metal ion system	Zn (II) – total Fe (II, III)								
% removal (Fe II, III)		1.81	11.16	14.04	22.18	33.18	23.88	12.91	8.59
Metal ion system	Zn (II) – total Fe (II, III) – Cu (II)								
% removal (Cu)		9.46	15.61	24.19	42.31	59.64	38.56	31.18	5.54
% removal (Fe II, III)		1.36	9.24	10.11	13.16	21.86	18.56	8.94	4.48

Table 5.2.1 (h) Influence of pH on biosorption of Fe (II, III) and Cu (II) ions in presence of Zn (II) on the surface of Eggshell and membrane powder

pH	1	2	3	4	5	6	7	8
Metal ion system	Zn (II) – Cu (II)							
% removal (Cu)	10.21	14.19	26.35	46.18	65.91	56.12	45.31	34.41
Metal ion system	Zn (II) – total Fe (II, III)							
% removal (Fe II, III)	1.08	10.21	13.04	19.56	27.57	17.32	13.81	7.31
Metal ion system	Zn (II) – total Fe (II, III) – Cu (II)							
% removal (Cu)	8.31	12.36	19.61	36.59	48.97	39.61	31.85	21.36
% removal (Fe II, III)	1.09	6.61	15.11	16.35	24.51	13.52	8.91	4.49

Table 5.2.1 (i) Influence of pH on biosorption of Fe (II, III) and Cu (II) ions in presence of Zn (II) on the surface of *Zinc sequestering bacterium VMSDCM* accession no. HQ108109

pH	1	2	3	4	5	6	7	8
Metal ion system	Zn (II) – Cu (II)							
% removal (Cu)	18.19	26.14	43.68	56.14	73.14	84.19	88.19	88.19
Metal ion system	Zn (II) – total Fe (II, III)							
% removal (Fe II, III)	11.21	21.36	36.52	44.57	64.19	72.13	81.1	81.12
Metal ion system	Zn (II) – total Fe (II, III) – Cu (II)							

% removal (Cu)	16.14	21.1	40.68	49.18	61.21	76.11	81.23	81.23
% removal (Fe II, III)	9.21	16.51	28.16	34.11	51.22	60.74	73.34	73.34

Table 5.2.2 (a) Influence of temperature on biosorption of Fe (II, III) and Cu (II) ions in presence of Zn (II) on the surface of Mango bark sawdust

Temperature (K)	298	303	308	313	318
Metal ion system Zn (II) – Cu (II)					
% removal Cu (II)	55.16	84.16	58.07	42.14	36.6
Metal ion system Zn (II) – total Fe (II, III)					
% removal (Fe II, III)	28.11	48.11	31.18	25.61	19.21
Metal ion system Zn (II) – total Fe (II, III) – Cu (II)					
% removal (Cu)	31.84	80.16	32.68	20.14	11.31
% removal (Fe II, III)	17.36	26.11	20.11	9.81	5.54

Table 5.2.2 (b) Influence of temperature on biosorption of Fe (II, III) and Cu (II) ions in presence of Zn (II) on the surface of Orange peel

Temperature (K)	298	303	308	313	318
Metal ion system Zn (II) – Cu (II)					
% removal Cu (II)	52.38	76.18	37.84	25.24	14.16
Metal ion system Zn (II) – total Fe (II, III)					
% removal (Fe II, III)	30.20	32.11	29.11	22.61	9.36
Metal ion system Zn (II) – total Fe (II, III) – Cu (II)					
% removal (Cu)	32.86	71.16	32.61	23.81	12.19
% removal (Fe II, III)	21.11	21.31	19.36	10.31	4.31



Table 5.2.2 (c) Influence of temperature on biosorption of Fe (II, III) and Cu (II) ions in presence of Zn (II) ion on Pineapple peel

Temperature (K)	298	303	308	313	318
Metal ion system Zn (II) – Cu (II)					
%removal Cu (II)	60.16	80.18	62.11	43.1	18.19
Metal ion system Zn (II) – total Fe (II, III)					
% removal (Fe II, III)	12.16	30.33	21.11	16.32	7.41
Metal ion system Zn (II) – total Fe (II, III) – Cu (II)					
% removal (Cu)	31.18	58.21	30.61	24.11	16.31
% removal (Fe II, III)	9.36	22.14	19.36	10.31	4.31

Table 5.2.2 (d) Influence of temperature on biosorption of Fe (II, III) and Cu (II) ions in presence of Zn (II) ion on Jackfruit peel powder

Temperature (K)	298	303	308	313	318
Metal ion system Zn (II) – Cu (II)					
%removal Cu (II)	28.16	68.16	36.18	43.1	24.56
Metal ion system Zn (II) – total Fe (II, III)					
% removal (Fe II, III)	18.24	28.16	21.11	16.32	7.41
Metal ion system Zn (II) – total Fe (II, III) – Cu (II)					
% removal (Cu)	31.18	55.51	30.61	24.11	16.31
% removal (Fe II, III)	5.58	20.24	11.25	8.85	3.36

Table 5.2.2 (e) Influence of temperature on biosorption of Fe (II, III) and Cu (II) ions in presence of Zn (II) ion on *Cedrus deodara* sawdust

Temperature (K)	298	303	308	313	318
Metal ion system	Zn (II) – Cu (II)				
%removal Cu (II)	55.18	71.11	45.36	36.12	19.61
Metal ion system	Zn (II) – total Fe (II, III)				
% removal (Fe II, III)	49.16	37.19	32.14	25.61	13.36
Metal ion system	Zn (II) – total Fe (II, III) – Cu (II)				
% removal (Cu)	42.18	65.5	27.19	19.36	24.18
% removal (Fe II, III)	30.18	32.14	19.28	10.36	3.36

Table 5.2.2 (f) Influence of temperature on biosorption of Fe (II, III) and Cu (II) ions in presence of Zn (II) ion on *Eucalyptus* bark sawdust

Temperature (K)	298	303	308	313	318
Metal ion system	Zn (II) – Cu (II)				
%removal Cu (II)	48.16	65.91	51.58	44.59	32.64
Metal ion system	Zn (II) – total Fe (II, III)				
% removal (Fe II, III)	28.16	27.57	30.76	25.14	11.26
Metal ion system	Zn (II) – total Fe (II, III) – Cu (II)				
% removal (Cu)	33.21	48.97	30.52	28.74	19.26
% removal (Fe II, III)	18.13	24.51	22.61	20.14	8.49

Table 5.2.2 (g) Influence of temperature on biosorption of Fe (II, III) and Cu (II) ions in presence of Zn (II) ion on Eggshell and membrane in liquid phase

Temperature (K)	298	303	308	313	318
Metal ion system Zn (II) – Cu (II)					
%removal Cu (II)	48.16	74.19	55.16	36.19	24.56
Metal ion system Zn (II) – total Fe (II, III)					
% removal (Fe II, III)	19.28	27.19	13.33	9.18	4.31
Metal ion system Zn (II) – total Fe (II, III) – Cu (II)					
% removal (Cu)	36.18	53.12	32.19	24.25	19.34
% removal (Fe II, III)	15.56	20.22	15.11	13.11	9.36

Table

5.2.2 (h) Influence of temperature on biosorption of Fe (II, III) and Cu (II) ions in presence of Zn (II) ion on *Zinc sequestering bacterium VMSDCM*

Temperature (K)	298	303	308	313	318
Metal ion system Zn (II) – Cu (II)					
%removal Cu (II)	74.39	88.19	88.19	83.36	74.19
Metal ion system Zn (II) – total Fe (II, III)					
% removal (Fe II, III)	78.59	81.1	81.1	77.31	68.14
Metal ion system Zn (II) – total Fe (II, III) – Cu (II)					
% removal (Cu)	65.36	81.23	81.23	64.37	48.17
% removal (Fe II, III)	51.18	73.34	73.34	40.36	22.81

Table 5.2.3 (a) Influence of biosorbent dose on biosorption of Fe (II, III) and Cu (II) ions in presence of Zn (II) ion on Mango bark sawdust in liquid phase

Biosorbent dose (g l <sup>-1</sup> )	0.1	0.2	0.3	0.4	0.5	1	2	3	4	5
Metal ion system Zn (II) – Cu (II)										
%removal Cu (II)	25.64	44.16	59.68	68.91	78.81	84.16	84.17	84.18	84.18	84.18
Metal ion system Zn (II) – total Fe (II, III)										
% removal (Fe II, III)	18.44	26.19	38.55	45.37	46.84	48.11	48.14	48.19	48.19	48.19
Metal ion system Zn (II) – total Fe (II, III) – Cu (II)										
% removal (Cu)	18.84	26.67	39.61	55.92	71.36	80.16	80.18	80.19	80.20	80.20
% removal (Fe II, III)	7.69	11.31	14.31	20.14	24.16	26.11	26.13	26.16	26.18	26.18

Table 5.2.3 (b) Influence of biosorbent dose on biosorption of Fe (II, III) and Cu (II) ions in presence of Zn (II) ion on Orange peel in liquid phase.

Biosorbent dose (g l <sup>-1</sup> )	0.1	0.2	0.3	0.4	0.5	1	2	3	4	5
Metal ion system Zn (II) – Cu (II)										
%removal Cu (II)	15.68	30.51	44.39	56.18	72.18	76.18	76.24	76.25	76.25	76.25
Metal ion system Zn (II) – total Fe (II, III)										

	III)										
% removal (Fe II, III)		10.18	21.31	28.18	30.14	31.19	32.11	32.36	32.34	32.39	32.39
Metal ion system	Zn (II) – total Fe (II, III) – Cu (II)										
% removal (Cu)		24.18	33.64	48.16	54.36	65.36	71.16	71.27	71.39	71.42	71.42
% removal (Fe II, III)		8.83	15.32	18.36	19.31	20.36	21.31	21.37	21.45	21.51	21.51

Table 5.2.3 (c) Influence of biosorbent dose on biosorption of Fe (II, III) and Cu (II) ions in presence of Zn (II) ion on Pineapple peel in liquid phase

Biosorbent dose (g l <sup>-1</sup> )		0.1	0.2	0.3	0.4	0.5	1	2	3	4	5
Metal ion system	Zn (II) – Cu (II)										
%removal Cu (II)		12.38	18.36	30.28	44.19	65.39	80.18	81.92	82.38	82.43	82.43
Metal ion system	Zn (II) – total Fe (II, III)										
% removal (Fe II, III)		8.16	12.88	19.47	24.61	26.60	30.33	31.29	31.65	31.65	31.65
Metal ion system	Zn (II) – total Fe (II, III) – Cu (II)										
% removal (Cu)		16.36	21.61	30.29	38.67	51.58	58.21	59.91	60.11	60.11	60.11
% removal (Fe II, III)		4.43	14.38	19.21	21.38	22.91	22.14	23.18	23.26	23.26	23.26

Table 5.2.3 (d) Influence of biosorbent dose on biosorption of Fe (II, III) and Cu (II) ions in presence of Zn (II) ion on Jackfruit peel in liquid phase

Biosorbent dose (g l <sup>-1</sup> )	0.1	0.2	0.3	0.4	0.5	1	2	3	4	5
Metal ion system Zn (II) – Cu (II)										
%removal Cu (II)	18.91	21.59	34.38	48.19	59.21	68.16	68.26	68.91	68.94	68.94
Metal ion system Zn (II) – total Fe (II, III)										
% removal (Fe II, III)	6.91	10.11	21.36	25.29	27.34	28.16	28.41	28.49	28.52	28.52
Metal ion system Zn (II) – total Fe (II, III) – Cu (II)										
% removal (Cu)	11.34	18.36	28.88	38.36	49.38	55.51	55.63	55.71	55.82	55.82
% removal (Fe II, III)	4.43	6.18	11.36	16.34	19.36	20.24	20.61	20.82	20.91	20.91

Table 5.2.3 (e) Influence of biosorbent dose on biosorption of Fe (II, III) and Cu (II) ions in presence of Zn (II) ion on *Cedrus deodara* sawdust in liquid phase

Biosorbent dose (g l <sup>-1</sup> )	0.1	0.2	0.3	0.4	0.5	1	2	3	4	5
Metal ion system Zn (II) – Cu (II)										
%removal Cu (II)	18.11	29.36	50.26	62.36	70.36	71.11	71.36	71.44	71.52	71.52
Metal ion system Zn (II) – total Fe (II, III)										

% removal (Fe II, III)	9.31	20.33	33.16	36.58	36.92	37.19	37.36	37.85	37.94	37.94
Metal ion system	Zn (II) – total Fe (II, III) – Cu (II)									
% removal (Cu)	12.36	23.26	36.79	49.33	57.65	65.5	65.65	65.78	65.91	65.91
% removal (Fe II, III)	6.36	15.47	21.36	28.77	301.81	32.14	32.61	32.76	32.91	32.91

Table 5.2.3 (f) Influence of biosorbent dose on biosorption of Fe (II, III) and Cu (II) ions in presence of Zn (II) ion on Eucalyptus bark sawdust in liquid phase

Biosorbent dose (g l <sup>-1</sup> )	0.1	0.2	0.3	0.4	0.5	1	2	3	4	5
Metal ion system	Zn (II) – Cu (II)									
%removal Cu (II)	12.38	26.34	39.33	50.19	65.18	74.19	74.32	74.46	74.59	74.59
Metal ion system	Zn (II) – total Fe (II, III) – Cu (II)									
% removal (Fe II, III)	6.11	12.89	20.39	25.69	26.91	27.19	27.43	27.78	27.95	27.95
Metal ion system	Zn (II) – total Fe (II, III) – Cu (II)									
% removal (Cu)	12.36	20.38	32.33	41.64	48.92	53.12	53.28	53.50	53.69	53.69
% removal (Fe II, III)	4.11	9.31	15.31	18.91	19.52	20.22	20.38	20.54	20.68	20.68

Table 5.2.3 (g) Influence of biosorbent dose on biosorption of Fe (II, III) and Cu (II) ions in presence of Zn (II) ion on Eucalyptus leaf powder in liquid phase

Biosorbent dose (g l <sup>-1</sup> )	0.1	0.2	0.3	0.4	0.5	1	2	3	4	5
Metal ion system	Zn (II) – Cu (II)									
%removal Cu (II)	10.11	20.18	35.54	49.56	59.88	68.38	68.42	68.61	68.74	68.74
Metal ion system	Zn (II) – total Fe (II, III)									
% removal (Fe II, III)	7.36	14.44	30.61	32.18	33.07	33.18	33.21	33.24	33.28	33.28
Metal ion system	Zn (II) – total Fe (II, III) – Cu (II)									
% removal (Cu)	9.36	14.58	24.56	38.44	51.26	59.64	59.88	59.92	59.96	52.96
% removal (Fe II, III)	2.41	8.48	10.11	15.31	19.24	21.86	21.91	21.93	21.96	21.96

Table 5.2.3 (h) Influence of biosorbent dose on biosorption of Fe (II, III) and Cu (II) ions in presence of Zn (II) ion on Eggshell and membrane in liquid phase

Biosorbent dose (g l <sup>-1</sup> )	0.1	0.2	0.3	0.4	0.5	1	2	3	4	5
Metal ion system	Zn (II) – Cu (II)									
%removal Cu (II)	10.58	25.59	39.88	52.36	60.21	65.91	65.93	65.96	65.96	65.96
Metal ion system	Zn (II) – total Fe (II, III)									
% removal (Fe II, III)	8.56	17.39	25.36	26.89	27.53	27.57	27.59	27.66	27.66	27.66
Metal ion system	Zn (II) – total Fe (II,									



	III) – Cu (II)										
% removal (Cu)		9.32	20.89	28.39	37.77	46.11	48.97	49.21	49.33	49.44	49.66
% removal (Fe II, III)		4.41	12.36	18.66	22.34	23.98	24.51	24.56	24.59	24.62	24.62

Table 5.2.3 (i) Influence of biosorbent dose on biosorption of Fe (II, III) and Cu (II) ions in presence of Zn (II) ion on dead cells of *Zinc sequestering bacterium VMSDCM* accession no HQ108109

Biosorbent dose (g l <sup>-1</sup> )		0.1	0.2	0.3	0.4	0.5	1	2	3	4	5
Metal ion system	Zn (II) – Cu (II)										
%removal Cu (II)		12.36	42.44	69.84	82.18	87.89	88.19	88.24	88.29	88.31	88.31
Metal ion system	Zn (II) – total Fe (II, III)										
% removal (Fe II, III)		9.91	24.18	44.31	61.31	77.81	81.1	81.31	81.39	81.58	81.58
Metal ion system	Zn (II) – total Fe (II, III) – Cu (II)										
% removal (Cu)		10.36	22.36	42.11	68.81	79.34	81.23	81.41	81.52	81.78	81.78
% removal (Fe II, III)		6.63	15.65	30.33	48.64	63.14	73.34	73.56	73.69	73.71	73.71

Table 5.2.4(a) Influence of initial concentration of Zn (II) ion on biosorption of Zn (II) ions in presence of total Fe (II, III) and Cu (II) on Mango bark sawdust

Initial concentration of Zn (II) ion (mg/l)	1	2	4	8	10	20	40	80	100	120	150
Metal ion system Zn (II) – Cu (II)											
%removal Cu (II)	98.61	99.64	99.88	97.11	96.33	92.12	91.33	90.67	89.33	87.67	84.16
Metal ion system Zn (II) – total Fe (II, III)											
% removal (Fe II, III)	94.33	95.11	97.35	96.19	95.33	94.19	93.66	79.66	65.33	59.36	48.11
Metal ion system Zn (II) – total Fe (II, III) – Cu (II)											
% removal (Cu)	95.61	96.19	97.33	95.36	94.31	95.56	94.33	88.71	86.34	84.08	80.16
% removal (Fe II, III)	90.36	91.55	92.36	91.58	90.31	89.63	88.19	71.33	60.11	49.67	26.11

Table 5.2.4 (b) Influence of initial concentration of Zn (II) ion on biosorption of Zn (II) ions in presence of total Fe (II, III) and Cu (II) on Orange peel.

Initial concentration of Zn (II) ion (mg/l)	1	2	4	8	10	20	40	80	100	120	150
Metal ion system Zn (II) – Cu (II)											
%removal Cu (II)	95.14	96.77	97.17	98.11	99.18	97.66	96.33	89.51	84.81	81.11	76.18

Metal ion system	Zn (II) – total Fe (II, III)											
% removal (Fe II, III)		93.36	94.51	95.69	96.77	98.88	95.33	90.41	77.36	71.19	49.33	32.11
Metal ion system	Zn (II) – total Fe (II, III) – Cu (II)											
% removal Cu(II)		94.18	95.64	96.36	97.11	98.11	93.36	92.18	85.61	82.31	78.77	71.16
% removal (Fe II, III)		88.41	89.36	90.11	91.36	92.34	88.61	85.34	74.41	60.31	41.23	21.31

Table 5.2.4 (c) Influence of of initial concentration of Zn (II) ion on biosorption of Zn (II) ions in presence of total Fe (II, III) and Cu (II) on Pineapple peel.

Initial concentration of Zn (II) ion (mg/l)		1	2	4	8	10	20	40	80	100	120	150
Metal ion system	Zn (II) – Cu (II)											
%removal Cu (II)		93.6	94.19	95.66	96.64	97.33	98.34	95.11	94.33	92.19	90.31	82.43
Metal ion system	Zn (II) – total Fe (II, III)											
% removal (Fe II, III)		86.69	87.77	88.19	89.97	90.33	92.36	87.71	74.41	66.68	49.33	31.65
Metal ion system	Zn (II) – total Fe (II, III) –											

	Cu (II)											
% removal Cu(II)	90.34	91.33	92.61	93.33	94.18	95.66	93.31	77.31	70.14	65.55	60.11	
% removal (Fe II, III)	80.33	81.19	82.37	83.39	84.55	85.44	80.66	69.66	64.33	43.19	23.26	

Table 5.2.4 (d) Influence of initial concentration of Zn (II) ion on biosorption of Zn (II) ions in presence of total Fe (II, III) and Cu (II) on Jackfruit peel powder.

Initial concentration of Zn (II) ion (mg/l)	1	2	4	8	10	20	40	80	100	120	150
Metal ion system Zn (II) – Cu (II)											
%removal Cu (II)	96.39	97.88	98.36	99.34	97.36	95.3	92.06	85.36	80.36	77.84	68.94
Metal ion system Zn (II) – total Fe (II, III)											
% removal (Fe II, III)	92.44	93.68	94.55	95.61	90.33	85.55	69.91	55.19	49.34	39.88	28.16
Metal ion system Zn (II) – total Fe (II, III) – Cu (II)											
% removal Cu(II)	94.33	95.66	96.38	98.11	95.5	92.24	82.33	73.11	69.18	64.44	55.51
% removal (Fe II, III)	88.74	89.61	90.11	91.33	81.36	78.14	69.33	54.49	44.16	36.61	20.24

Table 5.2.4 (e) Influence of initial concentration of Zn (II) ion on biosorption of Zn (II) ions in presence of total Fe (II, III) and Cu (II) on *Cedrus deodara* sawdust.

Initial concentration of Zn (II) ion (mg/l)	1	2	4	8	10	20	40	80	100	120	150
Metal ion system Zn (II) – Cu (II)											
%removal Cu (II)	90.24	91.29	92.33	93.36	94.11	95.66	96.33	97.11	98.14	84.4	74.11
Metal ion system Zn (II) – total Fe (II, III)											
% removal (Fe II, III)	88.71	89.36	90.31	91.34	92.36	93.33	94.11	95.64	96.33	64.19	37.19
Metal ion system Zn (II) – total Fe (II, III) – Cu (II)											
% removal Cu(II)	87.77	88.61	89.14	90.31	91.32	92.33	93.36	94.55	95.61	80.81	65.5
% removal (Fe II, III)	82.11	83.65	84.55	85.44	86.91	87.77	88.91	89.64	90.11	66.51	32.14

Table 5.2.4 (f) Influence of initial concentration of Zn (II) ion on biosorption of Zn (II) ions in presence of total Fe (II, III) and Cu (II) on *Eucalyptus* bark sawdust.

Initial concentration of Zn (II) ion (mg/l)	1	2	4	8	10	20	40	80	100	120	150
Metal ion system Zn (II) – Cu (II)											
%removal Cu (II)	85.66	86.33	87.77	88.88	89.92	90.22	92.22	92.24	82.33	77.36	74.19

Metal ion system	Zn (II) – total Fe (II, III)											
% removal (Fe II, III)		80.33	81.34	82.66	83.33	84.54	85.55	86.61	87.07	77.24	66.34	27.19
Metal ion system	Zn (II) – total Fe (II, III) – Cu (II)											
% removal Cu(II)		80.11	81.24	82.26	83.35	84.65	85.51	86.11	87.14	79.66	68.84	53.12
% removal (Fe II, III)		70.14	71.44	72.35	73.36	74.44	75.68	76.44	78.84	59.63	58.44	20.22

Table 5.2.4 (g) Influence of initial concentration of Zn (II) ion on biosorption of Zn (II) ions in presence of total Fe (II, III) and Cu (II) on Eucalyptus leaf powder.

Initial concentration of Zn (II) ion (mg/l)		1	2	4	8	10	20	40	80	100	120	150
Metal ion system	Zn (II) – Cu (II)											
%removal Cu (II)		92.36	93.34	94.5	95.51	96.11	97.38	98.01	85.56	82.11	78.84	68.38
Metal ion system	Zn (II) – total Fe (II, III)											
% removal (Fe II, III)		85.54	86.33	87.71	88.19	89.64	90.22	92.14	74.45	76.33	50.08	33.18
Metal ion system	Zn (II) – total Fe (II, III) – Cu											

	(II)										
% removal Cu(II)	90.44	91.36	92.33	93.34	94.55	95.54	96.61	78.81	75.50	64.48	59.64
% removal (Fe II, III)	80.04	81.19	82.33	84.44	85.69	86.33	87.18	65.33	52.11	38.66	21.86

Table 5.2.4 (h) Influence of initial concentration of Zn (II) ion on biosorption of Zn (II) ions in presence of total Fe (II, III) and Cu (II) on Eggshell and membrane

Initial concentration of Zn (II) ion (mg/l)	1	2	4	8	10	20	40	80	100	120	150
Metal ion system Zn (II) – Cu (II)											
% removal Cu (II)	80.21	84.56	88.19	92.33	95.54	86.12	80.11	78.18	76.44	73.13	65.91
Metal ion system Zn (II) – total Fe (II, III)											
% removal (Fe II, III)	82.16	83.14	84.19	85.66	86.19	59.34	51.33	44.61	40.11	39.19	27.57
Metal ion system Zn (II) – total Fe (II, III) – Cu (II)											
% removal Cu(II)	78.11	79.36	82.46	90.34	94.33	78.84	70.11	64.19	57.16	53.11	48.97
% removal (Fe II, III)	70.11	71.34	72.33	73.31	74.4	61.33	53.33	44.15	39.66	31.4	24.51

Table 5.2.4 (i) Influence of initial concentration of Zn (II) ion on biosorption of Zn (II) ions in presence of total Fe (II, III) and Cu (II) on *Zinc sequestering bacterium VMSDCM* accession no HQ108109.

Initial concentration of Zn (II) ion (mg/l)	1	2	4	8	10	20	40	80	100	120	150
Metal ion system Zn (II) – Cu											

	(II)											
%removal Cu (II)		76.31	77.31	78.14	79.16	79.88	80.14	82.33	84.19	85.66	86.19	88.19
Metal ion system	Zn (II) – total Fe (II, III)											
% removal (Fe II, III)		73.31	74.51	74.58	75.51	76.16	77.71	77.78	78.84	79.33	80.11	81.1
Metal ion system	Zn (II) – total Fe (II, III) – Cu (II)											
% removal Cu(II)		71.91	72.33	73.14	74.33	75.19	76.81	77.36	78.14	78.36	79.11	81.23
% removal (Fe II, III)		60.13	61.36	62.32	63.34	65.61	66.61	68.11	69.3	70.19	71.19	73.24

Table 5.2.6 (a) Influence of particle size on biosorption of total Fe (II, III) and Cu (II) ions on Mango bark sawdust.

Particle size (mm)		0.05	0.1	0.2	0.4	0.5	1	2	3	4
Metal ion system	Zn (II) – Cu (II)									
%removal Cu (II)		84.16	82.16	80.11	79.69	78.84	75.54	73.36	70.11	68.44
Metal ion system	Zn (II) – total Fe (II, III)									
% removal (Fe II, III)		48.11	41.36	40.34	39.39	36.64	34.41	32.22	30.36	25.54
Metal ion system	Zn (II) – total Fe (II, III) – Cu (II)									
% removal Cu(II)		80.16	79.64	78.14	77.6	73.34	72.11	69.81	68.55	64.55



% removal (Fe II, III)	26.11	18.14	15.44	13.36	14.11	11.34	10.36	9.31	8.85
---------------------------	-------	-------	-------	-------	-------	-------	-------	------	------

Table 5.2.6 (b) Influence of particle size on biosorption of total Fe (II, III) and Cu (II) ions on Orange peel

Particle size (mm)	0.05	0.1	0.2	0.4	0.5	1	2	3	4
Metal ion system Zn (II) – Cu (II)									
%removal Cu (II)	76.18	73.36	72.11	70.64	68.84	65.55	62.21	55.55	44.39
Metal ion system Zn (II) – total Fe (II, III)									
% removal (Fe II, III)	32.11	30.11	28.61	25.54	20.11	18.33	17.71	16.64	15.18
Metal ion system Zn (II) – total Fe (II, III) – Cu (II)									
% removal Cu(II)	71.16	69.41	68.31	65.54	60.11	57.77	52.12	47.34	40.19
% removal (Fe II, III)	21.31	19.24	18.71	17.77	15.59	12.36	10.31	8.34	7.59

Table 5.2.6 (c) Influence of particle size on biosorption of total Fe (II, III) and Cu (II) ions on Pineapple peel

Particle size (mm)	0.05	0.1	0.2	0.4	0.5	1	2	3	4
Metal ion system Zn (II) – Cu (II)									
%removal Cu (II)	82.43	80.19	79.91	78.33	77.41	75.33	74.19	70.36	66.34
Metal ion system Zn (II) – total Fe									

	(II, III)									
% removal (Fe II, III)		31.65	25.54	23.34	22.19	20.11	18.34	17.33	15.41	13.66
Metal ion system	Zn (II) – total Fe (II, III) – Cu (II)									
% removal Cu (II)		60.11	58.33	55.51	50.19	45.55	40.41	31.66	29.33	28.14
% removal (Fe II, III)		23.26	20.11	15.11	12.19	8.36	6.66	4.36	2.19	1.08

Table 5.2.6 (d) Influence of particle size on biosorption of total Fe (II, III) and Cu (II) ions on Jackfruit peel powder

Particle size (mm)		0.05	0.1	0.2	0.4	0.5	1	2	3	4
Metal ion system	Zn (II) – Cu (II)									
%removal Cu (II)		68.94	66.51	61.33	62.16	60.36	58.55	55.54	50.99	46.66
Metal ion system	Zn (II) – total Fe (II, III)									
% removal (Fe II, III)		28.16	25.11	21.16	18.88	15.51	13.30	11.01	9.36	8.88
Metal ion system	Zn (II) – total Fe (II, III) – Cu (II)									
% removal Cu (II)		55.51	54.55	52.47	50.36	47.71	44.31	40.19	38.33	35.61
% removal (Fe II, III)		20.24	18.33	15.61	13.33	10.36	9.09	8.88	7.76	6.03

Figure 5.2.6 (e) Influence of particle size on biosorption of total Fe (II, III) and Cu (II) ions on *Cedrus deodara* sawdust.

Particle size (mm)	0.05	0.1	0.2	0.4	0.5	1	2	3	4
Metal ion system Zn (II) – Cu (II)									
%removal Cu (II)	74.11	73.36	72.19	71.19	70.33	68.19	65.66	63.33	62.19
Metal ion system Zn (II) – total Fe (II, III)									
% removal (Fe II, III)	37.19	35.54	32.19	30.16	28.87	25.54	23.36	22.19	20.36
Metal ion system Zn (II) – total Fe (II, III) – Cu (II)									
% removal Cu (II)	65.5	59.91	55.51	50.16	48.19	45.55	44.19	40.33	38.33
% removal (Fe II, III)	32.14	27.33	25.61	23.36	20.11	15.36	13.61	10.11	9.93

Table 5.2.6 (f) Influence of particle size on biosorption of total Fe (II, III) and Cu (II) ions on *Eucalyptus* bark sawdust

Particle size (mm)	0.05	0.1	0.2	0.4	0.5	1	2	3	4
Metal ion system Zn (II) – Cu (II)									
%removal Cu (II)	74.19	72.11	70.16	69.33	68.41	65.55	60.33	51.36	45.77
Metal ion system Zn (II) – total Fe (II, III)									
% removal (Fe II, III)	27.19	23.36	22.18	20.19	15.66	13.4	11.36	10.11	9.95

Metal ion system	Zn (II) – total Fe (II, III) – Cu (II)									
% removal Cu (II)		53.12	48.19	45.66	42.33	40.36	38.84	32.19	26.39	22.19
% removal (Fe II, III)		20.22	17.19	15.66	13.33	12.10	10.11	8.87	8.83	7.77

Table 5.2.6 (g) Influence of particle size on biosorption of total Fe (II, III) and Cu (II) ions on Eucalyptus Leaf powder

Particle size (mm)		0.05	0.1	0.2	0.4	0.5	1	2	3	4
Metal ion system	Zn (II) – Cu (II)									
%removal Cu (II)		68.38	66.34	65.33	64.5	63.38	62.11	60.11	58.33	55.5
Metal ion system	Zn (II) – total Fe (II, III)									
% removal (Fe II, III)		33.18	32.11	30.6	28.51	25.33	24.01	18.31	15.03	12.60
Metal ion system	Zn (II) – total Fe (II, III) – Cu (II)									
% removal Cu (II)		59.64	55.53	52.12	50.66	48.33	46.34	42.33	40.19	46.34
% removal (Fe II, III)		21.86	18.33	15.06	14.33	13.11	12.16	10.19	9.36	8.81

Table 5.2.7 (a) Influence of contact time on biosorption of total Fe (II, III) and Cu (II) ions on Mango bark sawdust

Contact time (hours)		0.5	1	2	4	6	10	14	18	22	26	32	36
----------------------	--	-----	---	---	---	---	----	----	----	----	----	----	----

Metal ion system	Zn (II)													
	-													
	Cu (II)													
%removal Cu (II)		72.16	75.19	78.36	80.18	82.33	83.41	83.36	83.42	83.61	84.90	84.05	84.16	8
Metal ion system	Zn (II)													
	-													
	total Fe (II, III)													
% removal (Fe II, III)		37.74	40.19	42.18	45.33	46.41	47.08	47.29	47.81	47.39	47.81	48.09	48.11	4
Metal ion system	Zn (II)													
	-													
	total Fe (II, III)													
	-													
	Cu (II)													
% removal Cu (II)		51.33	60.19	73.55	76.89	77.83	78.55	79.46	79.51	79.63	79.70	79.86	80.16	8
% removal (Fe II, III)		11.96	16.33	20.33	22.4	24.51	25.33	25.61	25.77	25.84	25.89	25.92	26.11	2

Table 5.2.7 (b) Influence of contact time on biosorption of total Fe (II, III) and Cu (II) ions on Orange peel.

Contact time (hours)	0.5	1	2	4	6	10	14	18	
Metal ion system	Zn (II)								
	-								
	Cu (II)								
%removal Cu (II)		36.34	40.39	46.19	58.88	62.33	69.46	76.18	76.18
Metal ion system	Zn (II)								
	-								
	total Fe								

	(II, III)								
% removal (Fe II, III)		25.33	28.61	30.19	31.16	31.88	31.96	32.11	32.11
Metal ion system	Zn (II) - total Fe (II, III) - Cu (II)								
% removal Cu (II)		42.33	49.88	59.77	67.77	68.42	70.11	71.16	71.16
% removal (Fe II, III)		14.11	17.11	19.66	20.66	20.74	20.88	21.31	21.31

Table 5.2.7 (c) Influence of contact time on biosorption of total Fe (II, III) and Cu (II) ions on Pineapple peel

Contact time (hours)		0.5	1	2	4	6	10	14
Metal ion system	Zn (II) - Cu (II)							
%removal Cu (II)		71.36	75.66	78.19	80.11	81.33	82.41	82.43
Metal ion system	Zn (II) - total Fe (II, III)							
% removal (Fe II, III)		25.51	26.33	27.88	28.39	29.40	31.65	31.65
Metal ion system	Zn (II) - total Fe (II, III)							

	-							
	Cu							
	(II)							
% removal Cu (II)		51.19	52.33	53.66	54.81	59.32	60.11	60.11
% removal (Fe II, III)		15.64	18.33	21.36	21.91	22.03	23.26	23.26

Table 5.2.7 (d) Influence of contact time on biosorption of total Fe (II, III) and Cu (II) ions on Jackfruit peel

Contact time (hours)		0.5	1	2	4	6	10	14	18	22
Metal ion system	Zn (II)									
	-									
	Cu (II)									
% removal Cu (II)		35.5	41.36	45.54	49.36	50.11	55.36	65.31	68.36	68.94
Metal ion system	Zn (II)									
	-									
	total Fe (II, III)									
% removal (Fe II, III)		21.36	24.19	26.33	26.77	26.86	28.05	28.11	28.16	28.16
Metal ion system	Zn (II)									
	-									
	total Fe (II, III)									
	-									
	Cu (II)									
% removal Cu (II)		30.11	34.66	38.19	44.66	45.31	47.11	50.36	55.51	55.51
% removal (Fe II, III)		13.36	15.19	17.36	19.55	19.59	19.66	19.87	20.24	20.24

Table 5.2.7 (e) Influence of contact time on biosorption of total Fe (II, III) and Cu (II) ions on *Cedrus deodara* sawdust

Contact time (hours)	0.5	1	2	4	6
Metal ion system Zn (II) – Cu (II)					
%removal Cu (II)	47.77	53.39	69.11	74.11	74.11
Metal ion system Zn (II) – total Fe (II, III)					
% removal (Fe II, III)	31.03	34.44	36.49	37.19	37.19
Metal ion system Zn (II) – total Fe (II, III) – Cu (II)					
% removal Cu (II)	56.61	59.33	62.33	65.5	65.5
% removal (Fe II, III)	22.19	26.33	28.34	32.14	32.14

Table 5.2.7 (f) Influence of contact time on biosorption of total Fe (II, III) and Cu (II) ions on *Eucalyptus* bark sawdust

Contact time (hours)	0.5	1	2	4	6	10	14
Metal ion system Zn (II) – Cu (II)							
%removal Cu (II)	66.61	68.55	71.44	72.33	73	73.6	73.69
					3	4	



Metal ion system	Zn (II) – total Fe (II, III)							
% removal (Fe II, III)		20.33	22.39	25.64	26.33	26.	26.55	26.81
						39		

Metal ion system	Zn (II) – total Fe (II, III) – Cu (II)							
% removal Cu (II)		42.33	44.39	47.77	48.19	50.	51.33	52.11
						33		
% removal (Fe II, III)		13.33	16.39	17.22	18.21	19.	19.59	19.81
						33		

Table 5.2.7 (g) Influence of contact time on biosorption of total Fe (II, III) and Cu (II) ions on Eucalyptus leaf powder

Contact time (hours)		0.5	1	2	4	6	10	14	18
Metal ion system	Zn (II) – Cu (II)								
%removal Cu (II)		58.6	62.19	65.55	66.34	66.84	67.71	68.38	68.38
Metal ion system	Zn (II) – total Fe (II, III)								
% removal (Fe II, III)		24.33	26.39	29.31	31.33	32.66	32.86	33.18	33.18

Metal ion system	Zn (II) – total Fe (II, III) – Cu (II)							
% removal Cu (II)		50.19	54.59	56.77	57.77	58.11	58.63	59.64
% removal (Fe II, III)		13.33	15.66	17.77	19.24	20.11	20.64	21.86

Table 5.2.7 (h) Influence of contact time on biosorption of total Fe (II, III) and Cu (II) ions on Eggshell and membrane

Contact time (hours)		0.5	1	2	4	6
Metal ion system	Zn (II) – Cu (II)					
% removal Cu (II)		49.39	52.36	54.39	57.71	59.22
Metal ion system	Zn (II) – total Fe (II, III)					
% removal (Fe II, III)		21.19	23.64	25.66	26.91	27.10
Metal ion system	Zn (II) – total Fe (II, III) – Cu (II)					
% removal Cu (II)		42.19	43.36	44.18	45.53	46.57
% removal (Fe II, III)		17.36	18.36	19.33	20.5	21.36

Table 5.2.7 (i) Influence of contact time on biosorption of total Fe (II, III) and Cu (II) ions on *Zinc sequestering bacterium VMSDCM* accession no. HQ108109

Contact time (hours)		0.5	1	2	4
Metal ion system	Zn (II) – Cu (II)				
%removal Cu (II)		80.19	82.36	88.19	88.19
Metal ion system	Zn (II) – total Fe (II, III)				
% removal (Fe II, III)		74.11	78.19	81.1	81.1
Metal ion system	Zn (II) – total Fe (II, III) – Cu (II)				
% removal Cu (II)		75.52	78.84	81.23	81.23
% removal (Fe II, III)		67.12	69.56	73.24	73.24

Table 5.2.8 (a) Influence of agitation rate on biosorption of total Fe (II, III) and Cu (II) ions on Mango bark sawdust

Agitation rate (RPM)		25	50	75	100	200	300
Metal ion system	Zn (II) – Cu (II)						
%removal Cu (II)		70.68	75.69	80.33	82.39	84.16	84.16
Metal ion system	Zn (II) – total Fe (II, III)						
% removal (Fe II, III)		33.31	39.44	46.59	47.11	48.11	48.11
Metal ion system	Zn (II) – total Fe (II, III) – Cu (II)						
% removal Cu (II)		69.66	77.34	79.54	80.03	80.16	80.16
% removal (Fe II, III)		17.33	20.36	24.33	25.69	26.11	26.11

Table 5.2.8 (b) Influence of agitation rate on biosorption of total Fe (II, III) and Cu (II) ions on Orange peel

Agitation rate (RPM)	25	50	75	100	200	300	400
Metal ion system Zn (II) – Cu (II)							
%removal Cu (II)	63.39	66.88	70.33	73.39	75.64	75.88	75.93
Metal ion system Zn (II) – total Fe (II, III)							
% removal (Fe II, III)	20.33	26.18	29.64	30.39	31.34	31.55	31.79
Metal ion system Zn (II) – total Fe (II, III) – Cu (II)							
% removal Cu (II)	50.11	55.74	60.19	66.13	70.19	70.55	70.91
% removal (Fe II, III)	12.19	15.36	19.34	20.36	20.54	20.68	20.89

Table 5.2.8 (c) Influence of agitation rate on biosorption of total Fe (II, III) and Cu (II) ions on Pineapple peel

Agitation rate (RPM)	25	50	75	100	200	300	400
Metal ion system Zn (II) – Cu (II)							
%removal Cu (II)	51.33	60.34	68.54	73.36	81.59	82.43	82.43
Metal ion system Zn (II) – total Fe (II, III)							
% removal (Fe II, III)	20.33	26.39	28.34	30.59	30.87	31.65	31.65
Metal ion system Zn (II) – total Fe (II, III) – Cu (II)							
% removal Cu (II)	40.91	44.33	49.39	55.59	59.64	60.11	60.11
% removal (Fe II, III)	13.36	16.81	19.33	22.36	22.44	23.26	23.26

Table 5.2.8 (d) Influence of agitation rate on biosorption of total Fe (II, III) and Cu (II) ions on Jackfruit peel

Agitation rate (RPM)	25	50	75	100	200	300	400
Metal ion system Zn (II) – Cu (II)							
%removal Cu (II)	67.36	67.45	67.58	67.88	68.31	68.91	68.94
Metal ion system Zn (II) – total Fe (II, III)							
% removal (Fe II, III)	27.15	27.33	27.44	27.88	28.03	28.16	28.16
Metal ion system Zn (II) – total Fe (II, III) – Cu (II)							
% removal Cu (II)	54.66	54.74	54.89	54.95	55.33	55.51	55.51
% removal (Fe II, III)	19.66	19.87	19.98	20.12	20.19	20.24	20.24

Table 5.2.8 (e) Influence of agitation rate on biosorption of total Fe (II, III) and Cu (II) ions on *Cedrus deodara* sawdust

Agitation rate (RPM)	25	50	75	100	200	300	400	500	600
Metal ion system Zn (II) – Cu (II)									
%removal Cu (II)	33.1	45.64	50.19	55.36	60.33	68.77	72.16	73.36	74.09
Metal ion system Zn (II) – total Fe (II, III)									
% removal (Fe II, III)	25.55	30.39	33.88	35.19	36.33	36.58	36.77	36.92	37.05
Metal ion system Zn (II) – total Fe (II, III) – Cu (II)									
% removal Cu (II)	30.19	38.77	40.11	49.36	55.19	60.19	62.33	64.48	65.93
% removal (Fe II, III)	15.66	19.33	25.65	27.36	29.88	31.33	31.91	32.02	32.08

Table 5.2.8 (f) Influence of agitation rate on biosorption of total Fe (II, III) and Cu (II) ions on Eucalyptus bark sawdust

Agitation rate (RPM)	25	50	75	100	200	300	400	500
Metal ion system	Zn (II) – Cu (II)							
%removal Cu (II)	37.38	54.59	69.36	73.34	73.55	74.08	74.09	74.19
Metal ion system	Zn (II) – total Fe (II, III)							
% removal (Fe II, III)	20.33	23.36	24.91	26.61	27.08	27.11	27.19	27.19
Metal ion system	Zn (II) – total Fe (II, III) – Cu (II)							
% removal Cu (II)	30.63	35.34	48.11	52.66	52.9	53.06	53.12	53.12
% removal (Fe II, III)	13.36	16.64	18.77	20.07	20.02	20.11	20.22	20.22

Table 5.2.8 (g) Influence of agitation rate on biosorption of total Fe (II, III) and Cu (II) ions on Eucalyptus leaf powder

Agitation rate (RPM)	25	50	75	100	200	300	400	500
Metal ion system	Zn (II) – Cu (II)							
%removal Cu (II)	62.55	62.84	62.92	63.05	63.11	63.21	63.38	63.38
Metal ion system	Zn (II) – total Fe (II, III)							
% removal (Fe II, III)	32.16	32.58	32.88	32.95	33.02	33.11	33.18	33.18
Metal ion system	Zn (II) – total Fe (II, III) – Cu (II)							
% removal Cu (II)	58.55	58.85	58.93	58.09	58.33	58.5	59.64	59.64
% removal (Fe II, III)	20.11	20.52	20.68	20.82	21.33	21.58	21.86	21.86

Table 5.2.8 (h) Influence of agitation rate on biosorption of total Fe (II, III) and Cu (II) ions on Eggshell and membrane

Agitation rate (RPM)	25	50	75	100	200	300	400	500	600
Metal ion system	Zn (II) – Cu (II)								
%removal Cu (II)	33.61	41.36	52.36	58.33	64.55	64.88	65.49	65.91	65.91
Metal ion system	Zn (II) – total Fe (II, III)								
% removal (Fe II, III)	22.38	24.55	26.33	26.92	27.09	27.19	27.33	27.57	27.57
Metal ion system	Zn (II) – total Fe (II, III) – Cu (II)								
% removal Cu (II)	30.31	35.58	42.33	46.41	48.11	48.29	48.56	48.97	48.97
% removal (Fe II, III)	17.44	20.26	22.26	23.61	23.84	23.96	24.12	24.51	24.51

Table 5.2.8 (i) Influence of agitation rate on biosorption of total Fe (II, III) and Cu (II) ions on *Zinc sequestering bacterium VMSDCM* accession no HQ108109

Agitation rate (RPM)	25	50	75	100	200	300
Metal ion system	Zn (II) – Cu (II)					
%removal Cu (II)	62.16	71.16	79.55	86.69	88.19	88.19
Metal ion system	Zn (II) – total Fe (II, III)					
% removal (Fe II, III)	38.36	53.36	74.6	78.92	81.1	81.1
Metal ion system	Zn (II) – total Fe (II, III) – Cu (II)					
% removal Cu (II)	45.19	56.61	60.33	78.41	81.23	81.23
% removal (Fe II, III)	32.19	44.56	59.63	67.33	73.24	73.24

## ANNEXURE (A-3)

---

```
#include<iostream>
#include<math.h>
using namespace std;
int main()
{
double c, average2, av1, av2, n, t;
double s=0;
for(int i=0;i<3;i++)
{
cout<<"Enter how many times the user want to enter the value of n:"<<endl;
cin>>n;
cout<<"Enter the temperature in Kelvin:"<<endl;
cin>>t;
if (t==298 || t==303)
{
double av1=0;
double c1,b,k,a,average1, q;
cout<<"Enter the value of 'D':"<<endl;
cin>>b;
cout<<"Enter the value of 'ln H':"<<endl;
cin>>k;
for (int i=0;i<n;i++)
{
cout<<"Enter the value of qe:"<<endl;
```



```

cin>>q;
cout<<"Enter the value of Ce:"<<endl;
cin>>c;
double r= log (c);
c1=q - ( (b*k) + (b*2.303*r) );
av1=av1+c1;
}
average1=av1/4;
cout<<"The value of the constant for"<<t<<" Kelvin is:"<<endl;
s=s+average1;
cout<<"The summed value of the constant for 298 K and 303 K is:"<<s<<endl;
}
else
if (t==308)
{
double av2=0;
double c2,b1,b2, s, m, e, b, k, c, q;
for (int i=0;i<n;i++)
{
cout<<"Enter the value of Cbm:"<<endl;
cin>>s;
cout<<"Enter the value of Qm:"<<endl;
cin>>m;
cout<<"Enter the value of Qe:"<<endl;
cin>>e;
cout<<"Enter the value of Vm:"<<endl;
cin>>b;

```

```
cout<<"Enter the value of Ce:"<<endl;
cin>>c;
b1=(m*b*c);
b2=(2*b*c)-(b*b*c)-(s);
c2=e-(b1/b2);
av2=av2+c2;
}
average2=av2/4;
cout<<"The value of the constant, 'Aa' is:"<<average2<<endl;
}
else
{
cout<<"Temperature Not in the required range"<<endl;
}
}
c=(s+average2);
cout<<"The value of the constant, 'DVM' is :"<<c<<endl;
return 0;
system("pause");
}
```

## APPENDIX (A-1)

$$q_e = (q_{\max} b C_e) / (1 + b C_e) \quad (\text{A-1})$$

$q_{\max}$  and  $b$  are the maximum uptake capacity (mg/g) and langmuir constant or sorption equilibrium constant (L/mg) respectively. The value of  $q_{\max}$  and  $b$  can be calculated from the slope and intercept of plot extrapolated between  $C_e/q_e$  and  $C_e$ .

$$q_e = q_{\max} (b C_e) / 1 + b C_e \quad (\text{A-2})$$

$$1/q_e = (1/b q_m) 1/C_e + 1/q_m \quad (\text{A-3})$$

$$q_e = q_m - (1/b) q_e / C_e \quad (\text{A-4})$$

$$q_e / C_e = b q_m - K_L q_e \quad (\text{A-5})$$

In the Langmuir model, the saturation capacity of the adsorbent ( $q_{\max}$ ) is equal to the saturation of the identical sites. The Langmuir constant  $b$  has special relationship with temperature. The increase or decrease in the value of  $b$  with the increase of temperature explains the thermodynamic feasibility of the biosorption mechanism as endothermic or exothermic indeed (Ho and Ofamaja, 2006, Padmavathy, 2008, Shaker, 2007, Vilar et al., (2008), Ruiz et al., 2008).

Freundlich isotherm, an empirical relationship between equilibrium concentration of metal ion in liquid phase and solid phase. The assumptions of Freundlich model are as follows

- (i) Adsorbent surface is heterogeneous and
- (ii) Multilayer adsorbent surface coverage by adsorbate

Nonlinear exponential form Freundlich equation has been represented in equation (A-6).

$$q_e = K_f C_e^{1/n} \quad (\text{A-6})$$

Linear form of Freundlich model can be represented as follows:

$$\text{Log } [q_e] = \text{Log } [K_f] + 1/n \log [C_e] \quad (\text{A-7})$$

$K_f$  and  $1/n$  are Freundlich constant (mg/g) and parameter for surface heterogeneity (Febrianto et al., (2009)).

Temkin isotherm assumes the temperature dependent linear decrease in heat of sorption. The relation has been represented in equation (A-8) (Febrianto et al., 2009).

$$q_e = B_t \ln(K_t C_e) \quad (\text{A-8})$$

Where,  $B_t$  constant related to the heat of adsorption and  $K_t$  ( $\text{lg}^{-1}$ ) are model constants. Usually this model is used to explain the sorption of metal ion on heterogeneous surface.

Dubinin- Radushkevich (D-R) model assumes the heterogeneous surface characteristic of the adsorbent. The model equation has been shown in equation (A-9) (Sari and Tuzen, 2009).

$$q_e = q_{\max} \exp \left[ \frac{\left( -RT \ln \left( \frac{C_e}{C_s} \right)^2 \right)}{\beta \varepsilon^2} \right] \quad (\text{A-9})$$

where  $R$  is gas constant (8.314 J/mole K),  $T$  is absolute temperature (K),  $\beta$  is model constant,  $\varepsilon$  is polayni potential and  $C_s$  is Zn (II) ion solubility at given temperature.

The non-linear form of pseudo first order reaction model has been shown in equation (A-10) (Sari and Tuzen, 2009).

$$\left[ \frac{dq_t}{dt} \right] = K_1 (q_e - q_t) \quad (\text{A-10})$$

where,  $q_e$  and  $q_t$  are uptake capacities of metal ion per unit of adsorbent at equilibrium and at time  $t$  and  $K_1$  is the Zn (II) ion biosorption constant. On integrating the equation (4) at boundary conditions  $q = 0$  at  $t = 0$  and  $q = q_t$  at  $t = t$  we get equation (A-11)

$$\log(q_e - q_t) = \log q_e - \frac{K_1 t}{2.303} \quad (\text{A - 11})$$

The slope and intercept of plot between  $\log (q_e - q_t)$  and time yields the value of reaction constant  $K_1$  ( $\text{min}^{-1}$ ) and  $\log q_e$  ( $\text{mgg}^{-1}$ ) respectively.

Assuming the binding of metal ions with adsorbate molecule by chemisorption mechanism, the non-linear form of pseudo second order has been represented in equation (A -12) (Abdelwaha, 2007).

$$\frac{dq_t}{dt} = K_2 (q_e - q_t)^2 \quad (\text{A -12})$$

Integrating equation (6) at boundary conditions reproduces equation (A -13)

$$\frac{t}{q_t} = \frac{t}{q_e} + \frac{1}{K_2 q_e^2} \quad (\text{A -13})$$

Extrapolation of the plot between  $t/q_t$  and  $t$  calculates the value of  $K_2$  and  $q_e$  as intercept and slope of the curve respectively.

Equation no. (A-14) represents linearized form of intra particle diffusion model (Vagheti et al., 2008).

$$q_e = K_{id} (t)^{0.5} + I \quad (\text{A-14})$$

where,  $K_{id}$  is intra particle diffusion constant and  $I$  is the intercept of the model.

Equation no. (A-15) (Srinivasan and Hema, 2009) represents the linearized form of Bangham's model.

$$\log \left| \log \left\{ \frac{C_0}{C_0 - qm} \right\} \right| = \log \left( \frac{K_0 m}{2.303V} \right) + \alpha \log(t) \quad (\text{A-15})$$

where  $q$  is uptake capacity at time ( $t$ ),  $m$  is mass of biomass in grams,  $V$  volume of solution in liters,  $\alpha > 1$  and  $K_0$  are constants.

## FTIR and SEM photographs of metal loaded selected biomass and latest references survey

The SEM photograph of *Cedrus deodara* sawdust (CDS) after adsorption of metal ion has been shown below.

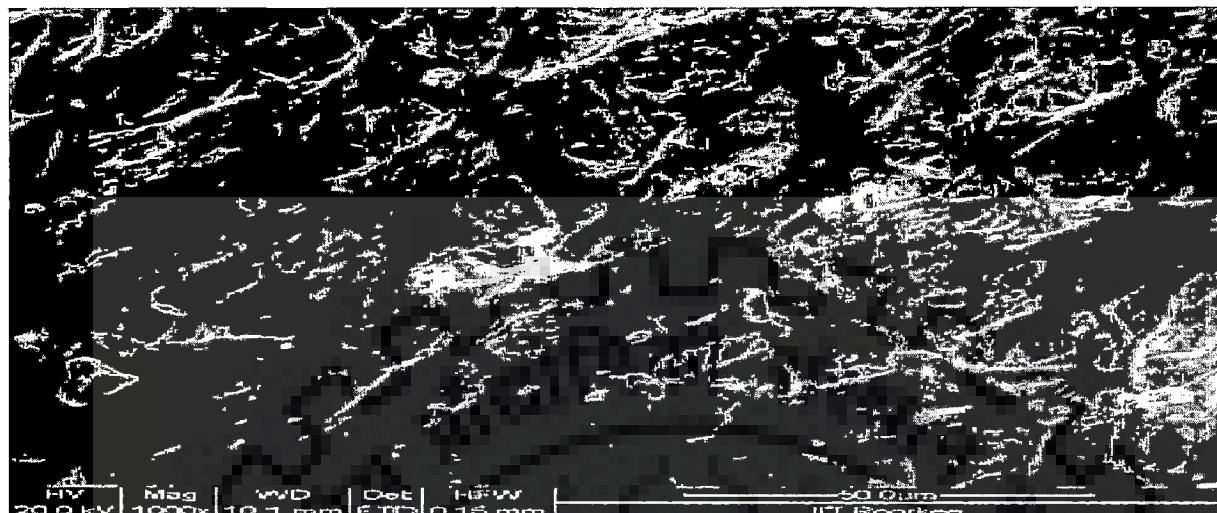


Figure 1: Metal loaded *Cedrus deodara* sawdust

Explanation of figure 1: The surface of the CDS after the sorption of metal ion (metal loaded) seemed to be smooth, homogeneous and crystalline. The surface of the sawdust became impregnated with Zn (II) ion leading to filling of pores present on the surface of CDS. Figure 2 and table 1 represents the FTIR spectrum of metal loaded *Cedrus deodara* sawdust.

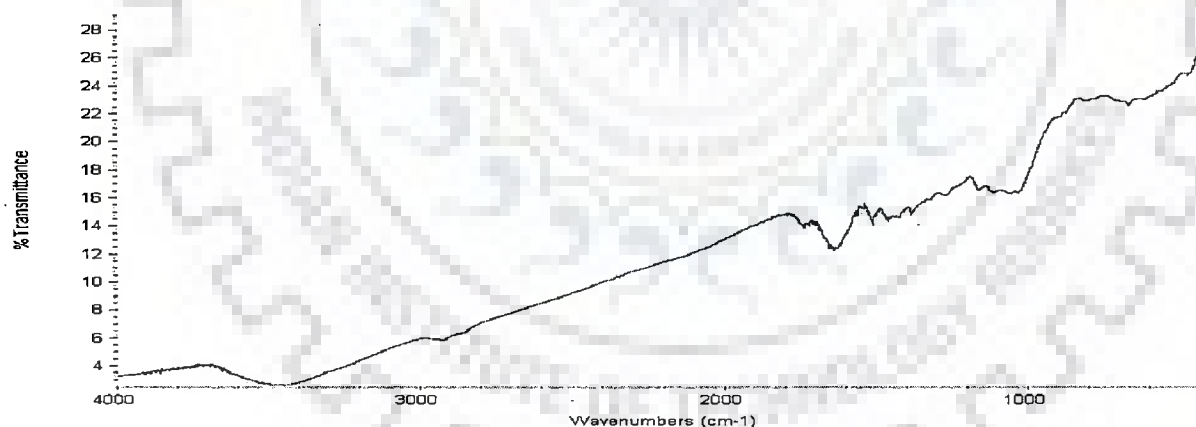


Figure 2: FTIR spectrum of *Cedrus deodara* sawdust

Table 1: Study of FTIR spectrum of metal loaded *Cedrus deodara* sawdust biomass

Metal loaded biomass (Wave numbers $\text{cm}^{-1}$ )	Functional group
3500 – 3000	Very weak reflectance, diminished, overlapping of -NH and -OH vibrations
2000-1000	Very weak reflectance

Weak and diminished reflectance pattern between  $3500 - 3000 \text{ cm}^{-1}$  and  $2000 - 1000 \text{ cm}^{-1}$  after the metal ion binding on biomass surface. Compared to unloaded biomass almost all the peaks of functional groups having affinity for Zn (II) ion were disappeared or diminished in metal loaded biomass, indicating the involvement of biosorbent surface chemistry in metal ion adsorption across liquid phase. The FTIR spectrums of metal unloaded and loaded microbial strain have been shown in figure 3 and figure 4.

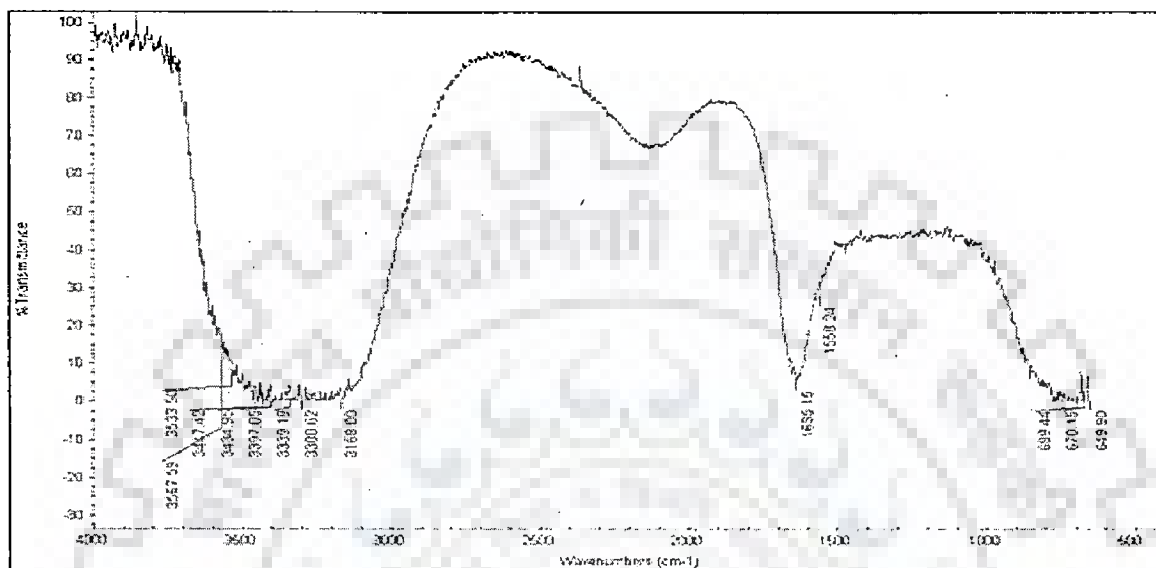


Figure 3: FTIR Spectrum of *zinc sequestering bacterium VMSDCM* Accession no. HQ 108109 before the biosorption of metal ion.

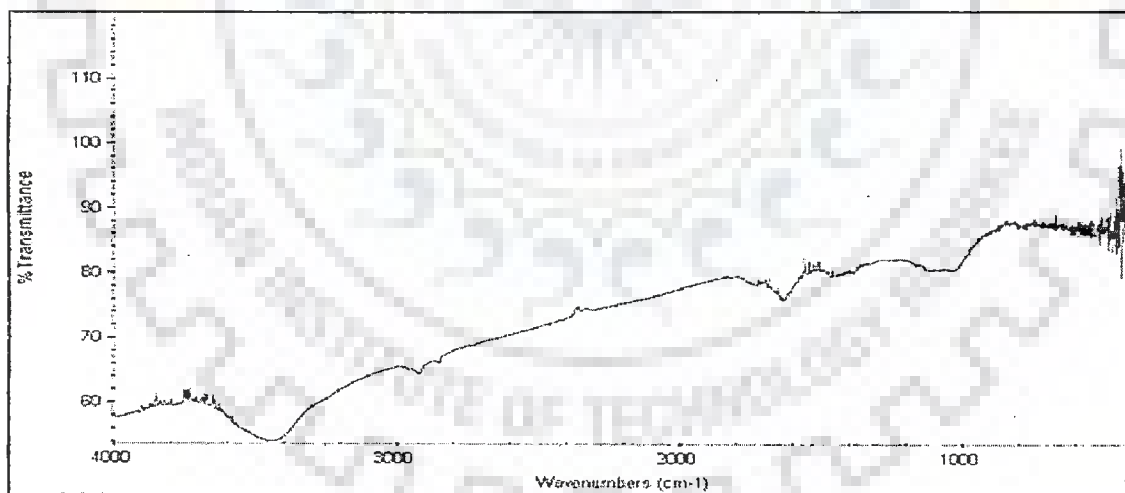


Figure 4: FTIR Spectrum of *zinc sequestering bacterium VMSDCM* Accession no. HQ108109 after the biosorption of metal ion.

The strong reflectance of FTIR spectrum between  $3500 - 3000 \text{ cm}^{-1}$  of the wave number indicates the presence of hydroxyl (-OH) and amide (-NH) negatively charged functional groups (Ozacan et al. 2009, Zakaria et al. 2009, Shen et al. 2009) on the surface of *zinc sequestering bacterium VMSDCM* Accession no. HQ108109. The broad peak reflectance/ vibration in range of  $3500 -$

3000  $\text{cm}^{-1}$  wave number indicated the overlapping of amide and hydroxyl vibrations (Mishra et al. 2010). Contrary to this, the FTIR spectrum shown in figure 4 indicated the weak reflectance of the functional groups. The weak reflectance of functional groups in *zinc sequestering bacterium VMSDCM* Accession no. HQ108109 after the sorption of Zn (II) compared to spectrum pattern of *zinc sequestering bacterium VMSDCM* Accession no. HQ108109 before the biosorption of metal ion was due to the involvement of functional groups in biosorption of Zn (II) ion on to bacterium VMSDCM surface.

### Reference

Ozcan, S. A. Tunali, S. Akar, T. and Ozacan, A., Biosorption of lead (II) ions onto waste biomass of *Phaseolus vulgaris L.*: Estimation of the equilibrium, kinetic and thermodynamic parameters, *Desalination*, vol 244, pp. 188–198, 2009.

Zakaria, A. Z. Suratman, M. Mohammed, N. and Ahmad, A. W., Chromium (VI) removal from aqueous solution by untreated rubber sawdust, *Desalination*, 244, pp. 109 – 121, 2009.

Shen, W. Chen, S. Shi, S. Li, X. Zhang, X. Hu, W. and Wang, H., Adsorption of Cu (II) and Pb (II) onto diethylenetriamine-bacterial cellulose, *Carbohydr. Polymers*, vol 75, pp. 110 – 114, 2009.

### Latest References Survey

Name of adsorbent	Metal ion	pH	Temp ( $^{\circ}\text{C}$ )	Initial concentration of metal ion	% removal	References
Line stone Sample S	Zn (II)	3-6	25, 30, 35	10(mg/l)	63.0 -86.8	Sidiri et al., 2012
Lime stone Sample C	Zn (II)	3-6	25, 30, 35	10(mg/l)	30.7 – 88.2	Sidiri et al., 2012
Lime stone Sample G	Zn (II)	3-6	25, 30, 35	10(mg/l) (mg/l)	25.3-88.6	Sdiri et al., 2012
Lime stone Sample Z	Zn (II)	3-6	25, 30, 35	10(mg/l)	6.5-37.8	Sdiri et al., 2012
Chitosan	Zn (II)	6	25 $\pm$ 2	0.1 – 750 (mg/l)	<70	Benavente et al., 2011
Purolite S-920	Zn (II)	5	25	0.001 mol/l	88.36	Jachula et al. 2012
Activated carbon derived from eucalyptus bark	Zn (II)	5	25	1.52 mmol/l	93.42	Mishra et al., 2012
Immobilized bacterium cells	Zn (II)	7	30 $\pm$ 2	33to 70 g/l	NA	Mishra et al., 2012



### Latest References

Benavente, M., Moreno, L., Martinez, J., Sorption of heavy metals from gold mining wastewater using chitosan, *J. Taiwan Institute Chem. Eng.*, vol 42, pp. 976 – 988, 2011.

Sdiri, A., Higashi, T., Jamoussi, F., Bouaziz, S., Effect of impurities on the removal of heavy metals by natural lime stones in aqueous systems, *J. Env. Manag.*, vol 93, pp. 245 – 253, 2012.

Jachula, J., Kolodynska, D., Hubicki, Z., Sorption of Zn (II) and Pb (II) ions in the presence of the biodegradable complexing agent of a new generation, *Chem. Eng. Res. Design.*, doi: 10.1016/j.cherd.2012.01.015, 2012.

Mishra, V., Balomajumder, C., Agarwal, V. K., Sorption of Zn (II) ion onto surface of activated carbon derived from eucalyptus bark saw dust from industrial wastewater: Isotherm, kinetics, mechanistic modeling and thermodynamics, *Desalination and Water Treatment*, vol 46, Issue 1-3, pp. 332 – 352, 2012.

Mishra, V., Balomajumder, C., Agarwal, V. K., Simultaneous adsorption and bioaccumulation: A study on continuous mass transfer in column reactor, *Environmental Progress and Sustainable Energy*, AICHE, DOI: 10.1002/ep.11671, 2012.

### MODELING OF CONTINUOUS COLUMN STUDY

Mishra, V., Balomajumder, C., Agarwal, V. K., Simultaneous adsorption and bioaccumulation: A study on continuous mass transfer in column reactor, *Environmental Progress and Sustainable Energy*, AICHE, DOI: 10.1002/ep.11671, 2012.